Oxidative Medicine and Cellular Longevity

Oxidative Stress in Disease and Aging: Mechanisms and Therapies 2016

Guest Editors: Claudio Cabello-Verrugio, Felipe Simon, Capucine Trollet, and Juan F. Santibanez

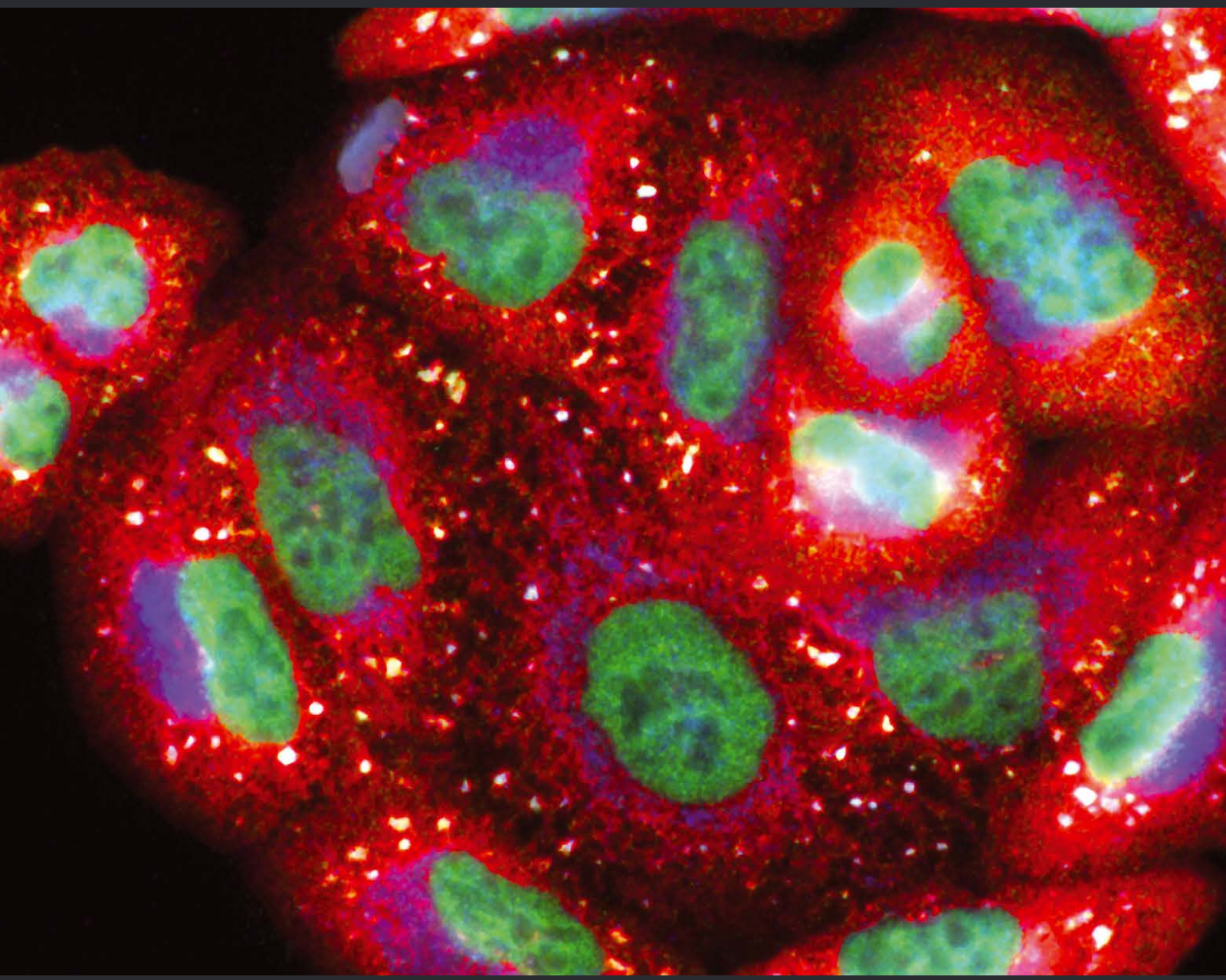

Oxidative Stress in Disease and Aging: Mechanisms and Therapies 2016

Oxidative Medicine and Cellular Longevity

Oxidative Stress in Disease and Aging: Mechanisms and Therapies 2016

Guest Editors: Claudio Cabello-Verrugio, Felipe Simon, Capucine Trollet, and Juan F. Santibanez

Editorial Board

Contents

Hindawi Publishing Corporation
Oxidative Medicine and Cellular Longevity
Volume 2017, Article ID 4310469, 2 pages
http://dx.doi.org/10.1155/2017/4310469

Editorial

Oxidative Stress in Disease and Aging: Mechanisms and Therapies 2016

Claudio Cabello-Verrugio,[1,2] Felipe Simon,[2,3] Capucine Trollet,[4] and Juan F. Santibañez[5,6]

[1]*Laboratorio de Biología y Fisiopatología Molecular, Departamento de Ciencias Biológicas, Facultad de Ciencias Biológicas and Facultad de Medicina, Universidad Andres Bello, Santiago, Chile*
[2]*Millennium Institute on Immunology and Immunotherapy, Santiago, Chile*
[3]*Laboratorio de Fisiología Integrativa, Departamento de Ciencias Biológicas, Facultad de Ciencias Biológicas and Facultad de Medicina, Universidad Andres Bello, Santiago, Chile*
[4]*Sorbonne Universités, UPMC Univ Paris 06, Centre de Recherche en Myologie, INSERM UMRS974, CNRS FRE3617, Institut de Myologie, 47 bd de l'Hôpital, 75013 Paris, France*
[5]*Laboratory for Experimental Hematology and Stem Cells, Institute for Medical Research, University of Belgrade, Serbia*
[6]*Laboratorio de Bionanotecnologia, Universidad Bernardo O'Higgins, Santiago, Chile*

Correspondence should be addressed to Claudio Cabello-Verrugio; claudio.cabello@unab.cl

Received 9 January 2017; Accepted 10 January 2017; Published 26 January 2017

Oxidative stress (OS) is an imbalance between the formation of reactive oxygen species (ROS) and antioxidant defense mechanisms. This phenomenon increases with age and affects the normal functioning of several tissues. Furthermore, numerous chronic diseases associated with older age, such as diabetes and cardiovascular, renal, pulmonary, and skeletal muscle disorders, are also directly related to OS. Considering this relationship, the aim of many ongoing studies is to elucidate the underlying mechanisms and role of OS in disease onset and development. In particular, there is considerable emphasis on finding new therapeutic strategies for decreasing OS.

This special issue presents new and relevant research regarding the mechanisms by which OS induces oxidative damage in the contexts of chronic disease and aging. Focus is given to the use of novel antioxidant strategies. The manuscripts within this special issue are all equally recommended by the editors, but the following contain especially interesting points worth comment.

X. H. Yang et al. evaluated the effect of epigallocatechin-3-gallate (EGCG), a component derived from green tea, on OS in the kidney of diabetic db/db mice. They demonstrated that EGCG ameliorated the levels of several parameters associated with OS and of signaling pathways related to oxidative damage and renal fibrosis (e.g., RAS axis, NOX, MAPK, TGF-b, and a-SMA). Overall, a renoprotector effect was found in diabetic mice.

N. Mihailović-Stanojević et al. studied the effect of wild thyme, a spice plant rich in polyphenolic compounds, on the development of hypertension. The authors demonstrated that wild thyme decreased OS and blood pressure in hypertensive rats, probably by increasing heme oxygenase 1.

E.-M. Noh et al. investigated how ROS production in senescent fibroblasts is generated by the modulation of phosphatidylinositol 3,4,5-triphosphate metabolism. The study showed in replicative senescent cells that increased ROS production was blocked by inhibiting three key signaling pathways: PI3K, protein kinase C, and NADPH oxidase. Additionally, the results indicated that a reduction in PTEN levels is important for abolishing increased ROS levels in human dermal fibroblasts.

J. Abrigo et al. studied the effect of mesenchymal stem cell administration on skeletal muscle damage induced by a high fat diet. The authors demonstrated that muscle wasting was produced by activating the ubiquitin proteasome pathway increased OS levels and myonuclear apoptosis. The main

finding was that mesenchymal stem cells abolished these three mechanisms involved in the muscle damage induced by a high fat diet.

All of these highlighted studies, as well as the other manuscripts contained in this special issue, advance improvements on pathological statuses by using diverse antioxidant strategies. We firmly believe that these findings will be of relevance to research concerning OS, chronic diseases, and aging.

Acknowledgments

The editors thank all of the authors who submitted their research to this special issue. The editors also thank each reviewer for their valuable contributions. The lead guest editor thanks all of the collaborating guest editors for their critical and exhaustive reviews and support, which were critical for the successful publication of this special issue.

Claudio Cabello-Verrugio
Felipe Simon
Capucine Trollet
Juan F. Santibañez

Hindawi Publishing Corporation
Oxidative Medicine and Cellular Longevity
Volume 2017, Article ID 6542631, 14 pages
http://dx.doi.org/10.1155/2017/6542631

Research Article

Semipurified Ethyl Acetate Partition of Methanolic Extract of *Melastoma malabathricum* Leaves Exerts Gastroprotective Activity Partly via Its Antioxidant-Antisecretory-Anti-Inflammatory Action and Synergistic Action of Several Flavonoid-Based Compounds

Noor Wahida Ismail Suhaimy,[1] Ahmad Khusairi Noor Azmi,[1] Norhafizah Mohtarrudin,[2] Maizatul Hasyima Omar,[3] Siti Farah Md. Tohid,[1] Manraj Singh Cheema,[1] Lay Kek Teh,[4] Mohd. Zaki Salleh,[4] and Zainul Amiruddin Zakaria[1,4]

[1]*Department of Biomedical Science, Faculty of Medicine and Health Science, Universiti Putra Malaysia, 43400 Serdang, Selangor, Malaysia*
[2]*Department of Pathology, Faculty of Medicine and Health Science, Universiti Putra Malaysia, 43400 Serdang, Selangor, Malaysia*
[3]*Phytochemistry Unit, Herbal Medicine Research Centre, Institute for Medical Research, Jalan Pahang, 50588 Kuala Lumpur, Malaysia*
[4]*Integrative Pharmacogenomics Institute (iPROMISE), Universiti Teknologi MARA, Level 7, FF3 Building, 42300 Puncak Alam, Selangor, Malaysia*

Correspondence should be addressed to Zainul Amiruddin Zakaria; dr_zaz@yahoo.com

Received 9 May 2016; Accepted 26 October 2016; Published 11 January 2017

Academic Editor: Francisco J. Romero

Recent study has demonstrated the gastroprotective activity of crude methanolic extract of *M. malabathricum* leaves. The present study evaluated the gastroprotective potential of semipurified extracts (partitions): petroleum ether, ethyl acetate (EAMM), and aqueous obtained from the methanolic extract followed by the elucidation of the gastroprotective mechanisms of the most effective partition. Using the ethanol-induced gastric ulcer assay, all partitions exerted significant gastroprotection, with EAMM being the most effective partition. EAMM significantly (i) reduced the volume and acidity (free and total) while increasing the pH of gastric juice and enhanced the gastric wall mucus secretion when assessed using the pylorus ligation assay, (ii) increased the enzymatic and nonenzymatic antioxidant activity of the stomach tissue, (iii) lost its gastroprotective activity following pretreatment with N-omega-nitro-L-arginine methyl ester (L-NAME; NO blocker) or carbenoxolone (CBXN; NP-SH blocker), (iv) exerted antioxidant activity against various in vitro oxidation assays, and (v) showed moderate in vitro anti-inflammatory activity via the LOX-modulated pathway. In conclusion, EAMM exerts a remarkable NO/NP-SH-dependent gastroprotective effect that is attributed to its antisecretory and antioxidant activities, ability to stimulate the gastric mucus production and endogenous antioxidant system, and synergistic action of several gastroprotective-induced flavonoids.

1. Introduction

Gastric ulcer is an injury that occurs in the stomach lining. The ulcer disrupts the mucosa integrity of the stomach with extension beyond the submucosa into the muscularis mucosa due to the active inflammation. 5% of human population suffers from gastric ulcer [1]. Current treatments available to treat ulcer work by reducing acid secretions or increasing mucosal protection such as proton pump inhibitor (PPI), histamine antagonist (H2) blocker, and antacids. Nevertheless,

it comes with undesirable side effects such as gynecomastia, arrhythmias, and haematopoietic changes [2].

Hence, there is a shift in interest in using natural products as an alternative source of medicine with promising results in treating diseases. With regard to gastric ulcer treatments, various studies have shown the ability of plant-based extracts to exert gastroprotective activity such as *Bauhinia purpurea* [3], *Muntingia calabura* [4], and *Annona reticulate* [5].

Melastoma malabathricum L. belongs to the family Melastomataceae. This shrub is commonly found throughout Southeast Asia region including Malaysia and is known among the Malay community as "Senduduk." Various parts of *M. malabathricum* have been used to treat different types of diseases with the leaves, in particular, have been used to treat gastric ulcers [6]. Various other parts of *M. malabathricum* in various forms of extraction have been reported to exhibit various types of pharmacological activities such as antibacterial, antiviral, antinociceptive, anti-inflammatory, antipyretic, antioxidant, anticoagulant, inhibitor of platelet-activating factor, antidiarrheal, and wound healing activities [6]. We have recently reported on the antiulcer potential of the methanolic extract of *Melastoma malabathricum* (MEMM) leaves [7]. In an attempt to identify the bioactive compound(s) that is responsible for MEMM-exerted antiulcer activity, the present study was designed to use the semipurified extracts, namely, petroleum ether (PEMM), ethyl acetate (EAMM), and aqueous (AQMM) partitions obtained through the partitioning of water-dissolved MEMM using petroleum ether followed by ethyl acetate to determine the gastroprotective activity of these partitions and to elucidate the mechanisms of gastroprotection exerted by the most effective partition and thereafter to identify the compound(s) in the most effective partition.

2. Materials and Methods

2.1. Plant Materials. *M. malabathricum* leaves were collected from their natural habitat in Serdang, Selangor, Malaysia, between August and September 2013 and identified by a botanist (Dr. Shamsul Khamis) from the Institute of Bioscience (IBS), Universiti Putra Malaysia (UPM), Serdang, Selangor, Malaysia. A voucher specimen (SK 1095/05) was issued and deposited in the Herbarium of the Laboratory of Natural Products, IBS, UPM.

2.2. Preparation of Methanol Extract of M. malabathricum and the Various Semipurified Extracts. Eight hundred grams of dried *M. malabathricum* leaves was grinded and soaked in methanol for 72 h at room temperature and this was repeated three times. The methanol supernatant was collected, pooled together, and then evaporated to yield approximately 40 g of dried crude MEMM [7]. The dried crude extract was first added with distilled water (ratio of 1 : 20; m/v) and then shaken to dissolve them well and then successively partitioned with the same volume of petroleum ether followed by ethyl acetate as described elsewhere [8]. The process of partitioning was repeated for the respective solvent until no changes in color could be seen in the supernatant. Each supernatant was then pooled together and evaporated leading to the yield of semipurified extracts of petroleum ether, ethyl acetate, and distilled water (aqueous partition).

2.3. Phytochemical Screening of Various Semipurified Extracts of MEMM. Each partition was subjected to phytochemical screening according to standard conventional screening tests as described by Ikhiri et al. [9]. The phytochemical screening was performed to identify the presences of alkaloids, flavonoids, triterpenes, tannins, saponins, and steroids by using 100 mg of each partition.

2.4. Antioxidant Potential of Various Semipurified Extracts of MEMM Assessed Using Several Oxidation Assays

2.4.1. Superoxide Anion (SOA) Radical Scavenging. The SOA radical scavenging activity was determined according to Liu et al. [10] but with slight modification. A mixture of 3 mL of Tris-HCl buffer (16 mM, pH 8), 1 mL of NBT (50 μM), 1 mL NADH (78 μM), and each of the respective partition (25–50 μg) was first prepared. The reaction was initiated by adding 1 mL of PMS solution (10 μM) and the mixture solution was incubated at 25°C for 5 min. The activity was read at absorbance 560 nm using a spectrophotometer (Shimadzu UV-Vis 1700) against blank samples and using l-ascorbic acid as a control.

2.4.2. 2,2-Diphenyl-1-picrylhydrazyl (DPPH) Radical Scavenging Assay. The DPPH-radical scavenging assay was performed according to the method of Blois [11] but with slight modification. Approximately, 50 μL of each partition (1.0 mg/mL) was loaded and followed by 50 μL of DPPH (1 mM in ethanolic solution) and 150 μL of absolute ethanol was added in 96-well microtiter plate in triplicate. The mixtures were mixed vigorously for 15 s at 500 rpm and incubated at room temperature for 30 min and the absorbance was measured spectrophotometrically at 515 nm.

2.4.3. Oxygen Radical Absorbance Capacity (ORAC) Assay. The ORAC assay was performed according to the method of Huang et al. [12] but with slight modification. The sample was assayed in 96-well plate and was measured every 60 s. The ORAC value was analyzed using MARS Data Analysis Reduction Software.

2.4.4. Total Phenolic Content (TPC). The TPC of each partition was determined using the Folin-Ciocalteu reagent with gallic acid used as a standard in accordance to the method of Singleton and Rossi Jr. [13] but with slight modification. One milligram of each partition was extracted with 1.0 mL of 80% methanol containing 1.0% hydrochloric acid and 1.0% of distilled water. The mixtures were put on the shaker set at 200 rpm at room temperature and then were centrifuged at 6000 rpm for 15 min. A 200 mL of each supernatant was mixed with 400 mL of the Folin-Ciocalteu reagent (0.1 mL/0.9 mL). The mixtures were incubated at room temperature for 5 min followed by the addition of 400 mL of sodium bicarbonate (60 mg/mL) and incubated at room temperature for 90 min. Absorbance readings were taken spectrophotometrically at 725 nm. The TPC level in

each partition was expressed as Gallic acid equivalent (GAE: mg/100 g).

2.5. In Vitro Effect of Various Semipurified Extracts of M. malabathricum against Several Inflammatory Mediators

2.5.1. Xanthine Oxidase (XO) Assay. The XO assay was performed as described by Noro et al. [14]. Ten microlitre of each partition was dissolve in DMSO along with 130 μL potassium phosphate buffer (0.05 M, pH 7.5) and 10 μL of the XO solution and thereafter was incubated for 10 min at 25°C. The assay was measured at absorbance of 295 nm.

2.5.2. Lipoxygenase (LOX) Assay. The LOX activity was determined according to Azhar-Ul-Haq et al. [15]. A mixture of 10 mL of each partition, 160 mL sodium phosphate buffer (0.1 M, pH 8), and 20 mL of soy bean LOX solution was incubated for 10 min at 25°C. The reaction was then initiated by the addition of 10 mL substrate in the form of sodium linoleic acid solution. The absorbance was measured at 234 nm.

2.6. Gastroprotective Activity of Various Semipurified Extracts of MEMM Assessed Using Several Gastric Ulcer Models

2.6.1. Experimental Animals. Healthy male Sprague-Dawley rats weighing between 180 and 200 g were used in this study. Rats were maintained under controlled conditions (22 ± 2°C, 12 h light/dark) in the Animal House, Faculty of Medicine, Universiti Putra Malaysia. Free access to food and water was allowed. The experimentation was approved by the Institutional Animal Care and Use Committee, Universiti Putra Malaysia (Ref. UPM/IACUC/AUP-R032/2014).

2.6.2. Ethanol-Induced Gastric Ulcer Model. The gastroprotective activity of each partition was determined against ethanol-induced gastric ulcer in male Sprague-Dawley rats ($n = 6$). The rats were orally administered with 10% DMSO as negative control, 100 mg/kg of ranitidine as positive control or, the semipurified extracts (PEMM, EAMM, or AQMM), in the doses ranging from 50, 250, or 500 mg/kg, for 7 consecutive days prior to the administration of ethanol. Another group of rats received 10% DMSO without ethanol-induced gastric ulcer, which served as the normal control. At the end of the treatment (7th day), gastric ulcers were induced by oral administration of absolute ethanol according to the method described by Zabidi et al. [16]. All rats were euthanized in CO_2 chamber and the stomachs were removed.

(1) Macroscopic and Microscopic Evaluations of Treated Stomachs. The stomachs were dissected along the greater curvature and rinsed with cold saline to remove the contents. The ulcer areas of each stomach were measured and the sum of the area was expressed as the ulcer area (mm^2) according to Zabidi et al. [16]. The percentage of gastroprotection was calculated using the following equation:

$$\text{Gastroprotection (\%)} = \left[\frac{(\text{Ulcer Area (control)} - \text{Ulcer Area (treated)})}{\text{Ulcer Area (control)}}\right] \times 100. \quad (1)$$

Each of the stomach samples was fixed with 10% buffered formalin before proceeding with tissue processing. The fixed stomachs were embedded in paraffin block and sectioned using optical rotary microtome to approximately 4 μ thickness and stained with hematoxylin and eosin prior to histological evaluation [16].

2.7. Pylorus Ligation-Induced Gastric Ulcer Assay on the Most Effective Semipurified Extract of MEMM. The most effective partition determined following the ethanol-induced gastric ulcer assay was further subjected to the pylorus ligation-induced gastric ulcer assay according to the method described by Shay et al. [17] but with some modification. Pylorus ligation was performed 1 h after the administration of the test solutions. The rat's stomach was ligated for 4 h and then the stomach content was collected wherein the volume, pH, free acidity, and total acidity of gastric juice as well as the gastric wall mucus content were measured.

2.7.1. Determination of Gastric Juice's Volume and pH. The gastric content was collected from the stomach of each rat and centrifuged at 2500 rpm for 10 min. The gastric content volume was measured and pH of the supernatant was determined using a pH meter [18].

2.7.2. Determination of Free Acidity and Total Acidity. The free acidity of gastric content was determined by titration of 0.01 N NaOH with methyl orange until the color changes to yellowish. Meanwhile, total acidity was determined by titration with 0.1 N NaOH by using 2% phenolphthalein as acid-base indicator. Total acidity was expressed as mEq/L [18].

2.7.3. Determination of Gastric Wall Mucus. The stomachs were rinsed to clear off any residues and weighed. The stomachs were then immersed in 10 mL of 0.1% Alcian blue in 0.16 M sucrose/0.05 M sodium acetate, pH 5.8 for 2 h, and shaken every 30 min interval. Then the stomachs were rinsed twice with 0.25 M sucrose solution. The remaining dye complexed with gastric mucus was extracted with 0.5 M magnesium chloride and shaken for 2 h at every 15 min intervals. Diethyl ether was added and centrifuged at 3600 rpm for 10 min. Samples were read at 580 nm using spectrophotometer [19].

2.8. Effects of Most Effective Semipurified Extract of MEMM on Antioxidant Enzymes of Gastric Tissues. The gastric tissues were washed thoroughly with ice-cold saline and cut into small pieces. The tissue was then homogenized on ice cold with phosphate-buffered saline (PBS) buffer (50 mM phosphate buffer, pH 7.4) containing a mammalian protease inhibitor cocktail using Teflon Homogenizer. The homogenized gastric tissues were centrifuged at 18 000 ×g for 15 min at 4°C. The supernatant, which was collected and stored at −80°C prior to analysis, was used to measure the activities of catalase (CAT), superoxide dismutase (SOD), glutathione (GSH), prostaglandin E_2 (PGE_2), and malondialdehyde (MDA) content. These assays were performed according to the respective manufacturer protocols (Cayman, USA).

2.8.1. Evaluation of Catalase Level. Measurement of CAT level was performed using the catalase assay kit (Cayman Chemical, USA) according to the protocol provided by the manufacturer. Briefly, the collected supernatant was assayed using a microtiter plate wherein each well contains 100 μL of diluted assay buffer, 30 μL of methanol, 20 μL of formaldehyde standard, 20 μL of catalase (positive control), and 20 μL of samples wells, respectively. Approximately 20 μL of diluted hydrogen peroxide was added to all the wells to initiate the reactions for 20 min. The reaction was stopped by adding 30 μL of diluted potassium hydroxide for 10 min at room temperature. Ultimately, 10 μL of catalase potassium periodate was added and incubated for 5 min before the absorbance was read at 540 nm using a plate reader.

2.8.2. Evaluation of Superoxide Dismutase Level. According to the instruction on the SOD kit (Cayman Chemical, USA) provided by the manufacturer, the collected supernatant (10 μL) was mixed with the tetrazolium salt solution (200 μL) to dilute the SOD activity of the supernatants. The reaction was initiated by adding 20 μL of xanthine oxidase and incubated for 20 min in a shaker. The absorbance was then read using the ELISA reader at 440 nm. In this assay bovine erythrocyte SOD (Cu/Zn) was used as the standard. According to this assay procedure, xanthine oxidase and hypoxanthine detected superoxide radicals. In brief, the kit could measure the amount of enzyme that caused 50% dismutation of the superoxide radical.

2.8.3. Evaluation of Glutathione Level. The GSH assay test was assayed according to the protocol provided by the manufacturer (Cayman Chemical, USA). Briefly, the collected supernatant (50 μL) was mixed with a solution containing 0.1 M sodium phosphate, 2 mM ethylenediaminetetraacetic acid (EDTA), 0.4 M 2-(N-morpholino) ethanesulfonic acid, reconstituted NADP+ and glucose-6-phosphate, and reconstituted glutathione reductase and glucose-6-phosphate dehydrogenase. In this study GSH was quantified using glutathione reductase. Following the reduction of hydroperoxides by glutathione peroxidase, oxidized glutathione (GSSG) was produced and used to create the standard curve. The absorbance was read at 405 nm.

2.8.4. Evaluation of Prostaglandin E_2 Level. The level of PGE_2 in the collected supernatant was analyzed using the enzyme immunoassay in 96-well plate according to the procedure provided by the manufacturer (Cayman Chemical, USA). Briefly, the supernatant and standards were added to the plate, which was precoated with goat polyclonal anti-mouse immunoglobulin G (IgG). The plate was then incubated with PGE_2 acetylcholinesterase conjugated with the PGE_2 Tracer and later applied with Ellman's reagent for 60 min. The kit converted PGE_2 into Bicyclo PGE_2 (stable derivative) which was measurable by the kit. The product of this enzymatic reaction had a distinct yellow color and absorbs strongly at 412 nm. Results were calculated using the standard curve which was expressed as picogram per milliliter (pg/mL).

2.8.5. Evaluation of MDA Level. The level of lipid peroxidation in gastric tissues was estimated by determining the MDA content using a thiobarbituric acid reactive substances (TBARS) assay kit (Cayman Chemical, USA). Briefly, 100 μL of SDS solution, 100 μL of the supernatant, and 4 mL color reagent were mixed in a vial and then incubated for 1 h (100°C). This was followed by an incubation of the vial on ice for 10 min after which the vial was centrifuged at 1,600 ×g for 10 min at 4°C. Within 30 min, 150 μL of each vial content was placed on a 96-well plate and the absorbance was read at 530 nm.

2.9. Determination of Endogenous Antiulcer Mechanisms of the Most Effective Semipurified Extract of MEMM

2.9.1. Role of Nonprotein Sulfhydryl Groups on the Gastroprotection Exerted by the Most Effective Semipurified Extract of MEMM. To investigate the involvement of the endogenous sulfhydryls compounds in the modulation of gastroprotective effect of the most effective semipurified extract, the procedure by Andreo et al. [20] was used but with slight modifications. Briefly, all groups of rats ($n = 6$) were subjected to intraperitoneal treatment with 10 mg/kg N-ethylmaleimide (NEM). After 30 min, either vehicle (10% DMSO), 100 mg/kg carbenoxolone (CBNX) or 500 mg/kg semipurified extract was orally administered. After 60 min, ethanol (5 mL/kg) was administered orally to all rats for gastric ulcer induction. All groups of rat were euthanized 60 min later and the stomachs were removed to measure the gastric ulcer area.

2.9.2. Role of Nitric Oxide on the Gastroprotection Exerted by the Most Effective Semipurified Extract of MEMM. To investigate the involvement of endogenous NO in the modulation of gastroprotective effect of the most effective semipurified extract of MEMM, the procedure by Andreo et al. [20] was used but with a slight modifications. Six groups of animals were treated intraperitoneally with 70 mg/kg of L-NAME or 500 mg/kg semipurified extract. After 60 min, gastric ulcer in all groups was induced using 5 mL/kg ethanol. All groups of rats were euthanized 60 min later and the stomach was removed for ulcer area measurement.

2.10. HPLC Analysis of the Most Effective Semipurified Extract of MEMM and Comparison against the HPLC Profile of Crude Extract MEMM or Pure Flavonoids.

The partitions of MEMM, namely, PEMM, EAMM, and AQMM, were also subjected to the HPLC analysis to identify the compound of interest, which could be associated with the extract's gastroprotective effect. In brief, 10 mg of sample was suspended in 1 mL methanol and then filtered through a filter cartridge (pore size of 0.45 μm) prior to use. The filtered sample was then analyzed using the HPLC system (Thermo Scientific Dionex Ultimate 3000 series, Thermo Scientific, Germering, Germany) with Waters 996 photodiode array detector. A Phenomenex RP-Max C_{18} column (4.6 mm i.d. × 250 mm) packed with 5 μm diameter particles was used. The mobile phase used in this procedure contained 0.1% formic acid in water (A) and 0.1% formic acid in acetonitrile (B) and the initial conditions were 90% A and 10% B with a linear

Table 1: Phytochemical screening of PEMM, EAMM, and AQMM.

Phytoconstituents	PEMM	EAMM	AQMM
Alkaloids	—	—	—
Saponins	1+	2+	2+
Flavonoids	1+	1+	—
Tannins	1+	2+	3+
Triterpenes	2+	—	—
Steroids	3+	1+	—

Phytoconstituent content scoring.
Alkaloids: + negligible amount of precipitate; ++ weak precipitate; +++ strong precipitate.
Saponins: + 1-2 cm froth; ++ 2-3 cm froth; +++ >3 cm froth.
Flavonoids, tannins, and triterpenes: + weak color; ++ mild color; +++ strong color.

gradient reaching 50% B at $t = 25$ min. This condition was maintained for another 5 min and then B was increased from 50% to 95%, within the next 5 min ($t = 35$ min). When the programme reached $t = 35$ min, B was returned to the initial composition (10%) until the programmed reached $t = 37$ min. The flow rate was 1.2 mL/min, injection volume was 10 μL, and the wavelength was 280 nm. The column oven was set at 27°C. Stock solutions of standards references were prepared in methanol at the concentration of 0.3 mg/mL. The chromatography peaks were confirmed by comparing its retention time with those of reference standards and by the respective UV-Vis spectra. All chromatography operations were carried out at ambient temperature and in triplicate.

2.11. Statistical Analysis. The data were expressed as means ± SEM and statistical significance was analyzed using ANOVA, followed by Dunnett's post hoc test. Data with the value of $p < 0.05$ were considered statistically significant.

3. Result

3.1. Pharmacological Activities Observations

3.1.1. Phytochemical Screening of Various Semipurified Extracts of MEMM. The phytochemical screening of the PEMM, EAMM, and AQMM revealed the presence of saponins and tannins, but not alkaloids, in all semipurified extracts (Table 1). Flavonoids were detected only in PEMM and EAMM while triterpenes were detected only in PEMM.

3.1.2. Antioxidant Potential of Various Semipurified Extracts of MEMM. The antioxidant activities of each partition at the concentration of 200 μg/mL are illustrated in Table 2. All partitions exhibited high SOA- and DPPH-radical scavenging activities while only the EAMM followed by AQMM demonstrated high ORAC value. Further analysis showed that EAMM possessed the highest TPC value followed by PEMM and AQMM. According to the standard procedure, a substance with a TPC value that is ≥1000 mg GAE/100 g is considered to have high total phenolic content.

3.1.3. Effects of Various Semipurified Extracts of MEMM on Inflammatory Mediators. The effects of various semipurified extracts of MEMM, at the concentration of 100 mg/mL, on inflammatory mediators, namely, LOX and XO, are shown in Table 3. From the results obtained, all semipurified extracts showed that lack of inhibitory activity towards XO with the highest percentage of inhibition, which is ≤11%, was recorded for EAMM. As for LOX activity, only EAMM and AQMM produced significant percentage of inhibition with the former causing a moderate inhibition with the recorded percentage of inhibition that is greater than 50%.

3.2. Gastroprotective Potential of Various Semipurified Extracts of MEMM

3.2.1. Effect of Various Semipurified Extracts of MEMM against Ethanol-Induced Gastric Ulcer. The gastroprotective activity of various semipurified extracts of MEMM against ethanol-induced gastric ulcer in rats is shown in Table 4. All extracts demonstrated significant ($p < 0.05$) reduction in ulcer formation in a dose-dependent manner. However, based on the percentage of ulcer inhibition, EAMM exhibited the greatest protection followed by the AQMM and PEMM with the approximate percentage of inhibition ranging between 15–98%, 7–91%, and 12–67%, respectively. Interestingly, the 250 mg/kg EAMM produced gastroprotection that was equally effective when compared to the 100 mg/kg ranitidine (approximately 60% inhibition).

3.2.2. Macroscopic and Microscopic Findings of Treated Stomachs. Macroscopic examination of the gastric mucosa of the negative control group (ulcer control) showed extensive and visible hemorrhagic necrosis of gastric mucosa (Figure 1(b)) in comparison to the normal untreated group that show no signs of hemorrhage or lesion (Figure 1(b)). Pretreatment with 100 mg/kg ranitidine reduced the formation of hemorrhages and lesions (Figure 1(c)) while pretreatment with PEMM, EAMM, or AQMM at the dose of 50–500 mg/kg also caused a dose-dependent decreased in the severity and visibility of hemorrhagic necrosis of gastric mucosa (Figures 1(d)–1(l)). These findings were further supported by the microscopic observations as shown in Figures 2(a)–2(e2). The negative control group demonstrated severe hemorrhages and necrosis at mucosa epithelium and destruction of the surface epithelium and edema at the submucosa layer (Figure 2(a)). The 100 mg/kg ranitidine-treated group (positive control) demonstrated moderate ulcer formation with the mild hemorrhage seen at the mucosa epithelium and moderate oedema at the submucosa layer (Figure 2(b)). Pretreatment with all semipurified extracts, at the concentration of 50 mg/kg failed to reversed the toxic effect of ethanol as indicated by the presence of severe mucosal disruption with ulcer and hemorrhage seen at the mucosa epithelium and severe oedema at the submucosa level (Figures 2(c1)–2(e1)). Increase in the dose of each partition was found to improve their gastroprotective effect towards the action of ethanol. At 500 mg/kg, pretreatment with EAMM demonstrated almost no disruption at the epithelium mucosa with the presence of mild edema but the absence of hemorrhage (Figure 2(d2)). On the other hand, pretreatment with AQMM exerted mild ulceration at the epithelium mucosa with moderate presence

Table 2: Antioxidant activity and TPC value of various partitions of MEMM measured using different assay.

Sample	SOA scavenging (%)	DPPH radical scavenging (%)	ORAC Value (μM TE/100 g)	TPC (mg/100 g GAE)
Sample concentration	200 μg/mL	200 μg/mL	200 μg/mL	200 μg/mL
Standard	Superoxide dismutase 6 × 10^{-3} U/mL	Ascorbic acid (AA) 200 μg/mL	Trolox standard curve	Gallic acid (GAE) standard curve
PEMM	100 ± 0.0 (H)	96.29 ± 1.9 (H)	32,000 ± 3,000	279.53 ± 7.93
EAMM	98.03 ± 0.74 (H)	97.94 ± 0.4 (H)	198,000 ± 9,800	963.10 ± 35.96
AQMM	98.17 ± 1.83 (H)	98.95 ± 0.1 (H)	185,000 ± 7,300	177.57 ± 14.26

Data expressed as mean ± SEM.
SOA scavenging and DPPH radical scavenging; H: high (70–100%), M: moderate (50–69%), and L: low (0–49%).
TPC value > 1000 mg GAE/100 g is considered higher total phenolic content.
The ORAC value of triplicate wells in duplicate experiments, SEM < 20%.

Table 3: Anti-inflammatory effect of various partitions of MEMM against in vitro xanthine oxidase and lipoxygenase assays.

Sample concentration 100 mg/mL	Xanthine oxidase assay (%)	Lipoxygenase assay (%)
PEMM	3.32 ± 1.68 (L)	NA
EAMM	10.23 ± 2.58 (L)	59.15 ± 4.43 (M)
AQMM	NA	32.84 ± 3.65 (L)

Data expressed as mean ± SEM.
Note: H: high (71–100%), M: moderate (41–70%), L: low (0–40%), and NA: not active.

Table 4: Gastroprotective effect of various partitions of MEMM against ethanol-induced in rats.

Pretreatment	Dose (mg/kg)	Ulcer area (mm^2)	Gastroprotection (%)
10% DMSO	—	27.00 ± 0.71	—
Ranitidine	100 mg	9.80 ± 1.11*	63.70
PEMM	50 mg	23.60 ± 1.36	12.59
	250 mg	18.00 ± 0.71*	33.33
	500 mg	12.40 ± 0.68*	54.07
EAMM	50 mg	19.80 ± 1.07	26.67
	250 mg	10.00 ± 1.18*	62.96
	500 mg	0.80 ± 0.20*	97.04
AQMM	50 mg	22.80 ± 0.86	15.56
	250 mg	15.40 ± 0.68*	42.96
	500 mg	3.80 ± 0.37*	85.93

Data were expressed as mean ± SEM and analyzed by one-way ANOVA followed by Dunnett's post hoc test ($n = 6$).
* $p < 0.05$ as compared to control (10% DMSO).

of edema and the absence of hemorrhage (Figure 2(e2)) while pretreatment with PEMM demonstrated moderate disruption of the epithelium mucosa with the presence of moderate hemorrhages and edema (Figure 2(c2)). Overall, the gastric mucosa tissue pretreated by EAMM showed intact appearance of histological structure when compared with the normal control group.

3.2.3. Effect of EAMM against the Pylorus Ligation-Induced Gastric Lesion. Based on the ethanol-induced gastric ulcer test, EAMM was found to exert the most effective gastroprotective activity. This effective semipurified extract was then subjected to further analysis to elucidate the possible mechanisms of gastroprotection. In the first stage of this study, EAMM was tested in the pyloric ligation assay to evaluate its potential in modulating the gastric content parameters such as gastric juice's volume, pH, free and total acidity, and gastric wall mucus content. From the results obtained, EAMM provides gastroprotection by causing significant ($p < 0.05$) reduction in the volume of gastric juice and significant ($p < 0.05$) decrease in the production of free acidity and total acidity. Moreover, EAMM also significantly ($p < 0.05$) increased the pH of gastric juice and enhanced the gastric wall mucus secretion (Table 5).

3.3. Effect of EAMM on the Enzymatic and Nonenzymatic Antioxidant Levels of Ethanol-Induced Gastric Ulcer Tissue. Gastric tissue of negative control group treated only with ethanol demonstrated significant ($p < 0.05$) reduction in the level of SOD, CAT, GSH, and PGE_2 but increase in the level

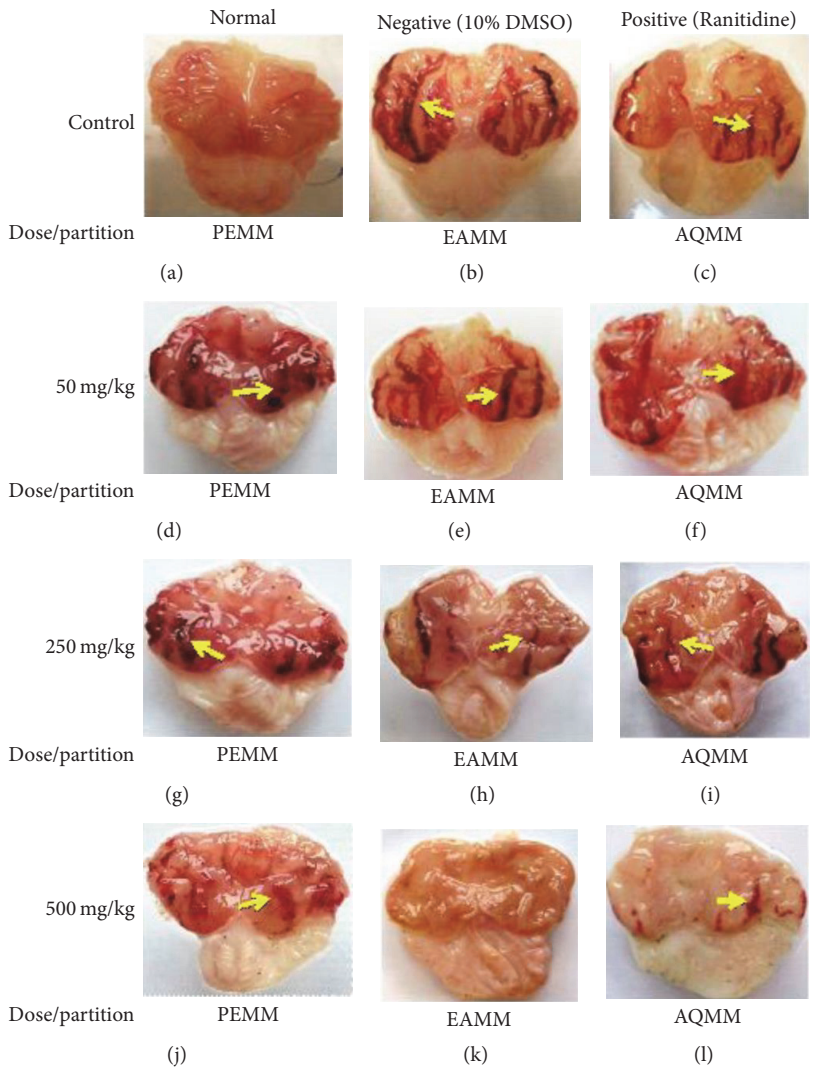

Figure 1: Effect of various partitions, namely, PEMM, EAMM, and AQMM, obtained from methanol extract of *M. malabathricum* (MEMM) against the ethanol-induced gastric ulcer in rats. Arrow (yellow) indicates lesions.

of TBARS, when compared to the normal untreated group. On the other hand, EAMM significantly ($p < 0.05$) reversed the enzymatic and nonenzymatic antioxidant levels of ulcer-bearing gastric tissue when compared to the negative control group (Table 6). As can be seen from the presented table, EAMM increased the level of SOD, CAT, GSH, and PGE_2 but reduced the level of TBARS when compared to the negative control group.

3.4. Role of Endogenous Factors of Gastroprotection on the Action of EAMM

3.4.1. Effect of Nonprotein Sulfhydryl Group on the Gastroprotective Activity of EAMM Assessed Using the Ethanol-Induced Gastric Ulcer in Rats. Investigation on the role of NP-SH in the gastroprotective effect of EAMM was carried out by prechallenging the EAMM or CBNX (positive control) with NEM (NP-SH blocker). From the results obtained, NEM administration was found to significantly ($p < 0.05$) worsen the ethanol-induced gastric ulcer formation in the negative control group. Prechallenging the EAMM- and CBNX-treated group with NEM also resulted in significant ($p < 0.05$) decrease of gastroprotective potential of both compounds (Table 7).

3.4.2. Effect of N-Omega-nitro-L-arginine Methyl Ester on the Gastroprotective Activity of EAMM Assessed Using the Ethanol-Induced Gastric Ulcer in Rats. The role of NO in the modulation of gastroprotective activity of EAMM was also investigated by prechallenging the extract with L-NAME, an NO blocker (Table 7). From the results obtained, the absence of NO following the preadministration of L-NAME significantly ($p < 0.05$) increased the severity of gastric ulcer formed in comparison to the saline-treated negative control group. Further, pretreatment with L-NAME significantly ($p < 0.05$) reversed the gastroprotective action of saline-pretreated EAMM and CBNX.

Table 5: Gastroprotective effect of EAMM against the pylorus ligation assay.

Pretreatment	Dose (mg/kg)	Gastric juice (mL)	pH	Free Acidity (mEq/L)	Total acidity (mEq/L)	Gastric wall mucus (Alcian blue μg/g wet tissue)
10% DMSO	—	9.67 ± 0.67	1.51 ± 0.12	1061.00 ± 205.70	1513 ± 122.30	263.10 ± 35.43
Ranitidine	100	2.30 ± 0.37*	4.18 ± 0.81*	243.00 ± 39.56*	644.00 ± 89.61*	592.60 ± 31.84*
EAMM	50	13.33 ± 1.15	1.99 ± 0.17	528.00 ± 37.70*	692.60 ± 95.98*	404.10 ± 48.31
	250	6.75 ± 0.93	3.40 ± 0.49*	319.20 ± 46.76*	553.40 ± 43.89*	636.90 ± 41.33*
	500	5.17 ± 0.50	4.00 ± 0.27*	292.10 ± 47.87*	579.50 ± 38.42*	659.30 ± 41.15*

Data were expressed as mean ± SEM and analyzed by one-way ANOVA followed by Dunnett's post hoc test ($n = 6$).
* $p < 0.05$ as compared to control (10% DMSO).

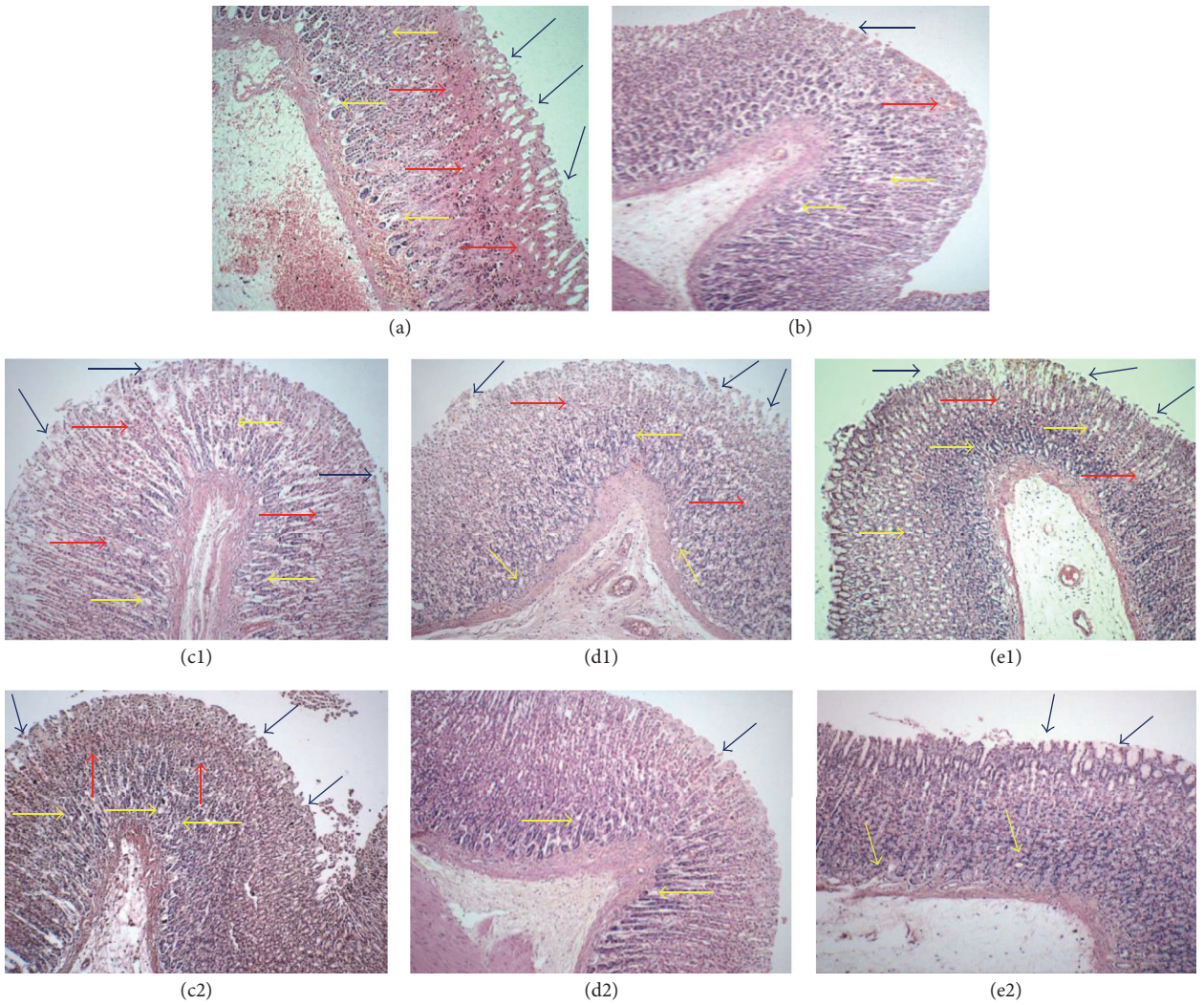

Figure 2: Microscopic analysis of the ethanol-induced gastric ulcer tissues following pretreatment of rats with the respective partition of *M. malabathricum* (magnification at ×20). (a) The negative control group (10% DMSO-pretreated) displayed severe hemorrhage (red arrow), ulcer (blue arrow), and necrosis at mucosa epithelium and edema (yellow arrow) at submucosa layer. (b) The positive control group (ranitidine-pretreated) demonstrated mild ulcer and hemorrhage at mucosa and moderate oedema at submucosa layer. (c1), (d1), and (e1) The groups pretreated with the respective PEMM, EAMM, or AQMM, at the dose of 50 mg/kg, demonstrated severe disruption with ulcer and hemorrhage at mucosa epithelium and severe oedema at submucosa layer with the presence of severe to moderate hemorrhage, ulcer, and necrosis at mucosa epithelium layer. and (c2), (d2), and (e2) At the dose of 500 mg/kg, the group pretreated with EAMM showed the mildest tissue damage when compared to the PEMM or AEMM indicated by the presence of mild ulcer, moderate edema, and the absence of hemorrhage.

Table 6: Effect of EAMM on SOD, CAT, GSH, PGE_2, and TBARS level in rat gastric tissues.

Pretreatment	Dose (mg/kg)	SOD (U/mg protein)	Catalase (nmol/min/mL)	GSH (μM/mg protein)	TBARS (μmol/mL)	PGE_2 (ng/mg)
Normal (untreated)	—	2.51 ± 0.07*	127.60 ± 0.62*	13.57 ± 0.55*	0.12 ± 0.00*	11.30 ± 0.67*
10% DMSO	—	1.28 ± 0.04	198.21 ± 1.60	2.51 ± 0.34	0.37 ± 0.03	4.74 ± 0.25
Ranitidine	100	1.79 ± 0.04*	117.80 ± 0.80*	4.69 ± 0.40*	0.16 ± 0.09*	8.27 ± 1.01*
EAMM	50	1.30 ± 0.07	104.40 ± 1.48*	3.29 ± 0.36	0.22 ± 0.01	4.75 ± 0.31
	250	1.71 ± 0.10*	122.30 ± 1.62*	5.12 ± 0.29*	0.16 ± 0.08*	8.37 ± 0.84*
	500	1.71 ± 0.12*	120.30 ± 1.91*	5.93 ± 0.42*	0.16 ± 0.01*	5.94 ± 0.61*

Data were expressed as mean ± SEM and analyzed by one-way ANOVA followed by Dunnett's post hoc test ($n = 6$).
* $p < 0.05$ as compared to control (10% DMSO).

Table 7: Gastroprotective effect of EAMM following pretreatment with L-NAME or NEM assessed using the ethanol-induced gastric ulcer model.

Pretreatment	Treatment	Dose (mg/kg)	Ulcer area (mm^2)
Saline	10% DMSO	—	27.68 ± 1.69
	CBXN	100	6.83 ± 0.60[a]
	EAMM	500	1.67 ± 0.33[a]
L-NAME	10% DMSO	—	36.67 ± 2.78[a]
	CBXN	100	12.00 ± 0.73[bc]
	EAMM	500	8.83 ± 0.60[bd]
NEM	10% DMSO	—	41.67 ± 1.75[a]
	CBXN	100	18.50 ± 2.26[ef]
	EAMM	500	11.25 ± 0.54[eg]

Data were expressed as mean ± SEM and analyzed by one-way ANOVA followed by Dunnett's post hoc test ($n = 6$).
[a] $p < 0.05$ as compared to control (saline + 10% DMSO).
[b] $p < 0.01$ as compared to control (L-NAME + 10% DMSO).
[cf] $p < 0.05$ as compared to control (saline + CBXN).
[dg] $p < 0.05$ as compared to control (saline + EAMM).
[e] $p < 0.05$ as compared to control (NEM + 10% DMSO).

3.5. HPLC Profile of EAMM and Comparison against the HPLC Profile of Crude MEMM and Standard Pure Flavonoids. The HPLC profile of crude methanolic extract (MEMM) and its most effective semipurified partition (EAMM) are shown in Figures 3(a) and 3(b), respectively. The peaks obtained and their respective retention time (R_T) in each chromatograms were compared with that of several pure flavonoid-based compounds. From the comparison made, several compounds with their respective R_T, namely, gallocatechin ($R_T = 3.92$ min) (1), epigallocatechin ($R_T = 4.91$ min) (2), catechin ($R_T = 8.89$ min) (3), chlorogenic acid ($R_T = 10.47$ min) (4), caffeic acid ($R_T = 10.70$ min) (5), quercetin ($R_T = 11.63$ min) (6), quercetin-3-O-glucoside ($R_T = 11.66$ min) (7), *p*-coumaric acid ($R_T = 14.28$ min) (8), and hesperidin ($R_T = 16.43$ min) (9) were postulated to be presented in MEMM and EAMM.

4. Discussion

Ulcer formation on the stomach lining is caused by the imbalance between the protective and aggressive factors and is also associated with living conditions. The major factors of gastric ulcer are bacterial infection by *Helicobacter pylori*, medications such as NSAIDs, chemical factor such as hydrochloric acid or ethanol, and gastric cancer [20]. Meanwhile, minor factors tend to be associated with the lifestyle of the patients such as stress, smoking, spicy food, and nutritional deficiency [20]. Despite the presence of various classes of antiulcer agents, their successes are often associated with various unwanted side effects that limit their usage. Attempts have been made to find an alternative replacement from current medications wherein plant-based compounds have been regarded as an important source of alternative new bioactive compounds.

One of the plants in Malaysia that has been used traditionally by the Malay to treat gastric ulcer is *M. malabathricum* and studies have demonstrated the gastroprotective potential of the aqueous [21], chloroform [22], and methanol [7, 16] extracts of its leaves. The methanolic extract showed the ability to attenuate ethanol- and indomethacin-induced gastric ulcer in rats [16]. Moreover, the extract showed a significant reduction in the volume and acidity of the gastric juice while increasing the pH and gastric mucus wall content by using the pylorus ligation model in rats [7].

The MEMM also modulates the level of several enzymatic and nonenzymatic antioxidant system within the gastric tissue wherein the levels of SOD, glutathione peroxidase (GTP), and glutathione reductase (GTR) were increased but

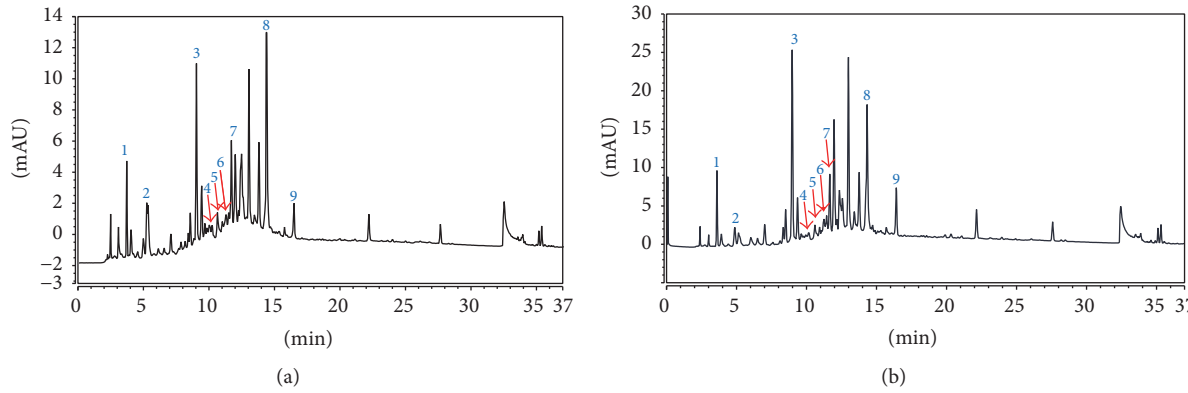

Figure 3: UHPLC analysis of MEMM and EAMM. (a) UHPLC profile of MEMM. (b) UHPLC profile of EAMM.

the levels of CAT, myeloperoxidase (MPO), and TBARS were decreased. Moreover, the gastroprotective activity of MEMM was reduced by an inhibitor of NO synthase and SH blocker. Methanol is an intermediate solvent, which is able to extract all the polar-, nonpolar-, and intermediate-based biocompounds that exert the gastroprotective activity. This has triggered our interest to segregate the biocompounds according to their polarity to further understand their activity.

The PEMM, EAMM, and AQMM were tested for their antioxidant, anti-inflammatory, and gastroprotective potentials using various standard assays. Although all partitions exerted remarkable antioxidant activity when assessed using the SOA- and DPPH-radical scavenging assays, EAMM exerts the most effective activity when measured using the ORAC assay and possesses the highest TPC value with significant LOX- but not XO-mediated in vitro anti-inflammatory action. All partitions were tested using the ethanol-induced gastric ulcer model in rats and macroscopic observations demonstrated that EAMM exert the most effective gastroprotective activity, followed by AQMM and PEMM. The EAMM exerted almost complete protection (≈98% reduction in ulcer area formation) against the action of ethanol and was further supported by the microscopic observations, which showed only slight epithelial sloughing off but no presence of hemorrhage, edema, or necrosis. Taking these findings into consideration, the EAMM was determined as the most effective partition and subjected to further analysis. In the pylorus ligation assay, EAMM was shown to modulate several parameters of gastric content wherein the semipurified extract reduces the volume and free acidity and total acidity while increasing the pH of gastric juice. Moreover, EAMM was also found to enhance the secretion of gastric wall mucus. These findings suggest that EAMM triggered gastroprotective effect partly by reducing the volume and acidity and at the same time increasing the pH of the gastric juice. Further attempt to elucidate the ability of EAMM to affect the enzymatic and nonenzymatic antioxidant system within the gastric tissues following ethanol-induced ulcer formation revealed the ability of the semipurified extract to modulate the enzymatic and nonenzymatic antioxidant system. EAMM was found to increase the level of SOD, CAT, GSH, and PGE_2 while reducing the level of TBARS. It also revealed the role of endogenous factors such as NP-SH group and NO in the modulation of gastroprotective activity of EAMM. The NEM (NP-SH blocker) decreases the extract's gastroprotective activity remarkably and the ability of L-NAME (NO blocker) to reverse the EAMM gastroprotection suggests the role of NO in the EAMM's mechanisms of gastroprotection.

The pathogenesis of gastric ulcers have been widely known to involve oxidative stress. Ingestion of these necrotic agents may trigger the formation and release of free radicals or reactive oxygen species (ROS), which are known to contribute to the damage of gastric mucosa. Therefore, any compounds that were able to reduce oxidative stress or possess antioxidant potential are essential to the gastrointestinal tract as they can provide protection against the action of necrotic agents such as ethanol [23]. Those antioxidant biocompounds may act as radical scavengers thus protecting the gastric mucosa from oxidative damage. EAMM exert the most notable antioxidant potential and possess the highest TPC value in comparison to other partitions, which makes it a potential candidate to further investigate the antiulcer activity of *M. malabathricum*. The antioxidant and free radical scavenging properties of EAMM may have contributed to the observed gastroprotective effect.

The role of anti-inflammatory action in the modulation of EAMM induced gastroprotection should also be considered based on the fact that *M. malabathricum* exerts an effective anti-inflammatory activity when assessed using various COX-mediated animal inflammatory models [24, 25]. The EAMM was found to cause over 50% inhibition of LOX-mediated in vitro inflammation, therefore, suggesting the anti-inflammatory potential against the LOX-mediated inflammation that might contribute towards the effective gastroprotection of EAMM [26]. LOX is known to take part in the oxidation of arachidonic acid into a family of eicosanoid inflammatory mediators known as leukotrienes. Leukotrienes are believed to contribute to gastric mucosal damage by promoting tissue ischaemia and inflammation and play an imperative role in blood coagulation and gastrointestinal tract irritation [27]. Therefore, inhibition of LOX as seen with EAMM is believed to be vital in attenuating the formation of ethanol-induced gastric ulcer [28].

Despite the ability to exert anti-inflammatory activity, EAMM has been shown in the presence study to exert antiulcer activity and was effective in increasing the level of PGE_2 following subjection to the ethanol-induced gastric ulcer assay. The discrepancy in the action of EAMM is therefore worth discussing. Prostaglandins synthesis depends on the activity of COXs, which exist as distinct isoforms referred to as COX-1 and COX-2. COX-1, which is the dominant source of prostanoids that subserve housekeeping functions, such as gastric epithelial cytoprotection and homeostasis, expressed constitutively in most cells. On the other hand, COX-2 which is the more important source of prostanoid formation in inflammation and in proliferative diseases is induced by inflammatory stimuli, hormones, and growth factors. There is a dramatic increase of COX-2 expression upon provocation of inflammatory cells and in inflamed tissues. However, both enzymes contribute to the generation of autoregulatory and homeostatic prostanoids and both can contribute to prostanoid release during inflammation. Thus, with regard to its anti-inflammatory activity, EAMM is suggested to act preferentially towards inhibiting the COX-2 action, which lead to the inhibition of PGE_2 synthesis and inflammatory action. In terms of its antiulcer activity, EAMM is postulated to activate the COX-1 action leading to increase synthesis of local PGE_2 and PGI_2, which provides protection towards the gastroduodenal epithelial integrity. The disruption of this pathway via inhibition of COX-1 will lead to ulcer formation. Moreover, EAMM may be able to activate the gastroduodenal epithelial COX-2-dependent prostanoids (i.e., PGE_2 and PGI_2) that hasten ulcer healing. Both PGs, in particular, are vasodilators in the gastrointestinal mucosa, which may increase mucus production and reduce acid and pepsin levels in the stomach, thereby contributing to the gastric mucosal defense and facilitate the repair of preexisting ulcers in the gastrointestinal mucosa [29, 30].

The ethanol-induced gastric ulcer model is frequently used to evaluate the antiulcerogenic activity of drugs. Ethanol acts by rapidly penetrating the gastric mucosa and damaging the cell and plasma membranes leading to increase in intracellular membrane permeability to sodium and water. This, in turn, leads to massive accumulation of calcium that clarifies the pathogenesis of gastric mucosal injury [31]. Continuous ingestion of ethanol resulted in the development of gastric lesions in the form of multiple hemorrhagic red bands of different sizes along the glandular stomach. The gastric mucosal lesions incited by ethanol ingestion might decelerate the mechanism of gastric defense [32], which include the depletion of gastric mucus content, mucosal cell injury, and damaged mucosal blood flow [33]. Other than direct action on the gastric mucosa, ethanol also augments the production of ROS (i.e., superoxide anion and hydroxyl radicals) and enhances release of arachidonate metabolites [34, 35]. The ROS, in particular triggers lipid peroxidation that will cause disturbance in cellular activities leading ultimately to membrane cell damage, cell death, exfoliation, and epithelial erosion. This may explain the ability of EAMM to attenuate the ethanol-induced gastric ulcer formation due to its high antioxidant and anti-inflammatory capacities.

The ability of any compound to control the contraction and relaxation of gastric circular muscles might also contribute to the enhancement of gastroprotective effect [36, 37]. The contraction of circular muscles of the rat fundus strip caused by ethanol ingestion may lead to compression of the mucosa at the crest of the mucosal folds, causing ulceration and necrosis [36]. On the other hand, circular muscles relaxation will cause the gastric mucosa folds to flatten as part of the gastric mucosa defense by increasing the exposure of mucosal area to necrotizing agents while reducing the volume of gastric irritants on the rugal crest [37]. From the macroscopic observation, a flattening of the mucosal folds was observed following pretreatment with EAMM. This suggest that the EAMM also promotes gastroprotective action by decreasing the gastric motility as these alterations may also contribute to the development and prevention of gastric lesions.

The possible mechanisms of gastroprotection involving the role of NO and NP-SH were also investigated using the ethanol-induced gastric ulcer assay in rats. The rats were pretreated with L-NAME or NEM followed by EAMM before inducing with ethanol, respectively. Both the L-NAME and NEM caused significant reduction in the gastroprotective activity of EAMM suggesting that the semipurified extract works in the presence of NO and NP-SH. NO is one of the vital defensive endogenous factors in the gastric mucosa [38] and is important for the modulation of gastric mucosal integrity. Moreover, NO is vital for the regulation of mucus secretion, acid and alkaline secretion, and gastric mucosal blood flow [39]. The endothelium is the main and most preferred target of gastric ethanol damage [40]. In addition, L-NAME when given systemically inhibits NO synthesis/action leading to an increase in systemic blood pressure and the vasoconstriction of several vascular beds that damage the gastric mucosa and its endothelium [41]. Pretreatment of rats with L-NAME followed by EAMM reversed the gastroprotective effects exerted by the semipurified extract against ethanol-induced injury. These findings indicate the possible participation of the NO-mediated system in the gastroprotective activity elicited by EAMM. Mucus is important in gastroprotection as it helps to strengthen the mucosal barrier against harmful agents. At the molecular level, the mucus subunits are connected via disulfide bridges and reduction in this bridges will cause the mucus to be more water soluble [42]. The disulfide bridges help to maintain continuous adherence of the stable, undisturbed mucus layer, which serves to protect the underlying mucosa from proteolytic digestion [43]. The NP-SH compound exerts its protective effects against prooxidant agents by binding the free radicals synthesized following the ingestion of noxious agents [40].

In regard to the phytochemical constituents of EAMM, several classes of biocompounds were detected, namely, saponins, tannins, flavonoids, and steroids. This finding was concurrent with our previous report on the presence of those classes of biocompounds in the crude MEMM [44]. A number of biocompounds from the classes of flavonoids, saponins, and tannins are known to act as antioxidants [45–47] and anti-inflammatory [48–50] and are, therefore, suggested to act synergistically to exert both activities in all

models used. The synergistic action of those biocompounds is believed to be accountable towards the effectiveness of gastroprotective activity shown by EAMM. Therefore, the presence of these phytochemical substances may partly protect against gastric lesions by enhancing the antioxidant and anti-inflammatory activities of EAMM. In addition, flavonoid-based biocompounds have been reported to promote gastroprotection by increasing the gastric blood flow, stimulating the synthesis of mucosubstances of the gastric mucosa, increasing the PGs content and mucus thickness [51, 52]. Flavonoid-based biocompounds were also reported to promote formation of the gastric mucosa, inhibit pepsinogen production, decrease acid mucosal secretion, and reduce ulcerogenic lesions [53]. The ability of tannin-based biocompounds to prevent ulcer formation is by promoting protein precipitation layer on the ulcer site to form a protective pellicle, which helps to prevent the absorption of toxic substances and withstand the effects of proteolytic enzymes [54–56]. Meanwhile, the saponin-based biocompounds have been reported to demonstrate its gastroprotective effect by activating the mucus membrane protective factors [57] and by selectively inhibiting $PGF_{2\alpha}$ [31].

Several types of bioactive compounds have been identified in the MEMM as well as EAMM [6]. The closest findings that mimic the present extract, MEMM, were made by Nazlina et al. [58], who successfully isolated rutin, quercitrin, and quercetin using the TLC assay while those that mimic the present partition, EAMM, were made by Susanti et al. [59], who managed to isolate quercetin and quercitrin. Recent study on the hepatoprotective activity of MEMM also demonstrated the presence of rutin and quercitrin. Interestingly, quercetin, quercitrin, and rutin have been reported to play a role in gastroprotection elsewhere [53, 60, 61]. Therefore, these compounds are suggested to act together synergistically to produce the observed gastroprotective effect. Following the latest HPLC analysis of MEMM and EAMM, which used different set of HPLC equipment, conditions, eluants, and so forth in comparison to our previous study on MEMM [7, 44], several bioactive flavonoid-based compounds were identified, namely, gallocatechin (1), epigallocatechin (2), catechin (3), chlorogenic acid (4), caffeic acid (5), quercetin (6), quercetin-3-*O*-glucoside (7), *p*-coumaric acid (8), and hesperidin (9). Interestingly, some of these compounds like catechin [62], chlorogenic acid [63], caffeic acid [64], quercetin [65], and hesperidin [66] have been reported to exert antiulcer activity and are, therefore, expected to act synergistically to demonstrate the antiulcer activity as observed in MEMM and EAMM.

5. Conclusion

In conclusion, the ethyl acetate partition of MEMM or EAMM demonstrates the most effective gastroprotective activity against ethanol-induced gastric ulcer model, which could be attributed to the extract's (i) high antioxidant and anti-inflammatory activities; (ii) capability to modulate the gastric tissue's enzymatic and nonenzymatic antioxidant system; (iii) potential to regulate the PGE_2 synthesis, and (iv) ability to work via pathways involving the NO and NP-SH. Moreover, this activity could be plausibly linked to the presence of gastroprotective agents such as catechin, chlorogenic acid, caffeic acid, quercetin, and hesperidin, which might act synergistically to produce the observed activity.

Competing Interests

The authors declare that there is no conflict of interests regarding the publication of this article.

References

[1] D. Bandyopadhyay, K. Biswas, M. Bhattacharyya, R. J. Reiter, and R. K. Banerjee, "Gastric toxicity and mucosal ulceration induced by oxygen-derived reactive species: protection by melatonin," *Current Molecular Medicine*, vol. 1, no. 4, pp. 501–513, 2001.

[2] K. R. Mcquaid, "Drugs used in the treatment of gastrointestinal disease," in *Basic and Clinical Pharmacology*, B. G. Katzung, Ed., pp. 1009–1040, McGraw-Hill, Singapore, 2007.

[3] M. F. F. Kamarolzaman, F. Yahya, S. S. Mamat et al., "Gastroprotective activity and mechanisms of action of *Bauhinia purpurea* Linn. (Leguminoseae) leaf methanol extract," *Tropical Journal of Pharmaceutical Research*, vol. 13, no. 11, pp. 1889–1898, 2014.

[4] Z. A. Zakaria, T. Balan, V. Suppaiah, S. Ahmad, and F. Jamaludin, "Mechanism(s) of action involved in the gastroprotective activity of *Muntingia calabura*," *Journal of Ethnopharmacology*, vol. 151, no. 3, pp. 1184–1193, 2014.

[5] J. Singh, V. R. Santhosh Kumar, and V. Kadam, "Antiulcer activity of annona reticulate leaves extract in rats," *International Journal of Pharmacy and Pharmaceutical Sciences*, vol. 4, no. 1, pp. 412–414, 2012.

[6] S. M. Joffry, N. J. Yob, M. S. Rofiee et al., "*Melastoma malabathricum* (L.) smith ethnomedicinal uses, chemical constituents, and pharmacological properties: a review," *Evidence-Based Complementary and Alternative Medicine*, vol. 2012, Article ID 258434, 48 pages, 2012.

[7] Z. A. Zakaria, T. Balan, S. S. Mamat, N. Mohtarrudin, T. L. Kek, and M. Z. Salleh, "Mechanisms of gastroprotection of methanol extract of *Melastoma malabathricum* leaves," *BMC Complementary and Alternative Medicine*, vol. 15, no. 1, article 135, 15 pages, 2015.

[8] T. Balan, M. H. M. Sani, S. H. Mumtaz Ahmad, V. Suppaiah, N. Mohtarrudin, and Z. A. Zakaria, "Antioxidant and anti-inflammatory activities contribute to the prophylactic effect of semi-purified fractions obtained from the crude methanol extract of *Muntingia calabura* leaves against gastric ulceration in rats," *Journal of Ethnopharmacology*, vol. 164, no. 1, pp. 1–15, 2015.

[9] K. Ikhiri, D. Boureima, and D.-D. Dan-Koulodo, "Chemical screening of medicinal plants used in the traditional pharmacopoeia of Niger," *International Journal of Pharmacognosy*, vol. 30, no. 4, pp. 251–262, 1992.

[10] F. Liu, V. E. C. Ooi, and S. T. Chang, "Free radical scavenging activities of mushroom polysaccharide extracts," *Life Sciences*, vol. 60, no. 10, pp. 763–771, 1997.

[11] M. S. Blois, "Antioxidant determinations by the use of a stable free radical," *Nature*, vol. 181, no. 1, pp. 1199–1200, 1958.

[12] D. Huang, B. Ou, M. Hampsch-Woodill, J. A. Flanagan, and R. L. Prior, "High-throughput assay of oxygen radical absorbance capacity (ORAC) using a multichannel liquid handling system coupled with a microplate fluorescence reader in 96-well format," *Journal of Agricultural and Food Chemistry*, vol. 50, no. 16, pp. 4437–4444, 2002.

[13] V. L. Singleton and J. A. Rossi Jr., "Colorimetry of total phenolics with phosphomolybdic-phosphotungstic acid reagents," *American Journal of Enology and Viticulture*, vol. 16, no. 1, pp. 144–158, 1965.

[14] T. Noro, T. Miyase, M. Kuroyanagi, A. Ueno, and S. Fukushima, "Monoamine oxidase inhibitor from the rhizomes of *Kaempferia galanga* L.," *Chemical and Pharmaceutical Bulletin*, vol. 31, no. 8, pp. 2708–2711, 1983.

[15] Azhar-Ul-Haq, A. Malik, I. Anis et al., "Enzymes inhibiting lignans from *Vitex negundo*," *Chemical and Pharmaceutical Bulletin*, vol. 52, no. 11, pp. 1269–1272, 2004.

[16] Z. Zabidi, W. N. Wan Zainulddin, S. S. Mamat et al., "Antiulcer activity of methanol extract of *Melastoma malabathricum* leaves in rats," *Medical Principles and Practice*, vol. 21, no. 5, pp. 501–503, 2012.

[17] H. Shay, S. A. Komarov, S. S. Fels, D. Meranze, M. Gruenstein, and H. Siplet, "A simple method for the uniform production of gastric ulceration in the rat," *Gastroenterology*, vol. 5, no. 1, pp. 43–61, 1945.

[18] E. E. A. Hisam, Z. A. Zakaria, N. Mohtaruddin, M. S. Rofiee, H. A. Hamid, and F. Othman, "Antiulcer activity of the chloroform extract of Bauhinia purpurea leaf," *Pharmaceutical Biology*, vol. 50, no. 12, pp. 1498–1507, 2012.

[19] S. J. Corne, S. M. Morrissey, and R. J. Woods, "Proceedings: a method for the quantitative estimation of gastric barrier mucus," *Journal of Physiology*, vol. 242, no. 2, pp. 116P–117P, 1974.

[20] M. A. Andreo, K. V. R. Ballesteros, C. A. Hiruma-Lima, L. R. Machado da Rocha, A. R. M. Souza Brito, and W. Vilegas, "Effect of *Mouriri pusa* extracts on experimentally induced gastric lesions in rodents: role of endogenous sulfhydryls compounds and nitric oxide in gastroprotection," *Journal of Ethnopharmacology*, vol. 107, no. 3, pp. 431–441, 2006.

[21] W. N. W. Zainulddin, Z. Zabidi, F. H. Kamisan et al., "Anti-ulcer activity of the aqueous extract of *Melastoma malabathricum* L. leaf in rats," *Pakistan Journal of Pharmaceutical Sciences*, vol. 29, no. 1, pp. 35–38, 2016.

[22] Z. A. Zakaria, A. S. N. Zainol, A. Sahmat et al., "Gastroprotective activity of chloroform extract of *Muntingia calabura* and *Melastoma malabathricum* leaves extracts," *Pharmaceutical Biology*, vol. 54, no. 5, pp. 812–826, 2016.

[23] N. F. M. Rocha, G. V. D. Oliveira, F. Y. R. D. Araújo et al., "(−)-α-Bisabolol-induced gastroprotection is associated with reduction in lipid peroxidation, superoxide dismutase activity and neutrophil migration," *European Journal of Pharmaceutical Sciences*, vol. 44, no. 4, pp. 455–461, 2011.

[24] Z. A. Zakaria, C. A. Fatimah, A. M. Mat Jais et al., "The *in vitro* antibacterial activity of *Muntingia calabura* extracts," *International Journal of Pharmacology*, vol. 2, no. 4, pp. 439–442, 2006.

[25] Z. A. Zakaria, M. R. Sulaiman, A. M. M. Jais et al., "The antinociceptive activity of *Muntingia calabura* aqueous extract and the involvement of L-arginine/nitric oxide/cyclic guanosine monophosphate pathway in its observed activity in mice," *Fundamental and Clinical Pharmacology*, vol. 20, no. 4, pp. 365–372, 2006.

[26] S. Fiorucci, E. Distrutti, O. M. de Lima et al., "Relative contribution of acetylated cyclo-oxygenase (COX)-2 and 5-lipooxygenase (LOX) in regulating gastric mucosal integrity and adaptation to aspirin," *The FASEB Journal*, vol. 17, no. 9, pp. 1171–1173, 2003.

[27] J. Martel-Pelletier, D. Lajeunesse, P. Reboul, and J.-P. Pelletier, "Therapeutic role of dual inhibitors of 5-LOX and COX, selective and non-selective non-steroidal anti-inflammatory drugs," *Annals of the Rheumatic Diseases*, vol. 62, no. 6, pp. 501–509, 2003.

[28] Y. Yonei and P. H. Guth, "Ethanol-induced gastric injury: role of submucosal venoconstriction and leukotrienes," *Digestive Diseases and Sciences*, vol. 36, no. 5, pp. 601–608, 1991.

[29] J. L. Wallace, "Prostaglandins, NSAIDs, and gastric mucosal protection: why doesn't the stomach digest itself?" *Physiological Reviews*, vol. 88, no. 4, pp. 1547–1565, 2008.

[30] E. Ricciotti and G. A. Fitzgerald, "Prostaglandins and inflammation," *Arteriosclerosis, Thrombosis, and Vascular Biology*, vol. 31, no. 5, pp. 986–1000, 2011.

[31] A. Kumar, V. Singh, and A. K. Chaudhary, "Gastric antisecretory and antiulcer activities of *Cedrus deodara* (Roxb.) Loud. in Wistar rats," *Journal of Ethnopharmacology*, vol. 134, no. 2, pp. 294–297, 2011.

[32] M. Kinoshita, T. Noto, and H. Tamaki, "Effect of a combination of ecabet sodium and cimetidine on experimentally induced gastric lesions and gastric mucosal resistance to ulcerogenic agents in rats," *Biological and Pharmaceutical Bulletin*, vol. 18, no. 2, pp. 223–226, 1995.

[33] V. J. Galani, S. S. Goswami, and M. B. Shah, "Antiulcer activity of *Trichosanthes cucumerina* Linn. Against experimental gastroduodenal ulcers in rats," *Oriental Pharmacy and Experimental Medicine*, vol. 10, no. 1, pp. 222–230, 2010.

[34] D. Bagchi, O. R. Carryl, M. X. Tran et al., "Stress, diet and alcohol-induced oxidative gastrointestinal mucosal injury in rats and protection by bismuth subsalicylate," *Journal of Applied Toxicology*, vol. 18, no. 1, pp. 3–13, 1998.

[35] M. Rachchh and S. Jain, "Gastroprotective effect of *Benincasa hispida* fruit extract," *Indian Journal of Pharmacology*, vol. 40, no. 6, pp. 271–275, 2008.

[36] A. Jamal, K. Javed, M. Aslam, and M. A. Jafri, "Gastroprotective effect of cardamom, *Elettaria cardamomum* Maton. fruits in rats," *Journal of Ethnopharmacology*, vol. 103, no. 2, pp. 149–153, 2006.

[37] S. I. Abdelwahab, S. Mohan, M. A. Abdulla et al., "The methanolic extract of *Boesenbergia rotunda* (L.) Mansf. and its major compound pinostrobin induces anti-ulcerogenic property in vivo: possible involvement of indirect antioxidant action," *Journal of Ethnopharmacology*, vol. 137, no. 2, pp. 963–970, 2011.

[38] T. Brzozowski, P. C. Konturek, Z. Śliwowski et al., "Interaction of nonsteroidal anti-inflammatory drugs (NSAID) with *Helicobacter pylori* in the stomach of humans and experimental animals," *Journal of Physiology and Pharmacology*, vol. 57, no. 3, pp. 67–79, 2006.

[39] S. I. Chandranath, S. M. A. Bastaki, and J. Singh, "A comparative study on the activity of lansoprazole, omeprazole and PD-136450 on acidified ethanol- and indomethacin-induced gastric lesions in the rat," *Clinical and Experimental Pharmacology and Physiology*, vol. 29, no. 3, pp. 173–180, 2002.

[40] F. M. De-Faria, A. C. A. Almeida, A. Luiz-Ferreira et al., "Antioxidant action of mangrove polyphenols against gastric damage induced by absolute ethanol and ischemia-reperfusion

in the rat," *The Scientific World Journal*, vol. 2012, Article ID 327071, 9 pages, 2012.

[41] P. Sikirić, S. Seiwerth, Ž. Grabarević et al., "The influence of a novel pentadecapeptide, BPC 157, on N-G-nitro-L-arginine methylester and L-arginine effects on stomach mucosa integrity and blood pressure," *European Journal of Pharmacology*, vol. 332, no. 1, pp. 23–33, 1997.

[42] J. R. Avila, C. Alarcón De La Lastra, M. J. Martín et al., "Role of endogenous sulphydryls and neutrophil infiltration in the pathogenesis of gastric mucosal injury induced by piroxicam in rats," *Inflammation Research*, vol. 45, no. 2, pp. 83–88, 1996.

[43] A. Allen and G. Flemström, "Gastroduodenal mucus bicarbonate barrier: protection against acid and pepsin," *American Journal of Physiology—Cell Physiology*, vol. 288, no. 1, pp. C1–C19, 2005.

[44] S. S. Mamat, M. F. F. Kamarolzaman, F. Yahya et al., "Methanol extract of *Melastoma malabathricum* leaves exerted antioxidant and liver protective activity in rats," *BMC Complementary and Alternative Medicine*, vol. 13, Article ID 326, 12 pages, 2013.

[45] R. Baharfar, R. Azimi, and M. Mohseni, "Antioxidant and antibacterial activity of flavonoid-, polyphenol- and anthocyanin-rich extracts from *Thymus kotschyanus* boiss & hohen aerial parts," *Journal of Food Science and Technology*, vol. 52, no. 10, pp. 6777–6783, 2015.

[46] Y.-F. Zheng, J.-H. Xie, Y.-F. Xu et al., "Gastroprotective effect and mechanism of patchouli alcohol against ethanol, indomethacin and stress-induced ulcer in rats," *Chemico-Biological Interactions*, vol. 222, no. 1, pp. 27–36, 2014.

[47] L.-L. Zhang and Y.-M. Lin, "Tannins from *Canarium album* with potent antioxidant activity," *Journal of Zhejiang University Science B*, vol. 9, no. 5, pp. 407–415, 2008.

[48] M. Funakoshi-Tago, K. Okamoto, R. Izumi et al., "Anti-inflammatory activity of flavonoids in Nepalese propolis is attributed to inhibition of the IL-33 signaling pathway," *International Immunopharmacology*, vol. 25, no. 1, pp. 189–198, 2016.

[49] Y. Yao, X. Yang, Z. Shi, and G. Ren, "Anti-inflammatory activity of saponins from quinoa (Chenopodium quinoa Willd.) seeds in lipopolysaccharide-stimulated RAW 264.7 macrophages cells," *Journal of Food Science*, vol. 79, no. 5, pp. H1018–H1023, 2014.

[50] M. L. Mota, G. Thomas, and J. M. Barbosa Filho, "Anti-inflammatory actions of tannins isolated from the bark of *Anacardium occidentale* L," *Journal of Ethnopharmacology*, vol. 13, no. 1, pp. 289–300, 1985.

[51] K. S. L. Mota, G. E. N. Dias, M. E. F. Pinto et al., "Flavonoids with gastroprotective activity," *Molecules*, vol. 14, no. 3, pp. 979–1012, 2009.

[52] R. Saziki, I. Arai, Y. Isobe, H. Hirose, and H. Aihara, "Effects of sofalcone on necrotizing agents-induced gastric lesions and on endogenous prostaglandins in rats stomachs," *Journal of Pharmacobio-Dynamics*, vol. 7, no. 11, pp. 791–797, 1984.

[53] C. La Casa, I. Villegas, C. Alarcón De La Lastra, V. Motilva, and M. J. Martín Calero, "Evidence for protective and antioxidant properties of rutin, a natural flavone, against ethanol induced gastric lesions," *Journal of Ethnopharmacology*, vol. 71, no. 1-2, pp. 45–53, 2000.

[54] T. A. John and A. O. Onabanjo, "Gastroprotective effects of an aqueous extract of *Entandrophragma utile* bark in experimental ethanol-induced peptic ulceration in mice and rats," *Journal of Ethnopharmacology*, vol. 29, no. 1, pp. 87–93, 1990.

[55] D. A. Lewis and G. P. Shaw, "A natural flavonoid and synthetic analogues protect the gastric mucosa from aspirin-induced erosions," *Journal of Nutritional Biochemistry*, vol. 12, no. 2, pp. 95–100, 2001.

[56] P. A. Nwafor, K. D. Effraim, and T. W. Jacks, "Gastroprotective effect of aqueous extract of *Khaya senegalensis* bark on indomethacin-induced ulceration in rats," *West African Journal of Pharmacology and Drug Research*, vol. 12, no. 1, pp. 46–50, 1996.

[57] M. K. Choudhary, S. H. Bodakhe, and S. K. Gupta, "Assessment of the antiulcer potential of *Moringa oleifera* root-bark extract in rats," *Journal of Acupuncture and Meridian Studies*, vol. 6, no. 4, pp. 214–220, 2013.

[58] I. Nazlina, S. Norha, A. W. Noor Zarina, and I. B. Ahmad, "Cytotoxicity and antiviral activity of *Melastoma malabathricum* extracts," *Malaysian Journal of Applied Biology*, vol. 37, no. 1, pp. 53–55, 2008.

[59] D. Susanti, H. M. Sirat, F. Ahmad, and R. M. Ali, "Bioactive constituents from the leaves of *Melastoma malabathricum* L.," *Jurnal Ilmiah Farmasi*, vol. 5, no. 1, pp. 1–8, 2008.

[60] C. A. De La Lastra, M. J. Martín Calero, and V. Motilva, "Antiulcer and gastroprotective effects of quercetin: a gross and histologic study," *Pharmacology*, vol. 48, no. 1, pp. 56–62, 1994.

[61] M. Abreu Miranda, M. Lemos, K. Alves Cowart et al., "Gastroprotective activity of the hydroethanolic extract and isolated compounds from the leaves of *Solanum cernuum* Vell," *Journal of Ethnopharmacology*, vol. 172, no. 1, pp. 421–429, 2015.

[62] K. Hamaishi, R. Kojima, and M. Ito, "Anti-ulcer effect of tea catechin in rats," *Biological and Pharmaceutical Bulletin*, vol. 29, no. 11, pp. 2206–2213, 2006.

[63] A. T. Shimoyama, J. R. Santin, I. D. MacHado et al., "Antiulcerogenic activity of chlorogenic acid in different models of gastric ulcer," *Naunyn-Schmiedeberg's Archives of Pharmacology*, vol. 386, no. 1, pp. 5–14, 2013.

[64] Y.-T. Cheng, C.-Y. Ho, J.-J. Jhang, C.-C. Lu, and G.-C. Yen, "DJ-1 plays an important role in caffeic acid-mediated protection of the gastrointestinal mucosa against ketoprofen-induced oxidative damage," *Journal of Nutritional Biochemistry*, vol. 25, no. 10, pp. 1045–1057, 2014.

[65] Y. Suzuki, M. Ishihara, T. Segami, and M. Ito, "Anti-ulcer effects of antioxidants, quercetin, α-tocopherol, nifedipine and tetracycline in rats," *Japanese Journal of Pharmacology*, vol. 78, no. 4, pp. 435–441, 1998.

[66] D. I. Hamdan, M. F. Mahmoud, M. Wink, and A. M. El-Shazly, "Effect of hesperidin and neohesperidin from bittersweet orange (*Citrus aurantium* var. *bigaradia*) peel on indomethacin-induced peptic ulcers in rats," *Environmental Toxicology and Pharmacology*, vol. 37, no. 1, pp. 907–915, 2014.

Hindawi Publishing Corporation
Oxidative Medicine and Cellular Longevity
Volume 2016, Article ID 6354261, 9 pages
http://dx.doi.org/10.1155/2016/6354261

Research Article

Skin Aging-Dependent Activation of the PI3K Signaling Pathway via Downregulation of PTEN Increases Intracellular ROS in Human Dermal Fibroblasts

Eun-Mi Noh,[1] Jinny Park,[2] Hwa-Ryung Song,[3] Jeong-Mi Kim,[1] Minok Lee,[1] Hyun-Kyung Song,[1] On-Yu Hong,[4] Pyoung H. Whang,[5] Myung-Kwan Han,[3] Kang-Beom Kwon,[1,6] Jong-Suk Kim,[4] and Young-Rae Lee[1,7]

[1]*Center for Metabolic Function Regulation, Wonkwang University School of Medicine, Iksan 570-749, Republic of Korea*
[2]*Division of Hematology/Oncology, Gachon University Gil Medical Center, Incheon 405-760, Republic of Korea*
[3]*Department of Microbiology & Immunology, Institute of Medical Science, Chonbuk National University Medical School, Jeonju 560-182, Republic of Korea*
[4]*Department of Biochemistry, Institute of Medical Science, Chonbuk National University Medical School, Jeonju 560-182, Republic of Korea*
[5]*Department of Pediatrics, Institute of Clinical Science, Chonbuk National University Medical School, Jeonju 560-182, Republic of Korea*
[6]*Department of Korean Physiology, Wonkwang University School of Korean Medicine, Iksan 570-749, Republic of Korea*
[7]*Department of Oral Biochemistry and Institute of Biomaterials, Implant, School of Dentistry, Wonkwang University, Iksan 570-749, Republic of Korea*

Correspondence should be addressed to Jong-Suk Kim; jsukim@jbnu.ac.kr and Young-Rae Lee; mindyr@wku.ac.kr

Received 25 March 2016; Revised 4 July 2016; Accepted 26 July 2016

Academic Editor: Juan F. Santibanez

Reactive oxygen species (ROS) play a major role in both chronological aging and photoaging. ROS induce skin aging through their damaging effect on cellular constituents. However, the origins of ROS have not been fully elucidated. We investigated that ROS generation of replicative senescent fibroblasts is generated by the modulation of phosphatidylinositol 3,4,5-triphosphate (PIP3) metabolism. Reduction of the PTEN protein, which dephosphorylates PIP3, was responsible for maintaining a high level of PIP3 in replicative cells and consequently mediated the activation of the phosphatidylinositol-3-OH kinase (PI3K)/Akt pathway. Increased ROS production was blocked by inhibition of PI3K or protein kinase C (PKC) or by NADPH oxidase activating in replicative senescent cells. These data indicate that the signal pathway to ROS generation in replicative aged skin cells can be stimulated by reduced PTEN level. Our results provide new insights into skin aging-associated modification of the PI3K/NADPH oxidase signaling pathway and its relationship with a skin aging-dependent increase of ROS in human dermal fibroblasts.

1. Introduction

Changes in the skin are the most prominent signs of aging. Skin aging can be divided into intrinsic or chronologic aging, which is the process of senescence that affects all body organs, and extrinsic aging (photoaging), which occurs because of exposure to environmental factors. One of the most important factors influencing intrinsic aging is a gradual loss of function or degeneration that occurs at the cellular level [1]. Cellular senescence, a state of essentially irreversible growth arrest of cells, can be triggered *in vitro* by phenotypic changes in morphology, gene expression, and function [2, 3]. Primary cultured cells undergo replicative senescence, which is characterized by telomere shortening, genomic damage, epigenomic damage, and activation of tumor suppressors [1].

Reactive oxygen species (ROS), primarily arising from oxidative cell metabolism, play a major role in both chronological aging and photoaging of skin [4]. Despite the presence

of several antioxidative mechanisms that deteriorate with increasing age, ROS damage to cellular components still abounds. This damage leads to increasing ROS, decreasing antioxidative capacities, and finally cellular aging [4, 5]. ROS in extrinsic and intrinsic skin aging may be assumed to induce transcription factors (NF-κB and c-Jun); this induction activates the decisive transcription factors, leads to the expression of matrix metalloproteinases, and prevents the expression of procollagen-1 [6]. It is still unclear what earlier events in ROS generation are involved in the progression of cellular aging. Accordingly, in this study we investigated the source of ROS in the skin cellular aging process.

The NOX family NADPH oxidases are proteins that transfer electrons across biological membranes. In general, NADPH oxidases have been thought to generate superoxide at the plasma membrane and release it into the extracellular space where it is converted into hydrogen peroxide. The biological function of NOX enzymes is the generation of ROS [7, 8]. Recent studies indicated that NADPH oxidase family members are found in a wide array of tissues [9]. NADPH oxidase is closely linked with phosphatidylinositol 3-OH kinase (PI3K) signaling [10, 11]. Protein kinase C (PKC), a downstream molecule of PI3K, is essential for superoxide generation by NADPH oxidase [10, 12].

The tumor suppressor PTEN dephosphorylates the lipid second messenger, phosphoinositol 3,4,5-trisphosphate (PIP3), an enzymatic product PI3K, and negatively regulates survival signaling mediated by PI3K/Akt (PI3K/Akt) [13, 14].

In this study, we demonstrated that PTEN downregulation and resultant activation of PI3K signaling caused PKCζ activation, which in turn increased ROS production through NADPH oxidase expression and its activity modulation in replicative aged human dermal fibroblasts (HDFs). Our results provide new insights into skin aging-associated modification of the PI3K/PKCζ/NADPH oxidase signaling pathway and its relationship with senescence-dependent increases of ROS in HDFs.

2. Materials and Methods

2.1. Cell Culture. HDFs isolated from neonatal foreskin were purchased from GIBCO (Invitrogen, CA). The dermal fibroblasts were cultured in Medium 106 with low serum growth supplement and 1% antibiotics at 37°C in a 5% CO2 incubator. The cells were subcultured in an atmosphere of 5% CO2 at 37°C by passaging them at a ratio of 1 : 5 in regular intervals. At later passages, the splitting ratio was reduced to 1 : 3 and 1 : 2, respectively. Cells were passaged such that the monolayers never exceeded 70–80% confluence. Population doublings (PD) were estimated using the following equation: $n = (\log 10F - \log 10I)/0.301$ (with n = population doublings, F = number of cells at the end of one passage, I = number of cells that were seeded at the beginning of one passage). The senescent status was verified by *in situ* staining for SA-β-galactosidase. 90–100% percent of the cells at PD 55 stained positive for SA-β-galactosidase.

2.2. Quantification of Intracellular Reactive Oxygen Species. The intracellular concentration of reactive oxygen species of HDFs was measured by using an oxidation-sensitive fluorescent probe dye, 2′,7′-dichlorodihydrofluorescein diacetate (DCF-DA) and hydroethidine (Sigma Co.) [15]. To measure intracellular ROS, the cells were incubated for 1 hr at 37°C with HBSS containing 33 μM DCF-DA (Molecular Probes) or 1 μM hydroethidine (Sigma Co.). The samples were then immediately observed under confocal fluorescence microscope (Olympus, Japan). The images were obtained by overlaying fluorescent images to differential interference contrast images. Also, DCF fluorescence was detected by FACStar flow cytometer (Becton Dickinson). For each sample, 10,000 events were collected. Reactive oxygen species production was expressed as mean fluorescence intensity (MFI), which was calculated by CellQuest software. Additionally, the cells were incubated for 1 hr at 37°C with HBSS containing 33 mM DCF-DA (Invitrogen Molecular Probes, Eugene, OR). The samples were then immediately observed under fluorescence microscopy.

2.3. Measurement of NADPH Oxidase. HDFs were lysed with the lysis buffer (20 mM Hepes, pH 7.2, 1% Triton X-100, 150 mM NaCl, 0.1 mM phenylmethylsulfonyl fluoride (PMSF), 1 mM EDTA, and 1 μg/mL aprotinin). After incubation for 30 min at 4°C, cellular debris was removed by centrifugation at 10,000 ×g for 30 min. NADPH oxidase in the supernatant was measured by lucigenin chemiluminescence in the presence of 500 μM NADPH (Sigma-Aldrich, St. Louis, MO) and 25 μM lucigenin (Sigma-Aldrich, St. Louis, MO) as described previously [16].

2.4. Western Blot Analysis. Cells were lysed with ice-cold M-PER® Mammalian Protein Extraction Reagent (Pierce Biotechnology, Rockford, IL), samples (30 μg) were separated by sodium dodecyl sulfate-polyacrylamide gel electrophoresis (GE Healthcare Life Sciences, Buckinghamshire, UK), and subsequent immunoblotting was performed by incubation with primary antibodies against PTEN, p85, $gp91^{phox}$, $p67^{phox}$, PKCζ, Akt, β-actin (Santa Cruz, CA), phosphor-Akt (Cell Signaling Technology, Beverly, MA), and phospho-PKCζ (Millipore Co., Ltd., Bedford, MA) and PIP3 (Abcam Co., MA) followed by further incubation with HRP-conjugated IgG secondary antibody. Protein expression levels were determined by signal analysis using an image analyzer (Fuji-Film, Tokyo, Japan).

2.5. Immunocytochemical Methods for PIP3 Analysis. Intracellular PIP_3 levels were directly determined using an immunocytochemical method with a recently developed monoclonal antibody to PIP_3 as described by Niswender et al. [17] Slide glasses containing HDFs were equilibrated in phosphate buffered saline at room temperature. Cells were fixed for 5–10 min at room temperature in 4% paraformaldehyde. After blocking in 5% normal goat serum and 2% bovine serum albumin, samples were incubated with mouse anti-PIP_3 monoclonal antibody (Echelon Biosciences, UT) at a 1 : 100 dilution overnight at 4°C. The negative control for the antibody was an equivalent concentration of nonimmune

mouse IgM. Primary antibodies were detected with goat anti-mouse IgM-TRITC at a 1 : 200 dilution 1 h at 4°C. Specimens were viewed using an Olympus FluoView laser scanning confocal microscope.

2.6. Preparation of Ectopic Expression of PTEN. To generate adenoviral constructs, the PTEN entry vector (pENTR-*PTEN*, Invitrogen, CA) and a control entry vector (pENTR-*GUS*->lacZ) were recombined with pAD/CMV/V5 (Invitrogen, Carlsbad, CA) using LR Clonase II (Invitrogen, Carlsbad, CA) to generate pAD/CMV/*GUS*->lacZ/V5 and pAD/CMV/*PTEN*/V5, respectively. The plasmid was linearized with Pac 1 and was transfected into 283A cells using lipofectamin 2000. Viruses from the culture supernatants of 293A cells that showed cytopathogenic effects were purified by cesium chloride banding. A confluent culture of HDFs was infected with recombinant adenovirus at a concentration of 1.0 plaque-forming units (pfu) per cell for 48–72 hours.

2.7. Statistical Analysis. Data are expressed as mean ± SEM. Statistical comparisons were performed using one-way ANOVA followed by the Fisher test. The significance of differences between groups was determined using Student's unpaired t-test. A value of $p < 0.05$ was accepted as an indication of statistical significance.

3. Results

3.1. Intracellular ROS Levels Are Increased by Activation of NADPH Oxidase in Replicative Aged HDFs. Skin cells in the human body have limited replication potential *in vivo*. This is reflected by the finite replicative lifespan *in vitro* termed "replicative cellular senescence," which has been proposed as an experimental model for human aging [18]. We also made an *in vitro* skin aging model by replicative subculturing with HDFs. We first analyzed whether ROS would change during extended passaging of HDFs. The level of intracellular ROS was determined using Dichlorofluorescin diacetate (DCF-DA) and Hydroethidine Fluorescence. Additionally, both of fluorescence was elevated in cells with extended HDF passages. Senescent status was verified by *in situ* staining for SA-β-galactosidase; 90–100% percent of the cells at PD 55 stained positive for SA-β-galactosidase (Figure 1(a)). Intracellular ROS levels increased during the passage progression by 4.9 ± 0.2 fold from passage 17 to 55 when ROS was quantified using a flow cytometer (Figure 1(b)). Interestingly, the increased ROS in replicative aged skin cells was not extinguished by the treatment with rotenone, an inhibitor of mitochondrial electron transfer (Figure 1(c)). However, ROS increase in replicative aged HDFs was inhibited by diphenyleneiodonium (DPI) and apocynin, inhibitors of NADPH oxidase (Figure 1(c)). Allopurinol, an inhibitor of xanthine oxidase, had no effect on aging-induced ROS (Figure 1(c)). The increased ROS in aged HDF was inhibited by superoxide dismutase (SOD) (Figure 1(c)). It is likely that the major source of ROS in replicative aged HDFs is not the mitochondria, but rather NADPH oxidase. These findings are further supported by our data that NADPH oxidase activity was elevated in replicative aged HDFs (Figure 1(d)). Additionally, we confirmed that elevated NADPH oxidase activity decreased by DPI and SOD in time-dependent manner (Supplementary Figure 1). The increase in NADPH oxidase activity can be induced by the increase of NADPH oxidase expression or modulation of NADPH activity. The expression of $p67^{phox}$ and $gp91^{phox}$ of NADPH oxidase increased in replicative aged HDFs. However, the expression of superoxide degrading enzymes, Cu, Zn-SOD, and Mn-SOD, did not change during the progression of cellular aging (Figure 1(e)). Together, these results indicated that increased ROS was elevated by NADPH oxidase activation in replicative aged HDFs. These results suggest that ROS increase in aged HDFs might be caused by increased NADPH expression rather than modulation of NADPH oxidase activity.

3.2. ROS Generation in Replicative Aged HDFs Is Induced by PI3K Signaling, Phosphorylation of PKCζ, and NADPH Oxidase Activation. In order to understand the signaling pathways via ROS generation, we tested whether wortmannin and calphostin, inhibitors of PI3K and PKC, respectively, inhibited the enhanced NADPH oxidase activity and ROS levels in replicative aged HDFs (Figures 2(a) and 2(b)). These findings suggest that ROS generation through the activation of NADPH oxidase in replicative aged HDFs might be mediated by PI3K and PKC signaling. From this finding we expected that PI3K and PKC signaling could be activated in replicative aged HDFs. Indeed, the phosphorylation of Akt, a hallmark of PI3K signal activation, increased in replicative aged HDFs (Figure 2(c)). PKCζ phosphorylation, an indicator of PKC activation, was also elevated in replicative aged HDFs (Figure 2(c)). PKCζ phosphorylation is likely to be mediated by activation of the PI3K-Akt pathway because PKCζ phosphorylation was inhibited by treatment with wortmannin (Figure 2(d)). Also, the expression of $p67^{phox}$ and $gp91^{phox}$ was decreased by 6 h treatment with wortmannin (Figure 2(e)). Thus, we conclude that the activation of the PI3K-Akt pathway induces phosphorylation of PKCζ, leading to enhanced NADPH oxidase activity and resulting in an increase in ROS generation.

3.3. Replicative Aged HDFs Exhibit Increased Intracellular PIP3 Levels through PTEN Downregulation. To determine what activates the PI3K-Akt pathway, we tested whether the protein levels of PI3K increase as HDFs age. We determined that the PI3K p85 subunit protein levels showed a slight decrease in replicative aged HDFs (Figure 3(a)). PI3K signaling can be affected by PTEN since the PIP3 level is controlled directly by the balance of activities between PI3K, the synthetic enzyme of PIP3, and PTEN, its degradative enzyme [18, 19]. We found that the protein level of PTEN was reduced much more than that of PI3K as the cells aged (Figure 3(a)). These data suggest that the imbalance between PI3K and PTEN levels induces modulation of PIP3 metabolism, which results in the activation of PI3K-Akt pathway. To confirm this, we measured intracellular PIP3 levels in HDFs of various ages. Intracellular levels of PIP3 increased with increasing passages of HDF indicating that the elevation of PIP3 levels

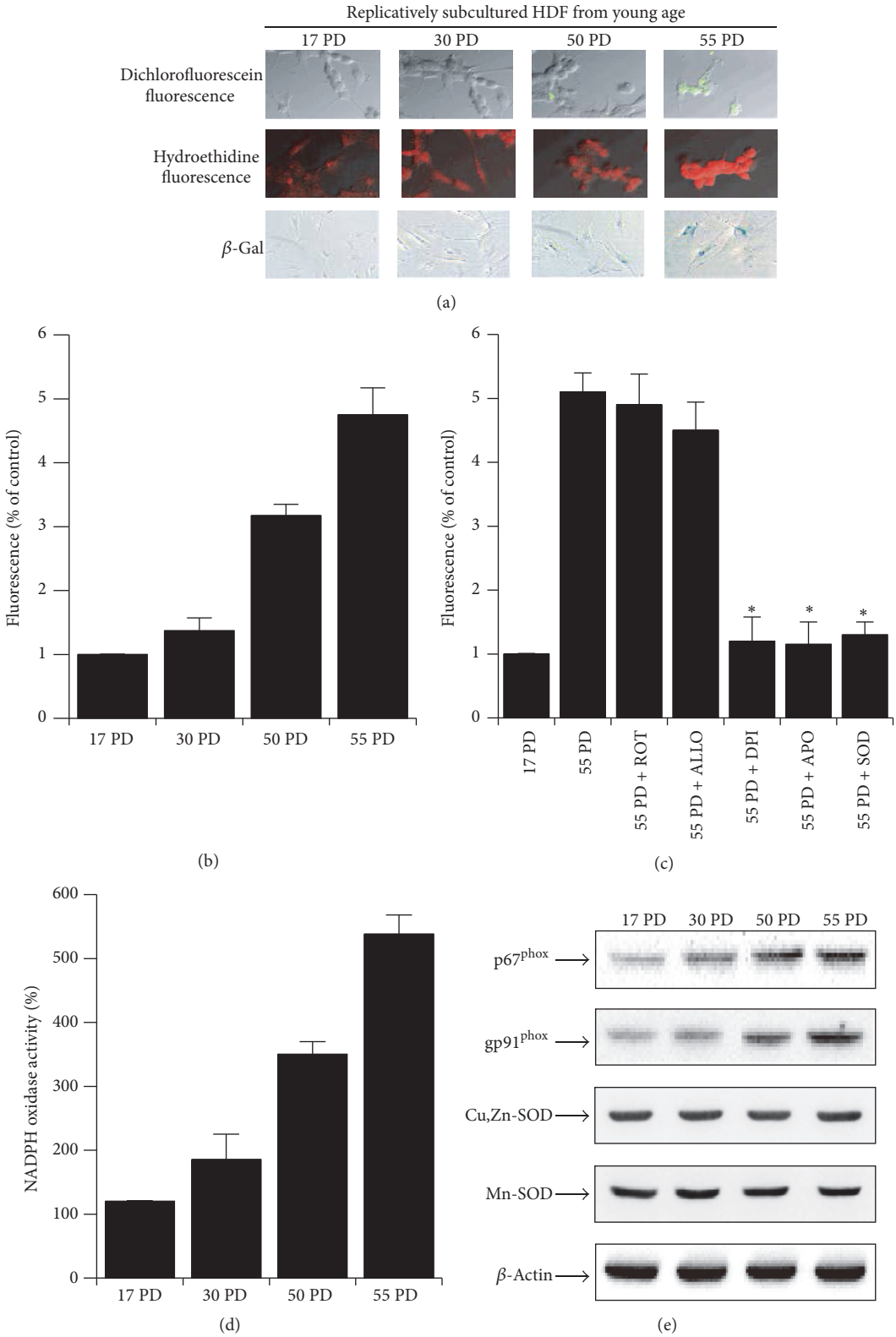

Figure 1: Elevation of cellular ROS levels in replicative aged HDFs through the activation of NADPH oxidase. (a) Increase in ROS with increasing PD of HDFs determined by ROS-sensitive fluorescent dyes. Various PDs of HDFs were stained with DCF-DA for 30 min and visualized with fluorescence microscopy. Senescent status was verified by *in situ* staining for SA-β-galactosidase. (b) ROS was measured by flow cytometry using DCFH-DA in various PDs of HDFs. (c) ROS in replicative aged HDFs (55 PD) under control conditions and in the presence of superoxide dismutase (SOD, 200 U/mL), rotenone (ROT, 10 mM), allopurinol (ALLO, 100 μM), diphenyleneiodonium (DPI, 100 μM), and apocynin (APO, 300 μM). (d) Increase in NADPH oxidase activity with increasing PDs of HDFs. NADPH oxidase activity was measured by lucigenin activity in the presence of 500 μM NADPH. (e) Multiple PDs of HDFs were analyzed by western blot for $gp91^{phox}$, $p67^{phox}$, and β-actin. Error bars, SD; $n = 5$ in each group. $^{*}P < 0.001$, compared with 55 PD.

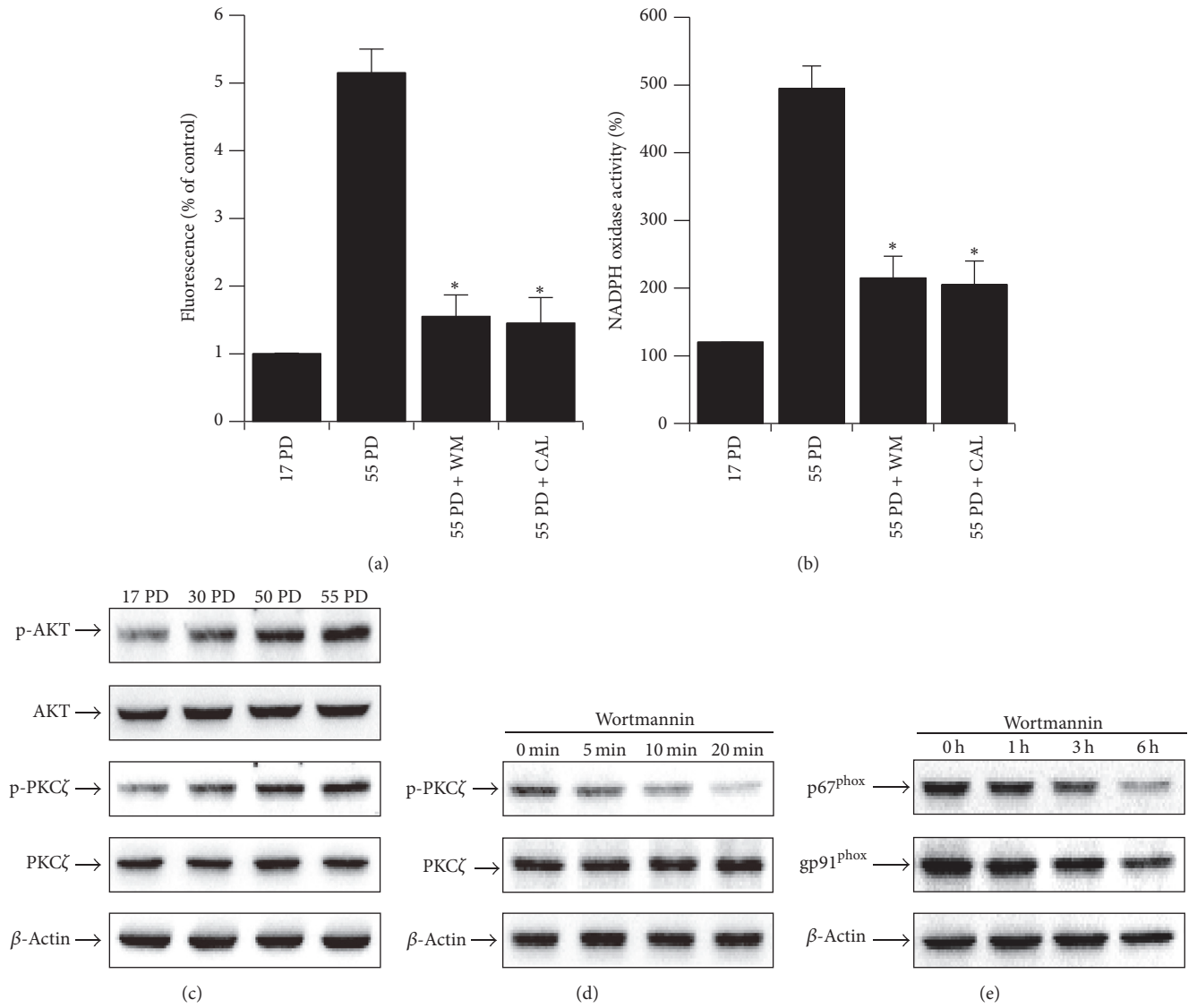

Figure 2: The elevation of cellular ROS levels in replicative aged HDFs through activation of PI3K, PKCζ, and NADPH oxidase. (a) Blockage of aging-induced increase of ROS by incubating 55 PD HDFs with medium alone or with 100 nM wortmannin or 100 nM calphostin for 30 min. Blockage was measured by flow cytometry using DCF-DA. (b) Blockage of aging-induced increase of NADPH oxidase activity by wortmannin and calphostin C. NADPH oxidase activity was measured by lucigenin activity with medium alone or with 100 nM wortmannin or 100 nM calphostin C in the presence of 500 μM NADPH. (c) Aging-induced increase of PKCζ and Akt phosphorylation. Various PDs of HDFs were lysed, and western blots for phospho-Akt, phospho-PKCζ, and β-actin were performed with the cell lysates (see Methods). (d) Inhibition of PKCζ phosphorylation by wortmannin. 35 PD HDFs were treated with 100 nM wortmannin for the indicated times and the cells were analyzed with western blots for phospho-PKCζ and β-actin. (e) Inhibition of gp91^{phox} and p67^{phox} expression by wortmannin. 55 PD HDFs were treated with 100 nM wortmannin for the indicated times. The cells were analyzed by western blotting for gp91^{phox}, p67^{phox}, and β-actin. Error bars, SD; $n = 5$ in each group. $^{*}P < 0.005$, compared with 55 PD.

in replicative aged HDFs is induced by a decrease in PIP3 breakdown through greater downregulation of PTEN than of PI3K (Figure 3(b)). Additionally, we confirmed elevation of PIP3 protein expression with increasing passage of HDF using western blotting analysis (Supplementary Figure 2). And we examined the effect of PI3K on PIP3 production. Treatment of Wortmannin (PI3K inhibitor) decreased PIP3 expression in aged cells (Supplementary Figure 3).

3.4. Overexpression of PTEN Decreases Cellular ROS Levels by Inhibiting NADPH Oxidase through PIP3 Downregulation. To confirm the effect of PTEN on NADPH oxidase/ROS, we infected replicative aged HDFs with adenovirus containing the PTEN gene (Ad/PTEN) or control lacZ (Ad/LacZ). PTEN protein levels were elevated by infection with Ad/PTEN (Figure 4(b)). PTEN overexpression in replicative aged HDFs abolished the aging-induced increases in PIP3 concentration

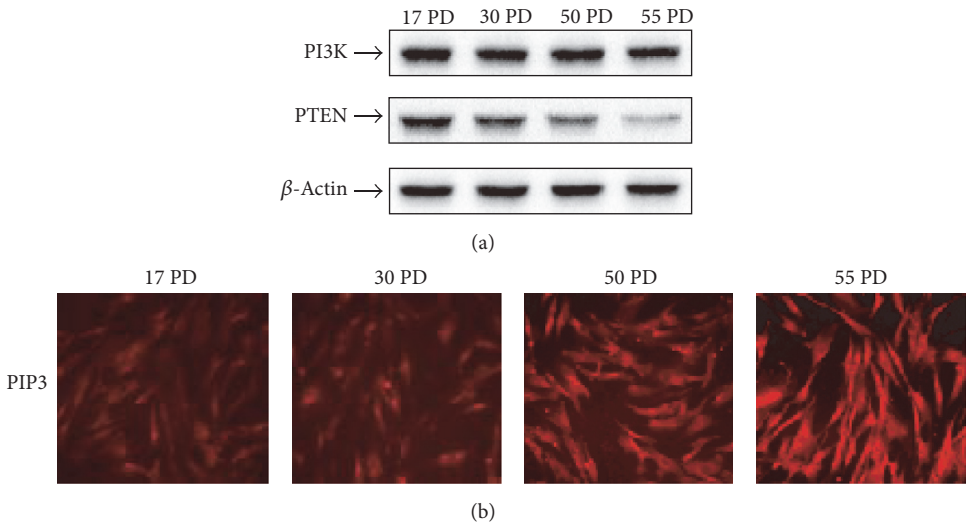

Figure 3: Replicative senescence-dependent increase in intracellular PIP_3 levels through PTEN downregulation. (a) Expression levels of PI3K and PTEN, in various PDs of HDFs. Various PDs of HDFs were analyzed by western blotting for PTEN, PI3K p85 subunit, and β-actin. (b) PIP_3 immunofluorescence staining in various PDs of HDFs. Various PDs of HDFs were fixed with 4% paraformaldehyde, incubated with anti-PIP_3 antibody and stained with TRITC-labeled anti-mouse IgM antibody. Images were acquired using an Olympus FluoView™ laser scanning confocal microscope.

(Figure 4(a)) and NADPH oxidase expression (Figure 4(b)) as well as the resultant aging-induced ROS generation (Figure 4(c)). On the contrary, inactivation of PTEN increased PIP3 expression (Supplementary Figure 4). Our data show that enhanced ROS further activates PI3K signaling by the inactivation of PTEN.

4. Discussion

ROS induces skin aging by damaging cellular constituents; however, the origins of ROS have not been elucidated in intrinsic skin aging. In this study, we showed that ROS in replicative aged HDFs are generated by the modulation of PIP3 metabolism. The decrease in PTEN protein, which dephosphorylates PIP3, was responsible for maintaining high levels of PIP3 in replicative aged HDFs and consequently mediated the activation of the PI3K/Akt pathway. PI3K/Akt pathway activation led to PKCζ activation and in turn increased ROS production through increases in NADPH expression. Therefore, we investigated whether the pathway leading to ROS generation is initiated by increased PIP3 level through regulation of PTEN in replicative aged HDFs.

Skin aging, a progressive and multifactorial but not yet fully understood process, is particularly interesting because of the continuously increasing life expectancy in many countries [20, 21]. Changes in the skin are the most prominent signs of aging. Skin aging can be divided into intrinsic or chronologic aging, which is the process of senescence that affects all body organs, and extrinsic aging caused by environmental factors. Intrinsic or natural mechanisms play a role in the way an individual ages, and both intrinsic and extrinsic mechanisms share molecular pathways. In this study, we investigated the signal pathway of ROS generation with a focus on the mechanisms of skin aging.

ROS, byproducts of normal cellular oxidative processes, increase as cellular senescence progresses [22, 23] and have been shown to contribute to cellular senescence [24]. ROS primarily arise from oxidative cell metabolism and play a major role in both chronological aging and photoaging [20]. However, it remains unclear what earlier events lead to increased ROS during the skin aging. Skin cells in the human body have a limited replication potential *in vivo*. This is reflected by the finite replicative lifespan *in vitro* termed "replicative cellular senescence," which has been proposed as an experimental model for human aging [18]. We created an *in vitro* skin aging model by replicative subculture of HDFs. We analyzed whether ROS would change during extended passaging of HDFs (Figure 1). Interestingly, the increased ROS in replicative aged HDFs was not extinguished by treatment with rotenone, an inhibitor of mitochondrial electron transfer. The ROS increase in replicative aged skin cells was inhibited by diphenyleneiodonium and apocynin, inhibitors of NADPH oxidase. Allopurinol, an inhibitor of xanthine oxidase also had no effect on aging-induced ROS. It is likely that the major source of ROS in replicative aged skin cells is not mitochondria but NADPH oxidase. These findings are further supported by data suggesting that NADPH oxidase activity was elevated in replicative aged HDFs.

NADPH oxidases (NOX) have been thought to generate superoxide at the plasma membrane and release it into the extracellular space where it is converted into hydrogen peroxide. The biological function of NOX enzymes is the generation of ROS [7, 8]. Recent studies indicate that NADPH oxidase family members are found in a wide array of tissues [9]. ROS produced by the NOX proteins Nox1–5 and Duox1/2 play essential roles in the physiology of the brain, the immune system, the vasculature, and the digestive

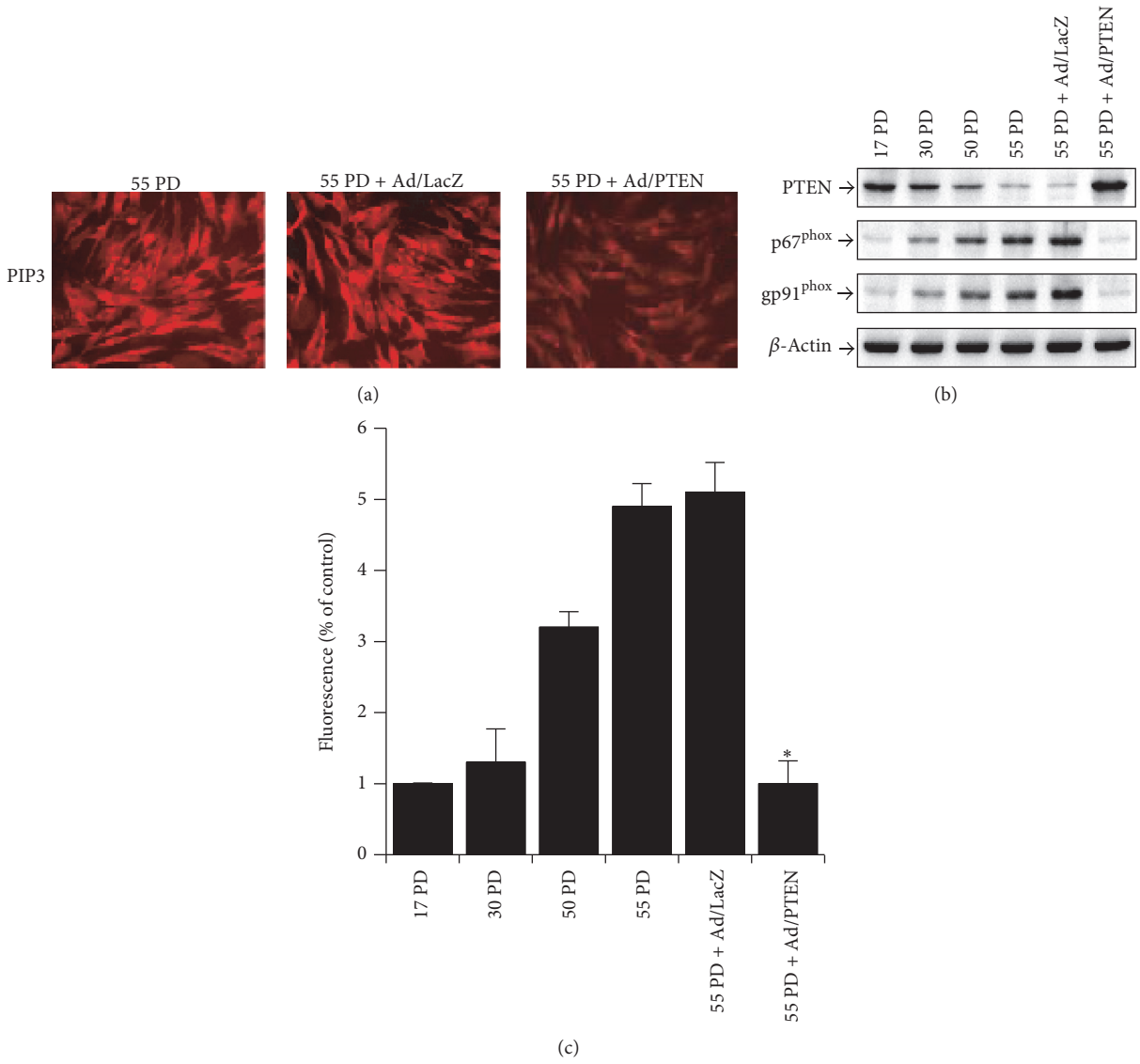

Figure 4: ROS generation in replicative aged HDFs is induced by the activation of PI3K signaling through aging-induced downregulation of PTEN and activation of PI3K/PKC. (a) The inhibition of aging-induced increases in PIP3 levels by PTEN gene transfer. Replicative aged HDFs (55 PD) were cultured in standard medium and infected with Ad/LacZ and Ad/PTEN. After 48 h, the cells were fixed with 4% paraformaldehyde, incubated with anti-PIP3 antibody, and stained with TRITC-labeled anti-mouse IgM antibody. Images were acquired with an Axiovert S100 fluorescence microscope (Zeiss, Germany) equipped with a DP70 digital camera (Olympus, Japan). (b) Inhibition of $p91^{phox}$ and $p67^{phox}$ expression by PTEN gene transfer. Replicative aged HDFs (55 PD) were cultured in standard medium and infected with Ad/LacZ or Ad/PTEN. After 48 h, the cells were lysed and blotted with antibody for PTEN, $gp91^{phox}$, $p67^{phox}$, and β-actin. (c) Inhibition of ROS generation by PTEN gene transfer. Replicative aged HDFs (55 PD) were cultured under standard medium and infected with vector alone (Ad/LacZ) or PTEN viral vector (Ad/PTEN). After 48 h, ROS was measured by flow cytometry using DCF-DA. Error bars, SD; $n = 5$ in each group. $^{*}P < 0.005$, compared with 55 PD.

tract as well as in hormone synthesis. In particular, NADPH oxidase-2 is a key regulator of human dermal fibroblasts [25]. We confirmed that expression of NOXs in aged HDFs was increased (Supplementary Figure 5). NADPH oxidase is a multicomponent enzyme; the classical phagocytic NADPH oxidase is composed of membrane-bound subunits $p22^{phox}$ and $gp91^{phox}$ (also referred to as NOX2) as well as cytosolic subunits, including $p67^{phox}$ and $p47^{phox}$ [8, 26]. In our results, we confirmed that the expression of $p67^{phox}$ and $gp91^{phox}$ increased during the extended passaging of HDFs (Figure 1). These results indicate that the elevation of ROS levels in replicative aged HDFs is induced by an increase in NADPH oxidase-2 protein expression.

PKCζ was originally discovered as a unique PKC isotype. It is classified into the atypical PKC (aPKC) subfamily [27]. PKCζ is also activated by lipid components, such as phosphatidylinositols (PIs), phosphatidic acid, arachidonic acid, and ceramide. Among these lipids, PIP3 has been the focus of much interest with regard to its regulation of aPKCs

in various cells. aPKCs can be regulated by PI3K, which produces PIP3 from PIP2 [28].

NADPH oxidase is closely linked with PI3K signaling [10, 11]. PKCζ, a downstream molecule of PI3K, is essential for superoxide generation by NADPH oxidase [10, 12]. Thus, we tested the effect of PI3K and PKC inhibitors on aging-induced increase of ROS generation, NADPH oxidase activity and protein expression (Figure 2). In addition, we confirmed that PKC inhibitor inhibits NADPH oxidase activity in a time-dependent manner in replicative aged HDFs (Supplementary Figure 6). From our results, we conclude that activation of the PI3K/Akt pathway induces phosphorylation of PKCζ, leads to enhance of NADPH oxidase expression and activity, and thereby results in increased ROS generation.

To determine what activates the PI3K-Akt pathway, we first tested whether the protein levels of PI3K increased as HDFs aged. Contrary to our expectations, the protein levels of the PI3K p85 subunit showed a slight decrease in replicative aged HDFs (Figure 3(a)). PI3K signaling can be affected by PTEN since PIP3 levels are controlled directly by a balance of activities between the PI3K, the synthetic enzyme of PIP3, and PTEN, its degradative enzyme [18, 19]. We found that, as the cells aged, the protein levels of PTEN were much more reduced than those of PI3K. These data suggest that the imbalance between PI3K and PTEN levels induces modulation of PIP3 metabolism, which results in the activation of the PI3K-Akt pathway. To confirm this, we measured intracellular PIP3 levels in HDFs of various ages and found that intracellular levels of PIP3 increased with increasing passage of HDFs. These results indicate that the elevation of PIP3 levels in replicative aged HDFs is induced by a decrease in PIP3 breakdown through greater downregulation of PTEN than of PI3K.

PTEN downregulation might be an initiation step of the signal pathway leading to ROS production. To confirm this, we examined whether the signal pathway could be stopped by restoring PTEN levels in replicative aged HDFs to the level of young HDFs. We infected replicative aged HDFs with adenovirus containing the PTEN gene (Ad/PTEN) or adenovirus containing the lacZ gene (Ad/LacZ). PTEN overexpression in replicative aged HDFs by the PTEN gene abolished the aging-induced increase in PIP3 concentration, NADPH oxidase-2 related protein expression, and consequent aging-induced ROS generation (Figure 4). These data indicate that the signal pathway for ROS generation in replicative aged HDFs can be stimulated by reduced PTEN levels. Taking that report and our results together, enhanced ROS production might further activate the PI3K/Akt pathway by PTEN inactivation, thus establishing a self-perpetuating cycle leading to further aging.

In conclusion, we demonstrated that PTEN downregulation and resultant activation of PI3K signaling caused PKC activation, which in turn increased ROS production through NADPH oxidase protein expression and activity modulation. Thus, our results provide novel evidence that ROS in replicative aged HDFs might be produced by aging-induced modifications of related cellular signal pathways. We also demonstrated that PTEN downregulation initiates the signal pathway leading to ROS generation in the progress of replicative skin aging.

Competing Interests

The authors do not have any conflict of interests to disclose.

Authors' Contributions

Eun-Mi Noh, and Jinny Park contributed equally to this work.

Acknowledgments

This work was supported by a National Research Foundation of Korea [NRF] grant funded by the Korean government [MEST] [no. 2011-0030130] and [MSIP] [no. 2016R1CB1014413].

References

[1] J. Campisi, "Aging, cellular senescence, and cancer," *Annual Review of Physiology*, vol. 75, pp. 685–705, 2013.

[2] L. Hayflick, "The limited in vitro lifetime of human diploid cell strains," *Experimental Cell Research*, vol. 37, no. 3, pp. 614–636, 1965.

[3] Q. M. Chen, K. R. Prowse, V. C. Tu, S. Purdom, and M. H. K. Linskens, "Uncoupling the senescent phenotype from telomere shortening in hydrogen peroxide-treated fibroblasts," *Experimental Cell Research*, vol. 265, no. 2, pp. 294–303, 2001.

[4] G. J. Fisher, S. Kang, J. Varani et al., "Mechanisms of photoaging and chronological skin aging," *Archives of Dermatology*, vol. 138, no. 11, pp. 1462–1470, 2002.

[5] E. Makrantonaki and C. C. Zouboulis, "William J. Cunliffe Scientific Awards. Characteristics and pathomechanisms of endogenously aged skin," *Dermatology*, vol. 214, no. 4, pp. 352–360, 2007.

[6] J. H. Chung, S. Kang, J. Varani, J. Lin, G. J. Fisher, and J. J. Voorhees, "Decreased extracellular-signal-regulated kinase and increased stress-activated MAP kinase activities in aged human skin in vivo," *Journal of Investigative Dermatology*, vol. 115, no. 2, pp. 177–182, 2000.

[7] F. Jiang, Y. Zhang, and G. J. Dusting, "NADPH oxidase-mediated redox signaling: roles in cellular stress response, stress tolerance, and tissue repair," *Pharmacological Reviews*, vol. 63, no. 1, pp. 218–242, 2011.

[8] K. Bedard and K.-H. Krause, "The NOX family of ROS-generating NADPH oxidases: physiology and pathophysiology," *Physiological Reviews*, vol. 87, no. 1, pp. 245–313, 2007.

[9] J. D. Lambeth, "NOX enzymes and the biology of reactive oxygen," *Nature Reviews Immunology*, vol. 4, no. 3, pp. 181–189, 2004.

[10] N. G. Shenoy, G. J. Gleich, and L. L. Thomas, "Eosinophil major basic protein stimulates neutrophil superoxide production by a class IA phosphoinositide 3-kinase and protein kinase C-ζ-dependent pathway," *The Journal of Immunology*, vol. 171, no. 7, pp. 3734–3741, 2003.

[11] Y. S. Bae, J.-Y. Sung, O.-S. Kim et al., "Platelet-derived growth factor-induced H_2O_2 production requires the activation of phosphatidylinositol 3-kinase," *The Journal of Biological Chemistry*, vol. 275, no. 14, pp. 10527–10531, 2000.

[12] P. M.-C. Dang, A. Fontayne, J. Hakim, J. El Benna, and A. Périanin, "Protein kinase C ζ phosphorylates a subset of selective sites of the NADPH oxidase component p47phox and

participates in formyl peptide-mediated neutrophil respiratory burst," *The Journal of Immunology*, vol. 166, no. 2, pp. 1206–1213, 2001.

[13] D. Haas-Kogan, N. Shalev, M. Wong, G. Mills, G. Yount, and D. Stokoe, "Protein kinase B (PKB/Akt) activity is elevated in glioblastoma cells due to mutation of the tumor suppressor PTEN/MMAC," *Current Biology*, vol. 8, no. 21, pp. 1195–1198, 1998.

[14] T. Maehama and J. E. Dixon, "The tumor suppressor, PTEN/MMAC1, dephosphorylates the lipid second messenger, phosphatidylinositol 3,4,5-trisphosphate," *The Journal of Biological Chemistry*, vol. 273, no. 22, pp. 13375–13378, 1998.

[15] S. Ramachandran, N. Rajendra Prasad, and S. Karthikeyan, "Sesamol inhibits UVB-induced ROS generation and subsequent oxidative damage in cultured human skin dermal fibroblasts," *Archives of Dermatological Research*, vol. 302, no. 10, pp. 733–744, 2010.

[16] M. M. Tarpey and I. Fridovich, "Methods of detection of vascular reactive species: nitric oxide, superoxide, hydrogen peroxide, and peroxynitrite," *Circulation Research*, vol. 89, no. 3, pp. 224–236.

[17] K. D. Niswender, B. Gallis, J. E. Blevins, M. A. Corson, M. W. Schwartz, and D. G. Baskin, "Immunocytochemical detection of phosphatidylinositol 3-kinase activation by insulin and leptin," *Journal of Histochemistry and Cytochemistry*, vol. 51, no. 3, pp. 275–283, 2003.

[18] M. P. Myers, I. Pass, I. H. Batty et al., "The lipid phosphatase activity of PTEN is critical for its tumor supressor function," *Proceedings of the National Academy of Sciences of the United States of America*, vol. 95, no. 23, pp. 13513–13518, 1998.

[19] K. Kurose, X.-P. Zhou, T. Araki, S. A. Cannistra, E. R. Maher, and C. Eng, "Frequent loss of PTEN expression is linked to elevated phosphorylated Akt levels, but not associated with p27 and cyclin D1 expression, in primary epithelial ovarian carcinomas," *The American Journal of Pathology*, vol. 158, no. 6, pp. 2097–2106, 2001.

[20] E. Kohl, J. Steinbauer, M. Landthaler, and R.-M. Szeimies, "Skin ageing," *Journal of the European Academy of Dermatology and Venereology*, vol. 25, no. 8, pp. 873–884, 2011.

[21] G. Jenkins, "Molecular mechanisms of skin ageing," *Mechanisms of Ageing and Development*, vol. 123, no. 7, pp. 801–810, 2002.

[22] E. Hütter, H. Unterluggauer, F. Überall, H. Schramek, and P. Jansen-Dürr, "Replicative senescence of human fibroblasts: the role of Ras-dependent signaling and oxidative stress," *Experimental Gerontology*, vol. 37, no. 10-11, pp. 1165–1174, 2002.

[23] H. T. Kang, H. I. Lee, and E. S. Hwang, "Nicotinamide extends replicative lifespan of human cells," *Aging Cell*, vol. 5, no. 5, pp. 423–436, 2006.

[24] Q. Chen, A. Fischer, J. D. Reagan, L.-J. Yan, and B. N. Ames, "Oxidative DNA damage and senescence of human diploid fibroblast cells," *Proceedings of the National Academy of Sciences of the United States of America*, vol. 92, no. 10, pp. 4337–4341, 1995.

[25] G.-Y. Zhang, L.-C. Wu, T. Dai et al., "NADPH oxidase-2 is a key regulator of human dermal fibroblasts: a potential therapeutic strategy for the treatment of skin fibrosis," *Experimental Dermatology*, vol. 23, no. 9, pp. 639–644, 2014.

[26] B. M. Babior, "NADPH oxidase: an update," *Blood*, vol. 93, no. 5, pp. 1464–1476, 1999.

[27] Y. Ono, T. Fujii, K. Ogita, U. Kikkawa, K. Igarashi, and Y. Nishizuka, "Protein kinase C ζ subspecies from rat brain: its structure, expression, and properties," *Proceedings of the National Academy of Sciences of the United States of America*, vol. 86, no. 9, pp. 3099–3103, 1989.

[28] T. Hirai and K. Chida, "Protein kinase Cζ (PKCζ): activation mechanisms and cellular functions," *The Journal of Biochemistry*, vol. 133, no. 1, pp. 1–7, 2003.

Hindawi Publishing Corporation
Oxidative Medicine and Cellular Longevity
Volume 2016, Article ID 7570489, 13 pages
http://dx.doi.org/10.1155/2016/7570489

Research Article

Protective Effects of Hydrogen Sulfide in the Ageing Kidney

Cui-Lan Hou, Ming-Jie Wang, Chen Sun, Yong Huang, Sheng Jin, Xue-Pan Mu, Ying Chen, and Yi-Chun Zhu

Research Center on Aging and Medicine, Fudan University, Shanghai Key Laboratory of Bioactive Small Molecules, Department of Physiology and Pathophysiology, Shanghai Medical College, Fudan University, Shanghai, China

Correspondence should be addressed to Yi-Chun Zhu; yczhu@shmu.edu.cn

Received 4 June 2016; Revised 22 September 2016; Accepted 3 October 2016

Academic Editor: Claudio Cabello-Verrugio

Aims. The study aimed to examine whether hydrogen sulfide (H_2S) generation changed in the kidney of the ageing mouse and its relationship with impaired kidney function. *Results*. H_2S levels in the plasma, urine, and kidney decreased significantly in ageing mice. The expression of two known H_2S-producing enzymes in kidney, cystathionine γ-lyase (CSE) and cystathionine-β-synthase (CBS), decreased significantly during ageing. Chronic H_2S donor (NaHS, 50 μmol/kg/day, 10 weeks) treatment could alleviate oxidative stress levels and renal tubular interstitial collagen deposition. These protective effects may relate to transcription factor Nrf2 activation and antioxidant proteins such as HO-1, SIRT1, SOD1, and SOD2 expression upregulation in the ageing kidney after NaHS treatment. Furthermore, the expression of H_2S-producing enzymes changed with exogenous H_2S administration and contributed to elevated H_2S levels in the ageing kidney. *Conclusions*. Endogenous hydrogen sulfide production in the ageing kidney is insufficient. Exogenous H_2S can partially rescue ageing-related kidney dysfunction by reducing oxidative stress, decreasing collagen deposition, and enhancing Nrf2 nuclear translocation. Recovery of endogenous hydrogen sulfide production may also contribute to the beneficial effects of NaHS treatment.

1. Introduction

Population ageing is a global phenomenon and exerts heavy demands on the healthcare system and society. The aged population, 65 years or older, will reach 1 billion people, accounting for 13% of the total worldwide population in 2030 [1]. Ageing is a natural process accompanied by gradual declining in physiological functions. Impaired renal function in ageing people is of great clinical relevance and usually associates with cardiovascular diseases and even mortality. The characteristics of the ageing kidney include nephrosclerosis, nephron hypertrophy, cortical volume reduction, and cyst formation [2]. On the other hand, the high frequency of underlying diseases among ageing people, such as concurrent diabetes, complicates the treatment of nephropathy. Therefore, understanding the process of kidney ageing might help to improve the quality of life of the ageing population and to provide precise treatment for senile nephropathy.

Hydrogen sulfide (H_2S) is a gasotransmitter generated endogenously by cystathionine-γ-lyase (CSE), cystathionine-β-synthase (CBS), and 3-mercaptopyruvate sulfurtransferase (3-MST). H_2S has diverse physiological functions such as relaxing blood vessels, lowering blood pressure [3, 4], anti-apoptosis [5], anti-inflammation [6], and antioxidative stress [7]. In recent years, emerging studies have focused on the possibility of life span elongation by H_2S. Miller and Roth firstly reported the regulatory role of H_2S (50 ppm) in *C. elegans* ageing [8], and Wei and Kenyon recently confirmed this effect [9].

The beneficial effects of H_2S on lifespan elongation involve both direct and indirect mechanisms. Some key regulatory molecules, such as Sirtuins [8] and Klotho [10], contribute to the direct effects of H_2S, whereas the antioxidative nature of H_2S protects the ageing heart or brain indirectly [11, 12]. Organ-specific mechanisms are of great clinical value for treating ageing-related diseases as well as pursuing healthy ageing. Our previous study showed that heart H_2S levels in long-term fructose-fed ageing mice decreased from 0.020 μmol/g protein to 0.013 μmol/g protein, which may play some roles in the pathogenesis of diabetic cardiomyopathy [13]. The aim of this study was to investigate the endogenous production of H_2S in the ageing kidney and the effect of

chronic H_2S supplements in protecting the kidney from ageing-related damage.

2. Materials and Methods

2.1. Animals and NaHS Administration. Eight-week-old male C57BL/6 mice were purchased from Department of Laboratory Animal Science of Fudan University and raised under controlled conditions (22 ± 2°C, 45–55% relative humidity, and 12 h dark-light cycle), with unrestricted access to diet and water until 16 months of age (old group). Another group of 8-week-old male C57BL/6 mice were purchased and raised until 3 months of age (young control group). We further divided the old mice into four groups: old control with normal saline, old with low-dose NaHS (10 μmol/kg/day), old with medium-dose NaHS (50 μmol/kg/day), and old with high-dose NaHS (100 μmol/kg/day). The treatment, which consisted of intraperitoneal injection of NaHS or normal saline once a day, lasted for 10 weeks. All animal studies were approved by the Ethics Committee of Experimental Research, Fudan University Shanghai Medical College.

2.2. Metabolism and Biochemical Analyses. Mice were placed in metabolic cages (Tecniplast, Italy) separately for metabolism evaluation. After 3 days' acclimation, 24-hour water and food intake were measured and urine was collected. Glucose strips (OneTouch, Johnson) were used to determine fasting plasma glucose with blood collected from the tail vein before euthanasia. Plasma was obtained by centrifuging a blood sample at 3000 rpm, 4°C for 15 minutes (min). Plasma levels of creatinine (Crea), blood urea nitrogen (BUN), total cholesterol (CHOL), triglycerides (TG), low-density lipoprotein cholesterol (LDL-C), and high-density lipoprotein cholesterol (HDL-C) were determined by automatic biochemical analyser (Cobas 6000, Roche, Basel, Switzerland).

2.3. Detection of Reactive Oxygen Species (ROS) Levels. ROS levels in the kidney were measured using dihydroethidium (DHE) staining (Sigma-Aldrich) [14]. Briefly, DHE powder was dissolved in dimethyl sulfoxide and further diluted with phosphate-buffered saline (PBS) at 55°C until fully dissolution. Mice were injected with DHE solution (100 μL, 27 mg/kg) maintained at 37–40°C and reinjected after 30 min. Eighteen hours later, mice were anesthetized and the kidney tissues were embedded in optimum cutting temperature compound (OCT). Mice kidney tissue sections (7 μm) were obtained by using a frozen tissue slicer and observed under a laser confocal microscope (Zeiss LSM710) at the wavelength of 488/610 nm. Florescence values were normalized to the old groups.

2.4. Morphological and Histological Analyses. The kidney tissues were excised, fixed in 10% formalin, and embedded in paraffin. Kidney sections (4 μm) were stained with Masson's, hematoxylin and eosin (HE), and TUNEL stain, according to the manufacturer's instructions. Renal pathological changes were observed under an optical microscope. Apoptosis was determined through TUNEL staining.

2.5. Measurement of H_2S Levels and the Activity of H_2S-Producing Enzymes. H_2S levels in plasma, urine, and kidney tissues were determined as previously described [15]. The activity of CSE/CBS in the kidney tissues was measured by the method described by Tao et al. [16]. Briefly, 260 μL homogenized kidney tissues were incubated together with 20 μL L-cysteine (10 mmol/L) and 20 μL pyridoxal-5′ phosphate (2 mmol/L) in an EP tube for 30 min at 37°C. Then 30 μL supernatant obtained after centrifugation (10 min at 12000 rpm) was incubated with 80 μL monobromobimane (MBB) for 40 min on a shaker at room temperature. Reaction was terminated by adding 20% formic acid and tested by gas chromatography-mass spectrometry (GC-MS). It should be borne in mind that this method can only test the overall activity of CSE and CBS because they share the same substrates.

2.6. Enzymatic Activity Assay. SIRT1 activity was determined by using the SIRT1 Fluorometric Drug Discovery Kit (BML-AK555-0001, Enzo) according to the manufacturer's protocol [17]. Briefly, for cell-free measurement of the reaction between H_2S and recombinant SIRT1, 10 μL SIRT1 protein (0.25 U) and 5 μL NaHS (0, 12.5, 25, 50, and 100 μmol/L) were incubated with 5 μL substrate (0.25 mmol/L) and 5 μL NAD (0.25 mmol/L) plus 25 μL assay buffer. For tissue SIRT1 activity measurement, the reaction system contains 10 μL kidney tissue homogenate, 5 μL substrate (0.25 mmol/L), and 5 μL NAD (0.25 mmol/L) plus 30 μL assay buffer. Both reactions were carried out at 37°C for 40 min and stopped by addition of 1x Fluor de Lys® Developer II plus nicotinamide (50 μL per well) (every 1 mL stop solution contains 760 μL assay buffer, 40 μL 50 mmol/L nicotinamide, and 200 μL 5x Developer II). Fifteen mins later, fluorescence values were measured on a fluorometric reader (Synergy™ Mx, USA) with excitation at 360 nm and emission at 460 nm.

2.7. Western Blot Analysis. The kidney cytoplasm nuclear proteins were collected under the kit protocol (Nuclear and Cytoplasmic Protein Extraction Kit, Beyotime Biotechnology, Nanjing) and quantified using a BCA reagent (Shen Neng Bo Cai Corp, Shanghai). The proteins were resolved on a sodium dodecyl sulfate 10% polyacrylamide gel and transferred onto polyvinylidene fluoride membrane (Millipore, Bedford, MA, USA) and incubated with primary antibodies (1 : 1000 dilution) against Bcl-2, Bax, CSE, CBS, 3-MST, SIRT1 (Santa Cruz, CA, USA), Collagen I (Col I), Collagen III (Col III), Fibronectin (FN), SOD1, SOD2 (Abcam Company, USA), or Nrf2, HO-1 (Proteintech, China) at 4°C overnight. The blots were washed with phosphate buffer saline (TBST) for three times and then incubated with horseradish peroxidase-conjugated secondary antibodies for another 1 hour at room temperature. After washing, the blots were visualized by using chemiluminescent substrate (ECL). The densities of immunoblot bands were analysed using a scanning densitometer (model GS-800, Bio-Rad Laboratories, Hercules, CA, USA) coupled with Bio-Rad personal computer analysis software.

2.8. Statistical Analysis. Results are expressed as mean ± SEM. Statistical analysis was performed using SPSS software,

Table 1: Results are means ± SE. Old groups were treated with a variety of NaHS (0, 10, 50, and 100 μmol/kg/day) treatments for 10 weeks. $^{*}P < 0.05$ and $^{**}P < 0.01$ compared with old control (young group, $N = 14$; old groups, $N = 18$).

	Old	Young	Old-10	Old-50	Old-100
Body weights (bw) (g)	29.26 ± 3.03	20.88 ± 02.30**	2939 ± 0.46	27.37 ± 1.7	27.17 ± 2.69
Fasting plasma glucose (mmol/L)	3.8429 ± 0.4315	3.9143 ± 0.4140	3.9600 ± 0.5771	3.8833 ± 0.5419	4.1200 ± 0.5762
Heart mass/bw	0.0052 ± 0.0003	0.0058 ± 0.0008	0.0062 ± 0.0008**	0.0061 ± 0.0008**	0.0058 ± 0.0007**
Liver mass/bw	0.0446 ± 0.0041	0.0464 ± 0.0046	0.0465 ± 0.0037	0.0457 ± 0.0017	0.0454 ± 0.0024
Left kidney mass/bw	0.0064 ± 0.0007	0.0066 ± 0.0011	0.0067 ± 0.0007	0.0072 ± 0.0003**	0.0073 ± 0.0004**
Right kidney mass/bw	0.0065 ± 0.0007	0.0059 ± 0.0016	0.0069 ± 0.0008	0.0074 ± 0.0004**	0.0073 ± 0.0004*

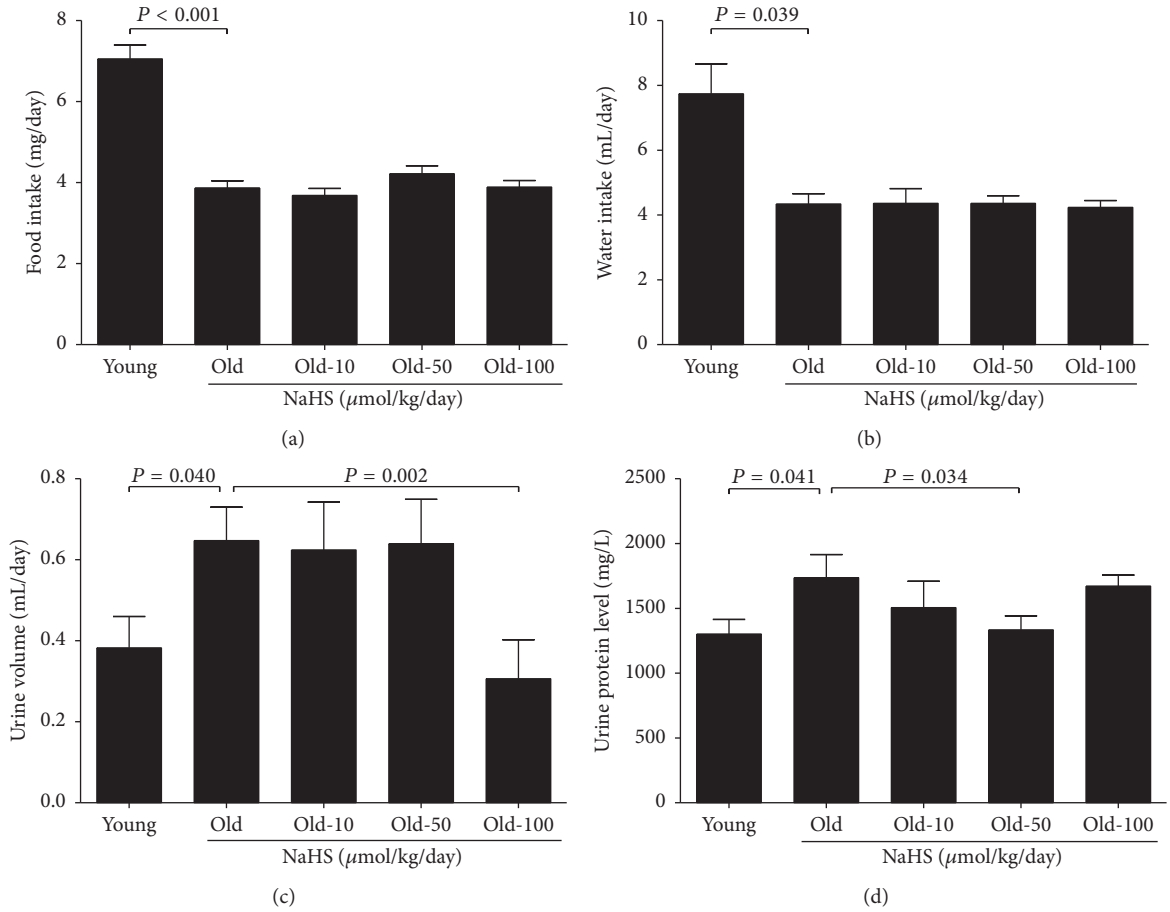

Figure 1: Twenty-four-hour metabolic characteristics of young and old mice. The old groups were treated with different doses of NaHS or saline as the control for 10 weeks. (a) Food intake. (b) Water intake. (c) Urine volume. (d) The level of urinary protein. Values are mean ± SE. $P < 0.05$ was considered significant (young groups, $N = 12$; old groups, $N = 14$).

version 21.0 (SPSS, Inc., Chicago, IL, USA). Comparisons among groups were performed by one-way ANOVA. Paired data were evaluated by two-tailed Student's t-test. Statistical significance was considered when $P < 0.05$.

3. Results

3.1. Hydrogen Sulfide Donor NaHS Has a Protective Effect in Ageing Mice Metabolism. There was no significant difference in fasting blood-glucose between the young and old groups, and NaHS (10, 50, and 100 μmol/kg/day) treatment changed neither the fasting blood-glucose nor the body weight among old groups (Table 1). Compared with young mice, food and water intake were decreased whereas the urine volume increased in old control mice. Chronic NaHS treatment for 10 weeks did not change the food and water intake (Figures 1(a) and 1(b)) but could decrease the 24-hour urine volume and the contents of urine protein (Figures 1(c) and 1(d)). The maximum effect of NaHS in decreased urine volume was achieved in the 100 μmol/kg/day NaHS treatment group, whereas the 50 μmol/kg/day NaHS treatment group decreased urine protein contents the most (Figures 1(c) and 1(d)). The blood level of Crea and LDL-C did not change (Figures 2(a) and 2(e)), whereas the contents of BUN, CHOL,

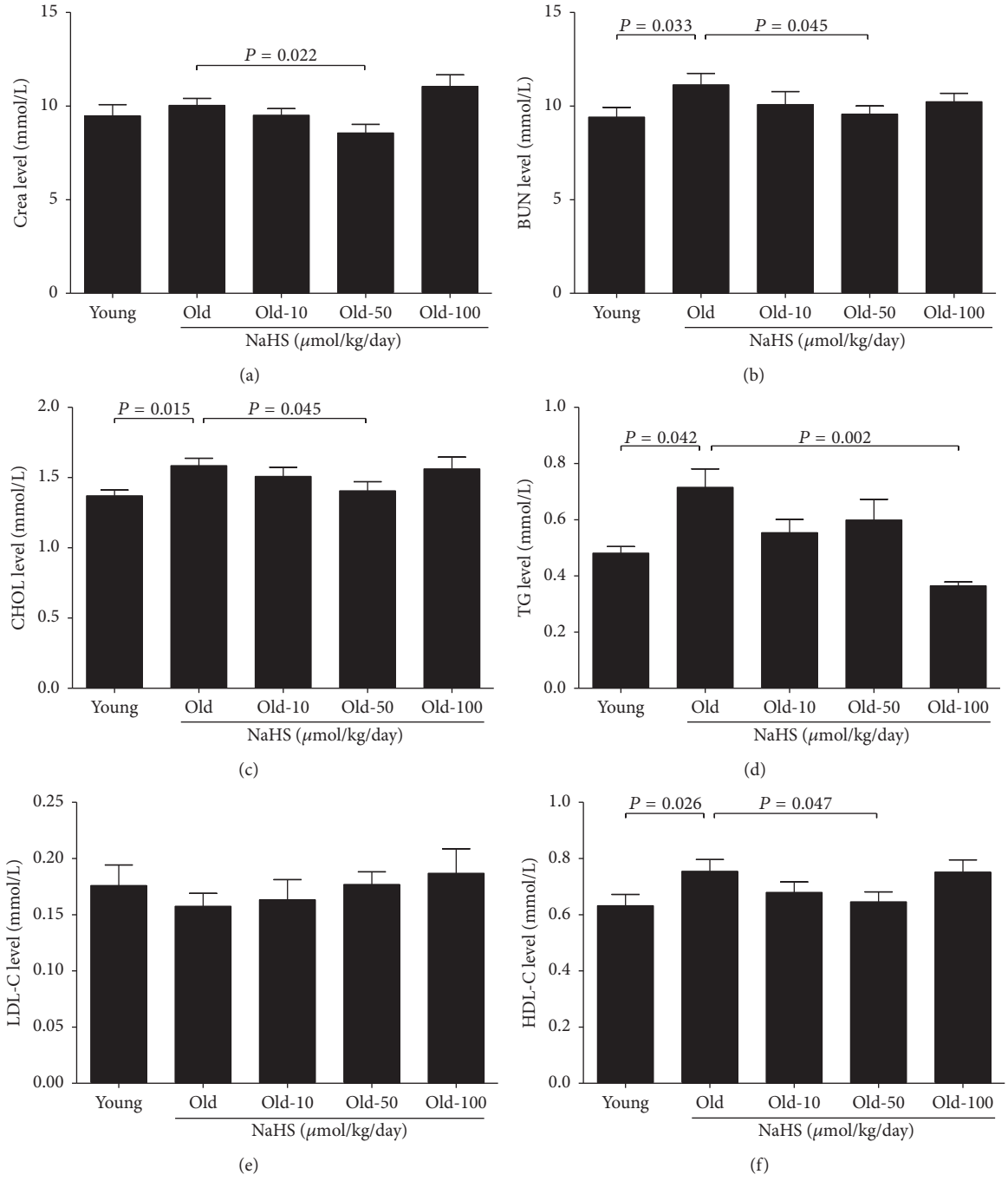

Figure 2: Blood biochemical results for young and old mice. (a) Crea: creatinine. (b) BUN: blood urea nitrogen. (c) CHOL: total cholesterol. (d) TG: triglycerides. (e) LDL-C: low-density lipoprotein. (f) HDL-C: high-density lipoprotein. Values are mean ± SE. $P < 0.05$ was considered significant (young groups, $N = 12$; old groups, $N = 14$).

TG, and HDL-C increased dramatically in old control mice compared with young mice (Figures 2(b), 2(c), 2(d), and 2(f)). Ten weeks of 50 μmol/kg/day NaHS treatment significantly alleviated the increase of Crea, BUN, CHOL, and HDL-C (Figures 2(a), 2(b), 2(c), and 2(f)), and 100 μmol/kg/day NaHS therapy decreased the TG contents (Figure 2(d)). Our results indicate that there is impaired kidney function during ageing, and exogenous H_2S treatment could partially reverse such impairment.

3.2. NaHS Alleviates the Level of Oxidative Stress in the Ageing Kidney. ROS levels in the kidney were examined after 10 weeks of NaHS therapy. DHE fluorescence intensity and malondialdehyde (MDA) levels were elevated significantly in the old control group compared with young mice, and chronic NaHS treatment could mitigate these changes (Figures 3(a), 3(b), and 3(c)). Accordingly, SOD activity and glutathione peroxidase (GPx) levels were decreased in old mice, and 50 μmol/kg/day NaHS treatment could partially rescue these

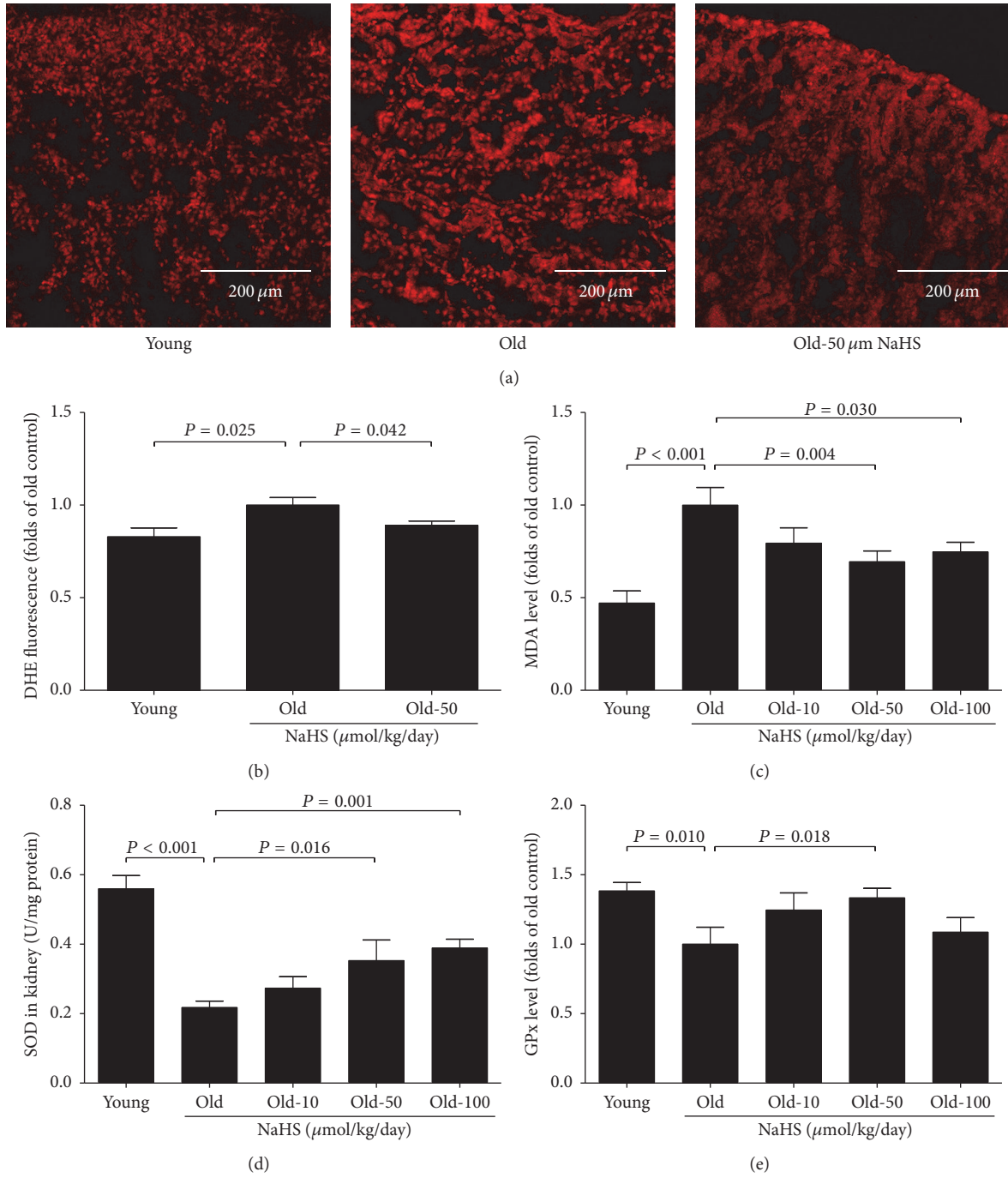

FIGURE 3: H_2S donor NaHS protected the ageing kidney from oxidative stress. ((a) and (b)) DHE staining and the DHE fluorescence in the kidney tissue. (c) Malondialdehyde (MDA) levels in the kidney. (d) Total SOD activity renal tissue. (e) Glutathione peroxidase (GPx) levels in the kidney. Values are mean ± SE. $P < 0.05$ was considered significant (young groups, $N = 6$; old groups, $N = 8$).

changes (Figures 3(d) and 3(e)). Our results indicated that the H_2S donor could protect the ageing kidney from oxidative stress.

3.3. Ageing Mice Exhibit Kidney Remodeling and Apoptosis and Chronic NaHS Treatment Mitigates These Processes. Masson staining showed significantly increased interstitial fibrosis compared with young groups, and 10 weeks of 50 μmol/kg/day NaHS treatment could partially reduce collagen deposition (Figures 4(a) and 4(b)). There was higher expression of Col III and FN in the ageing kidney, and this trend became less significant with chronic NaHS treatment (Figures 4(d) and 4(e)). Col I expression was also increased in the ageing kidney, but with no significant difference between the NaHS-treated and nontreated groups (Figure 4(c)). In addition, mRNA levels of Col I, Col III, and FN also increased

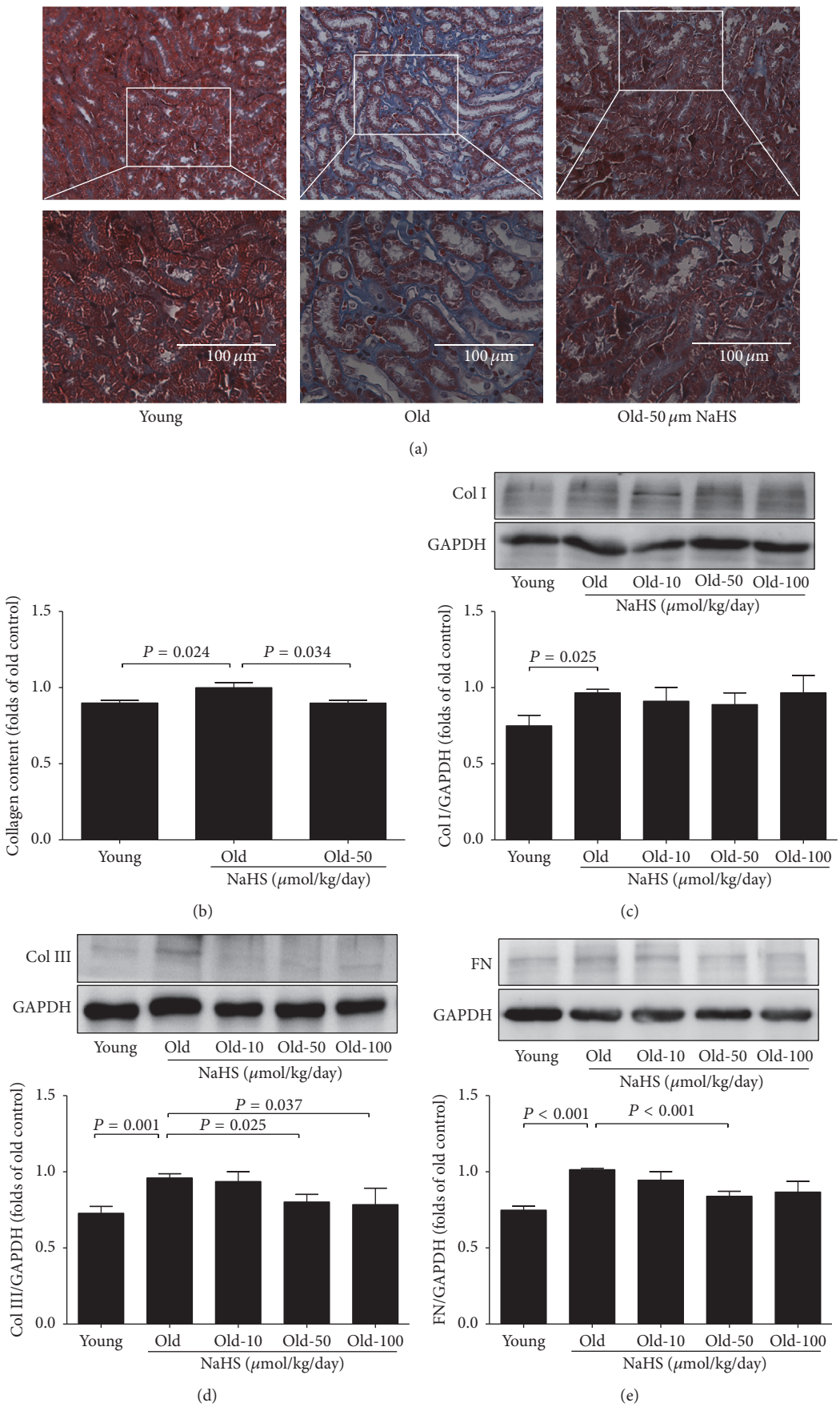

Figure 4: Renal pathological changes of ageing mice. ((a) and (b)) Masson staining of the kidney tissue. (c) Col I and (d) Col III expression in ageing mice ($N = 8$). (e) FN expression in ageing mice ($N = 10$). $P < 0.05$ was considered significant.

during ageing (Figure S1 in Supplementary Material available online at http://dx.doi.org/10.1155/2016/7570489).

The ageing kidney appeared to have a higher apoptosis level compared with that of the young group, evidenced by increased expression of proapoptotic Bax and decreased expression of antiapoptotic Bcl-2 (Figure 5(b)). TUNEL staining revealed the same changes (Figure 5(a)). HE staining showed tubular dilation and inflammatory infiltration among ageing mice, whereas chronic NaHS therapy could mitigate this damage (Figure 5(c)). Our results indicated that kidney remodeling and apoptosis had occurred in ageing mice, and chronic NaHS treatment could mitigate these processes.

3.4. Endogenous Hydrogen Sulfide Production Is Decreased in Ageing Mice; NaHS Treatment Alleviates the Reduction by Increasing the Expression and Activity of Hydrogen Sulfide-Producing Enzymes. Compared with young groups, ageing mice showed lower CSE and CBS expression, although 3-MST expression remained unchanged. Ten weeks of NaHS treatments (50 μmol/kg/day) significantly increased the expression of CSE and CBS, but not the 3-MST (Figures 6(a1), 6(a2), and 6(a3)). Plasma, urine, and kidney H_2S levels decreased significantly during ageing (Figures 6(b1), 6(b2), and 6(b3)), whereas 10 weeks of NaHS (50 μmol/kg/day) treatment alleviated the plasma and urine H_2S levels (Figures 6(b2) and 6(b3)). H_2S levels in ageing kidney tissues were also increased to some extent after NaHS treatment, but without statistical significance (Figure 6(b1)). CSE/CBS activity in the ageing kidney decreased, and 100 μmol/kg/day NaHS treatment diminished this reduction (Figure 6(c)).

3.5. NaHS Activates SIRT1 in the Ageing Kidney. To determine whether H_2S protects the ageing kidney through the SIRT1-mediated pathway, the protein and transcriptional levels of SIRT1 were examined. Both the protein expression and mRNA transcription of SIRT1 were decreased in ageing mice compared with young ones, and NaHS (50 μmol/kg/day) treatment could improve SIRT1 protein expression but not the mRNA levels (Figure 7(a)). SIRT1 is a deacetylase, and 10 weeks of NaHS treatment did not affect total deacetylase activity in the ageing kidney (Figure 7(b)), but 25 μmol/L NaHS could directly increase the activity of recombinant SIRT1 protein in vitro (Figure 7(c)). Measurement of SIRT1 activity in the ageing kidney will help to make clear whether chronic NaHS treatment selectively influences SIRT1 activity while total deacetylase activity remains the same.

3.6. Effects of Chronic NaHS Treatment on the Expression of Antioxidant-Related Proteins in the Ageing Kidney. The expression of antioxidant proteins in kidney tissue was examined by western blot analysis at the end of chronic NaHS treatment. Ten weeks of NaHS (50 μmol/kg/day) treatment could increase the Nrf2 expression and improve its downstream antioxidative proteins such as HO-1, SOD1, and SOD2 (Figure 8(a)). Moreover, compared with young groups, both the nuclear and cytosol Nrf2 levels were decreased, and NaHS (50 μmol/kg/day) treatment could selectively increase nuclear Nrf2 (Figure 8(b)). As shown in Figure S2A, the Nrf2 nuclear translation in the kidney tissue was insufficient. As shown in Figure S2B, Nrf2 translocation in the NRK-52E cells treated with NaHS (50 μmol/L) was significantly induced from cytosol to nucleus and peaked at 60 min. The translocation of Nrf2 from cytoplasm into nuclear may be one of the protective mechanisms of H_2S against ageing-related oxidative stress.

4. Discussion

In this study, we employed an ageing mouse model to investigate chronic NaHS treatment in the process of kidney senescence. Our work reveals two important findings: (1) lower plasma, urine, and kidney H_2S levels and reduction of kidney CSE and CBS expression and activity are accompanied with ageing; (2) exogenous administration of H_2S donor NaHS mitigates ageing-related kidney dysfunction, and the protective effect of NaHS may at least partially relate to improved endogenous H_2S production and its antioxidative nature.

During ageing, an elevated amount of ROS generated from glycolysis, specifically caused by the defects in the polyol pathway, uncoupling of nitric oxide synthase, xanthine oxidase, and advanced glycation, results in the progressive deterioration of renal function [18]. Emerging data suggest that ROS are related to the pathophysiology of glomerular dysfunction, interstitial fibrosis, and glomerulosclerosis [19, 20]. In streptozotocin-induced diabetic rats, H_2S therapy (14 μmol/kg/day) improved renal function and decreased glomerular basement thickening, mesangial expansion, and interstitial fibrosis [18]. Our previous study showed that chronic NaHS treatment (30, 60, and 120 μmol/kg/day) significantly reduced ROS levels in the kidney of GK rats [21]. Consistently, we found that chronic NaHS treatment could reduce ROS levels (50 μmol/kg/day) and MDA contents (50 and 100 μmol/kg/day) and increase GPx levels and SOD activity in the kidney of ageing mice. H_2S takes part in a great variety of physiological and pathophysiological processes because of its antiapoptotic, antioxidative, anti-inflammatory, and proangiogenic activities in mammals, and the reduction of endogenous H_2S levels has been related to various diseases. Zhou et al. reported that endogenous H_2S generation and CSE protein expression decreased significantly in the streptozotocin-induced diabetic rat model and that exogenous H_2S (14 μmol/kg/day) protected against diabetic nephropathy [18]. Our previous study also showed that chronic NaHS (30 μmol/kg/day) treatment might ameliorate diabetic complications of the kidney [21].

In this study, we confirmed intensified interstitial fibrosis in the ageing kidney and observed decreased accumulation of Col III (50 and 100 μmol/kg/day) and FN (at 50 μmol/kg/day) with exogenous NaHS. We also observed increased apoptosis in the ageing kidney, and chronic NaHS treatment could partially reverse this deterioration. Age-related kidney damage might reversely correlate with endogenous H_2S production. We found that both H_2S levels in the plasma, urine, and kidney and the kidney expression of CSE and CBS decreased significantly with ageing. As part of our body's antioxidative defense, an insufficient H_2S system may decrease the overall ability of ROS scavenging and render the kidney to be

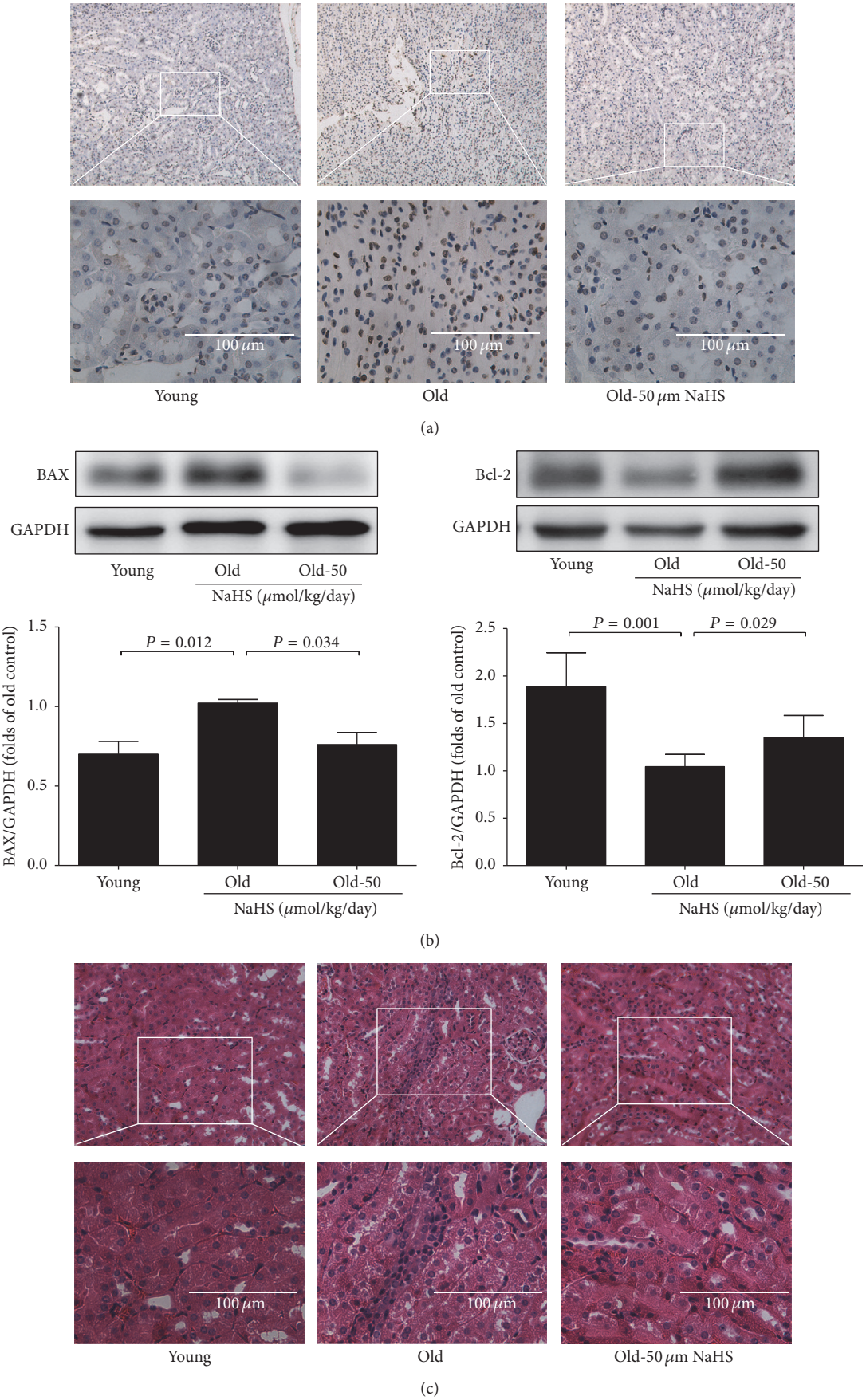

FIGURE 5: Renal pathological changes of ageing mice. (a) TUNEL staining of the kidney tissue. (b) Bax ($N = 6$) and Bcl-2 ($N = 7$) expression in ageing mice. (c) HE staining of the kidney tissue. Values are means ± SE. $P < 0.05$ was considered significant.

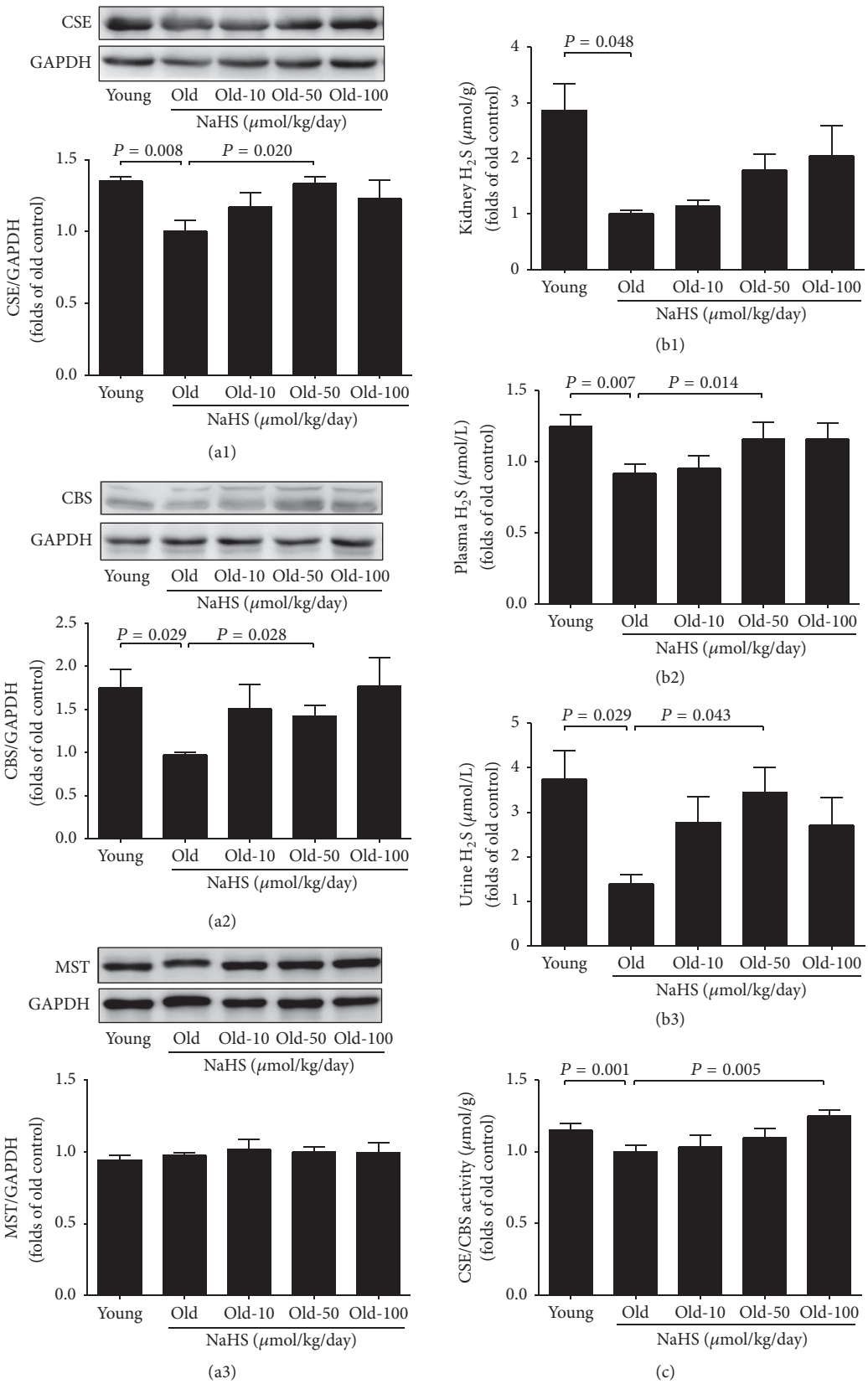

Figure 6: Exogenous H_2S alleviated ageing-related decreasing of H_2S production. (a1)–(a3) Kidney expression of CSE ($N = 11$) and CBS decreased significantly, whereas 3-MST kept constant during ageing ($N = 10$). (b1)–(b3) Plasma, urine, and kidney tissue H_2S levels decreased significantly during ageing and rose again after chronic NaHS treatment. (c) The activity of CSE/CBS in the ageing kidney declined, whereas 100 μmol/kg/day NaHS treatment could mitigate the reduction. Values are means ± SE. $P < 0.05$ was considered significant ($N = 12$).

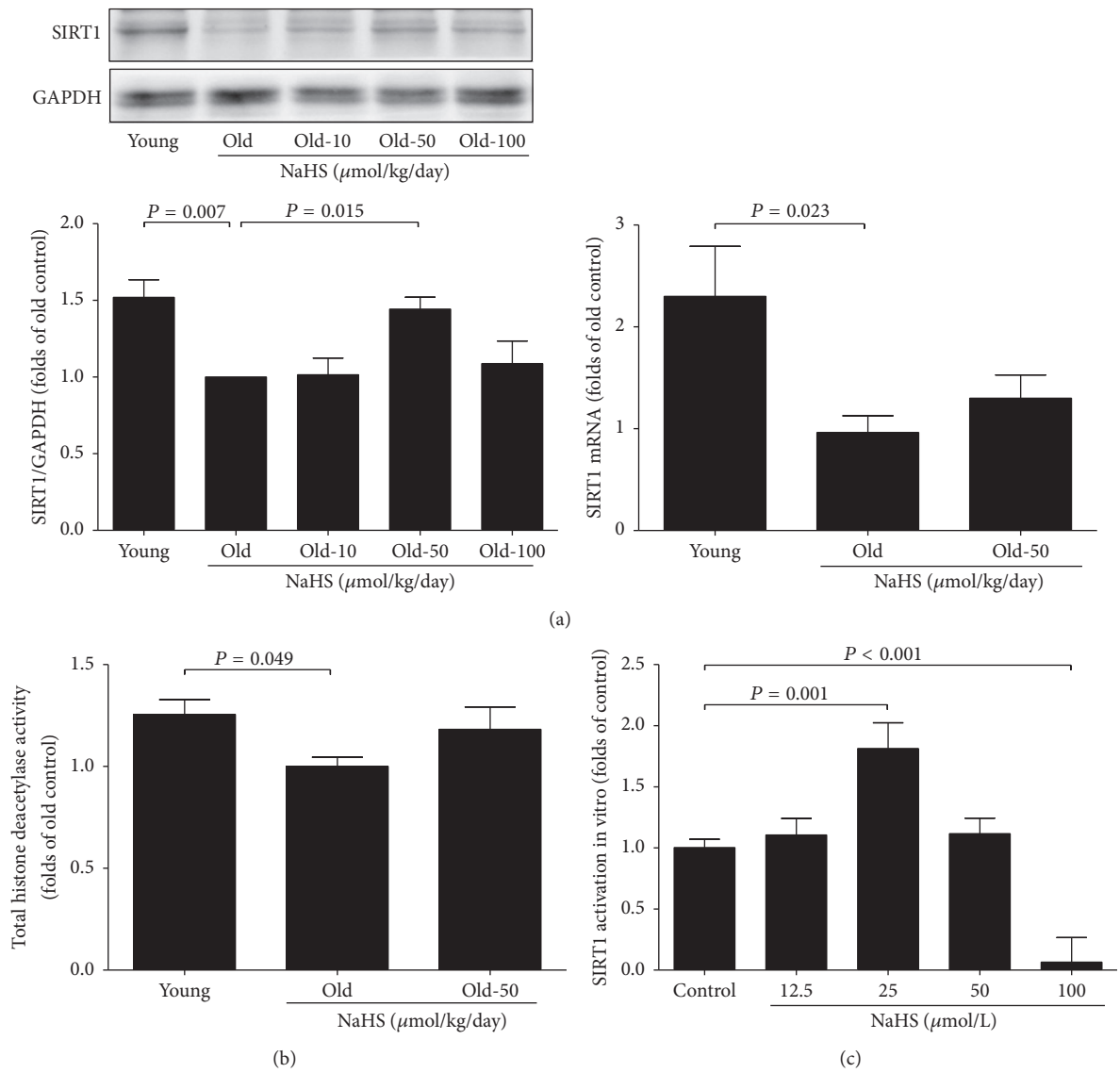

Figure 7: SIRT1 was involved in NaHS-mediated ageing kidney protection. (a) SIRT1 protein and mRNA expressions in the kidney after chronic NaHS treatment for 10 weeks ($N = 8$). (b) Total deacetylase activity exchangeable in the kidney ($N = 10$). (c) NaHS-activated recombinant protein SIRT1 activity in vitro ($N = 10$). Values are mean ± SE. $P < 0.05$ was considered significant.

under oxidative stress. Reasonably, chronic NaHS treatment protects the ageing kidney by ROS scavenging and enhancing endogenous H_2S production in kidney tissue as reported previously in myocardium [22]. Decreased CBS activity in the ageing kidney may also lead to homocysteine accumulation. Because the latter plays an important role in chronic renal failure [23, 24], further study is needed to explore whether homocysteine metabolism disorder is involved in ageing-related kidney damage and whether exogenous NaHS could help restore the normal metabolic pathway.

Christopher Hine reported that sulfur amino acid restriction could alter H_2S production and protect the liver from ischemia-reperfusion injury [25], indicating the beneficial role of endogenous H_2S. SIRT1, which emerges as a major life span regulator, has been widely explored in the cardiovascular system and nervous system, but it is rare in the urinary system. SIRT1 has robust biological effects and can affect metabolic homeostasis and ageing. Consistent with previous studies [26, 27], we found that both the expression and activity of SIRT1 decreased rapidly in the ageing kidney. The reduction of NAD^+ biosynthesis may be responsible for reduced SIRT1 activity [26]. Here we report an interesting finding that a low concentration of NaHS (25 μmol/L) could directly induce SIRT1 activation in a cell-free system, whereas chronic treatment of NaHS (50 μmol/kg/day) selectively improves the expression but not the activity of SIRT1 in the ageing kidney. SIRT1 also regulates lipid metabolism by manipulating PPAR-α, LXR, FXR, and SREBP signals [28, 29]. For example, SIRT1 positively regulates LXR proteins, which act as cholesterol sensor and adjust whole body cholesterol and lipid homeostasis [30]. Our blood biochemical tests showed that chronic NaHS treatment could

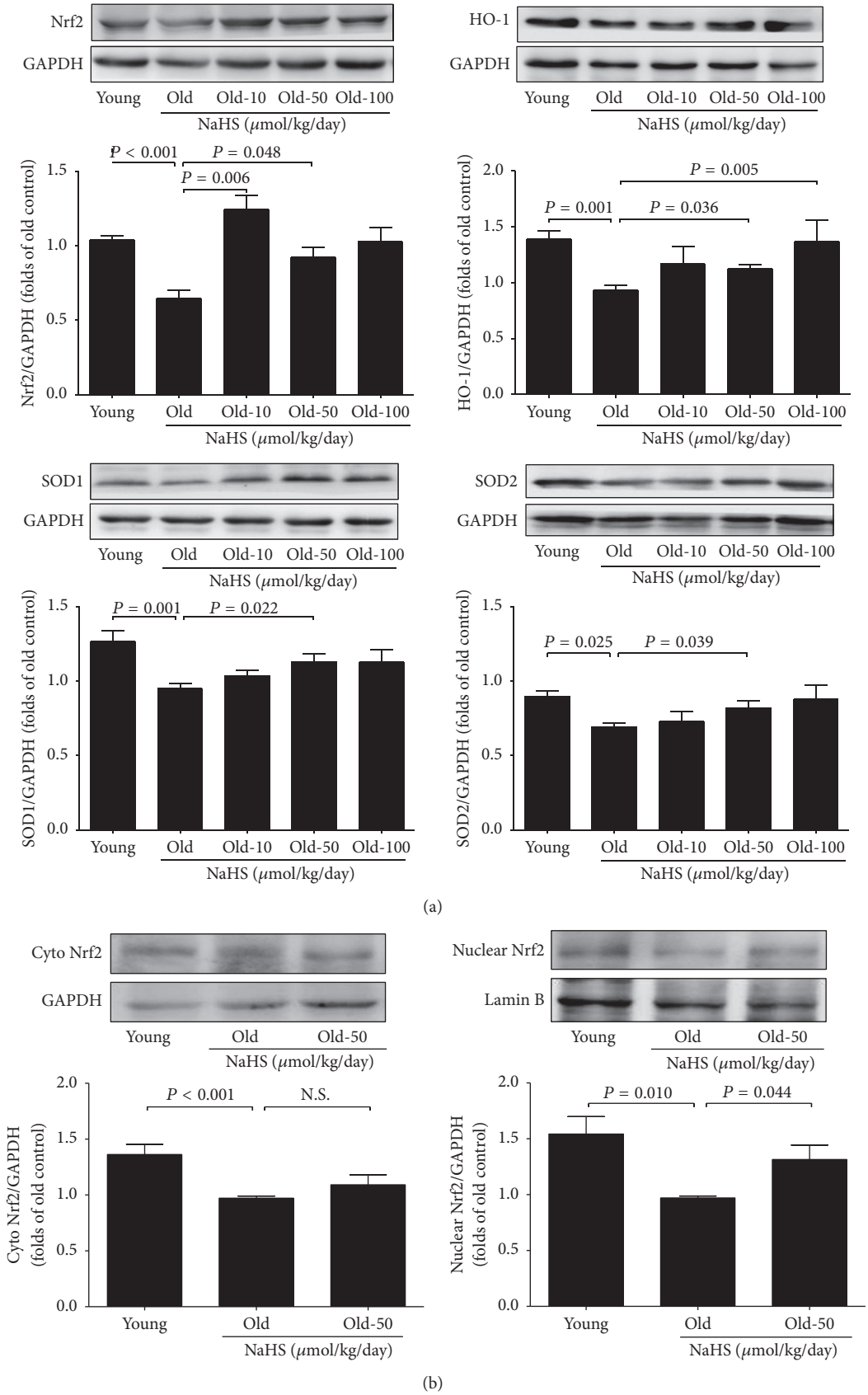

Figure 8: The protective effects of the H_2S donor on the expression of antioxidant-related proteins in the ageing kidney tissue. (a) The expression change of Nrf2 ($N = 11$), HO-1 ($N = 10$), SOD1 ($N = 11$), and SOD2 ($N = 10$) after 10 weeks of exogenous H_2S donor. (b) Nrf2 was translocated from cytosol to nucleus, Lamin B was used as nuclear control, and GAPDH was used as cytosol control ($N = 6$). Values are mean ± SE. $P < 0.05$ was considered significant.

decrease CHOL and TG. Therefore, H_2S may modulate liver and renal lipid metabolism through an enhanced SIRT1 signal and contribute to the prevention of renal disease progression.

Nrf2 is an important antioxidative molecule that modulates the expression of antioxidant genes [30] and thus prevents age-related oxidative stress [31, 32]. Here we showed that the kidney Nrf2 expression decreased during ageing and that chronic NaHS treatment could rescue Nrf2 expression (10 and 50 μmol/kg/day) and enhance its nuclear translocation (50 μmol/kg/day). The precise mechanism of excessive oxidative stress in ageing is not clear, but the decreased expression of Nrf2/antioxidant stress element-linked antioxidant genes is thought to play a role [32–34]. We found that chronic NaHS treatment could activate Nrf2 downstream genes such as HO-1, SOD1, and SOD2, which consequently enhanced resistance to oxidative stress in the ageing kidney. Taken together, our data support the idea that H_2S plays a crucial role in protecting the ageing kidney from antifibrosis and antiapoptosis through the regulation of redox homeostasis.

5. Conclusion

In summary, we demonstrated that 3-MST was expressed in the ageing kidney and that endogenous H_2S levels decreased because of the impaired expression of H_2S-producing enzymes. Chronic exogenous H_2S treatment could protect the ageing kidney by reducing oxidative stress, decreasing collagen deposition, and enhancing Nrf2 nuclear translocation, as well as increasing endogenous H_2S production.

Competing Interests

The authors declare no conflict of interests regarding the publication of this paper.

Authors' Contributions

Cui-Lan Hou and Ming-Jie Wang contributed equally to this work.

Acknowledgments

The authors thank Bo Tan for his excellent technical assistance in H_2S measurements. This present study was supported by the National Natural Science Foundation of China (NSFC) (no. 81230003 to Yi-Chun Zhu, no. 81670248 to Ming-Jie Wang, and no. 81402917 to Bo Tan), the Ministry of Education (20110071130009 to Yi-Chun Zhu), the Shanghai Pujiang Program (15PJ1400700 to Ming-Jie Wang), the Research Center on Ageing and Medicine, Fudan University (13dz2260700 to Ming-Jie Wang), and Key Laboratory Program of the Education Commission of Shanghai Municipality (ZDSYS14005 to Yi-Chun Zhu).

References

[1] J. Volkert, H. Schulz, M. Härter, O. Wlodarczyk, and S. Andreas, "The prevalence of mental disorders in older people in Western countries—a meta-analysis," *Ageing Research Reviews*, vol. 12, no. 1, pp. 339–353, 2013.

[2] A. Denic, R. J. Glassock, and A. D. Rule, "Structural and functional changes with the aging kidney," *Advances in Chronic Kidney Disease*, vol. 23, no. 1, pp. 19–28, 2016.

[3] G. Yang, L. Wu, B. Jiang et al., "H_2S as a physiologic vasorelaxant: hypertension in mice with deletion of cystathionine γ-lyase," *Science*, vol. 322, no. 5901, pp. 587–590, 2008.

[4] Y. Sun, Y. Huang, R. Zhang et al., "Hydrogen sulfide upregulates KATP channel expression in vascular smooth muscle cells of spontaneously hypertensive rats," *Journal of Molecular Medicine*, vol. 93, no. 4, pp. 439–455, 2015.

[5] C. Guo, F. Liang, W. Shah Masood, and X. Yan, "Hydrogen sulfide protected gastric epithelial cell from ischemia/reperfusion injury by Keap1 s-sulfhydration, MAPK dependent anti-apoptosis and NF-κB dependent anti-inflammation pathway," *European Journal of Pharmacology*, vol. 725, no. 1, pp. 70–78, 2014.

[6] J. Du, Y. Huang, H. Yan et al., "Hydrogen sulfide suppresses oxidized low-density lipoprotein (Ox-LDL)-stimulated monocyte chemoattractant protein 1 generation from macrophages via the nuclear factor κb (NF-κB) pathway," *The Journal of Biological Chemistry*, vol. 289, no. 14, pp. 9741–9753, 2014.

[7] J. Zheng, T. Zhao, Y. Yuan, N. Hu, and X. Tang, "Hydrogen sulfide (H_2S) attenuates uranium-induced acute nephrotoxicity through oxidative stress and inflammatory response via Nrf2-NF-κB pathways," *Chemico-Biological Interactions*, vol. 242, no. 1, pp. 353–362, 2015.

[8] D. L. Miller and M. B. Roth, "Hydrogen sulfide increases thermotolerance and lifespan in *Caenorhabditis elegans*," *Proceedings of the National Academy of Sciences of the United States of America*, vol. 104, no. 51, pp. 20618–20622, 2007.

[9] Y. Wei and C. Kenyon, "Roles for ROS and hydrogen sulfide in the longevity response to germline loss in Caenorhabditis elegans," *Proceedings of the National Academy of Sciences*, vol. 113, no. 20, pp. e2832–e2841, 2016.

[10] Y. Zhang, Z.-H. Tang, Z. Ren et al., "Hydrogen sulfide, the next potent preventive and therapeutic agent in aging and age-associated disease," *Molecular and Cellular Biology*, vol. 33, no. 6, pp. 1104–1113, 2013.

[11] C. Wei, Y. Zhao, L. Wang et al., "H_2S restores the cardioprotection from ischemic post-conditioning in isolated aged rat hearts," *Cell Biology International*, vol. 39, no. 10, pp. 1173–1176, 2015.

[12] R. E. Sandu, A. Buga, A. T. Balseanu, M. Moldovan, and A. Popa-Wagner, "Twenty-four hours hypothermia has temporary efficacy in reducing brain infarction and inflammation in aged rats," *Neurobiology of Aging*, vol. 38, no. 1, pp. 127–140, 2016.

[13] S. Jin, S. X. Pu, C. L. Hou et al., "Cardiac H_2S generation is reduced in ageing diabetic mice," *Oxidative Medicine and Cellular Longevity*, vol. 2015, Article ID 758358, 14 pages, 2015.

[14] K. L. Quick and L. L. Dugan, "Superoxide stress identifies neurons at risk in a model of ataxia-telangiectasia," *Annals of Neurology*, vol. 49, no. 5, pp. 627–635, 2001.

[15] X. Shen, C. B. Pattillo, S. Pardue, S. C. Bir, R. Wang, and C. G. Kevil, "Measurement of plasma hydrogen sulfide in vivo and in vitro," *Free Radical Biology and Medicine*, vol. 50, no. 9, pp. 1021–1031, 2011.

[16] B.-B. Tao, S.-Y. Liu, C.-C. Zhang et al., "VEGFR2 functions as an H_2S-targeting receptor protein kinase with its novel Cys1045-Cys1024 disulfide bond serving as a specific molecular switch for hydrogen sulfide actions in vascular endothelial cells," *Antioxidants & Redox Signaling*, vol. 19, no. 5, pp. 448–464, 2013.

[17] K. J. Bitterman, R. M. Anderson, H. Y. Cohen, M. Latorre-Esteves, and D. A. Sinclair, "Inhibition of silencing and accelerated aging by nicotinamide, a putative negative regulator of yeast Sir2 and human SIRT1," *The Journal of Biological Chemistry*, vol. 277, no. 47, pp. 45099–45107, 2002.

[18] X. Zhou, Y. Feng, Z. Zhan, and J. Chen, "Hydrogen sulfide alleviates diabetic nephropathy in a streptozotocin-induced diabetic rat model," *The Journal of Biological Chemistry*, vol. 289, no. 42, pp. 28827–28834, 2014.

[19] P. Wang, C. K. Isaak, Y. L. Siow, and K. O, "Downregulation of cystathionine β-synthase and cystathionine γ-lyase expression stimulates inflammation in kidney ischemia—reperfusion injury," *Physiological Reports*, vol. 24, no. 12, article e12251, 2014.

[20] F. Yi and P.-L. Li, "Mechanisms of homocysteine-induced glomerular injury and sclerosis," *American Journal of Nephrology*, vol. 28, no. 2, pp. 254–264, 2008.

[21] R. Xue, D.-D. Hao, J.-P. Sun et al., "Hydrogen sulfide treatment promotes glucose uptake by increasing insulin receptor sensitivity and ameliorates kidney lesions in type 2 diabetes," *Antioxidants & Redox Signaling*, vol. 19, no. 1, pp. 5–23, 2013.

[22] N. Li, M.-J. Wang, S. Jin et al., "The H_2S donor NaHS changes the expression pattern of H_2S-producing enzymes after myocardial infarction," *Oxidative Medicine and Cellular Longevity*, vol. 2016, Article ID 6492469, 11 pages, 2016.

[23] U. Sen, W. E. Rodriguez, N. Tyagi, M. Kumar, S. Kundu, and S. C. Tyagi, "Ciglitazone, a PPARγ agonist, ameliorates diabetic nephropathy in part through homocysteine clearance," *American Journal of Physiology—Endocrinology and Metabolism*, vol. 295, no. 5, pp. E1205–E1212, 2008.

[24] W. E. Rodriguez, U. Sen, N. Tyagi et al., "PPAR gamma agonist normalizes glomerular filtration rate, tissue levels of homocysteine, and attenuates endothelial-myocyte uncoupling in alloxan induced diabetic mice," *International Journal of Biological Sciences*, vol. 4, no. 4, pp. 236–244, 2008.

[25] C. Hine, E. Harputlugil, Y. Zhang et al., "Endogenous hydrogen sulfide production is essential for dietary restriction benefits," *Cell*, vol. 160, no. 1-2, pp. 132–144, 2015.

[26] S.-I. Imai, "Dissecting systemic control of metabolism and aging in the NAD World: the importance of SIRT1 and NAMPT-mediated NAD biosynthesis," *FEBS Letters*, vol. 585, no. 11, pp. 1657–1662, 2011.

[27] N. Braidy, G. J. Guillemin, H. Mansour, T. Chan-Ling, A. Poljak, and R. Grant, "Age related changes in NAD^+ metabolism oxidative stress and sirt1 activity in wistar rats," *PLoS ONE*, vol. 6, no. 4, Article ID e19194, pp. 1–18, 2011.

[28] A. Purushotham, T. T. Schug, Q. Xu, S. Surapureddi, X. Guo, and X. Li, "Hepatocyte-specific deletion of SIRT1 alters fatty acid metabolism and results in hepatic steatosis and inflammation," *Cell Metabolism*, vol. 9, no. 4, pp. 327–338, 2009.

[29] A. K. Walker, F. Yang, K. Jiang et al., "Conserved role of SIRT1 orthologs in fasting-dependent inhibition of the lipid/cholesterol regulator SREBP," *Genes and Development*, vol. 24, no. 13, pp. 1403–1417, 2010.

[30] X. Li, S. Zhang, G. Blander, J. G. Tse, M. Krieger, and L. Guarente, "SIRT1 deacetylates and positively regulates the nuclear receptor LXR," *Molecular Cell*, vol. 28, no. 1, pp. 91–106, 2007.

[31] M. M. Sachdeva, M. Cano, and J. T. Handa, "Nrf2 signaling is impaired in the aging RPE given an oxidative insult," *Experimental Eye Research*, vol. 119, no. 1, pp. 111–114, 2014.

[32] A. Loboda, M. Damulewicz, E. Pyza, A. Jozkowicz, and J. Dulak, "Role of Nrf2/HO-1 system in development, oxidative stress response and diseases: an evolutionarily conserved mechanism," *Cellular and Molecular Life Sciences*, vol. 73, no. 17, pp. 3221–3247, 2016.

[33] G. Yang, K. Zhao, Y. Ju et al., "Hydrogen sulfide protects against cellular senescence via *S*-sulfhydration of Keap1 and activation of Nrf2," *Antioxidants & Redox Signaling*, vol. 18, no. 15, pp. 1906–1919, 2013.

[34] A. J. Done, M. J. Gage, N. C. Nieto, and T. Traustadóttir, "Exercise-induced Nrf2-signaling is impaired in aging," *Free Radical Biology and Medicine*, vol. 96, no. 1, pp. 130–138, 2016.

Hindawi Publishing Corporation
Oxidative Medicine and Cellular Longevity
Volume 2016, Article ID 6190504, 12 pages
http://dx.doi.org/10.1155/2016/6190504

Research Article

Activation of ALDH2 with Low Concentration of Ethanol Attenuates Myocardial Ischemia/Reperfusion Injury in Diabetes Rat Model

Pin-Fang Kang,[1] Wen-Juan Wu,[2] Yang Tang,[1] Ling Xuan,[1] Su-Dong Guan,[3] Bi Tang,[1] Heng Zhang,[1] Qin Gao,[3] and Hong-Ju Wang[1]

[1]*Department of Cardiovascular Disease, The First Affiliated Hospital of Bengbu Medical College, Bengbu 233004, China*
[2]*Department of Biochemistry and Molecular Biology, Bengbu Medical College, Bengbu 233030, China*
[3]*Department of Physiology, Bengbu Medical College, Bengbu 233030, China*

Correspondence should be addressed to Qin Gao; bbmcgq@126.com and Hong-Ju Wang; docwhj1101@163.com

Received 10 May 2016; Revised 9 August 2016; Accepted 24 August 2016

Academic Editor: Ryuichi Morishita

The aim of this paper is to observe the change of mitochondrial aldehyde dehydrogenase 2 (ALDH2) when diabetes mellitus (DM) rat heart was subjected to ischemia/reperfusion (I/R) intervention and analyze its underlying mechanisms. DM rat hearts were subjected to 30 min regional ischemia and 120 min reperfusion in vitro and pretreated with ALDH2 activator ethanol (EtOH); cardiomyocyte in high glucose (HG) condition was pretreated with ALDH2 activator Alda-1. In control I/R group, myocardial tissue structure collapse appeared. Compared with control I/R group, left ventricular parameters, SOD activity, the level of Bcl-2/Bax mRNA, ALDH2 mRNA, and protein expressions were decreased and LDH and MDA contents were increased, meanwhile the aggravation of myocardial structure injury in DM I/R group. When DM I/R rats were pretreated with EtOH, left ventricular parameters, SOD, Bcl-2/Bax, and ALDH2 expression were increased; LDH, MDA, and myocardial structure injury were attenuated. Compared with DM + EtOH I/R group, cyanamide (ALDH2 nonspecific blocker), atractyloside (mitoPTP opener), and wortmannin (PI3K inhibitor) groups all decreased left ventricular parameters, SOD, Bcl-2/Bax, and ALDH2 and increased LDH, MDA, and myocardial injury. When cardiomyocyte was under HG condition, CCK-8 activity and ALDH2 protein expression were decreased. Alda-1 increased CCK-8 and ALDH2. Our findings suggested enhanced ALDH2 expression in diabetic I/R rats played the cardioprotective role, maybe through activating PI3K and inhibiting mitoPTP opening.

1. Introduction

Diabetes mellitus (DM) is a common metabolic disorder that can affect patient life and survival quality with acute and chronic complications [1–3]. It is associated with a high cardiovascular mortality, and it is also the most common cause of end-stage heart disease [4]. The morbidity and mortality of diabetes show an increasing trend, and the incidence of heart failure after myocardial infarction in diabetic patients is more than 2-3 times than nondiabetic. Myocardial ischemia/reperfusion (I/R) injury can cause cardiac glucose metabolism disorders, calcium overload, and cardiac fibrosis, resulting in accumulation of harmful products, easily leading to apoptosis and necrosis [5]. Therefore, how to protect ischemic myocardium effectively, promote myocardial functional recovery, and reduce myocardial apoptosis become a research hotspot.

Mitochondrial aldehyde dehydrogenase 2 (ALDH2) is one of the key enzymes of alcohol metabolism, which catalyzes the conversion of aldehyde to acetic acid [6]. ALDH2 plays a crucial metabolic role in the detoxification and oxidation of aldehyde, such as inhibiting the production of 4-hydroxynon-2-enal [7–9]. ALDH2 was found to attenuate ethanol exposure-induced myocardial dysfunction, and activation of ALDH2 led to cardiac protection against ischemia and reperfusion injury [10–15]. Previous studies also indicated that, with the development of diabetes, cardiac ALDH2 activity was further decreased, and inhibition of

ALDH2 by oxidative stress leads to cardiac dysfunction in diabetes mellitus [16]. What changes of ALDH2 expression that appeared and what mechanisms involved in diabetic rat myocardial I/R injury spark our interest.

At the beginning of I/R, the signal transduction pathways were activated by various means of myocardial protection proactively, especially phosphatidylinositol-3-kinase serine/threonine kinase (PI3K-Akt). PI3K-Akt signaling pathway is an important pathway which regulates cell proliferation, cell division, apoptosis, and other activities. Heart was protected by ischemic preconditioning via activated PI3K-Akt signaling pathway; however, the effect of myocardial protection was abolished by PI3K inhibitor, wortmannin. It is suggested that PI3K-Akt signal transduction pathway was involved in myocardial protection.

Mitochondrial permeability transition pore (mitoPTP) is located in the inner and outer mitochondrial membrane multiprotein complexes, which plays an important role in maintaining mitochondrial membrane potential and protecting the structure and function of mitochondrion [17, 18]. Under physiological condition, mitoPTP is closed, and it has almost no permeability for all mitochondrial metabolites and ions. Opening of mitoPTP is involved in cell death induced by a variety of causes, for example, I/R, endotoxin, and anticancer agents [19]. Opening mitoPTP leads to mitochondrial swelling and outer membrane rupture; the proapoptotic factors and cytochrome C were released into the cytoplasm, inducing energy metabolism unbalance, intracellular calcium overload, and exacerbated ischemic cell damage. The opening of mitoPTP in reperfusion is a sign of myocardial injury from reversible to irreversible [20, 21]. mitoPTP is considered to be the terminal effector of cell death in I/R injury, while delaying or blocking the opening of mitoPTP may reduce I/R injury [22, 23]. A large number of reports suggested that ischemic preconditioning, ischemic postconditioning, and drug pretreatment could protect heart against injury by inhibiting of the opening of mitoPTP [24–26].

Based on above background, we were prompted to investigate the effects of pretreatment with ethanol (EtOH) as a tool to induce ALDH2 activity in myocardial I/R injury of diabetic rats and give drug intervention, including ALDH2 inhibitor cyanimide, PI3K inhibitor wortmannin, and the opener of mitoPTP atractyloside, to determine its underlying mechanisms.

2. Materials and Methods

2.1. Animals. Male Sprague-Dawley rats (200~250 g) were purchased from the Animal Center of Bengbu Medical College, Anhui. The rats were fed normal chow and had free access to water. Housing was at a constant temperature of (21 ± 1)°C with a fixed 12 h light/dark cycle. All animal procedures were in accordance with United States National Institutes of Health Guide and were approved by the Animal Use and Care Committee of Bengbu Medical College.

2.2. Chemicals and Reagents. Streptozotocin (STZ), cyanamide (CYA), wortmannin (Wor), atractyloside (Atr), and Alda-1 were purchased from Sigma (St. Louis, MO, USA). Ethanol (EtOH) was obtained from Bengbu New Chemical Reagent Factory, China. 10% fetal bovine serum was obtained from Zhe Jiang Tianhang Biological corporation, China. Lactate dehydrogenase (LDH), Malondialdehyde (MDA), and superoxide dismutase (SOD) assay kits were purchased from Nanjing Jiancheng Bioengineering Institute, China. CCK-8 assay kit was from Shanghai Bestbio Life Technology, China. The primers used were as follows: for ALDH2 forward: 5′-GTG TTC GGA GAC GTC AAA GA-3′ and reverse 5′-GCA GAG CTT GGG ACA GGT AA-3′, the amplified fragment length was 187 bp; for Bcl-2 forward: 5′-CTG GTG GAC AAC ATC GCT CTG-3′ and reverse: 5′-GGT CTG CTG ACC TCA CTT GTG-3′, the amplified fragment length was 227 bp; for Bax forward: 5′-GGA TCG AGC AGA GAG GAT GG-3′ and reverse: 5′-GCT CAT TGC CGA TAG TGA TGA CT-3′, the amplified fragment length was 464 bp; for β-actin forward: 5′-GAT GGT GGG TAT GGG TCA GAA-3′ and reverse: 5′-GGC CAT CTC TTG CTC GAA GTC-3′, the amplified fragment length was 630 bp. Mouse anti-ALDH2, anti-Bcl-2, anti-Bax, and anti-β-actin monoclonal antibodies were purchased from Santa Cruz Biotechnology (CA). Goat anti-mouse secondary antibodies were from Boston Co., Ltd., Wuhan, China.

2.3. Induction of Diabetes and Experimental Protocol. Diabetes was induced in overnight fasted rats by administering a single intraperitoneal (i.p.) injection of 55 mg/kg streptozotocin (STZ) freshly dissolved in 0.1 mol/L sodium citrate buffer (pH 4.5). The rats in control group were injected with a similar volume of sodium citrate buffer alone. The rats whose fasting blood glucose level was more than 16.7 mmol/L after 72 h of injection were as diabetic [27]. All rats were fed for eight weeks. Animals were randomly divided into control, diabetes (DM), and DM + EtOH groups, respectively. In DM + EtOH group, DM rats were fed with 2.5% EtOH in their drinking water for one week to initiate drinking and then changed to 5% EtOH continuous access through seven weeks.

2.4. Ischemia and Reperfusion and Drugs Intervention in Isolated Perfused Heart. All rat hearts were subjected to regional ischemia and reperfusion intervention (I/R) in vitro. After the rats were anesthetized (chloral hydrate, 4 g/kg, i.p.), hearts were excised rapidly, placed in ice-cold Krebs-Henseleit (K-H) buffer, mounted on a Langendorff apparatus, and perfused at 37°C with K-H buffer. The buffer was equilibrated with 95% O_2/5% CO_2 (pH 7.4) and had the following composition (mmol/L): NaCl 118.0, KCl 4.7, $CaCl_2$ 1.25, KH_2PO_4 1.2, $NaHCO_3$ 25.0, and glucose 11.0. A latex, fluid-filled balloon was introduced into the left ventricle through the left atrial appendage and the balloon catheter was linked to a pressure transducer connected to a data acquisition system (Medlab, Nanjing, China) to assess contractile function. The left ventricular end diastolic pressure (LVEDP) was adjusted to 4~8 mmHg for 30 min. Myocardial infarction (MI) was created by ligation of the left anterior descending artery (LAD). MI was induced by LAD ligation 2~3 mm from the origin with 5-0 silk suture. Then 30 min of

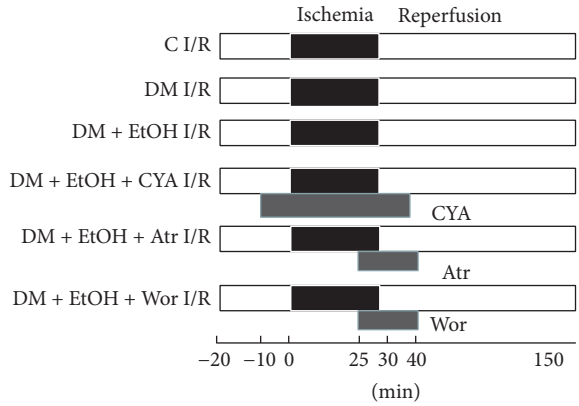

Figure 1: Protocol of various drugs intervention on rat myocardial ischemia/reperfusion model in vitro. C I/R: control ischemia and reperfusion; DM I/R: diabetes rats subjected to myocardial ischemia and reperfusion; DM + EtOH I/R: diabetes + ethanol subjected to myocardial ischemia and reperfusion; DM + EtOH + CYA I/R: diabetes + ethanol + cyanamide subjected to myocardial ischemia and reperfusion; DM + EtOH + Atr I/R: diabetes + ethanol + atractyloside subjected to myocardial ischemia and reperfusion; DM + EtOH + Wor I/R: diabetes + ethanol + wortmannin subjected to myocardial ischemia and reperfusion.

regional myocardial ischemia (i.e., MI) followed by 120 min of reperfusion was done in all rats. The cardiac parameters including HR, left ventricular developed pressure (LVDP: difference between left ventricular end systolic pressure and end diastolic pressure), maximal rise/fall rate of left ventricular pressure ($\pm dp/dt_{max}$), left ventricular end diastolic pressure (LVEDP), and rate-pressure product (RPP: LVDP × HR) were monitored continuously. The rats were divided into control I/R ($n = 6$), DM I/R ($n = 6$), and DM + EtOH I/R ($n = 6$). Other EtOH treated rats were subjected to three different drugs' intervention, respectively ($n = 6$/group). The ALDH2 inhibitor cyanamide (CYA) at 1 mmol/L was given from 10 min before ischemia to the first 10 min of reperfusion, with total perfusing for 50 min (DM + EtOH + CYA I/R); the mitoPTP opener atractyloside (Atr) at 20 mmol/L was given from the last 5 min of ischemia to the early 10 min of reperfusion, with total perfusing for 15 min (DM + EtOH + Atr I/R). The inhibitor of PI3K, 100 nmol/L wortmannin (Wor), was given at the end ischemia for 5 min and early reperfusion for 10 min (DM + EtOH + Wor I/R) (Figure 1).

2.5. Detection of LDH Release in Coronary Flow. Coronary flow was collected at 5 min and 10 min of reperfusion, and LDH release was measured by commercially available kits according to the manufacturer's instructions.

2.6. Detection of MDA Content and SOD Activity in Heart Tissue. At the end of the experimental period, 0.1 g heart tissue was homogenized in ice-cold PBS buffer. Malondialdehyde (MDA) content and superoxide dismutase (SOD) activity were measured by commercially available kits according to the manufacturer's instructions.

2.7. Detection of Cardiac ALDH2, Bax, and Bcl-2 at mRNA Level by RT-PCR. RT-PCR was used to detect the levels of ALDH2, Bax, and Bcl-2 mRNA expression in heart. Briefly, total RNA was extracted with TRIzol according to the manufacturer's instructions. Two micrograms of total RNA was reverse-transcribed to cDNA, and PCR was performed by a routine method. PCR products were analyzed on 1% agarose gel. Densitometry results for ALDH2, Bax, and Bcl-2 gene were compared with corresponding β-actin levels to account for loading differences.

2.8. Ultrastructure Observation of Myocardial Cell by Transmission Electron Microscope. Cardiac tissue was dissected and small pieces were fixed with 2.5% glutaraldehyde in 0.1% mol/L cacodylate buffer for 1 h. Ultrathin sections were cut and contrasted with uranylacetate buffer by lead citrate and observed with JEM-1230 transmission electron microscope (JEOL, Japan).

2.9. Cell Culture and Drug Treatment. Rat neonatal cardiomyocytes were isolated from 1~2 d old Sprague-Dawley rats by digestion with trypsin. Briefly, ventricular tissue was aseptically removed from neonatal rats, minced, and then digested with mixed protease (0.25% trypsin, 0.2% collagenase II, 100 μg/mL DNA enzyme I, and D-Hanks solution) (Solarbio, Beijing, China) at 37°C in a shaking water bath. The cells were released after the first digestion was discarded, whereas the cells from subsequent digestion were added to an equal volume of Dulbecco's modified Eagle's medium (DMEM) supplemented with 10% fetal bovine serum until all cells were collected. Cells were pelleted by centrifugation at 1000 rpm for 6 min and resuspended in DMEM supplemented 10% fetal bovine serum. The isolated cells were first plated in culture disks of 95% air and 5% CO_2 at 37°C for 2 h to exclude nonmuscle cells. The suspended cells were then collected and plated at a density of 5×10^5 cells/cm^2 and maintained under the same conditions as above. The cells were used for outlined experiments after 4~5 days later.

2.10. Immunofluorescence Analysis. Cardiomyocytes cultured on coverslips were seeded in 6-well plates and fixed in 4% paraformaldehyde in PBS for 15 min at room temperature, followed by washing with PBS, three times per 5 min. Then, cardiomyocytes were incubated with 0.1% TritonX-100 in PBS for 30 min, followed by washing with PBS, three times per 5 min again. After blocking with 1% bovine serum albumin in PBS for 1 h, the cells were incubated in BSA blocking buffer containing primary antibody-α-SMA (1 : 200, Boster, China), and the cells were washed and then incubated in secondary anti-mouse antibody (1 : 200; Boster, China) for 1 h. Furthermore, cardiomyocytes were incubated for 15 min with 4,6-diamidino-2-phenylindole (DAPI; ZSGB, Beijing, China) for nuclear staining, and fluorescence micrographs were obtained using Olympus FSX100 microscope.

2.11. Grouping. The cardiomyocytes were divided into 3 groups as follows: control (C) group, HG group, and Alda-1 + HG group. In C group, cardiomyocytes were incubated

in DMEM medium including 5.5 mmol/L glucose for 48 h. In HG group, cardiomyocytes were incubated in high glucose medium (25 mmol/L glucose) for 48 h; and in Alda-1 + HG group cardiomyocytes were pretreated with HG and ALDH2 activator Alda-1 (20 μmol/L) for 48 h.

2.12. Cell Counting Kit- (CCK-) 8 Assay. Cardiomyocytes (100 μL/well) were seeded into 96-well plate at a density of (0.5~1.0) $\times$ 10^4 cells/mL and incubated at 37°C, 5% CO_2 overnight. A CCK-8 assay kit was used to detect cell viabilities according to the manufacturer's instructions. Following treatment, test samples and CCK-8 were added to each well 10 μL, respectively. After 1~4 h incubation, cells viability was determined by measuring the absorbance at 450 nm using microplate reader. The activity levels were determined according to the manufacturer's instructions.

2.13. Detection of Cardiac and Cardiomyocyte ALDH2 Protein Expression by Western Blot. The ALDH2 protein in cardiac tissue and cardiomyocyte was detected by western blot [1]. Anti-ALDH2 (1 : 500) antibody was used. Mouse anti-β-actin antibody (1 : 500) was used as an internal control. The immunoblots were exposed to X-ray film and analyzed with a digital image system.

2.14. Statistical Analysis. All values are expressed as mean ± SD. Statistical comparisons were performed by one-way analysis of variance and the Newman-Keuls test. Differences of $p < 0.05$ were regarded as significant.

3. Results

3.1. Changes of Ventricular Hemodynamic Parameters. In C I/R group, compared with baseline, LVDP, $\pm dp/dt_{max}$, and RPP were decreased, and LVEDP was increased during ischemia period; during reperfusion period, LVDP, $\pm dp/dt_{max}$, and RPP were lower and LVEDP was higher. During ischemia and reperfusion period, in contrast to C I/R rat, in DM I/R rat, LVDP, $\pm dp/dt_{max}$, and RPP were decreased, and LVEDP was increased; compared with DM I/R group, LVDP, $\pm dp/dt_{max}$, and RPP were increased, and LVEDP was decreased in DM + EtOH I/R group; compared with DM + EtOH I/R group, in DM + EtOH + CYA I/R group, LVDP, $\pm dp/dt_{max}$, and RPP were furtherly decreased, and LVEDP was increased; the changes in DM + EtOH + Atr I/R and DM + EtOH + Wor I/R groups were similar to DM + EtOH + CYA I/R group (Table 1). There were no differences among the three groups, in DM + EtOH + cyanamide + I/R versus DM + EtOH + wortmannin + I/R versus DM + EtOH + atractyloside + I/R.

3.2. Changes of LDH Content. The changes of LDH content in different groups were shown in Table 2. In contrast to C I/R group, in DM I/R group rats, LDH release was increased. Compared with DM I/R group, LDH release was decreased in DM + EtOH I/R group. Compared with DM + EtOH I/R group, LDH release was increased in DM + EtOH + CYA I/R, DM + EtOH + Atr I/R, and DM + EtOH + Wor I/R groups (Table 2).

3.3. Changes of MDA Content and SOD Activity in Heart Tissue. Compared with C I/R group, in DM I/R group, MDA content was increased, and SOD activity was decreased. Compared with DM I/R group, in DM + EtOH I/R group, MDA content was decreased, accompanied with the increase of SOD activity. Compared with DM + EtOH I/R group, MDA content was increased, and SOD activity was decreased in DM + EtOH + CYA I/R, DM + EtOH + Atr I/R, and DM + EtOH + Wor I/R groups (Figure 2).

3.4. Change of Bax and Bcl-2 at mRNA Level in Heart. Compared with C I/R group, Bax mRNA was increased; Bcl-2 mRNA and the ratio of Bcl-2/Bax were significantly decreased in DM I/R group. Compared with DM I/R group, in DM + EtOH I/R group, Bax mRNA was decreased; Bcl-2 mRNA and the ratio of Bcl-2/Bax were increased. Compared with DM + EtOH I/R group, Bax mRNA was decreased; Bcl-2 mRNA and the ratio of Bcl-2/Bax were decreased in DM + EtOH + CYA I/R, DM + EtOH + Atr I/R, and DM + EtOH + Wor I/R groups (Figure 3).

3.5. Change of ALDH2 mRNA and Protein Level in Heart. Compared with C I/R group, ALDH2 mRNA and protein expressions were significantly decreased in DM I/R group. Compared with DM I/R group, ALDH2 mRNA and protein expressions were increased significantly in DM + EtOH I/R group; compared with DM + EtOH I/R group, ALDH2 mRNA and protein expressions were decreased in DM + EtOH + CYA I/R and DM + EtOH + Atr I/R and DM + EtOH + Wor I/R groups (Figures 4(a), 4(b), 4(c), and 4(d)).

3.6. CCK-8 Assay and ALDH2 Protein Level in Cardiomyocyte. Compared with C group, cardiomyocyte activity and ALDH2 protein expressions were significantly decreased in HG group. Compared with HG group, cardiomyocyte activity and ALDH2 protein expression were increased significantly in Alda-1 + HG group (Figures 5(a), 5(b), and 5(c)).

3.7. Ultrastructural Changes of Myocardial Cell. In C I/R group, mitochondrial dense membrane was uncompleted, mild swelling, and myocardial myofilament was fractured, no large tracts of dissolution; in DM I/R group, mitochondrial swelling was aggravated, myocardial cytoplasmic muscle fiber was ruptured, and large areas of dissolution and vacuolation occurred. Compared with DM I/R group, in DM + EtOH I/R group, the degree of derangement of the cardiac myofilament and mitochondrial swelling was lessened; compared with DM + EtOH I/R group, in DM + EtOH + CYA I/R, DM + EtOH + Atr I/R, and DM + EtOH + Wor I/R groups, the injury was increased (Figure 6).

4. Discussion

In the current study, we mimicked myocardial ischemia/reperfusion (I/R) injury in diabetic rats. Compared with C I/R group, LDH levels were increased, cardiac systolic and diastolic dysfunction were aggravated, as indicated by the decreases of LVDP, $\pm dp/dt_{max}$, and RPP and increases

Table 1: Hemodynamic parameters in the isolated perfused rat hearts subjected to ischemia and reperfusion (I/R) (mean ± SD, $n = 5$).

Variable	Baseline	Ischemia	Reperfusion		
		30 min	5 min	10 min	120 min
LVDP (% of baseline)					
C I/R	100 ± 0	59 ± 13	63 ± 13	65 ± 14	58 ± 4
DM I/R	100 ± 0	$33 \pm 7^{**}$	$42 \pm 12^{*}$	$48 \pm 5^{**}$	$32 \pm 5^{**}$
DM + EtOH I/R	100 ± 0	$59 \pm 15^{\#\#}$	$93 \pm 12^{**\#\#}$	$90 \pm 7^{**\#\#}$	$58 \pm 13^{\#\#}$
DM + EtOH + CYA I/R	100 ± 0	$36 \pm 7^{**\wedge\wedge}$	$44 \pm 8^{**\wedge\wedge}$	$44 \pm 8^{**\wedge\wedge}$	$35 \pm 9^{**\wedge\wedge}$
DM + EtOH + Atr I/R	100 ± 0	$38 \pm 8^{**\wedge}$	$48 \pm 8^{*\wedge\wedge}$	$47 \pm 8^{**\wedge\wedge}$	$30 \pm 4^{**\wedge\wedge}$
DM + EtOH + Wor I/R	100 ± 0	$39 \pm 6^{**\wedge\wedge}$	$47 \pm 8^{*\wedge\wedge}$	$44 \pm 7^{**\wedge\wedge}$	$32 \pm 3^{**\wedge\wedge}$
LVEDP (% of baseline)					
C I/R	100 ± 0	101 ± 1	116 ± 2	120 ± 10	177 ± 11
DM I/R	100 ± 0	$151 \pm 15^{**}$	$177 \pm 14^{**}$	$159 \pm 9^{**}$	$262 \pm 27^{**}$
DM + EtOH I/R	100 ± 0	$104 \pm 7^{\#\#}$	$143 \pm 6^{**\#\#}$	$141 \pm 8^{**\#\#}$	$182 \pm 14^{\#\#}$
DM + EtOH + CYA I/R	100 ± 0	$155 \pm 11^{**\wedge\wedge}$	$182 \pm 11^{**\wedge\wedge}$	$160 \pm 12^{**\wedge\wedge}$	$254 \pm 20^{**\wedge\wedge}$
DM + EtOH + Atr I/R	100 ± 0	$147 \pm 20^{**\wedge\wedge}$	$166 \pm 3^{**\wedge\wedge}$	$166 \pm 5^{**\wedge\wedge}$	$251 \pm 16^{**\wedge\wedge}$
DM + EtOH + Wor I/R	100 ± 0	$168 \pm 19^{**\wedge\wedge}$	$176 \pm 7^{**\wedge\wedge}$	$170 \pm 11^{**\wedge\wedge}$	$281 \pm 45^{**\wedge\wedge}$
$+dp/dt_{max}$ (% of baseline)					
C I/R	100 ± 0	64 ± 10	80 ± 15	78 ± 12	55 ± 8
DM I/R	100 ± 0	48 ± 8	$43 \pm 9^{**}$	$46 \pm 5^{**}$	$34 \pm 6^{**}$
DM + EtOH I/R	100 ± 0	60 ± 14	$91 \pm 17^{\#\#}$	$91 \pm 19^{\#\#}$	$62 \pm 11^{\#\#}$
DM + EtOH + CYA I/R	100 ± 0	47 ± 7	$46 \pm 6^{**\wedge\wedge}$	$47 \pm 6^{**\wedge\wedge}$	$32 \pm 7^{**\wedge\wedge}$
DM + EtOH + Atr I/R	100 ± 0	48 ± 6	$45 \pm 2^{**\wedge\wedge}$	$47 \pm 4^{**\wedge\wedge}$	$34 \pm 7^{**\wedge\wedge}$
DM + EtOH + Wor I/R	100 ± 0	49 ± 9	$43 \pm 6^{**\wedge\wedge}$	$44 \pm 4^{**\wedge\wedge}$	$33 \pm 5^{**\wedge\wedge}$
$-dp/dt_{max}$ (% of baseline)					
C I/R	100 ± 0	59 ± 13	59 ± 10	59 ± 1	41 ± 5
DM I/R	100 ± 0	$42 \pm 9^{**}$	$42 \pm 6^{**}$	$46 \pm 9^{**}$	$31 \pm 4^{**}$
DM + EtOH I/R	100 ± 0	$62 \pm 5^{\#\#}$	$85 \pm 10^{**\#\#}$	$84 \pm 12^{**\#\#}$	$48 \pm 6^{**\#\#}$
DM + EtOH + CYA I/R	100 ± 0	$45 \pm 4^{*\wedge\wedge}$	$46 \pm 7^{*\wedge\wedge}$	$44 \pm 4^{**\wedge\wedge}$	$35 \pm 4^{*\wedge\wedge}$
DM + EtOH + Atr I/R	100 ± 0	$43 \pm 5^{**\wedge\wedge}$	$49 \pm 5^{*\wedge\wedge}$	$45 \pm 4^{**\wedge}$	$33 \pm 4^{**\wedge\wedge}$
DM + EtOH + Wor I/R	100 ± 0	$46 \pm 4^{*\wedge}$	$44 \pm 5^{**\wedge\wedge}$	$43 \pm 4^{**\wedge\wedge}$	$30 \pm 5^{**\wedge\wedge}$
RPP (% of baseline)					
C I/R	100 ± 0	59 ± 6	62 ± 17	62 ± 8	33 ± 3
DM I/R	100 ± 0	$26 \pm 7^{**}$	$32 \pm 8^{**}$	$28 \pm 7^{**}$	$18 \pm 4^{**}$
DM + EtOH I/R	100 ± 0	$55 \pm 13^{\#\#}$	$76 \pm 7^{**\#\#}$	$79 \pm 19^{**\#\#}$	$37 \pm 6^{\#\#}$
DM + EtOH + CYA I/R	100 ± 0	$29 \pm 5^{**\wedge\wedge}$	$28 \pm 5^{**\wedge\wedge}$	$25 \pm 6^{**\wedge\wedge}$	$15 \pm 5^{**\wedge\wedge}$
DM + EtOH + Atr I/R	100 ± 0	$28 \pm 4^{**\wedge\wedge}$	$34 \pm 6^{**\wedge\wedge}$	$31 \pm 6^{**\wedge\wedge}$	$16 \pm 4^{**\wedge\wedge}$
DM + EtOH + Wor I/R	100 ± 0	$32 \pm 8^{**\wedge\wedge}$	$30 \pm 3^{**\wedge\wedge}$	$25 \pm 4^{**\wedge\wedge}$	$18 \pm 2^{**\wedge\wedge}$

$^{*}p < 0.05$, $^{**}p < 0.01$ versus C I/R; $^{\#\#}p < 0.01$ versus DM I/R; $^{\wedge}p < 0.05$, $^{\wedge\wedge}p < 0.01$ versus DM + EtOH I/R.

Table 2: Effect of different drugs on LDH release in the coronary effluent in the isolated rat hearts subjected to ischemia and reperfusion (I/R) (mean ± SD, $n = 5$).

Group	5 min (U/L)	10 min (U/L)
C I/R	66.08 ± 7.60	60.50 ± 6.93
DM I/R	$154.58 \pm 16.50^{**}$	$129.58 \pm 22.23^{**}$
DM + EtOH I/R	$77.92 \pm 11.62^{\#\#}$	$61.58 \pm 5.63^{\#\#}$
DM + EtOH + CYA I/R	$139.83 \pm 20.41^{**\wedge\wedge}$	$107.92 \pm 27.42^{**\wedge\wedge}$
DM + EtOH + Atr I/R	$137.17 \pm 22.14^{**\wedge\wedge}$	$112.67 \pm 24.02^{**\wedge\wedge}$
DM + EtOH + Wor I/R	$136.25 \pm 29.42^{**\wedge\wedge}$	$113.75 \pm 18.40^{**\wedge\wedge}$

$^{**}p < 0.01$ versus C I/R; $^{\#\#}p < 0.01$ versus DM I/R; $^{\wedge\wedge}p < 0.01$ versus DM + EtOH I/R.

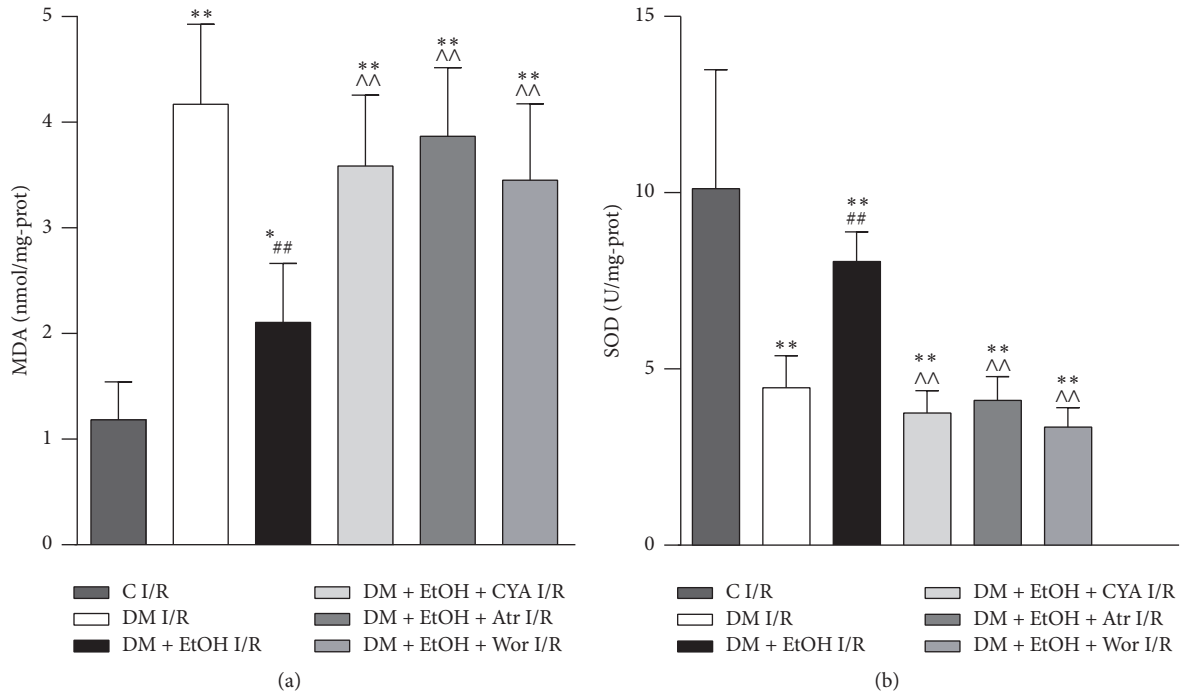

Figure 2: The levels of MDA (a) and SOD (b) of rats myocardium in each group (mean ± SD $n = 5$). $^{*}p < 0.05$, $^{**}p < 0.01$ versus C I/R; $^{\#\#}p < 0.01$ versus DM I/R; $^{\wedge\wedge}p < 0.01$ versus DM + EtOH I/R.

of LVEDP, cardiac oxidative stress injury was aggravated, as indicated by the decrease of SOD activity and increase of MDA content, and the expression of Bcl-2 mRNA was decreased while Bax mRNA was increased, also indicating that myocyte apoptosis was aggravated. Meanwhile, we also found that myocardial ultrastructure was damaged in DM I/R group. Myocardial ALDH2 at mRNA and protein levels were decreased in DM I/R group. When diabetes rats were pretreated with low concentration of EtOH, which was used as a tool to induce ALDH2 activity, LDH level was decreased; whereas LVDP, $\pm dp/dt_{\max}$, RP, SOD activity and Bcl-2 mRNA level were increased, MDA content and Bax mRNA level were decreased. Also, the injury to myocardial ultrastructure was attenuated. The effect of EtOH was associated with increased myocardial ALDH2 mRNA and protein levels. When the diabetic rats were treated with CYA, Wor, or Atr after EtOH intervention, the injury was increased, and ALDH2 activity was reduced, and LDH level was decreased; whereas LVDP, $\pm dp/dt_{\max}$, RPP, SOD activity and Bcl-2 mRNA level were increased, MDA content and Bax mRNA levels were decreased. At the same time, the injury to myocardial ultrastructure was aggravated in DM + EtOH + CYA I/R group, and the changes in DM + EtOH + Atr I/R group and DM + EtOH + Wor I/R group were similar to DM + EtOH + CYA I/R group. These results suggested that decreases in ALDH2 expression may play a key role in myocardial I/R injury in diabetic rats. Upregulation of ALDH2 can protect the heart against myocardial I/R injury, and the mechanism may be through activation of PI3K-Akt signaling pathway and inhibiting mitoPTP opening.

Cardiovascular complications remain the leading cause of diabetes related mortality and morbidity. The oxidative stress of diabetes can increase myocardial I/R injury; myocardial I/R injury produced excessive amounts of reactive oxygen species and increasingly aggravated the injury of myocardial reperfusion. Several reports in recent years had discussed the association between ALDH2 and myocardial injury. Overexpression of ALDH2 offers myocardial protection maybe against alcohol-induced cardiac tissue and cellular injury. Enhanced ALDH2 activity by the direct effect of ALDH2 activator-1 or ethanol preconditioning led to cardiac protection against I/R injury; on the other hand, myocardial I/R injury may be exacerbated after ALDH2 knockout in mice [28, 29]. Earlier findings from our group also indicated that activation of ALDH2 with ethanol attenuated diabetes-induced myocardial injury in rats [27]. However, there are few researches on the relationship of myocardial ALDH2 and diabetes myocardial ischemia/reperfusion injury. Recent evidence revealed that ALDH2 prevented ROS-induced vascular contraction in angiotensin-II induced hypertensive mice [30]. ALDH2 overexpression attenuated hyperoxia-induced cell death in lung epithelial cells through reduction of ROS, activation of ERK/MAPK, and PI3K-Akt signaling pathways [31]. Thus far, there have been no reports about the changes of ALDH2 in diabetes myocardial I/R injury, and the underlying cellular mechanisms are not clear.

Therefore, in the present study, we firstly sought to determine whether ALDH2 expression also changed in diabetes myocardial I/R injury model. In previous study, we observed that, with the progression of diabetes, myocardial ALDH2

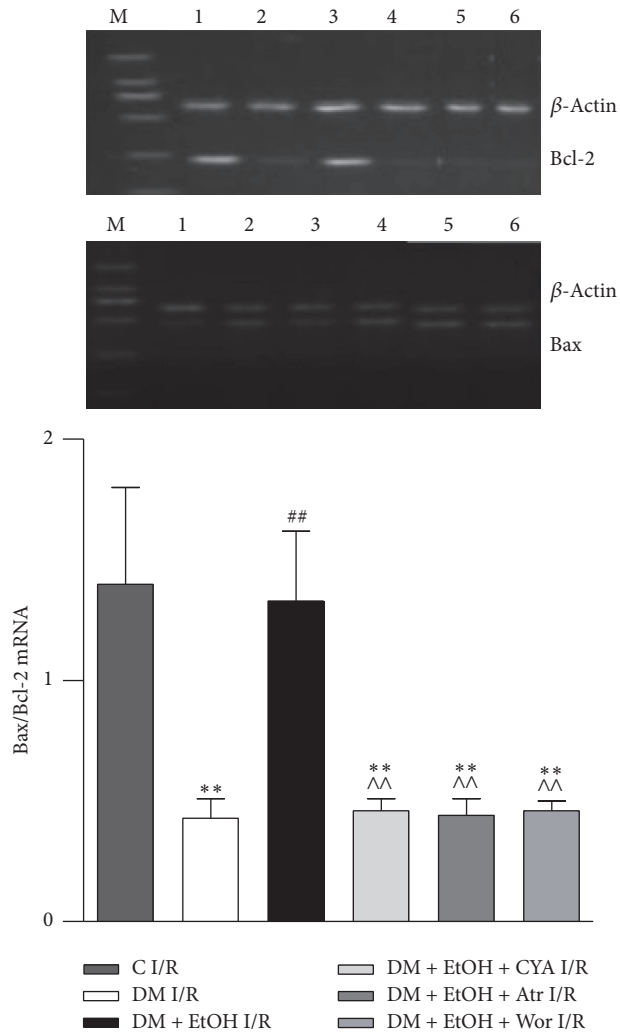

Figure 3: The expressions of Bcl-2 and Bax mRNA of heart tissue in rats (mean ± SD of 5 separate experiments). $^{**}p < 0.01$ versus C I/R; $^{\#\#}p < 0.01$ versus DM I/R; $^{\wedge\wedge}p < 0.01$ versus DM + EtOH I/R. (1) C I/R; (2) DM I/R; (3) DM + EtOH I/R; (4) DM + EtOH + CYA I/R; (5) DM + EtOH + Atr I/R; (6) DM + EtOH + Wor I/R.

expression was further decreased accompanying decreased ventricular function, and activation of ALDH2 can decrease diabetes- induced myocardial injury. In the present study, we used diabetic I/R model and observed cardiac systolic and diastolic function was destroyed, and myocardial ultrastructure was damaged accompanied with the aggravation of oxidative stress. At the same time, myocardial ALDH2 at mRNA and protein levels were decreased, and LDH release in the coronary effluent was increased. It is suggested that the expression of ALDH2 was related to the cardiac I/R injury induced by diabetes.

ALDH2 as an antioxidant enzyme may be easily inactivated by free radicals. Recently, ALDH2 was identified as a target for oxidative modification during glyceryl trinitrate tolerance [32, 33]; and ALDH2 activity was correlated inversely with cardiac infarct size in rat hearts subjected to ischemia and reperfusion ex vivo [34]. We used low concentration of EtOH as a tool to induce ALDH2 activity to investigate whether upregulation of ALDH2 expression could benefit recovery from myocardial function; it is likely that increasing ALDH2 expression can attenuate the happening of oxidative stress and the destroying of myocardial function. These findings suggest that, compared with diabetic I/R group, ALDH2 overexpression can exert the protective effect against cardiac I/R injury of diabetes. However, the ALDH2 inhibitor CYA, which was involved in ALDH2, conferred protection against cardiac I/R injury, and LDH release was increased, and the expressions of ALDH2 at mRNA and protein level were decreased. The result showed that ALDH2 overexpression reconciled diabetes-induced contractile dysfunction, whereas cardioprotection elicited by ALDH2 was blocked by the inhibitor CYA. Further study is required to better elucidate the mechanism of ALDH2. Mitochondrial permeability transition pore (mitoPTP) is a nonselective highly conductive channel which exists between mitochondrial inner and outer membranes, playing an important role in apoptosis. The opening of mitoPTP is an ultimate target of all kinds of damage; ischemia/reperfusion induced mitoPTP to open and also induced the overload of intracellular calcium, accumulation of ROS, and increase in PH and other factors [35]. Argaud et al. reported in the rabbit myocardial ischemia model that when the rabbits were given preconditioning, postconditioning, and mitoPTP inhibitor, respectively, during reperfusion, the effects were similar in reducing myocardial infarct size, and the tolerance of myocardial mitochondria was decreased for calcium overload in I/R injury. However, the myocardial mitochondria resistance was increased after postconditioning or mitoPTP inhibitor treatment [36]. These studies indicated that postconditioning may be via inhibiting the opening of mitoPTP resulting in reducing the myocardial damage by overload of calcium. It is suggested that the myocardial protection of preconditioning and postconditioning was involved in suppression of open mitoPTP. In the present paper, we further investigate the role of ALDH2 in the diabetic rat hearts. In our study, we used the specific openers of mitoPTP atractyloside (Atr). The result suggested that Atr canceled the protection of EtOH; indeed, we found the ALDH2 mRNA and protein levels were reduced; meanwhile, cardiac LV contractile function was declining and myocardial ultrastructure was damaged accompanied with the aggravation of oxidative stress. Zhou et al. reported on hydrogen peroxide-induced myocardial injury model. Low concentration of ethanol can inhibit the opening of mitoPTP induced by oxidative stress via GSK-3β pathway and PI3K/Akt; however, high concentration of ethanol-fed rats can induce the cell apoptosis and opening of mitoPTP [37, 38]. These results displayed that promoting the opening of mitoPTP might be via inhibiting ALDH2 generation against its protection.

It is well known that PI3K/Akt signaling is a key mediator of cell survival. Akt is also implicated in the cardioprotection for cardiac myocyte survival [39]. However, the role of Akt signaling in regulation of diabetic rat myocardial I/R injury is not clear. Activation of Akt was found to rescue the cardiac mechanical function defect induced by ER stress [40]. In the study, we used the PI3K/Akt inhibitor wortmannin

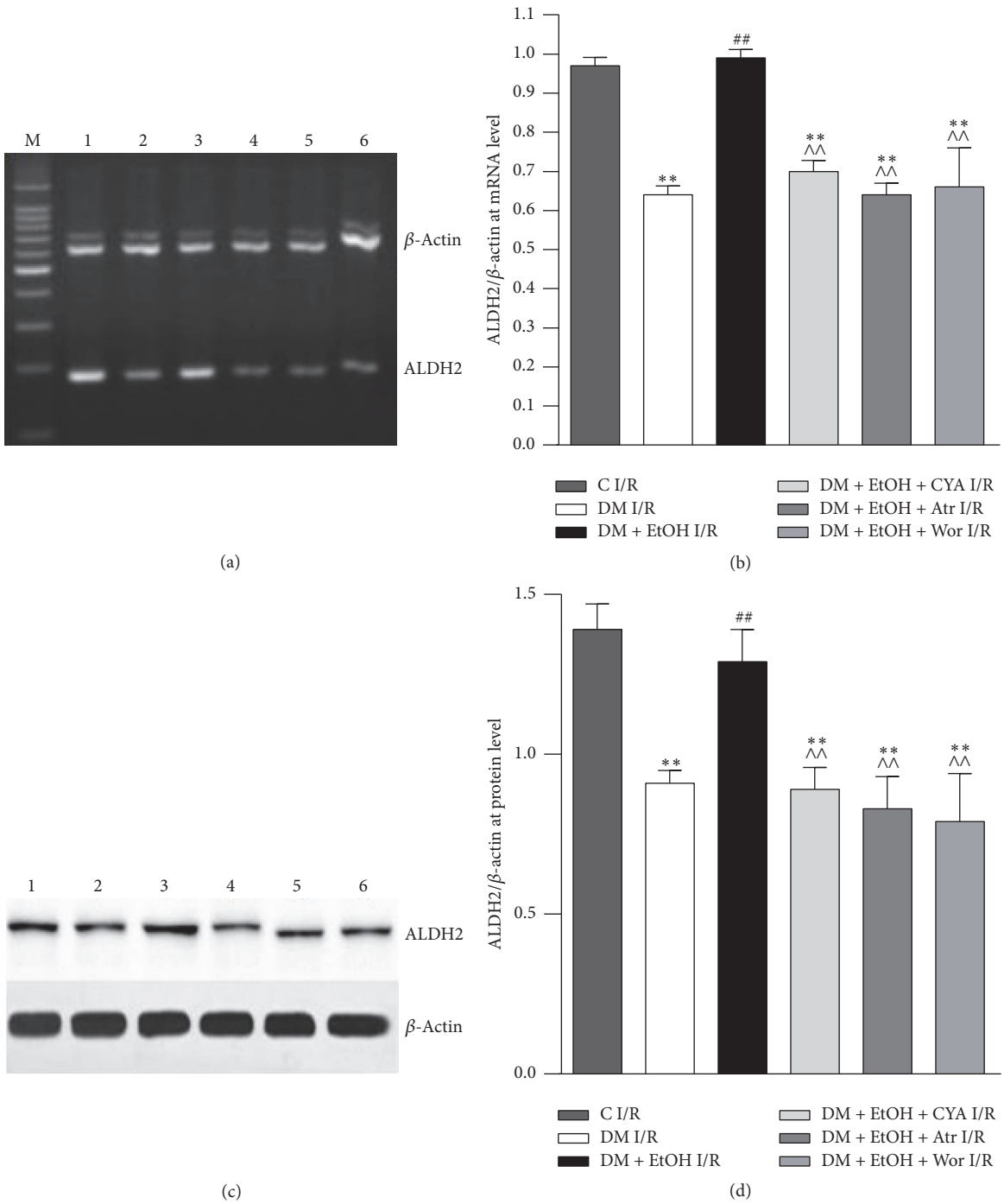

Figure 4: Expressions of ALDH2 at mRNA (a, b) and protein (c, d) level of heart tissue in rats (mean ± SD of 5 separate experiments). $^{**}p < 0.01$ versus C I/R; $^{\#\#}p < 0.01$ versus DM I/R; $^{\wedge\wedge}p < 0.01$ versus DM + EtOH I/R. (1) C I/R; (2) DM I/R; (3) DM + EtOH I/R; (4) DM + EtOH + CYA I/R; (5) DM + EtOH + Atr I/R; (6) DM + EtOH + Wor I/R.

(Wor); compared with DM + EtOH I/R group, ALDH2 mRNA and protein levels were decreased; meanwhile, cardiac LV contractile function and myocardial ultrastructure were damaged accompanied with the aggravation of oxidative stress. Data depicted that ALDH2 induced cell survival was blocked by inhibition of PI3K. These results suggested that the protection of ALDH2 was at least partially mediated by PI3K/Akt pathway. However, further study is required to better elucidate the mechanism of ALDH2 cardiac protection.

I/R injury is a complex process and results in oxidative stress in myocardium, such as O_2^- and H_2O_2 accumulating and resulting in cellular toxicity, finally due to imbalance between production and removal of ROS. The survival myocardial cells after myocardial infarction were more prone

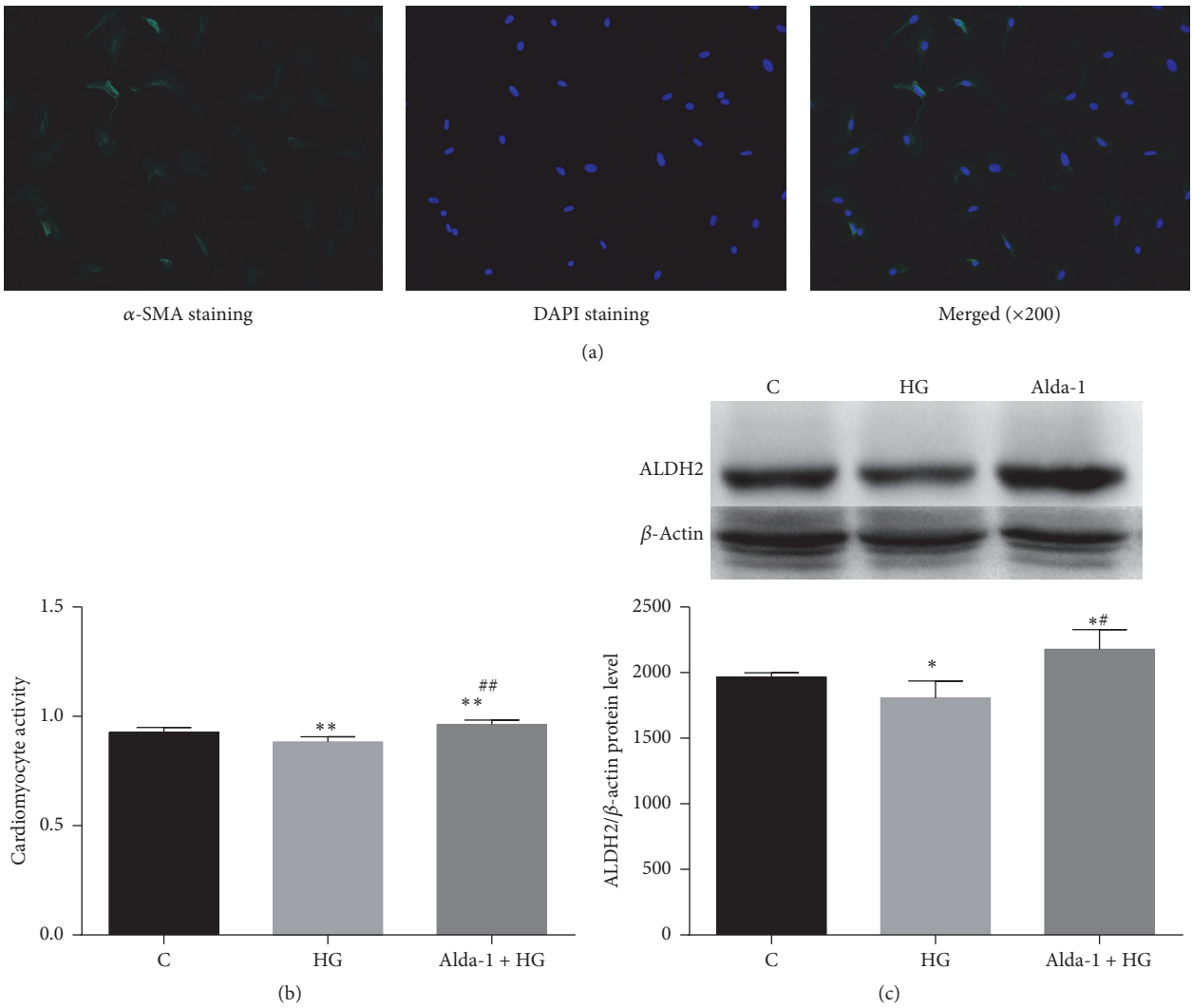

FIGURE 5: Identify cardiomyocytes by immunofluorescence (a), CCK-8 activity (b), and expressions of ALDH2 protein level of cardiomyocyte in rats (c) (mean ± SD of five separate experiments). $^{*}p < 0.05$, $^{**}p < 0.01$ versus C, $^{\#}p < 0.05$, and $^{\#\#}p < 0.01$ versus HG.

to calcium overload and therefore more susceptible to I/R injury; accumulating evidence proved that overproduction of ROS triggered myocyte apoptosis by upregulating proapoptotic members of Bcl-2 family. In addition, investigators have shown that Bcl-2 gene family is known to modulate the permeability of the mitochondrial membrane and the release of cytochrome C [41]. Therefore, we investigated whether the expressions of Bax and Bcl-2 genes are related to ALDH2 induced protection in diabetic myocardial I/R injury. In our study, we detected Bax and Bcl-2 at mRNA levels. The result showed that the expression of cardiac Bcl-2 at mRNA level was decreased, the expression of Bax at mRNA level was increased, Bcl-2/Bax mRNA was decreased in DM I/R group, and LDH release in the coronary effluent of diabetic rats was increased. Meanwhile, ALDH2 mRNA and protein were decreased. However, compared with DM I/R group, the ratio of Bax to Bcl-2 mRNA and LDH levels were decreased in DM + EtOH I/R group, and the expressions of ALDH2 mRNA and protein were increased, which suggested that the increase of myocardial cells apoptosis may be associated with the decrease of ALDH2. To further prove our hypothesis, via given drug intervention, ALDH2 inhibitor CYA, PI3K inhibitor Wor, and the opener of mitoPTP Atr, the result suggests the ratio of Bax to Bcl-2 mRNA was decreased; meanwhile, ALDH2 levels were decreased accompanied with the changes of cardiac LV contractile function, oxidative stress, and myocardial ultrastructure.

To verify whether cardiac ALDH2 directly participates in diabetes-induced cardiomyocyte injury, in this study, we also applied high glucose induced cardiomyocyte injury to mimic diabetes. We found that, in cardiomyocytes model, compared with C group, CCK-8 activity and the ALDH2 protein expression were decreased in HG group; when cardiomyocytes were pretreated with Alda-1, the specific activator of ALDH2 in HG condition, CCK-8 activity was increased accompanied with the increase of ALDH2 protein expression. It is suggested that direct activation of cardiomyocyte ALDH2 attenuated high glucose induced myocardial injury. It is worthwhile to note

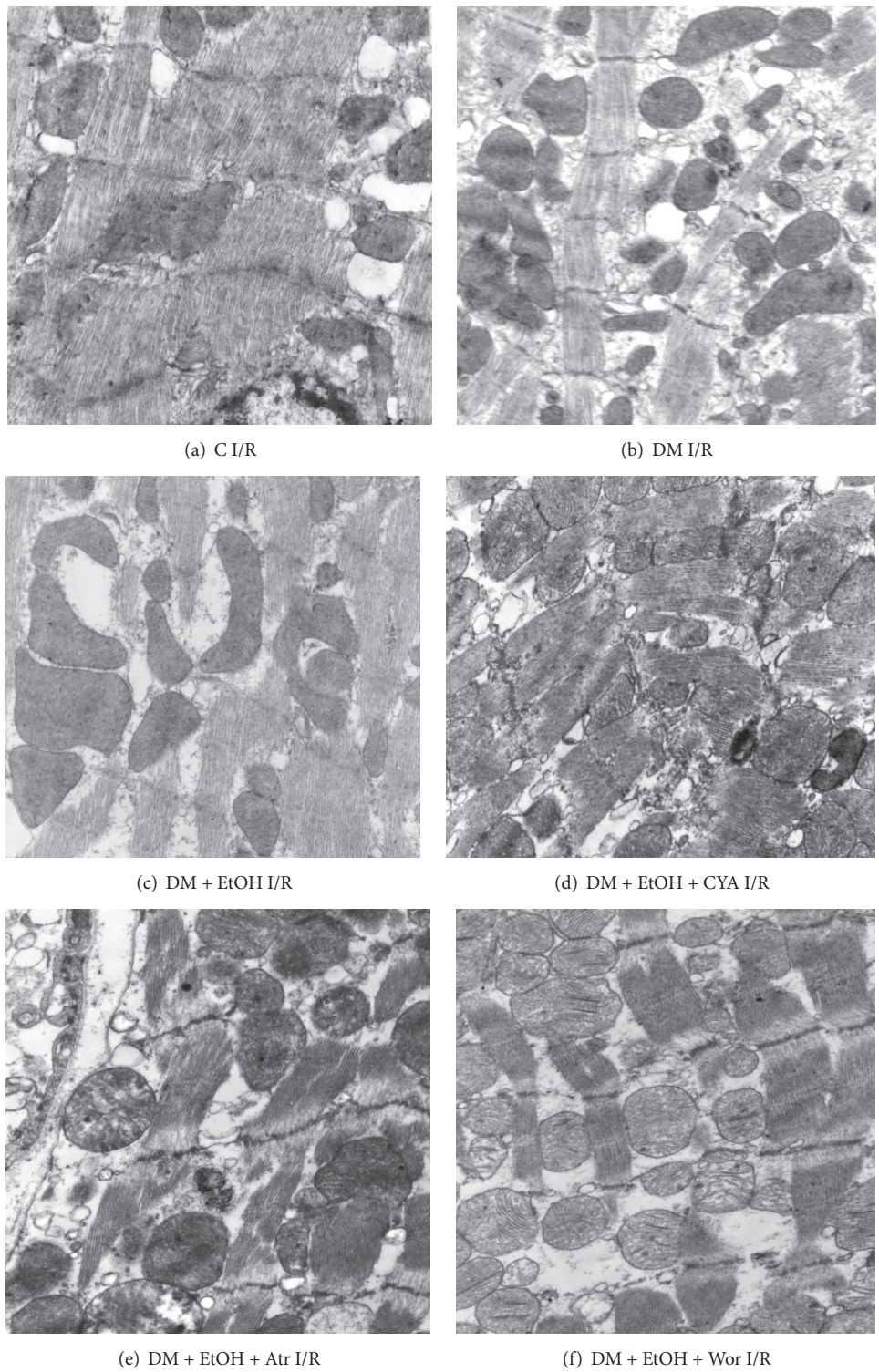

(a) C I/R (b) DM I/R

(c) DM + EtOH I/R (d) DM + EtOH + CYA I/R

(e) DM + EtOH + Atr I/R (f) DM + EtOH + Wor I/R

Figure 6: Changes of rat myocardium ultrastructural organization in each group (magnification: 10K).

that there were some limitations in our study. In cardiomyocyte model, we only observed the protection of enhanced ALDH2 expression in HG condition. To better understand the mechanism involved, we will investigate the effect of cardiomyocytes ALDH2 in hypoxia and reoxygenation status and further validate our hypothesis.

In conclusion, activation of ALDH2 participates in the regulation of diabetic I/R injury induced cardiac myocyte apoptosis via mitochondrial pathway. ALDH2 may play an antiapoptotic effect through decreasing the ratio of Bax/Bcl-2, activation of PI3K/Akt signaling pathway, and inhibiting mitoPTP opening. Promoting ALDH2 expression may

become a new pathway for the clinical treatment DM with CHD patients, and further studies are necessary to confirm this hypothesis.

Competing Interests

The authors declare that they have no competing interests.

Authors' Contributions

Pin-Fang Kang, and Wen-Juan Wu contributed equally to this work.

Acknowledgments

This work was supported by research grants from National China Natural Science Foundation (nos. 81000074 and 81550036) and from Anhui Province Natural Science Foundation (no. 1508085MH169) and Anhui Province Education Key Projects (no. KJ2016A484), China, and Key Project of Top-Notch Talent of Discipline (specialty) of the higher Education Institute of Anhui Province 2016 (no. gxbjZD2016072), China.

References

[1] E. Adeghate, P. Schattner, and E. Dunn, "An update on the etiology and epidemiology of diabetes mellitus," *Annals of the New York Academy of Sciences*, vol. 1084, pp. 1–29, 2006.

[2] C. Gremizzi, A. Vergani, V. Paloschi, and A. Secchi, "Impact of pancreas transplantation on type 1 diabetes-related complications," *Current Opinion in Organ Transplantation*, vol. 15, no. 1, pp. 119–123, 2010.

[3] S. Boudina and E. D. Abel, "Diabetic cardiomyopathy revisited," *Circulation*, vol. 115, no. 25, pp. 3213–3223, 2007.

[4] M. Kooistra, M. I. Geerlings, W. P. T. M. Mali, K. L. Vincken, Y. Van Der Graaf, and G. J. Biessels, "Diabetes mellitus and progression of vascular brain lesions and brain atrophy in patients with symptomatic atherosclerotic disease. The SMART-MR study," *Journal of the Neurological Sciences*, vol. 332, no. 1-2, pp. 69–74, 2013.

[5] Y. Zhang and J. Ren, "ALDH2 in alcoholic heart diseases: molecular mechanism and clinical implications," *Pharmacology and Therapeutics*, vol. 132, no. 1, pp. 86–95, 2011.

[6] J. Ren, "Acetaldehyde and alcoholic cardiomyopathy: lessons from the ADH and ALDH2 transgenic models," *Novartis Foundation Symposium*, vol. 285, pp. 69–76, 2007.

[7] G. R. Budas, M.-H. Disatnik, and D. Mochly-Rosen, "Aldehyde dehydrogenase 2 in cardiac protection: a new therapeutic target?" *Trends in Cardiovascular Medicine*, vol. 19, no. 5, pp. 158–164, 2009.

[8] H. J. Forman, J. M. Fukuto, T. Miller, H. Zhang, A. Rinna, and S. Levy, "The chemistry of cell signaling by reactive oxygen and nitrogen species and 4-hydroxynonenal," *Archives of Biochemistry and Biophysics*, vol. 477, no. 2, pp. 183–195, 2008.

[9] D. R. Petersen and J. A. Doorn, "Reactions of 4-hydroxynonenal with proteins and cellular targets," *Free Radical Biology and Medicine*, vol. 37, no. 7, pp. 937–945, 2004.

[10] H. Ma, J. Li, F. Gao, and J. Ren, "Aldehyde dehydrogenase 2 ameliorates acute cardiac toxicity of ethanol: role of protein phosphatase and forkhead transcription factor," *Journal of the American College of Cardiology*, vol. 54, no. 23, pp. 2187–2196, 2009.

[11] T. A. Doser, S. Turdi, D. P. Thomas, P. N. Epstein, S.-Y. Li, and J. Ren, "Transgenic overexpression of aldehyde dehydrogenase-2 rescues chronic alcohol intake-induced myocardial hypertrophy and contractile dysfunction," *Circulation*, vol. 119, no. 14, pp. 1941–1949, 2009.

[12] W. Ge, R. Guo, and J. Ren, "AMP-dependent kinase and autophagic flux are involved in aldehyde dehydrogenase-2-induced protection against cardiac toxicity of ethanol," *Free Radical Biology and Medicine*, vol. 51, no. 9, pp. 1736–1748, 2011.

[13] E. N. Churchill, M. H. Disatnik, and D. Mochly-Rosen, "Time-dependent and ethanol-induced cardiac protection from ischemia mediated by mitochondrial translocation of varepsilonPKC and activation of aldehyde dehydrogenase 2," *Journal of Molecular and Cellular Cardiology*, vol. 46, no. 2, pp. 278–284, 2009.

[14] C.-H. Chen, G. R. Budas, E. N. Churchill, M.-H. Disatnik, T. D. Hurley, and D. Mochly-Rosen, "Activation of aldehyde dehydrogenase-2 reduces ischemic damage to the heart," *Science*, vol. 321, no. 5895, pp. 1493–1495, 2008.

[15] G. R. Budas, M.-H. Disatnik, C.-H. Chen, and D. Mochly-Rosen, "Activation of aldehyde dehydrogenase 2 (ALDH2) confers cardioprotection in protein kinase C epsilon (PKCε) knockout mice," *Journal of Molecular and Cellular Cardiology*, vol. 48, no. 4, pp. 757–764, 2010.

[16] J. Wang, H. Wang, P. Hao et al., "Inhibition of aldehyde dehydrogenase 2 by oxidative stress is associated with cardiac dysfunction in diabetic rats," *Molecular Medicine*, vol. 17, no. 3-4, pp. 172–179, 2011.

[17] H.-J. Wang, P.-F. Kang, W.-J. Wu et al., "Changes in cardiac mitochondrial aldehyde dehydrogenase 2 activity in relation to oxidative stress and inflammatory injury in diabetic rats," *Molecular Medicine Reports*, vol. 8, no. 2, pp. 686–690, 2013.

[18] S.-B. Ong, S. Subrayan, S. Y. Lim, D. M. Yellon, S. M. Davidson, and D. J. Hausenloy, "Inhibiting mitochondrial fission protects the heart against ischemia/reperfusion injury," *Circulation*, vol. 121, no. 18, pp. 2012–2022, 2010.

[19] A. Rasola and P. Bernardi, "The mitochondrial permeability transition pore and its involvement in cell death and in disease pathogenesis," *Apoptosis*, vol. 12, no. 5, pp. 815–833, 2007.

[20] D. B. Zorov, M. Juhaszova, Y. Yaniv, H. B. Nuss, S. Wang, and S. J. Sollott, "Regulation and pharmacology of the mitochondrial permeability transition pore," *Cardiovascular Research*, vol. 83, no. 2, pp. 213–225, 2009.

[21] C. Wang and R. J. Youle, "The role of mitochondria in apoptosis," *Annual Review of Genetics*, vol. 43, pp. 95–118, 2009.

[22] S. M. Davidson, D. Hausenloy, M. R. Duchen, and D. M. Yellon, "Signalling via the reperfusion injury signalling kinase (RISK) pathway links closure of the mitochondrial permeability transition pore to cardioprotection," *International Journal of Biochemistry and Cell Biology*, vol. 38, no. 3, pp. 414–419, 2006.

[23] S. Y. Lim, S. M. Davidson, D. J. Hausenloy, and D. M. Yellon, "Preconditioning and postconditioning: the essential role of the mitochondrial permeability transition pore," *Cardiovascular Research*, vol. 75, no. 3, pp. 530–535, 2007.

[24] Z. H. Li, C. R. Jiang, M. L. Xia et al., "Activation of mitochondrial aldehyde dehydrogenase 2 and inhibition of mitochondrial permeability transition pore involved in cardioprotection of ethanol postconditioning," *Zhe Jiang Da Xue Xue Bao Yi Xue Ban*, vol. 39, no. 6, pp. 566–571, 2010.

[25] J. Liao, A. Sun, Y. Xie et al., "Aldehyde dehydrogenase-2 deficiency aggravates cardiac dysfunction elicited by endoplasmic reticulum stress induction," *Molecular Medicine*, vol. 18, no. 5, pp. 785–793, 2012.

[26] E. K. Iliodromitis, C. Gaitanaki, A. Lazou et al., "Differential activation of mitogen-activated protein kinases in ischemic and nitroglycerin-induced preconditioning," *Basic Research in Cardiology*, vol. 101, no. 4, pp. 327–335, 2006.

[27] Q. Gao, H.-J. Wang, X.-M. Wang et al., "Activation of ALDH2 with ethanol attenuates diabetes induced myocardial injury in rats," *Food and Chemical Toxicology*, vol. 56, pp. 419–424, 2013.

[28] N. S. Chandel, D. S. McClintock, C. E. Feliciano et al., "Reactive oxygen species generated at mitochondrial complex III stabilize hypoxia-inducible factor-1α during hypoxia: a mechanism of O_2 sensing," *The Journal of Biological Chemistry*, vol. 275, no. 33, pp. 25130–25138, 2000.

[29] R. Aikawa, M. Nawano, Y. Gu et al., "Insulin prevents cardiomyocytes from oxidative stress-induced apoptosis through activation of PI3 kinase/Akt," *Circulation*, vol. 102, no. 23, pp. 2873–2879, 2000.

[30] H. Choi, R. C. Lee, H. Y. Wong et al., "Lipid peroxidation dysregulation in ischemiac stroke:plasma 4-HNE as a potential bio-marker?" *Biochemical and Biophysical Research Communications*, vol. 425, no. 4, pp. 842–847, 2012.

[31] D. Xu, J. R. Guthrie, S. Mabry, T. M. Sack, and W. E. Truog, "Mitochondrial aldehyde dehydrogenase attenuates hyperoxia-induced cell death through activation of ERK/MAPK and PI3K-Akt pathways in lung epithelial cells," *American Journal of Physiology—Lung Cellular and Molecular Physiology*, vol. 291, no. 5, pp. L966–L975, 2006.

[32] K. Sydow, A. Daiber, M. Oelze et al., "Central role of mitochondrial aldehyde dehydrogenase and reactive oxygen species in nitroglycerin tolerance and cross-tolerance," *The Journal of Clinical Investigation*, vol. 113, no. 3, pp. 482–489, 2004.

[33] P. Wenzel, U. Hink, M. Oelze et al., "Role of reduced lipoic acid in the redox regulation of mitochondrial aldehyde dehydrogenase (ALDH-2) activity: implications for mitochondrial oxidative stress and nitrate tolerance," *The Journal of Biological Chemistry*, vol. 282, no. 1, pp. 792–799, 2007.

[34] W. Ge and J. Ren, "MTOR-STAT3-notch signalling contributes to ALDH2-induced protection against cardiac contractile dysfunction and autophagy under alcoholism," *Journal of Cellular and Molecular Medicine*, vol. 16, no. 3, pp. 616–626, 2012.

[35] F. Di Lisa and P. Bernardi, "Mitochondria and ischemia-reperfusion injury of the heart: fixing a hole," *Cardiovascular Research*, vol. 70, no. 2, pp. 191–199, 2006.

[36] L. Argaud, O. Gateau-Roesch, O. Raisky, J. Loufouat, D. Robert, and M. Ovize, "Postconditioning inhibits mitochondrial permeability transition," *Circulation*, vol. 111, no. 2, pp. 194–197, 2005.

[37] K. Zhou, L. Zhang, J. Xi, W. Tian, and Z. Xu, "Ethanol prevents oxidant-induced mitochondrial permeability transition pore opening in cardiac cells," *Alcohol and Alcoholism*, vol. 44, no. 1, pp. 20–24, 2009.

[38] A. L. King, T. M. Swain, D. A. Dickinson, M. J. Lesort, and S. M. Bailey, "Chronic ethanol consumption enhances sensitivity to Ca^{2+}-mediated opening of the mitochondrial permeability transition pore and increases cyclophilin D in liver," *American Journal of Physiology—Gastrointestinal and Liver Physiology*, vol. 299, no. 4, pp. G954–G966, 2010.

[39] T. L. Yuan, G. Wulf, L. Burga, and L. C. Cantley, "Cell-to-cell variability in PI3K protein level regulates PI3K-AKT pathway activity in cell populations," *Current Biology*, vol. 21, no. 3, pp. 173–183, 2011.

[40] Y. Zhang and J. Ren, "Thapsigargin triggers cardiac contractile dysfunction via NADPH oxidase-mediated mitochondrial dysfunction: role of Akt dephosphorylation," *Free Radical Biology and Medicine*, vol. 51, no. 12, pp. 2172–2184, 2011.

[41] R. M. Kluck, E. Bossy-Wetzel, D. R. Green, and D. D. Newmeyer, "The release of cytochrome c from mitochondria: a primary site for Bcl-2 regulation of apoptosis," *Science*, vol. 275, no. 5303, pp. 1132–1136, 1997.

Hindawi Publishing Corporation
Oxidative Medicine and Cellular Longevity
Volume 2016, Article ID 1973834, 18 pages
http://dx.doi.org/10.1155/2016/1973834

Review Article

New Insights into the Role of Oxidative Stress Mechanisms in the Pathophysiology and Treatment of Multiple Sclerosis

Bożena Adamczyk and Monika Adamczyk-Sowa

Department of Neurology in Zabrze, Medical University of Silesia, ul. 3 Maja 13-15, 41-800 Zabrze, Poland

Correspondence should be addressed to Bożena Adamczyk; bozena.m.adamczyk@gmail.com

Received 18 May 2016; Revised 5 August 2016; Accepted 19 September 2016

Academic Editor: Capucine Trollet

Multiple sclerosis (MS) is a multifactorial disease of the central nervous system (CNS) characterized by an inflammatory process and demyelination. The etiology of the disease is still not fully understood. Therefore, finding new etiological factors is of such crucial importance. It is suspected that the development of MS may be affected by oxidative stress (OS). In the acute phase OS initiates inflammatory processes and in the chronic phase it sustains neurodegeneration. Redox processes in MS are associated with mitochondrial dysfunction, dysregulation of axonal bioenergetics, iron accumulation in the brain, impaired oxidant/antioxidant balance, and OS memory. The present paper is a review of the current literature about the role of OS in MS and it focuses on all major aspects. The article explains the mechanisms of OS, reports unique biomarkers with regard to their clinical significance, and presents a poorly understood relationship between OS and neurodegeneration. It also provides novel methods of treatment, including the use of antioxidants and the role of antioxidants in neuroprotection. Furthermore, adding new drugs in the treatment of relapse may be useful. The article considers the significance of OS in the current treatment of MS patients.

1. Introduction

Multiple sclerosis (MS) is a multifactorial disease of the central nervous system (CNS) in which both inflammatory and neurodegenerative processes occur simultaneously. In the course of the disease inflammation is decreased whereas the degeneration of the CNS progresses [1]. Several forms of MS are distinguished. These are the following: RRMS (relapsing-remitting MS), SPMS (secondary progressive MS), and PPMS (primary progressive MS). In RRMS an inflammatory process predominates whereas in SPMS and PPMS a neurodegenerative process is more strongly expressed. Relapses defined as episodic exacerbations of neurological signs or symptoms are characteristic of RRMS [2]. Between the relapses patients fully or partially recover from the deficit. The most common form of MS is RRMS which may progress into SPMS after years of remission; SPMS is a natural consequence of RRMS in which relapses decrease and finally disappear over time. In PPMS relapses do not occur from the onset of MS. Progressive axonal loss typically accompanies the PPMS form [3]. As a result, in the course of progressive forms the dominance of neurodegeneration is related to a lack of functional improvement [4, 5].

The ultimate causative factor of this process remains unknown. However, it is suspected that the development of MS may be affected by genetic and environmental factors. Recent observations confirm the fact that oxidative stress (OS) became an important factor associated with the development of demyelination [1, 6, 7].

2. The Importance of OS in MS

The inflammatory component in MS is important not only due to axonal and neuronal loss but also due to the fact that it starts the degenerative cascade in the early stage of MS [6]. Interestingly, persistent hyperactivation of oxidative enzymes suggests an "OS memory" in chronic neuroinflammation [62]. The induction of the activation of microglia and mitochondrial dysfunction plays a particular role in inflammatory processes. Microglia activated by T-lymphocytes release proteolytic enzymes, cytokines, oxidative products, and free radicals. On the other hand, microglia have a number of

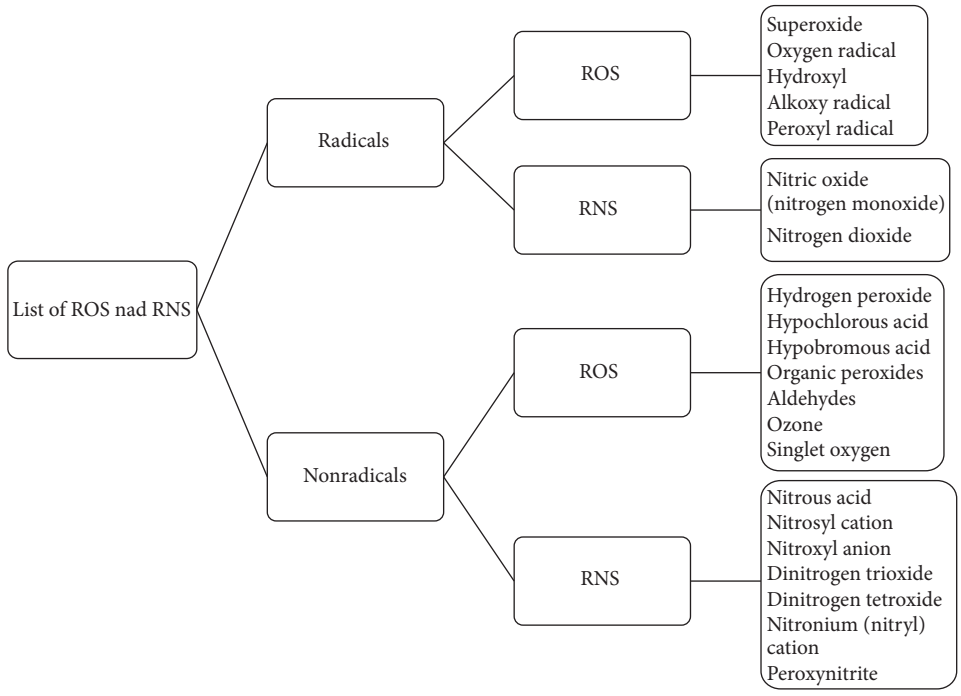

Figure 1: Reactive oxygen species (ROS) and reactive nitrogen species (RNS) [5, 59–61]. The classification of ROS and RNS depended on having an unpaired electron. Nonradial species exists without an unpaired electron.

protective properties [59] such as a positive role in the promotion of neuroprotection, lowering inflammation, and stimulation of tissue repair [60].

The development of neurodegeneration in MS is a complex process that may be related to primary apoptosis, synaptopathy, and excitotoxicity associated with glutamate overload, ionic channel dysfunction, calcium overload, mitochondriopathy, proteolytic enzyme production, and activation of apoptotic pathways. It is also important that mitochondrial dysfunction results in an increased production of reactive oxygen species (ROS), which is detrimental to neurons and glia [12, 61]. On the other hand, OS damages the mitochondria, which disrupts the transport of adenosine triphosphate along the axon, and consequently leads to neurodegeneration [63–65]. Importantly, the neurodegenerative process is complicated and still poorly understood.

For a better understanding of the redox processes in the course of MS, some general issues related to OS need to be addressed.

2.1. The Mechanisms of OS. The brain tissue is very sensitive to the action of radicals due to its high demand for oxygen and a limited possibility of obtaining antioxidants. An imbalance between free radical production and antioxidative defense results in OS and nitrosative stress [18, 66].

A free radical can be defined as an unstable, short-lived, and highly reactive atom or molecule [18]. Free radicals, ROS and reactive nitrogen species (RNS), can affect important classes of biological molecules, thus leading to multiple lipid and protein damage via peroxidation and nitration processes [18].

The levels of ROS/RNS are involved in various physiological functions such as the immune function (i.e., defense against pathogenic microorganisms). They are also involved in a number of cellular signaling pathways, in the mitogenic response, and in the redox regulation [18, 67, 68]. Both ROS and RNS can be classified into two groups, that is, radicals and nonradicals [8, 10, 18, 69] (Figure 1).

The endogenous sources of ROS include mitochondria, peroxisomes, endoplasmic reticulum, and phagocytic cells. Macrophages constitute a major factor responsible for the production of ROS [10] due to high oxygen consumption [6, 18].

The redox reaction involves mainly a superoxide radical, hydrogen peroxide, hydroxyl radical anion, nitric oxide (NO), peroxynitrite [10, 13], peroxyl radical, singlet oxygen, ozone, and hypochlorous acid [18]. Some of these free radicals are described in more detail below.

The superoxide radical exists in two forms such as superoxide or hydroperoxyl radical anion [18]. The enzymes that can produce superoxide include xanthine oxidase [63], lipoxygenase, cyclooxygenase [9, 21], and nicotinamide adenine dinucleotide phosphate- (NADPH-) dependent oxidase [30].

Hydrogen peroxide is formed by the enzyme superoxide dismutase (SOD). It can easily penetrate the biological membranes and damage DNA by producing the hydroxyl radical [29]. The hydroxyl radical can strongly react with both organic and inorganic molecules [17].

Nitric oxide is generated by different nitric oxide synthases (NOSs). Three types of NOS isoforms are distinguished, that is, neuronal NOS (nNOS), endothelial NOS

(eNOS), and inducible NOS (iNOS). Nitric oxide is an important intracellular second messenger [18]. It is involved in a number of biological functions such as blood pressure regulation, smooth muscle relaxation, neurotransmission, defense mechanisms, and immune regulation [11].

Peroxynitrite, which is highly toxic, is formed by the reaction between the superoxide radical and NO (nitrogen monoxide) [61]. During the subsequent reaction, new reactive compounds lead to oxidation processes of lipids, proteins (methionine and tyrosine), and DNA [24].

2.2. Redox Processes in MS. Researchers suggest that dysregulation of axonal bioenergetics plays a critical role in OS and subsequent axonal injury [25, 64].

Interestingly, the examination of the cerebrospinal fluid (CSF) during exacerbation of MS revealed a bioenergetic failure that was associated with an increased mitochondrial proton leak and an increased expression of genes involved in oxidative damage [35–37]. Moreover, the presence of proinflammatory cytokines in the CSF and prooxidative markers (e.g., nitrotyrosine) led to cytokine-induced synaptic hyperexcitability and consequent glutamate-dependent neurotoxicity [34, 40].

Recent studies suggest the importance of ceramides in the CSF as signaling molecules leading to impaired mitochondrial function. The short-chain ceramides stimulated oxygen species production and led to neuronal death [23, 39].

Iron accumulation in the brain is of great importance. This process leads to chronic cell stress, resulting in axonal and neuronal death [70]. Abnormal iron accumulation was found in MS plaques. Extracellular hemoglobin oxidized and led to local OS through the globin radical which was responsible for myelin basic protein oxidative cross-linking and heme involved in lipid peroxidation [70].

The process of neurodegeneration depends on the liberation of iron from the myelin sheath during demyelination [22]. A diffuse neurodegenerative process is related to the high iron content in the basal ganglia [20]. Ferrous iron may strengthen oxidative injury in the presence of oxygen radicals produced by the oxidative burst [16, 26, 33]. Oxidative stress, mitochondrial injury, and energy failure may be involved in plaque formation and neurodegeneration in white and grey matter lesions [41, 56, 71]. Another scientific report suggested that neurodegeneration in MS was associated with chronic subclinical extravasation of hemoglobin into lesions, the dysfunction of different cellular protective mechanisms against extracellular hemoglobin reactivity and OS [57].

Other studies stressed that alterations in the oxidant/antioxidant balance contributed to the pathophysiology of MS. Consideration was given to the balance between the concentration of compounds such as lipid peroxidation levels, carbonyl protein content, DNA damage and SOD, CAT activities, vitamins C and E, and nonprotein thiol content [42]. Also, the presence of free radicals in the nervous tissue may be toxic; for example, peroxynitrite increases inflammation and in the chronic phase leads to such a high concentration that it may lead to neurodegeneration [13].

Due to a constant lack of useful markers of the disease, it is important to find compounds whose levels are easy to mark, which may bring vast clinical implications. The review of the literature presented below is an attempt to collect biomarkers.

2.3. Markers of OS for Assessment: Serum, Erythrocytes, CSF, Saliva, Urine. Free radicals can damage biological molecules including nucleic acids, proteins, and lipids [18, 66]. The products of these reactions can become markers of OS. Serum is the most common material for the evaluation of the components of OS. It allows the estimation of most enzymes, substrates, and products of redox reactions. These enzymes include xanthine oxidase, NOS, lipoxygenase, cyclooxygenase, myeloperoxidase [47], prolyl oligopeptidase [51], nicotinamide adenine dinucleotide phosphate-oxidase 1 (NOX1), and NADPH-dependent oxidase [30]. The following may become the markers of oxidative lipid damage: isoprostanes (IsoP-prostaglandin like substances), for example, 8-iso-prostaglandin (F2α-8-iso-PGF2α) which constitutes the product of lipid peroxidation of arachidonic acid, malondialdehyde (MDA) [18], the formation of fluorescent peroxidized lipid-protein covalent adducts, and the increase in conjugated diene [70]. Oxidative stress involves the oxidation of proteins and glycoxidation. The following are the results of this reaction: the glycophore content, the total level of advanced protein oxidation (AOPP), protein carbonyls, dityrosine level, N′-formylkynurenine, and a decreased level of serum protein thiol groups [55].

The other specific markers of protein oxidation such as tyrosine (a marker for hydroxyl radical) and 3-nitrotyrosine (a marker for RNS) [43] are also considered. Furthermore, 3-nitrotyrosine is a specific marker of peroxynitrite-induced cellular damage [18].

Another study showed a possibility of using parameters such as ketodienes and Schiff bases [46]. Other indicators in the serum included kynurenine, N′-formylkynurenine, thioredoxin [32], and 8-hydroxy-2′-deoxyguanosine [47].

The parameters used for the measurement of the overall level of OS among healthy individuals and patients with MS are as follows: the total oxidant status (TOS), the oxidative stress index (OSI), and the total antioxidant status (TAS). This reflects the overall level of OS. In turn, OSI is defined as the ratio of TOS to TAS. The total antioxidant status shows the overall level of antioxidant capacity of the human body [72]. The oxidative stress index determines the oxidant/antioxidant balance more reliably in the body.

Following further research, more mediators may be determined in the serum, such as thiobarbituric acid reactive substances, advanced oxidation protein products, fructosamine [73], and activated α-2-macroglobulin level [51]. Both AOPP and MDA may be also marked in erythrocytes [74, 75]. Furthermore, the following are also measured in the CSF: levels of MDA and IsoP [54, 76, 77], ceramides [78], chemokine 11 (CCL11) [79], AOPP, and a decreased level of total thiol groups [80].

Both saliva and urine may serve as a useful material. The levels of thiobarbituric acid reactive substances and advanced glycation end-products can be assessed in saliva [73]. Urine may be a good material for the assessment of urinary 8-iso-PGF2α, which is a marker of lipid peroxidation in vivo [81].

Researchers reported that acrolein (2-propenal) might strengthen OS [59]. Acrolein antibody strategy was indicated to measure local acrolein levels but quantification of urinary 3-hydroxypropylmercapturic acid (3-HPMA) was the best marker for measuring global acrolein accumulation when glutathione levels were not depleted [82].

Other biomarkers are serum levels of IL-6, tumor necrosis factor (TNF-α), interferon γ (IFN-γ), IL-4, IL-10, and IL-17, albumin, ferritin, plasma levels of lipid hydroperoxides (CL-LOOH), carbonyl protein, and nitric oxide metabolites (NOx) [83]. Lipophilic fluorescent end-CL-products of free radicals may be an interesting marker [84]. Oxidative stress is also evaluated by tert-butyl hydroperoxide-initiated chemiluminescence [85] or the formation of ROS from $2'$,$7'$-dichlorodihydrofluorescein-diacetate fluorescence [86].

The oxidative stress factors possible for assessment in serum, erythrocytes, CSF, saliva, and urine are collectively presented in Table 1.

2.4. Linking OS Markers with Disease Course, Relapses, Disability, and MRI Lesions. A number of researchers try to find OS markers which are connected with MS. The review of the literature shows that there are some OS markers of the disease course; for example, studies demonstrated a significant increase in the levels of 8-iso-PGF2α in the CSF of patients with SPMS [86]. Guan et al. showed high levels of urinary 8-iso-PGF2α (a marker of lipid peroxidation in vivo) in MS patients. The concentration of urinary 8-iso-PGF2α was significantly higher in patients with SPMS and PPMS as compared to the control group [81]. It was also shown that a reduced level of prolyl oligopeptidase activity and activated α-2-macroglobulin level in the plasma were characteristic of PPMS and RRMS [51]. In addition, in another study plasmatic AOPPs were equally higher in RRMS and SPMS patients [87].

Recently acrolein, an endogenously produced toxic compound and a pathological factor in MS, underwent analysis [88]. It may be used as a potential biomarker for diagnosis and prognosis of MS [82].

Results from the study of Fiorini et al. showed that proteins such as hemopexin, alpha-1-B glycoprotein, inter-a-trypsin inhibitor heavy chain H4, complement C3, and antithrombin III were found to be more oxidized in pathological samples. Oxidation of these proteins might be used to determine the level of OS in the body [1].

Recent scientific findings, which offer the first evidence of increased RNA oxidation in normal-appearing cortex of MS brain, seem to be of great importance. However, further studies are needed to clarify the role of RNA oxidation in MS brain [89].

Cerebrospinal fluid IsoP, which is an OS marker of relapse, was higher in patients with a first clinical attack suggestive of MS as compared to the controls [77]. In turn, lower vitamin D levels may be responsible for the development of MS [42]. It may be related to vitamin D-binding protein (DBP) which was found to be more oxidized in both remitting and relapsing phases. However, higher levels of oxidation rate of DBP were observed during relapses. The increased oxidation rate of DBP already observed in the remitting course showed that some molecular pathways were not completely suppressed during remission as compared to the controls [1].

The degree of oxidation of clusterin was upregulated in MS patients as compared to the healthy controls [1]. This protein was responsible for chaperone-activity already increased in the remitting phase and kept upregulated in the relapsing phase [1].

Karlík et al. reported higher levels of thiobarbituric acid reactive substances and advanced glycation end-products in the saliva of patients with relapse. The study also demonstrated an increase in other OS markers of relapses in the plasma such as thiobarbituric acid reactive substances, advanced oxidation protein products, and fructosamine [73].

Oxidative stress markers of disability included platelet hemostatic function which was advanced in SPMS patients and positively correlated with an increased production of the superoxide radical and with the Expanded Disability Status Scale (EDSS). It seems that the platelet function is activated by a high level of OS [90].

Furthermore, in one of the studies it was demonstrated that inflammation, oxidative and nitrosative stress biomarkers such as serum levels of IL-6, TNF-α, IFN-γ, IL-4, IL-10, and IL-17, albumin, ferritin, and plasma levels of CL-LOOH, carbonyl protein, AOPPs, NOx, TRAP, and NcoI TNFβ genotypes might be considered potential predictive biomarkers of high disability in MS (EDSS) and were associated with different aspects of disease progression (higher pyramidal symptoms, sensitive symptoms, and cerebellar symptoms) [83].

Another study, including 110 patients with MS, demonstrated that patients with insulin resistance (IR) had a higher level of disability (EDSS), higher levels of interleukin IL-6 and IL-17 and OS evaluated by tert-butyl hydroperoxide-initiated chemiluminescence and AOPPs compared to patients without IR. It appears that IR and adiposity could contribute to more OS and disability [85].

Other studies indicated that the EDSS and gadolinium enhancement lesion volume-Gd+ were affected by increased levels of OS in erythrocytes in CIS, RRMS, and SPMS patients (increased level of AOPP and MDA) [74, 75].

Summarizing the above observations, the following may become OS markers of disability (EDSS): advanced platelet hemostatic function and increased level of AOOPs and MDA in erythrocytes and plasma levels of CL-LOOH, carbonyl protein, AOPPs, NOx, and TRAP. Additionally, IL-6, IL-17, TNF-α, IFN-γ, IL-4, IL-10, IL-17, and OS were evaluated by tert-butyl hydroperoxide-initiated chemiluminescence.

Data on OS and MRI lesions reported that a higher level of AOPP and a decreased level of total thiol groups in the plasma and in the CSF were involved in the clinically isolated syndrome (CIS) and RRMS pathophysiology but not with total T2 weighted lesions number and Gd enhancement lesion volume [80].

3. The Importance of Antioxidants in MS

Oxidative stress at each stage of MS is a key element in the pathogenesis of the disease. At the time of relapse all these processes are intensified, leading to the loss of neurons

Table 1: Biomarkers of oxidative stress. Free radicals can damage biological molecules including nucleic acids, proteins, carbohydrates, and lipids with the participation of various enzymes. As a result of these reactions new compounds are formed which may become biomarkers. Most of the available biological materials can be used to measure the level of these compounds in MS patients.

(a)

The biological material: serum											
Enzyme	Reference	Lipid damage	Reference	Protein damage	Reference	RNA/DNA damage	Reference	Carbohydrate damage	Reference	Other	Reference
Xanthine oxidase	[8]	Isoprostanes	[5]	Nitrotyrosine	[5, 9]	8-Hydroxy-2′-deoxy guanosine	[10]	Fructosamine	[11]	Peroxynitrite	[12]
NADPH dependent oxidase	[13]	MDA	[5, 14, 15]	O-Tyrosine	[9]					TOS	[16, 17]
Monoamino oxidase	[18]	Fluorescent peroxidized lipid-protein covalent adducts	[19, 20]	Glycophore	[21]					OSI	[17]
Alpha-ketoglutarat dehydrogenase	[18]	CL-LOOH	[22]	AOPP	[21–27]					Thiobarbituric acid reacting substances	[11]
Glycerol phosphate dehydrogenase	[18]	Conjugated diene	[19]	Protein carbonyls	[21, 22]					α-2-Macroglobulin	[13]
Lipoxygenase	[10]			Dityrosine	[21]					Acrolein	[28]
Cyclooxygenase	[10]			N′-Formylkynurenine	[21, 29]					Schiff bases	[30]
Myeloperoxidase	[10]			Kynurenine	[29]					Lipophilic fluorescent end-CL-products	[20]
Prolyl oligopeptidase	[31]			Decreased proteins thiol groups	[21, 32]					Tert-Butyl hydroperoxide-initiated chemilumines-cence	[26]
Nitric oxide synthase	[31]									2′,7′-Dichlorodi: hydrofluorescein: diacetate fluorescence	[33]
										NOx	[22]
										CCL11	[34]
										IL-6	[22, 26]
										IL-17	[22, 26]
										TNF-α	[22]

(a) Continued.

The biological material: serum											
Enzyme	Reference	Lipid damage	Reference	Protein damage	Reference	RNA/DNA damage	Reference	Carbohydrate damage	Reference	Other	Reference
										IFN-γ	[22]
										IL-4	[22]
										IL-10	[22]

(b)

	The biological material							
	CSF	References	Erythrocyte	References	Urine	References	Saliva	References
Lipid damage	Isoprostanes 8-iso-PGF2α MDA	[35–37] [38] [35–37]	MDA	[24, 25]	8-Iso-PGF2α	[39]		
Protein damage	AOPP total thiol groups	[21, 23] [21, 23]	AOPP	[24, 25]			Advanced glycation end-products	[11]
Other	Ceramides CCL11	[40] [34]			3-Hydroxy propyl-mercapturic acid (acrolein metabolic)	[28]	Thiobarbituric acid reacting substances	[11]

SOD: superoxide dismutase, NOX1: nicotinamide adenine dinucleotide phosphate-oxidase 1, MDA: malondialdehyde, CL-LOOH: lipid hydroperoxides, NOx: nitric oxide metabolites, TOS: total oxidant status, OSI: oxidative stress index, TNF-α: tumor necrosis factor, IFN-γ: interferon γ, AOPP: advanced oxidation protein products, 8-iso-PGF2α: isoprostane, CCL11: chemokine 11, and CSF: cerebrospinal fluid.

Table 2: The types of antioxidants. The types of antioxidants depend on molecular structure. The table lists the most important barrier antioxidant enzymes and other compounds and ions which are not enzymes.

Enzymes oxidants [16, 29, 41–44]	Nonenzymatic antioxidants [13]	
	Low molecular weight antioxidants	Antioxidant elements
CAT	Uric acid	Ions: Cu, Fe, Zn, Mn
GPx	Vitamin C	
GR	Vitamin D	
SOD	Vitamin E	
Paraoxonase	Glutathione	
Arylesterase	Coenzyme Q	
GSTs	B-Carotene	
NQO1	AU	
Peroxiredoxin-3		
Thioredoxin-2, 6		
FeOx		
δ-ALA-D		

CAT: catalase, GPx: glutathione peroxidase, GR: glutathione reductase, SOD: superoxide dismutase, GSTs: glutathione-S-transferases, NQO1: NAD(P)H:quinone oxidoreductase 1, FeOx: ferroxidase, δ-ALA-D: δ aminolevulinate dehydratase, and AU: uric acid.

over years. Current treatment is focused on decreasing inflammation, however only partially on preventing neurodegeneration. It is possible that a new target of treatment will focus on neutralizing free radicals. The course of the disease is affected by the use of antioxidants and substances that affect antioxidant pathways which reduce the severity and cause faster remission and less pronounced course of neuroinflammation and neurodegeneration [76, 91].

The following is a short description of antioxidants and their practical application in MS.

3.1. Enzymatic and Nonenzymatic Antioxidants. Antioxidants, which are divided into enzymatic and nonenzymatic, are substances that protect the body against free radicals (Table 2). Among enzymes the most important include catalase (CAT), glutathione peroxidase (GPx), glutathione reductase (GR), superoxide dismutase (SOD), serum paraoxonase, arylesterase [45], and δ-aminolevulinate dehydratase (δ-ALA-D) activity [42]. Superoxide dismutase has three isoforms that is, copper/zinc SOD (SOD-1), manganese SOD (SOD-2), and extracellular EC-SOD [13]. It needs to be stressed that in the serum the major antioxidant enzymes include CAT, GPx, peroxiredoxins [18, 92, 93], glutathione-S-transferases (GSTs), and nitrite reductase NAD(P)H quinone oxidoreductase 1 (NQO1) [38]. The concentration of these enzymes in the serum may reflect the status of an antioxidant line of defense.

Nonenzymatic antioxidants may be classified into low molecular weight and antioxidant elements (ions). Low molecular weight antioxidants include uric acid (UA), vitamins C, D, and E, glutathione, coenzyme Q, and b-carotene [13]. Iron (Fe), copper (Cu), zinc (Zn), and manganese (Mn) are the most important ions with antioxidant properties. The general and nonprotein thiol groups represent a nonenzymatic segment of the antioxidant defense system [46].

3.2. Antioxidant Factors Possible for Assessment: Serum, Erythrocytes, CSF, Saliva, and Urine. The following can be assessed in the serum: UA [13], nonprotein thiol groups [42, 46], and the total glutathione and reduced glutathione [47]. The lowest molecular weight antioxidants can be used. Other markers of antioxidant ability in the body may be determined in the CSF, for example, concentration of Klotho (an antiaging protein) [94] and total thiol groups [80]. Uric acid may be determined in the CSF; however its concentration depends on the leakage of UA molecules from the serum through the blood-brain-barrier (BBB) and the balance between consumption and production within the CNS [27].

Furthermore, an impaired iron metabolism plays a major role in the pathogenesis of MS [18]. One of a few studies reported that in the saliva of patients with MS ferric reducing ability (FRA) was decreased by 38% as compared to the controls [73]. Ferroxidase (FeOx) activity of ceruloplasmin prevents OS by promoting the connection of free radicals from iron ions to transferrin. A reduced serum FeOx activity was noted in 69 RRMS patients and in 62 patients with other inflammatory neurological disorders [95]. To summarize, FRA can be measured in saliva [73] whereas the ferroxidase (FeOx) activity may be determined in the serum [95].

Erythrocyte SOD and GPx can be marked in erythrocytes [74]. Urine assessment is a noninvasive method useful in the measurement of the oxidative status. Gholipour et al. showed that urine 6-sulphatoxymelatonin (aMT6s, major metabolite of melatonin) levels were significantly lower in MS patients as compared to the control group [96].

Two parameters appear to be significant, that is, the total radical-trapping antioxidant parameter (TRAP) and the total antioxidant status (TAS). The first parameter may be measured by a fluorescence-based method (TRAPm) or calculated (TRAPc) by a mathematical formula, considering antioxidant levels in the serum, that is, protein-bound thiol groups, UA, and vitamins E and C [97]. What is important, TRAP was recently proposed to measure the antioxidant level in the plasma [83]. The difference between TRAPm and TRAPc is due to antioxidants, which are still unidentified

[97]. Furthermore, TAS can be determined in the serum and it reflects the overall level of antioxidant capacity of the patient [45].

The antioxidant factors possible for assessment in serum, erythrocytes, CSF, saliva, and urine are collectively presented in Table 3.

3.3. The Impact of External and Internal Antioxidant Factors on the Course of Disease, Disability, and MRI Lesions. It was reported that melatonin (10 mg daily/30 days) caused a statistically significant increase in antioxidative enzymes such as SOD and GPx and a decrease in MDA in erythrocytes of SPMS patients [74]. This suggests the possibility of a positive impact of melatonin on the course of severe forms of MS. Glutathione is an antioxidant in the brain which might be a marker of the oxidative line of defense in MS patients and also might serve to monitor the disease course [31].

Another study showed that an expression of antioxidant power such as plasmatic ferric reducing ability (FRA) and thiol group dosage were significantly lower in patients with active disease [87], which may worsen the prognosis. Interestingly, the GSTP1 polymorphism and quinone oxidoreductase 1 (NQO1) variant genotypes in MS patients suggested that a defective function of detoxification enzymes might be a determinant of susceptibility and the clinical manifestation of the disease [38].

One of the studies examined coenzyme Q10 and antioxidized low-density lipoproteins (anti-oxLDL) antibodies, which may help to maintain the BBB integrity and might result in a mild disease course [98].

Aleagha et al. indicated that a decreased concentration of Klotho in the CSF of patients with RRMS showed a significant negative correlation with the disability [94]. Recent reports indicated that decreased urine aMT6s levels significantly correlated with the MS Functional Composite Score. The authors believe that there might be some new hope in developing a quantitative and objective measure to assess the severity of MS [96]. The urine aMT6s levels were not correlated with the level of disability measured by the EDSS scale [96].

Serum UA concentrations in 30 MS patients and 20 controls with noninflammatory neurological diseases supported the significance of UA in the pathogenesis of MS. Serum UA concentrations were found to be significantly lower in MS patients as compared to the controls [27]. However, CSF UA concentrations might not be a reliable marker of disease activity in MS which was assessed by MRI lesions and the CSF/serum albumin quotient [27].

On the other hand, the relationship between disability, MRI Gd + lesions and SOD concentration in erythrocytes in CIS and RRMS patients is not clear and requires further studies [74, 75].

3.4. Opportunities for Antioxidant Supplementation in MS: What Can Be Supplemented? Neuroprotection seems to be a vast area to explore, common to a number of neurodegenerative diseases, including MS. The role of OS in MS appears to be vital. Currently, a large therapeutic potential lies in antioxidants. Research focuses on finding new substances with antioxidant properties.

The melatonin supplementation appears to be useful [74, 75, 99] and may scavenge the hydroxyl, carbonate, alkoxyl, peroxyl, and aryl cation radicals and stimulate the activities of antioxidative enzymes (GPx, SOD, etc.) [74]. It was confirmed that melatonin also plays an important role in improving the antioxidant defense in MS through upregulation of sirtuin 1 (SIRT1) and its target genes for MnSOD and CAT [100]. Moreover, melatonin is selectively taken up by mitochondrial membranes, which makes it a potential therapeutic tool in treating neurodegenerative disorders [50].

In vitro studies demonstrated that dihydroasparagusic acid prevented lipopolysaccharide-induced production of neurotoxic mediators such as NO, TNF-α, prostaglandin E2, inducible NOS, cyclooxygenase-2 protein expression, and lipoxygenase activity in microglial cells [101].

Oxidative stress is also responsible for depletion of n-3 polyunsaturated fatty acid (PUFA), leading to disruptions in the lipid-based signaling, intracellular signal dysfunction and increased neurotoxicity. Consequently, n-3 PUFA supplementation is a rational therapeutic approach [102].

α- (alpha-) Lipoic acid (ALA) is a natural, endogenous antioxidant that acts as a peroxisome-proliferator-activated receptor-γ (PPAR-γ) [49]. The researchers showed that increased δ-ALA-D activity may be a protective agent against OS [42]. The data provided the first evidence that ALA might increase the production of PPAR-γ in vivo in experimental autoimmune encephalomyelitis (EAE) and might reveal antioxidative and immunomodulatory mechanisms for the application of ALA in human MS [49]. Khalili et al. suggested that 1200 mg of lipoic acid daily improved serum TAC among RRMS patients without affecting other biomarkers [103]. On the other hand, one of the systematic reviews showed that over-the-counter antioxidants such as epigallocatechin-3-gallate and ALA offered benefits, however only in preclinical studies. There is no evidence that they alter MS relapses or the disease progression [14].

Interestingly, a randomized study conducted on a sample of 24 patients with RRMS proved that supplementation of coenzyme Q10 for 12 weeks resulted in an increase SOD activity, plasma TAC, and a decrease in MDA levels as compared to the controls [104].

Idebenone, an organic compound known as a synthetic analog of coenzyme Q10, was proven to be beneficial in Friedreich's ataxia and Leber's hereditary optic neuropathy. In these diseases idebenone protected neuronal HT22 cells from glutamate-induced death in vitro. Fiebiger et al. reported that the histopathological examination of the CNS of idebenone-treated mice showed no improvement in inflammation, demyelination, or axonal damage. It seems that this is not a preferred method of MS treatment [105].

It was also shown that serum lipophilic antioxidants, that is, γ-tocopherol, β-carotene, and coenzyme Q10 were deficient or moved within the border of lower physiological value in a vast majority of MS patients. Researchers suggested that the deficit of lipophilic antioxidants in the blood of MS patients could have a negative impact on bioenergetics of reparative demyelinating processes and could promote neurodegeneration [25].

Table 3: The Biomarkers of antioxidant capacity. The serum is assayed for enzymes with antioxidant properties. There are also other compounds and important parameters which can be assessed in the serum. In addition, new possibilities for the use of other biological materials occurred. All these markers provide knowledge about the antioxidant status of the organism.

The biological material											
Serum	References		References	Saliva	References	CSF	References	Erythrocytes	References	Urine	References
Enzymes		*Other*									
CAT	[31, 45]	TAC	[22, 46]	FRA	[11, 16]	Klotho protein	[47]	SOD	[24, 25]	aMT6s	[46]
GPx	[8, 48]	TRAP	[11, 14, 16, 47, 49, 50]			Total thiol groups	[21, 23]	GPx	[24]		
GR	[8]	FRA	[27]			AU	[51]				
SOD	[13–15]	Nonproteins thiol group	[30, 47]								
Paraoxonase 1	[45, 160, 162]	γ-Tocopherol	[54]								
Arylesterase	[16]	β-Carotene	[12, 54]								
GSTs	[42]	Coenzyme Q10	[54]								
NQO1	[42]	Ceruloplasmin	[55]								
Peroxiredoxin-3	[5, 56–58]	Ferritin	[5]								
Thioredoxin-2, 6	[29]	AU	[12]								
FeOx	[55]										
δ-ALA-D	[41]										

GPx: glutathione peroxide, SOD: superoxide dismutase, CAT: catalase, GPx: glutathione peroxidase, GR: glutathione reductase, SOD: superoxide dismutase, GSTs: glutathione-S-transferases, NQO1: NAD(P)H:quinone oxidoreductase 1, FeOx: ferroxidase, δ-ALA-D-δ: aminolevulinate dehydratase, TAC: total antioxidant capacity, TRAP: total radical-trapping antioxidant parameter, FRA: ferric reducing ability, AU: uric acid, aMT6s: 6-sulphatoxymelatonin levels, CSF: cerebrospinal fluid.

3.5. Antioxidants of Plant Origin. Ghaffari et al. reported that treatment with two doses of saffron extract (5 and 10 μg/rat) weekly resulted in a growth of total antioxidant reactivity capacity, lipid peroxidation products, and antioxidant enzymes activity in the hippocampus of experimental models of MS compared to the controls [106]. Other studies demonstrated that the administration of Nigella sativa seeds in EAE induced in Wistar rats suppressed inflammation, enhanced remyelination in the cerebellum, and reduced the expression of transforming growth factor beta 1 (TGF β1) [107]. In turn, a nanodroplet formulation of pomegranate seed oil (denominated nano-PSO) dramatically reduced oxidation of lipids in the brains of rats [48, 108].

A small number of MS patients ($n = 9$) demonstrated a protective effect of hypericum perforatum, which resulted in an increase in neutrophil GPx activity and a decrease in intracellular free calcium ions [109]. Some studies indicated that a low fat diet and antioxidant supplements could reduce levels of free radicals [110–112]. Dietary flavonoids have a potential to protect neurons against OS, an ability to suppress neuroinflammation and modulate cell signaling pathways [112]. Flavonoids such as luteolin, quercetin, and fisetin at concentrations of 20–80 μM decrease the amount of myelin phagocytosed by macrophages [113].

Other studies described a number of potential antioxidants, such as cerium oxide nanoparticles, and sulforaphane, which is an organosulfur compound present in vegetables, ginseng, hemp seed, and evening primrose oils [114–116]. Matrine (MAT) is another antioxidant of plant origin. It is a quinolizidine alkaloid derived from the herb Radix Sophorae Flave. In EAE MAT treatment significantly upregulated the expression of the transcription factor such as nuclear factor (erythroid-derived 2) like 2 (Nrf2) which plays a role in inhibiting OS [58].

Following further studies, synthetic inhibitors of phospholipase A2 (PLA2) from plants including curcumin, ginkgo biloba, and *Centella asiatica* extracts were also used for the treatment of neurological disorders [108].

4. Inflammatory Mediators and Antioxidants

New findings suggest that chemokine 11 (CCL11) in the serum and in the CSF released from activated astrocytes promoted OS via microglial NOX1 activation and glutamate-mediated neurotoxicity. These findings proposed using inhibitor of NOX1 in therapy [79]. Another study explained how TNF-α inhibited the differentiation of progenitor cells. The effect depended on a number of factors such as increased ROS production, altered mitochondrial calcium uptake, mitochondrial membrane potential, and respiratory complex I activity. The accumulation of progenitor cells at the lesion sites was observed in MS patients [117] and suggested that failed remyelination was a consequence of the inhibition of differentiation [118–120]. In another study, authors presented the possibility of using a TNFR2 agonist as a factor protecting oligodendrocyte progenitor against OS [121].

Scientists suggested that enhanced astrocytic peroxisome proliferator-activated receptor gamma coactivator 1-alpha (PGC-1α) levels reduced the production of proinflammatory mediators such as IL-6 and chemokine (C-C motif) ligand 2 and increased the expression of antioxidant enzymes, including peroxiredoxin-3 and thioredoxin-2 in generated human primary astrocytes. Activation of PGC-1α may be a protective factor for neurons [44].

The results from the study of EL Andaloussi et al. presented the use of exosomes, biologically active nanovesicles (30–120 nm) that could be easily delivered across the BBB [122] as an improvement to induce postinjury remyelination processes. They stimulated primary dendritic cells cultures with low-level IFNγ. Exosomes (IFNγ-DC-Exos) contain microRNA species which are involved in oligodendrocyte development pathways and can increase baseline myelination, reduce OS, and improve remyelination. Researchers also found that IFNγ-DC-Exos increased oxidative tolerance and antioxidant levels in microglia and potentially included anti-inflammatory miRNAs. Furthermore, IFNγ-DC-Exos nasally administered to animals increased CNS myelination in vivo [123].

5. The New Possibilities in the Treatment of MS: Neuroprotection

A number of substances are tested for a possible ability to protect the brain against neurodegeneration. In addition, the development of neuroprotective drugs is more problematic [6]. A limited response to the application of ROS scavengers results from their short half-life, on the order of milliseconds and the degree of instability of ROS [3, 59, 124, 125].

Hydralazine may become a potential target for therapy due to the fact that it protects cells from the damaging effects of acrolein [59, 126–128].

Novel agents/approaches could offer help in preventing mitochondrial dysfunction and in improving neurodegeneration. The following are considered: CDDO-ethyl amide, CDDO-trifluroethylamide, pioglitazone, rosiglitazone, resveratrol, 5-aminoimidazole-4-carboxamide ribonucleotide (AICAR), and bezafibrate [129].

Other findings suggested that neural stem cells (NSCs) exposed to 125 μM H_2O_2 for 30 min and pretreated with different doses of lovastatin for 48 h were protected against OS-induced cell death by the expression of PGC-1α, which is a master regulator of mitochondrial function controlling energy metabolism and Nrf2. It is possible that in the future lovastatin may be used to promote the survival rate of NSCs [130]. The former group which can readily cross the BBB includes simvastatin, atorvastatin, and cerivastatin while hydrophilic statins include rosuvastatin and pravastatin [131].

The experimental results of the effects of exendin-4 and glucagon-like peptide-1 (GLP-1) in several mouse models of MS were reported by Hölscher. The main inflammatory responses were much reduced, as well as the intensity of demyelination. The cytokine release in the spleen was also reduced. It was shown that most GLP-1 mimetics such as exendin-4, liraglutide, and lixisenatide crossed the BBB and showed neuroprotective effects [132, 133]. However, further studies are needed to clarify the relationship with OS.

Novel treatments can be rated in EAE, a mouse model of MS. One of the scientific reports showed the effect of

polymerized form of nanocurcumin (PAP) on EAE, which might have a therapeutic effect as an anti-inflammatory and antioxidative stress agent with significant effects on myelin repair mechanisms [133]. Using nontoxic inhibition of myeloperoxidase might restore the BBB integrity thereby limiting migration of myeloid cells into the CNS that drive EAE pathogenesis. These inhibitors may be an effective therapeutic agent for the treatment of MS [134]. Yun et al. discovered a new molecule with a neuroprotective activity, that is, antioxidant protein peroxiredoxin 6 (PRDX6), which can reduce the inflammation in the CNS and potentiate oligodendrocyte survival [135]. The modulation of glutamate release and transport may also become a new therapeutic target [136].

The process, known as "remote damage" may have a significant effect on neurodegeneration. This process can damage neurons functionally related to the primary focus for months and years after the original damage such as stroke, multiple sclerosis, amyotrophic lateral sclerosis, and traumatic injury to the brain and the spinal cord. "Remote damage" may be defined as a variety of pathological processes, such as apoptosis, inflammation, glial activation, oxidative damage, neuronal changes in receptor mosaics, and autophagy. The impact of these factors is important at different times. Viscomi et al. attempted to investigate this process using the hemicerebellectomy (HCB) experimental paradigm. The researchers presented the idea of new therapies based on blocking "remote damage." The therapeutic window that occurs between the primary and secondary damage can be used to implement new neuroprotective treatment [137–139].

As it can be seen, not all the studies on the role of antioxidants in MS are consistent and further research should be done to test new substances for their effectiveness.

6. The Relationship between Immunomodulatory Therapy, OS, and Antioxidants

Immunomodulatory therapies are used to protect from relapses whereas corticosteroids are commonly used in the acute treatment of relapses.

The relationship between OS and dimethyl fumarate (DMF) is partially explained. The transcription factor (Nrf2) is a key regulator of antioxidative defense. Oral DMF activates anti-inflammatory and antioxidative pathways to upregulate the expression of this molecule [15, 52, 140]. A differential expression is involved in the defense against OS, predominantly in actively demyelinating white matter lesions [140–142]. Treatment of oligodendrocytes with DMF induces changes in citric acid cycle intermediates, glutathione, and lipids, indicating that this compound can protect oligodendrocyte metabolism and provide protection from OS [140].

Dimethyl fumarate and monomethyl fumarate (MMF), the immediate metabolite of DMF, activate Nrf2 transcriptional pathways. Target genes of Nrf2 include glutamate cysteine ligase transcription factor 1 and NAD(P)H oxidoreductase-1, resulting in cytoprotective effects against oxidative cellular injury. It is a potential novel mode of action differentiating this drug from other immune-modifying drugs [143]. This mechanism explains the possibility of using this drug in other degenerative diseases of the CNS, such as Parkinson's disease [144]. It is possible that dimethyl fumarate activates the prostaglandin EP2 receptor and consequently inhibits the progression of MS via the cAMP signaling pathway. This is another recently discovered mechanism of action which needs to be clarified due to OS in MS [145]. Dimethyl fumarate attenuates overproduction of ROS, which results in a decrease in a lipid peroxidation product, 7-ketocholesterol induced by ROS. It can protect murine oligodendrocytes 158N (myelin synthesizing cells) against apoptosis and autophagy. It may be responsible for neuroprotection [53]. Another effect of DMF may be associated with the activation of heme oxygenase-1 [146]. The use of a signaling pathway of the Kelch-like ECH-associated protein 1-nuclear factor erythroid 2-related factor 2-antioxidant-responsive element (Keap1-Nrf2-ARE) in vivo and in vitro leads to the downregulation of OS and inflammation, activated by DMF which may protect the nervous tissue against subarachnoid hemorrhage induced brain injury in rats [147]. In addition, it is suspected that DMF could strengthen the BBB by targeting interendothelial junctions in an Nrf2-dependent manner, thus protecting against cerebral edema during ischemic stroke [148]. On the other hand, in one of the studies on the Nrf2 pathway DMF enhanced the severity of lung carcinogenesis in mice [149].

It was also shown that therapies aiming at stimulating endogenous antioxidant pathway, for example, by inducing the Nrf2 pathway [65], may be quite effective in a situation of moderate OS such as the one in classical EAE models. However, they might be ineffective or even counterproductive in the case of extensive oxidative injury. It was proposed that the amplification of oxidative injury in MS was only reflected to a limited degree in the studied rodent models [150].

A new study reported that treatment with fingolimod reduced hyperoxia-induced OS, activation of microglia, and associated proinflammatory cytokine expression in neonatal oxygen-induced brain injury. The thesis could in part explain the efficacy of fingolimod in MS, in which OS plays an essential role [151].

IFNγ can damage myelin by spreading depression as in migraine with aura. In contrast, the physiological level of IFNγ as produced by environmental enrichment protected against demyelination and OS and was associated with a moderate and phasic increase in a number of proinflammatory cytokines. The controlled administration of pulsed IFNγ to brain slice cultures imitating environmental enrichment reduced OS, increased the concentration of myelin basic protein, and reduced spreading depression. Furthermore, stimulation of brain slice cultures with IFNγ induced the release of exosomes that had most likely neuroprotective functions [152].

Some studies attempted to prove the efficacy of IFN-β which was connected with other immunomodulatory therapies or antioxidant therapies. For instance, it was reported that treatment with IFN-β and glatiramer acetate

significantly reduced TNF-α. However, it did not affect other ROS/NRS biomarkers or disease progression [83].

In another study the level of protein carbonyls was elevated in RRMS patients treated with interferon β-1b and glatiramer acetate, whereas the serum protein thiol groups were decreased. Following the same study in RRMS patients without immunomodulatory therapy the same markers of OS were significantly elevated [55]. Sadowska-Bartosz et al. demonstrated an increase in oxidation parameters in the serum in RRMS patients treated with interferon β-1a and interferon β-1b. However, this increase was less significant compared to untreated RRMS patients or SPMS patients treated with mitoxantrone [32].

Treatment with the combination of glatiramer acetate and N-acetylcysteine had a favorable safety profile. Moreover, it had a positive effect on the redox state [153]. The administration of glatiramer acetate to female BALB/c mice under stress conditions resulted in normalization of ROS levels, restored nNOS activity, and resulted in clinical improvement in learning [154].

Another study demonstrated that melatonin supplementation at a dose of 5 mg over 90 days resulted in a significantly decreased MDA concentration in INF-β and glatiramer acetate-treated groups, however not in the mitoxantrone-treated group. In turn, a significant increase in SOD activity was observed only in glatiramer acetate-treated group as compared to the controls [155]. Interestingly, melatonin may also have implications for the treatment of severe MS. One of the studies indicated that the TAC level was significantly lower in the mitoxantrone-treated group and it increased after melatonin supplementation [156].

Using C-phycocyanin, a biliprotein from Spirulina platensis with antioxidant, anti-inflammatory, and cytoprotective properties and INF-β improved the redox status in mice with EAE, although they also differentially modulated another subset of genes. C-phycocyanin mainly modulated the expression of genes related to remyelination, gliogenesis, and axon-glia processes, which may be significant in neuroregeneration [157]. Therefore, a combined use of immunomodulatory therapies with antioxidants may prove beneficial.

Attempts were also made to explain some of the beneficial effects of natalizumab and its antioxidant capacity. Researchers studied serum melatonin levels in 18 patients with RRMS treated with natalizumab and noted that it caused significant increases in serum melatonin concentrations [158]. In one of the studies 22 MS patients were assigned to the treatment with 300 mg of natalizumab. After 14 months it was observed that natalizumab prompted a decrease in oxidative-damage biomarker levels, induced nuclear translocation of Nrf2 which was responsible for the activation of the antioxidant pathway, and a fall in serum vascular cell adhesion molecule-1 levels [47]. In addition, it was found that a decrease in carbonylated protein levels was connected with the patients with the highest levels of severity in the process (EDSS > 5) and treatment with natalizumab [159]. Consequently, it resulted in an increase of antioxidants and a reduction in OS biomarkers.

It should be borne in mind that mitoxantrone is potentially associated with an increased level of OS but on the other hand, the study demonstrated that mitoxantrone did not have an effect on the activity of paraoxonase 1 (an enzyme that protects the cell from OS) [160].

Arnold et al. evaluated the suicidal erythrocyte death induced by mitoxantrone. The study proved that mitoxantrone triggered cell apoptosis, partially due to the formation of ROS and ceramide thus increasing OS. Additionally, the authors assessed the effect of adding the antioxidant N-acetylcysteine, which significantly reduced the effect of mitoxantrone [86].

Due to the fact that the studies were not conclusive, it appears that treatment with interferon and mitoxantrone does not reduce OS [32].

To conclude, it appears that most of the drugs used in MS are directly or indirectly associated with OS.

7. Corticosteroids in Relapses: The Importance of OS and Antioxidants

The role of corticosteroids in OS is poorly understood. Wang et al. examined levels of MDA and TAC in peripheral blood and the CSF of RRMS patients in 7 days before methylprednisolone (MP) treatment and one month after MP treatment. They found that the increase in OS markers preceded inflammatory response in MS patients and MP treatment reduced the neuroinflammatory attack by decreasing brain antioxidant enzymes [54].

Ozone autohemotherapy is an emerging therapeutic technique that can change the brain metabolism. It was recently shown that MS patients demonstrated a marked increase in cytochrome-c-oxidase (CYT-c) activity and concentration about 40 minutes after the end of the autohemotherapy, possibly revealing a reduction of the chronic OS level typical of MS sufferers [161].

A protective effect of ozone (O_3) therapy was reported in EAE in rats either alone or in combination with corticosteroids. Such a combination allowed reducing the dose of MP due to a decreased level of brain glutathione, paraoxonase 1 enzyme activity, brain MDA, TNF-α, IL-1β, IFN-γ, Cox-2 immunoreactivity, and p53 proteins [162]. The study showed that adding compounds that modulate redox pathways in the cell could increase the effectiveness of the therapy and reduce a dose of corticosteroids.

8. Conclusions

The brain tissue, with a considerable number of phospholipid membranes, is very sensitive to the action of radicals due to a significant presence of mitochondria and consequently massive oxygen metabolic processes. A number of studies document the participation of OS in MS pathophysiology. Oxidative stress processes participate in both inflammatory and neurodegenerative pathophysiological components of MS. Oxidative stress is associated with the dysregulation of axonal bioenergetics, cytokine-induced synaptic hyperexcitability, abnormal iron accumulation, and the oxidant/antioxidant balance. Markers of OS assessed in the serum, erythrocytes,

CSF, saliva, and urine may have diagnostic properties whereas antioxidants may have clinical application in the future. There are at least a couple of OS markers of the disease course which can be particularly useful in the diagnosis of severe forms of MS such as SPMS and PPMS. Other useful applications include markers of relapse and OS markers of disability. There might be some new hope in an objective assessment of the severity of MS.

Many antioxidants may have a positive impact on the course of MS. These substances include melatonin, dihydroasparagusic acid, n-3 polyunsaturated fatty acid (PUFA), α- (alpha-) lipoic acid (ALA) and others (including plant origin antioxidants). Innovative therapies are aimed in particular at neuroprotection and neurodegeneration. Potential drugs include compounds such as hydralazine, exendin-4, glucagon-like peptide-1 (GLP-1), and also lovastatin which protects against OS-induced cell death by the expression of PGC-1α and Nrf2.

Currently, a number of new studies focus on the immunotherapy and OS. Natalizumab and fingolimod have a positive effect on antioxidant capacity and may result in a reduction in OS markers. The relationship between DMF and OS is best known and is associated with the modulation of OS molecules. On the other hand, mitoxantrone is a drug that may be responsible for an increase in OS. There are new suggestions combining mitoxantrone therapy with antioxidant supplementation such as N-acetylcysteine and melatonin in order to alleviate the toxicity of mitoxantrone.

Summarizing, using OS markers as biomarkers of MS severity or relapse could be a long-awaited helpful diagnostic tool. Moreover, adding antioxidants to immunotherapy which is well-established in MS may be reasonable and highly beneficial for MS patients due to their ability to reduce OS. Further research should be done to test new antioxidants for their effectiveness.

Competing Interests

The authors declare that there is no conflict of interests regarding the publication of this paper.

References

[1] A. Fiorini, T. Koudriavtseva, E. Bucaj et al., "Involvement of oxidative stress in occurrence of relapses in multiple sclerosis: the spectrum of oxidatively modified serum proteins detected by proteomics and redox proteomics analysis," *PLoS ONE*, vol. 8, no. 6, article e65184, 2013.

[2] T. Kalincik, "Multiple sclerosis relapses: epidemiology, outcomes and management. A systematic review," *Neuroepidemiology*, vol. 44, no. 4, pp. 199–214, 2015.

[3] A. Compston and A. Coles, "Multiple sclerosis," *The Lancet*, vol. 372, no. 9648, pp. 1502–1517, 2008.

[4] B. D. Trapp, R. Ransohoff, and R. Rudick, "Axonal pathology in multiple sclerosis: relationship to neurologic disability," *Current Opinion in Neurology*, vol. 12, no. 3, pp. 295–302, 1999.

[5] B. D. Trapp, J. Peterson, R. M. Ransohoff, R. Rudick, S. Mörk, and L. Bö, "Axonal transection in the lesions of multiple sclerosis," *The New England Journal of Medicine*, vol. 338, no. 5, pp. 278–285, 1998.

[6] R. E. Gonsette, "Neurodegeneration in multiple sclerosis: the role of oxidative stress and excitotoxicity," *Journal of the Neurological Sciences*, vol. 274, no. 1-2, pp. 48–53, 2008.

[7] E. Miller, A. Walczak, J. Saluk, M. B. Ponczek, and I. Majsterek, "Oxidative modification of patient's plasma proteins and its role in pathogenesis of multiple sclerosis," *Clinical Biochemistry*, vol. 45, no. 1-2, pp. 26–30, 2012.

[8] R. Kohen and A. Nyska, "Oxidation of biological systems: Oxidative stress phenomena, antioxidants, redox reactions, and methods for their quantification," *Toxicologic Pathology*, vol. 30, no. 6, pp. 620–650, 2002.

[9] M. McIntyre, D. F. Bohr, and A. F. Dominiczak, "Endothelial function in hypertension: the role of superoxide anion," *Hypertension*, vol. 34, no. 4 I, pp. 539–545, 1999.

[10] M. Genestra, "Oxyl radicals, redox-sensitive signalling cascades and antioxidants," *Cellular Signalling*, vol. 19, no. 9, pp. 1807–1819, 2007.

[11] D. E. Koshland Jr., "The molecule of the year," *Science*, vol. 258, no. 5090, p. 1861, 1992.

[12] M. A. Friese, B. Schattling, and L. Fugger, "Mechanisms of neurodegeneration and axonal dysfunction in multiple sclerosis," *Nature Reviews Neurology*, vol. 10, no. 4, pp. 225–238, 2014.

[13] E. Miller, "Myostimulation as an antloxldatlve factor in sclerosis multiplex," *Polski Merkuriusz Lekarski*, vol. 31, no. 183, pp. 186–189, 2011.

[14] J. R. Plemel, C. A. Juzwik, C. A. Benson, M. Monks, C. Harris, and M. Ploughman, "Over-the-counter anti-oxidant therapies for use in multiple sclerosis: a systematic review," *Multiple Sclerosis*, vol. 21, no. 12, pp. 1485–1495, 2015.

[15] F. Kees, "Dimethyl fumarate: a Janus-faced substance?" *Expert Opinion on Pharmacotherapy*, vol. 14, no. 11, pp. 1559–1567, 2013.

[16] X. Zhang, M. Haaf, B. Todorich et al., "Cytokine toxicity to oligodendrocyte precursors is mediated by iron," *Glia*, vol. 52, no. 3, pp. 199–208, 2005.

[17] B. Halliwell, "Oxidants and human disease: some new concepts," *The FASEB Journal*, vol. 1, no. 5, pp. 358–364, 1987.

[18] A. Phaniendra, D. B. Jestadi, and L. Periyasamy, "Free radicals: properties, sources, targets, and their implication in various diseases," *Indian Journal of Clinical Biochemistry*, vol. 30, no. 1, pp. 11–26, 2015.

[19] P. Kuppusamy and J. L. Zweier, "Characterization of free radical generation by xanthine oxidase. Evidence for hydroxyl radical generation," *The Journal of Biological Chemistry*, vol. 264, no. 17, pp. 9880–9884, 1989.

[20] L. Haider, C. Simeonidou, G. Steinberger et al., "Multiple sclerosis deep grey matter: the relation between demyelination, neurodegeneration, inflammation and iron," *Journal of Neurology, Neurosurgery, and Psychiatry*, vol. 85, no. 12, pp. 1386–1395, 2014.

[21] H. A. Kontos, E. P. Wei, E. F. Ellis et al., "Appearance of superoxide anion radical in cerebral extracellular space during increased prostaglandin synthesis in cats," *Circulation Research*, vol. 57, no. 1, pp. 142–151, 1985.

[22] L. Haider, "Inflammation, iron, energy failure, and oxidative stress in the pathogenesis of multiple sclerosis," *Oxidative Medicine and Cellular Longevity*, vol. 2015, Article ID 725370, 10 pages, 2015.

[23] F. Darios, N. Lambeng, J.-D. Troadec, P. P. Michel, and M. Ruberg, "Ceramide increases mitochondrial free calcium levels via caspase 8 and Bid: role in initiation of cell death," *Journal of Neurochemistry*, vol. 84, no. 4, pp. 643–654, 2003.

[24] T. Douki and J. Cadet, "Peroxynitrite mediated oxidation of purine bases of nucleosides and isolated DNA," *Free Radical Research*, vol. 24, no. 5, pp. 369–380, 1996.

[25] Ľ. Kuračka, T. Kalnovičová, J. Kucharská, and P. Turčáni, "Multiple sclerosis: evaluation of purine nucleotide metabolism in central nervous system in association with serum levels of selected fat-soluble antioxidants," *Multiple Sclerosis International*, vol. 2014, Article ID 759808, 9 pages, 2014.

[26] H. Lassmann, J. Van Horssen, and D. Mahad, "Progressive multiple sclerosis: pathology and pathogenesis," *Nature Reviews Neurology*, vol. 8, no. 11, pp. 647–656, 2012.

[27] I. Dujmovic, T. Pekmezovic, R. Obrenovic et al., "Cerebrospinal fluid and serum uric acid levels in patients with multiple sclerosis," *Clinical Chemistry and Laboratory Medicine*, vol. 47, no. 7, pp. 848–853, 2009.

[28] V. V. Bamm, D. K. Lanthier, E. L. Stephenson, G. S. T. Smith, and G. Harauz, "In vitro study of the direct effect of extracellular hemoglobin on myelin components," *Biochimica et Biophysica Acta—Molecular Basis of Disease*, vol. 1852, no. 1, pp. 92–103, 2015.

[29] B. Halliwell, M. V. Clement, and L. H. Long, "Hydrogen peroxide in the human body," *FEBS Letters*, vol. 486, no. 1, pp. 10–13, 2000.

[30] A. A. Starkov, "The role of mitochondria in reactive oxygen species metabolism and signaling," *Annals of the New York Academy of Sciences*, vol. 1147, pp. 37–52, 2008.

[31] A. N. Carvalho, J. L. Lim, P. G. Nijland, M. E. Witte, and J. Van Horssen, "Glutathione in multiple sclerosis: more than just an antioxidant?" *Multiple Sclerosis Journal*, vol. 20, no. 11, pp. 1425–1431, 2014.

[32] I. Sadowska-Bartosz, M. Adamczyk-Sowa, A. Gajewska, and G. Bartosz, "Oxidative modification of blood serum proteins in multiple sclerosis after interferon or mitoxantrone treatment," *Journal of Neuroimmunology*, vol. 266, no. 1-2, pp. 67–74, 2014.

[33] F. Bagnato, S. Hametner, B. Yao et al., "Tracking iron in multiple sclerosis: a combined imaging and histopathological study at 7 Tesla," *Brain*, vol. 134, no. 12, pp. 3602–3615, 2011.

[34] S. Rossi, C. Motta, V. Studer et al., "Tumor necrosis factor is elevated in progressive multiple sclerosis and causes excitotoxic neurodegeneration," *Multiple Sclerosis Journal*, vol. 20, no. 3, pp. 304–312, 2014.

[35] K. Marballi, M. P. Quinones, F. Jimenez et al., "In vivo and in vitro genetic evidence of involvement of neuregulin 1 in immune system dysregulation," *Journal of Molecular Medicine*, vol. 88, no. 11, pp. 1133–1141, 2010.

[36] J. W. Hill, R. Poddar, J. F. Thompson, G. A. Rosenberg, and Y. Yang, "Intranuclear matrix metalloproteinases promote DNA damage and apoptosis induced by oxygen-glucose deprivation in neurons," *Neuroscience*, vol. 220, pp. 277–290, 2012.

[37] C. Tronel, G. Y. Rochefort, N. Arlicot, S. Bodard, S. Chalon, and D. Antier, "Oxidative stress is related to the deleterious effects of heme oxygenase-1 in an in vivo neuroinflammatory rat model," *Oxidative Medicine and Cellular Longevity*, vol. 2013, Article ID 264935, 10 pages, 2013.

[38] A. Alexoudi, S. Zachaki, C. Stavropoulou et al., "Combined *GSTP1* and *NQO1* germline polymorphisms in the susceptibility to Multiple Sclerosis," *International Journal of Neuroscience*, vol. 125, no. 1, pp. 32–37, 2015.

[39] A. Falluel-Morel, N. Aubert, D. Vaudry et al., "Opposite regulation of the mitochondrial apoptotic pathway by C2-ceramide and PACAP through a MAP-kinase-dependent mechanism in cerebellar granule cells," *Journal of Neurochemistry*, vol. 91, no. 5, pp. 1231–1243, 2004.

[40] S. Rossi, R. Furlan, V. De Chiara et al., "Interleukin-1β causes synaptic hyperexcitability in multiple sclerosis," *Annals of Neurology*, vol. 71, no. 1, pp. 76–83, 2012.

[41] D. Mahad, H. Lassmann, and D. Turnbull, "Review: mitochondria and disease progression in multiple sclerosis," *Neuropathology and Applied Neurobiology*, vol. 34, no. 6, pp. 577–589, 2008.

[42] C. R. N. Polachini, R. M. Spanevello, D. Zanini et al., "Evaluation of delta-aminolevulinic dehydratase activity, oxidative stress biomarkers, and vitamin D levels in patients with multiple sclerosis," *Neurotoxicity Research*, vol. 29, no. 2, pp. 230–242, 2016.

[43] M. Chevion, E. Berenshtein, and E. R. Stadtman, "Human studies related to protein oxidation: protein carbonyl content as a marker of damage," *Free Radical Research*, vol. 33, pp. S99–S108, 2000.

[44] P. G. Nijland, M. E. Witte, B. van het Hof et al., "Astroglial PGC-1alpha increases mitochondrial antioxidant capacity and suppresses inflammation: implications for multiple sclerosis," *Acta Neuropathologica Communications*, vol. 2, no. 1, article 170, 2014.

[45] A. Kirbas, S. Kirbas, O. Anlar, H. Efe, and A. Yilmaz, "Serum paraoxonase and arylesterase activity and oxidative status in patients with multiple sclerosis," *Journal of Clinical Neuroscience*, vol. 20, no. 8, pp. 1106–1109, 2013.

[46] M. A. Lutsky, A. M. Zemskov, and K. A. Razinkin, "[Biochemical markers of oxidative stress in different forms and phases of multiple sclerosis]," *Zhurnal nevrologii i psikhiatrii imeni S.S. Korsakova / Ministerstvo zdravookhraneniia i meditsinskoĭ promyshlennosti Rossiĭskoĭ Federatsii, Vserossiĭskoe obshchestvo nevrologov [i] Vserossiĭskoe obshchestvo psikhiatrov*, vol. 114, no. 11, pp. 74–77, 2014.

[47] I. Tasset, C. Bahamonde, E. Agüera et al., "Effect of natalizumab on oxidative damage biomarkers in relapsing-remitting multiple sclerosis," *Pharmacological Reports*, vol. 65, no. 3, pp. 624–631, 2013.

[48] O. Binyamin, L. Larush, K. Frid et al., "Treatment of a multiple sclerosis animal model by a novel nanodrop formulation of a natural antioxidant," *International Journal of Nanomedicine*, vol. 10, pp. 7165–7174, 2015.

[49] K.-C. Wang, C.-P. Tsai, C.-L. Lee et al., "α-lipoic acid enhances endogenous peroxisome-proliferator-activated receptor-γ to ameliorate experimental autoimmune encephalomyelitis in mice," *Clinical Science*, vol. 125, no. 7, pp. 329–340, 2013.

[50] S. A. Ganie, T. A. Dar, A. H. Bhat et al., "Melatonin: a potential anti-oxidant therapeutic agent for mitochondrial dysfunctions and related disorders," *Rejuvenation Research*, vol. 19, no. 1, pp. 21–40, 2016.

[51] J. Tenorio-Laranga, I. Peltonen, S. Keskitalo et al., "Alteration of prolyl oligopeptidase and activated α-2-macroglobulin in multiple sclerosis subtypes and in the clinically isolated syndrome," *Biochemical Pharmacology*, vol. 85, no. 12, pp. 1783–1794, 2013.

[52] C. B. Burness and E. D. Deeks, "Dimethyl fumarate: a review of its use in patients with relapsing-remitting multiple sclerosis," *CNS Drugs*, vol. 28, no. 4, pp. 373–387, 2014.

[53] A. Zarrouk, T. Nury, E. M. Karym et al., "Attenuation of 7-ketocholesterol-induced overproduction of reactive oxygen species, apoptosis, and autophagy by dimethyl fumarate on 158 N murine oligodendrocytes," *The Journal of Steroid Biochemistry and Molecular Biology*, 2016.

[54] P. Wang, K. Xie, C. Wang, and J. Bi, "Oxidative stress induced by lipid peroxidation is related with inflammation of demyelination and neurodegeneration in multiple sclerosis," *European Neurology*, vol. 72, no. 3-4, pp. 249–254, 2014.

[55] I. Sadowska-Bartosz, M. Adamczyk-Sowa, S. Galiniak, S. Mucha, K. Pierzchala, and G. Bartosz, "Oxidative modification of serum proteins in multiple sclerosis," *Neurochemistry International*, vol. 63, no. 5, pp. 507–516, 2013.

[56] M. T. Fischer, R. Sharma, J. L. Lim et al., "NADPH oxidase expression in active multiple sclerosis lesions in relation to oxidative tissue damage and mitochondrial injury," *Brain*, vol. 135, no. 3, pp. 886–899, 2012.

[57] V. V. Bamm and G. Harauz, "Hemoglobin as a source of iron overload in multiple sclerosis: does multiple sclerosis share risk factors with vascular disorders?" *Cellular and Molecular Life Sciences*, vol. 71, no. 10, pp. 1789–1798, 2014.

[58] N. Liu, Q.-C. Kan, X.-J. Zhang et al., "Upregulation of immunomodulatory molecules by matrine treatment in experimental autoimmune encephalomyelitis," *Experimental and Molecular Pathology*, vol. 97, no. 3, pp. 470–476, 2014.

[59] M. Tully and R. Shi, "New insights in the pathogenesis of multiple sclerosis-role of acrolein in neuronal and myelin damage," *International Journal of Molecular Sciences*, vol. 14, no. 10, pp. 20037–20047, 2013.

[60] J. Correale, "The role of microglial activation in disease progression," *Multiple Sclerosis*, vol. 20, no. 10, pp. 1288–1295, 2014.

[61] J. S. Beckman and W. H. Koppenol, "Nitric oxide, superoxide, and peroxynitrite: the good, the bad, and the ugly," *The American Journal of Physiology*, vol. 271, no. 5, pp. C1424–C1437, 1996.

[62] A. A. Mossakowski, J. Pohlan, D. Bremer et al., "Tracking CNS and systemic sources of oxidative stress during the course of chronic neuroinflammation," *Acta Neuropathologica*, vol. 130, no. 6, pp. 799–814, 2015.

[63] O. Errea, B. Moreno, A. Gonzalez-Franquesa, P. M. Garcia-Roves, and P. Villoslada, "The disruption of mitochondrial axonal transport is an early event in neuroinflammation," *Journal of Neuroinflammation*, vol. 12, article 152, 2015.

[64] H. Lassmann, "Pathology and disease mechanisms in different stages of multiple sclerosis," *Journal of the Neurological Sciences*, vol. 333, no. 1-2, pp. 1–4, 2013.

[65] H. Bros, J. M. Millward, F. Paul, R. Niesner, and C. Infante-Duarte, "Oxidative damage to mitochondria at the nodes of Ranvier precedes axon degeneration in ex vivo transected axons," *Experimental Neurology*, vol. 261, pp. 127–135, 2014.

[66] W. Dröge, "Free radicals in the physiological control of cell function," *Physiological Reviews*, vol. 82, no. 1, pp. 47–95, 2002.

[67] M. Valko, D. Leibfritz, J. Moncol, M. T. D. Cronin, M. Mazur, and J. Telser, "Free radicals and antioxidants in normal physiological functions and human disease," *International Journal of Biochemistry and Cell Biology*, vol. 39, no. 1, pp. 44–84, 2007.

[68] J. Nordberg and E. S. J. Arnér, "Reactive oxygen species, antioxidants, and the mammalian thioredoxin system," *Free Radical Biology and Medicine*, vol. 31, no. 11, pp. 1287–1312, 2001.

[69] B. Halliwell, *Free Radicals and Other Reactive Species in Disease*, National University of Singapore, 2001.

[70] D. H. Mahad, B. D. Trapp, and H. Lassmann, "Pathological mechanisms in progressive multiple sclerosis," *The Lancet Neurology*, vol. 14, no. 2, pp. 183–193, 2015.

[71] L. Haider, M. T. Fischer, J. M. Frischer et al., "Oxidative damage in multiple sclerosis lesions," *Brain*, vol. 134, no. 7, pp. 1914–1924, 2011.

[72] E. H. J. M. Jansen and T. Ruskovska, "Comparative analysis of serum (Anti)oxidative status para Cyrillicmeters in healthy persons," *International Journal of Molecular Sciences*, vol. 14, no. 3, pp. 6106–6115, 2013.

[73] M. Karlík, P. Valkovič, V. Hančinová, L. Krížová, Ľ. Tóthová, and P. Celec, "Markers of oxidative stress in plasma and saliva in patients with multiple sclerosis," *Clinical Biochemistry*, vol. 48, no. 1-2, pp. 24–28, 2015.

[74] E. Miller, A. Walczak, I. Majsterek, and J. Kedziora, "Melatonin reduces oxidative stress in the erythrocytes of multiple sclerosis patients with secondary progressive clinical course," *Journal of Neuroimmunology*, vol. 257, no. 1-2, pp. 97–101, 2013.

[75] S. Ljubisavljevic, I. Stojanovic, T. Cvetkovic et al., "Erythrocytes' antioxidative capacity as a potential marker of oxidative stress intensity in neuroinflammation," *Journal of the Neurological Sciences*, vol. 337, no. 1-2, pp. 8–13, 2014.

[76] V. Chiurchiù, "Novel targets in multiple sclerosis: to oxidative stress and beyond," *Current Topics in Medicinal Chemistry*, vol. 14, no. 22, pp. 2590–2599, 2014.

[77] E. Sbardella, A. Greco, M. L. Stromillo et al., "Isoprostanes in clinically isolated syndrome and early multiple sclerosis as biomarkers of tissue damage and predictors of clinical course," *Multiple Sclerosis Journal*, vol. 19, no. 4, pp. 411–417, 2013.

[78] O. G. Vidaurre, J. D. Haines, I. Katz Sand et al., "Cerebrospinal fluid ceramides from patients with multiple sclerosis impair neuronal bioenergetics," *Brain*, vol. 137, no. 8, pp. 2271–2286, 2014.

[79] B. Parajuli, H. Horiuchi, T. Mizuno, H. Takeuchi, and A. Suzumura, "CCL11 enhances excitotoxic neuronal death by producing reactive oxygen species in microglia," *GLIA*, vol. 63, no. 12, pp. 2274–2284, 2015.

[80] S. Ljubisavljevic, I. Stojanovic, S. Vojinovic et al., "The patients with clinically isolated syndrome and relapsing remitting multiple sclerosis show different levels of advanced protein oxidation products and total thiol content in plasma and CSF," *Neurochemistry International*, vol. 62, no. 7, pp. 988–997, 2013.

[81] J.-Z. Guan, W.-P. Guan, T. Maeda, X. Guoqing, W. GuangZhi, and N. Makino, "Patients with multiple sclerosis show increased oxidative stress markers and somatic telomere length shortening," *Molecular and Cellular Biochemistry*, vol. 400, no. 1-2, pp. 183–187, 2015.

[82] M. Tully, L. Zheng, and R. Shi, "Acrolein detection: potential theranostic utility in multiple sclerosis and spinal cord injury," *Expert Review of Neurotherapeutics*, vol. 14, no. 6, pp. 679–685, 2014.

[83] A. P. Kallaur, E. M. V. Reiche, S. R. Oliveira et al., "Genetic, immune-inflammatory, and oxidative stress biomarkers as predictors for disability and disease progression in multiple sclerosis," *Molecular Neurobiology*, 2016.

[84] J. Ivica and J. Wilhelm, "Lipophilic fluorescent products of free radicals," *Biomedical Papers*, vol. 158, no. 3, pp. 365–372, 2014.

[85] S. R. Oliveira, A. N. Colado Simão, A. P. Kallaur et al., "Disability in patients with multiple sclerosis: influence of insulin resistance, adiposity, and oxidative stress," *Nutrition*, vol. 30, no. 3, pp. 268–273, 2014.

[86] M. Arnold, R. Bissinger, and F. Lang, "Mitoxantrone-induced suicidal erythrocyte death," *Cellular Physiology and Biochemistry*, vol. 34, no. 5, pp. 1756–1767, 2014.

[87] L. Pasquali, C. Pecori, C. Lucchesi et al., "Plasmatic oxidative stress biomarkers in multiple sclerosis: relation with clinical and demographic characteristics," *Clinical Biochemistry*, vol. 48, no. 1-2, pp. 19–23, 2015.

[88] R. Shi, T. Rickett, and W. Sun, "Acrolein-mediated injury in nervous system trauma and diseases," *Molecular Nutrition and Food Research*, vol. 55, no. 9, pp. 1320–1331, 2011.

[89] P. Kharel, J. McDonough, and S. Basu, "Evidence of extensive RNA oxidation in normal appearing cortex of multiple sclerosis brain," *Neurochemistry International*, vol. 92, pp. 43–48, 2016.

[90] A. Morel, M. Bijak, E. Miller, J. Rywaniak, S. Miller, and J. Saluk, "Relationship between the increased haemostatic properties of blood platelets and oxidative stress level in multiple sclerosis patients with the secondary progressive stage," *Oxidative Medicine and Cellular Longevity*, vol. 2015, Article ID 240918, 10 pages, 2015.

[91] S. Ljubisavljevic, "Oxidative stress and neurobiology of demyelination," *Molecular Neurobiology*, vol. 53, no. 1, pp. 744–758, 2016.

[92] J. M. Matés, C. Pérez-Gómez, and I. N. De Castro, "Antioxidant enzymes and human diseases," *Clinical Biochemistry*, vol. 32, no. 8, pp. 595–603, 1999.

[93] H. Z. Chae, S. W. Kang, and S. G. Rhee, "Isoforms of mammalian peroxiredoxin that reduce peroxides in presence of thioredoxin," *Methods in Enzymology*, vol. 300, pp. 219–226, 1999.

[94] M. S. E. Aleagha, B. Siroos, M. Ahmadi et al., "Decreased concentration of Klotho in the cerebrospinal fluid of patients with relapsing-remitting multiple sclerosis," *Journal of Neuroimmunology*, vol. 281, pp. 5–8, 2015.

[95] C. Cervellati, A. Romani, E. Fainardi et al., "Serum ferroxidase activity in patients with multiple sclerosis: A Pilot Study," *In Vivo*, vol. 28, no. 6, pp. 1197–1200, 2014.

[96] T. Gholipour, T. Ghazizadeh, S. Babapour et al., "Decreased urinary level of melatonin as a marker of disease severity in patients with multiple sclerosis," *Iranian Journal of Allergy, Asthma and Immunology*, vol. 14, no. 1, pp. 91–97, 2015.

[97] A. Ceriello, N. Bortolotti, E. Falleti et al., "Total radical-trapping antioxidant parameter in NIDDM patients," *Diabetes Care*, vol. 20, no. 2, pp. 194–197, 1997.

[98] M. Gironi, B. Borgiani, E. Mariani et al., "Oxidative stress is differentially present in multiple sclerosis courses, early evident, and unrelated to treatment," *Journal of Immunology Research*, vol. 2014, Article ID 961863, 9 pages, 2014.

[99] E. Miller, A. Morel, L. Saso, and J. Saluk, "Melatonin redox activity. Its potential clinical applications in neurodegenerative disorders," *Current Topics in Medicinal Chemistry*, vol. 15, no. 2, pp. 163–169, 2015.

[100] S. Emamgholipour, A. Hossein-Nezhad, M. A. Sahraian, F. Askarisadr, and M. Ansari, "Evidence for possible role of melatonin in reducing oxidative stress in multiple sclerosis through its effect on SIRT1 and antioxidant enzymes," *Life Sciences*, vol. 145, pp. 34–41, 2016.

[101] A. Salemme, A. R. Togna, A. Mastrofrancesco et al., "Anti-inflammatory effects and antioxidant activity of dihydroasparagusic acid in lipopolysaccharide-activated microglial cells," *Brain Research Bulletin*, vol. 120, pp. 151–158, 2016.

[102] G. Morris, K. Walder, B. K. Puri, M. Berk, and M. Maes, "The deleterious effects of oxidative and nitrosative stress on palmitoylation, membrane lipid rafts and lipid-based cellular signalling: new drug targets in neuroimmune disorders," *Molecular Neurobiology*, vol. 53, no. 7, pp. 4638–4658, 2016.

[103] M. Khalili, S. Eghtesadi, A. Mirshafiey et al., "Effect of lipoic acid consumption on oxidative stress among multiple sclerosis patients: a randomized controlled clinical trial," *Nutritional Neuroscience*, vol. 17, no. 1, pp. 16–20, 2014.

[104] M. Sanoobar, S. Eghtesadi, A. Azimi, M. Khalili, S. Jazayeri, and M. Reza Gohari, "Coenzyme Q10 supplementation reduces oxidative stress and increases antioxidant enzyme activity in patients with relapsing-remitting multiple sclerosis," *The International Journal of Neuroscience*, vol. 123, no. 11, pp. 776–782, 2013.

[105] S. M. Fiebiger, H. Bros, T. Grobosch et al., "The antioxidant idebenone fails to prevent or attenuate chronic experimental autoimmune encephalomyelitis in the mouse," *Journal of Neuroimmunology*, vol. 262, no. 1-2, pp. 66–71, 2013.

[106] S. Ghaffari, H. Hatami, and G. Dehghan, "Saffron ethanolic extract attenuates oxidative stress, spatial learning, and memory impairments induced by local injection of ethidium bromide," *Research in Pharmaceutical Sciences*, vol. 10, no. 3, pp. 222–232, 2015.

[107] N. A. Noor, H. M. Fahmy, F. F. Mohammed, A. A. Elsayed, and N. M. Radwan, "Nigella sativa amliorates inflammation and demyelination in the experimental autoimmune encephalomyelitis-induced Wistar rats," *International Journal of Clinical and Experimental Pathology*, vol. 8, no. 6, pp. 6269–6286, 2015.

[108] W.-Y. Ong, T. Farooqui, G. Kokotos, and A. A. Farooqui, "Syntheti and natural inhibitors of phospholipases A2: their importance for understanding and treatment of neurological disorders," *ACS Chemical Neuroscience*, vol. 6, no. 6, pp. 814–831, 2015.

[109] M. Naziroglu, S. Kutluhan, I. S. Övey, M. Aykur, and V. A. Yurekli, "Modulation of oxidative stress, apoptosis, and calcium entry in leukocytes of patients with multiple sclerosis by Hypericum perforatum," *Nutritional Neuroscience*, vol. 17, no. 5, pp. 214–221, 2014.

[110] E. Mauriz, A. Laliena, D. Vallejo et al., "Effects of a low-fat diet with antioxidant supplementation on biochemical markers of multiple sclerosis long-term care residents," *Nutricion Hospitalaria*, vol. 28, no. 6, pp. 2229–2235, 2013.

[111] V. P. Dadhania, P. P. Trivedi, A. Vikram, and D. N. Tripathi, "Nutraceuticals against neurodegeneration: a mechanistic insight," *Current Neuropharmacology*, vol. 14, no. 6, pp. 627–640, 2016.

[112] L. González-González, J. G. Pérez-Cortéz, M. Flores-Aldana, N. Macías-Morales, and C. Hernández-Girón, "Antioxidant use as dietary therapy in patients with multiple sclerosis," *Medwave*, vol. 15, no. 1, Article ID e6065, 2015.

[113] J. J. A. Hendriks, H. E. De Vries, S. M. A. Van Der Pol, T. K. Van Den Berg, E. A. F. Van Tol, and C. D. Dijkstra, "Flavonoids inhibit myelin phagocytosis by macrophages; a structure-activity relationship study," *Biochemical Pharmacology*, vol. 65, no. 5, pp. 877–885, 2003.

[114] K. L. Heckman, W. Decoteau, A. Estevez et al., "Custom cerium oxide nanoparticles protect against a free radical mediated autoimmune degenerative disease in the brain," *ACS Nano*, vol. 7, no. 12, pp. 10582–10596, 2013.

[115] B. Li, W. Cui, J. Liu et al., "Sulforaphane ameliorates the development of experimental autoimmune encephalomyelitis by antagonizing oxidative stress and Th17-related inflammation in mice," *Experimental Neurology*, vol. 250, pp. 239–249, 2013.

[116] S. Rezapour-Firouzi, S. R. Arefhosseini, M. Ebrahimi-Mamaghani et al., "Activity of liver enzymes in multiple sclerosis patients with Hot-nature diet and co-supplemented hemp seed, evening primrose oils intervention," *Complementary Therapies in Medicine*, vol. 22, no. 6, pp. 986–993, 2014.

[117] N. Scolding, R. Franklin, S. Stevens, C.-H. Heldin, A. Compston, and J. Newcombe, "Oligodendrocyte progenitors are present in the normal adult human CNS and in the lesions of multiple sclerosis," *Brain*, vol. 121, no. 12, pp. 2221–2228, 1998.

[118] M. Bonora, E. De Marchi, S. Patergnani et al., "Tumor necrosis factor-α impairs oligodendroglial differentiation through a mitochondria-dependent process," *Cell Death and Differentiation*, vol. 21, no. 8, pp. 1198–1208, 2014.

[119] T. Kuhlmann, V. Miron, Q. Cuo, C. Wegner, J. Antel, and W. Brück, "Differentiation block of oligodendroglial progenitor cells as a cause for remyelination failure in chronic multiple sclerosis," *Brain*, vol. 131, no. 7, pp. 1749–1758, 2008.

[120] G. Wolswijk, "Oligodendrocyte precursor cells in the demyelinated multiple sclerosis spinal cord," *Brain*, vol. 125, no. 2, pp. 338–349, 2002.

[121] O. Maier, R. Fischer, C. Agresti, and K. Pfizenmaier, "TNF receptor 2 protects oligodendrocyte progenitor cells against oxidative stress," *Biochemical and Biophysical Research Communications*, vol. 440, no. 2, pp. 336–341, 2013.

[122] S. EL Andaloussi, S. Lakhal, I. Mäger, and M. J. A. Wood, "Exosomes for targeted siRNA delivery across biological barriers," *Advanced Drug Delivery Reviews*, vol. 65, no. 3, pp. 391–397, 2013.

[123] A. D. Pusic, K. M. Pusic, B. L. L. Clayton, and R. P. Kraig, "IFNγ-stimulated dendritic cell exosomes as a potential therapeutic for remyelination," *Journal of Neuroimmunology*, vol. 266, no. 1-2, pp. 12–23, 2014.

[124] R. Gold, C. Linington, and H. Lassmann, "Understanding pathogenesis and therapy of multiple sclerosis via animal models: 70 years of merits and culprits in experimental autoimmune encephalomyelitis research," *Brain*, vol. 129, no. 8, pp. 1953–1971, 2006.

[125] K. J. Smith, R. Kapoor, and P. A. Felts, "Demyelination: the role of reactive oxygen and nitrogen species," *Brain Pathology*, vol. 9, no. 1, pp. 69–92, 1999.

[126] G. Leung, W. Sun, L. Zheng, S. Brookes, M. Tully, and R. Shi, "Anti-acrolein treatment improves behavioral outcome and alleviates myelin damage in experimental autoimmune enchephalomyelitis mouse," *Neuroscience*, vol. 173, pp. 150–155, 2011.

[127] K. Hamann, G. Nehrt, H. Ouyang, B. Duerstock, and R. Shi, "Hydralazine inhibits compression and acrolein-mediated injuries in ex vivo spinal cord," *Journal of Neurochemistry*, vol. 104, no. 3, pp. 708–718, 2008.

[128] K. Hamann and R. Shi, "Acrolein scavenging: a potential novel mechanism of attenuating oxidative stress following spinal cord injury," *Journal of Neurochemistry*, vol. 111, no. 6, pp. 1348–1356, 2009.

[129] P. K. Kamat, A. Kalani, P. Kyles, S. C. Tyagi, and N. Tyagi, "Autophagy of mitochondria: a promising therapeutic target for neurodegenerative disease," *Cell Biochemistry and Biophysics*, vol. 70, no. 2, pp. 707–719, 2014.

[130] A. Abdanipour, T. Tiraihi, A. Noori-Zadeh, A. Majdi, and R. Gosaili, "Evaluation of lovastatin effects on expression of anti-apoptotic Nrf2 and PGC-1α genes in neural stem cells treated with hydrogen peroxide," *Molecular Neurobiology*, vol. 49, no. 3, pp. 1364–1372, 2014.

[131] M. Schachter, "Chemical, pharmacokinetic and pharmacodynamic properties of statins: an update," *Fundamental and Clinical Pharmacology*, vol. 19, no. 1, pp. 117–125, 2005.

[132] C. Hölscher, "Central effects of GLP-1: new opportunities for treatments of neurodegenerative diseases," *The Journal of Endocrinology*, vol. 221, no. 1, pp. T31–T41, 2014.

[133] C. Hölscher, "Potential role of glucagon-like peptide-1 (GLP-1) in neuroprotection," *CNS Drugs*, vol. 26, no. 10, pp. 871–882, 2012.

[134] H. Zhang, A. Ray, N. M. Miller, D. Hartwig, K. A. Pritchard, and B. N. Dittel, "Inhibition of myeloperoxidase at the peak of experimental autoimmune encephalomyelitis restores blood-brain barrier integrity and ameliorates disease severity," *Journal of Neurochemistry*, vol. 136, no. 4, pp. 826–836, 2016.

[135] H.-M. Yun, K.-R. Park, E.-C. Kim, and J. T. Hong, "PRDX6 controls multiple sclerosis by suppressing inflammation and blood brain barrier disruption," *Oncotarget*, vol. 6, no. 25, pp. 20875–20884, 2015.

[136] I. R. Stojanovic, M. Kostic, and S. Ljubisavljevic, "The role of glutamate and its receptors in multiple sclerosis," *Journal of Neural Transmission*, vol. 121, no. 8, pp. 945–955, 2014.

[137] M. T. Viscomi, L. Latini, E. Bisicchia, V. Sasso, and M. Molinari, "Remote degeneration: insights from the hemicerebellectomy model," *Cerebellum*, vol. 14, no. 1, pp. 15–18, 2015.

[138] M. T. Viscomi and M. Molinari, "Remote neurodegeneration: multiple actors for one play," *Molecular Neurobiology*, vol. 50, no. 2, pp. 368–389, 2014.

[139] P. Pacher and K. Mackie, "Interplay of cannabinoid 2 (CB2) receptors with nitric oxide synthases, oxidative and nitrative stress, and cell death during remote neurodegeneration," *Journal of Molecular Medicine*, vol. 90, no. 4, pp. 347–351, 2012.

[140] H. Huang, A. Taraboletti, and L. P. Shriver, "Dimethyl fumarate modulates antioxidant and lipid metabolism in oligodendrocytes," *Redox Biology*, vol. 5, pp. 169–175, 2015.

[141] Q. Wang, S. Chuikov, S. Taitano et al., "Dimethyl fumarate protects neural stem/progenitor cells and neurons from oxidative damage through Nrf2-ERK1/2 MAPK pathway," *International Journal of Molecular Sciences*, vol. 16, no. 6, pp. 13885–13907, 2015.

[142] S. Licht-Mayer, I. Wimmer, S. Traffehn et al., "Cell type-specific Nrf2 expression in multiple sclerosis lesions," *Acta Neuropathologica*, vol. 130, no. 2, pp. 263–277, 2015.

[143] T. Dehmel, M. Döbert, S. Pankratz et al., "Monomethylfumarate reduces in vitro migration of mononuclear cells," *Neurological Sciences*, vol. 35, no. 7, pp. 1121–1125, 2014.

[144] I. Lastres-Becker, A. J. García-Yagüe, R. H. Scannevin et al., "Repurposing the NRF2 activator dimethyl fumarate as therapy against synucleinopathy in Parkinson's disease," *Antioxidants & Redox Signaling*, vol. 25, no. 2, pp. 61–77, 2016.

[145] S. E. Fiedler, A. R. Kerns, C. Tsang, V. Tsang, D. Bourdette, and S. Salinthone, "Dimethyl fumarate activates the prostaglandin EP2 receptor and stimulates cAMP signaling in human peripheral blood mononuclear cells," *Biochemical and Biophysical Research Communications*, vol. 475, no. 1, pp. 19–24, 2016.

[146] T. Kume, A. Suenaga, Y. Izumi, and A. Akaike, "Protective effect of dimethyl fumarate on an oxidative stress model induced by sodium nitroprusside in mice," *Biological & Pharmaceutical Bulletin*, vol. 39, no. 6, pp. 1055–1059, 2016.

[147] Y. Liu, J. Qiu, Z. Wang et al., "Dimethylfumarate alleviates early brain injury and secondary cognitive deficits after experimental subarachnoid hemorrhage via activation of Keap1-Nrf2-ARE system," *Journal of Neurosurgery*, vol. 123, no. 4, pp. 915–923, 2015.

[148] R. Kunze, A. Urrutia, A. Hoffmann et al., "Dimethyl fumarate attenuates cerebral edema formation by protecting the blood-brain barrier integrity," *Experimental Neurology*, vol. 266, pp. 99–111, 2015.

[149] C. To, C. S. Ringelberg, D. B. Royce et al., "Dimethyl fumarate and the oleanane triterpenoids, CDDO-imidazolide and CDDO-methyl ester, both activate the Nrf2 pathway but have opposite effects in the A/J model of lung carcinogenesis," *Carcinogenesis*, vol. 36, no. 7, pp. 769–781, 2015.

[150] C. Schuh, I. Wimmer, S. Hametner et al., "Oxidative tissue injury in multiple sclerosis is only partly reflected in experimental disease models," *Acta Neuropathologica*, vol. 128, no. 2, pp. 247–266, 2014.

[151] M. Serdar, J. Herz, K. Kempe et al., "Fingolimod protects against neonatal white matter damage and long-term cognitive deficits caused by hyperoxia," *Brain, Behavior, and Immunity*, vol. 52, pp. 106–119, 2016.

[152] A. D. Pusic and R. P. Kraig, "Phasic treatment with interferon gamma stimulates release of exosomes that protect against spreading depression," *Journal of Interferon and Cytokine Research*, vol. 35, no. 10, pp. 795–807, 2015.

[153] H. M. Schipper, D. Arnold, F. Grand'Maison et al., "Tolerability and safety of combined glatiramer acetate and N-acetylcysteine in relapsing-remitting multiple sclerosis," *Clinical Neuropharmacology*, vol. 38, no. 4, pp. 127–131, 2015.

[154] C. G. Pascuan, E. H. Simon, A. M. Genaro, and M. L. Palumbo, "Involvement of nitric oxide in improving stress-induced behavioural alteration by glatiramer acetate treatment in female BALB/c mice," *Psychopharmacology*, vol. 232, no. 9, pp. 1595–1605, 2015.

[155] M. Adamczyk-Sowa, K. Pierzchala, P. Sowa, R. Polaniak, M. Kukla, and M. Hartel, "Influence of melatonin supplementation on serum antioxidative properties and impact of the quality of life in multiple sclerosis patients," *Journal of Physiology and Pharmacology*, vol. 65, no. 4, pp. 543–550, 2014.

[156] M. Adamczyk-Sowa, K. Pierzchala, P. Sowa et al., "Melatonin acts as antioxidant and improves sleep in MS patients," *Neurochemical Research*, vol. 39, no. 8, pp. 1585–1593, 2014.

[157] G. Pentón-Rol, N. Lagumersindez-Denis, L. Muzio et al., "Comparative neuroregenerative effects of C-phycocyanin and IFN-beta in a model of multiple sclerosis in mice," *Journal of Neuroimmune Pharmacology*, vol. 11, no. 1, pp. 153–167, 2016.

[158] C. Bahamonde, C. Conde, E. Agüera et al., "Elevated melatonin levels in natalizumab-treated female patients with relapsing-remitting multiple sclerosis: Relationship to oxidative stress," *European Journal of Pharmacology*, vol. 730, no. 1, pp. 26–30, 2014.

[159] I. Tasset, E. Agüera, F. Gascón et al., "Natalizumab and reduction of carbonylated proteins in patients with multiple sclerosis," *Revista de Neurologia*, vol. 54, no. 8, pp. 449–452, 2012.

[160] A. Jamroz-Wisniewska, J. Beltowski, Z. Stelmasiak, and H. Bartosik-Psujek, "Paraoxonase 1 activity in multiple sclerosis patients during mitoxantrone therapy," *Acta Neurologica Scandinavica*, vol. 127, no. 6, pp. e33–e36, 2013.

[161] F. Molinari, V. Simonetti, M. Franzini et al., "Ozone autohemotherapy induces long-term cerebral metabolic changes in multiple sclerosis patients," *International Journal of Immunopathology and Pharmacology*, vol. 27, no. 3, pp. 379–389, 2014.

[162] N. A. Salem, N. Assaf, M. F. Ismail, Y. A. Khadrawy, and M. Samy, "Ozone therapy in ethidium bromide-induced demyelination in rats: possible protective effect," *Cellular and Molecular Neurobiology*, vol. 36, no. 6, pp. 943–954, 2016.

Hindawi Publishing Corporation
Oxidative Medicine and Cellular Longevity
Volume 2016, Article ID 4797102, 11 pages
http://dx.doi.org/10.1155/2016/4797102

Review Article

Oxidative Stress and *Salvia miltiorrhiza* in Aging-Associated Cardiovascular Diseases

Cheng-Chieh Chang,[1] Yu-Chun Chang,[2] Wen-Long Hu,[1,3,4] and Yu-Chiang Hung[1,5]

[1]*Department of Chinese Medicine, Kaohsiung Chang Gung Memorial Hospital and Chang Gung University College of Medicine, Kaohsiung, Taiwan*
[2]*Department of Applied Cosmetology, Kao Yuan University, Kaohsiung, Taiwan*
[3]*Kaohsiung Medical University, College of Medicine, Kaohsiung, Taiwan*
[4]*Fooyin University College of Nursing, Kaohsiung, Taiwan*
[5]*School of Chinese Medicine for Post Baccalaureate, I-Shou University, Kaohsiung, Taiwan*

Correspondence should be addressed to Yu-Chiang Hung; hungyuchiang@gmail.com

Received 31 May 2016; Accepted 15 September 2016

Academic Editor: Capucine Trollet

Aging-associated cardiovascular diseases (CVDs) have some risk factors that are closely related to oxidative stress. *Salvia miltiorrhiza* (SM) has been used commonly to treat CVDs for hundreds of years in the Chinese community. We aimed to explore the effects of SM on oxidative stress in aging-associated CVDs. Through literature searches using Medicine, PubMed, EMBASE, Cochrane library, CINAHL, and Scopus databases, we found that SM not only possesses antioxidant, antiapoptotic, and anti-inflammatory effects but also exerts angiogenic and cardioprotective activities. SM may reduce the production of reactive oxygen species by inhibiting oxidases, reducing the production of superoxide, inhibiting the oxidative modification of low-density lipoproteins, and ameliorating mitochondrial oxidative stress. SM also increases the activities of catalase, manganese superoxide dismutase, glutathione peroxidase, and coupled endothelial nitric oxide synthase. In addition, SM reduces the impact of ischemia/reperfusion injury, prevents cardiac fibrosis after myocardial infarction, preserves cardiac function in coronary disease, maintains the integrity of the blood-brain barrier, and promotes self-renewal and proliferation of neural stem/progenitor cells in stroke. However, future clinical well-designed and randomized control trials will be necessary to confirm the efficacy of SM in aging-associated CVDs.

1. Introduction

Cardiovascular diseases (CVDs) are a group of disorders related to the heart or blood vessels. Major CVDs include stroke, ischemic heart disease, cardiomyopathy, rheumatic heart disease, hypertensive heart disease, endocarditis, atrial fibrillation, aortic aneurysm, and peripheral arterial disease [1]. Global life expectancy increased from 65.3 years in 1990 to 71.5 years in 2013. At the same time, the numbers of deaths from noncommunicable diseases increased steadily [2]. CVDs are the leading form of noncommunicable diseases [2]. In 2012 and 2013, 17.3 million deaths worldwide resulted from CVDs [3]. Among these deaths, coronary artery disease and stroke contributed most to the total global burden of CVDs [1]. It is estimated that 90% of CVDs are preventable [4]. The Framingham and World Health Organization MONICA studies found several risk factors for CVDs (e.g., age, smoking, physical inactivity, unhealthy diet, obesity, family history, hypertension, diabetes mellitus, and hyperlipidemia) [5–10]. Some of these risk factors are immutable; however, many important risk factors are modifiable. When relevant risk factors decrease, the incidence and mortality of CVDs improved.

Most CVD risk factors are related to oxidative stress. Reactive oxygen species (ROS) are the main cause of oxidative stress and are highly reactive with proteins, lipids, and DNA, damaging these cellular components [11]. Under normal conditions, the production of ROS during aerobic metabolism

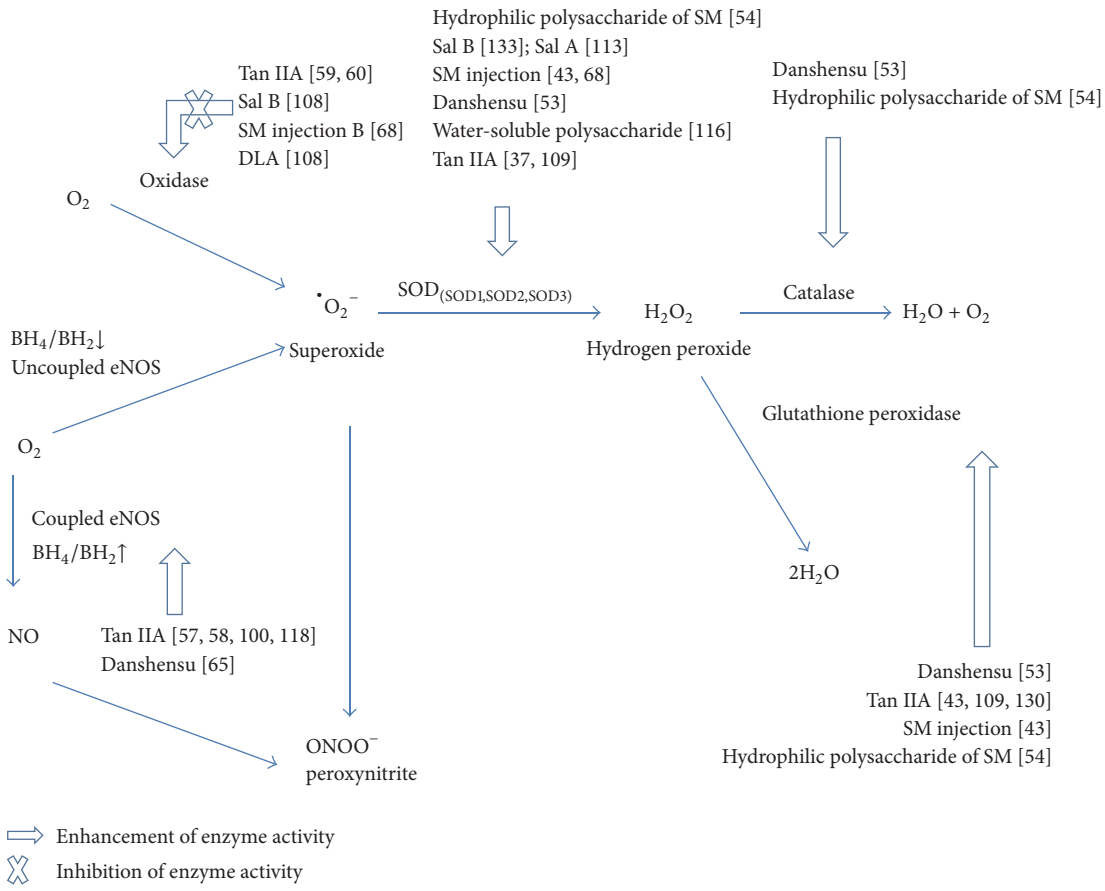

Figure 1: Vascular reactive oxygen species production. Oxidases convert oxygen to superoxide, which is then dismutated to H_2O_2 by superoxide dismutase (SOD). H_2O_2 can be converted to H_2O by catalase or glutathione peroxidase. In addition, coupled endothelial NO synthase (eNOS) catalyzes the formation of nitric oxide (NO). When tetrahydrobiopterin (BH4) generation is reduced, the uncoupled eNOS produces superoxide instead of NO. The superoxide can react rapidly with NO to form peroxynitrite ($ONOO^-$), a powerful oxidant and nitrating agent. Reference numbers are inside the parentheses. DLA: 3,4-dihydroxyphenyl lactic acid; SM: *Salvia miltiorrhiza*; Sal A: salvianolic acid A; Sal B: salvianolic acid B; Tan IIA: tanshinone IIA.

and the scavenging of ROS by tissue antioxidant systems are in balance [12]. This balance is shifted in favor of oxidative stress in the presence of cardiovascular risk factors [5, 13, 14].

The most important forms of ROS are nitric oxide (NO), superoxide, hydrogen peroxide, and peroxynitrite (Figure 1). NO is produced in normal physiologic conditions from L-arginine by coupled endothelial nitric oxide synthase (eNOS) that is activated via protein kinase A- or Akt-dependent phosphorylation [15]. NO is a crucial mediator of blood vessel homeostasis by inhibiting vascular smooth muscle contraction and growth, platelet aggregation, and leukocyte adhesion to the endothelium. Under some circumstances, such as hypertension, hyperglycemia, and hypercholesterolemia, eNOS becomes uncoupled and superoxide is synthesized rather than NO [16–20]. When normal NO production is impaired, CVDs may occur [21].

In aged vessels, endothelial dysfunction occurs owing to eNOS uncoupling by reducing the tetrahydrobiopterin to dihydrobiopterin ratio [22]. Superoxide is the product of a univalent reduction of oxygen by various oxidases [23]. The important oxidases include xanthine oxidase, uncoupled NO synthases, cytochrome P450 enzymes, and mitochondrial and NADPH oxidases [24–26]. Superoxide is toxic and possesses three main effects that contribute to the pathogenesis of CVDs [27]: (1) rapid inactivation and reaction with NO to form the more highly reactive peroxynitrite; (2) mediation of aberrant redox signaling in the vasculature to induce alterations of vascular function, and (3) direct oxidative damage to cell components [28].

Peroxynitrite is a powerful oxidant and nitrating agent. Peroxynitrite can damage a wide array of cellular molecules, including carbonate, proteins, low-density lipoproteins (LDL), and DNA to form nitration and nitrosation products that are involved in the pathogenesis of cardiovascular complications [29, 30].

The superoxide dismutases (SODs) are the major antioxidant enzymes that degrade superoxide. There are three isoforms of SOD in mammals: cytoplasmic Cu/ZnSOD (SOD1), mitochondrial MnSOD (SOD2), and extracellular Cu/ZnSOD (SOD3) [31]. All forms of SOD rapidly dismutate superoxide to the more stable ROS, hydrogen peroxide, that

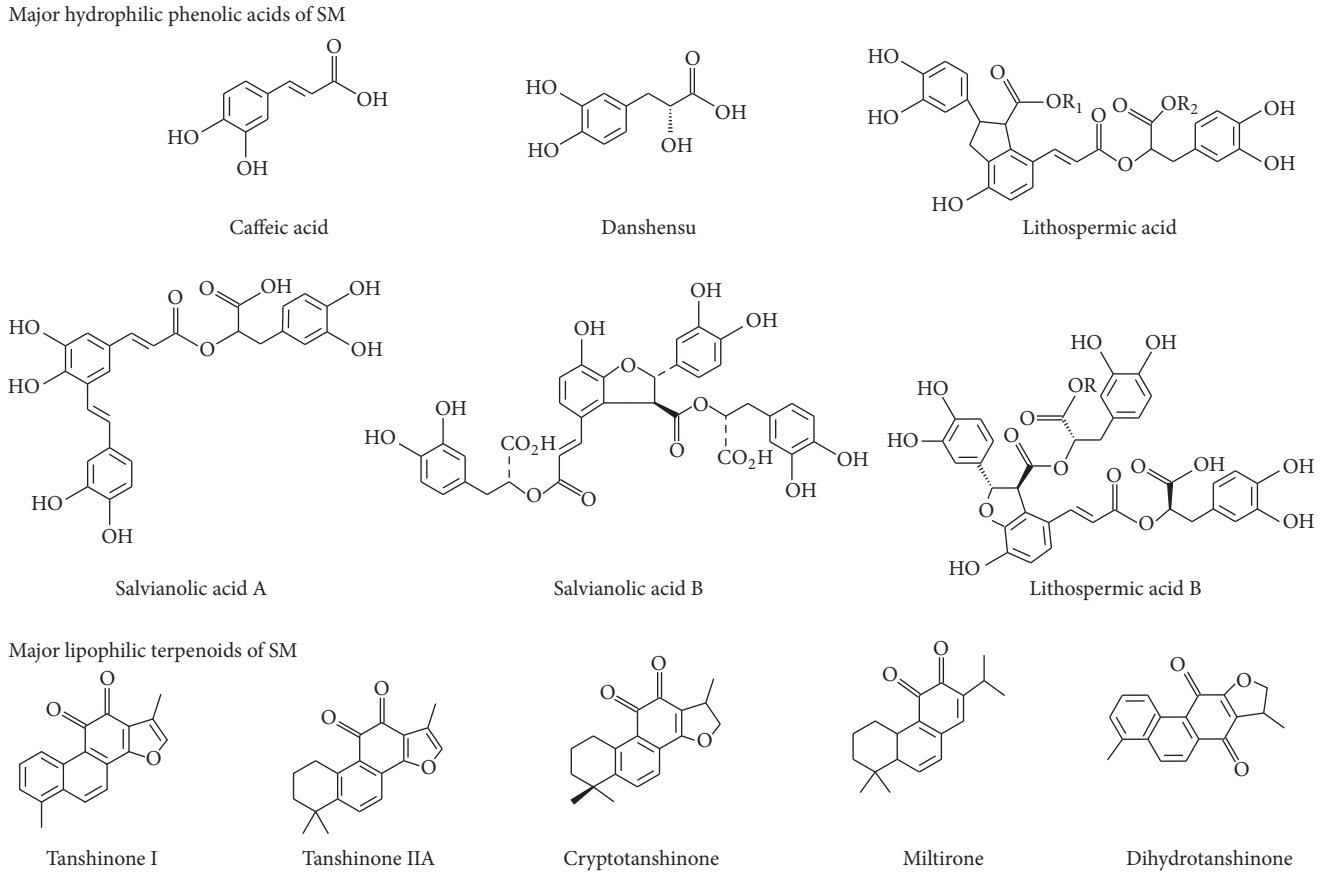

Figure 2: The chemical structure of major hydrophilic phenolic acids and lipophilic terpenoids of *Salvia miltiorrhiza*.

is then converted to water and oxygen by either catalase or glutathione peroxidase [32].

Salvia miltiorrhiza (SM) belongs to the family of Labiatae and its dried root, referred to as "Danshen" in traditional Chinese medicine, has been commonly used for hundreds of years in the treatment of CVDs [33]. Our previous population-based studies demonstrated that SM is the most common herbal drug used to treat ischemic heart disease [34] and ischemic stroke [35]. In traditional Chinese medicine, Danshen is regarded as an important herb for "activating circulation and dispersing stasis or sludging of blood." SM exhibits strong antioxidant activity by scavenging ROS [36]. SM also modulates endothelial cell permeability, inhibits platelet aggregation [37], and protects human umbilical vein endothelial cells against homocysteine-induced endothelial dysfunction [38] or vascular smooth muscle cells proliferation [39].

There are many active constituents found in alcohol and water extracts of SM (Figure 2). At least 49 diterpenoid quinones, more than 36 hydrophilic phenolic acids, and 23 essential oil constituents have been isolated and identified from SM [40]. Among the chemical components, tanshinone IIA (Tan IIA) and salvianolic acid B (Sal B) are usually chosen as markers to assess the quality of SM [41].

Terpenoids are the most important lipophilic components of SM. Most diterpenoids are present as tanshinones and their analogs, which are a class of abietane diterpene compounds found exclusively in the Salvia genus [42]. Tanshinone I, Tan IIA, and cryptotanshinone are the major constituents of the tanshinones and are studied mainly for their biological activity [43]. SM also contains some triterpenoids [44]. These terpenoids possess a wide range of biological activities including antioxidant [45], antibacterial [46], anti-inflammatory [47], antiatherogenic [36], neuroprotective [48], antitumor [49], and antidiabetic [50] effects.

Phenolic acids are the main type of hydrophilic component from SM. Most of the phenolic acids in SM are condensation derivatives of caffeic acid in different linkage forms and numbers [51]. The most prominent effects of the phenolic acids in SM are antioxidant, anticoagulant, and antithrombotic activities and protection of cells from ischemia-reperfusion (I/R) injury [33, 52, 53]. Moreover, over the past few years, there are several studies showing that the polysaccharides extracted from SM also have antioxidant and antitumor activities [54, 55].

Unfavorable changes in CVD risk factors are seen in aging individuals and will likely be reflected in worsening morbidity and mortality [56]. Thus, the minimization of risk factors is a key point for decreasing the incidence of aging-related CVD.

Many researchers have demonstrated that SM can reduce the impact of CVD risk factors and the injury caused by

oxidative stress. This article provides an overview of SM in terms of its ability to reduce oxidative stress-induced injury and aging-related risk factors associated with CVD. Studies of the effects of SM on the two most frequent CVDs, coronary artery disease and stroke, are also reviewed.

2. Materials and Methods

The current review focuses on the role of oxidative stress and SM (Danshen) in aging-associated CVDs. Literature searches were done using the Medicine, PubMed, EMBASE, Cochrane library, CINAHL, and Scopus databases, and the contents of the identified articles were summarized.

3. Results and Discussion

3.1. Hypertension. Hypertension is the most readily modifiable risk factor for CVDs [57]. Oxidative stress, an aberrant vascular redox system, and endothelial dysfunction can contribute to hypertension [13, 28]. In traditional Chinese medicine, Danshen is the most frequently prescribed single herb for hypertension [58]. Tan IIA has a vasodilatory effect through restoring eNOS coupling by increasing the ratio of tetrahydrobiopterin to dihydrobiopterin and reducing the production of superoxide by inhibiting the expression of NOX4, a member of the NADPH oxidase family [59, 60]. In addition to reducing ROS, Tan IIA protects against endothelial cell damage by decreasing the Bax/Bcl-2 ratio and inhibiting caspase-3 activation [61]. The water extract of SM that contains lithospermic acid B (also named tanshinoate B) and Sal B exhibits an antihypertensive effect through the inhibition of angiotensin-converting enzyme or the renin angiotensin system [62–65]. Sal B and danshensu, the major hydrophilic constituents of SM, can regulate vascular tone and reduce blood pressure by activating of the calcium-activated big potassium (BK_{CA}) channel [66, 67]. In addition, SM injection can decrease plasma levels of endothelin-1 and thromboxane B2 [68].

3.2. Smoking. Cigarette smoking is an important and reversible risk factor for CVDs but is ranked lower than hypertension because of the widespread implementation of smoke-free legislation [69]. However, in some countries, smoking remains the third leading risk factor for CVDs, behind dietary risks and hypertension. Smokers return to the risk level of never-smokers after cessation of smoking for at least 10 years [69].

Smoking may enhance oxidative stress not only through the production of ROS but also through weakening of the antioxidant defense systems [70]. Smoking-associated CVDs include abdominal aortic aneurysm, peripheral artery disease, unheralded coronary death, and subarachnoid hemorrhage [71]. SalA attenuates the formation of aortic aneurysms in apolipoprotein E-deficient mice by selectively inhibiting matrix metalloproteinase-9 (MMP-9) to maintain the integrity of blood vessels [72]. A crude extract of SM dilates isolated rat femoral arteries by opening tetraethylammonium-sensitive potassium channels in smooth muscle cells [73] and produces a vasorelaxant effect in the rat knee joint through the release of calcitonin gene-related peptide and the endothelium-derived relaxant factors NO and prostaglandins [74]. One recent study revealed that the injection of Danshen root could suppress cigarette smoking-induced lung inflammation by decreasing the levels of interleukin- (IL-) 8, IL-6, and tumor necrosis factor- (TNF-) α in Sprague-Dawley rats [75].

3.3. Hyperglycemia. Hyperglycemia and diabetes mellitus are strong, significant, and independent risk factors for CVDs [76, 77]. Hyperglycemia induces oxidative stress in diabetic patients, and the overproduction of ROS contributes to the development of CVDs [78, 79]. Peroxynitrite plays an important role in the pathogenesis of diabetic CVD complications through oxidative and nitrosative stress [29]. In the presence of hyperglycemia, vascular remodeling is augmented by uncoupled eNOS [80], increases in endothelial superoxide levels that inhibit vascular smooth muscle Na-K-ATPase activity [81], and downregulation of transient receptor potential cation channel subfamily V member 4 that regulates vascular function [82]. The hydrophilic extract of SM clearly ameliorates oxidative stress stimulated by hyperglycemia in diabetic patients with coronary heart disease [83]. The induction of vascular endothelial growth factor (VEGF) expression by high glucose levels is also reversed by the SM hydrophilic extract through amelioration of mitochondrial oxidative stress [84].

Sal B is the main bioactive component in the SM hydrophilic extract [85]. The tanshinones are insulin sensitizers that enhance the activity of insulin on tyrosine phosphorylation through the activation of Akt and extracellular signal-regulated kinase (ERK)1/2 and by glycogen synthase kinase (GSK)3β and glucose transporter (GLUT)4 translocation [86]. Furthermore, the hydrophilic polysaccharide of SM protects against the development of type 2 diabetes by attenuating insulin resistance through increases in the activities of catalase, MnSOD, and glutathione peroxidase in rats [54].

3.4. Hyperlipidemia. Hyperlipidemia is the most important risk factor for atherosclerosis and a major cause of CVDs [87, 88]. Increased transcytosis of lipoproteins is the initial event in atherogenesis. ROS generated by activated inflammatory cells and the production of oxidized lipoproteins are key points for atherosclerotic plaque erosion and rupture [89]. We showed that Tan IIA exhibits a strong antiatherosclerotic effect associated with reduced vascular cell adhesion molecule- (VCAM-) 1, intercellular adhesion molecule- (ICAM-) 1, and CX3CL1 expression through inhibition of the NF-κB signaling pathway in human vascular endothelial cells [90]. Sal B inhibits LDL oxidation and neointimal hyperplasia in endothelium-denuded hypercholesterolemic rabbits through inhibition of ROS production [91]. Magnesium tanshinoate B, an important aqueous component of SM, can also inhibit oxidative modification of LDLs, prevent the uptake of LDLs by macrophages [92], and protect endothelial cells against oxidized lipoprotein-induced apoptosis [93].

3.5. Overweight and Obesity. Obesity has become a global epidemic. The 2013 National Health and Nutrition Examination Survey (NHANES) guidelines recommended 64.5% of American adults for weight loss treatment [94]. Obesity is an independent risk factor for CVDs [95]. Adipose tissue is a significant source of TNF-α, IL-6, resistin, leptin, angiotensinogen, and adiponectin [96]. The production of these proinflammatory cytokines may contribute to the low-level systemic inflammation seen in obesity-associated chronic pathologies [97].

Endothelial dysfunction is present in obese individuals due to decreased NO and increased oxidative stress [98]. Cryptotanshinone inhibits phosphorylation of STAT3 during early adipogenesis and then downregulates the expression of the early transcription factors C/EBPβ and PPARγ to suppress preadipocyte differentiation [99]. Sal B can also suppress the expression of PPARγ and C/EBPα and increase the expression of GATA binding proteins 2 and 3 to prevent the differentiation of preadipocytes and weight gain in obese mice [100]. There is also a study in a rodent model demonstrating that a Chinese herbal extract (SK0506) containing SM possesses a favorable impact on the metabolic syndrome through suppression of visceral fat accumulation and regulation of lipid metabolism [101].

3.6. Coronary Artery and Ischemic Heart Diseases

3.6.1. Angina. Angina pectoris and coronary artery spasm are the most common coronary artery diseases. Tan IIA elicits a strong vasodilatory effect in rat and porcine coronary arterioles through the BK_{CA} channel and increased NO and cytochrome P450 metabolites [102, 103]. SalB also can relax the rat coronary artery by inhibiting calcium channels in vascular smooth muscle cells [104]. A systematic review of 60 eligible randomized controlled trials indicates that the Danshen dripping pill, in which SM is the main component, is more effective than isosorbide dinitrate in treating angina pectoris [105].

3.6.2. Myocardial Infarction (MI). Tan IIA prevents platelet activation by inhibiting the mitogen-activated protein kinase (MAPK) pathway, such as Erk-2 phosphorylation [106]. After MI, reperfusion of ischemic tissue provides oxygen and substrates that are necessary for tissue recovery. However, reperfusion may also induce I/R injury, including excessive production of ROS, enhanced biosynthesis of adhesion molecules, activation of leukocytes, and involvement of cytokines and other inflammatory mediators that cause target and remote organ damage [107]. Both the hydrophilic and lipophilic constituents of SM appear to improve the I/R-induced vascular damage multifactorially and synergistically [108]. The protective function of Tan IIA on myocardial I/R injury may be through inhibiting ROS production and attenuating the expression of high mobility group box B1 protein that results in the activation of proinflammatory pathways [109]. Tan IIA can also reduce monocyte chemoattractant protein-1 expression and macrophage infiltration.

The expression of transforming growth factor-β1 in cardiac fibroblasts is inhibited by Tan IIA via the NF-κB signaling pathway [110]. The water-soluble fraction of an SM root extract possesses antioxidant activity, and the hydrophilic components of SM, including protocatechuic aldehyde and Sal B, inhibit the TNF-α-induced expression of ICAM-1 and VCAM-1 and the NF-κB and activator protein-1 DNA binding activities in human umbilical vein endothelial cells [111].

Danshensu, the major water-soluble component of SM, protects isolated heart tissue against I/R injury through activation of Akt/ERK1/2/Nrf2 signaling [53]. Recent research shows that Sal A has antiapoptotic effects via activating ERK1/2 and downregulating c-Jun N-terminal kinase (JNK), with increased Bcl-2 and reduced Bax protein expression [112, 113]. A combination of SalB and ginsenoside Rg1 increases the viability of cardiac myocytes and reduces infarct size, thereby improving the functional parameters of the heart against I/R injury in rats [114]. The injection of SM containing water-soluble components such as Sal A shows a cardioprotective effect after infarction by inhibiting L-type Ca^{2+} channels and decreasing the contractility of adult rat cardiac myocytes [115]. Moreover, even the polysaccharide from SM possesses cardiac protective properties [116].

3.6.3. Cardiac Remodeling. Cardiac remodeling is an important aspect of the progression to heart failure observed after MI [117]. Patients with reverse remodeling during treatment have better outcomes and lower mortality than those without such remodeling [118]. Tanshinone VI protects the myocardium against I/R injury and attenuates the progression of myocardial remodeling in vitro [119]. Tan IIA attenuates the expression of angiotensin II-induced collagen type I, ROS formation, and the proliferation of cardiac fibroblasts [120, 121]. Recent research also demonstrates that Tan IIA inhibits extracellular matrix remodeling induced by angiotensin II in human cardiac fibroblasts through inhibition of Smad signaling and MMP-9 expression via nuclear localization of NF-κB [122]. Salvianolic acids, including SalA and Sal B, suppress ROS at the early stage of acute MI and then inhibit the subsequent transcription and posttranslational activation of MMP-9 [123, 124]. Sal B functions as a competitive inhibitor of MMP-9 and inhibits the migration, proliferation, collagen synthesis, and cytokine secretion of cardiac fibroblasts [125, 126].

3.7. Stroke. Stroke is the second leading global cause of death behind heart disease [3]. A nationwide population-based study surveyed the usage of traditional Chinese medicine for stroke patients in Taiwan. This study revealed that about 15% of stroke patients used traditional Chinese medicine and that SM was the most used single herb [127]. Disruption of the blood-brain barrier (BBB), inflammatory processes, and nerve cell apoptosis occur after stroke. Tan IIA decreases BBB permeability and suppresses the expression of ICAM-1 and MMP-9 significantly to reduce the infarct area [128]. Another study found that the protective effect of Tan IIA on I/R-induced nerve cells apoptosis involves suppression of excess

Table 1: The main antiapoptotic and anti-inflammatory mechanisms of SM.

	Mechanism	References
Antiapoptosis		
Salvianolic acid A	MAPK signaling pathway ↑ERK1/2; ↓JNK with ↓Bax/Bcl-2	[112, 113]
Salvianolic acid B	↑SIRT1; ↓Ac-FOXO1 with ↓Bax/Bcl-2	[134]
Magnesium tanshinoate B	↓JNK, ↓cytochrome c release, ↓caspase-3	[93]
Danshensu	↑PI3K/Akt signal pathway; ↑p-GSK-3β levels	[136]
Tanshinone IIA	↓Bax; ↓caspase-3, and ↓Bax/Bcl-2 ratio	[37]
Anti-inflammation		
Danshen root	↓IL 8; ↓IL-6 and ↓TNFα	[75]
Salvianolic acid B	↑SIRT1; ↓TNF-α; ↓IL-1β	[134]
Protocatechuic aldehyde	↓NF-κB; ↓AP-1; ↓VCAM-1; ↓ICAM-1	[111]
Tanshinone IIA	↓HMGB1; ↓NF-κB; ↓MCP-1; ↓TNF-α; ↓TGF-β1; ↓CX3CL1; ↓ICAM- 1; ↓VCAM-1	[90, 109, 110]
Albumin-conjugated PEGylated Tan IIA	↓p38 MAPK; ↓ERK1/2; ↓JNK; iNOS; ↓MPO; ↓TNF-α; ↓IL-1β; ↓IL-6; ↓TNF-α; ↓IL-8; ↓GFAP; ↓MMP-9; ↓COX-2; ↑PPARγ; ↑IL-10; ↑TGF-β1	[131, 132]

↑ means upregulation; ↓ means downregulation.
COX-2, cyclooxygenase-2; MAPK, mitogen-activated protein kinase; ERK, extracellular signal-regulated kinase; JNK, c-Jun N-terminal kinase; IL, interleukin; GFAP, glial fibrillary acidic protein; GSK-3β, glycogen synthase kinase-3β; interleukin; MPO, myeloperoxidase; MCP-1, monocyte chemoattractant protein-1; TNF-α, tumor necrosis factor-alpha; TGF-β1, transforming growth factor-β1; SIRT1, silent information regulator 1; PI3K, phosphoinositide 3-kinase; VCAM-1, vascular cell adhesion molecule; ICAM-1, intercellular adhesion molecule; MMP-9, matrix metalloproteinase-9; PPARγ, peroxisome proliferator activated receptor γ.

activation of glial cells, inhibiting the activities of caspase-3 and caspase-8, central regulators of apoptosis [129].

Tan IIA protects the integrity of the BBB through the increased expression of critical endothelial tight junction proteins [130]. Tan IIA is neuroprotective against ischemic stroke, but its short half-life and poor permeability across the BBB limits its effectiveness. There are reports demonstrating that albumin-conjugated PEGylated Tan IIA possesses better brain delivery efficacy and displays remarkable neuroprotective effects through modulation of the MAPK signal pathways and inflammatory cascades [131, 132]. SalB exhibits its neuroprotective effect through antioxidant and antiapoptotic activities by reducing the Bax/Bcl-2 ratio in hippocampal CA1 neurons in mice with I/R injury [133]. The expression of silent information regulator 1, a nicotinamide adenine dinucleotide-dependent deacetylase, is also upregulated by Sal B yielding an antiapoptotic effect after ischemia [134].

A novel derivative of Sal B exhibits a neuroprotective effect against cerebral ischemic injury through angiogenesis and nerve function recovery via the JAK2/STAT3 and VEGF/Flk-1 pathways [135]. Danshensu also possesses a neuroprotective effect against I/R injury by inhibiting apoptosis through activating the phosphoinositide 3-kinase (PI3K)/Akt signaling pathway [136]. Rehabilitation can facilitate some recovery of neurological function after a stroke with evidence of neurogenesis [137]. Sal B promotes neural stem/progenitor cell self-renewal and proliferation through the PI3K/Akt signaling pathway, resulting in improved cognitive function after stroke in rats [138]. These results suggest that SM may act as a potential drug in the treatment of brain injury or neurodegenerative diseases.

3.8. Future Prospects. Figures 1 and 2 illustrate the chemical structure and effects of SM on ROS. Table 1 lists the main antiapoptotic and anti-inflammatory mechanisms of SM. In addition, there are several clinical trials related to SM underway in the United States, including two phase III clinical trials. One is the "Phase III Trial of Dantonic® (T89) Capsule to Prevent and Treat Stable Angina." The other trial is the "Phase III Study of Compound Danshen Dripping Pills to Treat Diabetic Retinopathy." Both trials focus on oxidative stress and CVDs. The results will provide important new information about the clinical utility of SM.

The tanshinones are functionally active components in SM. However, they are poorly water-soluble with a low dissolution rate that results in low oral bioavailability. Many studies have focused on improving the drug delivery systems for tanshinones including the use of liposomes [139], nanoparticles [131, 140], and solid dispersions [141]. Further research in this area is needed to assure optimal delivery of SM products.

4. Conclusion

SM exhibits antioxidant, antiapoptotic, and anti-inflammatory effects. SM reduces ROS production through inhibiting oxidases, reducing the production of superoxide, inhibiting oxidative modification of LDLs, and ameliorating mitochondrial oxidative stress. It also increases the activities of catalase, MnSOD, glutathione peroxidase, and coupled eNOS. Moreover, in coronary artery disease and stroke, SM not only reduces the impact of I/R injury but also prevents cardiac fibrosis after MI, preserves cardiac function in coronary disease, and maintains the integrity of the BBB, thereby

promoting neural stem/progenitor cell self-renewal and proliferation following a stroke. Therefore, SM can be an effective agent for the prevention and treatment of CVDs. However, in accordance with in vitro and in vivo laboratory evidence, well-designed clinical studies are necessary to confirm the efficacy of SM in the treatment of CVDs.

Competing Interests

The authors declare no competing interests.

Authors' Contributions

Cheng-Chieh Chang and Yu-Chun Chang contributed equally to this work.

Acknowledgments

This work was supported partly by National Science Research Grant of Taiwan (NSC-96-2320-B-182-023-MY2) and Chang Gung Memorial Hospital (CMRPG83011; CMRPD32027).

References

[1] A. E. Moran, G. A. Roth, J. Narula, and G. A. Mensah, "1990–2010 Global cardiovascular disease atlas," *Global Heart*, vol. 9, no. 1, pp. 3–16, 2014.

[2] GBD 2013 Mortality and Causes of Death Collaborators, "Global, regional, and national age-sex specific all-cause and cause-specific mortality for 240 causes of death, 1990–2013: a systematic analysis for the Global Burden of Disease Study 2013," *The Lancet*, vol. 385, no. 9963, pp. 117–171, 2015.

[3] G. A. Roth, M. D. Huffman, A. E. Moran et al., "Global and regional patterns in cardiovascular mortality from 1990 to 2013," *Circulation*, vol. 132, no. 17, pp. 1667–1678, 2015.

[4] H. C. McGill Jr., C. A. McMahan, and S. S. Gidding, "Preventing heart disease in the 21st century: implications of the Pathobiological Determinants of Atherosclerosis in Youth (PDAY) study," *Circulation*, vol. 117, no. 9, pp. 1216–1227, 2008.

[5] J. R. Margolis, R. F. Gillum, M. Feinleib, R. C. Brasch, and R. R. Fabsitz, "Community surveillance for coronary heart disease: the framingham cardiovascular disease survey: methods and preliminary results," *American Journal of Epidemiology*, vol. 100, no. 6, pp. 425–436, 1974.

[6] R. F. Gillum, M. Feinleib, J. R. Margolis, R. R. Fabsitz, and R. C. Brasch, "Community surveillance for cardiovascular disease: the Framingham cardiovascular disease survey. Some methodological problems in the community study of cardiovascular disease," *Journal of Chronic Diseases*, vol. 29, no. 5, pp. 289–299, 1976.

[7] W. B. Kannel, D. McGee, and T. Gordon, "A general cardiovascular risk profile: the Framingham study," *The American Journal of Cardiology*, vol. 38, no. 1, pp. 46–51, 1976.

[8] R. F. Gillum, R. R. Fabsitz, M. Feinleib, P. A. Wolf, J. R. Margolis, and R. C. Brasch, "Community surveillance for cerebrovascular disease: the Framingham Cardiovascular Disease Survey," *Public Health Reports*, vol. 93, no. 5, pp. 438–442, 1978.

[9] U. Keil, "The worldwide WHO MONICA project: results and perspectives," *Gesundheitswesen*, vol. 67, supplement 1, pp. S38–S45, 2005.

[10] C. W. Tsao and R. S. Vasan, "Cohort Profile: the Framingham Heart Study (FHS): overview of milestones in cardiovascular epidemiology," *International Journal of Epidemiology*, vol. 44, no. 6, pp. 1800–1813, 2015.

[11] C. A. Papaharalambus and K. K. Griendling, "Basic mechanisms of oxidative stress and reactive oxygen species in cardiovascular injury," *Trends in Cardiovascular Medicine*, vol. 17, no. 2, pp. 48–54, 2007.

[12] B. Frei, "Reactive oxygen species and antioxidant vitamins: mechanisms of action," *The American Journal of Medicine*, vol. 97, no. 3, pp. 5S–13S, 1994.

[13] Q. N. Dinh, G. R. Drummond, C. G. Sobey, and S. Chrissobolis, "Roles of inflammation, oxidative stress, and vascular dysfunction in hypertension," *BioMed Research International*, vol. 2014, Article ID 406960, 11 pages, 2014.

[14] D. Tousoulis, A. Briasoulis, N. Papageorgiou et al., "Oxidative stress and endothelial function: therapeutic interventions," *Recent Patents on Cardiovascular Drug Discovery*, vol. 6, no. 2, pp. 103–114, 2011.

[15] M. Khazaei, F. Moien-afshari, and I. Laher, "Vascular endothelial function in health and diseases," *Pathophysiology*, vol. 15, no. 1, pp. 49–67, 2008.

[16] A. Bouloumié, J. Bauersachs, W. Linz et al., "Endothelial dysfunction coincides with an enhanced nitric oxide synthase expression and superoxide anion production," *Hypertension*, vol. 30, no. 4, pp. 934–941, 1997.

[17] F. Cosentino, K. Hishikawa, Z. S. Katusic, and T. F. Lüscher, "High glucose increases nitric oxide synthase expression and superoxide anion generation in human aortic endothelial cells," *Circulation*, vol. 96, no. 1, pp. 25–28, 1997.

[18] U. Landmesser, S. Dikalov, S. R. Price et al., "Oxidation of tetrahydrobiopterin leads to uncoupling of endothelial cell nitric oxide synthase in hypertension," *The Journal of Clinical Investigation*, vol. 111, no. 8, pp. 1201–1209, 2003.

[19] S. Kawashima and M. Yokoyama, "Dysfunction of endothelial nitric oxide synthase and atherosclerosis," *Arteriosclerosis, Thrombosis, and Vascular Biology*, vol. 24, no. 6, pp. 998–1005, 2004.

[20] K. A. Pritchard Jr., L. Groszek, D. M. Smalley et al., "Native low-density lipoprotein increases endothelial cell nitric oxide synthase generation of superoxide anion," *Circulation Research*, vol. 77, no. 3, pp. 510–518, 1995.

[21] K. Chen, R. N. Pittman, and A. S. Popel, "Nitric oxide in the vasculature: where does it come from and where does it go? A quantitative perspective," *Antioxidants and Redox Signaling*, vol. 10, no. 7, pp. 1185–1198, 2008.

[22] Y.-M. Yang, A. Huang, G. Kaley, and D. Sun, "eNOS uncoupling and endothelial dysfunction in aged vessels," *American Journal of Physiology—Heart and Circulatory Physiology*, vol. 297, no. 5, pp. H1829–H1836, 2009.

[23] I. Fridovich, "Superoxide anion radical ($O_2^{\cdot-}$), superoxide dismutases, and related matters," *The Journal of Biological Chemistry*, vol. 272, pp. 18515–18517, 1997.

[24] L. S. Terada, I. R. Willingham, M. E. Rosandich, J. A. Leff, G. W. Kindt, and J. E. Repine, "Generation of superoxide anion by brain endothelial cell xanthine oxidase," *Journal of Cellular Physiology*, vol. 148, no. 2, pp. 191–196, 1991.

[25] R. M. Clancy, J. Leszczynska-Piziak, and S. B. Abramson, "Nitric oxide, an endothelial cell relaxation factor, inhibits neutrophil superoxide anion production via a direct action on the NADPH oxidase," *The Journal of Clinical Investigation*, vol. 90, no. 3, pp. 1116–1121, 1992.

[26] J.-M. Li and A. M. Shah, "Differential NADPH- versus NADH-dependent superoxide production by phagocyte-type endothelial cell NADPH oxidase," *Cardiovascular Research*, vol. 52, no. 3, pp. 477–486, 2001.

[27] J.-M. Li and A. M. Shah, "Endothelial cell superoxide generation: regulation and relevance for cardiovascular pathophysiology," *American Journal of Physiology—Regulatory Integrative and Comparative Physiology*, vol. 287, no. 5, pp. R1014–R1030, 2004.

[28] M. Y. Lee and K. K. Griendling, "Redox signaling, vascular function, and hypertension," *Antioxidants & Redox Signaling*, vol. 10, no. 6, pp. 1045–1059, 2008.

[29] P. Pacher and C. Szabó, "Role of peroxynitrite in the pathogenesis of cardiovascular complications of diabetes," *Current Opinion in Pharmacology*, vol. 6, no. 2, pp. 136–141, 2006.

[30] Z. Cao and Y. Li, "Potent inhibition of peroxynitrite-induced DNA strand breakage by ethanol: possible implications for ethanol-mediated cardiovascular protection," *Pharmacological Research*, vol. 50, no. 1, pp. 13–19, 2004.

[31] T. Fukai and M. Ushio-Fukai, "Superoxide dismutases: role in redox signaling, vascular function, and diseases," *Antioxidants & Redox Signaling*, vol. 15, no. 6, pp. 1583–1606, 2011.

[32] J. Han, V. V. Shuvaev, and V. R. Muzykantov, "Catalase and superoxide dismutase conjugated with platelet-endothelial cell adhesion molecule antibody distinctly alleviate abnormal endothelial permeability caused by exogenous reactive oxygen species and vascular endothelial growth factor," *The Journal of Pharmacology and Experimental Therapeutics*, vol. 338, no. 1, pp. 82–91, 2011.

[33] X. Wang, S. L. Morris-Natschke, and K.-H. Lee, "New developments in the chemistry and biology of the bioactive constituents of Tanshen," *Medicinal Research Reviews*, vol. 27, no. 1, pp. 133–148, 2007.

[34] Y.-C. Hung, Y.-J. Tseng, W.-L. Hu et al., "Demographic and prescribing patterns of Chinese herbal products for individualized therapy for ischemic heart disease in Taiwan: population-based study," *PLoS ONE*, vol. 10, no. 8, Article ID e0137058, 2015.

[35] I. L. Hung, Y. C. Hung, L. Y. Wang et al., "Chinese herbal products for ischemic stroke," *The American Journal of Chinese Medicine*, vol. 43, no. 7, pp. 1365–1379, 2015.

[36] J. Fu, H. Huang, J. Liu, R. Pi, J. Chen, and P. Liu, "Tanshinone IIA protects cardiac myocytes against oxidative stress-triggered damage and apoptosis," *European Journal of Pharmacology*, vol. 568, no. 1–3, pp. 213–221, 2007.

[37] J.-Q. Liu, T.-F. Lee, M. Miedzyblocki, G. C. F. Chan, D. L. Bigam, and P.-Y. Cheung, "Effects of tanshinone IIA, a major component of *Salvia miltiorrhiza*, on platelet aggregation in healthy newborn piglets," *Journal of Ethnopharmacology*, vol. 137, no. 1, pp. 44–49, 2011.

[38] K. Chan, S. H. Chui, D. Y. L. Wong, W. Y. Ha, C. L. Chan, and R. N. S. Wong, "Protective effects of Danshensu from the aqueous extract of *Salvia miltiorrhiza* (Danshen) against homocysteine-induced endothelial dysfunction," *Life Sciences*, vol. 75, no. 26, pp. 3157–3171, 2004.

[39] Y.-C. Hung, P.-W. Wang, T.-L. Pan, G. Bazylak, and Y.-L. Leu, "Proteomic screening of antioxidant effects exhibited by *Radix Salvia miltiorrhiza* aqueous extract in cultured rat aortic smooth muscle cells under homocysteine treatment," *Journal of Ethnopharmacology*, vol. 124, no. 3, pp. 463–474, 2009.

[40] H. Pang, L. Wu, Y. Tang, G. Zhou, C. Qu, and J. Duan, "Chemical analysis of the herbal medicine salviae miltiorrhizae radix et rhizoma (Danshen)," *Molecules*, vol. 21, no. 1, article 51, 2016.

[41] J.-Z. Song, S.-L. Li, Y. Zhou, C.-F. Qiao, S.-L. Chen, and H.-X. Xu, "A novel approach to rapidly explore analytical markers for quality control of Radix Salviae Miltiorrhizae extract granules by robust principal component analysis with ultra-high performance liquid chromatography-ultraviolet-quadrupole time-of-flight mass spectrometry," *Journal of Pharmaceutical and Biomedical Analysis*, vol. 53, no. 3, pp. 279–286, 2010.

[42] Y. Zhang, P. Jiang, M. Ye, S.-H. Kim, C. Jiang, and J. Lü, "Tanshinones: sources, pharmacokinetics and anti-cancer activities," *International Journal of Molecular Sciences*, vol. 13, no. 10, pp. 13621–13666, 2012.

[43] C.-Y. Su, Q.-L. Ming, K. Rahman, T. Han, and L.-P. Qin, "Salvia miltiorrhiza: traditional medicinal uses, chemistry, and pharmacology," *Chinese Journal of Natural Medicines*, vol. 13, no. 3, pp. 163–182, 2015.

[44] Y.-B. Wu, Z.-Y. Ni, Q.-W. Shi et al., "Constituents from *Salvia* species and their biological activities," *Chemical Reviews*, vol. 112, no. 11, pp. 5967–6026, 2012.

[45] X.-L. Niu, K. Ichimori, X. Yang et al., "Tanshinone II-A inhibits low density lipoprotein oxidation in vitro," *Free Radical Research*, vol. 33, no. 3, pp. 305–312, 2000.

[46] D.-S. Lee, S.-H. Lee, J.-G. Noh, and S.-D. Hong, "Antibacterial activities of cryptotanshinone and dihydrotanshinone I from a medicinal herb, *Salvia miltiorrhiza* bunge," *Bioscience, Biotechnology and Biochemistry*, vol. 63, no. 12, pp. 2236–2239, 1999.

[47] S. Y. Kim, T. C. Moon, H. W. Chang, K. H. Son, S. S. Kang, and H. P. Kim, "Effects of tanshinone I isolated from *Salvia miltiorrhiza* Bunge on arachidonic acid metabolism and in vivo inflammatory responses," *Phytotherapy Research*, vol. 16, no. 7, pp. 616–620, 2002.

[48] T. Liu, H. Jin, Q.-R. Sun, J.-H. Xu, and H.-T. Hu, "The neuroprotective effects of tanshinone IIA on β-amyloid-induced toxicity in rat cortical neurons," *Neuropharmacology*, vol. 59, no. 7-8, pp. 595–604, 2010.

[49] M. A. Mosaddik, "In vitro cytotoxicity of Tanshinones isolated from Salvia miltiorrhiza Bunge against P388 lymphocytic leukemia cells," *Phytomedicine*, vol. 10, no. 8, pp. 682–685, 2003.

[50] F. Qiu, G. Wang, R. Zhang, J. Sun, J. Jiang, and Y. Ma, "Effect of danshen extract on the activity of CYP3A4 in healthy volunteers," *British Journal of Clinical Pharmacology*, vol. 69, no. 6, pp. 656–662, 2010.

[51] R.-W. Jiang, K.-M. Lau, P.-M. Hon, T. C. W. Mak, K.-S. Woo, and K.-P. Fung, "Chemistry and biological activities of caffeic acid derivatives from *Salvia miltiorrhiza*," *Current Medicinal Chemistry*, vol. 12, no. 2, pp. 237–246, 2005.

[52] G. Ge, Q. Zhang, J. Ma et al., "Protective effect of *Salvia miltiorrhiza* aqueous extract on myocardium oxidative injury in ischemic-reperfusion rats," *Gene*, vol. 546, no. 1, pp. 97–103, 2014.

[53] J. Yu, L. Wang, M. Akinyi et al., "Danshensu protects isolated heart against ischemia reperfusion injury through activation of Akt/ERK1/2/Nrf2 signaling," *International Journal of Clinical and Experimental Medicine*, vol. 8, no. 9, pp. 14793–14804, 2015.

[54] W. Zhang, L. Zheng, Z. Zhang, and C.-X. Hai, "Protective effect of a water-soluble polysaccharide from *Salvia miltiorrhiza* Bunge on insulin resistance in rats," *Carbohydrate Polymers*, vol. 89, no. 3, pp. 890–898, 2012.

[55] Y.-Y. Jiang, L. Wang, L. Zhang et al., "Characterization, antioxidant and antitumor activities of polysaccharides from *Salvia miltiorrhiza* Bunge," *International Journal of Biological Macromolecules*, vol. 70, pp. 92–99, 2014.

[56] D. A. Rhoades, T. K. Welty, W. Wang et al., "Aging and the prevalence of cardiovascular disease risk factors in older American Indians: the strong heart study," *Journal of the American Geriatrics Society*, vol. 55, no. 1, pp. 87–94, 2007.

[57] D. Peiris, S. R. Thompson, A. Beratarrechea et al., "Behaviour change strategies for reducing blood pressure-related disease burden: findings from a global implementation research programme," *Implementation Science*, vol. 10, no. 1, 2015.

[58] P.-R. Yang, W.-T. Shih, Y.-H. Chu, P.-C. Chen, and C.-Y. Wu, "Frequency and co-prescription pattern of Chinese herbal products for hypertension in Taiwan: A Cohort Study," *BMC Complementary and Alternative Medicine*, vol. 15, no. 1, article 163, 2015.

[59] Z.-W. Zhou, X.-L. Xie, S.-F. Zhou, and C. G. Li, "Mechanism of reversal of high glucose-induced endothelial nitric oxide synthase uncoupling by tanshinone IIA in human endothelial cell line EA.hy926," *European Journal of Pharmacology*, vol. 697, no. 1–3, pp. 97–105, 2012.

[60] P. Wang, X. Wu, Y. Bao et al., "Tanshinone IIA prevents cardiac remodeling through attenuating NAD (P)H oxidase-derived reactive oxygen species production in hypertensive rats," *Die Pharmazie*, vol. 66, no. 7, pp. 517–524, 2011.

[61] L.-Q. Jia, G.-L. Yang, L. Ren et al., "Tanshinone IIA reduces apoptosis induced by hydrogen peroxide in the human endothelium-derived EA.hy926 cells," *Journal of Ethnopharmacology*, vol. 143, no. 1, pp. 100–108, 2012.

[62] D. G. Kang, H. Oh, H. T. Chung, and H. S. Lee, "Inhibition of angiotensin converting enzyme by lithospermic acid B isolated from radix *Salviae miltiorrhiza* Bunge," *Phytotherapy Research*, vol. 17, no. 8, pp. 917–920, 2003.

[63] D. G. Kang, Y. G. Yun, J. H. Ryoo, and H. S. Lee, "Antihypertensive effect of water extract of Danshen on renovascular hypertension through inhibition of the renin angiotensin system," *American Journal of Chinese Medicine*, vol. 30, no. 1, pp. 87–93, 2002.

[64] X. Ouyang, K. Takahashi, K. Komatsu et al., "Protective effect of *Salvia miltiorrhiza* on angiotensin II-induced hypertrophic responses in neonatal rat cardiac cells," *Japanese Journal of Pharmacology*, vol. 87, no. 4, pp. 289–296, 2001.

[65] S. W. S. Leung, D.-Y. Zhu, and R. Y. K. Man, "Effects of the aqueous extract of *Salvia Miltiorrhiza* (danshen) and its magnesium tanshinoate B-enriched form on blood pressure," *Phytotherapy Research*, vol. 24, no. 5, pp. 769–774, 2010.

[66] F. F. Y. Lam, S. W. Seto, Y. W. Kwan, J. H. K. Yeung, and P. Chan, "Activation of the iberiotoxin-sensitive BKCa channels by salvianolic acid B of the porcine coronary artery smooth muscle cells," *European Journal of Pharmacology*, vol. 546, no. 1–3, pp. 28–35, 2006.

[67] Y. Tang, M. Wang, C. Chen, X. Le, S. Sun, and Y. Yin, "Cardiovascular protection with danshensu in spontaneously hypertensive rats," *Biological & Pharmaceutical Bulletin*, vol. 34, pp. 1596–1601, 2011.

[68] Z. Xia, J. Gu, D. M. Ansley, F. Xia, and J. Yu, "Antioxidant therapy with *Salvia miltiorrhiza* decreases plasma endothelin-1 and thromboxane B2 after cardiopulmonary bypass in patients with congenital heart disease," *The Journal of Thoracic and Cardiovascular Surgery*, vol. 126, no. 5, pp. 1404–1410, 2003.

[69] K. Pirie, R. Peto, G. K. Reeves, J. Green, and V. Beral, "The 21st century hazards of smoking and benefits of stopping: a prospective study of one million women in the UK," *The Lancet*, vol. 381, no. 9861, pp. 133–141, 2013.

[70] B. Isik, A. Ceylan, and R. Isik, "Oxidative stress in smokers and non-smokers," *Inhalation Toxicology*, vol. 19, no. 9, pp. 767–769, 2007.

[71] M. Pujades-Rodriguez, J. George, A. D. Shah et al., "Heterogeneous associations between smoking and a wide range of initial presentations of cardiovascular disease in 1937 360 people in England: lifetime risks and implications for risk prediction," *International Journal of Epidemiology*, vol. 44, no. 1, pp. 129–141, 2015.

[72] T. Zhang, J. Xu, D. Li et al., "Salvianolic acid A, a matrix metalloproteinase-9 inhibitor of Salvia miltiorrhiza, attenuates aortic aneurysm formation in apolipoprotein E-deficient mice," *Phytomedicine*, vol. 21, no. 10, pp. 1137–1145, 2014.

[73] F. F. Y. Lam, J. H. K. Yeung, and J. H. Y. Cheung, "Mechanisms of the dilator action of Danshen *(Salvia miltiorrhiza*) on rat isolated femoral artery," *Journal of Cardiovascular Pharmacology*, vol. 46, no. 3, pp. 361–368, 2005.

[74] F. Y. Lam, S. C. W. Ng, J. H. Y. Cheung, and J. H. K. Yeung, "Mechanisms of the vasorelaxant effect of Danshen (*Salvia miltiorrhiza*) in rat knee joints," *Journal of Ethnopharmacology*, vol. 104, no. 3, pp. 336–344, 2006.

[75] F. W. Yi-ju Cheng, Y. Hu, M.-X. Wu, J. Du, and M.-L. Cheng, "Compound injection of Danshen root suppresses cigarettes smoking-induced lung inflammation: a SD rat model," *Inflammation and Cell Signaling*, vol. 2, no. 4, pp. 1–6, 2015.

[76] D. E. Singer, D. M. Nathan, K. M. Anderson, P. W. F. Wilson, and J. C. Evans, "Association of HbA1c with prevalent cardiovascular disease in the original cohort of the Framingham heart study," *Diabetes*, vol. 41, no. 2, pp. 202–208, 1992.

[77] W. B. Kannel and D. L. McGee, "Diabetes and glucose tolerance as risk factors for cardiovascular disease: The Framingham Study," *Diabetes Care*, vol. 2, no. 2, pp. 120–126, 1979.

[78] A. Aydin, H. Orhan, A. Sayal, M. Özata, G. Şahin, and A. Isimer, "Oxidative stress and nitric oxide related parameters in type II diabetes mellitus: effects of glycemic control," *Clinical Biochemistry*, vol. 34, no. 1, pp. 65–70, 2001.

[79] G. S. Dave and K. Kalia, "Hyperglycemia induced oxidative stress in type-1 and type-2 diabetic patients with and without nephropathy," *Cellular and Molecular Biology*, vol. 53, no. 5, pp. 68–78, 2007.

[80] N. Sasaki, T. Yamashita, T. Takaya et al., "Augmentation of vascular remodeling by uncoupled endothelial nitric oxide synthase in a mouse model of diabetes mellitus," *Arteriosclerosis, Thrombosis, and Vascular Biology*, vol. 28, no. 6, pp. 1068–1076, 2008.

[81] S. Gupta, E. Chough, J. Daley et al., "Hyperglycemia increases endothelial superoxide that impairs smooth muscle cell Na^+-K^+-ATpase activity," *American Journal of Physiology—Cell Physiology*, vol. 282, no. 3, pp. C560–C566, 2002.

[82] K. Monaghan, J. McNaughten, M. K. McGahon et al., "Hyperglycemia and diabetes downregulate the functional expression of TRPV4 channels in retinal microvascular endothelium," *PLoS ONE*, vol. 10, no. 6, article e0128359, 2015.

[83] Q. Qian, S. Qian, P. Fan, D. Huo, and S. Wang, "Effect of *Salvia miltiorrhiza* hydrophilic extract on antioxidant enzymes in diabetic patients with chronic heart disease: a randomized controlled trial," *Phytotherapy Research*, vol. 26, no. 1, pp. 60–66, 2012.

[84] S. Qian, D. Huo, S. Wang, and Q. Qian, "Inhibition of glucose-induced vascular endothelial growth factor expression by *Salvia miltiorrhiza* hydrophilic extract in human microvascular

endothelial cells: evidence for mitochondrial oxidative stress," *Journal of Ethnopharmacology*, vol. 137, no. 2, pp. 985–991, 2011.

[85] M. Huang, P. Wang, S. Xu et al., "Biological activities of salvianolic acid B from *Salvia miltiorrhiza* on type 2 diabetes induced by high-fat diet and streptozotocin," *Pharmaceutical Biology*, vol. 53, no. 7, pp. 1058–1065, 2015.

[86] S. H. Jung, H. J. Seol, S. J. Jeon, K. H. Son, and J. R. Lee, "Insulin-sensitizing activities of tanshinones, diterpene compounds of the root of *Salvia miltiorrhiza* Bunge," *Phytomedicine*, vol. 16, no. 4, pp. 327–335, 2009.

[87] National Cholesterol Education Program (NCEP) Expert Panel on Detection-Evaluation and Treatment of High Blood Cholesterol in Adults (Adult Treatment Panel III), "Third Report of the National Cholesterol Education Program (NCEP) expert panel on detection, evaluation, and treatment of high blood cholesterol in adults (Adult Treatment Panel III) final report," *Circulation*, vol. 106, no. 25, pp. 3143–3421, 2002.

[88] K. Wouters, R. Shiri-Sverdlov, P. J. van Gorp, M. van Bilsen, and M. H. Hofker, "Understanding hyperlipidemia and atherosclerosis: lessons from genetically modified apoe and LDLR mice," *Clinical Chemistry and Laboratory Medicine*, vol. 43, no. 5, pp. 470–479, 2005.

[89] M. Hulsmans and P. Holvoet, "The vicious circle between oxidative stress and inflammation in atherosclerosis," *Journal of Cellular and Molecular Medicine*, vol. 14, no. 1-2, pp. 70–78, 2010.

[90] C.-C. Chang, C.-F. Chu, C.-N. Wang et al., "The anti-atherosclerotic effect of tanshinone IIA is associated with the inhibition of TNF-α-induced VCAM-1, ICAM-1 and CX3CL1 expression," *Phytomedicine*, vol. 21, no. 3, pp. 207–216, 2014.

[91] T.-L. Yang, F.-Y. Lin, Y.-H. Chen et al., "Salvianolic acid B inhibits low-density lipoprotein oxidation and neointimal hyperplasia in endothelium-denuded hypercholesterolaemic rabbits," *Journal of the Science of Food and Agriculture*, vol. 91, no. 1, pp. 134–141, 2011.

[92] O. Karmin, E. G. Lynn, R. Vazhappilly, K. K. Au-Yeung, D. Y. Zhu, and Y. L. Siow, "Magnesium tanshinoate B (MTB) inhibits low density lipoprotein oxidation," *Life Sciences*, vol. 68, no. 8, pp. 903–912, 2001.

[93] K. K. W. Au-Yeung, O. Karmin, P. C. Choy, D.-Y. Zhu, and Y. L. Siow, "Magnesium tanshinoate B protects endothelial cells against oxidized lipoprotein-induced apoptosis," *Canadian Journal of Physiology and Pharmacology*, vol. 85, no. 11, pp. 1053–1062, 2007.

[94] J. Stevens, E. E. Oakkar, Z. Cui, J. Cai, and K. P. Truesdale, "US adults recommended for weight reduction by 1998 and 2013 obesity guidelines, NHANES 2007–2012," *Obesity*, vol. 23, no. 3, pp. 527–531, 2015.

[95] P. Poirier and R. H. Eckel, "Obesity and cardiovascular disease," *Current Atherosclerosis Reports*, vol. 4, no. 6, pp. 448–453, 2002.

[96] B. L. Wajchenberg, "Subcutaneous and visceral adipose tissue: their relation to the metabolic syndrome," *Endocrine Reviews*, vol. 21, no. 6, pp. 697–738, 2000.

[97] S. Nishimura, I. Manabe, and R. Nagai, "Adipose tissue inflammation in obesity and metabolic syndrome," *Discovery Medicine*, vol. 8, no. 41, pp. 55–60, 2009.

[98] P. Poirier, T. D. Giles, G. A. Bray et al., "Obesity and cardiovascular disease: pathophysiology, evaluation, and effect of weight loss," *Arteriosclerosis, Thrombosis, and Vascular Biology*, vol. 26, no. 5, pp. 968–976, 2006.

[99] N. Rahman, M. Jeon, H.-Y. Song, and Y.-S. Kim, "Cryptotanshinone, a compound of *Salvia miltiorrhiza* inhibits pre-adipocytes differentiation by regulation of adipogenesis-related genes expression via STAT3 signaling," *Phytomedicine*, vol. 23, no. 1, pp. 58–67, 2016.

[100] P. Wang, S. Xu, W. Li et al., "Salvianolic acid B inhibited pparγ expression and attenuated weight gain in mice with high-fat diet-induced obesity," *Cellular Physiology and Biochemistry*, vol. 34, no. 2, pp. 288–298, 2014.

[101] Y. Tan, M. A. Kamal, Z.-Z. Wang, W. Xiao, J. P. Seale, and X. Qu, "Chinese herbal extracts (SK0506) as a potential candidate for the therapy of the metabolic syndrome," *Clinical Science*, vol. 120, no. 7, pp. 297–305, 2011.

[102] G. B. Wu, E. X. Zhou, and D. X. Qing, "TanshinoneII(A) elicited vasodilation in rat coronary arteriole: roles of nitric oxide and potassium channels," *European Journal of Pharmacology*, vol. 617, no. 1–3, pp. 102–107, 2009.

[103] Y. Yang, F. Cai, P.-Y. Li et al., "Activation of high conductance Ca^{2+}-activated K^+ channels by sodium tanshinoneII-A sulfonate (DS-201) in porcine coronary artery smooth muscle cells," *European Journal of Pharmacology*, vol. 598, no. 1–3, pp. 9–15, 2008.

[104] F. F. Y. Lam, J. H. K. Yeung, Y. W. Kwan, K. M. Chan, and P. M. Y. Or, "Salvianolic acid B, an aqueous component of danshen (*Salvia miltiorrhiza*), relaxes rat coronary artery by inhibition of calcium channels," *European Journal of Pharmacology*, vol. 553, no. 1–3, pp. 240–245, 2006.

[105] Y. Jia, F. Huang, S. Zhang, and S.-W. Leung, "Is danshen (*Salvia miltiorrhiza*) dripping pill more effective than isosorbide dinitrate in treating angina pectoris? A systematic review of randomized controlled trials," *International Journal of Cardiology*, vol. 157, no. 3, pp. 330–340, 2012.

[106] F. Maione, V. De Feo, E. Caiazzo, L. De Martino, C. Cicala, and N. Mascolo, "Tanshinone IIA, a major component of *Salvia milthorriza* Bunge, inhibits platelet activation via Erk-2 signaling pathway," *Journal of Ethnopharmacology*, vol. 155, no. 2, pp. 1236–1242, 2014.

[107] D. L. Carden and D. N. Granger, "Pathophysiology of ischaemia-reperfusion injury," *Journal of Pathology*, vol. 190, no. 3, pp. 255–266, 2000.

[108] J.-Y. Han, J.-Y. Fan, Y. Horie et al., "Ameliorating effects of compounds derived from *Salvia miltiorrhiza* root extract on microcirculatory disturbance and target organ injury by ischemia and reperfusion," *Pharmacology & Therapeutics*, vol. 117, no. 2, pp. 280–295, 2008.

[109] H. Hu, C. Zhai, G. Qian et al., "Protective effects of tanshinone IIA on myocardial ischemia reperfusion injury by reducing oxidative stress, HMGB1 expression, and inflammatory reaction," *Pharmaceutical Biology*, vol. 53, no. 12, pp. 1752–1758, 2015.

[110] Z. H. Ren, Y. H. Tong, W. Xu, J. Ma, and Y. Chen, "Tanshinone II A attenuates inflammatory responses of rats with myocardial infarction by reducing MCP-1 expression," *Phytomedicine*, vol. 17, no. 3-4, pp. 212–218, 2010.

[111] Z. Zhou, Y. Liu, A.-D. Miao, and S.-Q. Wang, "Protocatechuic aldehyde suppresses TNF-α-induced ICAM-1 and VCAM-1 expression in human umbilical vein endothelial cells," *European Journal of Pharmacology*, vol. 513, no. 1-2, pp. 1–8, 2005.

[112] T. Xu, X. Wu, Q. Chen et al., "The anti-apoptotic and cardioprotective effects of salvianolic acid a on rat cardiomyocytes following ischemia/reperfusion by DUSP-mediated regulation of the ERK1/2/JNK pathway," *PLoS ONE*, vol. 9, no. 7, Article ID e102292, 2014.

[113] H. Fan, L. Yang, F. Fu et al., "Cardioprotective effects of salvianolic acid a on myocardial ischemia-reperfusion injury in vivo

and in vitro," *Evidence-Based Complementary and Alternative Medicine*, vol. 2012, Article ID 508938, 9 pages, 2012.

[114] Y. Deng, M. Yang, F. Xu et al., "Combined salvianolic acid B and ginsenoside Rg1 exerts cardioprotection against ischemia/reperfusion injury in rats," *PLoS ONE*, vol. 10, no. 8, Article ID e0135435, 2015.

[115] Y. Gao, K. Zhang, F. Zhu et al., "*Salvia miltiorrhiza* (Danshen) inhibits L-type calcium current and attenuates calcium transient and contractility in rat ventricular myocytes," *Journal of Ethnopharmacology*, vol. 158, pp. 397–403, 2014.

[116] M. Song, L. Huang, G. Zhao, and Y. Song, "Beneficial effects of a polysaccharide from *Salvia miltiorrhiza* on myocardial ischemia-reperfusion injury in rats," *Carbohydrate Polymers*, vol. 98, no. 2, pp. 1631–1636, 2013.

[117] M. A. Konstam, D. G. Kramer, A. R. Patel, M. S. Maron, and J. E. Udelson, "Left ventricular remodeling in heart failure: current concepts in clinical significance and assessment," *JACC: Cardiovascular Imaging*, vol. 4, no. 1, pp. 98–108, 2011.

[118] J. R. D. A. R. Reis Filho, J. N. Cardoso, C. M. D. R. Cardoso, and A. C. Pereira-Barretto, "Reverse cardiac remodeling: a marker of better prognosis in heart failure," *Arquivos Brasileiros de Cardiologia*, vol. 104, no. 6, pp. 502–506, 2015.

[119] A. Yagi and S. Takeo, "Anti-inflammatory constituents, aloesin and aloemannan in Aloe species and effects of tanshinon VI in Salvia miltiorrhiza on heart," *Yakugakuzasshi: Journal of the Pharmaceutical Society of Japan*, vol. 123, no. 7, pp. 517–532, 2003.

[120] P. Chan, J.-C. Liu, L.-J. Lin et al., "Tanshinone IIA inhibits angiotensin II-induced cell proliferation in rat cardiac fibroblasts," *The American Journal of Chinese Medicine*, vol. 39, no. 2, pp. 381–394, 2011.

[121] L. Yang, X.-J. Zou, X. Gao et al., "Sodium tanshinone IIA sulfonate attenuates angiotensin II-induced collagen type I expression in cardiac fibroblasts in vitro," *Experimental and Molecular Medicine*, vol. 41, no. 7, pp. 508–516, 2009.

[122] S. Mao, W. Li, N. Qa'aty, M. Vincent, M. Zhang, and A. Hinek, "Tanshinone IIA inhibits angiotensin II induced extracellular matrix remodeling in human cardiac fibroblasts—implications for treatment of pathologic cardiac remodeling," *International Journal of Cardiology*, vol. 202, pp. 110–117, 2016.

[123] B. Jiang, W. Wu, M. Li et al., "Cardioprotection and matrix metalloproteinase-9 regulation of salvianolic acids on myocardial infarction in rats," *Planta Medica*, vol. 75, no. 12, pp. 1286–1292, 2009.

[124] B. Jiang, D. Li, Y. Deng et al., "Salvianolic acid A, a novel matrix metalloproteinase-9 inhibitor, prevents cardiac remodeling in spontaneously hypertensive rats," *PLoS ONE*, vol. 8, no. 3, Article ID e59621, 2013.

[125] B. Jiang, J. Chen, L. Xu et al., "Salvianolic acid B functioned as a competitive inhibitor of matrix metalloproteinase-9 and efficiently prevented cardiac remodeling," *BMC Pharmacology*, vol. 10, article 10, 2010.

[126] Y. Wang, F. Xu, J. Chen et al., "Matrix metalloproteinase-9 induces cardiac fibroblast migration, collagen and cytokine secretion: inhibition by salvianolic acid B from *Salvia miltiorrhiza*," *Phytomedicine*, vol. 19, no. 1, pp. 13–19, 2011.

[127] C. C. Chang, Y. C. Lee, C. C. Lin et al., "Characteristics of traditional Chinese medicine usage in patients with stroke in Taiwan: a nationwide population-based study," *Journal of Ethnopharmacology*, vol. 186, pp. 311–321, 2016.

[128] C. Tang, H. Xue, C. Bai, R. Fu, and A. Wu, "The effects of Tanshinone IIA on blood-brain barrier and brain edema after transient middle cerebral artery occlusion in rats," *Phytomedicine*, vol. 17, no. 14, pp. 1145–1149, 2010.

[129] L. Zhou, S. C. Bondy, L. Jian et al., "Tanshinone IIA attenuates the cerebral ischemic injury-induced increase in levels of GFAP and of caspases-3 and -8," *Neuroscience*, vol. 288, pp. 105–111, 2015.

[130] X. Yang, J. Yan, and J. Feng, "Treatment with tanshinone IIA suppresses disruption of the blood-brain barrier and reduces expression of adhesion molecules and chemokines in experimental autoimmune encephalomyelitis," *European Journal of Pharmacology*, vol. 771, pp. 18–28, 2016.

[131] X. Liu, M. Ye, C. An, L. Pan, and L. Ji, "The effect of cationic albumin-conjugated PEGylated tanshinone IIA nanoparticles on neuronal signal pathways and neuroprotection in cerebral ischemia," *Biomaterials*, vol. 34, no. 28, pp. 6893–6905, 2013.

[132] X. Liu, C. An, P. Jin, X. Liu, and L. Wang, "Protective effects of cationic bovine serum albumin-conjugated PEGylated tanshinone IIA nanoparticles on cerebral ischemia," *Biomaterials*, vol. 34, no. 3, pp. 817–830, 2013.

[133] Y.-F. Jiang, Z.-Q. Liu, W. Cui et al., "Antioxidant effect of salvianolic acid B on hippocampal CA1 neurons in mice with cerebral ischemia and reperfusion injury," *Chinese Journal of Integrative Medicine*, vol. 21, no. 7, pp. 516–522, 2015.

[134] H. Lv, L. Wang, J. Shen et al., "Salvianolic acid B attenuates apoptosis and inflammation via SIRT1 activation in experimental stroke rats," *Brain Research Bulletin*, vol. 115, pp. 30–36, 2015.

[135] H. Zhu, L. Zou, J. Tian, G. Du, and Y. Gao, "SMND-309, a novel derivative of salvianolic acid B, protects rat brains ischemia and reperfusion injury by targeting the JAK2/STAT3 pathway," *European Journal of Pharmacology*, vol. 714, no. 1–3, pp. 23–31, 2013.

[136] C. Guo, Y. Yin, J. Duan et al., "Neuroprotective effect and underlying mechanism of sodium danshensu [3-(3,4-dihydroxyphenyl) lactic acid from Radix and Rhizoma Salviae miltiorrhizae = Danshen] against cerebral ischemia and reperfusion injury in rats," *Phytomedicine*, vol. 22, no. 2, pp. 283–289, 2015.

[137] G.-L. Ming and H. Song, "Adult neurogenesis in the mammalian brain: significant answers and significant questions," *Neuron*, vol. 70, no. 4, pp. 687–702, 2011.

[138] P. Zhuang, Y. Zhang, G. Cui et al., "Direct stimulation of adult neural stem/progenitor cells in vitro and neurogenesis in vivo by salvianolic acid B," *PLoS ONE*, vol. 7, no. 4, Article ID e35636, 2012.

[139] T. A. Elbayoumi and V. P. Torchilin, "Current trends in liposome research," *Methods in Molecular Biology*, vol. 605, pp. 1–27, 2010.

[140] Y. Cai, W. Zhang, Z. Chen, Z. Shi, H. Chengwei, and M. Chen, "Recent insights into the biological activities and drug delivery systems of tanshinones," *International Journal of Nanomedicine*, vol. 11, pp. 121–130, 2016.

[141] X. Zhao, X. Liu, L. Gan, C. Zhou, and J. Mo, "Preparation and physicochemical characterizations of tanshinone IIA solid dispersion," *Archives of Pharmacal Research*, vol. 34, no. 6, pp. 949–959, 2011.

Hindawi Publishing Corporation
Oxidative Medicine and Cellular Longevity
Volume 2016, Article ID 4768541, 10 pages
http://dx.doi.org/10.1155/2016/4768541

Research Article

Weaning Induced Hepatic Oxidative Stress, Apoptosis, and Aminotransferases through MAPK Signaling Pathways in Piglets

Zhen Luo, Wei Zhu, Qi Guo, Wenli Luo, Jing Zhang, Weina Xu, and Jianxiong Xu

School of Agriculture and Biology, Shanghai Jiao Tong University, Shanghai Key Laboratory of Veterinary Biotechnology, Shanghai 200240, China

Correspondence should be addressed to Jianxiong Xu; jxxu1962@sjtu.edu.cn

Received 2 June 2016; Revised 7 August 2016; Accepted 25 August 2016

Academic Editor: Claudio Cabello-Verrugio

This study investigated the effects of weaning on the hepatic redox status, apoptosis, function, and the mitogen-activated protein kinase (MAPK) signaling pathways during the first week after weaning in piglets. A total of 12 litters of piglets were weaned at d 21 and divided into the weaning group (WG) and the control group (CG). Six piglets from each group were slaughtered at d 0 (d 20, referred to weaning), d 1, d 4, and d 7 after weaning. Results showed that weaning significantly increased the concentrations of hepatic free radicals H_2O_2 and NO, malondialdehyde (MDA), and 8-hydroxy-2′-deoxyguanosine (8-OHdG), while significantly decreasing the inhibitory hydroxyl ability (IHA) and glutathione peroxidase (GSH-Px), and altered the level of superoxide dismutase (SOD). The apoptosis results showed that weaning increased the concentrations of caspase-3, caspase-8, caspase-9 and the ratio of Bax/Bcl-2. In addition, aspartate aminotransferase transaminase (AST) and alanine aminotransferase (ALT) in liver homogenates increased after weaning. The phosphorylated JNK and ERK1/2 increased, while the activated p38 initially decreased and then increased. Our results suggested that weaning increased the hepatic oxidative stress and aminotransferases and initiated apoptosis, which may be related to the activated MAPK pathways in postweaning piglets.

1. Introduction

Weaning is abruptly stressful in the neonates' life, and that stress can result in growth retardation and susceptibility to diseases in mammals. These issues are especially serious in commercial swine husbandry during the first week after weaning, which often results in "postweaning stress syndrome (PWSD)" [1]. Previous studies have reported that weaning decreased intestinal digestive enzyme activities, damaged tight junction proteins, impaired immune response and barrier function, increased cytokines, and activated signaling pathways, both transiently and long term [2–5]. Our recent study indicated that weaning disrupted the physiologic equilibrium of oxidant and antioxidant and led to oxidative stress, eventually inducing enterocyte apoptosis and cell cycle arrest in the small intestine of postweaning piglets [6, 7].

The liver, which is located between the absorptive surfaces of the gastrointestinal tract, plays an important role in nutrients' metabolism and transformation. The liver's blood supply primarily originates from the intestine through the portal vein; so when the intestinal function is disrupted, an increase in intestinal permeability may contribute to the translocation of metabolites to the liver and impairment of liver function [8, 9]. Furthermore, the liver is more vulnerable to damage under particular kinds of stress [10]. The liver is a thermogenic organ that contains a large number of mitochondria in mammals, which is the place with high oxygen consumption and reactive oxygen species (ROS) formation [11, 12]. However, changes in hepatic function throughout the weaning period receive less attention from researchers compared to the intestine. One study showed that weaning induced endoplasmic reticulum stress in the liver of piglets [13]. Little data is available regarding weaning-induced oxidative injury, apoptosis, and loss of function in the potential mechanisms within the piglets' liver. The mitogen-activated protein kinases (MAPKs), the family of the serine-threonine protein kinases that transduce signals from the cell membrane to the nucleus, include extracellular signal-regulated kinases (ERKs), c-Jun N-terminal kinases (JNKs) and p38 and, in

particular, participate in oxidative stress-induced cell apoptosis and proliferation [14]. MAPKs have been shown to be activated in an ischemic-injured ileum and in a weaning jejunum in pigs [5, 15]. Whether weaning results in MAPKs activation in the liver remains unknown.

The present objective was to study the immediate effects of weaning on the markers of hepatic oxidative stress, apoptosis, function, and MAPK signaling pathways in postweaning piglets and then to evaluate whether there was a novel, promising method for preventing weaning stress in human beings and domestic animals.

2. Materials and Methods

2.1. Animals, Diets, and Sampling. The experiment was conducted according to the guidelines of Shanghai Jiao Tong University Institutional Animal Care and Use Committee. A total of 120 7-day-old piglets (Duroc × Landrace) from 12 litters were randomly assigned by litter to two groups: the normal suckling (control group, CG) and the weaning group (WG), resulting in six litters per group. All piglets were kept with their sows in gestation crates in the same farrowing pens, while they suckled, and they had free access to the basal diet from d 7 to d 28. The dietary ingredients and nutrition levels are shown in Table 1. At d 21, 6 litters of piglets were randomly selected, weaned, and then moved to nursery pens; the others remained with their mothers without mixing any litters. Water was consumed *ad libitum*, and the temperature in nursery pens was about 30°C with a relative humidity of 50–70%. Pens were regularly cleaned of the manure, and the pig house was well-ventilated. At d 20 after birth (d 0), before the separation of the piglets into the two study groups, six piglets with a similar body weight from six different litters were randomly selected and sacrificed for testing (half males and half females). At d 1, d 4, and d 7 after weaning, one piglet of similar body weight from each litter was selected and sacrificed for testing. All the selected pigs were anaesthetized by intramuscular injection of sodium pentobarbital (Merck, Germany) (40 mg/kg BW). Liver tissues were sampled and immediately stored at −80°C for analysis of redox status, enzyme activities, and protein expression.

Table 1: Dietary ingredients and nutrient levels.

Item	Amount
Ingredients (%)	
Corn	41.18
Fermented soybean meal	5.00
Peeled soybean meal	7.00
Extruded soybean	11.22
Fish meal	5.00
Plasma protein	4.00
Whey powder	15.00
Limestone	0.50
Monocalcium phosphate	0.90
Choline	0.10
Lactose	8.75
Sodium chloride	0.35
Vitamin premix[1]	0.50
Mineral premix[2]	0.50
Total	100.00
Nutrition levels	
Digestible Energy (MJ/kg)	14.48
Crude protein (%)	20.50
Ca (%)	0.85
Total P (%)	0.67
Available P (%)	0.55
Lysine (%)	1.55
Methionine (%)	0.42
Methionine + cysteine (%)	0.83
Tryptophan (%)	0.27
Threonine (%)	1.01

[1]Provided per kg of mixed diet: vitamin A, 12 000 IU/kg; vitamin D_3, 3200 IU/kg; vitamin K_3, 2.5 mg; vitamin E, 80 mg; vitamin B_1, 2.5 mg; vitamin B_2, 6.5 mg; vitamin B_6, 5 mg; vitamin B_{12}, 0.05 mg; niacin, 45 mg; and D-pantothenic acid, 20 mg.
[2] Provided per kg of mixed diet: folic acid, 1.5 mg; biotin, 0.15 mg; Fe, 150 mg as ferrous sulfate; Cu, 125 mg as copper sulfate; Zn, 200 mg as zinc oxide; Mn, 30 mg as manganous oxide; I, 0.3 mg as potassium iodide; and Se, 0.3 mg as selenium selenite.

2.2. Determination of H_2O_2 and NO in Liver Tissues. The liver tissues were weighed and homogenized in an H_2O_2 lysis buffer (1 : 20, w/v) according to the manufacturer's instructions (Beyotime Biotech, Shanghai, China). The supernatants were gathered by centrifuging at 12,000 ×g for 10 min. Briefly, the sample solution (50 μL) was incubated with reaction solution (100 μL) at room temperature for 30 min, and then the absorbance was read at 560 nm. The H_2O_2 concentration was calculated by the standard curve made from the standard solutions.

NO production in tissues was measured by the Griess method according to the specification of the NO assay kit (Beyotime Biotech, Shanghai, China). Briefly, liver tissues were weighed and homogenized in a RIPA lysis buffer (1 : 10, w/v). The supernatants were gathered by centrifuging at 12,000 ×g for 10 min. The sample solution (40 μL) and an equal volume of Griess reagents I and II were added to a 96-well microplate. The absorbance was measured at a wavelength of 540 nm. The NO concentration was calculated using a curve calibrated from sodium nitrite standards.

2.3. Determination of Lipid Peroxidation and Antioxidant Enzyme Activity. The activities of malondialdehyde (MDA) (Nanjing KeyGEN BioTech, Nanjing, China), the inhibitory hydroxyl ability (IHA), superoxide dismutase (SOD), glutathione peroxidase (GSH-Px) (Nanjing Jiancheng Bioengineering Institute, Nanjing, China) in the liver were determined through enzymatic colorimetric methods according to the commercial kits, respectively. Briefly, the concentration of MDA, which is an indicator of lipid peroxidation, was analyzed using the thiobarbituric acid (TBA) method to generate a colored product with an absorbance at 532 nm. The concentration of IHA was detected by the Fenton reaction method and the absorbance was read at 550 nm. Activity

of SOD was determined using the hydroxylamine method, and absorbance was recorded at 550 nm. GSH-Px activity was expressed by measuring the reduction of glutathione per min after the subtraction of the nonenzymatic reaction. All absorbance levels were determined using a UV-visible spectrophotometer (Tongfang, Inc., China) as described by Zhu et al. [6].

2.4. ELISA for DNA Injury, Caspases, and Indices of Hepatic Function. The activities of 8-hydroxy-2′-deoxyguanosine (8-OHdG), caspase-3, caspase-8, caspase-9 (Nanjing Jiancheng Bioengineering Institute, Nanjing, China), aspartate aminotransferase transaminase (AST) and alanine aminotransferase (ALT), alkaline phosphatase (ALP), and gamma glutamyltransferase (GGT) (Shanghai Yuanye Bioengineering Institute, Shanghai, China) were determined using commercially available enzyme-linked immune sorbent assay (ELISA) kits. Briefly, liver tissues were homogenized in 0.9% of saline solution and then centrifuged at 12,000 ×g for 15 min, to release the enzymes into the solution. Then, the microplates were coated of with anti-8-OHdG, caspase-3, caspase-8, caspase-9, AST, ALT, GGT, and ALP, followed by detection with a horseradish peroxidase-labeled substrate after incubation for 10 minutes at 37°C. Absorbance values were then read in a spectrophotometer at 450 nm.

2.5. Western Blot Analysis. Liver samples were homogenized in 500 μL of ice-cold RIPA lysis buffer (KGP703-100, KeyGEN Biotech, Nanjing, China), containing 1 mM of phenylmethylsulfonyl fluoride (PMSF, Amresco, Shanghai, China) and protease inhibitor cocktail tablets (05892791001, Roche, Germany) and incubating the suspension on ice for 30 min. The lysates were centrifuged for 10 min at 12,000 ×g, and the supernatants were collected. The protein content was measured using the BCA protein assay kit, according to the manufacturer's instructions (P0010, Beyotime Biotech, Shanghai, China). Tissue extracts (amounts equalized by protein concentration) were mixed with 5 × SDS-PAGE loading buffer (BL502A, Biosharp, US) and boiled for 3 min at 100°C. Protein (40 μg) was electrophoresed in 10% SDS-PAGE gels and transferred to polyvinylidene difluoride (PVDF) membranes (0.45 μm pore size, IPVH00010, Millipore, MA). The membranes were blocked for 2 h with 5% (w/v) skimmed milk powder (D8340, Solarbio, Shanghai, China) in Tris-Tween buffered saline (T-TBS) buffer [0.5 M NaCl (S7653, Sigma-Aldrich, Shanghai, China), 20 mM Tris (Amresco, Shanghai, China), pH 7.5, and 0.1% (v/v) Tween-20 (P7949, Sigma-Aldrich, Shanghai, China)], then washed three times with T-TBS, and incubated overnight at 4°C with primary antibodies following dilutions in 5% skimmed milk powder or BSA (0218054950, MP, US). The primary antibodies were JNK (1 : 2000, sc-571, Santa Cruz), p38α (1 : 200, sc-535, Santa Cruz), p-p38 (1 : 200, sc-7973, Santa Cruz), Bax (1 : 100, sc-493, Santa Cruz), Bcl-2 (1 : 200, sc-492, Santa Cruz), p-JNK (1 : 500, orb10951, Biorbyt Ltd, UK), ERK1/2 (1 : 1000, number 9102, Cell Signaling Technology), phospho-ERK1/2 (1 : 2000, number 4370, Cell Signaling Technology) (Thr202/Tyr204, Rabbit mAb) incubated overnight at 4°C, and then incubated with goat anti-rabbit (1 : 2000, ab97051, Abcam, UK) or goat anti-mouse IgG-HRP (1 : 2000, sc-2005, Santa Cruz) antibodies for 2 h. Image acquisition was performed on an enhanced chemiluminescence detection system (Tanon, Shanghai, China). Image J software was used to quantify the density of the specific protein bands.

Table 2: Concentrations of free radicals in liver homogenates of WG at d 1, d 4, and d 7 compared with CG ($n = 5$).

	CG	WG	P
H_2O_2 (μmol/g prot)			
d 0	11.75 ± 0.71		
d 1	11.38 ± 0.34	14.04 ± 0.83	0.000
d 4	11.46 ± 0.69	13.49 ± 1.21	0.012
d 7	13.24 ± 1.47	14.55 ± 0.97	0.134
NO (μmol/g prot)			
d 0	19.01 ± 0.64		
d 1	15.54 ± 0.32	19.46 ± 0.25	0.000
d 4	18.50 ± 1.32	19.10 ± 1.08	0.473
d 7	18.45 ± 0.90	21.11 ± 0.86	0.001

CG: control group; WG: weaning group. Differences were considered significant at $P < 0.05$.

2.6. Statistical Analysis. Data among groups both the CG and WG were tested for normal distribution using the statistical software SPSS 17.0 (SPSS Inc., Chicago, IL, US). If the data were not distributed normally, log transformation of variables was performed among treatment groups. No significant variance of data was found before the independent sample t-test method was conducted. All the data were presented as mean ± SD. P values < 0.05 were considered statistically significant.

3. Results

3.1. Concentrations of Free Radicals in the Liver. The concentrations of free radicals in liver homogenates are shown in Table 2. Compared with the CG, the content of H_2O_2 was significantly increased by 23.37% and 17.71% ($P < 0.05$) at d 1 and d 4 in the livers of the WG, but no difference was observed at d 7 between the CG and WG. Likewise, weaning increased the NO production at d 1 (by 25.23%) and d 7 (by 14.42%), while there was no significant difference at d 4.

3.2. Oxidant Injury and Antioxidant Enzyme Activity. We measured the concentrations of MDA and 8-OHdG and monitored the activities of IHA, SOD, and GSH-Px in the liver homogenates of CG and WG (shown in Figures 1 and 2). As the marker of lipid peroxidation, hepatic MDA levels in WG were no different from that found in the CG at d 1, but hepatic MDA levels were significantly higher ($P < 0.05$) at d 4 and d 7. Compared with the CG, 8-OHdG, as an indicator of DNA injury, was significantly higher ($P < 0.05$) in the WG at d 1, d 4, and d 7. The concentration of inhibitory hydroxyl radical (IHA) was significantly higher ($P < 0.05$) in the WG at d 1, d 4, and d 7, although IHA showed a downward curve

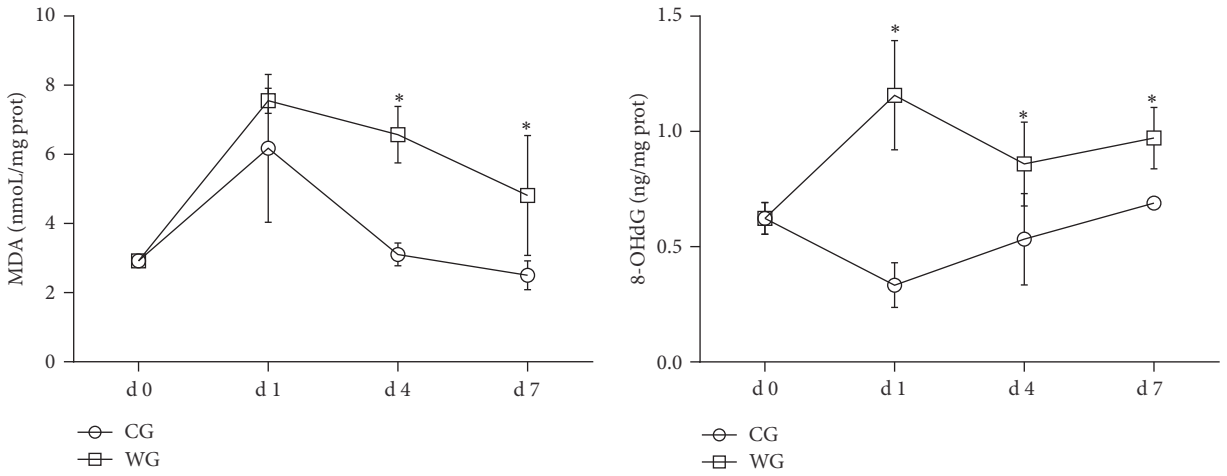

Figure 1: Oxidative injury obtained at d 0, d 1, d 4, and d 7 in the liver of WG compared with CG ($n = 5$). CG: control group; WG: weaning group. MDA: malondialdehyde (nmol/mg prot); 8-OHdG: 8-hydroxy-2-deoxyguanosine (ng/mg prot). *Means are significantly different ($P < 0.05$).

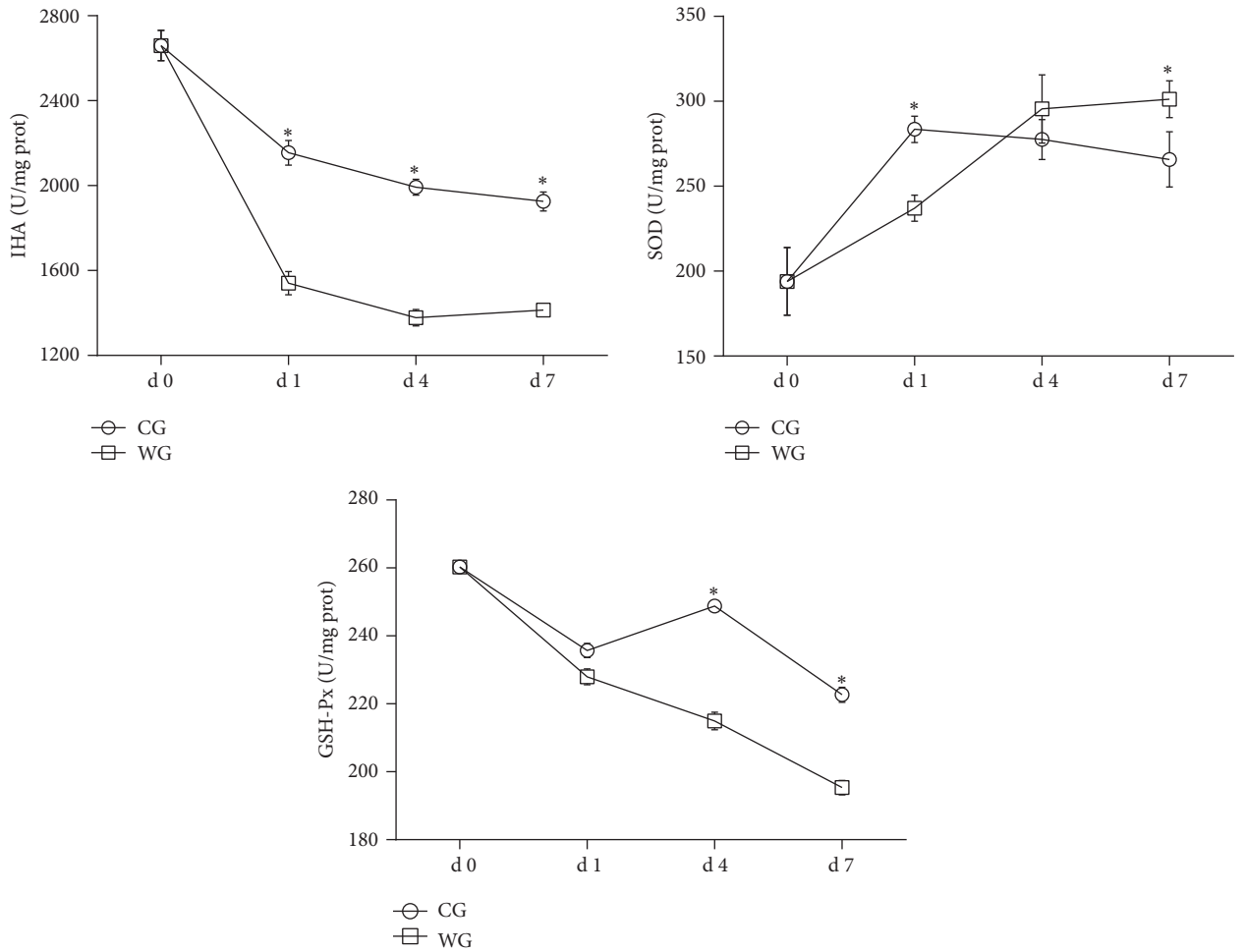

Figure 2: Antioxidant enzymes activities obtained at d 0, d 1, d 4, and d 7 in the liver of WG compared with CG. CG: control group; WG: weaning group. IHA: inhibitory hydroxyl ability (U/mg prot); SOD: superoxide dismutase (U/mg prot); GSH-Px: glutathione peroxidase (U/mg prot). *Means are significantly different ($P < 0.05$).

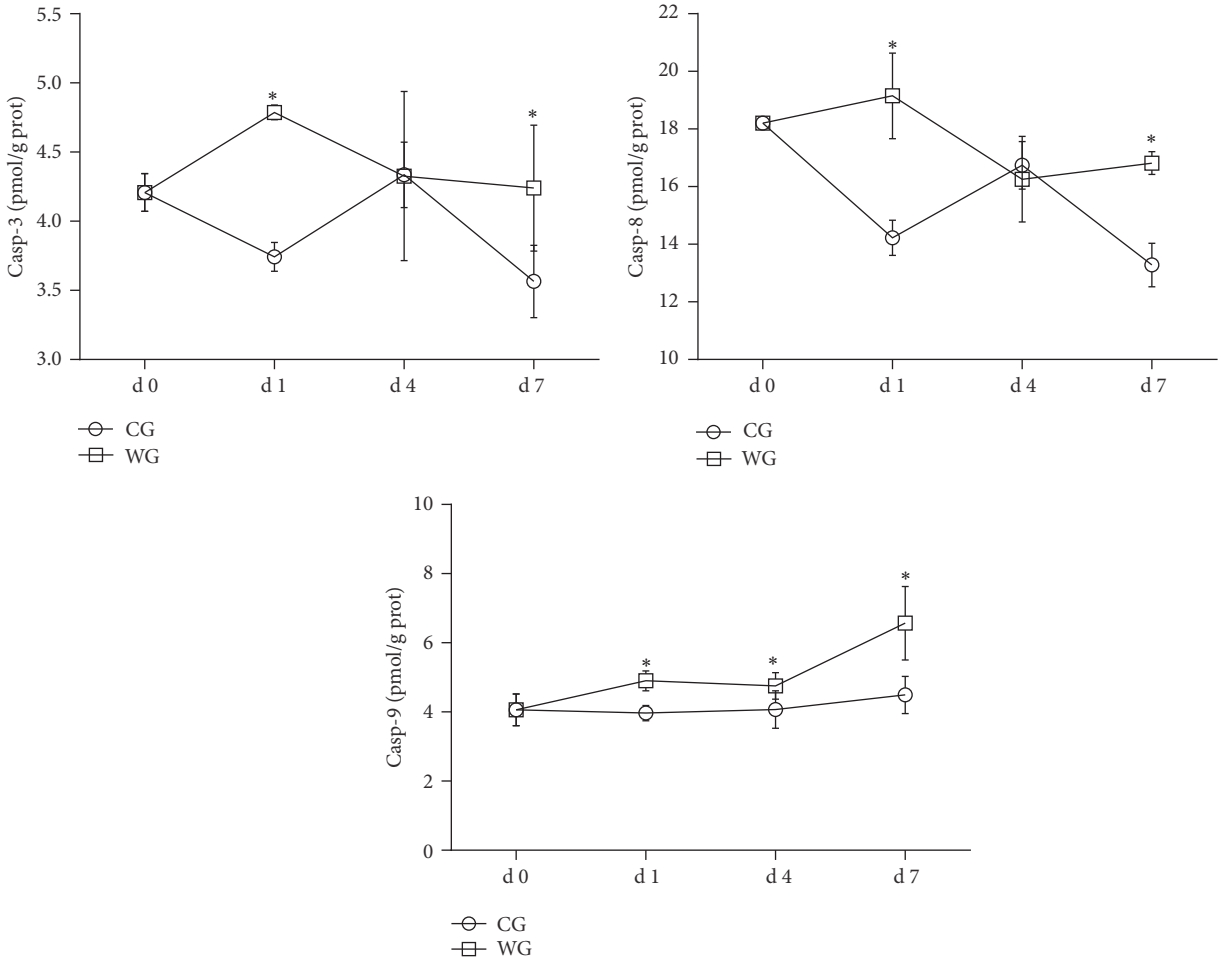

Figure 3: Caspase-3, caspase-8, and caspase-9 activities (pmol/g prot) at d 0, d 1, d 4, and d 7 in the liver of WG compared with CG. CG: control group; WG: weaning group. *Means are significantly different ($P < 0.05$).

over that time period. Contrarily, the concentration of SOD in the WG was much less at d 1 and then significantly ($P < 0.05$) higher than that found in the CG at d 7. No significant difference was observed in GSH-Px activity at d 1 after weaning, but the value was significantly lowered ($P < 0.05$) at d 4 and d 7 in the WG when compared with the CG.

3.3. ELISA Results for Caspase Activity. As shown in Figure 3, the levels of caspase-3 and caspase-8 were significantly higher ($P < 0.05$) in the livers of WG than those in the CG at d 1 and d 7. No difference was observed in the concentrations of caspase-3 and caspase-8 at d 4. Compared with the CG, the WG experienced a significantly increased concentration of caspase-9 ($P < 0.05$) in the liver at d 1, d 4, and d 7.

3.4. ELISA Results for Enzyme Activities of Hepatic Function. The effects of weaning on hepatic function at different time points are shown in Figure 4. The concentration of AST was significantly higher ($P < 0.05$) in WG than in the CG at d 1 and d 7 (by 5.35% and 8.08%, resp.). Meanwhile, the ALT activity was significantly increased ($P < 0.05$) in weaned piglets at d 1 (by 11.74%) and d 7 (by 10.29%). However, no significant differences were observed in the concentration of ALP and GGT in the WG when compared with the CG.

3.5. Protein Expression of MAPK Signaling Pathways and Regulator of Apoptosis. We measured the effects of weaning on the protein expressions of regulators of apoptosis (ratio of Bax/Bcl-2) and MAPK signaling pathways (Figure 5). Results showed that the ratio of Bax/Bcl-2 was significantly higher ($P < 0.05$) in the WG at d 1, but there were no differences between the WG and the CG at d 4 or d 7. Compared with the CG, the ratio of p-ERK/ERK was increased ($P < 0.05$) at d 4 and d 7, while the ratio of p-JNK/JNK was increased ($P < 0.05$) at d 1, d 4, and d 7 in the WG. Weaning lowered ($P < 0.05$) the ratio of p-p38/p38α at d 1 and 4, but the value was significantly higher at d 7.

4. Discussion

Weaning is the result of multiple factors involving physiological, environmental, and psychological changes in piglets, which often induces oxidative stress in vivo [6, 16]. Oxidative stress is a systematic response involving the pathophysiology

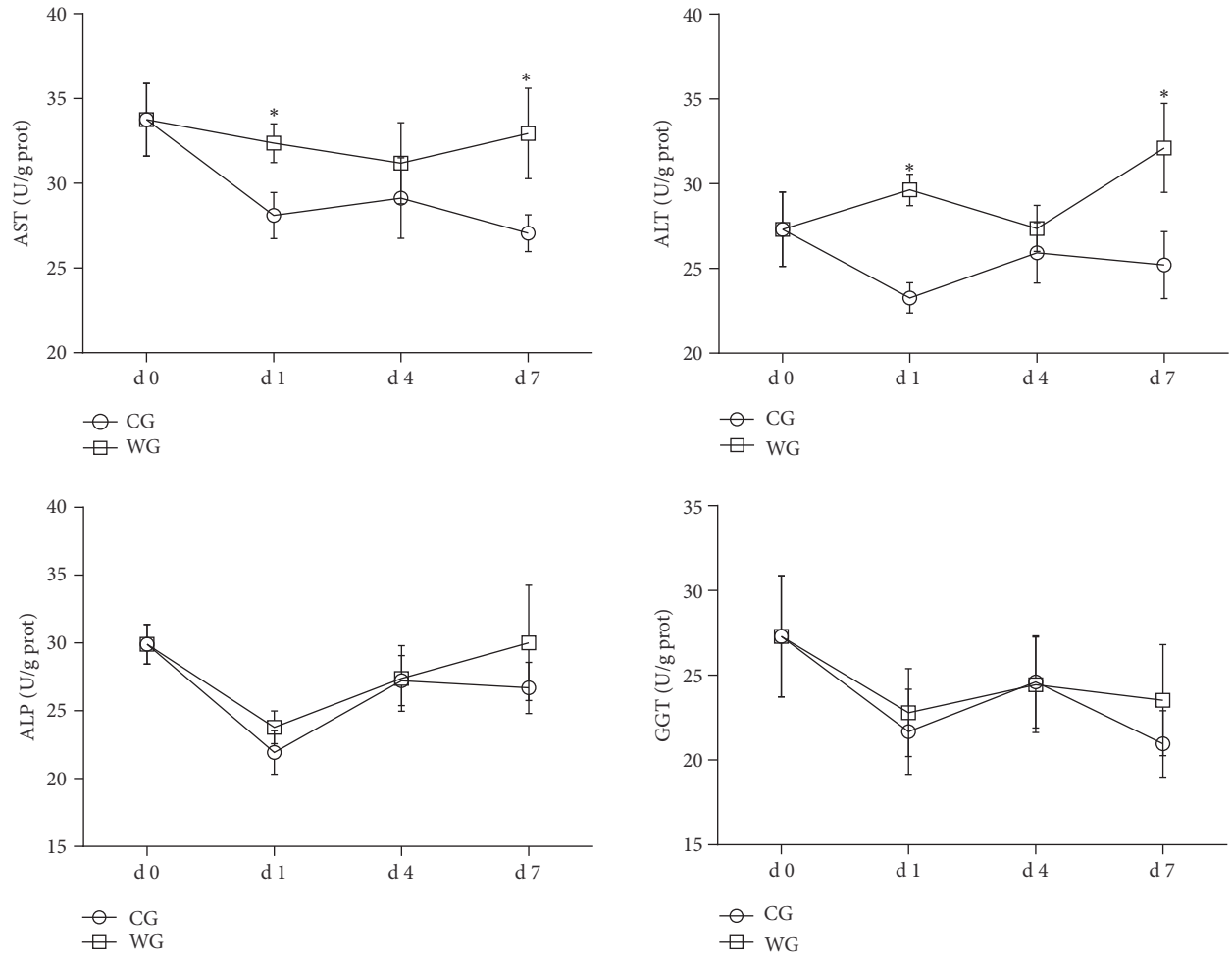

Figure 4: Indices of hepatic enzyme activities at d 0, d 1, d 4, and d 7 in WG compared with CG. CG: control group; WG: weaning group. AST: aspartate aminotransferase transaminase (U/g prot); ALT: alanine aminotransferase (U/g prot); ALP: alkaline phosphatase (U/g prot); GGT: gamma glutamyltransferase (U/g prot). *Means are significantly different ($P < 0.05$).

of many different disorders, including the hepatic redox status and function in piglets as shown in the present study [17].

H_2O_2 and NO are small, highly reactive molecules that play a dual role in normal cell progression, as both toxins and signaling molecules [18, 19]. In the present study, we found that NO and H_2O_2 were significantly increased in the liver homogenates of WG. The results were similar to our previous reports, which indicated that the concentrations of H_2O_2 and NO were increased in the serum, ileum, and colon of weaning piglets [6, 20]. Furthermore, to investigate whether the increased ROS led to oxidative injury caused by weaning, we determined the concentrations of MDA and 8-OHdG in the liver for both the CG and WG. MDA is derived by polyunsaturated fatty acid peroxidation and its contents have been considered a biological marker of lipid oxidative injury [21]. In this study, the concentration of MDA was significantly increased at d 4 and d 7 after weaning. However, our previous report found that the serum MDA increased only at d 14 after weaning, which indicated a postponed response [6]. We speculated that the liver was the major location for fatty acid β-oxidation, where MDA was produced as a decomposition product [22]. In addition, guanine is the most easily oxidized by the hydroxyl radical among the four DNA bases, because the oxidation potential of guanine is lower than the other three DNA bases [23]. Therefore, oxidative DNA damage can produce 8-OHdG in the nucleotide pool during DNA replication [24]. Findings of high 8-OHdG levels in the organs have been considered a biomarker of DNA oxidative injury [25]. Interestingly, we found that 8-OHdG was markedly increased after weaning at d 1, d 4, and d 7, which aligned with the resulting of inhibitory hydroxyl ability (IHA) (indirectly reflected the level of the hydroxyl radical).

The classical enzymatic antioxidants, such as SOD and GSH-Px, represented a first line of defense against ROS by detoxifying them; antioxidants can remove ROS rapidly and efficiently from the intracellular environment [26]. In the present study, we found that weaning led to decreased GSH-Px but increased SOD and an upward trend at d 7 after weaning. Similarly, Yin et al. reported that plasma GSH-Px decreased, but the enzyme activity and genes of SOD in the jejunum and ileum exhibited a significant upward trend at 7 d [27]. Indeed, the increased enzymatic activity of SOD

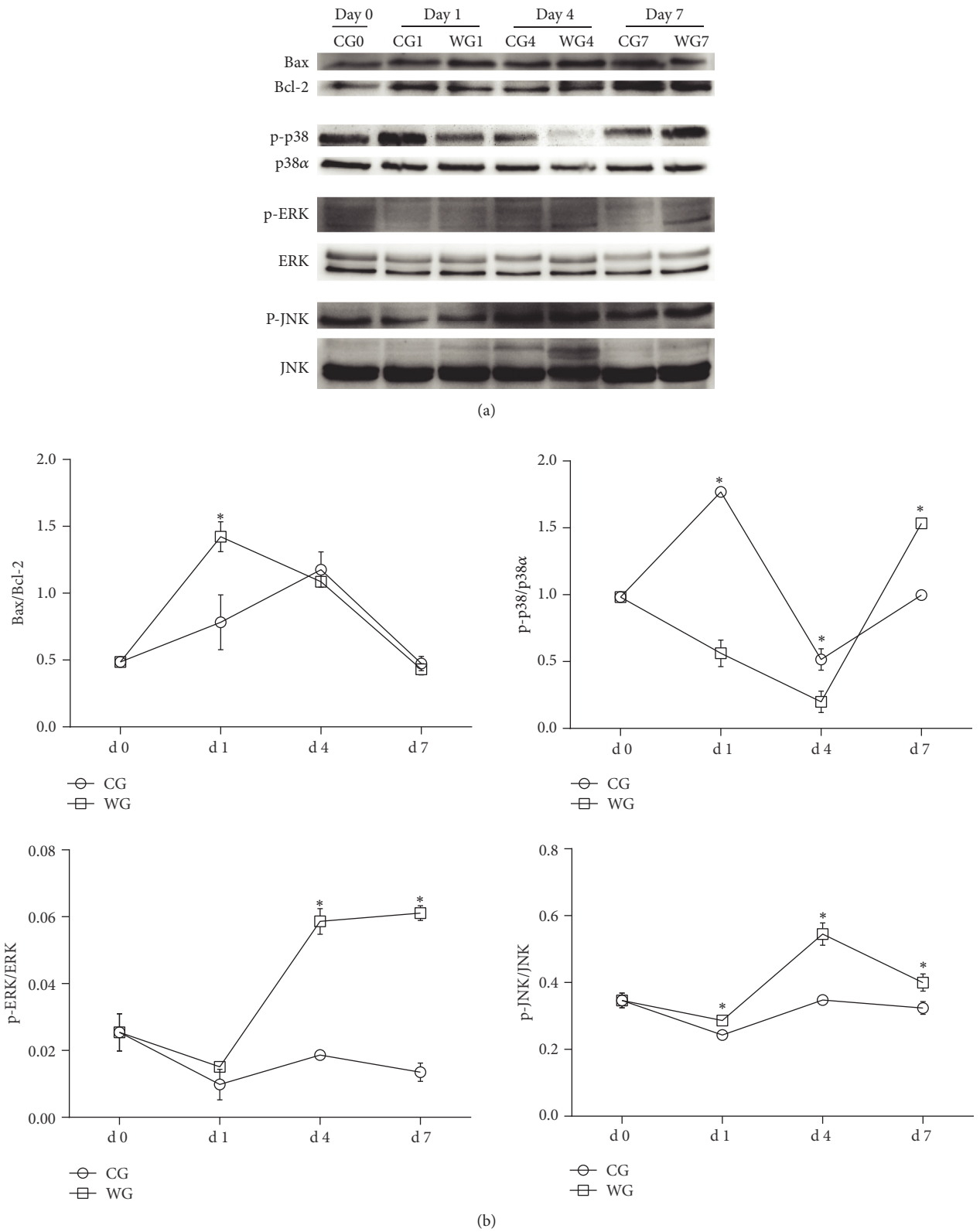

Figure 5: The protein expression of regulator of apoptosis and MAPK signaling pathways at d 0, 1, 4, and 7 in liver of WG compared with CG (a). The values are calculated as the ratios of Bax and Bcl-2 and their phosphorylation levels (p-JNK, p-p38, and p-ERK1/2) and the total levels of MAPK (b). CG: control group; WG: weaning group. *Means are significantly different ($P < 0.05$) ($n = 3$). Note: p38 [p38α (C20), SC-535, Santa Cruz] is recommended for detection of p38α as the total protein, while p-p38 [p-p38 (D-8) SC7379, Santa Cruz] is recommended for detection of p38α, p38β, and p38γ correspondingly.

suggested the process of enhanced resistance to oxidative stress within the piglets. These results might be explained by a compensatory response to reduce the oxidative stress caused by weaning. Our results showed that weaning led to the increase of hepatic ROS and caused oxidative injury and insufficiency of antioxidant enzyme activities in the WG, which suggested a higher risk of oxidative stress than that in CG. Recently, other research suggested that oxidative stress may accompany other stresses, such as endoplasmic reticulum (ER) stress [28]. Zhao reported that ER stress arose due to the increase of X-box binding protein 1 (XBP1) expression in the hepatocyte nucleus of weaning piglets [13], which was just in accordance with our results.

To further study whether weaning resulted in hepatic apoptosis, we investigated the concentrations of caspase-3, caspase-8, and caspase-9 and the protein expression of Bax and Bcl-2. Generally, the apoptosis response is regulated by either the death receptor pathway or the mitochondrial pathway in cells, depending on different stimuli sources [29]. Apoptosis is a vital component of various processes such as normal cell turnover and chemical-induced cell death, which played an important role in oxidative stress-induced injury. Although caspases are the central components of the apoptotic response, a high Bax/Bcl-2 ratio has been found to increase induction of caspases activation, such as caspase-9, representing the mitochondria pathway [30]. However, the activation of caspase-8 was involved in the death receptor pathway. Both of these pathways activated the effector caspase-3, an executioner caspase, which initiates the process of apoptosis [31, 32]. In the present study, from the protein expression and enzyme activity, we confirmed both that the ratio of Bax/Bcl-2 and the activities of caspase-3, caspase-8 and caspase-9 were significantly increased at d 1 after weaning. Likewise, a ratio of Bax/Bcl-2 was reported, in other research, as a regulator that determined the susceptibility to apoptosis in melanoma cells [33]. San-Miguel et al. reported that the relative expression of the ratio of Bax/Bcl-2 and the activity of caspase-3 were increased in the liver of infected rabbits [34]. Recently, we have reported that weaning may induce enterocyte apoptosis through the activation of Fas-dependent and mitochondria-dependent apoptosis [7]. Taken together, the results of this study proved the hypothesis that alteration in the Bax/Bcl-2 ratio caused by weaning regulated downstream caspase-driven apoptosis.

Additionally, we detected the enzymes in liver homogenates through ELISA. ALT, AST, ALP, and GGT were abundant intracellular enzymes in the liver, which were considered to be specific indicators for hepatic damage due to subsequent leakage of enzymes into blood circulation [35]. Elevated serum ALP and GGT have been associated with damaged liver function caused by hepatic cholestasis and some destruction of the hepatic cell membranes. Both of ALP and GGT were indicators that identified bile duct obstruction or cholestasis disease, both intra- and extrahepatic [36]. In the present study, constant ALP and GGT concentrations suggested that the hepatobiliary system was unobstructed after weaning. Aminotransferases are sensitive indicators of liver cell injury and are most helpful in identifying acute hepatocellular diseases such as hepatitis. High levels of AST and ALT in the liver homogenates of the WG were found, which suggested that oxidative stress was a common mechanism that damaged hepatocellular function [35, 37]. However, further studies are warranted to explore the changes within the serum concentrations and hepatic structure of weaning piglets.

Finally, the mechanisms involved in these changes in redox status, apoptosis, and function in the liver of weaning piglets were also investigated. The MAPK pathways including ERK1/2, p38, and JNK/SAPK were considered signaling cascades for regulation of various cellular processes, such as cell proliferation and apoptosis within a wide range of cell types [14]. In our study, we found that p-JNK/JNK and p-ERK/ERK were increased after weaning, but p-p38/p38α showed a different fluctuation curve. This finding was not consistent with Hu et al.'s research, which reported that the ratios of p-p38/p38, p-ERK/ERK, and p-JNK/JNK were increased by weaning in jejunum [5]. However, Campbell et al. found that phosphorylated p38 was found in normal mouse livers, while it was rapidly inactivated within 30 min after a partial hepatectomy [38], which supported our results. Therefore, we believed the difference between our results and Hu et al.'s may be attributed to tissue specificity. ERKs are important for cell survival and play an adaptive role in protecting cells from oxidative stress [39]. The increased expression of ERK in this study suggested a protective effect on the livers of postweaning piglets. However, the role of stress kinases p38-MAPK and JNK in connecting redox status and apoptosis remains controversial [14]. For example, Wang et al. reported that JNK activation, but not p38, was involved in methamphetamine-induced caspase-3 activation and neuronal cell death through the mitochondrial apoptosis pathway [40]. In other research, the proapoptotic p38-MAPK activated the downstream target Bax cascade in UVB irradiated human skin [41]. These data therefore indicate that the MAPK pathways are required for proliferation and apoptosis, depending on cell types and stimuli [14]. Further studies are suggested to use the inhibitors of MAPK pathways or through overexpression or knockout of these pathways to explore whether weaning can induce hepatic apoptosis in vitro.

5. Conclusion

Our study was the first to provide clear evidence that weaning induced hepatic oxidative stress and aminotransferases, which may be related to activated MAPK signaling pathways. A possible mechanism was suggested by this research that weaning increased the hepatic ROS production at first and then decreased antioxidant enzyme activities, which resulted in oxidative damage. Meanwhile, it initiated apoptosis by increasing the ratio of Bax/Bcl-2 and caspases involved in activating MAPK pathways (shown in Figure 6). The conclusions of this study may help to find suitable therapeutic strategies to relieve postweaning stress in both human beings and domestic animals.

Competing Interests

The authors declare that there are no competing interests in relation to this work.

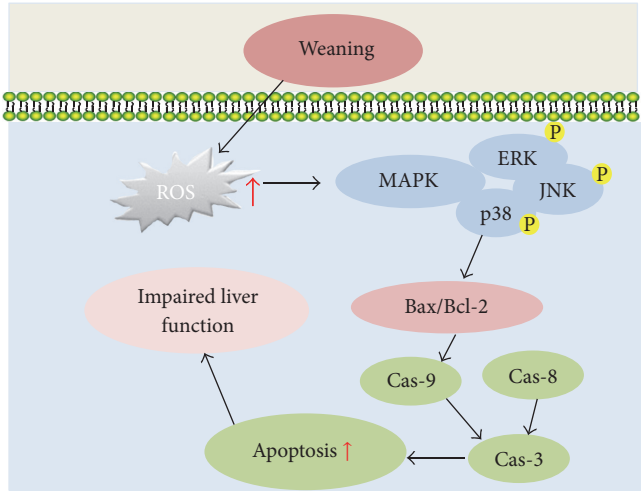

Figure 6: Schematic mechanisms illustrating the effects of weaning on hepatic redox status, apoptosis, and function in piglets.

Acknowledgments

This research was supported financially by the National Natural Science Foundation of China (Grant no. 30972103).

References

[1] J. M. Campbell, J. D. Crenshaw, and J. Polo, "The biological stress of early weaned piglets," *Journal of Animal Science and Biotechnology*, vol. 4, no. 1, article 19, 2013.

[2] G. Boudry, V. Péron, I. Le Huërou-Luron, J. P. Lallès, and B. Sève, "Weaning induces both transient and long-lasting modifications of absorptive, secretory, and barrier properties of piglet intestine," *The Journal of Nutrition*, vol. 134, no. 9, pp. 2256–2262, 2004.

[3] S. Pié, J. P. Lallès, F. Blazy, J. Laffitte, B. Sève, and I. P. Oswald, "Weaning is associated with an upregulation of expression of inflamatory cytokines in the intestine of piglets," *Journal of Nutrition*, vol. 134, no. 3, pp. 641–647, 2004.

[4] A. J. Moeser, C. Vander Klok, K. A. Ryan et al., "Stress signaling pathways activated by weaning mediate intestinal dysfunction in the pig," *American Journal of Physiology—Gastrointestinal and Liver Physiology*, vol. 292, no. 1, pp. G173–G181, 2007.

[5] C. H. Hu, K. Xiao, Z. S. Luan, and J. Song, "Early weaning increases intestinal permeability, alters expression of cytokine and tight junction proteins, and activates mitogen-activated protein kinases in pigs," *Journal of Animal Science*, vol. 91, no. 3, pp. 1094–1101, 2013.

[6] L. H. Zhu, K. L. Zhao, X. L. Chen, and J. X. Xu, "Impact of weaning and an antioxidant blend on intestinal barrier function and antioxidant status in pigs," *Journal of Animal Science*, vol. 90, no. 8, pp. 2581–2589, 2012.

[7] L. Zhu, X. Cai, Q. Guo, X. Chen, S. Zhu, and J. Xu, "Effect of N-acetyl cysteine on enterocyte apoptosis and intracellular signalling pathways' response to oxidative stress in weaned piglets," *British Journal of Nutrition*, vol. 110, no. 11, pp. 1938–1947, 2013.

[8] E. Seki and B. Schnabl, "Role of innate immunity and the microbiota in liver fibrosis: crosstalk between the liver and gut," *The Journal of Physiology*, vol. 590, no. 3, pp. 447–458, 2012.

[9] G. K. Michalopoulos, "Liver regeneration," *Journal of Cellular Physiology*, vol. 213, no. 2, pp. 286–300, 2007.

[10] Y. Ying, J. Yun, W. Guoyao, S. Kaiji, D. Zhaolai, and W. Zhenlong, "Dietary l-methionine restriction decreases oxidative stress in porcine liver mitochondria," *Experimental Gerontology*, vol. 65, pp. 35–41, 2015.

[11] J. F. Turrens, "Mitochondrial formation of reactive oxygen species," *The Journal of Physiology*, vol. 552, no. 2, pp. 335–344, 2003.

[12] H. Assaad, K. Yao, C. D. Tekwe et al., "Analysis of energy expenditure in diet-induced obese rats," *Frontiers in Bioscience*, vol. 19, pp. 967–985, 2014.

[13] L. Zhao, *The nutritional regulation of endoplasmic reticulum stress induced by early weaning stress in liver of piglets [M.S. thesis]*, 2014.

[14] T. Wada and J. M. Penninger, "Mitogen-activated protein kinases in apoptosis regulation," *Oncogene*, vol. 23, no. 16, pp. 2838–2849, 2004.

[15] D. E. Shifflett, S. L. Jones, A. J. Moeser, and A. T. Blikslager, "Mitogen-activated protein kinases regulate COX-2 and mucosal recovery in ischemic-injured porcine ileum," *American Journal of Physiology—Gastrointestinal and Liver Physiology*, vol. 286, no. 6, pp. G906–G913, 2004.

[16] J. R. Pluske, D. J. Hampson, and I. H. Williams, "Factors influencing the structure and function of the small intestine in the weaned pig: a review," *Livestock Production Science*, vol. 51, no. 1–3, pp. 215–236, 1997.

[17] A. Fernández-Sánchez, E. Madrigal-Santillán, M. Bautista et al., "Inflammation, oxidative stress, and obesity," *International Journal of Molecular Sciences*, vol. 12, no. 5, pp. 3117–3132, 2011.

[18] D. Armstrong, *Oxidative Stress in Applied Basic Research and Clinical Practice*, 2010.

[19] E. Schulz, T. Jansen, P. Wenzel, A. Daiber, and T. Münzel, "Nitric oxide, tetrahydrobiopterin, oxidative stress, and endothelial dysfunction in hypertension," *Antioxidants & Redox Signaling*, vol. 10, no. 6, pp. 1115–1126, 2008.

[20] C. C. Xu, S. F. Yang, L. H. Zhu et al., "Regulation of N-acetyl cysteine on gut redox status and major microbiota in weaned piglets," *Journal of Animal Science*, vol. 92, no. 4, pp. 1504–1511, 2014.

[21] D. Del Rio, A. J. Stewart, and N. Pellegrini, "A review of recent studies on malondialdehyde as toxic molecule and biological marker of oxidative stress," *Nutrition, Metabolism and Cardiovascular Diseases*, vol. 15, no. 4, pp. 316–328, 2005.

[22] E. N. Frankel and W. E. Neff, "Formation of malonaldehyde from lipid oxidation products," *Biochimica et Biophysica Acta (BBA)—Lipids and Lipid Metabolism*, vol. 754, no. 3, pp. 264–270, 1983.

[23] S. Kawanishi and Y. Hiraku, "Oxidative and nitrative DNA damage as biomarker for carcinogenesis with special reference to inflammation," *Antioxidants & Redox Signaling*, vol. 8, no. 5-6, pp. 1047–1058, 2006.

[24] A. G. Georgakilas, "Oxidative stress, DNA damage and repair in carcinogenesis: have we established a connection?" *Cancer Letters*, vol. 327, no. 1-2, pp. 3–4, 2012.

[25] M. Dizdaroglu, R. Olinski, J. H. Doroshow, and S. A. Akman, "Modification of DNA bases in chromatin of intact target human cells by activated human polymorphonuclear leukocytes," *Cancer Research*, vol. 53, no. 6, pp. 1269–1272, 1993.

[26] H. Zhang, K. J. Davies, and H. J. Forman, "Oxidative stress response and Nrf2 signaling in aging," *Free Radical Biology and Medicine*, vol. 88, pp. 314–336, 2015.

[27] J. Yin, M. M. Wu, H. Xiao et al., "Development of an antioxidant system after early weaning in piglets," *Journal of Animal Science*, vol. 92, no. 2, pp. 612–619, 2014.

[28] G. J. Burton and E. Jauniaux, "Oxidative stress," *Best Practice & Research: Clinical Obstetrics & Gynaecology*, vol. 25, no. 3, pp. 287–299, 2011.

[29] S. J. Riedl and Y. Shi, "Molecular mechanisms of caspase regulation during apoptosis," *Nature Reviews Molecular Cell Biology*, vol. 5, no. 11, pp. 897–907, 2004.

[30] J. C. Reed, "Bcl-2 and the regulation of programmed cell death," *The Journal of Cell Biology*, vol. 124, no. 1, pp. 1–6, 1994.

[31] I. Budihardjo, H. Oliver, M. Lutter, X. Luo, and X. Wang, "Biochemical pathways of caspase activation during apoptosis," *Annual Review of Cell and Developmental Biology*, vol. 15, no. 1, pp. 269–290, 1999.

[32] S. Elmore, "Apoptosis: a review of programmed cell death," *Toxicologic Pathology*, vol. 35, no. 4, pp. 495–516, 2007.

[33] M. Raisova, A. M. Hossini, J. Eberle et al., "The Bax/Bcl-2 ratio determines the susceptibility of human melanoma cells to CD95/Fas-mediated apoptosis," *Journal of Investigative Dermatology*, vol. 117, no. 2, pp. 333–340, 2001.

[34] B. San-Miguel, M. Alvarez, J. M. Culebras, J. González-Gallego, and M. J. Tuñón, "N-acetyl-cysteine protects liver from apoptotic death in an animal model of fulminant hepatic failure," *Apoptosis*, vol. 11, no. 11, pp. 1945–1957, 2006.

[35] A. R. Knudsen, K. J. Andersen, S. Hamilton-Dutoit, J. R. Nyengaard, and F. V. Mortensen, "Correlation between liver cell necrosis and circulating alanine aminotransferase after ischaemia/reperfusion injuries in the rat liver," *International Journal of Experimental Pathology*, vol. 97, no. 2, pp. 133–138, 2016.

[36] M. A. Hyder, M. Hasan, and A. H. Mohieldein, "Comparative levels of ALT, AST, ALP and GGT in liver associated diseases," *European Journal of Experimental Biology*, vol. 3, no. 2, pp. 280–284, 2013.

[37] M.-J. Kang and J.-I. Kim, "Protective effect of *Hedyotis diffusa* on lipopolysaccharide (LPS)-induced liver damage," *The FASEB Journal*, vol. 27, no. 1, supplement, p. 1155.5, 2013.

[38] J. S. Campbell, G. M. Argast, S. Y. Yuen, B. Hayes, and N. Fausto, "Inactivation of p38 MAPK during liver regeneration," *The International Journal of Biochemistry & Cell Biology*, vol. 43, no. 2, pp. 180–188, 2011.

[39] J. A. McCubrey, M. M. LaHair, and R. A. Franklin, "Reactive oxygen species-induced activation of the MAP kinase signaling pathways," *Antioxidants & Redox Signaling*, vol. 8, no. 9-10, pp. 1775–1789, 2006.

[40] S.-F. Wang, J.-C. Yen, P.-H. Yin, C.-W. Chi, and H.-C. Lee, "Involvement of oxidative stress-activated JNK signaling in the methamphetamine-induced cell death of human SH-SY5Y cells," *Toxicology*, vol. 246, no. 2-3, pp. 234–241, 2008.

[41] A. Van Laethem, S. Van Kelst, S. Lippens et al., "Activation of p38 MAPK is required for Bax translocation to mitochondria, cytochrome c release and apoptosis induced by UVB irradiation in human keratinocytes," *The FASEB Journal*, vol. 18, no. 15, pp. 1946–1948, 2004.

Hindawi Publishing Corporation
Oxidative Medicine and Cellular Longevity
Volume 2016, Article ID 1578235, 8 pages
http://dx.doi.org/10.1155/2016/1578235

Research Article

Impact of Oxidative Stress in Premature Aging and Iron Overload in Hemodialysis Patients

Blanca Murillo-Ortiz,[1] Joel Ramírez Emiliano,[2] Wendy Ivett Hernández Vázquez,[2] Sandra Martínez-Garza,[1] Sergio Solorio-Meza,[1] Froylán Albarrán-Tamayo,[1] Edna Ramos-Rodríguez,[1] and Luis Benítez- Bribiesca[3]

[1]*Unidad de Investigación en Epidemiología Clínica, Servicio de Hemodiálisis, Unidad Médica de Alta Especialidad (UMAE) No. 1 Bajío, Instituto Mexicano del Seguro Social (IMSS), León, GTO, Mexico*
[2]*Departamento de Investigaciones Médicas, Universidad de Guanajuato, León, GTO, Mexico*
[3]*Unidad de Investigación Médica en Enfermedades Oncológicas, CMN, SXXI, IMSS, 06720 Ciudad de México, Mexico*

Correspondence should be addressed to Blanca Murillo-Ortiz; bomo907@hotmail.com

Received 1 April 2016; Revised 15 July 2016; Accepted 23 August 2016

Academic Editor: Claudio Cabello-Verrugio

Background. Increased oxidative stress is a well described feature of patients in hemodialysis. Their need for multiple blood transfusions and supplemental iron causes a significant iron overload that has recently been associated with increased oxidation of polyunsaturated lipids and accelerated aging due to DNA damage caused by telomere shortening. *Methods.* A total of 70 patients were evaluated concomitantly, 35 volunteers with ferritin levels below 500 ng/mL (Group A) and 35 volunteers with ferritin levels higher than 500 ng/mL (Group B). A sample of venous blood was taken to extract DNA from leukocytes and to measure relative telomere length by real-time PCR. *Results.* Patients in Group B had significantly higher plasma TBARS ($p = 0.008$), carbonyls ($p = 0.0004$), and urea ($p = 0.02$) compared with those in Group A. Telomeres were significantly shorter in Group B, 0.66 (SD, 0.051), compared with 0.75 (SD, 0.155) in Group A ($p = 0.0017$). We observed a statistically significant association between relative telomere length and ferritin levels ($r = -0.37$, $p = 0.001$). Relative telomere length was inversely related to time on hemodialysis ($r = -0.27$, $p = 0.02$). *Conclusions.* Our findings demonstrate that iron overload was associated with increased levels of oxidative stress and shorter relative telomere length.

1. Introduction

Iron overload is a common complication in patients with renal chronic failure submitted to hemodialysis (HD). It results from the necessity that these patients undergo transfusions of red cells to treat symptomatic anemia, as well as from the administration of enteral and/or parenteral iron supplements [1]. Although it is still controversial, multiple clinical studies have found an association between iron overload and the oxidation of polyunsaturated lipids catalyzed by metallic ions in atherosclerotic disease and in the development of cardiovascular events [2, 3].

There are several studies that demonstrate that iron overload is related with oxidative stress. On both in vivo and in vitro models iron overload allowed us to study the oxidative stress induction through mechanisms which activate the increase on ROS. A study conducted in young women with low iron levels who were given daily supplements of iron found that serum ferritin levels were almost twice the basal levels after 6 weeks of treatment and that body iron was more than twice the basal level. However, plasma levels of malondialdehyde and exhaled ethane increased more than 40% [4].

Chai et al. confirmed that the hematopoietic inhibitory effects of iron overload in an iron-overloaded mouse model were parallel to clinical conditions. Secondly, its related mechanism was investigated. It was demonstrated that iron overload increased the ROS levels of HSPCs through the NOX4/ROS/P38 MAPK signaling pathways [5].

In an experimental study it was observed that taurine supplementation reduces oxidative stress and improves cardiovascular function in an iron-overload murine model [6]. The therapeutic effects of resveratrol in murine iron-overload models that showed cardiac iron overload, increased oxidative stress, altered Ca^{2+} homeostasis, and myocardial fibrosis resulting in heart disease have been recently reported, as well as increased nuclear and acetylated levels of FOXO1 with corresponding inverse changes in SIRT1 levels in the heart which are corrected by resveratrol therapy. Also they demonstrated that the iron mediated pathological effects on human cardiomyocytes and cardiofibroblast were prevented by resveratrol [7].

It also has been shown that iron-overloaded rats had significant increases in malonyl-dialdehyde (MDA), a marker of lipid peroxidation, and nitric oxide (NO) in liver and spleen compared to control group. The effects of iron overload on lipid peroxidation and NO levels were significantly reduced with the administration of curcumin ($p < 0.05$). Furthermore, the endogenous antioxidant activity in liver and spleen was also significantly decreased in chronic iron overload and after administration of curcumin was completely restored [8]. Sripetchwandee et al. demonstrated the first evidence of the effect of combining iron chelator therapy and antioxidants (deferiprone and N-acetylcysteine, resp.) for 4 weeks on the cerebral iron-overload inducted disfunction on Wistar rats which restored completely the cerebral function [9].

The oxidation of polyunsaturated fatty acids generates MDA and 4-hydroxyalkenals; MDA can be measured by TBARS test. Iron-induced oxidative stress may be key determinant in the significant increase of 8-OH-G, 2-hydroxyadenine, and 8-hydroxyadenine adducts [10]. These lesions, caused by hydroxyl radical attack, could significantly increase DNA damage as in the telomere region and/or impair its repair. Telomeres are the specialized DNA structures located at the end of eukaryotic chromosomes and consist of tandemly repeated DNA sequences. Telomeres shorten with each cell division, and it is well known that telomere length in peripheral blood mononuclear cells (PBMCs) decreases with age [11].

The telomere shortening rate is increased by oxidative stress. Boxall et al. suggest that the length of time on dialysis is independently associated with increased telomere shortening in HD patients and hypothesize that this is caused by the cumulative exposure of DNA to oxidative stress [12]. Telomere attrition, expressed in leukocytes (WBCs), can serve as a biomarker of cumulative oxidative stress and inflammation.

Chronic oxidative stress accelerates cellular aging, while telomere shortening has been associated with hypertension, endothelial dysfunction, atherosclerosis, and cardiovascular mortality [13]. A recent study showed that telomeres are shorter in patients with a diagnosis of DM2 with more years of evolution, compared with healthy subjects of the same age. The time of duration of the disease suggests a parallel and progressive increase of inflammation and oxidative stress that plays a direct role in telomere shortening [14].

With aging, the renal function decreases, showing an evidently lower glomerular flow rate. It has been shown that telomere shortening occurs first in cells of the cortex before it occurs in cells of the renal medulla [15]. The increased oxidative stress caused by iron overload may induce this telomere shortening, and this in turn may contribute to renal diseases such as glomerulosclerosis. Measuring telomere length provides evidence of the aging that occurs as a result of the oxidative stress caused by high body iron levels.

Sullivan was the first to suggest (1981) that the high incidence of cardiac disease may be related to elevated serum iron levels [16]. Subsequent investigations provided evidence that high levels of body iron may actually increase the risk of cardiovascular disease. Kiechl and colleagues found a strong correlation between the serum levels of body iron and the probability of developing new atherosclerotic carotid lesions [17].

The Rotterdam study indicated that high levels of body iron, evidenced by a serum ferritin concentration of 200 μg/L or greater, almost double the risk of acute myocardial infarction in elderly patients. In a number of patients in the Bruneck study, serum ferritin and LDL cholesterol showed synergistic effects associated with the progression of carotid atherosclerosis, suggesting that iron promotes lipid peroxidation [18]. Increased oxidative stress and inflammation are associated with atherosclerotic coronary artery disease in hemodialysis patients [19].

Patients with end stage renal disease have a markedly increased risk of presenting cardiovascular complications [20]. Recent evidence shows that there is a strong association between telomere shortening and heart failure [21]. Iron can contribute to cardiovascular complications through its oxidative effects on low-density lipoproteins and its induction of endothelial dysfunction [22–26].

This information has been used recently to enlighten the mechanisms and provide experimental bases to achieve new target therapies on the treatment of the complications generated by the iron overload and on one of its consequences: the oxidative stress. The purpose of our study was to evaluate the effect of iron overload on lipid oxidation and telomere length, as well as the incidence and/or progression of coronary artery disease compared with patients without iron overload, with nephropathy and undergoing renal replacement therapy in the hemodialysis program of our hospital unit.

2. Subjects and Methods

We included a total of 70 patients with nephropathy undergoing renal replacement therapy in the hemodialysis program of the High-Specialty Medical Unit No. 1 Bajío. The patients were of both genders and older than 18 years of age; 35 of them were volunteers with ferritin levels higher than 500 ng/mL (Group A) and 35 were volunteers with ferritin levels below 500 ng/mL (Group B), who were evaluated concomitantly. Patients with immune disorders and the habit of smoking and alcoholism were not included. A sample of venous blood was taken in order to extract DNA from leukocytes and to measure telomere length by real-time PCR. Serum levels of ferritin and oxidation markers were also determined. All patients underwent transthoracic echocardiography. This

protocol was approved by the local bioethics committee and a written informed consent was obtained from each volunteer.

2.1. Measurement of Biochemical Parameters. Serum levels of glucose were determined using the glucose oxidase-peroxidase method (Biosystems, Spain). Uric acid, urea, creatinine, cholesterol, and triglycerides were estimated using enzymatic methods (STANBIO Laboratory, Boerne, TX, USA). Ferritin levels in plasma were determined with an automated analyzer using dry chemistry technique. The analyzer is Johnson & Johnson's E60 IQ which is reported in units of the IS (ng/mL).

2.2. Telomere Measurement. DNA samples were extracted from white blood cells. The ratio of telomere repeat copy number to a single gene copy number (T/S) was determined by a previously described modified version of the quantitative real-time PCR telomere assay [27]. We performed PCR amplification with oligonucleotide primers designed to hybridize to the TTAGGG and CCCTAA repeats. The final concentrations of reagents in the PCR were 0.2 SYBR Green I (Molecular Probes), 15 mM Tris-HCl pH 8.0, 50 mM KCl, 2 mM $MgCl_2$, 0.2 mMeach dNTP, 5 mM DTT, 1% DMSO, and 1.25 U AmpliTaq Gold DNA polymerase. The final telomere primer concentrations were tel 1,270 nM and tel 2,900 nM. The final *36B4* (single copy gene) primer concentrations were 36B4u, 300 nM, 36B4d, and 500 nM. The primer sequences (written $5' \rightarrow 3'$) were tel 1, GGTTTTTGAGGGTGAGGGTGAGGGTGAGGGTGAGGGT, tel2, TCCCGACTATCCCTATCCCTATCCCTATCCCTATCCCTA, 36B4u, CAGCAAGTGGGAAGGTGTAATCC, 36B4d, and CCCATTCTATCATCAACGGGTACAA. All PCRs were performed on a LightCycler® 1.5 (Roche). The thermal cycling profile for both amplicons began with a 95°C incubation for 3 min to activate the AmpliTaq Gold DNA polymerase. The telomere PCR conditions were 40 cycles of 95°C for 15 s and 54°C for 2 min; for *36B4* PCR, they were 40 cycles of 95°C for 15 s and 58°C for 1 min. The LightCycler 1.5 (Roche) was then used to generate the standard curve for each run and to determine the dilution factors of standards corresponding to the amounts of T and S in each sample.

2.3. Measurement of Lipid Peroxidation and Oxidized Protein. Malondialdehyde levels and carbonyls content were quantified as we previously described [28]. The MDA levels were determined with the thiobarbituric acid-reactive substances (TBARS) assay using 30 μL of sera, whereas the carbonyl content was measured using 5 μL of sera.

2.4. Cardiovascular Evaluation

2.4.1. Echocardiogram. The echocardiogram was performed with a Hewlett Packard Sonos 5500 equipped with an electronic 3.5 MHz phased array probe and an 8 MHz linear array probe. The diameters of the left atrium, left ventricle, right ventricle, interventricular septum, and posterior wall of the left ventricle were measured. The image analysis was performed according to the criteria of the American Society of Echocardiography. The left ventricular mass was calculated using the Devereux method. The results of the echocardiographic studies were recorded on a CD for subsequent assessment by two experienced echocardiographers who determined by consensus whether the patient had ischemia or myocardial infarction.

2.5. Statistics. To determine the differences between groups, we used Student's t-test for independent samples. The Pearson correlation coefficient (r) was used to assess the association between relative telomere length and other variables. All data are presented as mean ± SE, with $p < 0.05$ as a cut-off for statistical significance.

3. Results

3.1. General Characteristics. We included 70 patients of both genders with nephropathy on renal replacement therapy, 35 of which had ferritin levels below 500 ng/mL, aged 46.48 ± 16.9 years (Group A), and the other 35 had ferritin levels higher than 500 ng/mL, aged 45.34 ± 16.57 years (Group B). Patients were receiving i.v. iron dextran at an average of ≥400 mg/month. Patient characteristics of the different groups are shown in Table 1.

3.2. Free Iron and Oxidative Stress: Lipid Peroxidation and Oxidized Protein. Serum levels of ferritin and oxidation markers were determined. The levels of ferritin were 308 ± 145 ng/dL (Group A) versus 3224±2078 ng/dL (Group B), $p < 0.001$. Patients with ferritin levels higher than 500 ng/mL had significant differences with higher levels of TBARS (11.7 ± 4.6 versus 9.4 ± 2.2 nmoles/mL, $p = 0.008$), carbonyls (27.2 ± 5.2 versus 22.5 ± 5.4 ng/μL, $p = 0.0004$), and urea (131.10 ± 50.77 versus 104.23 ± 46.36 mg/dL, $p = 0.02$) compared with patients with ferritin levels below 500 ng/mL (Group A) (Table 2).

Interestingly serum TBARS and carbonyls were positively associated with ferritin levels in all subjects ($r = 0.26$, $p = 0.02$, $r = 0.35$, $p = 0.01$, resp.); the relationship is shown in Figure 1. A length of time under hemodialysis demonstrated significant relationship with higher ferritin levels ($r = -0.27$, $p = 0.02$) as well (Figure 2).

3.3. Relative Telomere Length. A sample of venous blood was taken in order to extract DNA from leukocytes and to measure relative telomere length by PCR in real time. The length of telomeres was markedly shorter in the group with higher ferritin levels. Telomeres were significantly shorter in Group B than in Group A. The relative telomere length (T/S) in patients with higher ferritin levels was 0.66 (SD, 0.051), versus 0.75 (SD, 0.155) in controls ($p = 0.0017$) (Figure 3). We observed a statistically significant association between relative telomere length and ferritin levels ($r = -0.37$, $p = 0.001$) (Figure 4). We did not observe an inverse significant correlation between relative telomere length and age ($r = 0.01$, $p = 0.51$). Relative telomere length (T/S) was inversely related to the time under hemodialysis ($r = -0.27$, $p = 0.02$) (Figure 5).

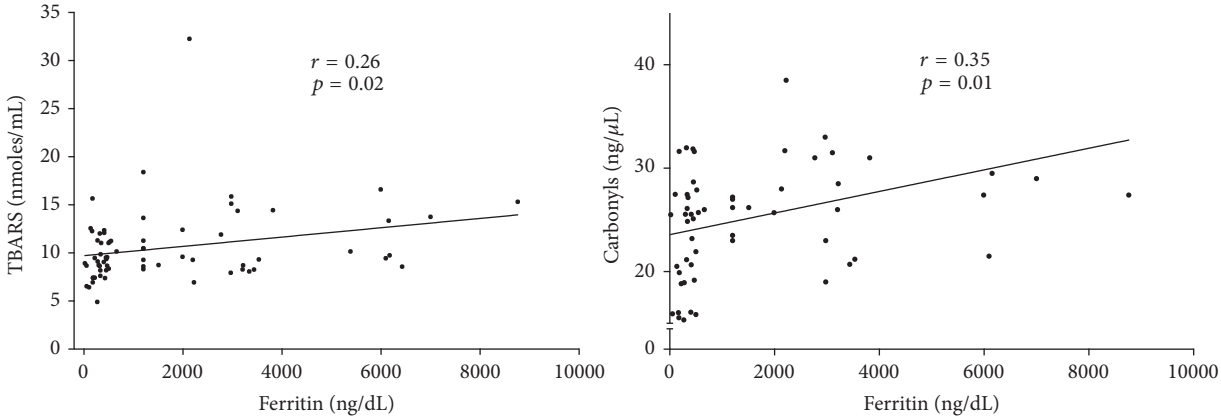

Figure 1: Serum TBARS and carbonyls were positively associated with ferritin levels in patients with nephropathy undergoing renal replacement therapy in hemodialysis ($n = 70$).

Table 1: Demographic and clinical characteristics in patients with high ferritin levels (Group A) and low ferritin levels (Group B).

	Group A ($n = 35$) n (%)	Group B ($n = 35$) n (%)	p
Female (%)	51.42 (18)	51.42 (18)	Ns
Male (%)	48.57 (17)	48.57 (17)	Ns
Age in years	45.4 ± 16.6	46.5 ± 16.9	0.77
Duration on HD (months)	40.87 ± 41.65	20.17 ± 29.00	0.01*
Diabetes (%)	68.57 (24)	51.42 (18)	0.22
Hypertension (%)	11.43 (4)	17.14 (6)	0.73
Other (%)	20 (7)	31.42 (11)	0.41

Data shown as mean ± SD. Student's t-test was used to determine the differences.

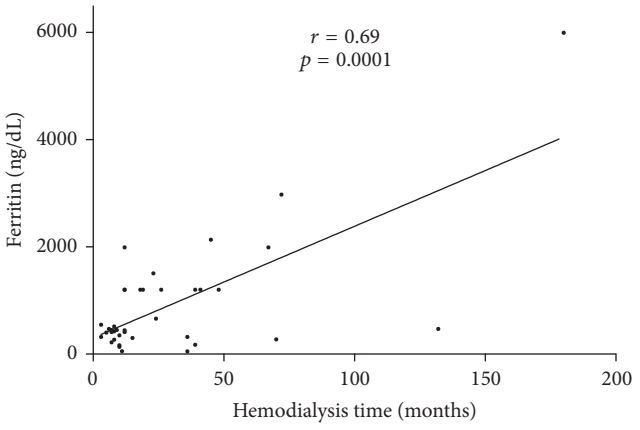

Figure 2: The relationship between ferritin (ng/dL) and length of time on hemodialysis in all subjects ($n = 70$).

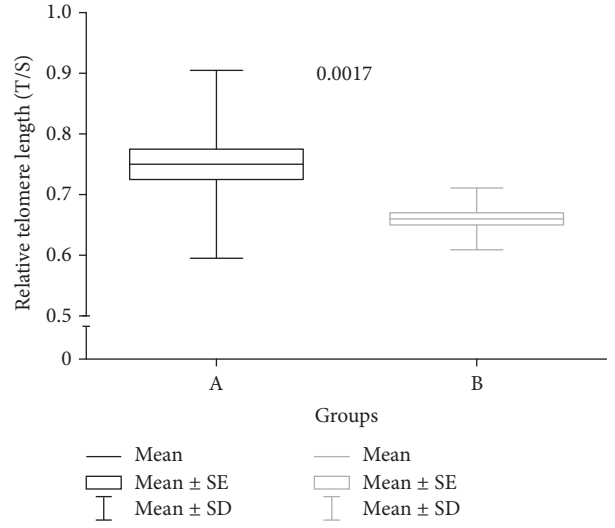

Figure 3: Comparison of relative telomere lengths (T/S) between groups.

3.4. Iron and Cardiovascular Disease. We found through the analysis of echocardiographic parameters that hypertrophy of the left ventricle, related to the Left Ventricular Mass Index (LVMI), was higher in the high ferritin level group (29 patients, 82.86%, versus 8 patients, 22.86%, $p = 0.01$). The results of echocardiographic examination are summarized in Table 3.

In this study, the shortening of telomeres was associated with a significant increase in left ventricular mass ($r = 0.40$, $p = 0.01$). The linear regression analysis between serum levels of ferritin with left ventricular mass observed was $p = 0.002$.

Table 2: Comparison of biochemical indices of iron status and oxidative markers between groups.

	Group A ($n = 35$) Mean ± SD	Group B ($n = 35$) Mean ± SD	p
Uric acid (mg/dL)	5.83 ± 1.04	5.45 ± 1.44	0.24
Creatinine (mg/dL)	7.81 ± 2.42	8.97 ± 2.65	0.06
Urea (mg/dL)	104.2 ± 46.3	131.10 ± 50.7	0.02*
Glucose (mg/dL)	100.9 ± 34.1	90.7 ± 30.3	0.18
Hemoglobin (g/dL)	11.23 ± 1.93	12.54 ± 1.85	0.01*
Ferritin (ng/mL)	308 ± 145	3224 ± 2078	<0.0001*
Iron (μg/dL)	78.5 ± 38.7	152.7 ± 86.1	<0.0001*
Iron saturation percentage (%)	48.3 ± 33.5	82.8 ± 39.2	0.0002*
TBARS (nmol/mL)	9.4 ± 2.2	11.7 ± 4.6	0.008*
Carbonyls (ng/μL)	22.5 ± 5.4	27.2 ± 5.2	0.0004*

*Data shown as mean ± SD. Student's t-test was used to determine the differences.

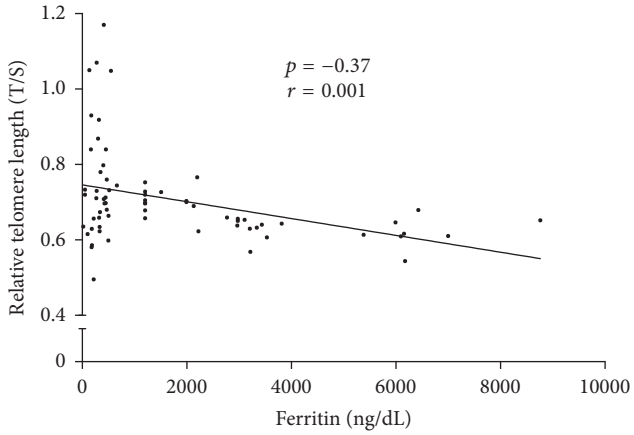

Figure 4: The relationship between relative telomere length (T/S) and ferritin.

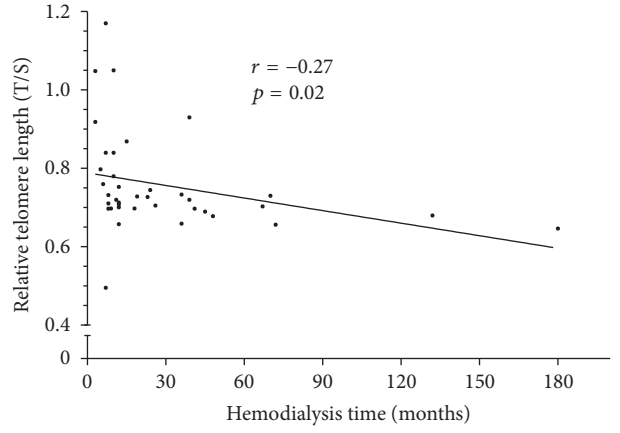

Figure 5: The relationship between relative telomere length (T/S) and time under hemodialysis.

Table 3: Echocardiographic examination results.

Parameter	($n = 70$)
LV mass (gr)	186.6 ± 67.4
LV systolic pressure (mm)	32.2 ± 5.6
LV diastolic pressure (mm)	50.7 ± 7.0
Ejection fraction (%)	65.2 ± 6.1
Fractional shortening (%)	36.6 ± 5.9

4. Discussion

The results of this study suggest that higher ferritin levels are associated with increased telomere shortening in hemodialysis patients. On this matter oxidative stress and inflammation are well-established key factors in the pathogenesis of atherosclerosis and vascular disease among chronic kidney disease patients [29].

Moreover, oxidative stress has also been related to immune system dysregulation in patients with uremia, indicated by increased oxidative biomarkers and activation of circulating leukocytes [30]. Uremia has been determined as an important factor in premature aging in patients with end stage renal disease [31]. Importantly, in our study serum urea levels were significantly higher in the group with higher ferritin levels (Group B); this metabolic condition induces various abnormalities in the patient, increasing the risk of developing uremic encephalopathy and other complications associated with poor prognosis.

Iron overload is a common complication in patients submitted to hemodialysis; the process of lipid peroxidation is catalyzed by iron and results in the formation of peroxyl radicals. We found a strong correlation between iron overload and increased oxidative biomarkers. The group with higher ferritin levels showed more telomere shortening; relative telomere length (T/S) in patients with higher ferritin levels was 0.66 (SD, 0.051), versus 0.75 (SD, 0.155) in controls ($p = 0.0017$); the telomere shortening rate was increased by oxidative stress. There is no immediate explanation of this phenomenon, but the relative increase in oxidative markers observed in patients with iron overload could be a contributing factor. The most significant finding of our study was the observation that hemodialysis patients with higher ferritin levels (Group B) showed increased telomere shortening.

Oxidative stress, in association with chronic inflammation, has been suggested as a possible contributory factor for this increase in mortality as well [32]. The increased oxidative stress caused by iron overload may induce this telomere shortening, which may contribute to renal diseases such as glomerulosclerosis, and prevent renal regeneration [33, 34].

Patients with chronic kidney disease have significantly increased morbidity and mortality from cardiovascular disease. Previous studies demonstrated a potential role of anemia in the pathogenesis of left ventricular hypertrophy [35]. Moreover several previous studies have documented that key cardiovascular diseases that increase with age (coronary atherosclerosis, arterial stiffening, increased carotid intima/media thickness, and clinically overt cardiovascular disease events such as myocardial infarction and stroke) are all associated with shortened telomere length. Likewise, vascular risk factors such as smoking, body mass index, and hypertension are inversely associated with telomere length [36].

Iron-overload cardiomyopathy is a prevalent cause of heart failure on a worldwide basis and is a major cause of mortality and morbidity in patients with secondary iron overload. In this study the analysis of echocardiographic parameters showed that higher ferritin levels in hemodialysis patients are associated with a significant increase in left ventricular mass which has been associated with higher cardiovascular risk in other studies. Murine iron-overload models showed cardiac iron overload, increased oxidative stress, altered Ca^2 homeostasis, and myocardial fibrosis resulting in heart disease [37].

Premature cardiovascular disease is a significant cause of morbidity and mortality [38], while end stage renal disease, and particularly its treatment with hemodialysis, is a condition of increased oxidative stress [39, 40].

Iron-induced oxidative stress plays a fundamental role in the pathogenesis of iron-overload mediated heart disease. The basic molecular mechanism of iron-overload cardiomyopathy has not been elucidated and strategies to treat this global epidemic are limited. Iron overload in humans leads to an advanced cardiomyopathy [41–44] and the development and validation of preclinical models of iron-overload cardiomyopathy are important for the discovery of new therapies [45, 46].

Monitoring the serum levels of ferritin has several benefits for patients with renal disease that are at increased risk of cardiovascular events, such as limiting the damage caused by oxidative stress [47, 48] and thus allowing the initiation of appropriate preventive therapeutic measures such [49] as the use of iron chelators. Telomere attrition, expressed in white blood cells (WBCs), can serve as a biomarker of the cumulative oxidative stress.

5. Conclusions

Our findings demonstrate that iron overload was associated with increased levels of oxidative stress and shorter relative telomere length. Identifying factors that accelerate the aging process in end stage renal disease can provide important therapeutic targets to revert this process. High levels of ferritin are related to signs of increased oxidative stress as reflected by increased TBARS and carbonyl levels in hemodialysis patients. Iron overload was found to be a major contributing factor to left ventricular hypertrophy. In addition iron overload is a potential therapeutic target to prevent premature aging and iron chelation agents may limit the increased oxidative stress in these patients.

Competing Interests

The authors declare that they have no competing interests.

Acknowledgments

Dr. Luis Benitez was an active part on the production of the present work, unfortunately he passed away in the final process of the manuscript.

References

[1] G. Weiss and L. T. Goodnough, "Anemia of chronic disease," *The New England Journal of Medicine*, vol. 352, no. 10, pp. 1011–1023, 2005.

[2] S. M. Lynch and B. Frei, "Mechanisms of metal ion-dependent oxidation of human low density lipoprotein," *Journal of Nutrition*, vol. 126, no. 4, 1996.

[3] E. Wieland, S. Parthasarathy, and D. Steinberg, "Peroxidase-dependent metal-independent oxidation of low density lipoprotein in vitro: a model for in vivo oxidation?" *Proceedings of the National Academy of Sciences of the United States of America*, vol. 90, no. 13, pp. 5929–5933, 1993.

[4] S. M. King, C. M. Donangelo, M. D. Knutson et al., "Daily supplementation with iron increases lipid peroxidation in young women with low iron stores," *Experimental Biology and Medicine*, vol. 233, no. 6, pp. 701–707, 2008.

[5] X. Chai, D. Li, X. Cao et al., "ROS-mediated iron overload injures the hematopoiesis of bone marrow by damaging hematopoietic stem/progenitor cells in mice," *Scientific Reports*, vol. 5, Article ID 10181, 2015.

[6] G. Y. Oudit, M. G. Trivieri, N. Khaper et al., "Taurine supplementation reduces oxidative stress and improves cardiovascular function in an iron-overload murine model," *Circulation*, vol. 109, no. 15, pp. 1877–1885, 2004.

[7] S. K. Das, W. Wang, P. Zhabyeyev et al., "Iron-overload injury and cardiomyopathy in acquired and genetic models is attenuated by resveratrol therapy," *Scientific Reports*, vol. 5, article 18132, 2015.

[8] F. A. Badria, A. S. Ibrahim, A. F. Badria, and A. A. Elmarakby, "Curcumin attenuates iron accumulation and oxidative stress in the liver and spleen of chronic iron-overloaded rats," *PLoS ONE*, vol. 10, no. 7, Article ID e0134156, 2015.

[9] J. Sripetchwandee, N. Pipatpiboon, N. Chattipakorn, and S. Chattipakorn, "Combined therapy of iron chelator and antioxidant completely restores brain dysfunction induced by iron toxicity," *PLoS ONE*, vol. 9, no. 1, Article ID e85115, 2014.

[10] E. Skrzydlewska, S. Sulkowski, M. Koda, B. Zalewski, L. Kanczuga-Koda, and M. Sulkowska, "Lipid peroxidation and antioxidant status in colorectal cancer," *World Journal of Gastroenterology*, vol. 11, no. 3, pp. 403–406, 2005.

[11] A. Benetos, K. Okuda, M. Lajemi et al., "Telomere length as an indicator of biological aging—the gender effect and relation with pulse pressure and pulse wave velocity," *Hypertension*, vol. 37, no. 2, pp. 381–385, 2001.

[12] M. C. Boxall, T. H. J. Goodship, A. L. Brown, M. C. Ward, and T. von Zglinicki, "Telomere shortening and haemodialysis," *Blood Purification*, vol. 24, no. 2, pp. 185–189, 2006.

[13] E. Jeanclos, N. J. Schork, K. O. Kyvik, M. Kimura, J. H. Skurnick, and A. Aviv, "Telomere length inversely correlates with pulse pressure and is highly familial," *Hypertension*, vol. 36, no. 2, pp. 195–200, 2000.

[14] B. Murillo-Ortiz, F. Albarrán-Tamayo, D. Arenas-Aranda et al., "Telomere length and type 2 diabetes in males, a premature aging syndrome," *Aging Male*, vol. 15, no. 1, pp. 54–58, 2012.

[15] L. P. Wills and R. G. Schnellmann, "Telomeres and telomerase in renal health," *Journal of the American Society of Nephrology*, vol. 22, no. 1, pp. 39–41, 2011.

[16] J. L. Sullivan, "Iron and the sex difference in heart disease risk," *The Lancet*, vol. 317, no. 8233, pp. 1293–1294, 1981.

[17] S. Kiechl, J. Willeit, G. Egger, W. Poewe, and F. Oberhollenzer, "Body iron stores and the risk of carotid atherosclerosis: prospective results from the bruneck study," *Circulation*, vol. 96, no. 10, pp. 3300–3307, 1997.

[18] K. Klipstein-Grobusch, J. F. Koster, D. E. Grobbee et al., "Serum ferritin and risk of myocardial infarction in the elderly: the Rotterdam Study," *American Journal of Clinical Nutrition*, vol. 69, no. 6, pp. 1231–1236, 1999.

[19] E. Senol, A. Ersoy, S. Erdinc, E. Sarandol, and M. Yurtkuran, "Oxidative stress and ferritin levels in haemodialysis patients," *Nephrology Dialysis Transplantation*, vol. 23, no. 2, pp. 665–672, 2008.

[20] M. Laddha, V. Sachdeva, P. M. Diggikar, P. K. Satpathy, and A. L. Kakrani, "Echocardiographic assessment of cardiac dysfunction in patients of end stage renal disease on haemodialysis," *Journal of Association of Physicians of India*, vol. 62, pp. 28–33, 2014.

[21] L. S. M. Wong, P. van der Harst, R. A. de Boer et al., "Renal dysfunction is associated with shorter telomere length in heart failure," *Clinical Research in Cardiology*, vol. 98, no. 10, pp. 629–634, 2009.

[22] J. Kletzmayr and W. H. Hörl, "Iron overload and cardiovascular complications in dialysis patients," *Nephrology Dialysis Transplantation*, vol. 17, supplement 2, pp. 25–29, 2002.

[23] I. S. Vari, B. Balkau, A. Kettaneh et al., "Ferritin and transferrin are associated with metabolic syndrome abnormalities and their change over time in a general population: data from an Epidemiological Study on the Insulin Resistance syndrome (DESIR)," *Diabetes Care*, vol. 30, no. 7, pp. 1795–1801, 2007.

[24] K. A. Schwartz, Z. Li, D. E. Schwartz, T. G. Cooper, and W. Emmett Braselton, "Earliest cardiac toxicity induced by iron overload selectively inhibits electrical conduction," *Journal of Applied Physiology*, vol. 93, no. 2, pp. 746–751, 2002.

[25] A. G. Mainous III and V. A. Díaz, "Relation of serum ferritin level to cardiovascular fitness among young men," *The American Journal of Cardiology*, vol. 103, no. 1, pp. 115–118, 2009.

[26] B. de Valk and J. J. M. Marx, "Iron, atherosclerosis, and ischemic heart disease," *Archives of Internal Medicine*, vol. 159, no. 14, pp. 1542–1548, 1999.

[27] R. M. Cawthon, "Telomere measurement by quantitative PCR," *Nucleic Acids Research*, vol. 30, no. 10, article e47, 2002.

[28] E. Franco-Robles, A. Campos-Cervantes, B. O. Murillo-Ortiz et al., "Effects of curcumin on brain-derived neurotrophic factor levels and oxidative damage in obesity and diabetes," *Applied Physiology, Nutrition and Metabolism*, vol. 39, no. 2, pp. 211–218, 2014.

[29] B. Descamps-Latscha, P. Jungers, and V. Witko-Sarsat, "Immune system dysregulation in uremia: role of oxidative stress," *Blood Purification*, vol. 20, no. 5, pp. 481–484, 2002.

[30] S. Sela, R. Shurtz-Swirski, M. Cohen-Mazor et al., "Primed peripheral polymorphonuclear leukocyte: a culprit underlying chronic low-grade inflammation and systemic oxidative stress in chronic kidney disease," *Journal of the American Society of Nephrology*, vol. 16, no. 8, pp. 2431–2438, 2005.

[31] P. M. Honoré, R. Jacobs, W. Boer, and O. Joannes-Boyau, "Sepsis and AKI: more complex than just a simple question of chicken and egg," *Intensive Care Medicine*, vol. 37, no. 2, pp. 186–189, 2011.

[32] T. Von Zglinicki, "Oxidative stress shortens telomeres," *Trends in Biochemical Sciences*, vol. 27, no. 7, pp. 339–344, 2002.

[33] J. Galle, "Oxidative stress in chronic renal failure," *Nephrology Dialysis Transplantation*, vol. 16, no. 11, pp. 2135–2137, 2001.

[34] N. J. Samani, R. Boultby, R. Butler, J. R. Thompson, and A. H. Goodall, "Telomere shortening in atherosclerosis," *The Lancet*, vol. 358, no. 9280, pp. 472–473, 2001.

[35] A. Levin, C. R. Thompson, J. Ethier et al., "Left ventricular mass index increase in early renal disease: impact of decline in hemoglobin," *American Journal of Kidney Diseases*, vol. 34, no. 1, pp. 125–134, 1999.

[36] R. S. Vasan, S. Demissie, M. Kimura et al., "Association of leukocyte telomere length with echocardiographic left ventricular mass: the Framingham heart study," *Circulation*, vol. 120, no. 13, pp. 1195–1202, 2009.

[37] M. M. Sung, S. K. Das, J. Levasseur et al., "Resveratrol treatment of mice with pressure-overload-induced heart failure improves diastolic function and cardiac energy metabolism," *Circulation: Heart Failure*, vol. 8, no. 1, pp. 128–137, 2015.

[38] B. Franczyk-Skóra, A. Gluba, R. Olszewski, M. Banach, and J. Rysz, "Heart function disturbances in chronic kidney disease—echocardiographic indices," *Archives of Medical Science*, vol. 10, no. 6, pp. 1109–1116, 2014.

[39] G. A. Stewart, P. B. Mark, N. Johnston et al., "Determinants of hypertension and left ventricular function in end stage renal failure: a pilot study using cardiovascular magnetic resonance imaging," *Clinical Physiology and Functional Imaging*, vol. 24, no. 6, pp. 387–393, 2004.

[40] R. B. Devereux, D. R. Alonso, E. M. Lutas et al., "Echocardiographic assessment of left ventricular hypertrophy: comparison to necropsy findings," *The American Journal of Cardiology*, vol. 57, no. 6, pp. 450–458, 1986.

[41] C. J. Murphy and G. Y. Oudit, "Iron-overload cardiomyopathy: pathophysiology, diagnosis, and treatment," *Journal of Cardiac Failure*, vol. 16, no. 11, pp. 888–900, 2010.

[42] D. J. Pennell, J. E. Udelson, A. E. Arai et al., "Cardiovascular function and treatment in beta-thalassemia major: a consensus statement from the American Heart Association," *Circulation*, vol. 128, no. 3, pp. 281–308, 2013.

[43] N. F. Olivieri, D. G. Nathan, J. H. Macmillan et al., "Survival in medically treated patients with homozygous β-thalassemia," *The New England Journal of Medicine*, vol. 331, no. 9, pp. 574–578, 1994.

[44] G. M. Brittenham, P. M. Griffith, A. W. Nienhuis et al., "Efficacy of deferoxamine in preventing complications of iron overload in patients with thalassemia major," *The New England Journal of Medicine*, vol. 331, no. 9, pp. 567–573, 1994.

[45] F. W. Huang, J. L. Pinkus, G. S. Pinkus, M. D. Fleming, and N. C. Andrews, "A mouse model of juvenile hemochromatosis," *The Journal of Clinical Investigation*, vol. 115, no. 8, pp. 2187–2191, 2005.

[46] J. C. Wood, M. Otto-Duessel, M. Aguilar et al., "Cardiac iron determines cardiac T2*, T2, and T1 in the gerbil model of iron cardiomyopathy," *Circulation*, vol. 112, no. 4, pp. 535–543, 2005.

[47] H. Ghoti, E. A. Rachmilewitz, R. Simon-Lopez et al., "Evidence for tissue iron overload in long-term hemodialysis patients and the impact of withdrawing parenteral iron," *European Journal of Haematology*, vol. 89, no. 1, pp. 87–93, 2012.

[48] A. E. Gaweda, Y. Z. Ginzburg, Y. Chait, M. J. Germain, G. R. Aronoff, and E. Rachmilewitz, "Iron dosing in kidney disease: inconsistency of evidence and clinical practice," *Nephrology Dialysis Transplantation*, vol. 30, no. 2, pp. 187–196, 2015.

[49] I. C. Macdougall, A. J. Bircher, K. Eckardt et al., "Iron management in chronic kidney disease: conclusions from a 'kidney disease: improving global outcomes' (KDIGO) Controversies Conference," *Kidney International*, vol. 89, no. 1, pp. 28–39, 2016.

Hindawi Publishing Corporation
Oxidative Medicine and Cellular Longevity
Volume 2016, Article ID 1458793, 11 pages
http://dx.doi.org/10.1155/2016/1458793

Research Article

Upregulation of Heme Oxygenase-1 in Response to Wild Thyme Treatment Protects against Hypertension and Oxidative Stress

Nevena Mihailovic-Stanojevic,[1] Zoran Miloradović,[1] Milan Ivanov,[1] Branko Bugarski,[2] Đurđica Jovović,[1] Danijela Karanović,[1] Una-Jovana Vajić,[1] Draženka Komes,[3] and Jelica Grujić-Milanović[1]

[1]*Institute for Medical Research, University of Belgrade, Dr. Subotica 4, P.O. Box 102, 11129 Belgrade, Serbia*
[2]*Faculty of Technology and Metallurgy, Department of Chemical Engineering, University of Belgrade, Karnegijeva 4, Belgrade, Serbia*
[3]*Faculty of Food Technology and Biotechnology, University of Zagreb, Pierottijeva 6, 10 000 Zagreb, Croatia*

Correspondence should be addressed to Nevena Mihailovic-Stanojevic; nevena@imi.bg.ac.rs

Received 9 May 2016; Revised 20 July 2016; Accepted 23 August 2016

Academic Editor: Claudio Cabello-Verrugio

High blood pressure is the most powerful contributor to the cardiovascular morbidity and mortality, and inverse correlation between consumption of polyphenol-rich foods or beverages and incidence of cardiovascular diseases gains more importance. Reactive oxygen species plays an important role in the development of hypertension. We found that wild thyme (a spice plant, rich in polyphenolic compounds) induced a significant decrease of blood pressure and vascular resistance in hypertensive rats. The inverse correlation between vascular resistance and plasma heme oxygenase-1 suggests that endogenous vasodilator carbon monoxide generated by heme oxidation could account for this normalization of blood pressure. Next product of heme oxidation, bilirubin (a chain-breaking antioxidant that acts as a lipid peroxyl radical scavenger), becomes significantly increased after wild thyme treatment and induces the reduction of plasma lipid peroxidation in hypertensive, but not in normotensive rats. The obtained results promote wild thyme as useful supplement for cardiovascular interventions.

1. Introduction

High blood pressure is certainly the most prevalent and powerful contributor to the cardiovascular morbidity and mortality in the majority of industrialized countries, with essential hypertension accounting for about 95% of all cases of hypertension [1]. Hypertension is recognized as a highly significant risk factor, and many effective antihypertensive drugs are developed, including angiotensin converting enzyme inhibitors, angiotensin-II receptor antagonists, diuretics, beta blockers, calcium channels blockers, and nitric oxide (NO) donors [2, 3].

Yet, for various reasons, hypertension is still a poorly controlled disorder, even in countries with very efficient preventive medical services. At the same time, about 75 to 80% of the world population (particularly in developing countries) uses alternative treatment options, often herbal medicines for the treatment of various health problems [4]. It should also be noted that there is a growing body of evidence suggesting the effectiveness of alternative therapeutic approaches in the treatment of various disorders, including hypertension. Thus, epidemiological evidence suggests the existence of a negative correlation between consumption of polyphenol-rich foods (fruits, vegetables, cocoa, etc.) or beverages (wine, especially red wine, grape juice, tea, etc.) and the incidence of cardiovascular disease [5, 6]. *Thymus serpyllum* L. (wild thyme, TE) has traditionally been used as a spice plant, whose aqueous extract is rich in the polyphenolic compounds [7] that are considered to be responsible for their antioxidant effects. Also, the antihypertensive effect of

essential oils from Chinese medicinal plants was confirmed in experimental studies [8]. Similarly, water extracts of plants from Lamiaceae family, rich in phenolic acids, decreased systolic blood pressure after subcutaneous administration in conscious stroke-prone spontaneously hypertensive rats [9] and inhibit rabbit lung angiotensin I-converting enzyme *in vitro* [10]. In addition, our previous study showed that aqueous extract obtained from TE induces powerful NO-independent systemic vasodilatation in spontaneously hypertensive rats (SHR) [7].

On the other hand, it is well known that reactive oxygen species (ROS), amongst other factors, play an important role in the development of hypertension in many experimental models, as well as in patients with essential, renovascular, and malignant hypertension [11]. Several experiments in which the expression of heme oxygenase-1 (HO-1), inducible form of the rate-limiting enzyme in the degradation of heme [12], was upregulated by different modulators or by gene transfer suggested that HO-1 participates in defence mechanisms against agents that induce oxidative injury [13]. Heme oxygenase cleaves the heme ring to form the water-soluble 1-carbon fragment as carbon monoxide (CO), iron, and a biliverdin [14], which is reduced by biliverdin reductase to bilirubin (lipophilic linear tetrapyrrole), a compound with potent antioxidant capacity, abundant in blood plasma [15]. Further studies confirmed the circulating forms of bilirubin, such as free bilirubin, albumin-bound bilirubin, conjugated bilirubin, and unconjugated bilirubin as effective scavengers of peroxyl radicals able to protect human low-density lipoprotein against peroxidation [13]. The CO, generated in equimolar concentrations to biliverdin during heme oxidation by HO, like NO, inhibits platelet aggregation and acts as a vasodilator when bioavailability of NO is limited [16]. This relaxation of vascular smooth muscle cells results from activation of pathways, including the stimulation of soluble guanylyl cyclase, opening of calcium activated K^+ channel, inhibition of cytochrome P450-dependent monooxygenase, or blocking the production of constrictor substances like endothelin [17]. Furthermore, the increased ROS production that was observed in hypertensive animals and humans could be reduced by treatment with superoxide dismutase (SOD) mimetics or antioxidants, resulting in the improvement of vascular and renal function, regression of vascular remodelling, and reduction of blood pressure [11]. Considering all the above, we hypothesized that TE regulates blood pressure and oxidative stress of SHR through a mechanism that could involve HO-1.

Therefore, the aim of the present study was to evaluate the ability of TE treatment to upregulate the expression and activity of inducible form of HO-1 and its correlation with antihypertensive as well as antioxidant responses of SHR.

2. Material and Methods

2.1. Thyme Extract Preparation. Dry thyme extract (TE) from *Thymus serpyllum* L. was prepared as described previously [7]. Briefly, TE was extracted by pouring 200 mL of boiled distilled water over the herbal samples (10 g) at room temperature, filtered through a tea strainer, and freeze-dried. The yield of freeze-dried TE amounted to 1.67% (w/w). The total polyphenols content of the corresponding freeze-dried TE exhibited 20.08 mg GAE/100 mg of TE, while the HPLC analysis of the polyphenolic profile of the obtained extract showed rosmarinic (4.30 mg/100 mg of freeze-dried TE) and caffeic acids (0.08 mg/100 mg of freeze-dried TE) as predominant TE phenols. The antioxidant capacity of TE evaluated by the FRAP and ABTS assays amounted to 1.66 mmol Fe(II)/100 mg and 86.1 μmol Trolox/100 mg of freeze-dried TE, respectively. As the dose-dependent antihypertensive evaluations revealed only the dose of 100 mg/kg freeze-dried TE effective in reducing systolic blood pressure [7], the present study was carried out with this TE dose.

2.2. Animals. We used six-month-old male spontaneously hypertensive rats (SHR, descendants of breeders originally obtained through Taconic Farms, Germantown, NY, USA) and normotensive *Wistar* (W) rats, bred at the Institute for Medical Research, University of Belgrade, Serbia, weighing about 300 g. They were maintained in temperature and humidity controlled rooms on a twelve-hour light-dark cycle.

The experimental protocol was approved by the Ethic Committee of the Institute for Medical Research, University of Belgrade, Serbia (number 0312-1/10), according to the National Law on Animal Welfare.

Rats were divided in 4 groups: two control groups, normotensive W rats (W-C) and SHR-C, received vehicle (0.2 mL saline), and two treated groups, W-TE and SHR-TE, received i.v. bolus of TE (100 mg/kg b.w. dissolved in 0.2 mL saline).

2.3. Systemic Haemodynamic Measurements. For the direct haemodynamic measurements, after bolus injection of TE or vehicle, all rats were anesthetized with 35 mg/kg b.w. sodium pentobarbital, intraperitoneally. Mean arterial pressure (MAP) and heart rate (HR) were measured through a femoral artery catheter (PE–50, Clay-Adams Parsippany, NY, USA), connected to a physiological data acquisition system (Cardiomax III-TCR, Columbus Instruments, Columbus, OH, USA). A jugular vein was cannulated with polyethylene tubing PE-50 for the injection of solutions. The left carotid artery was catheterized with a thermo sensor, which was coupled to Cardiomax III for the determination of cardiac output. The second end of thermocouple sensor was placed in cold saline. Following 20 min for stabilization after surgery, rats were given a bolus injection of TE or vehicle, and haemodynamic parameters were recorded 30 minutes after injection. Cardiac output was normalized to body weight and expressed as cardiac index (CI, mL/min/kg). Total peripheral vascular resistance (TPVR, mmHg × min × kg/mL) was calculated from MAP and CI (assuming that the mean right atrial pressure is zero).

2.4. Regional Haemodynamic Measurements. For regional blood flow measurements left carotid artery was gently separated from the surrounding tissue. An ultrasonic flow probe, 1RB (internal diameter = 1 mm) was placed around the artery and total carotid blood flow (CBF) was recorded using

a Transonic T106 Small Animal Flowmeter (Transonic T106 Small Animal Flowmeter, Transonic System Inc., Ithaca, New York). After abdominal incision renal artery preparation was utilized and renal blood flow (RBF) was recorded. Vascular resistance in these two vascular beds (CVR and RVR) was calculated by dividing MAP with total blood flow through respective blood vessel, normalized for the body weight, and expressed as mmHg min kg/mL.

2.5. Plasma Sample and Tissue Isolation. Blood samples obtained by puncture of the abdominal aorta were collected under anaesthesia, 30 minutes after TE or vehicle application, into tubes containing lithium-heparin (Li-heparin, Sigma, USA) as an anticoagulant. The plasma was separated by centrifugation at 4000 rpm for 20 min. After plasma removing, the remaining erythrocytes were rinsed three times, aliquoted, and stored at −80°C. Liver and kidney tissues were removed immediately on ice, rinsed with cold saline, weighed, and then cut into portions, frozen in liquid nitrogen, and stored at −80°C for the later estimation of protein content and enzymatic antioxidant defence.

2.6. Enzyme-Linked Immunosorbent Assay for Heme Oxygenase-1. Plasma and liver HO-1, an inducible heme degrading enzyme with antioxidant properties, was detected and quantified using commercially available, rat specific, enzyme-linked immunosorbent assay kit (HO-1, rat, EIA. ADI-EKS-810A, Enzo Life Sciences International, Inc.). Plasma, previously stored at −20°C, was defrosted and in accordance with the manufacturer's recommendations prepared for analysis. On the day of analysis, tissue was homogenized and prepared for the assay procedure according to the manufacturer's instructions. All samples, including standard, were assayed in duplicate. The intensity of the colour was measured in a microplate reader at 450 nm. HO-1 concentrations from the sample were quantitated by interpolating absorbance readings from a standard curve generated with the calibrated HO-1 protein standard. Values were expressed as ng/mL for plasma HO-1 and as μg/g of liver tissue.

2.7. Heme Oxygenase Enzyme Activity. Plasma bilirubin serves as a marker for heme oxygenase activity. Direct bilirubin (BIL-D) and total bilirubin (BIL-T) levels were determined using commercial kits for automatic analyser COBAS INTEGRA 400 plus (Hoffmann-La Roche, Germany).

2.8. Superoxide Dismutase, Catalase, and Glutathione Peroxidase Enzyme Activities. Antioxidant enzyme activities of the erythrocytes (e) as well as liver (L) and kidney (k) homogenates were measured by following the spectrophotometric methods: catalase (CAT) was determined as previously described [18], glutathione peroxidase (GPx) was measured according to Paglia and Valentine [19], and superoxide dismutase (SOD) was determined according to McCord and Fridovich [20].

2.9. Lipid Peroxidation. For the assessment of lipid peroxidation in plasma (p), liver (L), and kidney (k) lipid peroxide levels were estimated by assaying thiobarbituric acid reactive substances (TBARS) at 540 nm using 2-thiobarbituric acid (4,6-dihydroxy-2-mercaptopyrimidine; TBA, Acros, Organic). An extinction coefficient of 156000 M^{-1} cm^{-1} was used for calculation [21]. The level of p-TBARS was expressed as nmol/mL, while L-TBARS and k-TBARS were expressed as μmol/g tissue.

2.10. Statistical Analysis. The data are given as mean ± SEM. Comparisons between the respective groups were made by using *Student's t-tests*. p values < 0.05 were considered significant. Correlations between obtained parameters in normotensive as well as in hypertensive rats were also examined, and p values < 0.05 were considered significant (Statistica 8.0 for Windows).

3. Results

3.1. Effects of TE on Haemodynamic Parameters. Haemodynamic parameters are shown in Figure 1. As expected, MAP, HR, and TPVR of SHR-C were significantly higher compared to the values of these parameters in W-C group ($p < 0.001$), but without changes of CI. Bolus injection of saline solution containing dry thyme extract resulted in a significant decrease of MAP ($p < 0.001$) only in the group of SHR-TE, while TPVR was reduced in both SHR-TE ($p < 0.01$) and W-TE ($p < 0.001$) rats compared to their respective controls (Figures 1(a) and 1(d)) without changes in CI (Figure 1(c)). Injection of TE did not affect HR of both rat strains (Figure 1(b)).

3.2. Effects of TE on Regional Haemodynamic Parameters. Regional haemodynamic parameters are presented in Figure 2. The resistance in both vascular beds, carotid and renal artery, were significantly elevated in SHR-C compared to W-C (Figures 2(b) and 2(d), $p < 0.001$ and $p < 0.05$), without changes of respective vascular blood flow (Figures 2(a) and 2(c)). Acute TE treatment led to a decrease of CBF in *Wistar* rats (Figure 2(a), $p < 0.05$), while in the SHR caused a significant reduction of CVR (Figure 2(b), $p < 0.05$). Despite marked reduction of MAP, RVR remained nonsignificantly changed due to acute TE treatment (Figure 2(d)) but still showed a tendency to get closer to W groups.

3.3. Effects of TE on Plasma and Liver HO-1 Enzyme Concentration. We found that plasma HO-1 concentration did not differ significantly between the examined groups, although the value in SHR-TE group was the highest (Figure 3(a)). The expression of liver HO-1 (Figure 3(b)) was lower in hypertensive than in normotensive rats (1.32 ± 0.10 versus 1.62 ± 0.10 mg/g tissue, $p = 0.0634$). TE treatment significantly increased the content of this enzyme in hypertensive rats (SHR-TE, 1.66 ± 0.09, versus SHR-C, 1.32 ± 0.10 mg/g tissue, $p < 0.05$). On the contrary, the application of TE into normotensive rats resulted in a prominent decrease of quantity of this enzyme (W-C: 1.62 ± 0.10 versus W-TE: 1.38 ± 0.04 mg/g tissue, $p = 0.0507$).

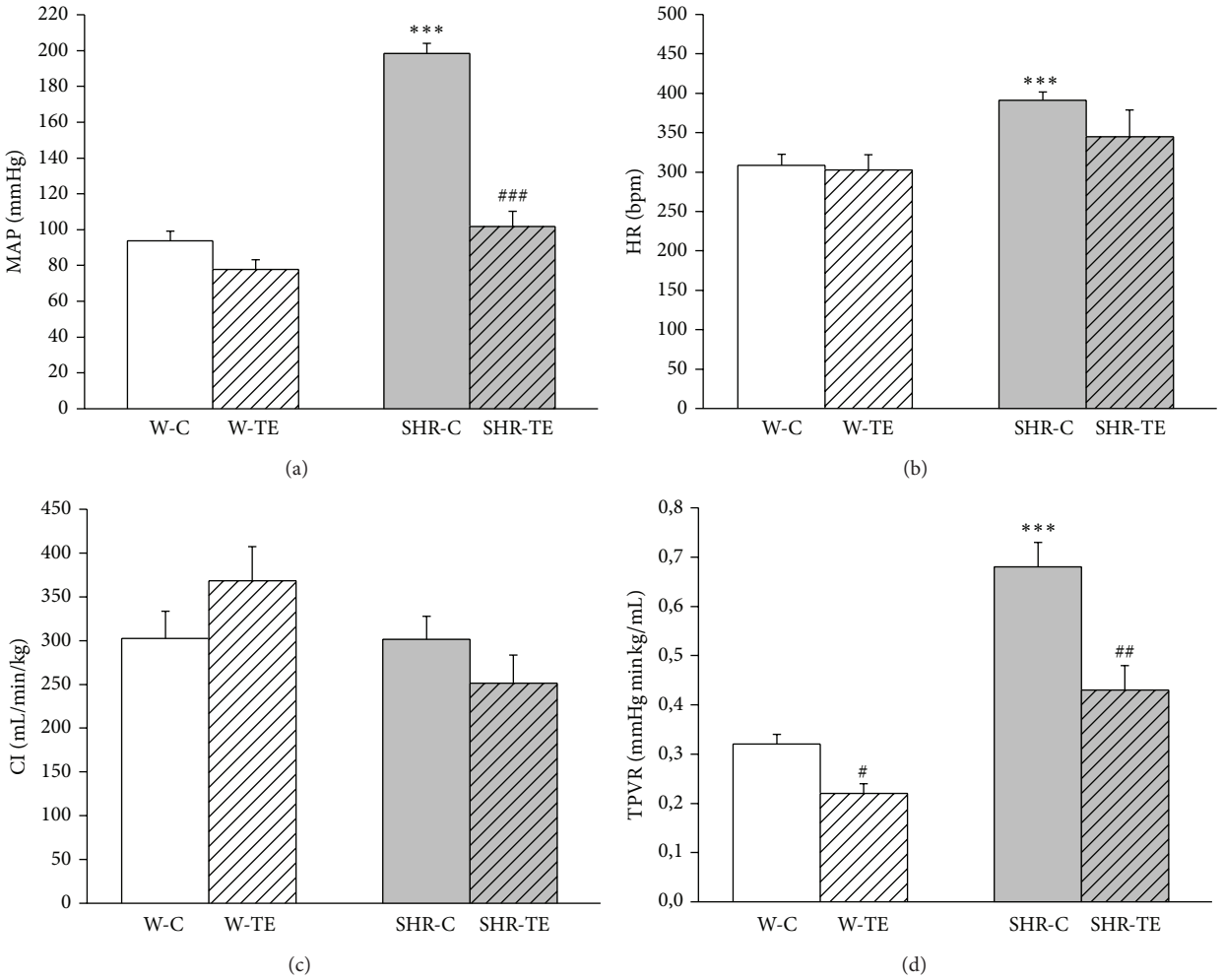

Figure 1: Haemodynamic parameters: (a) mean arterial pressure (MAP), (b) heart rate (HR), (c) cardiac index (CI), and (d) total peripheral vascular resistance (TPVR) in experimental groups. W-C, normotensive *Wistar* rats, and SHR-C, spontaneously hypertensive rats, received vehicle. W-TE and SHR-TE groups received thyme extract. $^{***}p < 0.001$, the significant difference between SHR-C and W-C; $^{###}p < 0.001$, $^{##}p < 0.01$, and $^{#}p < 0.05$, the significant difference between TE treated and appropriate control group.

3.4. Heme Oxygenase Enzyme Activity. Acute TE treatment significantly increased plasma BIL-D level in both rat strains (SHR-TE versus SHR-C: $p < 0.001$; W-TE versus W-C: $p < 0.05$, Figure 3(c)). Figure 3(d) shows that the plasma BIL-T content was not significantly different in W rats. However, the decreased BIL-T of hypertensive rats compared to age-matched normotensive rats was significantly reversed by TE treatment (SHR-TE versus SHR-C: $p < 0.05$).

3.5. Effects of TE on Plasma, Liver, and Kidney Lipid Peroxidation. SHR-C had higher p-TBARS then W-C rats ($p = 0.0772$, Figure 4(a)). Acute TE treatment significantly reduced the level of p-TBARS in SHR-TE group compared to SHR-C ($p < 0.01$, Figure 4(a)). On the contrary, in normotensive rats the value of p-TBARS became almost significantly elevated in response to TE treatment ($p = 0.0625$, Figure 4(a)). Liver homogenate TBARS levels did not differ amongst W-C, SHR-C, and W-TE groups. However, L-TBARS was markedly increased in SHR-TE than that in SHR-C group ($p < 0.01$ Figure 4(b)). The kidney TBARS level was significantly lower in SHR-C group compared to the W-C ($p < 0.001$ Figure 4(c)), and TE had no effects on it, in either hypertensive or normotensive rats.

3.6. Effects of TE on Antioxidant Enzymes Activities in Erythrocytes, Liver, and Kidney. SOD, CAT, and GPx enzyme activities in the erythrocytes, liver, and kidney from all experimental animals are shown in Figure 5. There were no differences in erythrocytes, liver, and kidney SOD activities between SHR-C and W-C rats (Figures 5(a), 5(d), and 5(g)). TE treatment significantly increased the kidney SOD activity in the SHR (SHR-TE versus SHR-C: $p < 0.001$), but not in the W rats (Figure 5(g)). Erythrocytes and liver CAT activity (Figures 5(b) and 5(e)) was unchanged in SHR-C as compared to W-C rats, but the treatment has led to the increases of erythrocytes CAT activity only in SHR-TE compared to SHR-C ($p < 0.05$). In contrast, CAT activity in kidney (Figure 5(h)) was found to be increased in both W-TE and SHR-C compared to W-C ($p < 0.05$, $p < 0.001$, resp.).

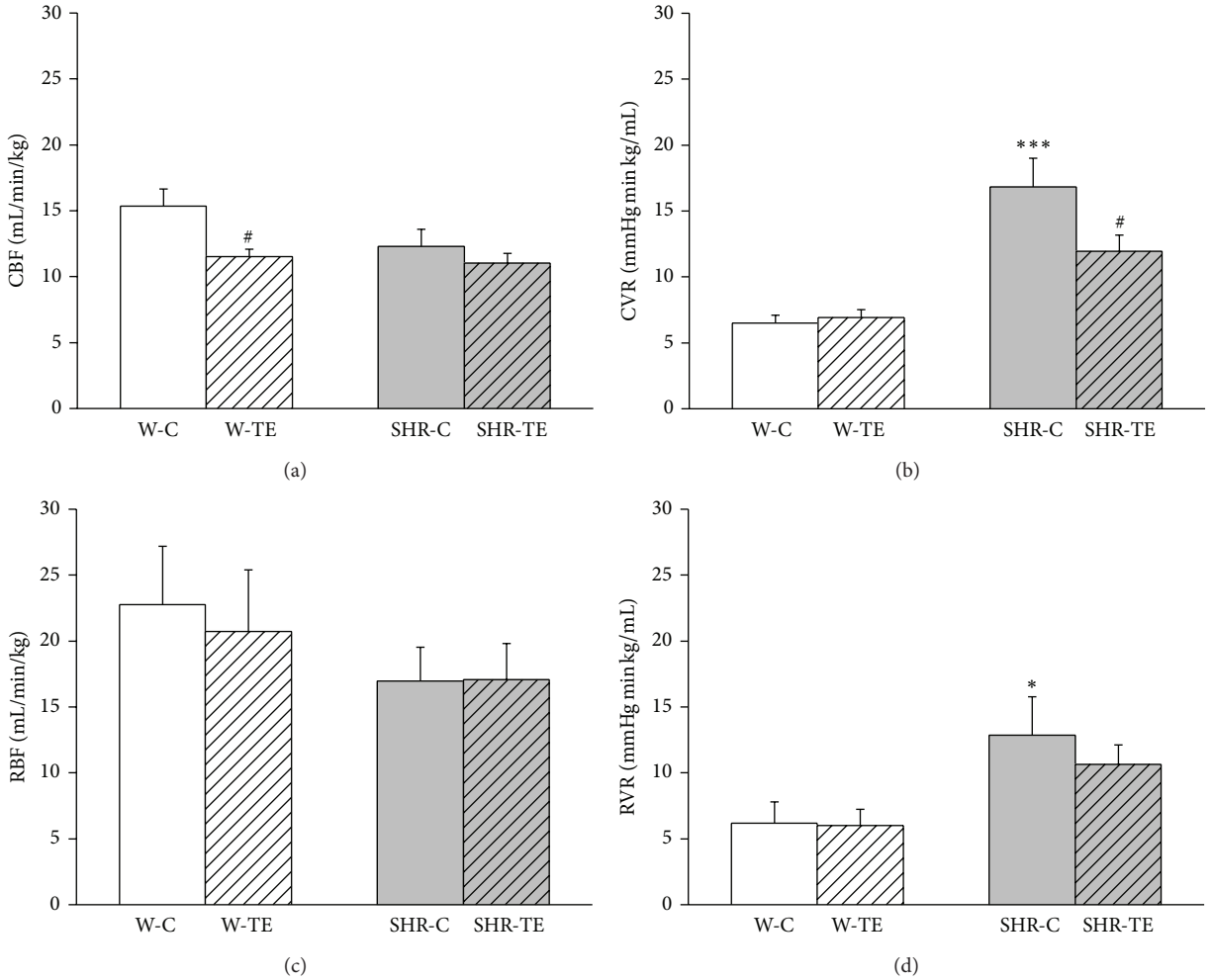

Figure 2: Regional haemodynamic parameters: (a) carotid blood flow (CBF), (b) carotid vascular resistance (CVR), (c) renal blood flow (RBF), and (d) renal vascular resistance (RVR) in experimental groups. W-C, normotensive Wistar rats, and SHR-C, spontaneously hypertensive rats, received vehicle. W-TE and SHR-TE groups received thyme extract. $^{*}p < 0.05$ and $^{***}p < 0.001$, the significant difference between SHR-C and W-C; $^{\#}p < 0.05$, the significant difference between TE treated and appropriate control group.

GPx activity from the erythrocytes of SHR-C was significantly lower compared to W-C ($p < 0.01$, Figure 5(c)). Bolus injection of TE induced a significant elevation of kidney GPx activities in normotensive rats ($p < 0.05$, Figure 5(i)). The opposite effect was found in kidney homogenates of SHR (Figure 5(e)). Namely, the activity of GPx was significantly reduced in SHR-TE compared to SHR-C ($p < 0.01$). In the liver homogenates the activity of this antioxidant enzyme was unchanged in both W-TE and SHR-TE groups compared to their controls (Figure 5(f)).

3.7. Correlation Analysis of Obtained Parameters. In SHR, vascular resistance of the systemic circulation was found to be positively correlated in relation to MAP ($r = 0.7546$, $p = 0.005$), whereas in normotensive rats the negative correlation of TPVR and CI ($r = -0.8027$, $p = 0.002$) was observed.

Correlation between haemodynamic parameters and oxidative status is shown in Table 1. MAP exhibits a significant positive correlation with p-TBARS. Also, MAP and TPVR showed strong negative correlation with regard to L-TBARS and HO-1 expression and activity in hypertensive but not in normotensive rats. In addition, in the group of hypertensive rats, we found a significant positive intercorrelation between L-TBARS, quantity of plasma and liver HO-1, and bilirubin concentrations, followed by strong and negative intercorrelation between these parameters with p-TBARS, while in the kidney we have not found a correlation between the examined parameters (Table 2). Table 3 represents the correlation of antioxidant enzyme activity and systemic haemodynamic parameters, with oxidative status in hypertensive and normotensive rats.

4. Discussion

Earlier, we suggested that a powerful vasodilator molecule, nitric oxide, is not liable for normalization of blood pressure in TE treated SHR [7].

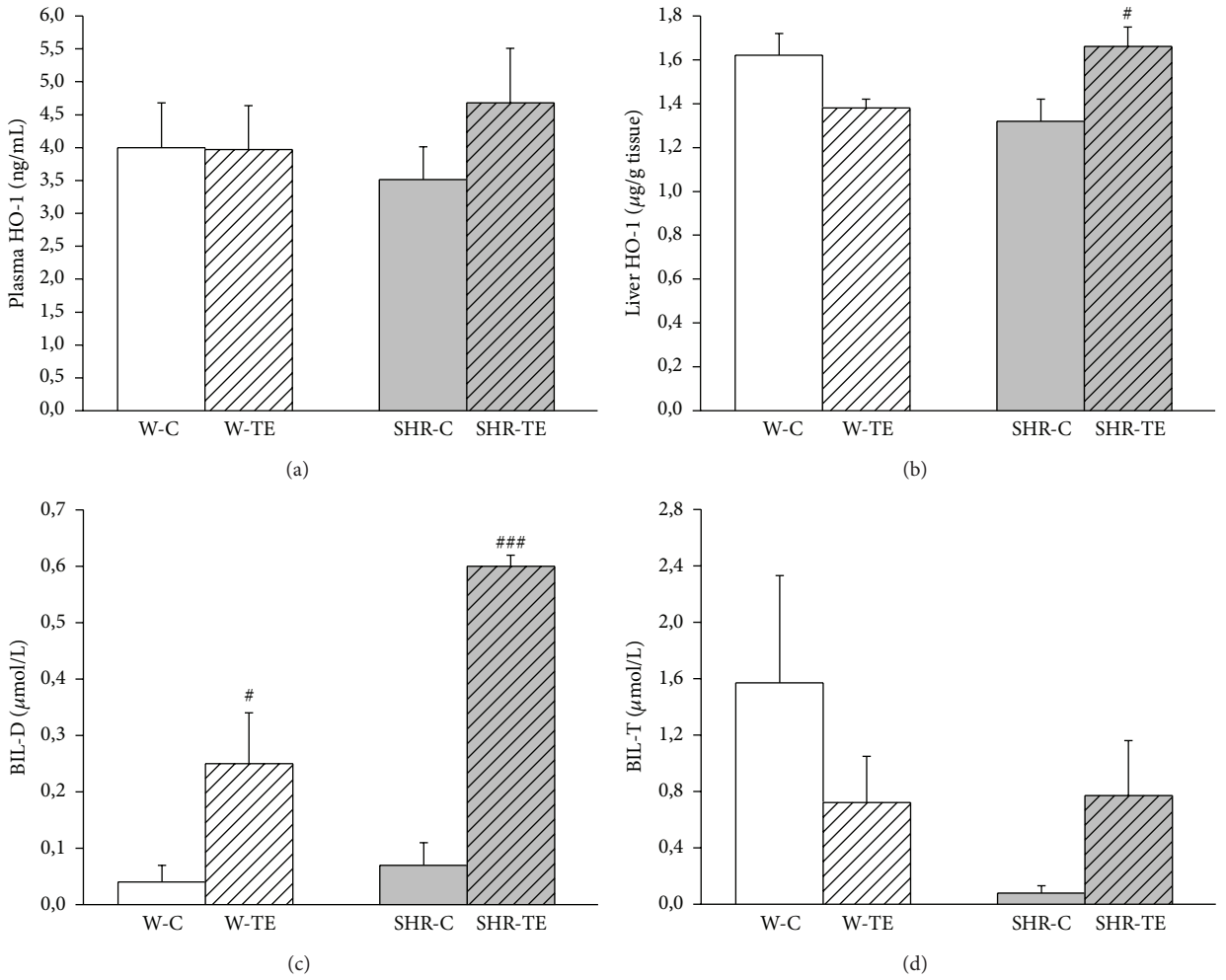

FIGURE 3: The quantity of (a) plasma and (b) liver heme oxygenase-1 (HO-1), (c) direct bilirubin (BIL-D) in plasma, and (d) total plasma bilirubin (BIL-T) in experimental groups. W-C, normotensive Wistar rats, and SHR-C, spontaneously hypertensive rats, received vehicle. W-TE and SHR-TE groups received thyme extract. $^{###}p < 0.001$ and $^{#}p < 0.05$, the significant difference between TE treated and appropriate control group.

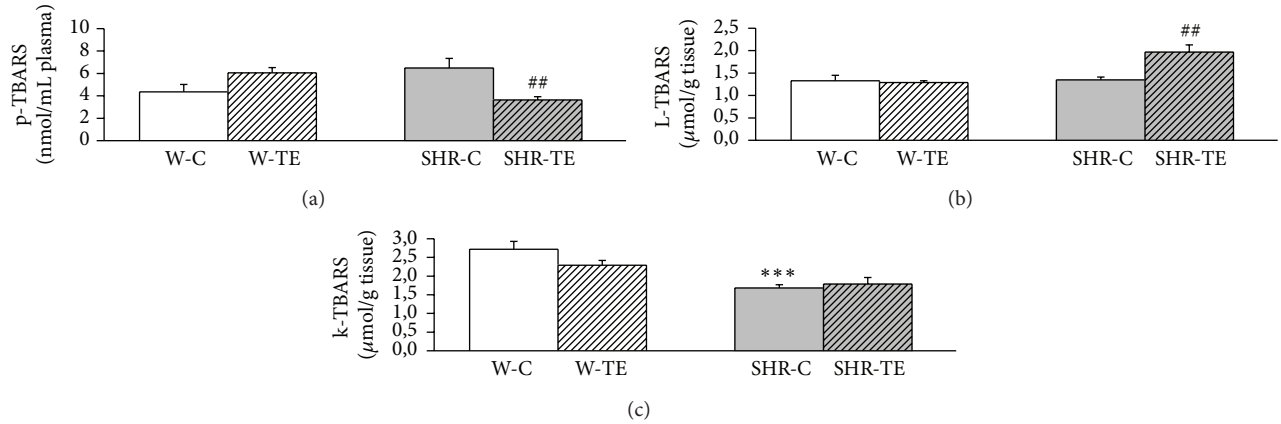

FIGURE 4: The quantity of (a) plasma (p), (b) liver (L), and (c) kidney (k) thiobarbituric acid reactive substances (TBARS) in experimental groups. W-C, normotensive Wistar rats, and SHR-C, spontaneously hypertensive rats received vehicle. W-TE and SHR-TE groups received thyme extract. $^{***}p < 0.001$, the significant difference between SHR-C and W-C; $^{##}p < 0.01$, the significant difference between TE treated and appropriate control group.

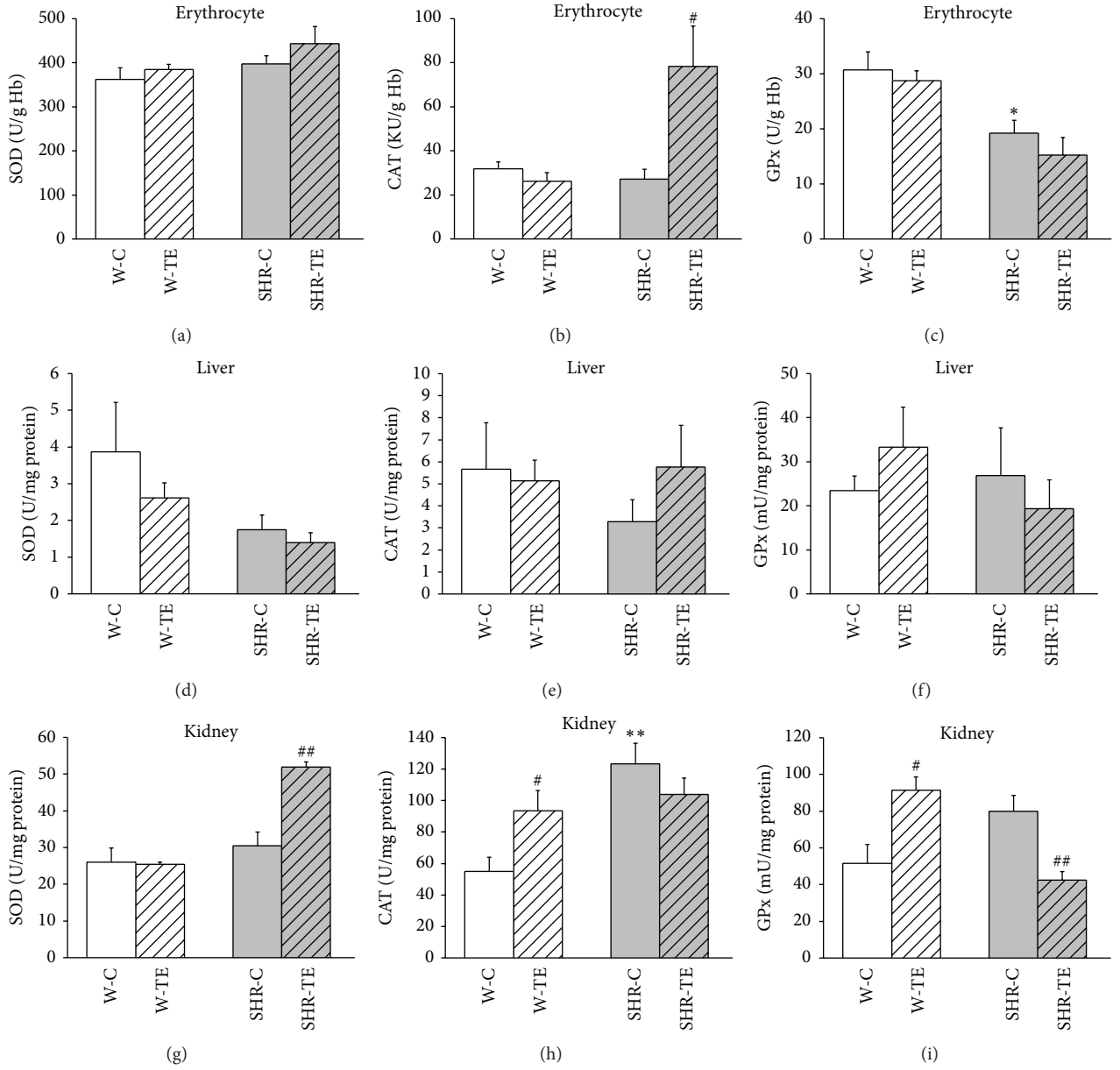

Figure 5: Antioxidant enzyme activities of (a), (b), and (c) erythrocytes, (d), (e), and (f) liver and (g), (h), and (i) kidney in experimental groups. W-C, normotensive *Wistar* rats, and SHR-C, spontaneously hypertensive rats, received vehicle. W-TE and SHR-TE groups received thyme extract, superoxide dismutase (SOD), catalase (CAT), and glutathione peroxidase (GPx). $^{*}p < 0.05$ and $^{**}p < 0.01$, the significant difference between SHR-C and W-C; $^{\#}p < 0.05$ and $^{\#\#}p < 0.01$, the significant difference between TE treated and appropriate control group.

Here, we hypothesized that induction of HO-1, due to TE treatment, may contribute to powerful blood pressure-lowering effect and reduction of systemic oxidative stress in SHR. In support of our hypothesis are the results by Jin et al. that identified rosmarinic acid as an inducer of HO-1 expression by increasing ROS production *in vitro* [22]. Further evidence identifies derivate of caffeic acid, caffeic acid phenethyl ester, as potent HO-1 inducer that can be used to markedly increase heme oxygenase activity in astrocytes [23]. To our knowledge, the present study is the first showing TE-induction of HO-1 *in vivo*, in hypertensive rats. Considering all the above and the composition of used TE, we suggest that this strong induction of HO-1 in SHR represents the response of the liver to TE-induced increase of ROS production. This assumption is supported with significant positive correlation between liver ROS measured by TBARS and the level of HO-1 in hypertensive rats.

In the present study, wild thyme induced significant and pronounced systemic vasorelaxation in both hypertensive and normotensive rats compared to vehicle, but only in hypertensive rats did such relaxation significantly and positively correlate with markedly reduced mean arterial pressure. As expected, results from SHR showed increased TPVR, CVR, and RVR accompanied with significant elevation of

Table 1: The correlation between haemodynamic parameters and oxidative status in hypertensive ($n = 12$) and normotensive rats ($n = 12$).

	L-TBARS		p-TBARS		k-TBARS		L-HO-1		p-HO-1		BIL-D		BIL-T	
	W	SHR	W	SHR	W	SHR	W	SHR	W	SHR	W	SHR	W	SHR
MAP	0.2830 $p = 0.373$	−0.7060 $p =$ **0.010**	−0.0489 $p = 0.880$	0.6251 $p =$ **0.030**	0.2371 $p = 0.458$	−0.1796 $p = 0.577$	0.4435 $p = 0.149$	−0.6159 $p =$ **0.033**	−0.4965 $p = 0.101$	−0.3846 $p = 0.217$	−0.3628 $p = 0.246$	−0.9249 $p =$ **0.000**	0.4006 $p = 0.197$	−0.6398 $p =$ **0.025**
TPVR	−0.1109 $p = 0.732$	−0.7578 $p =$ **0.004**	−0.1013 $p = 0.754$	0.4923 $p = 0.104$	0.3308 $p = 0.294$	−0.0962 $p = 0.766$	0.3023 $p = 0.340$	−0.4951 $p = 0.102$	0.1118 $p = 0.730$	−0.6518 $p =$ **0.022**	−0.5295 $p = 0.077$	−0.7001 $p =$ **0.011**	0.2704 $p = 0.395$	−0.4377 $p = 0.155$

SHR: spontaneously hypertensive rats that received vehicle or thyme extract; W: *Wistar* rats that received vehicle or thyme extract; MAP: mean arterial pressure; TPVR: total peripheral vascular resistance; L-TBARS, p-TBARS, and k-TBARS: liver thiobarbituric acid reactive substance, plasma thiobarbituric acid reactive substance, and kidney thiobarbituric acid reactive substances; quantity of L-HO-1 and p-HO-1: liver and plasma heme oxigenase-1 enzyme; BIL-D: direct bilirubin; BIL-T: total bilirubin. Marked correlations are significant at $p < 0.050$.

Table 2: The correlation of oxidative stress parameters with heme oxigenase-1 expression and activity in hypertensive (n = 12) and normotensive rats (n = 12).

	L-HO-1		HO-1		BIL-D		BIL-T	
	W	SHR	W	SHR	W	SHR	W	SHR
L-TBARS	0.0775 p = 0.811	0.6284 p = **0.029**	−0.1981 p = 0.537	0.6444 p = **0.024**	0.0034 p = 0.992	0.7475 p = **0.005**	0.2548 p = 0.424	0.5980 p = **0.040**
p-TBARS	−0.2623 p = 0.410	−0.7715 p = **0.003**	−0.0377 p = 0.908	−0.3397 p = 0.280	0.0890 p = 0.783	−0.7623 p = **0.004**	0.0614 p = 0.850	−0.5674 p = 0.054
k-TBARS	0.6801 p = **0.015**	0.4457 p = 0.147	0.1703 p = 0.597	0.4521 p = 0.140	−0.4280 p = 0.165	0.0775 p = 0.811	0.2146 p = 0.503	0.4398 p = 0.153

SHR: spontaneously hypertensive rats that received vehicle or thyme extract; W: *Wistar* rats that received vehicle or thyme extract; L-TBARS, p-TBARS, and k-TBARS: liver thiobarbituric acid reactive substance, plasma thiobarbituric acid reactive substance, and kidney thiobarbituric acid reactive substances; quantity of L-HO-1 and p-HO-1: liver and plasma heme oxigenase-1 enzyme; BIL-D: direct bilirubin; BIL-T: total bilirubin. Marked correlations are significant at $p < 0.050$.

Table 3: The correlation of antioxidant enzymes activity and systemic haemodynamic parameters, with oxidative status in hypertensive (n = 12) and normotensive rats (n = 12).

	e-CAT		k-SOD		k-CAT		k-GPx	
	W	SHR	W	SHR	W	SHR	W	SHR
MAP	0.3742 p = 0.231	−0.6178 p = **0.032**	−0.3627 p = 0.247	−0.7413 p = **0.006**	−0.6051 p = **0.037**	0.2260 p = 0.480	−0.3523 p = 0.261	0.7480 p = **0.005**
TPVR	0.3559 p = 0.256	−0.6041 p = **0.038**	0.2728 p = 0.391	−0.7791 p = **0.003**	−0.2638 p = 0.407	0.0124 p = 0.969	−0.3770 p = 0.227	0.5628 p = 0.057
L-TBARS	−0.0027 p = 0.993	0.6543 p = **0.021**	−0.1804 p = 0.575	0.7807 p = **0.003**	0.0896 p = 0.782	−0.1624 p = 0.614	0.0496 p = 0.878	−0.4627 p = 0.130
p-TBARS	0.0818 p = 0.800	−0.3587 p = 0.252	−0.5557 p = 0.061	−0.6479 p = **0.023**	0.3237 p = 0.305	0.2503 p = 0.433	0.2615 p = 0.412	0.2261 p = 0.480
k-TBARS	0.6637 p = **0.019**	−0.2964 p = 0.350	−0.0921 p = 0.776	0.3710 p = 0.235	−0.2610 p = 0.413	−0.0555 p = 0.864	−0.3946 p = 0.204	−0.2397 p = 0.453
BIL-D	−0.4345 p = 0.158	0.6818 p = **0.015**	−0.2737 p = 0.389	0.7989 p = **0.002**	0.1852 p = 0.564	−0.2638 p = 0.407	0.3991 p = 0.199	−0.6828 p = **0.014**

SHR: spontaneously hypertensive rats that received vehicle or thyme extract; W: *Wistar* rats that received vehicle or thyme extract; MAP: mean arterial pressure; TPVR: total peripheral vascular resistance; L-TBARS, p-TBARS, and k-TBARS: liver thiobarbituric acid reactive substance, plasma thiobarbituric acid reactive substance, and kidney thiobarbituric acid reactive substance; BIL-D: direct bilirubin; e-CAT and k-CAT: erythrocyte catalase and kidney catalase; k-SOD: kidney superoxide dismutase; k-GPx: kidney glutathione peroxidase. Marked correlations are significant at $p < 0.050$.

blood pressure and HR, without changes of CI, CBF, or RBF compared to *Wistar* rats. Our results in hypertensive rats treated with TE are in favour of previously obtained findings [24–26] that plant polyphenols decrease arterial pressure in SHR. Some studies showed that upregulating the HO/CO system lowers BP in young (8 weeks) but not in adult (20 weeks) spontaneously hypertensive rats (SHR) [27]. Other studies have demonstrated that either acute or chronic administration of HO-1 inducer was able to normalize blood pressure in SHR and that heme administration decreased blood pressure in SHR, while HO inhibitors produced an increase in systemic arterial pressure, even in normotensive rats [28]. The induction of HO-1 that we found in hypertensive rats was in significant negative correlation with the TPVR, indicating that HO-1 generated CO could be accountable for the intensive systemic vasorelaxation and the decrease of blood pressure that we observed in SHR-TE group. These results are in accordance with reports in which, like NO, HO-derived CO serves as a vasodilator to lower blood pressure, regardless of whether it operates via cGMP-dependent or cGMP-independent pathways, thus explaining a number of the potential actions of CO regarding the pathogenesis of cardiovascular diseases [28]. This vasodilator effect may also contribute to the improvement of regional haemodynamics in the carotid artery of hypertensive rats.

The increased iron concentration produced by the HO-1 activity is believed to cause the increased expression of ferritin and ferritin synthesis, which serves to sequester iron, a potent oxidant for cells [28]. Here, we did not determine ferritin content, but there is evidence that tea polyphenols could act as metal chelators [29] and therefore could remove ferrous ions, thereby protecting cells against metal ion-induced oxidative stress.

The next product of heme metabolism, biliverdin, becomes cleaved by biliverdin reductase to bilirubin, a chain-breaking antioxidant that acts as a lipid peroxyl radical (ROO·) scavenger [16]. Bilirubin is toxic in high concentration; however, it prevents adhesion molecule expression

and neutrophil adhesion and inhibits ROS and NADPH oxidase activity in biological systems [28]. Serum bilirubin circulates in the bloodstream in forms of direct and indirect bilirubin and has potent endogenous antioxidant properties that are found to have inverse associations with cardiovascular disease [30]. At physiologic oxygen pressure, bilirubin surpasses α-tocopherol, the most potent protector against lipid peroxidation. Increased levels of serum TBARS (a by-product of lipid peroxidation) have been previously reported in SHR [31], as well as in patients with hypertension and metabolic syndrome [32], ischemic heart disease [33], peripheral arterial disease [34], and diabetes mellitus [35]. In the present study, along with slight plasma and marked liver HO-1 elevation, plasma level of BIL-D became increased and was followed by reduction of plasma lipid peroxidation in SHR received TE. Also, there was significant negative intercorrelation between the p-TBARS and liver HO-1, as well as BIL-D, confirming the antioxidant defence properties of these endogenous products.

Interestingly, the liver HO system was nearly significantly suppressed in W-TE rats and that might be a possible reason for a moderate increase of plasma lipid peroxidation in this group.

The present study demonstrated almost similar SOD, CAT, and GPx enzyme activity in the liver of all experimental groups, which indicates that these antioxidant enzymes are not crucial for the oxidative status of the liver. Reduced activity of erythrocyte GPx from SHR in comparison to W rats failed to become corrected with TE, but TE induced the enhancement of erythrocyte CAT activity almost threefold and therefore protected SHR against hydrogen peroxide induced systemic oxidative stress. A similar kidney SOD activity that we found in SHR and W rats was in accordance with data obtained by Fortepiani and Reckelhoff [36] who showed that the expression of kidney Mn-SOD and Cu and Zn-SOD was similar in WKY and SHR despite higher ability of hypertensive kidney to produce superoxide. Also, they showed 30% lower expression of GPx and CAT in SHR than WKY and that WKY had increased expression of these enzymes in response to oxidative stress. We did not measure the expression of previously mentioned enzymes, but the activity of k-SOD that we observed was higher after TE in SHR, but not in W rats. At the same time, k-CAT and k-GPx enzyme activity was higher about 2-fold in hypertensive than in normotensive kidney. Further, we found the TE-induced increase of kidney CAT and GPx enzyme activity in normotensive rats. These data indicate that the increased activity of the k-CAT and k-GPx could have been a compensatory mechanism for the prevention of moderate plasma lipid peroxidation that we obtained in W-TE rats.

On the other hand, we found decreased activity of the kidney GPx enzyme in hypertensive rats after TE. Consequently, serum concentrations of bilirubin were high enough to account for a substantial portion of the total antioxidant capacity of serum [15], and bilirubin might alleviate oxidant stress in the blood [14]; we could assume that bilirubin ROO· scavenging activity in our study is sufficient to avoid oxidant stress in the hypertensive kidney. In addition to the direct effects of TE on HO system, the increased k-SOD activity due to the TE injection that we observed in hypertensive rats could be accountable for normalization of BP. Indeed, k-SOD was in significant negative correlation with MAP and TVR in this rat strain, but not in normotensive rats. Further, the increased k-SOD activity was in significant negative association with GPx that in turn negatively correlates against bilirubin, thus emphasizing the bilirubin (regardless of whether it is total or direct) responsible for plasma antioxidant defence.

The numerous polyphenolic substances and other chemical compounds that were found in the plants from the Lamiaceae family were speculated to account for the beneficial effects of these plant extracts on the cardiovascular system. However, the results of this experimental animal study indicate that strong and significant hypotensive and antioxidative activity of aqueous extract from *Thymus serpyllum* L. in hypertensive rats, at least partially, resulted due to targeting heme oxygenase system. Besides rosmarinic acid, used plant extract contains caffeic acid and quercetin and luteolin in trace [7]; thus further studies are needed to elucidate which of these polyphenolic compounds is responsible for those beneficial effects of TE or whether they are a consequence of their synergistic action.

Competing Interests

The authors have no competing interests to declare.

Acknowledgments

The authors gratefully acknowledge the professional English language assistance provided to them by Vladana Ivanov, M.A. in English language. This work was supported by grant from the Ministry of Education, Science and Technological Development, Republic of Serbia (Project no. III-46010).

References

[1] O. A. Carretero and S. Oparil, "Essential hypertension part I: definition and etiology," *Circulation*, vol. 101, no. 3, pp. 329–335, 2000.

[2] D. Jovanovic, D. Jovovic, N. Mihailovic-Stanojevic et al., "Effect of carvedilol on pulse pressure and left ventricular hypertrophy in spontaneously hypertensive rats with adriamycin nephropathy," *Biomedicine and Pharmacotherapy*, vol. 63, no. 8, pp. 571–576, 2009.

[3] N. Mihailovic-Stanojevic, Z. Miloradovic, J. Grujic-Milanovic, M. Ivanov, and D. Jovovic, "Effects of angiotensin II type-1 receptor blocker losartan on age-related cardiovascular risk in spontaneously hypertensive rats," *General Physiology and Biophysics*, pp. 112–118, 2009.

[4] N. Tabassum and F. Ahmad, "Role of natural herbs in the treatment of hypertension," *Pharmacognosy Reviews*, vol. 5, no. 9, p. 30, 2011.

[5] A. S. Kivimäki, P. I. Ehlers, A. M. Turpeinen, H. Vapaatalo, and R. Korpela, "Lingonberry juice improves endothelium-dependent vasodilatation of mesenteric arteries in spontaneously hypertensive rats in a long-term intervention," *Journal of Functional Foods*, vol. 3, no. 4, pp. 267–274, 2011.

[6] V. B. Schini-Kerth, C. Auger, J.-H. Kim, N. Étienne-Selloum, and T. Chataigneau, "Nutritional improvement of the endothelial control of vascular tone by polyphenols: role of NO and EDHF," *Pflugers Archiv—European Journal of Physiology*, vol. 459, no. 6, pp. 853–862, 2010.

[7] N. Mihailovic-Stanojevic, A. Belščak-Cvitanović, J. Grujić-Milanović et al., "Antioxidant and antihypertensive activity of extract from *Thymus serpyllum* L. in experimental hypertension," *Plant Foods for Human Nutrition*, vol. 68, no. 3, pp. 235–240, 2013.

[8] M. S. Kumar, S. Kumar, and B. Raja, "Antihypertensive and antioxidant potential of borneol-a natural terpene in L-NAME—induced hypertensive rats," *International Journal of Pharmaceutical and Biological Archive*, vol. 1, pp. 271–279, 2010.

[9] K. Ohashi, T. Bohgaki, and H. Shibuya, "Antihypertensive substance in the leaves of kumis kucing (Orthosiphon aristatus) in Java island," *Yakugaku Zasshi*, vol. 120, no. 5, pp. 474–482, 2000.

[10] Y.-I. I. Kwon, D. A. Vattem, and K. Shetty, "Evaluation of clonal herbs of Lamiaceae species for management of diabetes and hypertension," *Asia Pacific Journal of Clinical Nutrition*, vol. 15, no. 1, pp. 107–118, 2006.

[11] R. M. Touyz, "Reactive oxygen species, vascular oxidative stress, and redox signaling in hypertension: what is the clinical significance?" *Hypertension*, vol. 44, no. 3, pp. 248–252, 2004.

[12] A. L. Furfaro, N. Traverso, C. Domenicotti et al., "The Nrf2/HO-1 axis in cancer cell growth and chemoresistance," *Oxidative Medicine and Cellular Longevity*, vol. 2016, Article ID 1958174, 14 pages, 2016.

[13] M. Mayer, "Association of serum bilirubin concentration with risk of coronary artery disease," *Clinical Chemistry*, vol. 46, no. 11, pp. 1723–1727, 2000.

[14] T. W. Sedlak and S. H. Snyder, "Bilirubin benefits: cellular protection by a biliverdin reductase antioxidant cycle," *Pediatrics*, vol. 113, no. 6, pp. 1776–1782, 2004.

[15] V. Lobo, A. Patil, A. Phatak, and N. Chandra, "Free radicals, antioxidants and functional foods: impact on human health," *Pharmacognosy Reviews*, vol. 4, no. 8, p. 118, 2010.

[16] G. E. Mann, D. J. Rowlands, F. Y. L. Li, P. De Winter, and R. C. M. Siow, "Activation of endothelial nitric oxide synthase by dietary isoflavones: role of NO in Nrf2-mediated antioxidant gene expression," *Cardiovascular Research*, vol. 75, no. 2, pp. 261–274, 2007.

[17] J. F. Ndisang, L. Wu, W. Zhao, and R. Wang, "Induction of heme oxygenase-1 and stimulation of cGMP production by hemin in aortic tissues from hypertensive rats," *Blood*, vol. 101, no. 10, pp. 3893–3900, 2003.

[18] E. Beutler, "Catalase," in *Red Cell Metabolism, a Manual of Biochemical Methods*, Grune and Stratton, New York, NY, USA, 3rd edition, 1982.

[19] D. E. Paglia and W. N. Valentine, "Studies on the quantitative and qualitative characterization of erythrocyte glutathione peroxidase," *Journal of Laboratory and Clinical Medicine*, vol. 70, no. 1, pp. 158–169, 1967.

[20] J. M. McCord and I. Fridovich, "The utility of superoxide dismutase in studying free radical reactions. I. Radicals generated by the interaction of sulfite, dimethyl sulfoxide, and oxygen," *The Journal of Biological Chemistry*, vol. 244, no. 22, pp. 6056–6063, 1969.

[21] H. Ohkawa, N. Ohishi, and K. Yagi, "Assay for lipid peroxides in animal tissues by thiobarbituric acid reaction," *Analytical Biochemistry*, vol. 95, no. 2, pp. 351–358, 1979.

[22] C. H. Jin, H. S. Yang, D. S. Choi, M. W. Byun, W. G. Kim, and I. Y. Jeong, "Rosmarinic acid attenuated SIN-1-induced cytotoxicity in HepG2 cells through the HO-1 induction and radical scavenging activity," *Food Science and Biotechnology*, vol. 22, no. 2, pp. 549–556, 2013.

[23] G. Scapagnini, R. Foresti, V. Calabrese, A. M. Giuffrida Stella, C. J. Green, and R. Motterlini, "Caffeic acid phenethyl ester and curcumin: a novel class of heme oxygenase-1 inducers," *Molecular Pharmacology*, vol. 61, no. 3, pp. 554–561, 2002.

[24] J.-C. Liu, F.-L. Hsu, J.-C. Tsai et al., "Antihypertensive effects of tannins isolated from traditional Chinese herbs as non-specific inhibitors of angiontensin converting enzyme," *Life Sciences*, vol. 73, no. 12, pp. 1543–1555, 2003.

[25] N. Peng, J. T. Clark, J. Prasain, H. Kim, C. R. White, and J. M. Wyss, "Antihypertensive and cognitive effects of grape polyphenols in estrogen-depleted, female, spontaneously hypertensive rats," *American Journal of Physiology. Regulatory, Integrative and Comparative Physiology*, vol. 289, no. 3, pp. R771–R775, 2005.

[26] S. J. Thandapilly, J. L. LeMaistre, X. L. Louis, C. M. Anderson, T. Netticadan, and H. D. Anderson, "Vascular and cardiac effects of grape powder in the spontaneously hypertensive rat," *American Journal of Hypertension*, vol. 25, no. 10, pp. 1070–1076, 2012.

[27] J. F. Ndisang, W. Zhao, and R. Wang, "Selective regulation of blood pressure by heme oxygenase-1 in hypertension," *Hypertension*, vol. 40, no. 3, pp. 315–321, 2002.

[28] N. G. Abraham and A. Kappas, "Pharmacological and clinical aspects of heme oxygenase," *Pharmacological Reviews*, vol. 60, no. 1, pp. 79–127, 2008.

[29] V. Stangl, H. Dreger, K. Stangl, and M. Lorenz, "Molecular targets of tea polyphenols in the cardiovascular system," *Cardiovascular Research*, vol. 73, no. 2, pp. 348–358, 2007.

[30] J. Jo, J. E. Yun, H. Lee, H. Kimm, and S. H. Jee, "Total, direct, and indirect serum bilirubin concentrations and metabolic syndrome among the Korean population," *Endocrine*, vol. 39, no. 2, pp. 182–189, 2011.

[31] M. A. Newaz and N. N. A. Nawal, "Effect of γ-tocotreenol on blood pressure, lipid peroxtoation and total antioxtoant status in spontaneously hypertensive rats (SHR)," *Clinical and Experimental Hypertension*, vol. 21, no. 8, pp. 1297–1313, 1999.

[32] V. O. Palmieri, I. Grattagliano, P. Portincasa, and G. Palasciano, "Systemic oxidative alterations are associated with visceral adiposity and liver steatosis in patients with metabolic syndrome," *The Journal of Nutrition*, vol. 136, no. 12, pp. 3022–3026, 2006.

[33] B. R. Maharjan, J. C. Jha, D. Adhikari et al., "Oxidative stress, antioxidant status and lipid profile in ischemic heart disease patients from western region of Nepal," *Nepal Medical College Journal*, vol. 10, no. 1, pp. 20–24, 2008.

[34] J. Miquel, A. Ramirez-Bosca, A. Soler et al., "Increase with age of serum lipid peroxides: implications for the prevention of atherosclerosis," *Mechanisms of Ageing and Development*, vol. 100, no. 1, pp. 17–24, 1998.

[35] A. A. Osuntokl, O. A. Fasanmade, A. O. Adekola, and C. O. Amira, "Lipid peroxidation and erythrocyte fragility in poorly controlled type 2 diabetes mellitus," *Nigerian Quarterly Journal of Hospital Medicine*, vol. 17, no. 4, pp. 148–151, 2007.

[36] L. A. Fortepiani and J. F. Reckelhoff, "Increasing oxidative stress with molsidomine increases blood pressure in genetically hypertensive rats but not normotensive controls," *American Journal of Physiology—Regulatory Integrative and Comparative Physiology*, vol. 289, no. 3, pp. R763–R770, 2005.

Hindawi Publishing Corporation
Oxidative Medicine and Cellular Longevity
Volume 2016, Article ID 8045969, 6 pages
http://dx.doi.org/10.1155/2016/8045969

Research Article

Blood Levels of Oxidant/Antioxidant Parameters in Rats Infected with *Toxoplasma gondii*

Somayeh Bahrami,[1] Ali Shahriari,[2] Mehdi Tavalla,[3] Somayeh Azadmanesh,[1] and Hossein Hamidinejat[1]

[1]*Department of Parasitology, Faculty of Veterinary Medicine, Shahid Chamran University of Ahvaz, Ahvaz, Iran*
[2]*Department of Biochemistry, Faculty of Veterinary Medicine, Shahid Chamran University of Ahvaz, Ahvaz, Iran*
[3]*Department of Medical Parasitology, Faculty of Medicine, Jundishapur University of Medical Sciences, Ahvaz, Iran*

Correspondence should be addressed to Somayeh Bahrami; s.bahrami@scu.ac.ir

Received 6 April 2016; Revised 25 July 2016; Accepted 6 September 2016

Academic Editor: Claudio Cabello-Verrugio

Toxoplasmosis is a common parasitic infection in the world. Since increased free radicals and oxidative stress are reported in many parasitic diseases the purpose of the present study was to evaluate the oxidative stress in acute and chronic toxoplasmosis. RH strains of *Toxoplasma* tachyzoites were used in the present study. Twenty-five female rats were infected with the parasite while 25 other rats were as the control group that received normal saline. Zero-, 5-, 7-, 10-, and 45-day postinfection (DPI) blood samples were taken. Some parameters related to oxidant and antioxidants such as antioxidant enzymes, malondialdehyde, and total antioxidant capacity were measured. On day 7 after infection, GPX activity and GSH level were significantly increased and in the mentioned day the amount of total antioxidant capacity was significantly reduced. In other cases, there were no significant differences between the groups in different days. Overall, based on the results it seems that, on day 7 after infection, in infected rats responses to oxidative stress were triggered and led to decrease of total antioxidant capacity. Furthermore, glutathione was increased to cope with stress. It seems that probably antioxidant defense system entered the infection to the chronic phase and changed the parasites stage.

1. Introduction

Toxoplasma gondii is an obligate intracellular protozoan parasite responsible for toxoplasmosis, a disease that affects many mammals including man [1, 2]. Infection of an immunocompetent individual is usually asymptomatic; however, infection of immunocompromised individuals or congenital infection of a fetus can lead to debilitating or life-threatening illness. Infection generally occurs through either ingestion of oocysts shed in the faeces of a cat, which is the definitive host, or ingestion of viable tissue-cysts in undercooked meat. When primary infection occurs during pregnancy, congenital transmission could occur. Initial infection and acute disease are characterized by the presence of fast-replicating tachyzoites. Around 10–14 days after infection, tachyzoites differentiate into bradyzoites that replicate more slowly and form cysts in tissues throughout the body. Tissue cysts are long-lived and not associated with disease. However, in people with immunodeficiency, such as AIDS or malignancies, rupture of tissue cysts and the transformation of bradyzoites to tachyzoites result in disease reactivation. Congenitally infected individuals are also at risk of repeated disease reactivation, most notably in their brain and eyes, although the reason(s) for this has not been established. Recent investigations indicate that parasitic infections with high tolerance of the host are the result of defense mechanisms which include enhanced generation of reactive oxygen species (ROS) [3, 4]. Cells and biological fluids from an antioxidant defense system aid at suppression of ROS generation and prevention of ROS reactions with cellular components. A balance between oxidants and antioxidant is known to exist under physiological conditions. However, even small changes in oxidant or/and antioxidant levels may disturb its balance and leads to oxidative stress. This situation becomes dangerous when the antioxidant system is unable to prevent oxidative reactions triggered by ROS and directed oxidative modification of

lipids, proteins, and DNA [5–7]. Free radicals are produced continuously by normal metabolic processes, but their rate of production increases during certain parasitic infections.

Stage conversion between tachyzoite and bradyzoite forms of *Toxoplasma* is associated with morphological and molecular biological changes, including stage-specific antigen expression and alterations to metabolism [8]. Different studies confirmed that alkaline medium, heat shock protein, and acid conditions can induce stage conversion *in vitro*. These methods appear to rely on stressing the parasites. Having these facts in mind, the present study was designed to compare the antioxidant profile of rats during acute and chronic toxoplasmosis and investigate probable role of oxidative stress in *Toxoplasma gondii* tachyzoite-bradyzoite interconversion.

2. Materials and Methods

2.1. Parasite. The virulent RH strain of *T. gondii* was obtained from Jundishapur University of Medical Sciences, Ahvaz, Iran. Tachyzoites of this strain were collected by serial intraperitoneal passages in BALB/c mice. Parasites (1×10^5) were inoculated in the mice, and after 72 hours, tachyzoites were provided by repeated flushing of the peritoneal cavity by phosphate buffered saline (PBS). Tachyzoites were then harvested and centrifuged at 200 ×g for 5 min at room temperature to remove peritoneal cells and cellular debris. The supernatants were collected and centrifuged at 800 ×g for 10 min. The pellets, enriched with parasite tachyzoites, were recovered with PBS and used in the experiments [9].

2.2. In Vivo Study. Fifty female Wistar rats, 8 to 10 weeks old, approximately 250–280 g, were purchased from laboratory animal breeding council (Jundishapur University of Medical Science, Ahvaz, Iran). They were housed in a room under controlled temperature (24 ± 2°C), lighting (12 h light/dark cycle), and relative humidity 40–70% conditions. During experiment, all rats had free access to water and standard rat chow. After 1 week acclimation, firstly modified agglutination test was used to ensure rats were not already infected with *Toxoplasma*, and then they were divided randomly into two equal groups: The infected and control groups were each inoculated intraperitoneally with 1×10^7 organisms [10] and normal saline, respectively. On days 0, 5, 7, 10, and 45 after infection, five rats from each group were euthanized in a glass desiccator jar for open-drop anesthesia with chloroform following standard animal ethics guidelines of Iran. Blood samples were obtained by cardiac puncture into sterile vacuum tubes with and without anticoagulant (EDTA). Serum was separated by centrifuge and stored at −20°C until use. During the present study, the animals were handled according to the recommendation of the Ethics Committee, Shahid Chamran University of Ahvaz, Ahvaz, Iran (Ethical Approval number 29/6/94, 30 Sept. 2014). Acute and chronic toxoplasmosis of was confirmed by PCR and modified agglutination test (MAT), respectively.

2.3. DNA Extraction and Polymerase Chain Reaction (PCR) Amplification. Induction of acute toxoplasmosis was confirmed with PCR in infected rats on days 5, 7, and 10 after infection. DNA was extracted from whole blood using a genomic DNA purification kit (CinnaGen, Iran). For detection of *T. gondii* DNA, primers targeting the G529 gene were selected from the literature [11]. PCR reactions included a negative control, consisting of the reaction mix and 2 μL of DNase/RNase-free water and a positive control that consisted of a DNA sample from the tachyzoites of *T. gondii*. All PCR were performed in a 25 μL reaction containing 12.5 μL Taq DNA polymerase master mix Red (Amplicon, Denmark), 1 μM primers, and 50 ng DNA templates. PCR cycling included an initial denaturation at 94°C for 4 min, followed by 30 cycles of denaturation at 94°C for 50 s, annealing at 57°C for 50 s, and extension at 72°C for 60 s. This was followed by a final extension at 72°C for 5 min. PCR products were electrophoresed in 1.5% agarose (SinaClon Bioscience, Iran) in Tris-acetic acid-EDTA (TAE) buffer, stained with Green Safe stain (SinaClon Bioscience, Iran), and visualized under ultraviolet light. Positive samples showed a band of approximately 400 bp.

2.4. Modified Agglutination Test. To ensure that chronic toxoplasmosis occurred in rats on day 45 after infection, MAT was used as described by Desmonts and Remington and Dubey and Desmonts [12, 13]. The sera were diluted twofold (1 : 20 to 1 : 320) with phosphate buffered saline containing 0.2 M 2-mercaptoethanol and 50 μL of each dilution was put in a well of 96 U-bottom ELISA plates. Thereafter, 50 μL of the whole formalin-preserved *T. gondii* tachyzoites was added to each serum dilution. The wells were then mixed thoroughly by pipetting up and down several times, covered, and then incubated at 37°C overnight. The test was considered positive when a layer of agglutinated parasites was formed in wells at dilutions of 1 : 20 or higher. Positive and negative controls were included in each test.

2.5. Oxidant/Antioxidant Assessment. The determination of the SOD activity was based on the generation of superoxide radicals produced by xanthine and xanthine oxidase, which react with 2-(4-iodophenyl)-3-(4-nitrophenol)-5-phenyltetrazolium chloride to form a red formazon dye. Briefly, 300 μL of mixed substrate was added to 200 μL of diluted hemolysates. The samples were mixed well and 75 μL xanthine oxidase was added to reactions. The absorbance was measured at 505 nm and the SOD activity was then calculated according to the manufacturer's instruction (Ransod®-Randox Lab, Antrim, UK) and expressed as U/mL.

Glutathione peroxidase activity was determined based on the fact that GPX catalyzed the oxidation of glutathione by cumene hydroperoxide. In presence of the glutathione reductase and nicotinamide adenine dinucleotide phosphate (NADPH), the oxidized glutathione was immediately converted to the reduced form with concomitant oxidation of NADPH to $NADP^+$. To evaluate GPX activity in hemolysates 10 μL of samples was mixed with 500 μL reagent R1 and 20 μL cumene R2. The absorbance was measured at 340 nm

and the GPX activity was then calculated according to the manufacturer's instruction (Ransel®-Randox Lab, Antrim, UK). The enzymes activities were expressed as U/mL.

The procedure to estimate the reduced glutathione (GSH) level followed the method described by Ellman [14]. In this method thiols react with Ellman's reagent (5,5′-dithiobis-(2-nitrobenzoic acid) or DTNB), cleaving the disulfide bond to give 2-nitro-5-thiobenzoate (TNB^-), which ionizes to the TNB^{2-} dianion in water at neutral and alkaline pH.

To evaluate GSH level in samples, 15 μL of hemolysates was mixed with 260 μL assay buffer (0.1 M sodium phosphate and 1 mM EDTA, pH: 8) and 5 μL Ellman reagents. Samples were incubated for 15 min at room temperature and the TNB^{2-} formation was quantified in a spectrophotometer by measuring the absorbance of visible light at 412 nm. Absorbance values were compared with a standard curve generated from standard curve from known GSH.

Catalase activity was determined spectrophotometrically by the method of Koroliuk et al. [15]. Briefly, 10 μL of sample was incubated with 100 μmol/mL of H_2O_2 in 0.05 mmol/L Tris-HCl buffer pH = 7 for 10 min. The reaction was terminated by rapidly adding 50 μL of 4% ammonium molybdate. Yellow complex of ammonium molybdate and H_2O_2 was measured at 410 nm. One unit of catalase activity was defined as the amount of enzyme required to decompose 1 μmol H_2O_2 per min.

Total antioxidant capacity of serum was measured according to the method of Benzie and Strain [16]. Briefly, a working solution of FRAP (ferric reducing antioxidant power) was provided by mixing buffer acetate with TPTZ solution in HCl. After that $FeCl_3$ was added and mixed. 8 μL of serum and 240 μL of mentioned working solution were mixed and incubated for 10 min at room temperature. The optical density of samples was measured at 532 nm. Total antioxidant capacity was expressed as mmol/L.

Malondialdehyde levels in samples were measured using the thiobarbituric acid reaction method of Placer et al. [17]. Quantification of the thiobarbituric acid reactive substances was determined at 532 nm by comparing the absorption to the standard curve of MDA equivalents generated by acid-catalyzed hydrolysis of 1,1,3,3-tetramethoxypropane. To measure MDA level, a working solution containing 15% trichloroacetic acid, 0.375% thiobarbituric acid, and 0.25 N hydrochloric acid was prepared. For each sample, 250 μL serum and 500 μL working solution were mixed and placed in boiling water for 10 min. After cooling the samples were centrifuged at 3000 rpm for 10 min. Finally 200 μL of each supernatant was transferred to microplates and the optical density of samples was measured at 535 nm. The values of MDA were expressed as μmol/L.

2.6. Statistical Analysis. The mean value and standard error were calculated for each group of measurements. The Kolmogorov-Smirnov test was used to test the normal distribution of the data before statistical analysis was performed. Statistical analyses were conducted with the general linear model procedure of SAS for Windows version 9.1 (SAS, 1998) to determine if variables differed between groups. Whenever significant differences were found, mean values were compared by the Tukey test. A probability value of less than 0.05 was considered significant.

3. Results

After induction of experimental toxoplasmosis, acute toxoplasmosis was confirmed by PCR. In all the samples obtained 5 and 7 days after infection, DNA of *Toxoplasma* was detected in blood. Ten days after infection except for the two samples others were positive. Although in two samples DNA was not detected they were serologically positive. The accuracy of experimental chronic toxoplasmosis induction (samples obtained 45 days after infection) was serologically checked out. In all the samples complete carpet of agglutinated organisms was seen and considered as positive.

The antioxidant enzymes activities, total antioxidant capacity, and MDA level in blood of experimentally infected rats were compared to those of noninfected.

Changes of SOD activity in different days in infected ($p = 0.91$) and uninfected group ($p = 0.62$) were not significant. Also after comparing SOD activity in infected and uninfected groups on the days 0 ($p = 0.81$), 5 ($p = 0.36$), 7 ($p = 0.75$), 10 ($p = 0.35$), and 45 ($p = 0.80$) after infection, significant changes were not found (Table 1).

According to our data, level of GSH in noninfected rats in different days was not significantly changed while, in infected rats on the 7th day after infection, GSH was significantly increased comparing to 5th ($p = 0.002$), 10th ($p = 0.001$), and 45th ($p = 0.001$) day after infection. After comparing GSH level in infected and uninfected rats on the days 0 ($p = 0.57$), 5 ($p = 0.22$), and 45 ($p = 0.55$) after infection, significant changes were not found whereas on day 7 ($p = 0.019$) GSH level was substantially increased (Table 2).

Changes of GPX activity on days 5 ($p = 0.03$) and 7 ($p = 0.04$) after infection were significant in infected group. Also significant differences were detected in GPX activity between the infected rats and the controls on days 5 ($p = 0.03$) and 7 ($p = 0.02$) after infection (Table 3).

As shown in Table 4 the values for the activity of catalase in infected and uninfected rats were constant throughout the experiment. Also no significant differences were detected in catalase activity between the infected rats and the controls on days 0 ($p = 0.72$), 5 ($p = 0.57$), 7 ($p = 0.51$), 10 ($p = 0.53$), and 45 ($p = 0.75$) after infection.

The control value for the total antioxidant capacity in uninfected rats was constant throughout all stages of experiment whilst a statically significant decrease in the total antioxidant capacity was noticed on day 7 after infection in infected ones ($p = 0.004$). Significant difference was detected in total antioxidant capacity between the infected rats and the control ones on day 7 after infection ($p = 0.02$) (Table 5).

Changes of MDA level in different days in infected ($p = 0.57$) and uninfected rats ($p = 0.21$) were not significant. Also after comparing MDA level in infected and uninfected groups on days 0 ($p = 0.53$), 5 ($p = 0.49$), 7 ($p = 0.12$), 10 ($p = 0.15$), and 45 ($p = 0.28$) after infection, significant changes were not found (Table 6).

Table 1: Mean ± standard error of SOD activity (U/mL) in noninfected and *T. gondii* infected rats.

	Days after infection				
	0	5	7	10	45
Infected	98.2 ± 10.3^{Aa}	103.1 ± 9.3^{Aa}	114.2 ± 13.9^{Aa}	114.3 ± 15.3^{Aa}	104.6 ± 17.8^{Aa}
Noninfected	94.6 ± 8.7^{Aa}	85.1 ± 16.3^{Aa}	107.2 ± 16.2^{Aa}	91.1 ± 18.05^{Aa}	110 ± 10.8^{Aa}

Values in columns and rows with different uppercase and lowercase superscripts are significantly different ($p < 0.05$).

Table 2: Mean ± standard error of GSH level (μmol/mL) in noninfected and *T. gondii* infected rats.

	Days after infection				
	0	5	7	10	45
Infected	72.6 ± 5.3^{Aa}	78.6 ± 7.7^{Aa}	174.7 ± 16.4^{Bb}	52.1 ± 6.3^{Aa}	75.4 ± 18.3^{Aa}
Noninfected	70.3 ± 5.4^{Aa}	66.6 ± 4.9^{Aa}	98.4 ± 14.9^{Bb}	106.2 ± 20.4^{Aa}	90.4 ± 14.4^{Aa}

Values in columns and rows with different uppercase and lowercase superscripts are significantly different ($p < 0.05$).

Table 3: Mean ± standard error of GPX activity (U/mL) in noninfected and *T. gondii* infected rats.

	Days after infection				
	0	5	7	10	45
Infected	114.4 ± 11.6^{Aa}	313.5 ± 43.53^{Bb}	296.47 ± 42.1^{Bb}	128.1 ± 30.3^{Aa}	118.6 ± 28.7^{Aa}
Noninfected	117.3 ± 10.9^{Aa}	114.6 ± 14.4^{Aa}	107.4 ± 19.4^{Aa}	121.6 ± 23.4^{Aa}	107.1 ± 18.1^{Aa}

Values in columns and rows with different uppercase and lowercase superscripts are significantly different ($p < 0.05$).

Table 4: Mean ± standard error of catalase activity (U/mL) in noninfected and *T. gondii* infected rats.

	Days after infection				
	0	5	7	10	45
Infected	513.5 ± 82.3^{Aa}	466.8 ± 88.1^{Aa}	515.8 ± 63.2^{Aa}	551.5 ± 32.4^{Aa}	408.5 ± 78.8^{Aa}
Noninfected	532.5 ± 78.2^{Aa}	528.5 ± 75.6^{Aa}	427.5 ± 105.3^{Aa}	471.2 ± 88.7^{Aa}	449.7 ± 95.3^{Aa}

Values in columns and rows with different uppercase and lowercase superscripts are significantly different ($p < 0.05$).

Table 5: Mean ± standard error of total antioxidant capacity (mmol/L) in noninfected and *T. gondii* infected rats.

	Days after infection				
	0	5	7	10	45
Infected	987.2 ± 218.3^{Aa}	1016 ± 138.5^{Aa}	366.3 ± 53.6^{Bb}	1064.0 ± 70.7^{Aa}	1124.0 ± 105.3^{Aa}
Noninfected	874.1 ± 128.3^{Aa}	869.6 ± 125.5^{Aa}	895.6 ± 314.8^{Aa}	816.1 ± 169.9^{Aa}	961.72 ± 172.3^{Aa}

Values in columns and rows with different uppercase and lowercase superscripts are significantly different ($p < 0.05$).

Table 6: Mean ± standard error of MDA (μmol/L) in noninfected and *T. gondii* infected rats.

	Days after infection				
	0	5	7	10	45
Infected	20.6 ± 3.2^{Aa}	22.16 ± 5.4^{Aa}	13.56 ± 2.9^{Aa}	13.07 ± 1.2^{Aa}	15.5 ± 2.8^{Aa}
Noninfected	19.6 ± 3.2^{Aa}	18.2 ± 2.7^{Aa}	25.6 ± 6.01^{Aa}	18.5 ± 3.2^{Aa}	21.7 ± 4.1^{Aa}

Values in columns and rows with different uppercase and lowercase superscripts are significantly different ($p < 0.05$).

4. Discussion

A critical aspect of host defense to *Toxoplasma gondii* is the activation of parasiticidal mechanisms in host leukocytes. Mononuclear phagocytes, particularly macrophages that have been activated by lymphokines, are the principal defense against intracellular pathogens such as *T. gondii* and respiratory burst (rapid release of reactive oxygen species) plays an important role against *T. gondii* [18]. One of the mechanisms that protect the host cells against excess free radicals is the enzymatic antioxidant defense which includes SOD, catalase, peroxiredoxins, flavor hemoglobins, and glutathione S-transferase/GPX coupled to glutathione reductase. SOD is a key enzyme that appears to act as the first line defense against ROS but in the present study its activity was constant throughout all stages of experiment in infected rats.

Glutathione peroxidase and catalase are the two main enzymes involved in H_2O_2 detoxification [19]. Hydrogen peroxide (H_2O_2) is one of the main reactive oxygen species (ROS) leading to oxidative stress [20]. H_2O_2 is continuously generated by several enzymes (including superoxide dismutase, glucose oxidase, and monoamine oxidase) and must be degraded to prevent oxidative damage. The cytotoxic effect of H_2O_2 is thought to be caused by hydroxyl radicals generated from iron-catalyzed reactions, causing subsequent damage to DNA, proteins, and membrane lipids [21]. According to our results significant changes of catalase activity were not found during the experiment in infected rats while GSH level and GPX activity were substantially increased on the 7th day after infection. This is despite the fact that GSH elevation may be due to stimulation of antioxidant defense system against infection. GPX are a family of selenium-containing antioxidant enzymes that catalyze the reduction of hydrogen peroxide in the presence of reduced glutathione [22]. Glutathione exists in both reduced (GSH) and oxidized (GSSG) states. In the reduced state, the thiol group of cysteine is able to donate a reducing equivalent to unstable molecules such as reactive oxygen species. In donating an electron, glutathione itself becomes reactive but readily reacts with another reactive glutathione to form glutathione disulfide (GSSG). GSH can be regenerated from GSSG by the enzyme glutathione reductase (GSR) [23].

For reduction of glutathione via glutathione reductase, which converts reactive H_2O_2 into H_2O by glutathione peroxidase, NADPH is necessary. One of the most important metabolic pathways that generate NADPH is pentose phosphate pathway. It is possible that pentose phosphate pathway or other NADPH-generation pathways are increased in response to oxidative stress in acute toxoplasmosis (on day 7 after infection). However more detailed studies should be done to prove this claim. Based on the results of present study statistically significant decrease in the total antioxidant capacity was noticed on day 7 after infection in infected rats and significant difference was detected in total antioxidant capacity between the infected rats and the control ones on day 7 after infection. Total antioxidant capacity is based on the cumulative action of all the enzymatic (like SOD, catalase, GPX, etc.) and nonenzymatic antioxidants (like vitamins E and C, glutathione, melatonin, etc.) present in plasma and body fluids, thus providing an integrated parameter rather than the simple sum of measurable antioxidants.

Measuring serum TAC may help in the evaluation of physiological, environmental, and nutritional factors of the redox status in humans. Determining serum TAC may help to identify conditions affecting oxidative status *in vivo*. The measure of TAC considers the cumulative action of all the antioxidants present in serum and body fluids, thus providing an integrated parameter rather than the simple sum of measurable antioxidants. The capacity of known and unknown antioxidants and their synergistic interaction is therefore assessed, thus giving an insight into the delicate balance *in vivo* between oxidants and antioxidants [24]. In the present study GSH level was increased on day 7 after infection but TAC was decreased. Probably other antioxidants have been consumed to compensate and cope with oxidative stress and to prevent injuries from stress and effective infection control. Reduction of TAC is due to oxidative stress and returning to the basic state is probably due to the compatibility with stress. The enhanced production of ROS during infection can pose a threat to biomolecules by oxidation of proteins, damage to nucleic acids, and causing peroxidation of lipids [25]. MDA is a highly reactive aldehyde compound that results from lipid peroxidation of polyunsaturated fatty acids. The production of this aldehyde is used as a biomarker of oxidative stress [26]. In the present study MDA level was increased on day 7 after infection but it was not significant. Overall it seems that on day 7 after infection oxidative stress has occurred but it was not terminated to end product of lipid peroxidation elevation. Engin et al. have suggested that in toxoplasmosis MDA elevation is restricted to intracellular area and serum MDA level does not change [27].

In another point of view some studies have shown that inhibitors of mitochondrial function and inducers of oxidative stress can induce *Toxoplasma* encystment *in vitro* [28, 29]. Based on the present study perhaps antioxidant defense system is one of the effective mechanisms in tachyzoite-bradyzoite interconversion. However this study alone cannot confirm the above hypothesis. Understanding tachyzoite-bradyzoite interconversion process could help in designing new chemotherapeutic agents capable of eliminating tissue cysts. Therefore, further studies are required in this issue.

Competing Interests

The authors declare that they have no competing interests.

Acknowledgments

This study was supported by the research grant provided by Shahid Chamran University of Ahvaz.

References

[1] S.-Y. Wong and J. S. Remington, "Biology of *Toxoplasma gondii*," *AIDS*, vol. 7, no. 3, pp. 299–316, 1993.

[2] J. S. Remington and G. Desmonts, "Toxoplasmosis," in *Infectious Diseases of the Fetus and Newborn Infant*, J. S. Remington and J. O. Klein, Eds., pp. 89–195, WB Saunders, Philadelphia, Pa, USA, 1990.

[3] S. Sánchez-Campos, M. J. Tuñón, P. González, and J. González-Gallego, "Oxidative stress and changes in liver antioxidant enzymes induced by experimental dicroceliosis in hamsters," *Parasitology Research*, vol. 85, no. 6, pp. 468–474, 1999.

[4] K. Boczoń, E. Hadaś, E. Wandurska-Nowak, and M. Derda, "A stimulation of antioxidants in muscles of *Trichinella spiralis* infected rats," *Acta Parasitologica*, vol. 41, no. 3, pp. 136–138, 1996.

[5] S. Abo-Shousha, S. S. Khalil, and E. A. Rashwan, "Oxygen free radical and nitric oxide production in single or combined human schistosomiasis and fascioliasis," *Journal of the Egyptian Society of Parasitology*, vol. 29, no. 1, pp. 149–156, 1999.

[6] P. Sibille, O. Tliba, and C. Boulard, "Early and transient cytotoxic response of peritoneal cells from *Fasciola hepatica*-infected rats," *Veterinary Research*, vol. 35, no. 5, pp. 573–584, 2004.

[7] N. C. Smith, K. S. Ovington, and J. C. Boray, "*Fasciola hepatica*: free radical generation by peritoneal leukocytes in challenged rodents," *International Journal for Parasitology*, vol. 22, no. 3, pp. 281–286, 1992.

[8] H. Denton, C. W. Roberts, J. Alexander, K.-W. Thong, and G. H. Coombs, "Enzymes of energy metabolism in the bradyzoites and tachyzoites of *Toxoplasma gondii*," *FEMS Microbiology Letters*, vol. 137, no. 1, pp. 103–108, 1996.

[9] J. P. Dubey, S. K. Shen, O. C. H. Kwok, and J. K. Frenkel, "Infection and immunity with the RH strain of *Toxoplasma gondii* in rats and mice," *Journal of Parasitology*, vol. 85, no. 4, pp. 657–662, 1999.

[10] V. Lecomte, B. F. F. Chumpitazi, B. Pasquier, P. Ambroise-Thomas, and F. Santoro, "Brain-tissue cysts in rats infected with the RH strain of *Toxoplasma gondii*," *Parasitology Research*, vol. 78, no. 3, pp. 267–269, 1992.

[11] S. Rasti, M. Behrashi, B. Kazemi, A. Fatahian, G. Mousavi, and M. Namakchian, "Diagnosis of congenital toxoplasmosis by polymerase chain reaction," *Indian Journal of Medical Microbiology*, vol. 30, no. 2, p. 251, 2012.

[12] G. Desmonts and J. S. Remington, "Direct agglutination test for diagnosis of *Toxoplasma* infection: method for increasing sensitivity and specificity," *Journal of Clinical Microbiology*, vol. 11, no. 6, pp. 562–568, 1980.

[13] J. P. Dubey and G. Desmonts, "Serological responses of equids fed *Toxoplasma gondii* oocysts," *Equine Veterinary Journal*, vol. 19, no. 4, pp. 337–339, 1987.

[14] G. L. Ellman, "Tissue sulfhydryl groups," *Archives of Biochemistry and Biophysics*, vol. 82, no. 1, pp. 70–77, 1959.

[15] M. A. Koroliuk, L. I. Ivanova, I. G. Maiorova et al., "A method of determining catalase activity," *Laboratornoe Delo*, vol. 1988, no. 1, pp. 16–19, 1988.

[16] I. F. F. Benzie and J. J. Strain, "Ferric reducing/antioxidant power assay: direct measure of total antioxidant activity of biological fluids and modified version for simultaneous measurement of total antioxidant power and ascorbic acid concentration," *Methods in Enzymology*, vol. 299, pp. 15–27, 1998.

[17] Z. A. Placer, L. L. Cushman, and B. C. Johnson, "Estimation of product of lipid peroxidation (malonyl dialdehyde) in biochemical systems," *Analytical Biochemistry*, vol. 16, no. 2, pp. 359–364, 1966.

[18] A. Wochna, E. Niemczyk, C. Kurono et al., "Role of mitochondria in the switch mechanism of the cell death mode from apoptosis to necrosis—studies on ρ^0 cells," *Journal of Electron Microscopy*, vol. 54, no. 2, pp. 127–138, 2005.

[19] R. Dringen and B. Hamprecht, "Involvement of glutathione peroxidase and catalase in the disposal of exogenous hydrogen peroxide by cultured astroglial cells," *Brain Research*, vol. 759, no. 1, pp. 67–75, 1997.

[20] B. Halliwell and J. M. C. Gutteridge, "Antioxidant defense enzymes: the glutathione peroxidase family," in *Free Radicals in Biology and Medicine*, Clarendon Press, Oxford, UK, 3rd edition, 1999, pp. 140–146, 170–172, 1999.

[21] B. Halliwell, "Reactive oxygen species and the central nervous system," *Journal of Neurochemistry*, vol. 59, no. 5, pp. 1609–1623, 1992.

[22] J. W. E. Rush and S. D. Sandiford, "Plasma glutathione peroxidase in healthy young adults: influence of gender and physical activity," *Clinical Biochemistry*, vol. 36, no. 5, pp. 345–351, 2003.

[23] N. Couto, N. Malys, S. J. Gaskell, and J. Barber, "Partition and turnover of glutathione reductase from saccharomyces cerevisiae: a proteomic approach," *Journal of Proteome Research*, vol. 12, no. 6, pp. 2885–2894, 2013.

[24] A. Ghiselli, M. Serafini, F. Natella, and C. Scaccini, "Total antioxidant capacity as a tool to assess redox status: critical view and experimental data," *Free Radical Biology and Medicine*, vol. 29, no. 11, pp. 1106–1114, 2000.

[25] B. Halliwell and S. Chirico, "Lipid peroxidation: its mechanism, measurement, and significance," *The American Journal of Clinical Nutrition*, vol. 57, no. 5, pp. 715–725, 1993.

[26] F. J. Romero, F. Bosch-Morell, M. J. Romero et al., "Lipid peroxidation products and antioxidants in human disease," *Environmental Health Perspectives*, vol. 106, no. 5, pp. 1229–1234, 1998.

[27] A. B. Engin, F. Dogruman-Al, U. Ercin, B. Celebi, C. Babur, and N. Bukan, "Oxidative stress and tryptophan degradation pattern of acute *Toxoplasma gondii* infection in mice," *Parasitology Research*, vol. 111, no. 4, pp. 1725–1730, 2012.

[28] M. Soete, D. Camus, and J. F. Dubrametz, "Experimental induction of bradyzoite-specific antigen expression and cyst formation by the RH strain of *Toxoplasma gondii in vitro*," *Experimental Parasitology*, vol. 78, no. 4, pp. 361–370, 1994.

[29] W. Bohne, "Reduced replication of *Toxoplasma gondii* is necessary for induction of bradyzoite-specific antigens: a possible role for nitric oxide in triggering stage conversion," *Infection and Immunity*, vol. 62, no. 5, pp. 1761–1767, 1994.

Hindawi Publishing Corporation
Oxidative Medicine and Cellular Longevity
Volume 2016, Article ID 2968462, 14 pages
http://dx.doi.org/10.1155/2016/2968462

Research Article

Epigallocatechin-3-gallate Attenuates Renal Damage by Suppressing Oxidative Stress in Diabetic db/db Mice

Xiu Hong Yang,[1] Yu Pan,[2] Xiao Li Zhan,[1] Bao Long Zhang,[3] Li Li Guo,[4] and Hui Min Jin[1]

[1]*Division of Nephrology, Shanghai Pudong Hospital, Fudan University Pudong Medical Center, 2800 Gong Wei Road, Shanghai, China*
[2]*Division of Nephrology, Shanghai No. 9 People's Hospital, Shanghai Jiao Tong University School of Medicine, Shanghai, China*
[3]*The Institutes of Biomedical Sciences (IBS), Fudan University, Shanghai, China*
[4]*Hemodialysis Center, Bao Shan Branch of No. 1 People's Hospital, Shanghai Jiao Tong University, Shanghai, China*

Correspondence should be addressed to Li Li Guo; gflmei@hotmail.com and Hui Min Jin; hmjgli@163.com

Received 22 May 2016; Revised 14 July 2016; Accepted 9 August 2016

Academic Editor: Claudio Cabello-Verrugio

Epigallocatechin-3-gallate (EGCG), extracted from green tea, has been shown to have antioxidative activity. In the present study, we evaluated the effect of EGCG on the kidney function in db/db mice and also tried to investigate the underlying mechanism of the renoprotective effects of EGCG in both animals and cells. EGCG treatment could decrease the level of urinary protein, 8-iso-PGF2a, and Ang II. Moreover, EGCG could also change the level of several parameters associated with oxidative stress. In addition, the protein expression levels of AT-1R, p22-phox, p47-phox, p-ERK1/2, p-p38 MAPK, TGF-β1, and α-SMA in diabetic db/db mice were upregulated, and all of these symptoms were downregulated with the treatment of EGCG at 50 and 100 mg/kg/d. Furthermore, the pathological changes were ameliorated in db/db mice after EGCG treatment. HK-2 cell-based experiments indicated that EGCG could inhibit the expression of MAPK pathways, which is the downstream effector of Ang II mediated oxidative stress. All these results indicated that EGCG treatment could ameliorate changes of renal pathology and delay the progression of DKD by suppressing hyperglycemia-induced oxidative stress in diabetic db/db mice.

1. Introduction

Based on the survey of International Diabetes Federation (IDF), the number of people with diabetes mellitus (DM) was as high as 415.0 million in 2015 all over the world [1]. In China, there are more than 98.4 million patients with diabetes in 2013, ranking first in the world, and the number is estimated to reach 143.0 million in 2035 [1]. Diabetes, a worldwide health problem, is defined as a group of metabolic diseases characterized by hyperglycemia. Diabetes is always associated with long-term damage, dysfunction, and failure of different organs, leading to the development of several complications [2, 3]. Diabetic kidney disease (DKD) is a kind of chronic microvascular complications associated with diabetes, and 40% or more diabetic patients have developed DKD despite current treatments [2, 3]. DKD is also a major cause of chronic renal failure [2, 3]. Therefore, it is of great importance to find new approaches to delay the progression of DKD so as to reduce the number of dialysis patients.

Several recent studies have suggested that oxidative stress is involved in the procession and development of kidney injury, including DKD [2, 4–6]. Oxidative stress refers to the increase of reactive oxygen species (ROS) production and/or the decrease of antioxidant production disordering the balance between oxidation and antioxidation, leading to renal injury [2, 6]. Through multiple mechanisms, ROS can cause kidney damage, such as inducing the expression of angiotensin II (Ang II), increasing the production of transforming growth factor-β1 (TGF-β1) and smooth muscle actin-α (α-SMA), and activating the mitogen-activated protein kinase (MAPK) cascade [7–12]. In addition, it has been demonstrated that the major source for the generation of ROS is nicotinamide adenine dinucleotide phosphate (NADPH) oxidase in diabetic conditions [5, 6, 13–15]. As reported

previously, NADPH oxidase inhibitor can effectively restrain ROS generation, reduce the level of urinary protein, ameliorate the pathological changes of kidney, and delay the progression of DKD in the type 2 diabetic rat model [13].

Drinking tea is a common habit for Chinese people, which has a long history in China. Epigallocatechin-3-gallate (EGCG), a kind of green tea extract, is the major polyphenolic constituent present in green tea. Since it has been suggested to have anti-inflammatory, antioxidative, and hypoglycemic effects, EGCG has become a research hotpot in recent years [16–19]. But EGCG has been shown to exert prooxidative activities in some other studies [20, 21]. To date, a variety of studies have demonstrated that EGCG has salutary effects, but the precise mechanisms of EGCG are still unclear in DKD.

Therefore, we performed the present study to evaluate the effect of EGCG on the kidney function in db/db mice. Additionally, we also tried to investigate the underlying mechanism of the renoprotective effects of EGCG in both animals and cells.

2. Materials and Methods

2.1. Animals and Experimental Groups. Eight-week-old C57BLKS/J db/db mice (type 2 diabetic mice model) and their normal mice were purchased from Model Animal Research Center of Nanjing University (Nanjing, Jiangsu, China). The average weight of db/db mice was 33.7 ± 1.5 g. All the animal experimental procedures were approved by the Animal Care Committee of Fudan University. Mice were housed in plastic cages with a controlled temperature of 23–26°C, humidity of 50–55%, and a 12 h light/dark cycle. All the mice had free access to food and distilled water.

EGCG (>90% purity) was obtained from Sigma-Aldrich (St. Louis, MO, USA). Then Mice were allocated into 4 groups with the following treatment ($n = 16$, each): (1) normal, C57BLKS/J normal nontreated mice (gavage administration of 0.9% saline); (2) control, C57BLKS/J db/db nontreated mice (gavage administration of 0.9% saline); (3) EGCG A, C57BLKS/J db/db treated mice (gavage administration of EGCG 50 mg/kg/d); and (4) EGCG B, C57BLKS/J db/db treated mice (gavage administration of EGCG 100 mg/kg/d). The doses of EGCG were based on the previous researches [22]. Mice were sacrificed at week 4 and at week 8, with 8 animals killed each time in each group, respectively.

2.2. Oral Glucose Tolerance Test (OGTT). After fasting for 16 h, a basal blood sample was collected from the tip of the tail of mice ($t = 0$ min). Then mice from all groups were subjected to an OGTT. Briefly, animals were given glucose (1 g/kg) by gavage and blood samples were collected from the tail vein of mice at 0, 15, 30, 60, 90, and 120 minutes after administration for the measurement of glucose. Fasting blood glucose concentration was measured with the OneTouch Basic glucose meter (LifeScan Canada Ltd., Burnaby, BC, Canada) and fasting plasma insulin was measured with mouse insulin ELISA kits (Crystal Chem, Downers Grove, IL, USA).

2.3. Measurement of Urine Protein, 8-Iso-prostaglandin F2α (8-Iso-PGF2a), and Ang II in the Renal Homogenate. Mice, one per metabolic cage, were placed for 24 h urine collection. Urine samples from all mice were centrifuged at 12000 rpm for 5 minutes. Then, the clear supernatant from urine samples was collected and stored at −80°C for further analysis. The 24-hour urinary protein was determined by Coomassie Blue Plus Protein Assay Kit (Pierce, Rockford, IL, USA). Moreover, renal Ang II concentration was measured with Mouse Angiotensin II Elisa Kit, which was obtained from USCN Life Science, Inc. (Wuhan, Hubei, China). Furthermore, 8-iso-PGF2a concentration in urine was measured by a commercial ELISA kit (Cayman, Ann Arbor, MI, USA).

2.4. Measurement of Reactive Oxygen Species (ROS), 8-Hydroxy-2′-deoxyguanosine (8-OHdG), Superoxide Dismutase (SOD), Malondialdehyde (MDA), Catalase (CAT), and 3-Nitrotyrosine Concentration in Kidney Homogenates. After animals were killed, the kidney was excised immediately and placed in ice-cold RIPA buffer (CST, Beverly, MA, USA) for homogenization using a tissue homogenizer. After centrifugation, supernatant was collected and used for analysis of generation of following parameters in kidney homogenates: ROS level was detected by a fluorometric assay using the 2′7′-dichlorodihydrofluorescein diacetate (DCFH-DA, Sigma-Aldrich, St. Louis, MO, USA) as a fluorescence probe; the levels of SOD, MDA, CAT, and 8-OHdG in kidney were measured with commercial kits (Nanjing Jiancheng, Nanjing, Jiangsu, China); and 3-nitrotyrosine, a marker for oxidative stress in the kidney, was detected by ELISA using a commercial kit (Millipore, Bedford, MA, USA).

2.5. Cell Cultures and Treatments. HK-2 cells, a line of human renal proximal tubular epithelial cells obtained from Bioresource Collection and Research Center (BCRC), were maintained in Dulbecco's modified Eagle's medium (DMEM; Invitrogen, Carlsbad, CA, USA) supplemented with 10% fetal bovine serum (FBS, HyClone, South Logan, UT, USA) and 2% antibiotics (HyClone, South Logan, UT, USA). The medium was changed every three days. When HK-2 cells grew to 80% confluence, they were cultured in serum-free medium for 24 h.

To investigate the underlying mechanism of renoprotective effects of EGCG, cells were randomly divided into 4 groups: (1) untreated group, (2) Ang II group (cells were treated with 1 μM Ang II), (3) Ang II + EGCG A group (cells were first treated with 15 μM EGCG for 6 h, followed by 1 μM Ang II for 24 h), and (4) Ang II + EGCG B group (cells were first treated with 30 μM EGCG for 6 h, followed by 1 μM Ang II for 24 h). In addition, we also explored the role of PD98059 (ERK1/2 inhibitor, Sigma-Aldrich, St Louis, MO, USA) and SB202190 (p38 MAPK inhibitor, Sigma-Aldrich, St Louis, MO, USA) in Ang II mediated renal fibrosis; cells were then divided into five groups: (1) untreated group, (2) Ang II group (cells were treated with 1 μM Ang II), (3) Ang II + PD98059 group (cells were first treated with 10 mM PD98059 for 6 h, followed by 1 μM Ang II for 24 h), (4) Ang II + SB202190 group (cells were first treated with 10 mM SB202190 for 6 h, followed by 1 μM Ang II for 24 h), and (5) Ang II + both

groups (cells were first treated with 10 mM SB202190 and 10 mM PD98059 for 6 h, followed by 1 μM Ang II for 24 h Ang II). The doses of Ang II, EGCG, PD98059, and SB202190 were based on the previous researches [23, 24].

2.6. Western Blot Analysis. All protein samples of both kidney tissue and cultured HK-2 cells were centrifuged at 14000 rpm for 10 minutes, and the clear supernatants were collected. Total protein concentrations in the supernatants were determined by the BCA method. Then, the protein was boiled at 98°C for 5 to 10 minutes and stored at −80°C for later analysis.

Total of 45 μg protein (per sample) was electrophoresed via 10 or 12% SDS-PAGE and transferred onto nitrocellulose membranes (Bio-Rad, CA, USA). The membranes were then blocked with 5% nonfat milk or 5% BAS (bovine serum albumin) power and blocking buffer (1x Tris buffered saline and 0.1% Tween 20, Ph 7.4) at room temperature for 1 hour and next incubated with rabbit-anti-mouse primary antibodies overnight at 4°C: Ang II type 1 receptor (AT-1R, 1 : 1000), NADPH oxidase 1 (NOX-1, 1 : 1000), NOX-4 (1 : 1000), p22-phox (1 : 1000), p47-phox (1 : 1000), extracellular regulated protein kinases 1/2 (ERK1/2, 1 : 1000), p-ERK1/2 (1 : 1000), p38 MAPK (1 : 1000), p-p38 MAPK (1 : 500), TGF-β1 (1 : 100), α-SMA (1 : 100), and GAPDH (1 : 1000). The next day, after washing with Tris buffered saline for three times for 30 minutes (changed every 10 minutes), the membranes were incubated for 1 hour at room temperature with secondary antibodies (horseradish peroxidase-conjugated anti-rabbit IgG, 1 : 2000). For Western blot, the primary antibodies against AT-1R, p22-phox, p47-phox, TGF-β1, α-SMA, and GAPDH were purchased from Santa Cruz Biotechnology (Santa Cruz, CA, USA); those against p-ERK1/2, ERK1/2, p-p38 MAPK, p38 MAPK, and secondary antibodies were obtained from Cell Signaling Technology, Inc. (Beverly, MA, USA); antibodies against NOX1 and NOX4 were obtained from Abcam Company (Cambridge, MA, USA). Finally, the protein bands were visualized using SuperSignal West Femto Substrate (Pierce, Rockford, IL, USA).

2.7. Histopathology and Immunohistochemistry of Kidney. Histopathology and immunohistochemistry of kidney were performed as described previously [25]. The kidney tissue sections were kept in 4% paraformaldehyde solution and paraffin-embedded and then were cut into 3 μM thickness. The renal pathological changes were examined by Periodic Acid-Schiff (PAS) staining. The expressions of TGF-β1 (1 : 100) and α-SMA (1 : 100) were evaluated by immunohistochemistry. The percentage of positive staining area was quantified using Image-Pro Plus 6.0 software (Media Cybernetics, Silver Spring, MD, USA).

2.8. Statistical Analysis. The Stata 10.0 statistical software (Stata) was used for all statistical analysis. Results were expressed as means ± SEM. Differences among groups were subjected to a one-way analysis of variance (ANOVA) and $P < 0.05$ was considered significantly different.

3. Results

3.1. Detection of Body Weight (BW), Kidney Weight/Body Weight (KW/BW), Fasting Plasma Glucose, and Insulin Levels in Mice from Different Groups. Table 1 shows the changes in BW, KW/BW, the level of glucose, and insulin level in plasma of mice after administration by gavage with or without EGCG. At baseline, the BW of db/db mice was higher than normal mice. At four and eight weeks after oral administration of EGCG, the BW of db/db mice was still higher than normal mice, and there was no significant difference in db/db mice of each group. However, db/db mice treated with EGCG at 50 and 100 mg/kg/d had a significantly lower KW/BW when compared to nontreated db/db mice ($P < 0.01$). Compared with the normal group, the blood glucose level of db/db mice was obviously higher, which persistently increased during the whole study, whereas the level of fasting plasma glucose was obviously decreased ($P < 0.01$) and the level of fasting plasma insulin was significantly increased ($P < 0.01$) in db/db mice treated with EGCG compared to nontreated db/db mice ($P < 0.01$) after the treatment for 4 and 8 weeks.

In addition, the area under the curve (AUC) for OGTT in db/db mice was also higher than normal group, yet the AUC was significantly lower in db/db mice with the treatment of EGCG than nontreated db/db mice (Figures 1(a), 1(b), 1(c), and 1(d), $P < 0.05$). Furthermore, the AUC of db/db mice treated with EGCG at 100 mg/kg/d was lower in comparison with the group of db/db mice treated with EGCG at 50 mg/kg/d after the oral administration for 8 weeks (Figures 1(c) and 1(d), $P < 0.05$).

3.2. Changes in Urine Protein, 8-Iso-PGF2a, and Renal Homogenate Ang II after Different Treatment. Urine collection was performed 24 h after treatment in mice and levels of urine protein, 8-iso-PGF2a in urine, and Ang II of kidney were summarized in Table 2. The level of 24 h urine protein was reduced remarkably in db/db mice treated with EGCG compared to nontreated db/db mice during 8-week period ($P < 0.05$). Equally, EGCG treatment significantly decreased the level of 8-iso-PGF2a in urine compared to the nontreated db/db mice ($P < 0.05$). The significant decrease in Ang II level in kidney was also observed in db/db mice treated with EGCG compared to nontreated db/db mice ($P < 0.05$).

3.3. Changes in ROS, 8-OHdG, SOD, MDA, CAT, and 3-Nitrotyrosine in Kidney Homogenates in Mice after Different Treatment. We also explored the changes of several parameters in kidney homogenates in mice from different groups and the results were displayed in Table 3. Compared to the normal mice, there were significant changes (significant increase or decrease) in ROS, 8-OHdG, SOD, MDA, CAT, and 3-nitrotyrosine levels in db/db mice ($P < 0.05$). However, EGCG treatment (both concentrations of 50 mg/kg/d and 100 mg/kg/d) could obviously ameliorate the changes in the level of above parameters in db/db mice ($P < 0.05$) during the 8-week study period.

Table 1: Changes in BW, KW/BW, glucose, and insulin levels in mice after different treatment.

	Normal	Control	EGCG A	EGCG B
BW (g)				
Baseline	25.2 ± 0.6	33.2 ± 0.8$^{\#\#}$	33.4 ± 1.0$^{\#\#}$	33.3 ± 1.1$^{\#\#}$
Week 4	31.4 ± 1.3	39.8 ± 1.4$^{\#\#}$	38.9 ± 1.9$^{\#\#}$	39.5 ± 1.7$^{\#\#}$
Week 8	35.3 ± 1.1	45.6 ± 1.2$^{\#\#}$	44.2 ± 1.8$^{\#\#}$	44.3 ± 3.1$^{\#\#}$
KW/BW (mg/g)				
Baseline	3.5 ± 0.4	6.5 ± 0.2$^{\#\#}$	6.3 ± 0.5$^{\#\#}$	6.4 ± 0.4$^{\#\#}$
Week 4	3.6 ± 0.4	8.1 ± 0.3$^{\#\#}$	7.1 ± 0.8$^{\#\#**}$	7.3 ± 0.1$^{\#\#**}$
Week 8	4.0 ± 0.6	8.4 ± 0.1$^{\#\#}$	7.4 ± 0.2$^{\#\#**}$	7.5 ± 0.1$^{\#\#**}$
Glucose (mmol/L)				
Baseline	4.9 ± 0.3	11.5 ± 0.9$^{\#\#}$	11.3 ± 1.1$^{\#\#}$	11.5 ± 1.1$^{\#\#}$
Week 4	4.5 ± 0.9	15.1 ± 0.5$^{\#\#}$	12.8 ± 1.0$^{\#\#**}$	12.1 ± 0.6$^{\#\#**}$
Week 8	4.7 ± 0.8	17.2 ± 0.8$^{\#\#}$	14.4 ± 1.0$^{\#\#**}$	14.2 ± 0.7$^{\#\#**}$
Insulin (ng/mL)				
Baseline	3.3 ± 1.3	5.6 ± 1.4$^{\#}$	5.4 ± 1.1$^{\#}$	5.7 ± 0.8$^{\#}$
Week 4	3.2 ± 0.7	5.5 ± 1.1$^{\#}$	7.8 ± 0.8$^{\#\#*}$	8.0 ± 0.9$^{\#\#**}$
Week 8	3.5 ± 1.1	5.2 ± 1.7$^{\#}$	11.2 ± 2.2$^{\#\#**}$	12.4 ± 1.6$^{\#\#**}$

Note: normal, C57BLKS/J normal nontreated mice; control, C57BLKS/J db/db nontreated mice; EGCG A, db/db mice treated with EGCG of 50 mg/kg/d; EGCG B, db/db mice treated with EGCG of 100 mg/kg/d; BW, body weight; KW/BW, kidney weight/body weight; glucose, fasting plasma glucose; insulin, fasting plasma insulin; $^{\#}P < 0.05$ and $^{\#\#}P < 0.01$ versus normal; $^{*}P < 0.05$ and $^{**}P < 0.01$ versus control; values are means ± SEM. At baseline and at week 4, $n = 16$ in each group; at week 8, $n = 8$ in each group.

Table 2: Changes of 24-hour urinary protein, urinary 8-iso-PGF2a, and renal Ang II levels in urine 24 h after different treatment.

	Normal	Control	EGCG A	EGCG B
24-hour urinary protein (mg)				
Baseline	1.2 ± 0.3	5.8 ± 0.6$^{\#\#}$	5.9 ± 0.9$^{\#\#}$	5.7 ± 1.1$^{\#\#}$
Week 4	1.1 ± 0.7	7.5 ± 0.2$^{\#\#}$	6.7 ± 0.1$^{\#\#**}$	6.7 ± 0.5$^{\#\#**}$
Week 8	1.3 ± 0.5	11.9 ± 1.3$^{\#\#}$	8.8 ± 1.0$^{\#\#*}$	8.6 ± 1.1$^{\#\#*}$
Urinary 8-iso-PGF2a (ng/d)				
Baseline	38.5 ± 5.3	84.6 ± 8.5$^{\#\#}$	87.2 ± 11.3$^{\#\#}$	86.8 ± 12.1$^{\#\#}$
Week 4	39.8 ± 3.6	150.4 ± 11.9$^{\#\#}$	107.3 ± 12.1$^{\#\#**}$	110.6 ± 9.2$^{\#\#**}$
Week 8	38.7 ± 4.4	176.8 ± 10.1$^{\#\#}$	138.5 ± 8.3$^{\#\#**}$	126.7 ± 9.5$^{\#\#**}$
Renal Ang II (ng/L)				
Baseline	177.6 ± 20.2	238.3 ± 14.2$^{\#\#}$	240.5 ± 19.8$^{\#\#}$	238.9 ± 16.6$^{\#\#}$
Week 4	182.4 ± 12.1	346.2 ± 22.7$^{\#\#}$	297.5 ± 15.5$^{\#\#*}$	308.9 ± 7.3$^{\#\#*}$
Week 8	191.3 ± 23.9	405.8 ± 7.2$^{\#\#}$	367.4 ± 5.4$^{\#\#**}$	383.7 ± 9.6$^{\#\#*}$

Note: normal, C57BLKS/J normal nontreated mice; control, C57BLKS/J db/db nontreated mice; EGCG A, db/db mice treated with EGCG of 50 mg/kg/d; EGCG B, db/db mice treated with EGCG of 100 mg/kg/d; urinary 8-iso-PGF2a, urinary 8-iso-prostaglandin F2α; Ang II: the renal angiotensin II concentration; $^{\#\#}P < 0.01$ versus normal; $^{*}P < 0.05$ and $^{**}P < 0.01$ versus control; values are means ± SEM. At baseline and at week 4, $n = 16$ in each group; at week 8, $n = 8$ in each group.

3.4. Changes in Expression of AT-1R, TGF-β1, p22-phox, and p47-phox in Kidney Tissue in Mice after Different Treatment. As shown in Table 2, the renal Ang II level was increased in mice after treatment with EGCG. Moreover, we also explored the effects of EGCG on AT-1R, which is the receptor of Ang II. Following our results, the level of AT-1R was significantly downregulated in mice after oral administration of EGCG for 4 and 8 weeks (Figures 2(a) and 2(c), $P < 0.01$). Therefore, EGCG may play a role similar to Ang II type 1 receptor blocker. Likewise, the protein expression level of TGF-β1 in renal tissue was also obviously downregulated after treatment of EGCG (Figures 2(a) and 2(b), $P < 0.01$).

Hyperglycemia-induced oxidative stress plays an important role in the procession and development of DKD, which was confirmed by Western blot analysis in our study. Compared with the normal group, p22-phox and p47-phox (both were NADPH oxidase subunits) were upregulated in nontreated db/db mice, while EGCG treatment significantly reduced the protein expression of p22-phox and p47-phox in db/db mice (Figures 3(a), 3(b), and 3(c), $P < 0.05$).

3.5. Changes in the Expression of MAPK Signaling Pathway. Given that the oxidative stress may activate the MAPK cascade, we explored the changes in expression of p-ERK1/2 and

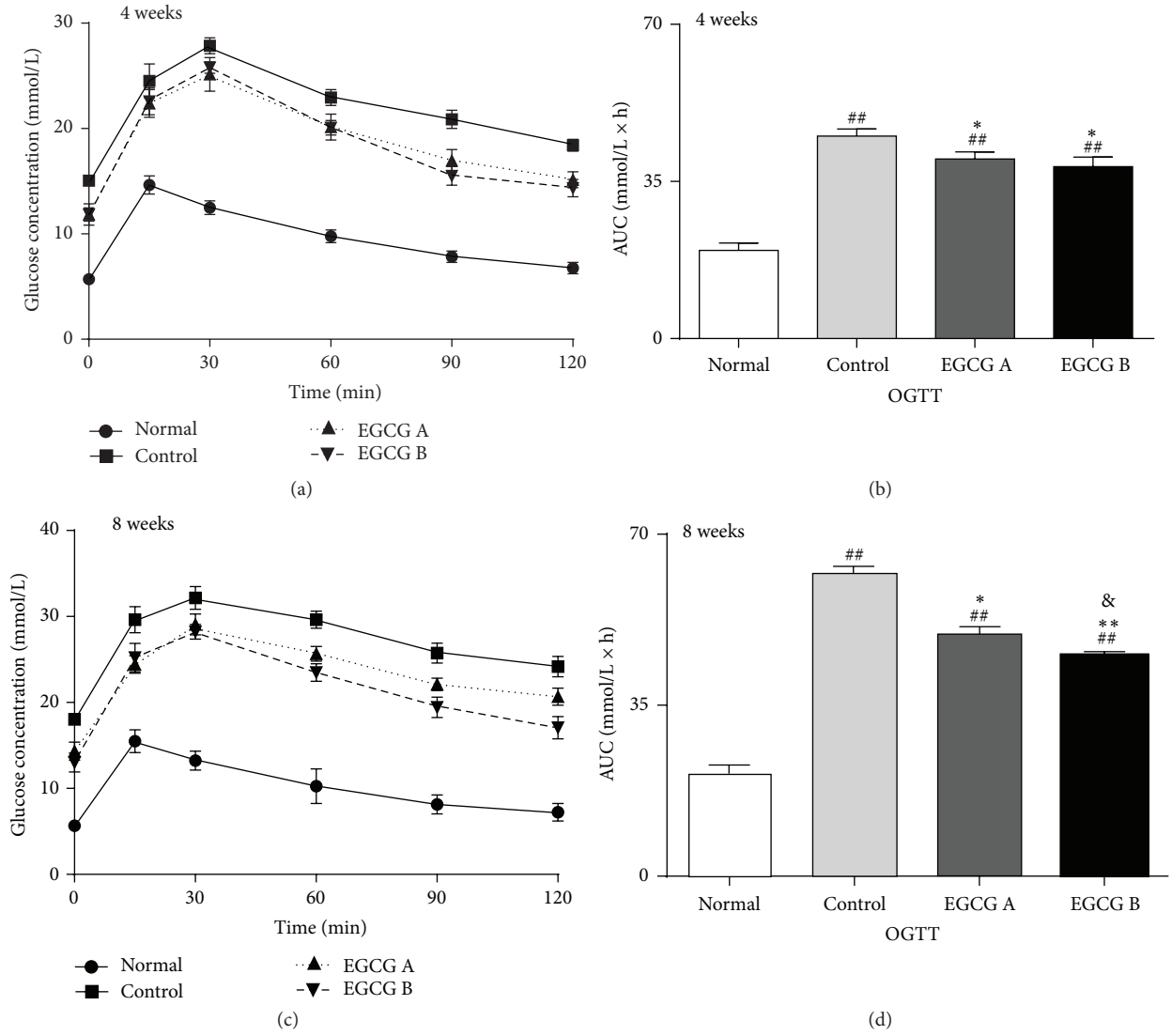

Figure 1: Glucose metabolic profile in db/db mice versus control mice. Diabetic db/db mice were treated with or without EGCG for 4 or 8 weeks, and OGTT (glucose, 1 g/kg) were performed. Glucose concentrations (a and c) and the AUC of OGTT (b and d) were shown. Normal: nontreated C57BL mice; control: C57BLKS/J db/db nontreated mice; EGCG A, db/db mice treated with EGCG of 50 mg/kg/d; EGCG B, db/db mice treated with EGCG of 100 mg/kg/d; values are means ± SEM. $^{\#\#}P < 0.01$ versus normal; $^{*}P < 0.05$ and $^{**}P < 0.01$ versus control; $^{\&}P < 0.05$ versus EGCG A. At week 4, $n = 16$ in each group; at week 8, $n = 8$ in each group.

p-p38 MAPK (both are important members of MAPK family) in kidney tissue in mice after EGCG treatment (Figure 4(a)). In this study, we found that the protein expressions of p-ERK1/2 and p-p38 MAPK were obviously increased in nontreated db/db mice compared to those in the kidney tissue in normal mice, and both of them were significantly reduced in mice after treatment of EGCG (Figures 4(b) and 4(c), $P < 0.05$).

3.6. EGCG Ameliorated Renal Damage and Fibrosis in db/db Mice. The renoprotective effects of EGCG in ameliorating renal damage and fibrosis were investigated by PAS and immunohistochemical staining (Figures 5(a), 5(b), and 5(c)). Compared to the normal mice, there was an increase of glomerular volume and mesangial matrix expansion, and EGCG treatment could attenuate these histological changes in db/db mice confirmed by PAS staining (Figure 5(a)). Results from statistical analysis indicated that EGCG could significantly reduce mesangial matrix index in db/db mice (Figure 5(d), $P < 0.05$). Additionally, the expression levels of TGF-β1 and α-SMA, which were associated with the development of fibrosis, were significantly downregulated after EGCG treatment in db/db mice compared to those in nontreated mice (Figures 5(b), 5(c), and 5(e), $P < 0.05$).

3.7. Effects of EGCG on Ang II Induced Renal Kidney Injury in HK-2 Cells. To explore the underlying mechanism of EGCG in renoprotection, we investigated the role of EGCG in Ang II mediated renal injury pathway in HK-2 cells. Following our results in Figure 6, after intervention with EGCG, the

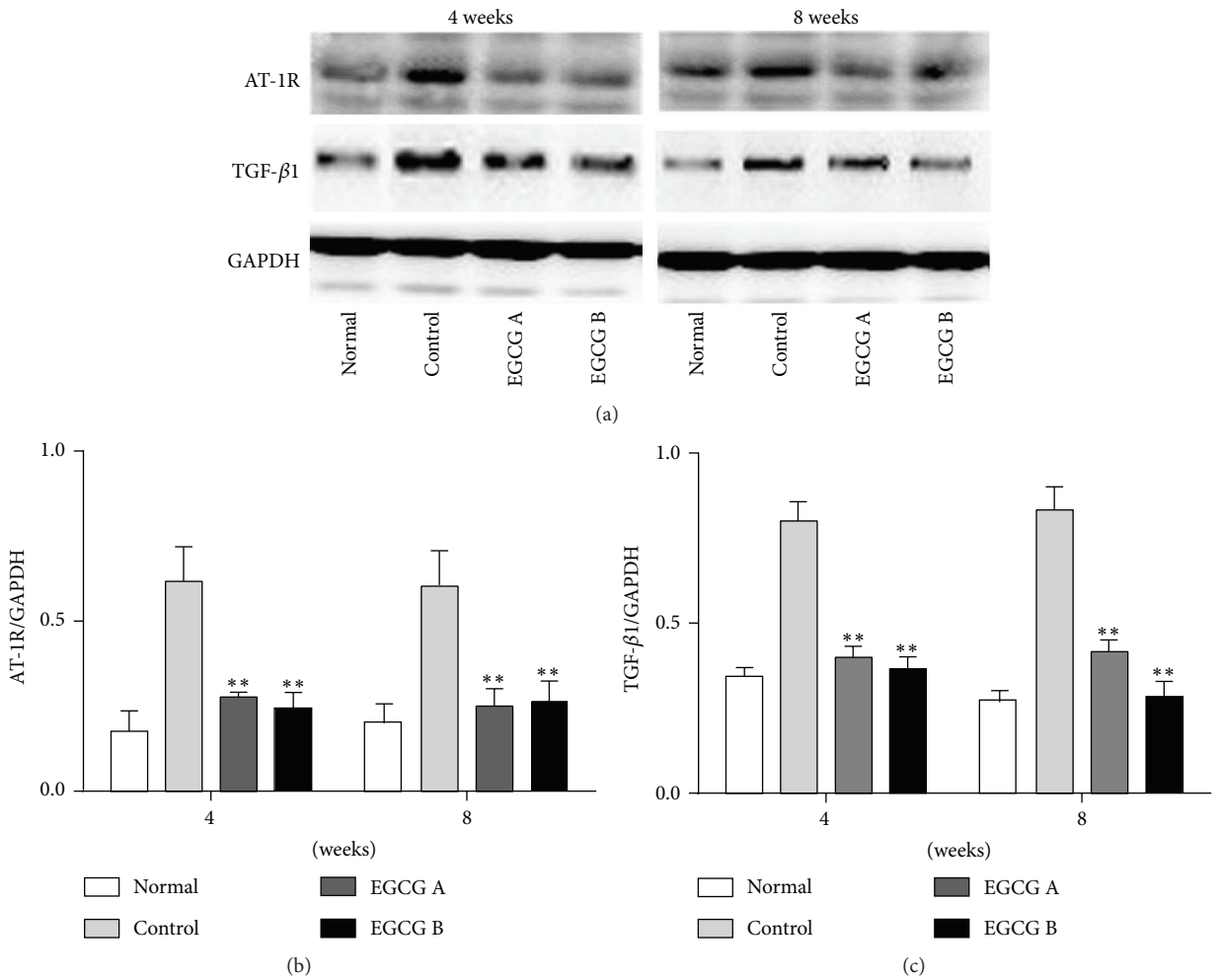

Figure 2: The protein expressions of AT-1R (b) and TGF-β1 (c) in renal tissue of mice detected by Western blot. Normal: nontreated C57BL mice; control: C57BLKS/J db/db nontreated mice; EGCG A, db/db mice treated with EGCG of 50 mg/kg/d; EGCG B, db/db mice treated with EGCG of 100 mg/kg/d; values are means ± SEM. $^{**}P < 0.01$ versus control. At both week 4 and week 8, $n = 8$ in each group.

increased expression of NOX-1 (Figures 6(a) and 6(b)), NOX-4 (Figures 6(a) and 6(b)), p22-phox (Figures 6(a) and 6(c)), p47-phox (Figures 6(a) and 6(c)), p-ERK1/2 (Figures 6(a) and 6(d)), p-P38 MAPK (Figures 6(a) and 6(e)), TGF-β1 (Figures 6(a) and 6(f)), and α-SMA (Figures 6(a) and 6(f)) induced by Ang II was significantly downregulated ($P < 0.05$). We also explored the role of PD98059 and SB202190 in Ang II mediated renal fibrosis. Based on our results, PD98059 and SB202190 can significantly decrease the expression of p-ERK1/2 (Figures 7(a) and 7(b)), p-P38 MAPK (Figures 7(a) and 7(c)), TGF-β1 (Figures 7(a) and 7(d)), and α-SMA (Figures 7(a) and 7(e)) even in the presence of Ang II ($P < 0.05$). Hence, EGCG is supposed to play a role in Ang II induced renal injury similar to PD98059 and SB202190.

4. Discussion

In this study, we founded that EGCG treatment at 50 or 100 mg/kg/d for 4 and 8 weeks could decrease the level of plasma glucose and also increase the level of plasma insulin in db/db mice. Moreover, 24 h urinary protein, 8-iso-PGF2a, and renal Ang II levels were also reduced by EGCG treatment. EGCG could also change the level of several parameters in renal homogenate including ROS, 8-OHdG, SOD, MDA, CAT, and 3-nitrotyrosine in db/db mice. In addition, EGCG treatment at dose of 50 and 100 mg/kg/d could also downregulate the expression of several factors involved in the signaling pathways activated by ROS production, including AT-1R, p22-phox, p47-phox, p-ERK1/2, p-p38 MAPK, TGF-β1, and α-SMA. Meanwhile, the pathological changes in diabetic db/db mice such as renal injury and fibrosis could be also ameliorated after EGCG treatment. Thus, we supposed that EGCG, a constituent of green tea, had beneficial effects on the kidney of diabetic db/db mice.

To date, numerous studies have suggested that oxidative stress can lead to kidney injury and accelerate the procession and development of DKD [2, 4–6]. Oxidative stress of DKD is mainly derived from hyperglycemia. Hence, controlling hyperglycemia is supposed to be an effective approach to slow the procession and development of DKD. Previous studies

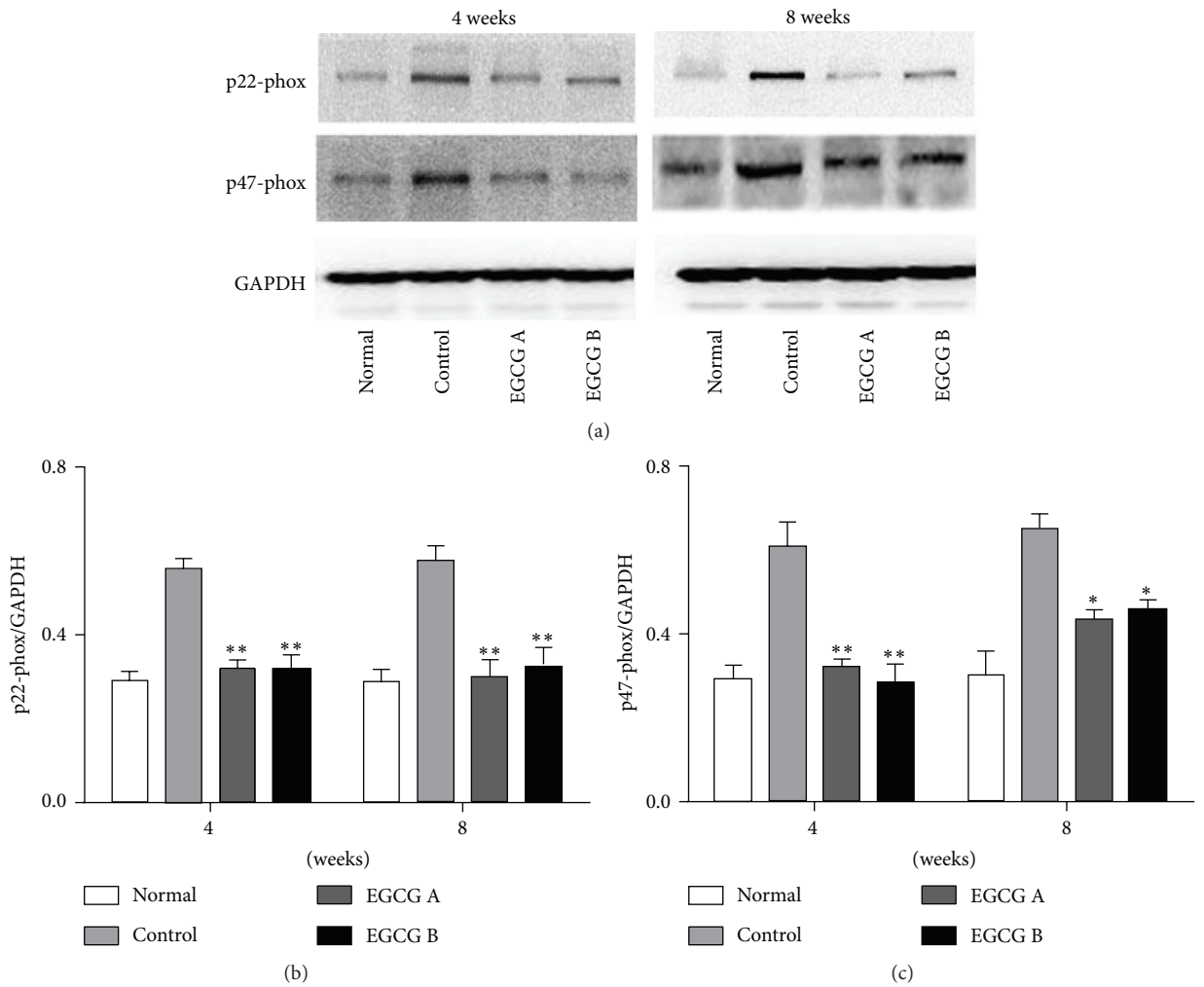

Figure 3: The protein expressions of p22-phox (b) and p47-phox (c) in renal tissue of mice detected by Western blot. Normal: nontreated C57BL mice; control: C57BLKS/J db/db nontreated mice; EGCG A, db/db mice treated with EGCG of 50 mg/kg/d; EGCG B, db/db mice treated with EGCG of 100 mg/kg/d; values are means ± SEM. $^{*}P < 0.05$ and $^{**}P < 0.01$ versus control. At both week 4 and week 8, $n = 8$ in each group.

have shown that EGCG has antihyperglycemia effect [16, 19, 26]. However, results from our study demonstrated that EGCG plays a role in regulating glycol metabolism. The level of fasting plasma glucose was decreased and the level of fasting plasma insulin was increased in db/db mice after treatment of EGCG. Furthermore, the AUC was significantly lower in db/db mice treated with EGCG compared to non-treated db/db mice. Interestingly, all these beneficial effects of EGCG were not obviously dose-dependent. On the other hand, there was no significant difference between the doses of 50 mg/kg/d and 100 mg/kg/d.

ROS production is a major process of oxidative stress, which has been shown to participate in DKD through various mechanisms, such as stimulating the expression of Ang II, inducing the production of TGF-β1 and α-SMA, and activating the MAPK cascade [7–11].

DKD is once considered to be caused by combined effects of hemodynamic changes and metabolic factors. This theory cannot clearly elucidate the pathogenesis of DKD, while hemodynamic factors are supposed to play an important role in the development of DKD [27, 28] learning from it. As described previously, the hemodynamic changes in kidney are related to the progression of DKD, and ROS takes part in these changes of renal hemodynamics in diabetic conditions, which stimulates the expression of renin angiotensin system (RAS) [27, 29, 30]. ROS-induced activation of Ang II, a crucial component of RAS, is able to increase intraglomerular pressure and activate the intracellular second messengers, which eventually results in the upregulation of urinary protein and renal fibrosis [31]. In addition, the increased level of Ang II accelerates the production of ROS [7]. AT-1R, the important receptor of Ang II, has been shown to play a significant role in increasing the urinary protein level [32]. It has been reported that, in diabetic conditions, there is a vicious circle: ROS-angiotensinogen-Ang II-AT-1R-ROS [33]. Moreover, studies have confirmed that AT-1R blocker remarkably alleviated the level of urinary protein of DKD patients [33]. Based on the results from our study, EGCG not only obviously

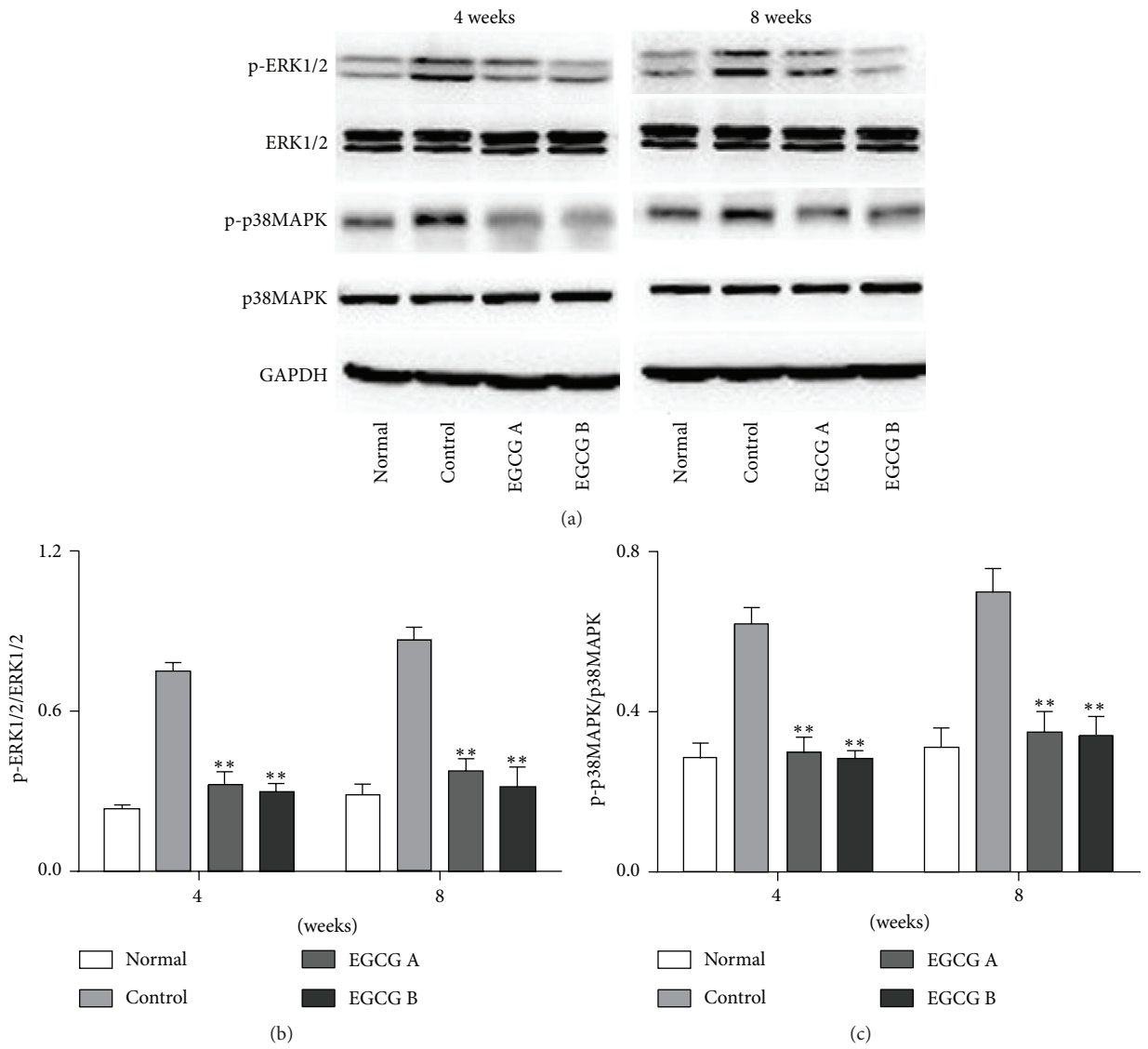

Figure 4: The protein expression of p-ERK1/2 (b) and p-P38 MAPK (c) in renal tissue of mice detected by Western blot. Normal: nontreated C57BL mice; control: C57BLKS/J db/db nontreated mice; EGCG A, db/db mice treated with EGCG of 50 mg/kg/d; EGCG B, db/db mice treated with EGCG of 100 mg/kg/d; values are means ± SEM. $^{**}P < 0.01$ versus control. At both week 4 and week 8, $n = 8$ in each group.

inhibited the level of ROS-induced Ang II expression in the renal homogenate but also significantly suppressed the protein expression of AT-1R. The effect of EGCG on AT-1R has been reported in only two studies. One study indicated that EGCG significantly reduced the expression of AT-1R mRNA in the liver of SHRSP-ZF rats [34], and the other demonstrated that EGCG could restore AT-1R mRNA expression to normal level which was decreased by Ang II stimulation in rat cardiac fibroblasts. In this study, it was the first time to show that EGCG decreased the protein expression of AT-1R in renal tissues of DKD [35]. Hence, EGCG may function as an AT-1R blocker. Further study should be performed to compare the effects of EGCG with olmesartan (AT-1R specific blocker) on kidney pathological changes in db/db mice.

Oxidative stress is considered the major culprit in kidney tissues. NADPH oxidase is abundantly distributed in mesangial cells, and renal tubular cells are also the targeted cells of ROS. ROS can induce the apoptosis of both mesangial cells and tubular cells in kidney, leading to pathological changes, eventually causing glomerular sclerosis and tubulointerstitial fibrosis. Studies have demonstrated that a major source for generation of ROS is NADPH oxidase in high-glucose conditions [5, 6, 13–15]. It has been reported that NADPH oxidase inhibitor can effectively inhibit the generation of ROS and delay the progression of DKD in the type 2 diabetic rat model [13]. In this study, our data demonstrated that the protein expression levels of p22-phox and p47-phox were significantly decreased in db/db mice after EGCG treatment. Similarly, the pathological changes in kidney were alleviated in mice after the oral administration with EGCG. Furthermore, the levels of 24 h urinary protein and 8-iso-PGF2a and renal Ang II were also reduced with the treatment of

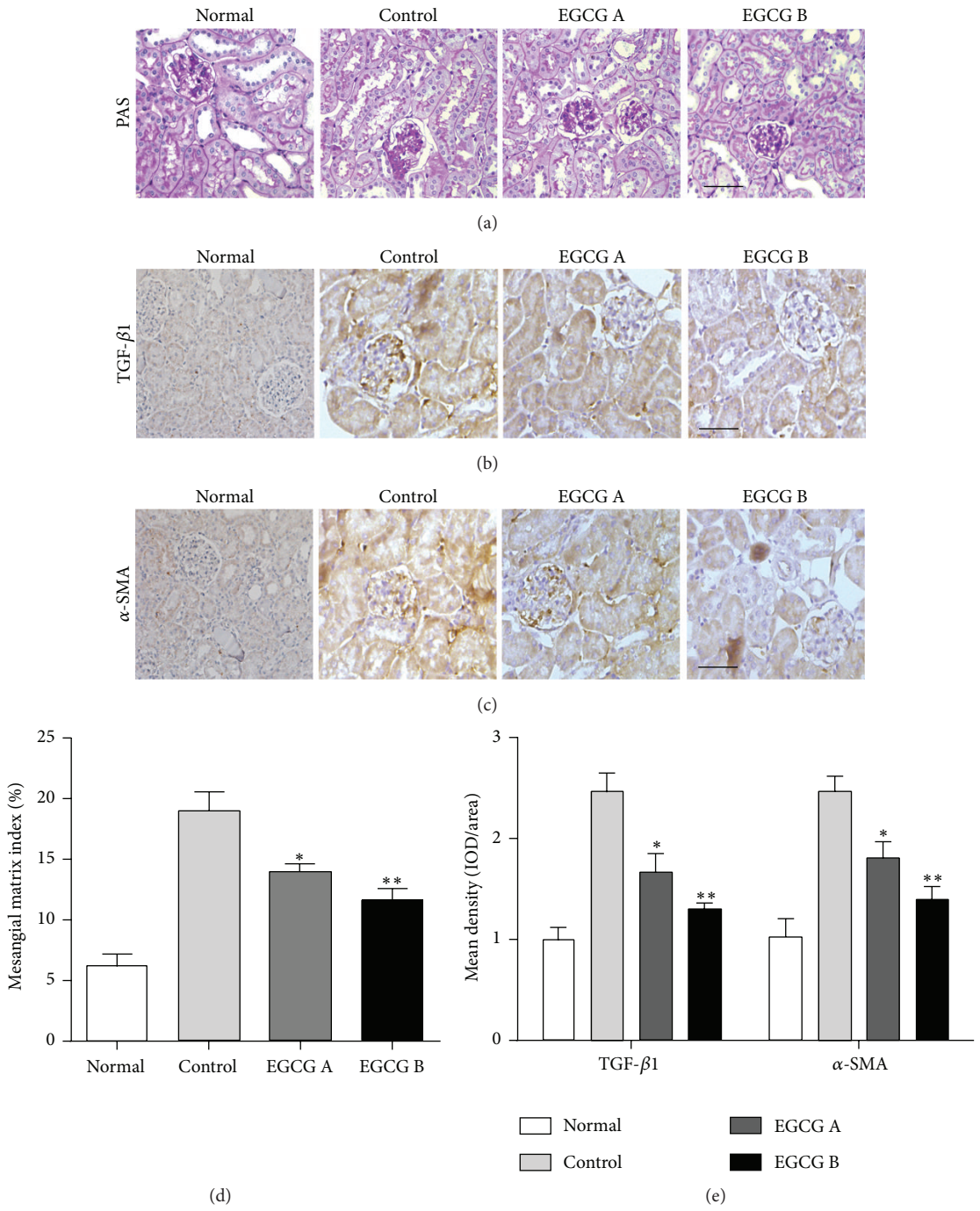

FIGURE 5: Effect of EGCG on renal pathological changes and fibrosis. Renal pathological changes were examined by PAS staining (a and d). The protein expression levels of TGF-β1 and α-SMA were evaluated by immunohistochemistry (b, c, and e). Scale bar: 50 μm; $n = 8$ in each group. Normal: nontreated C57BL mice; control: C57BLKS/J db/db nontreated mice; EGCG A, db/db mice treated with EGCG of 50 mg/kg/d; EGCG B, db/db mice treated with EGCG of 100 mg/kg/d; values are means ± SEM. $^{*}P < 0.05$ and $^{**}P < 0.01$ versus control.

EGCG. Considering these results, EGCG exerts antioxidant effect in DKD of db/db mice. However, some other studies show that EGCG has the ability to exert prooxidative activities [20, 21]. These discrepancies may be caused by the different mechanism of EGCG involved in different diseases. It is well known that molecules play different roles, even totally opposite roles, in different cells or tissues. EGCG may have prooxidative activities in other diseases, while it shows an antioxidative effect in renal injury.

Oxidative stress-induced inflammatory response is a major pathomechanism of DKD. Moreover, the increase of inflammatory cytokine levels under high glucose conditions in return could induce a further increase of oxidative stress forming a vicious cycle [36]. It has been reported that

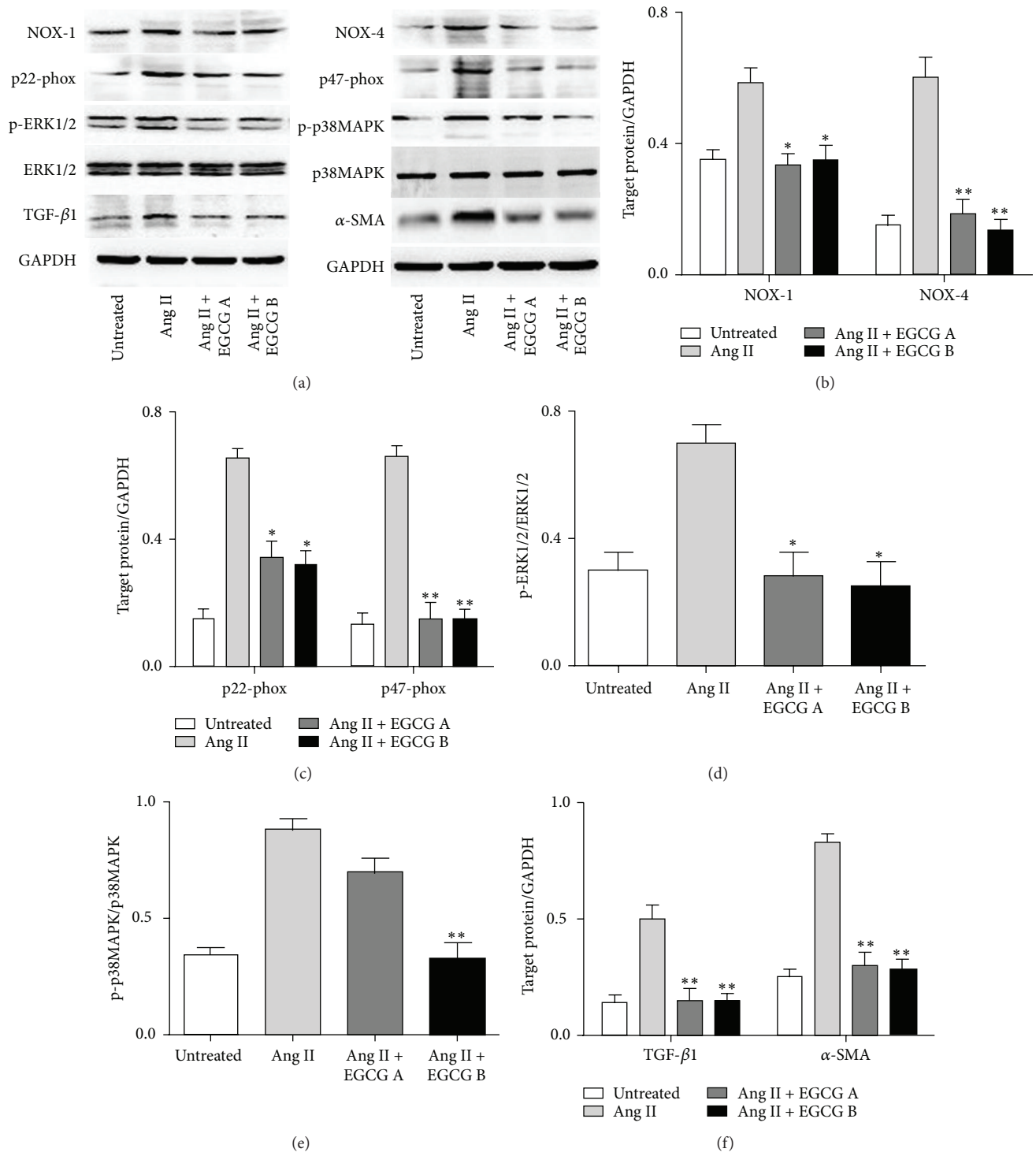

Figure 6: The protein expression of NOX-1 and NOX-4 (b), p22-phox and p47-phox (c), p-ERK1/2 (d), p-P38 MAPK (e), and TGF-β1 and α-SMA (f) of HK-2 cell after exposure to Ang II and EGCG detected by Western blot analyses. HK-2 cells were pretreated with 15 or 30 μM of EGCG for 6 h and then stimulated with Ang II (1 μM) for 24 hours. Values are means ± SEM. $^{*}P < 0.05$ and $^{**}P < 0.01$ versus control.

oxidative stress is a major contributor to the increase of TGF-β1 and α-SMA in DKD through direct or indirect ways [9, 36]. Both TGF-β1 and α-SMA are hypertrophic and fibrogenic cytokines which play a major role in glomerular hypertrophy and mesangial matrix expansion and finally lead to end-stage renal disease [36]. In addition, NADPH oxidase inhibitor effectively decreases TGF-β1 and α-SMA levels [37]. Furthermore, MAPK signaling pathways can be activated by ROS and participate in regulation of the inflammatory cytokines and processes [11]. It has been reported that ERK1/2

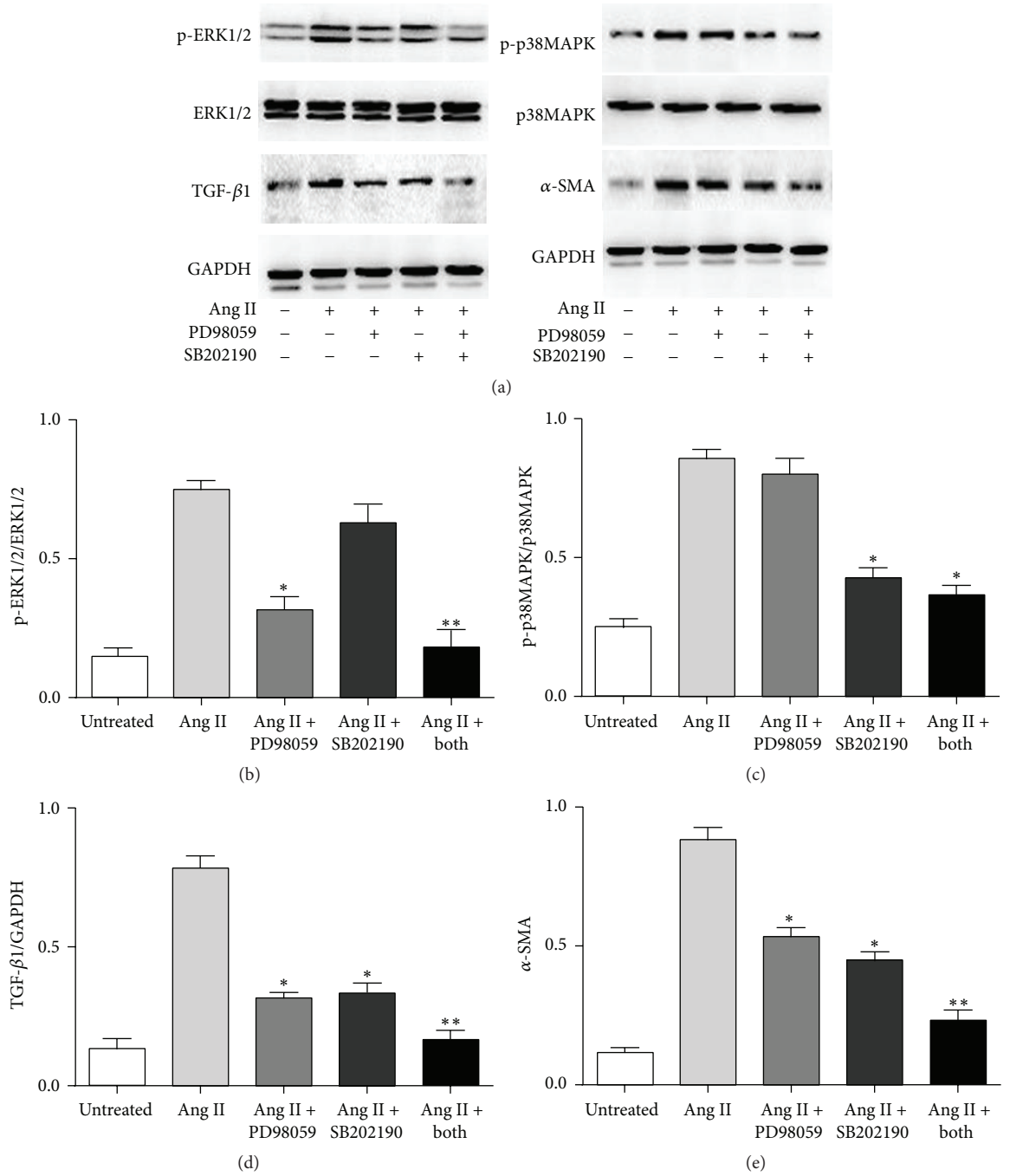

Figure 7: The protein expression of p-ERK1/2 (b), p-P38 MAPK (c), TGF-β1 (d), and α-SMA (e) of HK-2 cell after exposure to Ang II, PD98059, and SB202190. HK-2 cells were pretreated with PD98059 (ERK1/2 inhibitor) and/or SB202190 (p38 MAPK inhibitor) (all 10 mM) for 6 h and then stimulated with Ang II (1 μM) for 24 hours. Values are means ± SEM. $^{*}P < 0.05$ and $^{**}P < 0.01$ versus control.

and p38 MAPK, members of MAPK family, are crucial to mediate cellular responses such as inducing the proliferation, differentiation, and apoptosis of kidney cells and activating inflammatory processes [11, 33]. Therefore, TGF-β1, α-SMA, and MAPK signaling pathways which are stimulated by ROS are closely associated with the development of DKD. In this study, the db/db nontreated mice displayed obviously increased protein expression levels of p-ERK1/2 and p-p38 MAPK confirmed by Western blot and levels of TGF-β1 and α-SMA determined by immunohistochemistry compared to normal group. On the other hand, the increase levels of TGF-β1, α-SMA, p-ERK1/2, and p-p38 MAPK were inhibited by EGCG in diabetic conditions. Furthermore, in order to further explore the underlying molecular mechanism of

Table 3: Changes in ROS, 8-OHdG, SOD, MDA, CAT, and 3-nitrotyrosine in kidney homogenates in mice after different treatment.

	Normal	Control	EGCG A	EGCG B
ROS (U/mL)				
Baseline	201.4 ± 17.5	279.1 ± 17.8$^{\#\#}$	280.4 ± 20.7$^{\#\#}$	277.6 ± 23.2$^{\#\#}$
Week 4	203.9 ± 10.7	372.2 ± 20.2$^{\#\#}$	316.3 ± 18.1$^{\#\#**}$	304.5 ± 23.5$^{\#\#**}$
Week 8	218.4 ± 15.5	489.9 ± 20.3$^{\#\#}$	375.8 ± 21.4$^{\#\#**}$	352.6 ± 19.1$^{\#\#**}$
8-OHdG (pg/mg protein)				
Baseline	810.7 ± 32.6	958.3 ± 32.5$^{\#\#}$	975.2 ± 30.6$^{\#\#}$	969.2 ± 22.3$^{\#\#}$
Week 4	816.7 ± 35.4	1398.2 ± 33.7$^{\#\#}$	1179.5 ± 28.4$^{\#\#*}$	1163.6 ± 34.5$^{\#\#**}$
Week 8	823.1 ± 30.4	1757.8 ± 21.9$^{\#\#}$	1474.5 ± 25.3$^{\#\#**}$	1365.3 ± 28.6$^{\#\#**}$
SOD (U/mg protein)				
Baseline	60.8 ± 4.8	49.3 ± 7.1$^{\#}$	50.4 ± 5.5$^{\#}$	49.9 ± 6.2$^{\#}$
Week 4	61.3 ± 7.1	34.2 ± 7.2$^{\#\#}$	43.5 ± 3.5$^{\#*}$	44.9 ± 4.3$^{\#*}$
Week 8	59.1 ± 5.2	30.4 ± 4.7$^{\#\#}$	38.6 ± 6.4$^{\#**}$	41.4 ± 3.6$^{\#**}$
MDA (nM/mg protein)				
Baseline	14.6 ± 4.4	16.8 ± 3.3$^{\#}$	16.4 ± 3.7$^{\#}$	16.7 ± 5.6$^{\#}$
Week 4	15.3 ± 3.7	23.6 ± 3.5$^{\#}$	19.8 ± 1.6$^{\#*}$	18.5 ± 4.3$^{\#**}$
Week 8	15.7 ± 1.2	28.7 ± 4.1$^{\#}$	22.6 ± 2.9$^{\#*}$	21.2 ± 5.3$^{\#*}$
CAT (U/mg protein)				
Baseline	26.2 ± 2.2	23.0 ± 1.4$^{\#}$	23.3 ± 2.3$^{\#}$	23.1 ± 2.8$^{\#}$
Week 4	26.4 ± 1.2	15.9 ± 2.9$^{\#\#}$	21.5 ± 1.7$^{\#**}$	21.3 ± 2.1$^{\#**}$
Week 8	25.1 ± 1.8	13.6 ± 2.7$^{\#\#}$	17.4 ± 1.5$^{\#*}$	18.3 ± 2.4$^{\#**}$
3-nitrotyrosine (μg/mL)				
Baseline	18.7 ± 2.8	20.4 ± 1.1$^{\#}$	20.3 ± 1.0$^{\#}$	21.1 ± 2.4$^{\#}$
Week 4	18.5 ± 2.6	29.5 ± 3.3$^{\#\#}$	24.8 ± 0.9$^{\#*}$	22.3 ± 1.8$^{\#*}$
Week 8	20.4 ± 3.1	36.7 ± 2.8$^{\#\#}$	30.2 ± 1.5$^{\#*}$	31.4 ± 2.7$^{\#*}$

Note: normal, C57BLKS/J normal nontreated mice; control, C57BLKS/J db/db nontreated mice; EGCG A, db/db mice treated with EGCG of 50 mg/kg/d; EGCG B, db/db mice treated with EGCG of 100 mg/kg/d; ROS, reactive oxygen species; 8-OHdG, 8-hydroxy-2′-deoxyguanosine; SOD, superoxide dismutase; CAT, catalase; MDA, malondialdehyde. $^{\#}P < 0.05$ and $^{\#\#}P < 0.01$ versus normal; $^{*}P < 0.05$ and $^{**}P < 0.01$ versus control; values are means ± SEM. At baseline and at week 4, $n = 16$ in each group; at week 8, $n = 8$ in each group.

renoprotective effects of EGCG, we performed a cell-based study in HK-2 cells. Based on our results, EGCG could downregulate the expression of several factors involved in Ang II mediated oxidative stress in kidney including NOX-1, NOX-4, p22-phox, p47-phox, p-ERK1/2, p-P38 MAPK, TGF-β1, and α-SMA. EGCG is supposed to play a role in Ang II induced renal injury similar to PD98059 and SB202190, both of which are blockers of downstream molecules of Ang II pathway.

Considering the effects of EGCG in Ang II mediated oxidative stress in DKD in our study, we plotted a diagram elucidating the possible function of EGCG in Ang II regulated pathways, as shown in Figure 8. The renoprotective effects of EGCG might be realized by two pathways: one is functioning as a NADPH oxidase inhibitor, directly suppressing the production of ROS, and the other is inhibiting the expression of downstream molecules of Ang II mediated pathway, directly downregulating the production of effectors for renal fibrosis. Other possible mechanisms of EGCG such as function as an AT-1R blocker should be explored in further studies.

In summary, our results suggested that EGCG has renoprotective effects in diabetic db/db mice through disturbing Ang II mediated oxidative stress. These effects of EGCG are realized by several mechanisms including directly suppressing the activity of NADPH oxidase and inhibiting MAPK cascade involved in Ang II pathway.

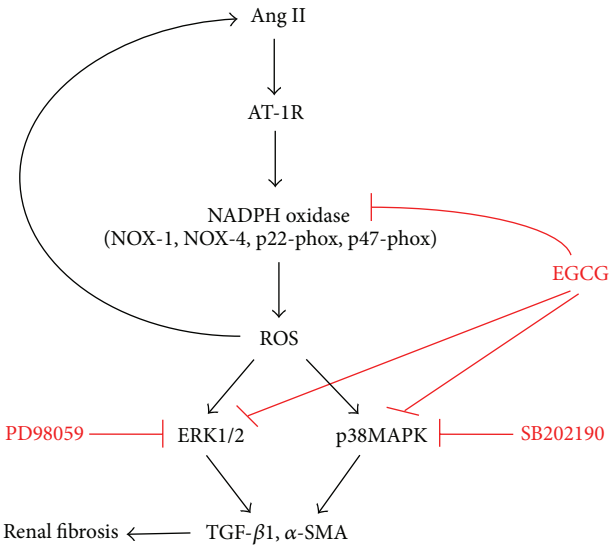

Figure 8: Diagram of the underlying mechanisms of EGCG disturbing Ang II induced oxidative stress and renal fibrosis.

Competing Interests

The authors declare that there are no competing interests.

Authors' Contributions

Xiu Hong Yang and Yu Pan contributed equally to this paper.

Acknowledgments

The study was supported by the Key Specialized Construction Project in Medicine of Shanghai (ZK2015A15), the Key Discipline Construction Project of the Pudong Health Bureau of Shanghai (PWZx2014-11), Outstanding Leaders Training Program of the Pudong Health Bureau of Shanghai (PWRl2012-05), the Shanghai Committee on Science and Technology (15ZR1437400), and grants from the National Natural Science Foundation of China (no. 81300652) for research resources.

References

[1] International Diabetes Federation, *IDF Diabetes Atlas*, International Diabetes Federation, Brussels, Belglum, 7th edition, 2015, http://www.diabetesatlas.org/.

[2] F. A. Hakim and A. Pflueger, "Role of oxidative stress in diabetic kidney disease," *Medical Science Monitor*, vol. 16, no. 2, pp. A37–A48, 2010.

[3] S. Tesfaye, L. Vileikyte, G. Rayman et al., "Painful diabetic peripheral neuropathy: consensus recommendations on diagnosis, assessment and management," *Diabetes/Metabolism Research and Reviews*, vol. 27, no. 7, pp. 629–638, 2011.

[4] R. C. Stanton, "Oxidative stress and diabetic kidney disease," *Current Diabetes Reports*, vol. 11, no. 4, pp. 330–336, 2011.

[5] Y. Gorin and F. Wauquier, "Upstream regulators and downstream effectors of NADPH oxidases as novel therapeutic targets for diabetic kidney disease," *Molecules and Cells*, vol. 38, no. 4, pp. 285–296, 2015.

[6] J. M. Forbes, M. T. Coughlan, and M. E. Cooper, "Oxidative stress as a major culprit in kidney disease in diabetes," *Diabetes*, vol. 57, no. 6, pp. 1446–1454, 2008.

[7] E. A. Jaimes, P. Hua, R.-X. Tian, and L. Raij, "Human glomerular endothelium: interplay among glucose, free fatty acids, angiotensin II, and oxidative stress," *American Journal of Physiology—Renal Physiology*, vol. 298, no. 1, pp. F125–F132, 2010.

[8] K. Fukami, S. Ueda, S.-I. Yamagishi et al., "AGEs activate mesangial TGF-β-Smad signaling via an angiotensin II type I receptor interaction," *Kidney International*, vol. 66, no. 6, pp. 2137–2147, 2004.

[9] K. Chopra, V. Tiwari, V. Arora, and A. Kuhad, "Sesamol suppresses neuro-inflammatory cascade in experimental model of diabetic neuropathy," *The Journal of Pain*, vol. 11, no. 10, pp. 950–957, 2010.

[10] M.-L. Brezniceanu, F. Liu, C.-C. Wei et al., "Attenuation of interstitial fibrosis and tubular apoptosis in db/db transgenic mice overexpressing catalase in renal proximal tubular cells," *Diabetes*, vol. 57, no. 2, pp. 451–459, 2008.

[11] H. B. Lee, M.-R. Yu, Y. Yang, Z. Jiang, and H. Ha, "Reactive oxygen species-regulated signaling pathways in diabetic nephropathy," *Journal of the American Society of Nephrology*, vol. 14, no. 3, pp. S241–S245, 2003.

[12] S. Fang, Y. Jin, H. Zheng et al., "High glucose condition upregulated Txnip expression level in rat mesangial cells through ROS/MEK/MAPK pathway," *Molecular and Cellular Biochemistry*, vol. 347, no. 1-2, pp. 175–182, 2011.

[13] S. M. Nam, M. Y. Lee, J. H. Koh et al., "Effects of NADPH oxidase inhibitor on diabetic nephropathy in OLETF rats: the role of reducing oxidative stress in its protective property," *Diabetes Research and Clinical Practice*, vol. 83, no. 2, pp. 176–182, 2009.

[14] L. Luo, D.-Z. Dai, Y.-S. Cheng, Q. Zhang, W.-J. Yuan, and Y. Dai, "Sildenafil improves diabetic vascular activity through suppressing endothelin receptor A, iNOS and NADPH oxidase which is comparable with the endothelin receptor antagonist CPU0213 in STZ-injected rats," *Journal of Pharmacy and Pharmacology*, vol. 63, no. 7, pp. 943–951, 2011.

[15] M. Xu, D.-Z. Dai, and Y. Dai, "Normalizing NADPH oxidase contributes to attenuating diabetic nephropathy by the dual endothelin receptor antagonist CPU0213 in rats," *American Journal of Nephrology*, vol. 29, no. 3, pp. 252–256, 2009.

[16] H.-J. Jang, S. D. Ridgeway, and J.-A. Kim, "Effects of the green tea polyphenol epigallocatechin-3-gallate on high-fat diet-induced insulin resistance and endothelial dysfunction," *American Journal of Physiology—Endocrinology and Metabolism*, vol. 305, no. 12, pp. E1444–E1451, 2013.

[17] C. E. N. Reiter, J.-A. Kim, and M. J. Quon, "Green tea polyphenol epigallocatechin gallate reduces endothelin-1 expression and secretion in vascular endothelial cells: roles for AMP-activated protein kinase, Akt, and FOXO1," *Endocrinology*, vol. 151, no. 1, pp. 103–114, 2010.

[18] S. P. Yoon, Y. H. Maeng, R. Hong et al., "Protective effects of epigallocatechin gallate (EGCG) on streptozotocin-induced diabetic nephropathy in mice," *Acta Histochemica*, vol. 116, no. 8, pp. 1210–1215, 2014.

[19] R. Gao, Y. Wang, Z. Wu, J. Ming, and G. Zhao, "Interaction of barley β-glucan and tea polyphenols on glucose metabolism in streptozotocin-induced diabetic rats," *Journal of Food Science*, vol. 77, no. 6, pp. H128–H134, 2012.

[20] L. Elbling, R.-M. Weiss, O. Teufelhofer et al., "Green tea extract and (-)-epigallocatechin-3-gallate, the major tea catechin, exert oxidant but lack antioxidant activities," *The FASEB Journal*, vol. 19, no. 7, pp. 807–809, 2005.

[21] G.-X. Li, Y.-K. Chen, Z. Hou et al., "Pro-oxidative activities and dose-response relationship of (−)-epigallocatechin-3-gallate in the inhibition of lung cancer cell growth: a comparative study in vivo and in vitro," *Carcinogenesis*, vol. 31, no. 5, pp. 902–910, 2010.

[22] N. Yamabe, T. Yokozawa, T. Oya, and M. Kim, "Therapeutic potential of (−)-epigallocatechin 3-O-gallate on renal damage in diabetic nephropathy model rats," *Journal of Pharmacology and Experimental Therapeutics*, vol. 319, no. 1, pp. 228–236, 2006.

[23] J. Gu, X. Liu, Q.-X. Wang et al., "Angiotensin II increases CTGF expression via MAPKs/TGF-β1/TRAF6 pathway in atrial fibroblasts," *Experimental Cell Research*, vol. 318, no. 16, pp. 2105–2115, 2012.

[24] D. Liu, J. T. Perkins, and B. Hennig, "EGCG prevents PCB-126-induced endothelial cell inflammation via epigenetic modifications of NF-κB target genes in human endothelial cells," *Journal of Nutritional Biochemistry*, vol. 28, pp. 164–170, 2016.

[25] A. Peng, T. Ye, D. Rakheja et al., "The green tea polyphenol (−)-epigallocatechin-3-gallate ameliorates experimental immune-mediated glomerulonephritis," *Kidney International*, vol. 80, no. 6, pp. 601–611, 2011.

[26] J. Yan, Y. Zhao, S. Suo, Y. Liu, and B. Zhao, "Green tea catechins ameliorate adipose insulin resistance by improving oxidative stress," *Free Radical Biology and Medicine*, vol. 52, no. 9, pp. 1648–1657, 2012.

[27] F. Pistrosch, J. Passauer, K. Herbrig, U. Schwanebeck, P. Gross, and S. R. Bornstein, "Effect of thiazolidinedione treatment on proteinuria and renal hemodynamic in type 2 diabetic patients with overt nephropathy," *Hormone and Metabolic Research*, vol. 44, no. 12, pp. 914–918, 2012.

[28] K. Reidy, H. M. Kang, T. Hostetter, and K. Susztak, "Molecular mechanisms of diabetic kidney disease," *The Journal of Clinical Investigation*, vol. 124, no. 6, pp. 2333–2340, 2014.

[29] Y. Li, G.-S. Shen, C. Yu et al., "Local bone interaction between renin-angiotensin system and kallikrein-kinin system in diabetic rat," *International Journal of Clinical and Experimental Pathology*, vol. 8, no. 2, pp. 1604–1612, 2015.

[30] H. Suzuki, T. Kikuta, T. Inoue, and U. Hamada, "Time to re-evaluate effects of renin-angiotensin system inhibitors on renal and cardiovascular outcomes in diabetic nephropathy," *World Journal of Nephrology*, vol. 4, no. 1, pp. 118–126, 2015.

[31] D. A. Long, K. L. Price, J. Herrera-Acosta, and R. J. Johnson, "How does angiotensin II cause renal injury?" *Hypertension*, vol. 43, no. 4, pp. 722–723, 2004.

[32] J. R. Ingelfinger, "Preemptive olmesartan for the delay or prevention of microalbuminuria in diabetes," *The New England Journal of Medicine*, vol. 364, no. 10, pp. 970–971, 2011.

[33] A. P. Lakshmanan, R. A. Thandavarayan, K. Watanabe et al., "Modulation of AT-1R/MAPK cascade by an olmesartan treatment attenuates diabetic nephropathy in streptozotocin-induced diabetic mice," *Molecular and Cellular Endocrinology*, vol. 348, no. 1, pp. 104–111, 2012.

[34] T. Kochi, M. Shimizu, D. Terakura et al., "Non-alcoholic steatohepatitis and preneoplastic lesions develop in the liver of obese and hypertensive rats: suppressing effects of EGCG on the development of liver lesions," *Cancer Letters*, vol. 342, no. 1, pp. 60–69, 2014.

[35] Y.-S. Han, L. Lan, J. Chu, W.-Q. Kang, and Z.-M. Ge, "Epigallocatechin gallate attenuated the activation of rat cardiac fibroblasts induced by angiotensin II via regulating β-arrestin1," *Cellular Physiology and Biochemistry*, vol. 31, no. 2-3, pp. 338–346, 2013.

[36] A. A. Elmarakby and J. C. Sullivan, "Relationship between oxidative stress and inflammatory cytokines in diabetic nephropathy," *Cardiovascular Therapeutics*, vol. 30, no. 1, pp. 49–59, 2012.

[37] X. Y. Shi, F. Hou, H. X. Niu et al., "Advanced oxidation protein products promote inflammation in diabetic kidney through activation of renal nicotinamide adenine dinucleotide phosphate oxidase," *Endocrinology*, vol. 149, no. 4, pp. 1829–1839, 1829.

Hindawi Publishing Corporation
Oxidative Medicine and Cellular Longevity
Volume 2016, Article ID 7894247, 12 pages
http://dx.doi.org/10.1155/2016/7894247

Research Article

Cathepsin B Regulates Collagen Expression by Fibroblasts via Prolonging TLR2/NF-κB Activation

Xue Li,[1] Zhou Wu,[2,3] Junjun Ni,[2] Yicong Liu,[2] Jie Meng,[2] Weixian Yu,[1] Hiroshi Nakanishi,[2] and Yanmin Zhou[1]

[1]*Department of Implantology, School of Stomatology, Jilin University, Changchun 130021, China*
[2]*Department of Aging Science and Pharmacology, Faculty of Dental Science, Kyushu University, Fukuoka 812-8582, Japan*
[3]*OBT Research Center, Faculty of Dental Science, Kyushu University, Fukuoka 812-8582, Japan*

Correspondence should be addressed to Zhou Wu; zhouw@dent.kyushu-u.ac.jp and Yanmin Zhou; zhouym62@126.com

Received 25 May 2016; Revised 29 July 2016; Accepted 8 August 2016

Academic Editor: Juan F. Santibanez

Fibroblasts are essential for tissue repair due to producing collagens, and lysosomal proteinase cathepsin B (CatB) is involved in promoting chronic inflammation. We herein report that CatB regulates the expression of collagens III and IV by fibroblasts in response to a TLR2 agonist, lipopolysaccharide from *Porphyromonas gingivalis* (*P.g.* LPS). In cultured human BJ fibroblasts, mRNA expression of CatB was significantly increased, while that of collagens III and IV was significantly decreased at 24 h after challenge with *P.g.* LPS (1 μg/mL). The *P.g.* LPS-decreased collagen expression was completely inhibited by CA-074Me, the specific inhibitor of CatB. Surprisingly, expression of collagens III and IV was significantly increased in the primary fibroblasts from CatB-deficient mice after challenge with *P.g.* LPS. The increase of CatB was accompanied with an increase of 8-hydroxy-2′-deoxyguanosine (8-OHdG) and a decrease of IκBα. Furthermore, the *P.g.* LPS-increased 8-OHdG and decreased IκBα were restored by CA-074Me. Moreover, 87% of CatB and 86% of 8-OHdG were colocalized with gingival fibroblasts of chronic periodontitis patients. The findings indicate the critical role of CatB in regulating the expression of collagens III and IV by fibroblasts via prolonging TLR2/NF-κB activation and oxidative stress. CatB-specific inhibitors may therefore improve chronic inflammation-delayed tissue repair.

1. Introduction

Fibroblasts are essential for tissue repair due to their activity in producing collagens. Collagen can be divided into fibrillar and nonfibrillar families. Collagens I and III, the major fibrillar collagens in connective tissues, play important roles in tissue repair [1]. In particular, collagen III is suggested to regulate collagen I synthesis [2], as a higher ratio of collagen III to collagen I is associated with scarless wound healing in mammal models [3, 4], and collagen III-deficient mice exhibit more pronounced wound contracture than those with collagen III [5]. However, the expression of collagen III is regulated by the activity of local fibroblasts [6]. Collagen IV, a nonfibrillar collagen, is a major component of the basement membrane (BM) [7, 8]. Recently, collagen IV has been shown to participate in the innate immune response by regulating cellular adhesion and migration [9], and Col4a1 (the human collagen IV gene) mutation-associated phenotypic features include chronic inflammation and immune activation [10–12].

Toll-like receptors (TLRs), which are expressed in fibroblasts [13, 14], have been observed to modulate tissue repair during chronic inflammation [15–17]. Furthermore, nuclear factor kappa B (NF-κB), the key transcription factor of TLR signaling, has been shown to inhibit collagen I gene expression directly [18] and mediate oxidative stress-decreased collagen biosynthesis [19].

Cathepsin B (CatB; EC 3.4.22.1), a typical cysteine lysosomal protease, promotes inflammation involved in the production of mature IL-1β [20–23]. CatB was recently found to be responsible for NF-κB activation through autophagy degradation of inhibitor of κBα (IκBα) in microglia/macrophages [24]. Naturally, as a protease, CatB degrades collagens in fibroblasts [25], but the role of CatB in regulating collagen

expression by fibroblasts during chronic inflammation is still unknown.

In the present study, we aimed to elucidate the involvement of CatB in the expression of collagens III and IV by fibroblasts after challenge with a TLR2 agonist, lipopolysaccharide from *Porphyromonas gingivalis* (*P.g.* LPS).

2. Materials and Methods

2.1. Reagents. *P.g.* LPS was purchased from InvivoGen (San Diego, CA, USA). Bay 11-7082 and SN50, the specific NF-κB inhibitors, were purchased from Sigma-Aldrich (St. Louis, MO, USA). CA-074Me, the specific CatB inhibitor, was purchased from Peptide Institute. Inc. (Osaka, Japan). Mouse anti-8-OHdG (N213120) was purchased from NOF Corporation (Kyoto, Japan). Antibodies of rabbit anti-fibronectin (H-300), goat anti-CatB (S-12), and rabbit anti-IκBα were purchased from Santa Cruz Biotechnology (Santa Cruz, CA, USA). Mouse anti-TLR2 (T 2.5) was purchased from eBioscience (San Diego, CA, USA). Mouse anti-Collagen III (Col-29) and mouse anti-Collagen IV (COL-94) were purchased from Abcam (Cambridge, UK).

2.2. Tissue Preparation from Periodontitis Patients. The gingival tissues were obtained from patients with periodontal surgery or extraction. The periodontal diagnosis of subjects with chronic periodontitis was established based on the clinical and radiographic criteria defined at the 1999 International World Workshop for a Classification of Periodontal Diseases and Conditions [26]. The samples included 7 cases diagnosed as chronic periodontitis (36–60 years of age, 3 males and 4 females), which were obtained from the Periodontology Department of the School of Stomatology, Jilin University. After periodontal surgery, the excised gingival specimens were immediately placed in liquid nitrogen and subsequently frozen at −80°C until use in experiments.

The gingival samples were immersed in a periodate lysine paraformaldehyde (PLP) fixative consisting of 0.01 M sodium metaperiodate, 0.075 M L-lysine-HCL, 4% paraformaldehyde, and 0.03% phosphate buffer (pH 6.2) for 6 h at 4°C. The specimens were protected for 2 days in 30% sucrose in phosphate-buffered saline (PBS) and then embedded in an optimal cutting temperature compound (Sakura Finetechnical Co., Ltd., Tokyo, Japan). The coronal frozen sections (thickness of 8 μm) were subjected to the immunohistochemical analyses.

2.3. BJ Human Fibroblast Cell Line Culture. BJ (CRL-2522) cells purchased from ATCC (Manassas, VA, USA) were cultured in Minimum Essential Medium (MEM; GIBCO, Grand Island, NY, USA) supplemented with 10% fetal bovine serum (FBS, GIBCO), 1% penicillin-streptomycin, 10 μg/mL insulin, and 450 mg/mL glucose. The cells were cultured at 37°C in a humidified atmosphere with 5% CO_2.

2.4. Primary CatB-Deficient ($CatB^{-/-}$) Fibroblast Culture. Three-day-old $CatB^{-/-}$ mice were sacrificed using an excessive amount of ether. The skin tissue was removed and immediately washed first in alcohol (75%) and then in PBS. The tissue was then cut and transferred into a 6-well plate. The fibroblasts were grown in MEM supplemented with 10% FBS, 1% penicillin-streptomycin, 10 μg/mL insulin, and 450 mg/mL glucose in a humidified atmosphere with 5% CO_2 at 37°C. The medium was changed after five days, and then the cells were cultivated with culture medium in a new plate. The experiments were performed using early passage fibroblasts before the second passage.

2.5. Determination of Cell Viability. BJ cells were cultured in a 96-well plate for 24 h (5×10^3 cells/well) and then incubated with various concentrations of *P.g.* LPS for 48 h. Cell viability was assessed using the cell-counting kit-8 (CCK-8; Dojindo, Kumamoto, Japan) in accordance with the manufacturer's instructions, as follows: After the treatment of *P.g.* LPS, 10 μL CCK-8 was added to each well of the 96-well plate and then incubated at 37°C for 2 h. In accordance with the instructions, the optical density was read at a wavelength of 450 nm using the microplate reader. Cell viability was calculated using the following formula: optical density of treated group/control group × 100%.

2.6. Immunofluorescence Imaging. The coronal frozen sections of periodontitis tissues were incubated with antibody diluent overnight at 4°C. The sections were then treated with primary rabbit anti-fibronectin (H-300, 1 : 1000), mouse anti-8-OHdG (N213120, 1 : 1000), goat anti-CatB (S-12, 1 : 1000), and mouse anti-TLR2 (T 2.5, 1 : 1000) for 12 h at 4°C. After washing with PBS, the sections were incubated with a mixture of FITC-conjugated and rhodamine-conjugated secondary antibodies for 2 h at 24°C. The sections were then washed again with PBS and mounted in Vectashield antifading medium (Vector Laboratory, CA, USA) and examined using a confocal laser scanning microscope (CLSM, C2si, Nikon, Japan). The CLSM images of individual sections were taken as a stack at a 1-μm step size in the z-direction with 20x objectives (numerical aperture = 0.5), zoom factor 1.0. A rectangle (1024 × 1024 pixels) corresponding to the size of 450 × 450 μm was used as the counting frame. The CLSM images were shown as the middle of the stacked images.

For the cultured BJ fibroblasts staining, the cells were seeded at 5×10^5 cells/mL in 24-well plates. 48 h after *P.g.* LPS (1 μg/mL) challenge or pretreatment with CA-074Me, the cells were fixed with 4% paraformaldehyde and then incubated with the mouse anti-p65 (1 : 500) and mouse anti-8-OHdG (1 : 1000) overnight at 4°C. After being incubated with anti-mouse Alexa 488 (1 : 1000, Jackson Immunoresearch Lab. Inc.) at room temperature for 2 h, they were then incubated with Hoechst (1 : 200, Sigma-Aldrich, Japan) and mounted in the antifading medium Vectashield. Fluorescence images were taken using a CLSM (C2si, Nikon, Japan).

2.7. Real-Time Quantitative Polymerase Chain Reaction Analysis (RT-qPCR). BJ cells were treated with *P.g.* LPS (1 μg/mL) for 3, 12, 24, and 48 h; primary $CatB^{-/-}$ fibroblast cells and primary wild type fibroblasts were treated with *P.g.* LPS (1 μg/mL) for 24 and 48 h. After treatment, the cells were collected. A set of the BJ cells was pretreated with Bay 11-7082 (20 μM, [27]), CA-074Me (50 μM, [22]), or SN50 (20 μM) for

1 h and then treated with *P.g.* LPS (1 μg/mL), incubated for 48 h, and harvested.

mRNA isolated from these cells was subjected to RT-qPCR. The total RNA was extracted with the Purelink RNA microkit (Invitrogen, Tokyo, Japan) in accordance with the manufacturer's instructions. A total of 1000 ng of extracted RNA was reverse transcribed to cDNA using the High Capacity RNA-to-cDNA Master Mix (Applied Biosystems, Foster City, CA, USA). The thermal cycling was held at 95°C for 5 min, followed by 40 cycles at 95°C for 5 sec and at 60°C for 10 sec. The cDNA was amplified in duplicate using TaqMan Universal PCR Master Mix (Applied Biosystems) with an Applied Biosystems 7500/7500 Fast Real-Time PCR System. The data were evaluated using the 7500 software program (version 2.0, Applied Biosystems). The primer sequences used were as follows: Human Actin: 5′-AGA GCT ACG AGC TGC CTG AC-3′ and 5′-AGC ACT GTG TTG GCG TAC AG-3′; Human TLR2: 5′-GCC AAA GTC TTG ATT GAT TGG-3′ and 5′-TTG AAG TTC TCC AGC TCC TG-3′; Human Collagen III: 5′-TGG TGT TGG AGC CGC TGC CA-3′ and 5′-CTC AGC ACT AGA ATC TGT CC-3′; Human Collagen IV: 5′-ATG TCA ATG GCA CCC ATC AC-3′ and 5′-CTT CAA GGT GGA CGG CGT AG-3′; Human CatB: 5′-TGA CGT GTT GGT ACA CTC CTG-3′ and 5′-TGG AGG GAG CTT TCT CTG TG-3′; Mouse Actin: 5′-CAA TAG TGA TGA CCT GGC CGT-3′ and 5′-AGA GGG AAA TCG TGC GTG AC-3′; Mouse Collagen III: 5′-CCA GCT GGG CCT TTG ATA CCT-3′ and 5′-TGC CCA CAG CCT TCT ACA CCT-3′; and Mouse Collagen IV: 5′-AGG CAG GTC AAG TTC TAG CG-3′ and 5′-CAA GCA TAG TGG TCC GAG TC-3′. For data normalization, an endogenous control (actin) was assessed to control for the cDNA input, and the relative units were calculated by a comparative Ct method. All of the RT-qPCR experiments were repeated three times, and the results are presented as the means of the ratios ± the standard error of the mean (SEM).

2.8. Electrophoresis and Immunoblotting. BJ cells were cultured in the 6-well plate at a density of 5×10^5 cells/mL. After treatment with *P.g.* LPS (1 μg/mL) for 12, 24, and 48 h, the cells were collected for experiments. A set of the BJ cells was pretreated with CA-074Me (50 μM) for 1 h, and then *P.g.* LPS (1 μg/mL) was added to the medium. The cells continued to be cultured for 48 h and were then harvested.

The cells were electrophoresed in 7.5% or 12% SDS-polyacrylamide gels, and the proteins on the SDS gels were transferred electrophoretically to nitrocellulose membranes, which were washed with PBS and then blocked for 1 h. The membranes were incubated with one of the following primary antibodies overnight at 4°C: rabbit anti-IκBα (1 : 1000), mouse anti-TLR2 (1 : 1000), rabbit anti-collagen III (1 : 500), rabbit anti-collagen IV (1 : 500) or goat anti-CatB (1 : 1000). After washing the membranes with PBS, the membranes were incubated with horseradish peroxidase- (HRP-) labeled anti-rabbit (1 : 1000, GE Healthcare, UK), anti-mouse (1 : 1000, GE Healthcare, UK), or anti-goat (1 : 1000, GE Healthcare, UK) antibodies for 2 h at 24°C, and then the protein bands were detected by an enhanced chemiluminescence detection system (ECK kit, Thermo Scientific, Rockford, IL, USA) using an image analyzer (LAS-4000; Fuji Photo Film, Tokyo, Japan).

2.9. 8-OHdG Assay. BJ cells were cultured in the 10 cm dish at a density of 5×10^5 cells/mL. After the cells adhering to the bottom of the dish, *P.g.* LPS (1 μg/mL) was treated or pretreated with CA-074Me (50 μM) for 1 h. After 48 h, the cells were collected and subjected to DNA extraction by DNA Extractor TIS Kit (Wako, Osaka, Japan) according to the manufacturer's protocol. The extracted DNA were calculated and prepared according to 8-OHdG Assay Preparation Reagent Set (Wako, Osaka, Japan), 200 μg/150 μL of each sample were heated at 98°C for 2 min. After chill in ice for 5 min, the samples were incubated with 19 μL acetic buffer and 10 μL of nuclease P1 solution at 37°C for 30 min. 20 μL of Tris buffer and 1 μL of Alkaline Phosphatase solution were added and incubated at 37°C for 30 min. Then, the samples were subjected to 8-OHdG ELISA kit (High sensitive-8-OHdG check; Japan Institute for the Control of Aging, Fukuroi, Japan) following the manufacturer's protocol.

2.10. Data Analysis. The data are represented as the means ± SEM. The statistical analyses were performed using a one- or two-way analysis of variance (ANOVA) with a post hoc Tukey's test using the GraphPad Prism software package (GraphPad Software Inc., San Diego, CA, USA). A value of $P < 0.05$ was considered to indicate statistical significance.

3. Results

3.1. The Expression of CatB as well as Collagen III and Collagen IV after P.g. LPS Challenge. First, we examined the suitable concentrations of *P.g.* LPS for challenging the cultured human BJ fibroblasts. The cell viability of BJ fibroblasts decreased significantly at 48 h after challenge with 1000 μg/mL *P.g.* LPS (Figure 1(a)). We therefore decided to use the concentration of *P.g.* LPS at 1 μg/mL in subsequent experiments, which was one-thousandth of the concentration that reduced the cell viability for the time course of the experiments.

During the time courses (3, 12, 24, and 48 h) challenged with *P.g.* LPS (1 μg/mL), the mean mRNA expression of CatB was significantly increased at 24 and 48 h (the late culture periods) but not at 3 or 12 h (the early culture periods) compared with the unchallenged cells (Figure 1(b)). In contrast, the mean mRNA expression of collagens III and IV was significantly increased at 3 and 12 h but was significantly decreased at 24 and 48 h after challenge with *P.g.* LPS compared with the unchallenged cells (Figures 1(c) and 1(d)). These observations provided the first evidence for a negative link between CatB and collagens III and IV during chronic activation of TLR2 signaling.

3.2. The Regulation of Collagens III and IV Expression by CatB in Fibroblasts after P.g. LPS Challenge. We next examined the roles of CatB in regulating the expression of collagens III and IV after challenge with *P.g.* LPS via two approaches: pharmacological inhibition using the specific CatB inhibitor CA-074Me and genetic deletion of CatB using primary fibroblasts from CatB-deficient ($CatB^{-/-}$) mice.

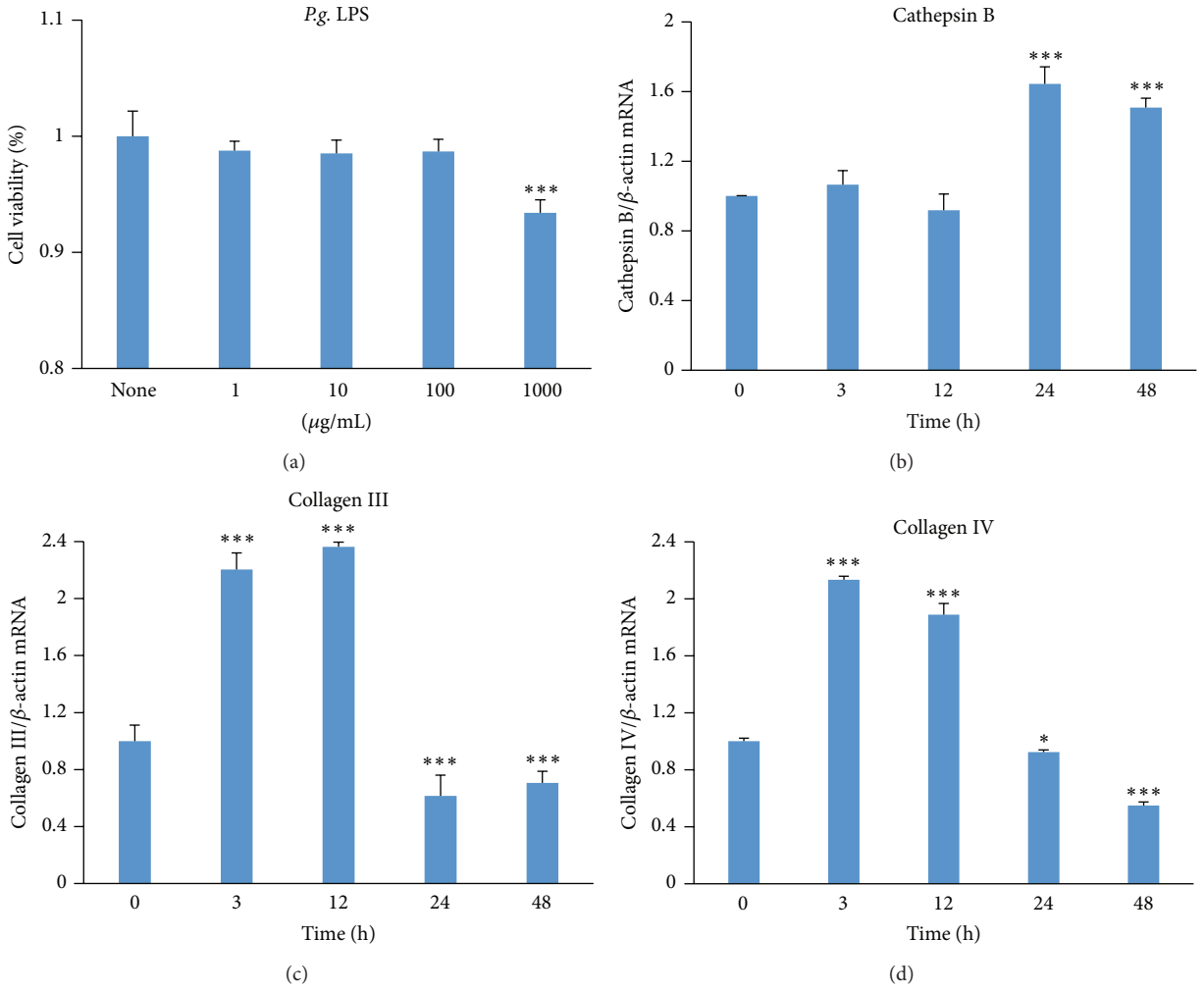

Figure 1: Expression of CatB and collagens III and IV by BJ fibroblasts after challenge with *P.g.* LPS. (a) The cell viability of BJ fibroblasts at 48 h after challenge with different dose of *P.g.* LPS by using cell-counting kit-8. (b) The mean mRNA expression level of CatB (3, 12, 24, and 48 h) after challenge with *P.g.* LPS (1 μg/mL). (c) The mean mRNA expression level of collagen III (3, 12, 24, and 48 h) after challenge with *P.g.* LPS (1 μg/mL). (d) The mean mRNA expression level of collagen IV (3, 12, 24, and 48 h) after challenge with *P.g.* LPS (1 μg/mL). Each column and bar represent the mean ± SEM ($n = 4$ each). The asterisks indicate a statistically significant difference from the value at the start of experiments (0 h) ($^{*}P < 0.05$, $^{***}P < 0.001$).

Pretreatment with CA-074Me (50 μM, 1 h) was able to restore the mean mRNA expression of both collagens III and IV to control levels at 48 h after challenge with *P.g.* LPS (Figures 2(a) and 2(b)). The protein expression levels of collagens III and IV were also restored by pretreatment with CA-074Me (50 μM, 1 h) after 48 h challenge with *P.g.* LPS (Figures 2(c)–2(e)). In the primary fibroblasts from wild type mice, the mean mRNA expression of collagens III and IV was significantly decreased at 24 and 48 h after challenge with *P.g.* LPS, findings which were consistent with those observed in human BJ fibroblasts (Figures 1(c) and 1(d)). To our surprise, the mean mRNA expression of collagens III and IV in the primary fibroblasts from CatB$^{-/-}$ mice was significantly increased compared with that of wild type mice at 24 and 48 h after challenge with *P.g.* LPS (Figures 2(f) and 2(g)). These observations clearly demonstrate that CatB has a critical role in regulating the expression of collagens III and IV by fibroblasts during chronic activation of TLR2 signaling.

3.3. The Regulation of NF-κB Activation and Oxidative Damage for Decreasing Collagens III and IV by CatB after P.g. LPS Challenge. Next, we investigated the molecular mechanisms by which CatB regulates the expression of collagens III and IV by fibroblasts after *P.g.* LPS challenge. Pretreatment with Bay 11-7082 or SN50, the specific inhibitors of NF-κB (1 h before *P.g.* LPS challenge), was able to inhibit the *P.g.* LPS-induced decrease in the mean mRNA expression of collagens III and IV by BJ fibroblasts at 48 h (Figures 3(a) and 3(b)), demonstrating that the *P.g.* LPS-induced decrease in the collagens was dependent on NF-κB activation. These results were consistent with those of a previous report showing that collagen I gene expression was dependent on NF-κB activation [18].

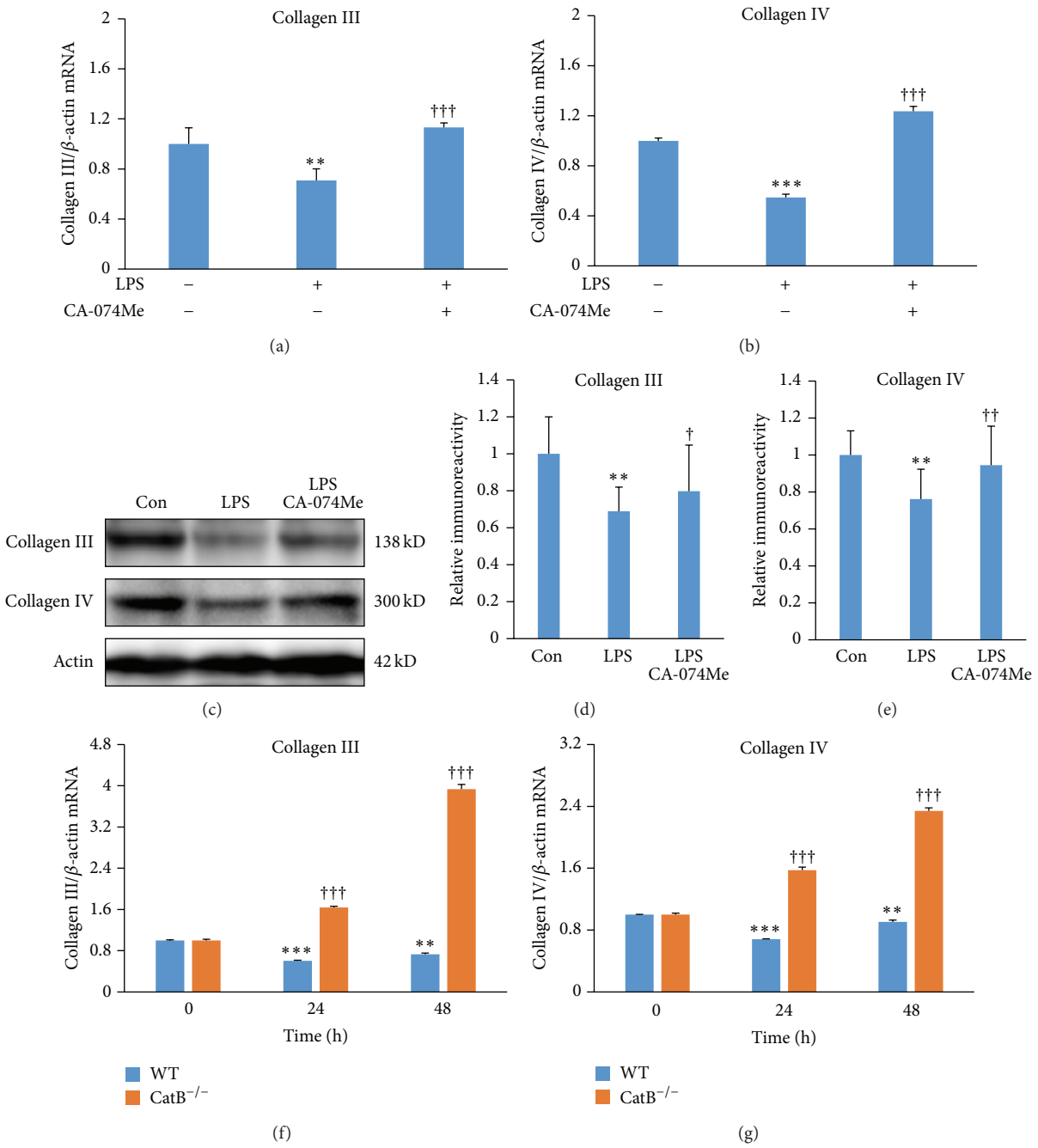

Figure 2: The effects of CatB on the expression of collagens III and IV by BJ fibroblasts after challenge with *P.g.* LPS. (a) The effect of CA-074Me (50 μM, 1 h before *P.g.* LPS challenge) on the expression of collagen III at 48 h after challenge with *P.g.* LPS (1 μg/mL). (b) The effect of CA-074Me on the expression of collagen IV at 48 h after challenge with *P.g.* LPS (1 μg/mL). Each column and bar represent the mean ± SEM ($n = 4$ each). The asterisks indicate a statistically significant difference from the value in untreated cells ($^{**}P < 0.01$, $^{***}P < 0.001$). The crosses indicate a statistically significant difference from the value in *P.g.* LPS-challenged cells without pretreatment with CA-074Me ($^{\dagger\dagger\dagger}P < 0.001$). (c) The effect of CA-074Me on the protein expression of collagen III and collagen IV at 48 h after challenge with *P.g.* LPS (1 μg/mL). ((d), (e)) The quantitative analyses of the immunoblotting for collagen III (d) and collagen IV (e). Each column and bar represent the mean ± SEM ($n = 4$ each). The asterisks indicate a statistically significant difference from the value in untreated cells ($^{**}P < 0.01$). The crosses indicate a statistically significant difference from the value in *P.g.* LPS-challenged cells without pretreatment with CA-074Me ($^{\dagger}P < 0.05$, $^{\dagger\dagger}P < 0.01$). (f) The expression of collagen III in the primary fibroblasts from wild type and CatB$^{-/-}$ mice at 24 and 48 h after challenge with *P.g.* LPS (1 μg/mL). (g) The expression of collagen IV in the primary fibroblasts from wild type and CatB$^{-/-}$ mice at 24 and 48 h after challenge with *P.g.* LPS (1 μg/mL). Each column and bar represent the mean ± SEM ($n = 4$ each). The asterisks indicate a statistically significant difference from the value in unchallenged cells from wild type mice ($^{**}P < 0.01$, $^{***}P < 0.001$). The crosses indicate a statistically significant difference from the value in the unchallenged cells from CatB$^{-/-}$ mice ($^{\dagger\dagger\dagger}P < 0.001$).

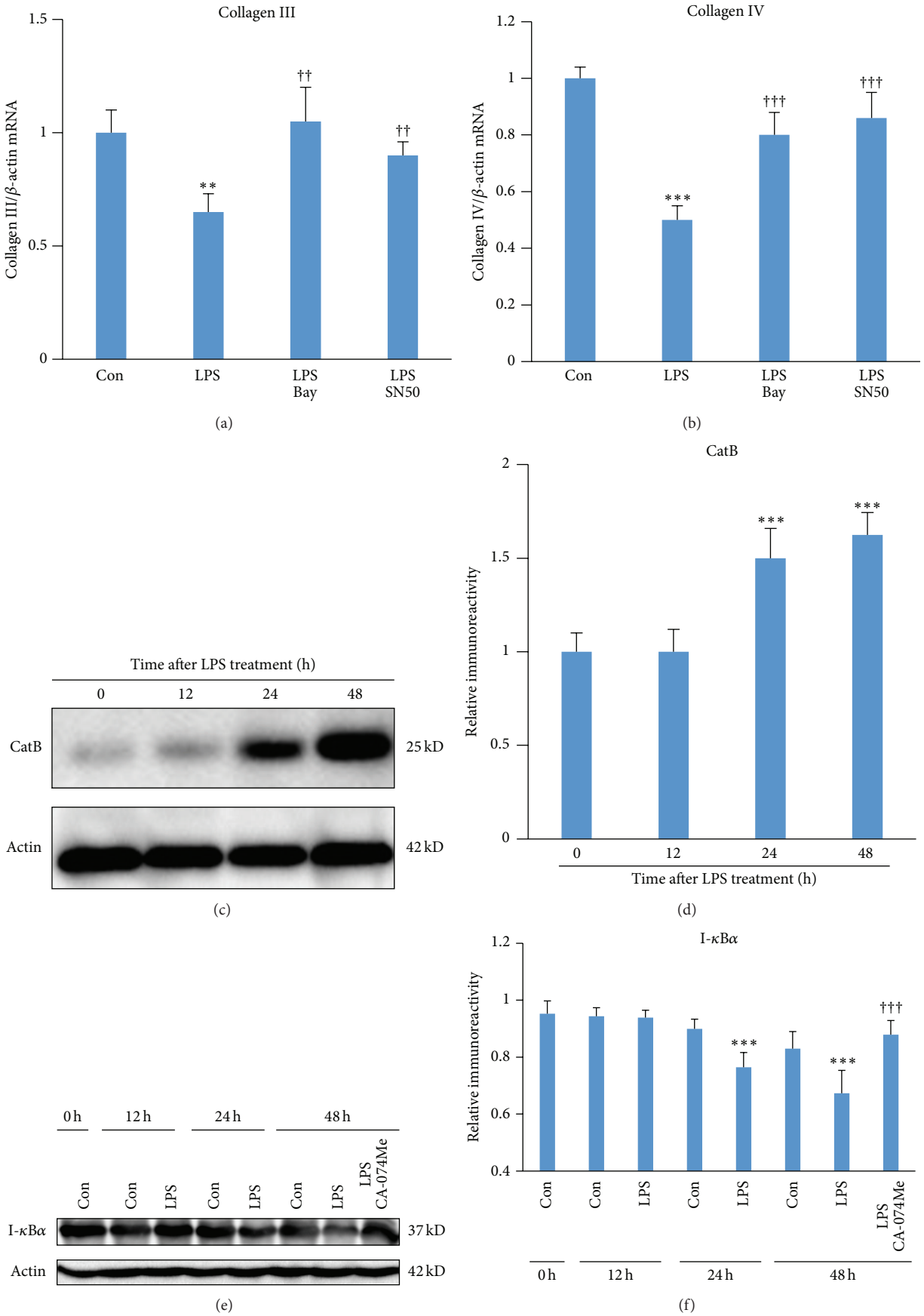

Figure 3: Continued.

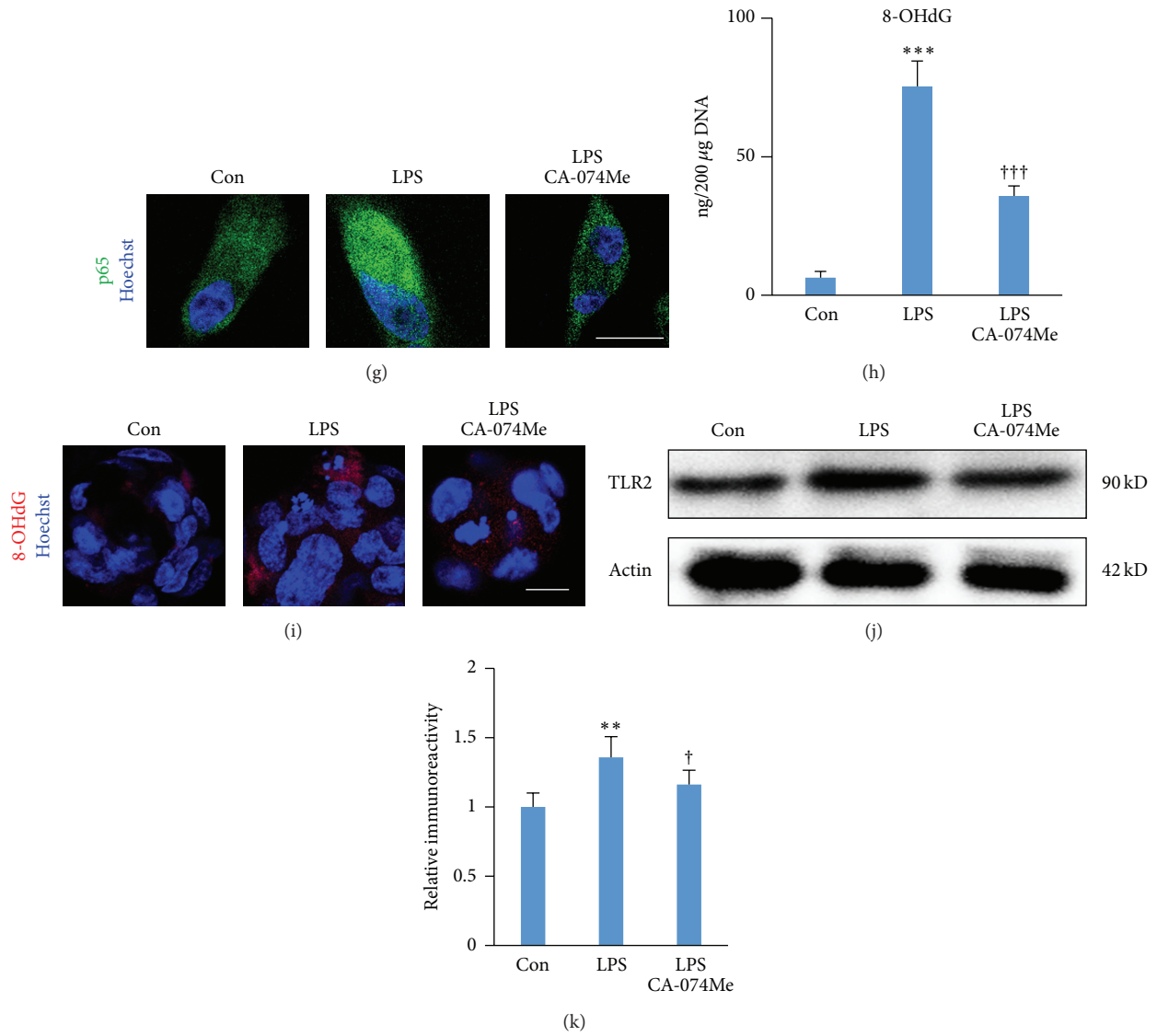

Figure 3: The effects of CatB on NF-κB activation and oxidative damage in BJ fibroblasts after challenge with *P.g.* LPS. ((a), (b)) The effect of Bay 11-7082 (Bay, 20 μM, 1 h before *P.g.* LPS challenge) and SN50 (20 μM, 1 h before *P.g.* LPS challenge) on the expression of collagen III (a) and collagen IV (b) at 48 h after challenge with *P.g.* LPS (1 μg/mL). Each column and bar represent the mean ± SEM ($n = 4$ each). The asterisks indicate a statistically significant difference from the value in unchallenged cells ($^{**}P < 0.01$, $^{***}P < 0.001$). The crosses indicate a statistically significant difference from the value in *P.g.* LPS-challenged cells without pretreatment with Bay 11-7082 ($^{\dagger\dagger}P < 0.01$, $^{\dagger\dagger\dagger}P < 0.001$). (c) The time course of the protein expression of CatB in BJ fibroblasts after challenge with *P.g.* LPS (1 μg/mL). (d) The quantitative analyses of the immunoblotting for CatB. Each column and bar represent the mean ± SEM ($n = 4$, each). The asterisks indicate a statistically significant difference from the value in the unchallenged cells ($^{***}P < 0.001$). (e) The time course of the protein expression of IκBα in BJ fibroblasts after challenge with *P.g.* LPS (1 μg/mL). (f) The quantitative analyses of the immunoblotting for IκBα. Each column and bar represent the mean ± SEM ($n = 4$, each). The asterisks indicate a statistically significant difference from the value in the unchallenged cells ($^{***}P < 0.001$). The crosses indicate a statistically significant difference from the value in 48 h *P.g.* LPS-challenged cells without pretreatment with CA-074Me ($^{\dagger\dagger\dagger}P < 0.001$). (g) The immunofluorescent CLSM images of p65 (green) in BJ fibroblasts after 48 h challenged with *P.g.* LPS or pretreatment with CA-074Me. Scale bar = 10 μm. (h) The amount of 8-OHdG in BJ fibroblasts 48 h after challenge with *P.g.* LPS. Each column and bar represent the mean ± SEM ($n = 4$, each). The asterisks indicate a statistically significant difference from the value in the unchallenged cells ($^{***}P < 0.001$). The crosses indicate a statistically significant difference from the value in 48 h *P.g.* LPS-challenged cells without pretreatment with CA-074Me ($^{\dagger\dagger\dagger}P < 0.001$). (i) The immunofluorescent CLSM images of 8-OHdG (green) in BJ fibroblasts after 48 h challenged with *P.g.* LPS or pretreatment with CA-074Me. Scale bar = 10 μm. (j) The protein expression of TLR2 in BJ fibroblasts 48 h after challenge with *P.g.* LPS (1 μg/mL). (k) The quantitative analyses of the immunoblotting for TLR2 in (j). Each column and bar represent the mean ± SEM ($n = 4$, each). The asterisks indicate a statistically significant difference from the value in the unchallenged cells ($^{**}P < 0.01$). The crosses indicate a statistically significant difference from the value in 48 h *P.g.* LPS-challenged cells without pretreatment with CA-074Me ($^{\dagger}P < 0.05$).

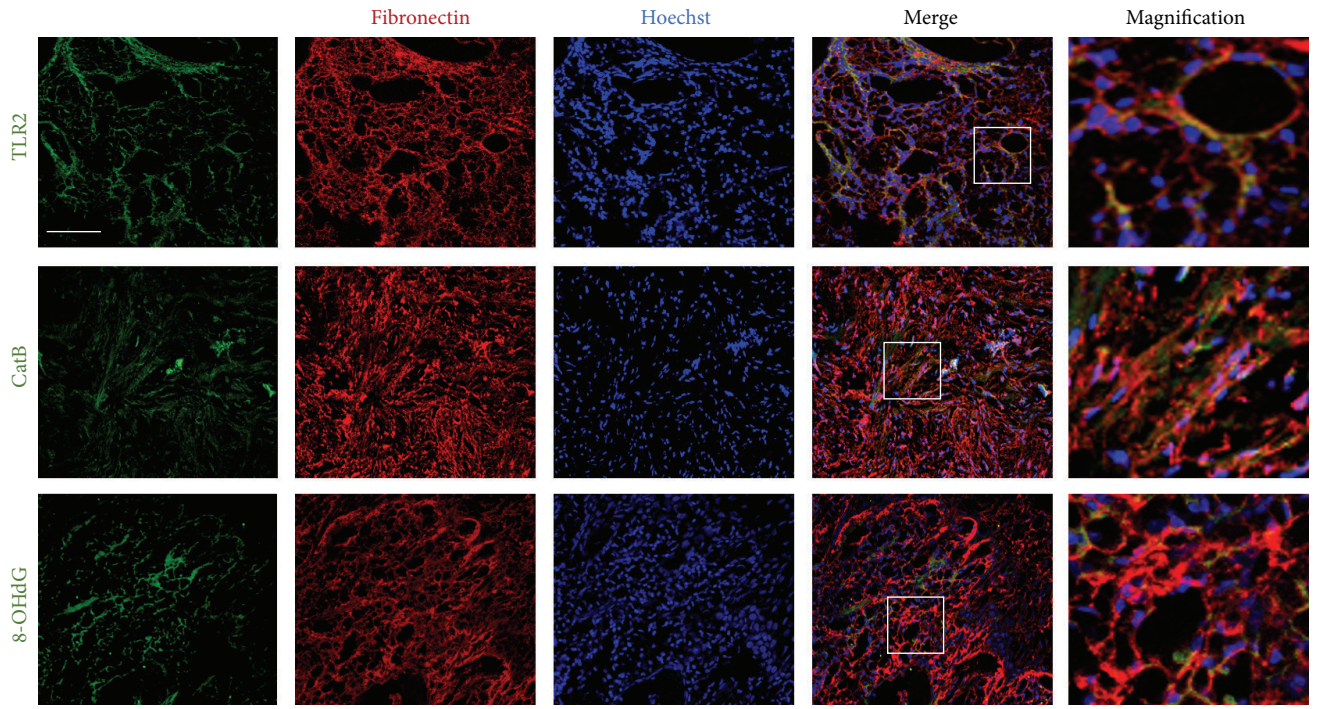

Figure 4: The immunofluorescent CLSM images of TLR2, CatB, and 8-OHdG (green) with fibronectin (red) and Hoechst-stained nuclei (blue) in the inflamed tissues of patients with chronic periodontitis. Scale bar = 50 μm. The magnifical images are made from the square areas. The increased CatB is closely related to the oxidative damage during the chronic activation of TLR2/NF-κB signaling.

We then further analyzed the expression of CatB, IκBα, and 8-OHdG (a critical biomarker of oxidative stress). The mean expression of CatB was significantly increased at 24 and 48 h (Figures 3(c) and 3(d)), while the mean expression of IκBα was significantly decreased compared with that of the control group at 24 and 48 h after *P.g.* LPS challenge (Figures 3(e) and 3(f)). The mean expression of the *P.g.* LPS-decreased IκBα was paralleled with the significant increase in the nuclear localization of p65 NF-κB at 24 after *P.g.* LPS challenge (Figure 3(g)). The mean amount of 8-OHdG was significantly increased at 48 h (Figure 3(h)) and the protein expression level of TLR2 was also increased at 48 h after *P.g.* LPS challenge (Figures 3(j) and 3(k)). These results suggest that an elevated level of CatB is positively associated with NF-κB activation and oxidative damage after challenge with *P.g.* LPS.

Interestingly, the *P.g.* LPS-induced increase in levels of 8-OHdG and decrease in levels of IκBα were significantly inhibited by CA-074Me at 48 h after *P.g.* LPS challenge (Figures 3(e)–3(i)). These observations demonstrate that CatB is involved in the proteolytic degradation of the IκBα and oxidative DNA damage during chronic *P.g.* LPS challenge. Therefore, the novel mechanism of CatB in regulating the expression of collagens by fibroblasts is via chronically activating TLR2/NF-κB signaling and subsequent oxidative damage.

3.4. Determination of CatB and Oxidative Damage in Fibroblasts of Inflamed Tissues with Chronic Periodontitis. TLR2, CatB, and 8-OHdG were expressed in the fibroblasts of inflamed tissues with chronic periodontitis and found to be localized in 89%, 87%, and 86% of fibronectin-positive fibroblasts, respectively (Figure 4). These results further demonstrate that the increased CatB is involved in oxidative damage in inflammatory tissues via the chronic activation of TLR2/NF-κB signaling. The critical role and novel mechanism of CatB in regulating the expression of collagens by fibroblasts via this activation and oxidative damage were summarized in Figure 5.

4. Discussion

The major finding of the present study was clarifying the critical role of CatB in regulating collagen expression by fibroblasts via prolonging TLR2/NF-κB activation (summarized in Figure 5). To our knowledge, this is the first study to demonstrate the involvement of CatB in collagen expression during chronic inflammation and oxidative stress, thereby adding to the available information regarding the mechanisms of delayed tissue repair during chronic inflammation.

We focused on collagens III and IV in fibroblasts because of their importance in wound healing and tissue remodeling. As the main fibrillar collagens in connective tissues [1], collagen III is suggested to regulate collagen I synthesis [2], since collagen III-deficit mice exhibit more pronounced wound contracture than those with collagen III [5], and upregulating collagen III expression using natural remedies accelerates cutaneous wound healing in rats [6]. However, the expression of collagen III is regulated by the activity of local fibroblasts [6]. Collagen IV, as a major component of

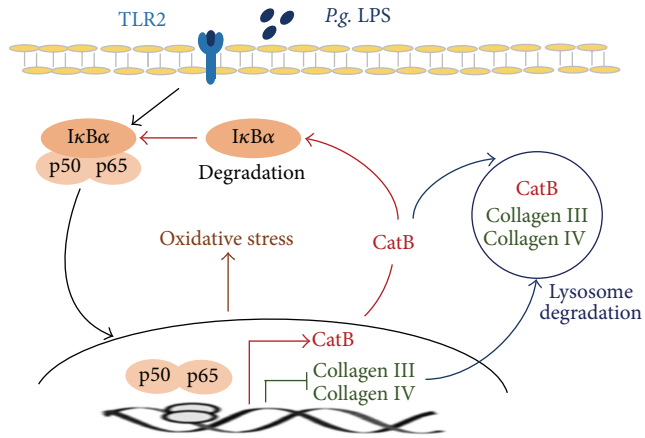

Figure 5: A schematic representation of the effects and the novel molecular mechanisms of CatB in regulating the expression of collagens III and IV via chronic activation of TLR2/NF-κB signaling and subsequent oxidative damage.

the BM, participates in the inflammatory responses during tissue repair [7, 28, 29], principally via cellular regulation and migration [9, 30]. Indeed, Col4a1 (human collagen IV gene) mutation-associated phenotypic features include chronic inflammation and immune activation [10, 11].

In the present study, the significant increase in the mRNA expression of collagens III and IV in fibroblasts at 3 and 12 h (the early culture periods) might have been a definitive response to challenge with the pathogenic agent TLR2 agonist *P.g.* LPS during the acute activation of TLR2 signaling [27], further demonstrating the expression of TLR2 in fibroblasts [13, 14]. In contrast, the mRNA expressions of both collagens III and IV in fibroblasts were significantly decreased at 24 and 48 h (the late culture periods) after challenge with *P.g.* LPS, possibly due to the chronic activation of TLR2 signaling. The concentration of *P.g.* LPS (1 μg/mL) used in the present experiments was one-thousandth of the concentration that reduced cell viability (1000 μg/mL), indicating that the *P.g.* LPS-induced decreases in collagen expression occurred in living fibroblasts (Figure 1(a)).

Of note, the *P.g.* LPS-induced decreases in collagen III and IV reflected the *P.g.* LPS-induced decrease in expression of IκBα and increase in expression of 8-OHdG. However, the *P.g.* LPS-induced decreases in expression of collagens were completely restored by Bay 11-7082 and SN50, the specific inhibitor of NF-κB (Figures 3(a) and 3(b)), suggesting that these reductions in collagen expression were dependent on NF-κB activation and oxidative damage, given that activated NF-κB exacerbates oxidative stress [31]. These results are consistent with a previous finding that NF-κB activation is necessary for UVC-decreased collagen biosynthesis [19] and that NF-κB inhibits collagen I gene expression [18]. The present findings suggest that TLR2/NF-κB-dependent decreases in the expression of collagen by fibroblasts may result in delayed tissue repair during chronic inflammation.

Elevated levels of CatB in fibroblasts are typically observed in many chronic inflammatory diseases, including rheumatoid arthritis as well as periodontitis [32–34]. Increased CatB expression in fibroblasts leads to tissue destruction, as fibroblasts are the prominent resident cells in the soft connective tissues [35]. In the present study, we determined that *P.g.* LPS increased the expression of CatB in fibroblasts, similar to the previous findings in macrophages [36]. Of note, the increased expression of CatB mRNA in the fibroblasts was observed at 24 and 48 h but not at 3 or 12 h after challenge with *P.g.* LPS, which agreed with the previous finding that CatB levels were not increased in the acute and intermediate stages of bacterial infection [37], implying that Cat B expression in fibroblasts might be induced by chronic activation of TLR2 signaling. Importantly, the *P.g.* LPS-induced increase in the CatB mRNA expression was paralleled by a *P.g.* LPS-induced decrease in the mRNA expression of both collagens III and IV, but this decrease was completely restored by pretreatment with CA-074Me. Surprisingly, the mean mRNA expression of collagens III and IV was significantly increased in the primary fibroblasts from $CatB^{-/-}$ mice from 24 h after challenge with *P.g.* LPS. The findings demonstrate the critical role of CatB in regulating collagen expression by fibroblasts during chronic activation of TLR2 signaling. CatB in *P.g.* LPS-challenged fibroblasts may not be involved in apoptosis [38], as the cell viabilities were not reduced with a *P.g.* LPS-induced increase in the expression of CatB. In addition, we also detected the expression of CatB in fibroblasts in the inflamed periodontal tissues from patients with chronic periodontitis (Figure 4), which was consistent with the findings in patients with rheumatoid arthritis [39, 40], inflammatory bowel disease [41], and polymyositis [42]. However, neither collagen III nor collagen IV was detected in these inflamed periodontal tissues (data not shown), strongly suggesting that CatB critically regulates collagen expression by fibroblasts during chronic inflammation.

CatB was recently found to regulate NF-κB activation [24]. However, conversely, CatB expression is believed to be NF-κB-dependent as the promoter of CatB has NF-κB binding site [43]. In almost all cell types, including fibroblasts, NF-κB exists as a dimer of a p50 and p65 subunit that is retained in an inactive cytoplasmic complex by binding to

the IκBα. NF-κB can be activated by TLR2 agonists as well as proinflammatory molecules, such as IL-1β, which induce phosphorylation acutely and proteolytic degradation of the IκB subunit chronically [21]. In the present study, an analysis of the whole cell extracts showed that the *P.g.* LPS-induced IκBα degradation in fibroblasts was paralleled by a *P.g.* LPS-induced increase in CatB in the late culture period; furthermore, the *P.g.* LPS-induced IκBα degradation was prevented by CA-074Me pretreatment (Figure 3). These results coincide with our previous observation of CatB-dependent IκBα degradation in microglia in a hypoxia/ischemia model [24] and strongly suggest that CatB is involved in the proteolytic degradation of the IκB subunit for slowing the migration out of the NF-κB complex from the nucleus, leading to sustained NF-κB activation in response to chronic *P.g.* LPS challenge.

This is the first report to clarify the novel mechanism of CatB involved in the downregulation of collagens III and IV via chronic activation of TLR2/NF-κB signaling. Furthermore, the *P.g.* LPS-induced increase in 8-OHdG might have been prevented by CA-074Me, suggesting the possible involvement of CatB in promoting oxidative stress through prolonging NF-κB activation, as activated NF-κB exacerbates oxidative stress [31].

CatB is considered a major lysosomal cysteine protease for the degradation of collagen in soft connective tissues, as it possesses both endopeptidase and exopeptidase activity which differs from other lysosomal cysteine proteases [44]. The increased expression of CatB by the chronic activation of TLR2/NF-κB signaling may also be involved in degrading the intercellular and extracellular collagen produced by fibroblasts, as CatB activities are required for the degradation of intracellular and extracellular collagen IV [45]. Furthermore, CatB is known to activate other collagenolytic matrix metalloproteinases for collagen degradation in fibroblasts at elevated levels during chronic inflammation [46].

5. Conclusion

CatB regulates the expression of collagens III and IV by fibroblasts via prolonging TLR2/NF-κB activation and oxidative stress (schematic illustration in Figure 5). Considering the role of CatB in collagen expression, CatB-specific inhibitors may be a useful approach for improving inflammation-delayed connective tissue repair, such as that found in dermatitis and periodontitis.

Competing Interests

The authors declare that they have no conflict of interests in association with this study.

Authors' Contributions

Xue Li and Zhou Wu contributed equally to this work.

Acknowledgments

This work was supported partly by The National Natural Science Foundation of China to Yanmin Zhou (81570983) and Grants-in-Aid for Scientific Research to Zhou Wu (16K11478).

References

[1] L. E. Tracy, R. A. Minasian, and E. J. Caterson, "Extracellular matrix and dermal fibroblast function in the healing wound," *Advances in Wound Care*, vol. 5, no. 3, pp. 119–136, 2016.

[2] X. Liu, T. H. Chang, S. M. Levenson, and M. Rojkind, "Wound fluids from saline solution- and *Staphylococcus aureus* peptidoglycan-inoculated sponges induce expression of matrix metalloproteinase 13 messenger ribonucleic acid by cultured rat fibroblasts," *Wound Repair and Regeneration*, vol. 5, no. 4, pp. 348–354, 1997.

[3] R. Carter, K. Jain, V. Sykes, and D. Lanning, "Differential expression of procollagen genes between mid- and late-gestational fetal fibroblasts," *Journal of Surgical Research*, vol. 156, no. 1, pp. 90–94, 2009.

[4] L. Cuttle, M. Nataatmadja, J. F. Fraser, M. Kempf, R. M. Kimble, and M. T. Hayes, "Collagen in the scarless fetal skin wound: detection with picrosirius-polarization," *Wound Repair and Regeneration*, vol. 13, no. 2, pp. 198–204, 2005.

[5] S. W. Volk, Y. Wang, E. A. Mauldin, K. W. Liechty, and S. L. Adams, "Diminished type III collagen promotes myofibroblast differentiation and increases scar deposition in cutaneous wound healing," *Cells Tissues Organs*, vol. 194, no. 1, pp. 25–37, 2011.

[6] M. Ganeshkumar, T. Ponrasu, R. Krithika, K. Iyappan, V. S. Gayathri, and L. Suguna, "Topical application of *Acalypha indica* accelerates rat cutaneous wound healing by up-regulating the expression of Type I and III collagen," *Journal of Ethnopharmacology*, vol. 142, no. 1, pp. 14–22, 2012.

[7] O. Chovar-Vera, V. Valenzuela-Muñoz, and C. Gallardo-Escárate, "Molecular characterization of collagen IV evidences early transcription expression related to the immune response against bacterial infection in the red abalone (*Haliotis rufescens*)," *Fish and Shellfish Immunology*, vol. 42, no. 2, pp. 241–248, 2015.

[8] W. J. Lennarz and M. D. Lane, *Encyclopedia of Biological Chemistry*, Academic Press, Cambridge, Mass, USA, 2013.

[9] K. Kühn, "Basement membrane (type IV) collagen," *Matrix Biology*, vol. 14, no. 6, pp. 439–445, 1995.

[10] M. Kiss, A. A. Kiss, M. Radics et al., "Drosophila type IV collagen mutation associates with immune system activation and intestinal dysfunction," *Matrix Biology*, vol. 49, pp. 120–131, 2016.

[11] D. S. Kuo, C. Labelle-Dumais, and D. B. Gould, "COL4A1 and COL4A2 mutations and disease: insights into pathogenic mechanisms and potential therapeutic targets," *Human Molecular Genetics*, vol. 21, no. 1, pp. R97–R110, 2012.

[12] J.-H. Ryu, S.-H. Kim, H.-Y. Lee et al., "Innate immune homeostasis by the homeobox gene *Caudal* and commensal-gut mutualism in *Drosophila*," *Science*, vol. 319, no. 5864, pp. 777–782, 2008.

[13] P. Proost, A.-K. Vynckier, F. Mahieu et al., "Microbial Toll-like receptor ligands differentially regulate CXCL10/IP-10 expression in fibroblasts and mononuclear leukocytes in synergy with IFN-γ and provide a mechanism for enhanced synovial chemokine levels in septic arthritis," *European Journal of Immunology*, vol. 33, no. 11, pp. 3146–3153, 2003.

[14] S. Hamidi, M. Schäfer-Korting, and G. Weindl, "TLR2/1 and sphingosine 1-phosphate modulate inflammation, myofibroblast differentiation and cell migration in fibroblasts," *Biochimica et Biophysica Acta—Molecular and Cell Biology of Lipids*, vol. 1841, no. 4, pp. 484–494, 2014.

[15] P. Huebener and R. F. Schwabe, "Regulation of wound healing and organ fibrosis by toll-like receptors," *Biochimica et Biophysica Acta—Molecular Basis of Disease*, vol. 1832, no. 7, pp. 1005–1017, 2013.

[16] M. Wu, D. J. Schneider, M. D. Mayes et al., "Osteopontin in systemic sclerosis and its role in dermal fibrosis," *Journal of Investigative Dermatology*, vol. 132, no. 6, pp. 1605–1614, 2012.

[17] S. Bhattacharyya, K. Kelley, D. S. Melichian et al., "Toll-like receptor 4 signaling augments transforming growth factor-β responses: a novel mechanism for maintaining and amplifying fibrosis in scleroderma," *The American Journal of Pathology*, vol. 182, no. 1, pp. 192–205, 2013.

[18] D. J. Kouba, K.-Y. Chung, T. Nishiyama et al., "Nuclear factor-κB mediates TNF-α inhibitory effect on α2(I) collagen (COL1A2) gene transcription in human dermal fibroblasts," *Journal of Immunology*, vol. 162, no. 7, pp. 4226–4234, 1999.

[19] L. Szoka, E. Karna, and J. A. Palka, "UVC inhibits collagen biosynthesis through up-regulation of NF-κB p65 signaling in cultured fibroblasts," *Journal of Photochemistry and Photobiology B: Biology*, vol. 129, pp. 143–148, 2013.

[20] A. Halle, V. Hornung, G. C. Petzold et al., "The NALP3 inflammasome is involved in the innate immune response to amyloid-β," *Nature Immunology*, vol. 9, no. 8, pp. 857–865, 2008.

[21] K. Terada, J. Yamada, Y. Hayashi et al., "Involvement of cathepsin B in the processing and secretion of interleukin-1β in chromogranin a-stimulated microglia," *Glia*, vol. 58, no. 1, pp. 114–124, 2010.

[22] L. Sun, Z. Wu, Y. Hayashi et al., "Microglial cathepsin B contributes to the initiation of peripheral inflammation-induced chronic pain," *The Journal of Neuroscience*, vol. 32, no. 33, pp. 11330–11342, 2012.

[23] Z. Wu, L. Sun, S. Hashioka et al., "Differential pathways for interleukin-1β production activated by chromogranin A and amyloid β in microglia," *Neurobiology of Aging*, vol. 34, no. 12, pp. 2715–2725, 2013.

[24] J. Ni, Z. Wu, C. Peterts, K. Yamamoto, H. Qing, and H. Nakanishi, "The critical role of proteolytic relay through cathepsins B and E in the phenotypic change of microglia/macrophage," *The Journal of Neuroscience*, vol. 35, no. 36, pp. 12488–12501, 2015.

[25] P. D. Arora, M. F. Manolson, G. P. Downey, J. Sodek, and C. A. G. McCulloch, "A novel model system for characterization of phagosomal maturation, acidification, and intracellular collagen degradation in fibroblasts," *The Journal of Biological Chemistry*, vol. 275, no. 45, pp. 35432–35441, 2000.

[26] G. C. Armitage, "Development of a classification system for periodontal diseases and conditions," *Annals of Periodontology*, vol. 4, no. 1, pp. 1–6, 1999.

[27] Y. Liu, Z. Wu, X. Zhang et al., "Leptomeningeal cells transduce peripheral macrophages inflammatory signal to microglia in reponse to *Porphyromonas gingivalis* LPS," *Mediators of Inflammation*, vol. 2013, Article ID 407562, 11 pages, 2013.

[28] B. Altincicek and A. Vilcinskas, "Metamorphosis and collagen-IV-fragments stimulate innate immune response in the greater wax moth, *Galleria mellonella*," *Developmental and Comparative Immunology*, vol. 30, no. 12, pp. 1108–1118, 2006.

[29] A. M. Abreu Velez and M. S. Howard, "Diagnosis and treatment of cutaneous paraneoplastic disorders," *Dermatologic Therapy*, vol. 23, no. 6, pp. 662–675, 2010.

[30] N. Ortega and Z. Werb, "New functional roles for non-collagenous domains of basement membrane collagens," *Journal of Cell Science*, vol. 115, part 22, pp. 4201–4214, 2002.

[31] H. L. Pahl, "Activators and target genes of Rel/NF-κB transcription factors," *Oncogene*, vol. 18, no. 49, pp. 6853–6866, 1999.

[32] G. Tettamanti, A. Grimaldi, L. Rinaldi et al., "The multifunctional role of fibroblasts during wound healing in *Hirudo medicinalis* (Annelida, Hirudinea)," *Biology of the Cell*, vol. 96, no. 6, pp. 443–455, 2004.

[33] S. W. Cox, B. M. Eley, M. Kiili, A. Asikainen, T. Tervahartiala, and T. Sorsa, "Collagen degradation by interleukin-1β-stimulated gingival fibroblasts is accompanied by release and activation of multiple matrix metalloproteinases and cysteine proteinases," *Oral Diseases*, vol. 12, no. 1, pp. 34–40, 2006.

[34] B. Tong, B. Wan, Z. Wei et al., "Role of cathepsin B in regulating migration and invasion of fibroblast-like synoviocytes into inflamed tissue from patients with rheumatoid arthritis," *Clinical and Experimental Immunology*, vol. 177, no. 3, pp. 586–597, 2014.

[35] P. Geraghty, M. P. Rogan, C. M. Greene et al., "Neutrophil elastase up-regulates cathepsin B and matrix metalloprotease-2 expression," *Journal of Immunology*, vol. 178, no. 9, pp. 5871–5878, 2007.

[36] J. Hannaford, H. Guo, and X. Chen, "Involvement of cathepsins B and L in inflammation and cholesterol trafficking protein NPC2 secretion in macrophages," *Obesity*, vol. 21, no. 8, pp. 1586–1595, 2013.

[37] I. S. Cha, J. Kwon, J. Y. Mun et al., "Cathepsins in the kidney of olive flounder, *Paralichthys olivaceus*, and their responses to bacterial infection," *Developmental and Comparative Immunology*, vol. 38, no. 4, pp. 538–544, 2012.

[38] A. Canbay, A. E. Feldstein, H. Higuchi et al., "Kupffer cell engulfment of apoptotic bodies stimulates death ligand and cytokine expression," *Hepatology*, vol. 38, no. 5, pp. 1188–1198, 2003.

[39] G. Cunnane, O. Fitzgerald, C. Beeton, T. E. Cawston, and B. Bresnihan, "Early joint erosions and serum levels of matrix metalloproteinase 1, matrix metalloproteinase 3, and tissue inhibitor of metalloproteinases 1 in rheumatoid arthritis," *Arthritis & Rheumatism*, vol. 44, no. 10, pp. 2263–2274, 2001.

[40] T. Mishiro, S. Nakano, S. Takahara et al., "Relationship between cathepsin B and thrombin in rheumatoid arthritis," *The Journal of Rheumatology*, vol. 31, no. 7, pp. 1265–1273, 2004.

[41] A. Baici, K. Müntener, A. Willimann, and R. Zwicky, "Regulation of human cathepsin B by alternative mRNA splicing: homeostasis, fatal errors and cell death," *Biological Chemistry*, vol. 387, no. 8, pp. 1017–1021, 2006.

[42] Y. Feng, L. Ni, and Q. Wang, "Administration of cathepsin B inhibitor CA-074Me reduces inflammation and apoptosis in polymyositis," *Journal of Dermatological Science*, vol. 72, no. 2, pp. 158–167, 2013.

[43] S. Bien, C. A. Ritter, M. Gratz et al., "Nuclear factor-κB mediates up-regulation of cathepsin B by doxorubicin in tumor cells," *Molecular Pharmacology*, vol. 65, no. 5, pp. 1092–1102, 2004.

[44] L. B. Creemers, I. D. C. Jansen, K. A. Hoeben, W. Beertsen, and V. Everts, "Involvement of V-ATPases in the digestion of soft connective tissue collagen," *Biochemical and Biophysical Research Communications*, vol. 251, no. 2, pp. 429–436, 1998.

[45] A. Mitrović, B. Mirković, I. Sosič, S. Gobec, and J. Kos, "Inhibition of endopeptidase and exopeptidase activity of cathepsin B impairs extracellular matrix degradation and tumour invasion," *Biological Chemistry*, vol. 397, no. 2, pp. 164–174, 2016.

[46] L. Zhang, J. Lin, J. Guo, W. Sun, and L. Pan, "Effects of 1, 25-(OH)2D3 on airway remodeling and airway epithelial cell apoptosis in a murine model of asthma," *Zhonghua Yi Xue Za Zhi*, vol. 95, no. 48, pp. 3945–3949, 2015.

Hindawi Publishing Corporation
Oxidative Medicine and Cellular Longevity
Volume 2016, Article ID 7813072, 8 pages
http://dx.doi.org/10.1155/2016/7813072

Review Article

Role of NADPH Oxidase in Metabolic Disease-Related Renal Injury: An Update

Cheng Wan, Hua Su, and Chun Zhang

Department of Nephrology, Union Hospital, Tongji Medical College, Huazhong University of Science and Technology, Wuhan, Hubei 430022, China

Correspondence should be addressed to Chun Zhang; drzhangchun@hust.edu.cn

Received 2 June 2016; Accepted 17 July 2016

Academic Editor: Juan F. Santibanez

Metabolic syndrome has been linked to an increased risk of chronic kidney disease. The underlying pathogenesis of metabolic disease-related renal injury remains obscure. Accumulating evidence has shown that NADPH oxidase is a major source of intrarenal oxidative stress and is upregulated by metabolic factors leading to overproduction of ROS in podocytes, endothelial cells, and mesangial cells in glomeruli, which is closely associated with the initiation and progression of glomerular diseases. This review focuses on the role of NADPH oxidase-induced oxidative stress in the pathogenesis of metabolic disease-related renal injury. Understanding of the mechanism may help find potential therapeutic strategies.

1. Introduction

Metabolic syndrome is a constellation of interconnected risk factors for cardiovascular diseases and type 2 diabetes, including dyslipidemia, hypertension, hyperglycemia, abdominal obesity, and insulin resistance [1, 2]. Along with cardiovascular diseases and type 2 diabetes, accumulating evidence shows that metabolic syndrome contributes to an increased risk of microalbuminuria and/or chronic kidney disease (CKD) [3–7]. However, it remains unclear whether there is a definitive cause-and-effect relationship between metabolic syndrome and renal injury.

Research on the underlying pathogenesis of metabolic disease-related renal injury has suggested an important role of oxidative stress, which is a result of reactive oxygen species (ROS) overproduction, mitochondrial dysfunction, and/or impaired antioxidant system [8]. There are numerous intrarenal sources of ROS, such as mitochondrial electron transport chain, xanthine oxidase, and uncoupled nitric oxide (NO) synthase, while nicotinamide adenine dinucleotide phosphate (NADPH) oxidase is generally accepted as the major producer [9–13].

NADPH oxidases are multisubunit enzymes composing membrane and cytosolic components that transfer electrons across biological membranes. There are seven members in the Nox family of NADPH oxidase, including Nox1–Nox5 and dual oxidases, Duox1 and Duox2, with different activation mechanisms and tissue distribution [13–16]. The Nox homologues are widely expressed throughout the kidney. Nox1, Nox2, Nox4, and Nox5 are predominantly expressed in glomerular endothelial cells, tubulointerstitial cells, and glomerular cells, that is, mesangial cells and glomerular epithelial cells [17]. Various homologue-specific mechanisms regulate the activity of the Nox family involving a complex series of protein/protein interactions, phosphorylation and translocation of its subunits, and Rac activation. Numerous stimuli and agonists like transforming growth factor-β (TGF-β), angiotensin II (Ang II), hyperglycemia, oxidized low density lipoprotein (oxLDL), insulin-like growth factor-1 (IGF-1), vascular endothelial growth factor (VEGF), and aldosterone are capable of upregulating the activity and/or the expression of NADPH oxidases, subsequently leading to overproduction of ROS including the immediate product superoxide and the following hydrogen peroxide.

The proposed functions of NADPH oxidase-derived ROS in the kidney are mainly regulation of renal blood flow, alteration of cell fate, and regulation of gene expression. Superoxide avidly reacts with nitric oxide (NO) limiting its relaxing

effect on afferent arterioles and mediates the activation of inflammasome, while hydrogen peroxide is involved in the activation of protein tyrosine kinases, phospholipases, serine/threonine kinases, and so forth, resulting in enhanced epithelial-to-mesenchymal transition (EMT), apoptosis of podocytes, and promotion of cellular hypertrophy [18–25].

The present review will focus on the role of NADPH oxidase-induced oxidative stress in the pathogenesis of metabolic disease-related renal injury.

2. NADPH Oxidase and Diabetic Nephropathy

Diabetic nephropathy (DN) is the major complication of type 1 and type 2 diabetes and is one of the leading causes of end-stage renal disease (ESRD) [26]. It is characterized by functional deficits with proteinuria and decreased glomerular filtration, as well as structural changes, such as loss of podocytes, proliferation and expansion of mesangial cells and matrix, thickening of glomerular and tubular basement membranes, tubular atrophy, interstitial fibrosis, and arteriosclerosis. Increasing evidence has demonstrated that NADPH oxidase-induced oxidative stress plays a pivotal role in the initiation and development of DN [11, 27]. Blockade of NADPH oxidase-derived ROS generation ameliorates diabetes-induced glomerular injury via reducing podocyte loss, proteinuria, glomerular hypertrophy, and mesangial matrix expansion [28–33].

Damage and depletion of podocytes due to apoptosis occur during early DN, presented as actin cytoskeleton rearrangement, podocyte foot process effacement, and slit diaphragm disruption [34]. Studies have highlighted the role of podocytes in DN pathogenesis and revealed the upregulation of the NADPH oxidase subunits expression, predominantly Nox4 and Nox1, in type 1 diabetic OVE26 mice and type 2 diabetic db/db mice, following excessive ROS generation and podocytes apoptosis which contributes to albuminuria [20, 35–37]. In vitro studies also have shown that high glucose induced the upregulation of NADPH oxidase expression, enhancement of NADPH oxidase activity, and apoptosis induction in podocytes at later time points [35, 37–39]. Eid et al. found that the increase of Nox4 expression was attributed to the inactivation of AMP-activated protein kinase (AMPK), and Nox4 promoted podocyte apoptosis via p53- and PUMA-dependent apoptotic pathway in high glucose condition [35, 40]. Other NADPH oxidase subunits, such as Nox2, p22phox, and p67phox, are also expressed on podocytes. However, very little is known concerning the regulation of these subunits in the presence of high glucose [11, 41–43].

Besides podocyte injury, two other morphological alterations during early DN are mesangial matrix accumulation and cell hypertrophy leading to thickening of glomerular basement membrane [27, 44]. The important role of NADPH oxidase in mesangial cell injury has been demonstrated in experimental models of diabetes as well as in cultured cells exposed to high glucose, while the molecular mechanisms remain speculative. High glucose induces upregulation of Nox4 and p22phox expression in mesangial cells as well as in diabetic kidney, and Nox4 and p22phox mediate cell hypertrophy and fibronectin expression [12, 45–48]. Since p22phox interacts with Nox4 and enhances its activity, Gorin and Wauquier suggested that p22phox and Nox4 might form a complex that contributed to high glucose-dependent oxidative stress and the subsequent fibrotic processes [13]. The role of other NADPH oxidase subunits in mesangial cell injury has been less studied and the findings are controversial.

Furthermore, NADPH oxidase also mediates the ROS generation induced by other mediators in DN such as Ang II and TGF-β [42, 49–51]. Induced by Ang II, an acute increase and prolonged upregulation of Nox4 expression both take place in mesangial cells, and Nox4 mediates ROS generation leading to activation of signalling, for instance, extracellular signal-regulated kinase-1/2 (ERK1/2) [52], Akt/protein kinase B (Akt/PKB) [50], and proline-rich tyrosine kinase-2 (Pyk-2)/Src/3-phosphoinositide-dependent protein kinase-1 (PDK-1) [22], which results in hypertrophy and increased fibronectin expression. Induced by TGF-β, Nox4 expression within mitochondria in podocytes is upregulated via the Sma and Mad homologue (Smad) 2/3 pathway and ultimately results in ROS overproduction, mitochondrial dysfunction, and podocyte apoptosis [53, 54].

3. NADPH Oxidase and Hyperhomocysteinemia-Associated Glomerular Injury

Hyperhomocysteinemia (hHcys) is defined as a pathological condition characterized by abnormal elevation of homocysteine (Hcys) plasma concentration and has been considered as a pivotal independent risk factor in the development of progressive glomerulosclerosis and/or ESRD [55–57]. Previous evidence has revealed that Hcys induces endothelial injury, vascular smooth muscle cells proliferation, and extracellular matrix (ECM) metabolism disturbance [58–61]. Considering the similarity of pathological alterations between Hcys-induced arterial injury and glomerular injury, the role of hHcys in glomerulosclerosis has been verified. Although the mechanism by which Hcys induces glomerular injury remains poorly understood, there is evidence that NADPH oxidase-derived oxidative stress is involved in the development of glomerular injury induced by Hcys [62–65]. An experimental model of hHcys was reported to develop glomerulosclerosis, characterized by local oxidative stress, podocyte dysfunction, mesangial expansion, and fibrosis, which could be significantly attenuated by treatment of NADPH oxidase inhibitors [64].

Podocyte injury is a critical early event leading to glomerulosclerosis. It has been revealed that Hcys induces podocyte damage and slit diaphragm disruption, causing proteinuria and glomerular sclerosis [66]. Zhang et al. [67] found that, in mice lacking Nox2 gene, hHcys induced by folate-free diet led to less severe podocyte injury and glomerulosclerosis, as shown by attenuated foot process effacement and podocyte loss, lower proteinuria, and glomerular damage index, as well as higher glomerular filtration rate. Thus, NADPH oxidase is suggested to be essential for Hcys-induced podocyte injury and glomerulosclerosis. Furthermore, Hcys stimulation was documented to upregulate NOX2 and p47phox expression

and induce their aggregation in lipid raft (LR) clusters in podocytes, while disrupting LR clustering markedly blocked the enrichment of the NADPH oxidase subunits, decreased the enzyme activity, and functionally attenuated Hcys-induced podocyte injury. These findings indicate that NADPH oxidase subunits aggregation and activation through LR clustering are important molecular mechanisms in Hcys-induced podocytes injury [68]. Hcys is also confirmed to induce podocytes to undergo EMT and inflammasome activation through NADPH oxidase-derived oxidative stress, which consequently leads to glomerular injury and sclerosis [69–71].

Ingram's research group and others also have clarified that Hcys induces alterations of ECM metabolism in mesangial cells, another important event leading to glomerulosclerosis and loss of renal function [72]. Hcys was reported to upregulate tissue inhibitor of metalloproteinase-1 and induce collagen type I accumulation, accompanied by enhanced cell proliferation and NADPH oxidase activity in rat mesangial cells [73]. Hcys-induced activation of NADPH oxidase is suggested to be mediated by enhanced ceramide synthesis and the subsequent increase of Rac GTPase activity [74]. There is also evidence showing that the N-methyl-D-aspartate (NMDA) receptor may mediate activation of NADPH oxidase in hHcys-associated glomerular injury [75]. In addition, Hcys has been found to cause mesangial apoptosis via oxidative stress and p38-mitogen-activated protein kinase activation, thereby suggesting another underlying mechanism of hHcys-associated glomerular injury [63].

4. NADPH Oxidase and Hyperlipidemia-Associated Glomerular Injury

The concern of the association between hyperlipidemia and renal diseases may date back to the 19th century. Since then, accumulating evidence in experimental findings and clinical observations has suggested an important role of hyperlipidemia in the progression of glomerulosclerosis [76–81]. Hyperlipidemia-associated glomerular injury is mainly characterized by lipid or lipoprotein deposition, macrophage infiltration, and mesangial expansion. As with other metabolic factors, such as hyperglycemia and hHcys, oxidative stress is proved to contribute to the deleterious effects of hyperlipidemia on renal injury. In high-fat diet fed mice, the expression of NADPH oxidase subunits, including p47phox, Nox2, and p67phox, was significantly upregulated, and the inhibitor could ameliorate hyperlipidemia-induced endothelial dysfunction via inhibition of NADPH oxidase expression [82]. However, in the study of Scheuer et al., it is reported that xanthine oxidoreductase rather than NADPH oxidase mainly accounted for the generation of ROS in glomeruli and tubulointerstitium induced by hyperlipidemia [83]. In addition, Joles et al. clarified that both hypercholesterolemia and hypertriglyceridemia aggravated renal injury predominantly via podocytes, accompanied by activation and injury of tubulointerstitial cells, lacking evidence of mesangial activation, proliferation, or matrix accumulation [80]. Furthermore, hyperlipidemia often coexists with other metabolic syndrome components and accelerates the progression of glomerular injury together [84, 85].

5. NADPH Oxidase and Hyperuricemia-Related Kidney Disease

Uric acid (UA) is an intermediate product in the purine degradation pathway in cells but is the final product of purine catabolism in humans, due to the loss of uricase activity during hominoid evolution [86]. The role of UA in CKD remains controversial, and the "UA debate" has been going on for decades [87]. UA has been considered as a major antioxidant in protecting cells from oxidative injury proved by abundant experimental and clinical evidence [88]. On the other hand, epidemiologic evidence and experimental models also have shown that hyperuricemia may impose detrimental effects as a prooxidant [89–92]. UA is often associated with other risk factors of CKD, including diabetes, hypertension, and inflammation [93], which makes it difficult to dissect the role of UA itself in the progression of CKD. However, a recent study showed an association between hyperuricemia and renal damage independently of hypertension and intrarenal renin-angiotensin system (RAS) activation [94].

In the past, hyperuricemia was thought to cause kidney disease by a crystal-dependent mechanism. The crystal of monosodium urate may induce potassium efflux, lysosomal rupture, and mitochondrial ROS production, which provoke inflammasome and induce the secretion of proinflammatory cytokines, eventually causing inflammation and renal injury. The crystal-independent mechanism of hyperuricemia-related kidney disease remains poorly understood. The main pathophysiological mechanisms of hyperuricemia-related kidney disease include endothelial dysfunction, activation of local RAS, oxidative stress, and proinflammatory and proliferative effects. NADPH oxidase is suggested to play a role in the pathogenesis of hyperuricemia-related kidney disease, as with other metabolic disease-related renal injuries. It has been revealed that hyperuricemia is associated with endothelial dysfunction, due to oxidative stress with activation of RAS and a decrease of NO bioavailability [95, 96]. In an experimental model of hyperuricemia, enhanced intrarenal oxidative stress, increased expression of NOX-4 and Ang II, and decreased NO bioavailability were observed [97]. The aging and apoptosis of endothelial cells induced by hyperuricemia were ameliorated by antioxidants [98]. Furthermore, there is evidence that mitochondrial alterations and decreased intracellular ATP are implicated in UA-induced endothelial dysfunction [99]. In cultured renal tubular cells, it has been shown that UA induces EMT and apoptosis of renal tubular cells which is ameliorated by antioxidants, suggesting a detrimental role of oxidative stress [100].

6. NADPH Oxidase and Obesity-Related Kidney Disease

Oxidative stress is also associated with other metabolic kidney diseases such as obesity-related kidney disease [101].

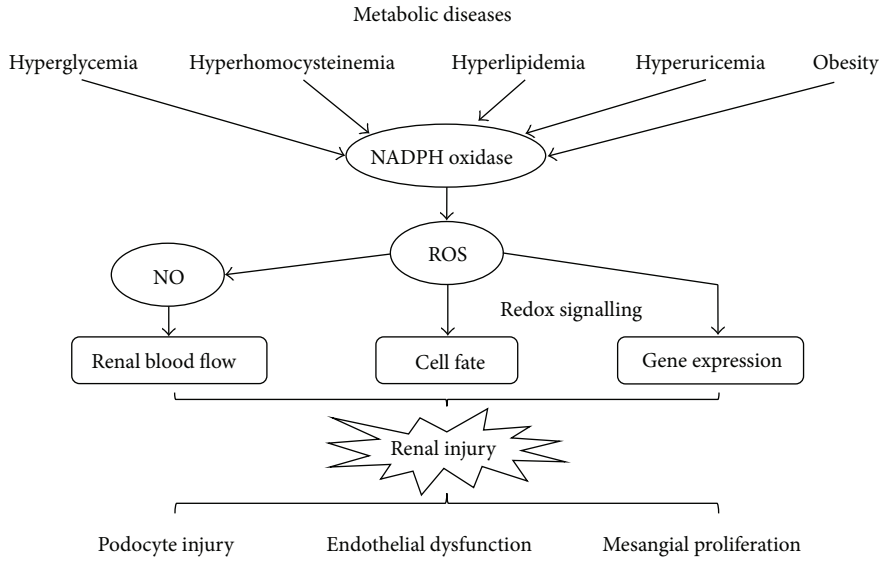

Figure 1: NADPH oxidase-derived ROS in the pathogenesis of metabolic disease-related renal injury. Metabolic stimuli may upregulate the expression of NADPH oxidase and enhance the activity of NADPH oxidase, which subsequently leads to overproduction of ROS. NADPH oxidase-derived oxidative stress is involved in podocyte injury, endothelial dysfunction, mesangial proliferation, and so forth, eventually resulting in renal injury. NADPH: nicotinamide adenine dinucleotide phosphate; ROS: reactive oxygen species; NO: nitric oxide.

It is well documented that the glomerular scarring in obesity-associated focal segmental glomerulosclerosis is driven by podocyte injury, which may partly be a result of the NADPH oxidase-derived oxidative stress induced by upregulated Ang II and TGF-β [102]. There is supplemental data supporting the fact that NADPH oxidase-mediated oxidative injury to the proximal tubule contributes to proteinuria in obese rats [103]. In addition, oxidative stress is demonstrated to play a role in the pathogenesis of renal injury through its contribution to progressive vascular dysfunction and remodeling [104, 105]. Collectively, NADPH oxidase-derived oxidative stress is suggested to trigger the progression of obesity-related kidney disease.

7. Conclusion

The NADPH oxidase is widely expressed throughout the kidney and is a major source of intrarenal oxidative stress. Metabolic stimuli elicit the upregulation of NADPH oxidase expression and the enhancement of NADPH oxidase activity. As depicted in Figure 1, ROS generated by NADPH oxidase plays a pivotal role in the pathogenesis of glomerular diseases related to metabolic diseases. Hence, approaches to reduce oxidative stress by antioxidants may be potential therapies to prevent and treat metabolic disease-related renal injury.

Competing Interests

The authors declare that they have no competing interests.

Acknowledgments

This work was supported by grants from the National Natural Science Foundation of China (no. 81170662, no. 31200872, no. 81470964, no. 81570671, and no. 81522010), a grant from Wuhan Science and Technology Bureau (no. 2015060101010039), and Specialized Research Fund for the Doctoral Program of Higher Education of China (no. 20130142110064).

References

[1] E. Kassi, P. Pervanidou, G. Kaltsas, and G. Chrousos, "Metabolic syndrome: definitions and controversies," *BMC Medicine*, vol. 9, article 48, 2011.

[2] K. G. M. M. Alberti, P. Zimmet, and J. Shaw, "The metabolic syndrome—a new worldwide definition," *The Lancet*, vol. 366, no. 9491, pp. 1059–1062, 2005.

[3] J. Chen, P. Muntner, L. L. Hamm et al., "The metabolic syndrome and chronic kidney disease in U.S. Adults," *Annals of Internal Medicine*, vol. 140, no. 3, pp. 167–174, 2004.

[4] M. Kurella, J. C. Lo, and G. M. Chertow, "Metabolic syndrome and the risk for chronic kidney disease among nondiabetic adults," *Journal of the American Society of Nephrology*, vol. 16, no. 7, pp. 2134–2140, 2005.

[5] J. Chen, P. Muntner, L. L. Hamm et al., "Insulin resistance and risk of chronic kidney disease in nondiabetic US adults," *Journal of the American Society of Nephrology*, vol. 14, no. 2, pp. 469–477, 2003.

[6] J. Chen, D. Gu, C.-S. Chen et al., "Association between the metabolic syndrome and chronic kidney disease in Chinese adults," *Nephrology Dialysis Transplantation*, vol. 22, no. 4, pp. 1100–1106, 2007.

[7] C. M. Hoehner, K. J. Greenlund, S. Rith-Najarian, M. L. Casper, and W. M. McClellan, "Association of the insulin resistance syndrome and microalbuminuria among nondiabetic native Americans. The Inter-Tribal Heart Project," *Journal of the American Society of Nephrology*, vol. 13, no. 6, pp. 1626–1634, 2002.

[8] M. Nita and A. Grzybowski, "The role of the reactive oxygen species and oxidative stress in the pathomechanism of the age-related ocular diseases and other pathologies of the anterior and posterior eye segments in adults," *Oxidative Medicine and Cellular Longevity*, vol. 2016, Article ID 3164734, 23 pages, 2016.

[9] Y. Gorin and K. Block, "Nox as a target for diabetic complications," *Clinical Science*, vol. 125, no. 8, pp. 361–382, 2013.

[10] P. S. Gill and C. S. Wilcox, "NADPH oxidases in the kidney," *Antioxidants and Redox Signaling*, vol. 8, no. 9-10, pp. 1597–1607, 2006.

[11] Y. Gorin and K. Block, "Nox4 and diabetic nephropathy: with a friend like this, who needs enemies?" *Free Radical Biology and Medicine*, vol. 61, pp. 130–142, 2013.

[12] Y. Gorin, K. Block, J. Hernandez et al., "Nox4 NAD(P)H oxidase mediates hypertrophy and fibronectin expression in the diabetic kidney," *Journal of Biological Chemistry*, vol. 280, no. 47, pp. 39616–39626, 2005.

[13] Y. Gorin and F. Wauquier, "Upstream regulators and downstream effectors of NADPH oxidases as novel therapeutic targets for diabetic kidney disease," *Molecules and Cells*, vol. 38, no. 4, pp. 285–296, 2015.

[14] K. Bedard and K.-H. Krause, "The NOX family of ROS-generating NADPH oxidases: physiology and pathophysiology," *Physiological Reviews*, vol. 87, no. 1, pp. 245–313, 2007.

[15] A. Panday, M. K. Sahoo, D. Osorio, and S. Batra, "NADPH oxidases: an overview from structure to innate immunity-associated pathologies," *Cellular and Molecular Immunology*, vol. 12, no. 1, pp. 5–23, 2015.

[16] S. Chen, X.-F. Meng, and C. Zhang, "Role of NADPH oxidase-mediated reactive oxygen species in podocyte injury," *BioMed Research International*, vol. 2013, Article ID 839761, 7 pages, 2013.

[17] S. A. Jones, J. T. Hancock, O. T. G. Jones, A. Neubauer, and N. Topley, "The expression of NADPH oxidase components in human glomerular mesangial cells: detection of protein and mRNA for p47phox, p67phox, and p22phox," *Journal of the American Society of Nephrology*, vol. 5, no. 7, pp. 1483–1491, 1995.

[18] A. Whaley-Connell, J. Habibi, R. Nistala et al., "Attenuation of NADPH oxidase activation and glomerular filtration barrier remodeling with statin treatment," *Hypertension*, vol. 51, no. 2, pp. 474–480, 2008.

[19] C. D. Bondi, N. Manickam, D. Y. Lee et al., "NAD(P)H oxidase mediates TGF-β1-induced activation of kidney myofibroblasts," *Journal of the American Society of Nephrology*, vol. 21, no. 1, pp. 93–102, 2010.

[20] A. A. Eid, Y. Gorin, B. M. Fagg et al., "Mechanisms of podocyte injury in diabetes: role of cytochrome P450 and NADPH oxidases," *Diabetes*, vol. 58, no. 5, pp. 1201–1211, 2009.

[21] K. Wingler, S. Wünsch, R. Kreutz, L. Rothermund, M. Paul, and H. H. H. W. Schmidt, "Upregulation of the vascular NAD(P)H-oxidase isoforms Nox1 and Nox4 by the renin-angiotensin system in vitro and in vivo," *Free Radical Biology and Medicine*, vol. 31, no. 11, pp. 1456–1464, 2001.

[22] K. Block, A. Eid, K. K. Griendling, D.-Y. Lee, Y. Wittrant, and Y. Gorin, "Nox4 NAD(P)H oxidase mediates Src-dependent tyrosine phosphorylation of PDK-1 in response to angiotensin II: role in mesangial cell hypertrophy and fibronectin expression," *The Journal of Biological Chemistry*, vol. 283, no. 35, pp. 24061–24076, 2008.

[23] D. Meng, D.-D. Lv, and J. Fang, "Insulin-like growth factor-I induces reactive oxygen species production and cell migration through Nox4 and Rac1 in vascular smooth muscle cells," *Cardiovascular Research*, vol. 80, no. 2, pp. 299–308, 2008.

[24] K. Miyata, M. Rahman, T. Shokoji et al., "Aldosterone stimulates reactive oxygen species production through activation of NADPH oxidase in rat mesangial cells," *Journal of the American Society of Nephrology*, vol. 16, no. 10, pp. 2906–2912, 2005.

[25] J. L. Barnes and Y. Gorin, "Myofibroblast differentiation during fibrosis: role of NAD(P)H oxidases," *Kidney International*, vol. 79, no. 9, pp. 944–956, 2011.

[26] F. A. Hakim and A. Pflueger, "Role of oxidative stress in diabetic kidney disease," *Medical Science Monitor*, vol. 16, no. 2, pp. RA37–RA48, 2010.

[27] D. K. Singh, P. Winocour, and K. Farrington, "Oxidative stress in early diabetic nephropathy: fueling the fire," *Nature Reviews Endocrinology*, vol. 7, no. 3, pp. 176–184, 2011.

[28] K. Asaba, A. Tojo, M. L. Onozato et al., "Effects of NADPH oxidase inhibitor in diabetic nephropathy," *Kidney International*, vol. 67, no. 5, pp. 1890–1898, 2005.

[29] S. M. Nam, M. Y. Lee, J. H. Koh et al., "Effects of NADPH oxidase inhibitor on diabetic nephropathy in OLETF rats: the role of reducing oxidative stress in its protective property," *Diabetes Research and Clinical Practice*, vol. 83, no. 2, pp. 176–182, 2009.

[30] M. Kitada, S. Kume, N. Imaizumi, and D. Koya, "Resveratrol improves oxidative stress and protects against diabetic nephropathy through normalization of Mn-SOD dysfunction in AMPK/SIRT1- independent pathway," *Diabetes*, vol. 60, no. 2, pp. 634–643, 2011.

[31] A. Tojo, K. Asaba, and M. L. Onozato, "Suppressing renal NADPH oxidase to treat diabetic nephropathy," *Expert Opinion on Therapeutic Targets*, vol. 11, no. 8, pp. 1011–1018, 2007.

[32] Y. Gorin, R. C. Cavaglieri, K. Khazim et al., "Targeting NADPH oxidase with a novel dual Nox1/Nox4 inhibitor attenuates renal pathology in type 1 diabetes," *American Journal of Physiology—Renal Physiology*, vol. 308, no. 11, pp. F1276–F1287, 2015.

[33] M. Fujii, T. Inoguchi, Y. Maeda et al., "Pitavastatin ameliorates albuminuria and renal mesangial expansion by downregulating NOX4 in db/db mice," *Kidney International*, vol. 72, no. 4, pp. 473–480, 2007.

[34] S. J. Shankland, "The podocyte's response to injury: role in proteinuria and glomerulosclerosis," *Kidney International*, vol. 69, no. 12, pp. 2131–2147, 2006.

[35] A. A. Eid, B. M. Ford, K. Block et al., "AMP-activated protein kinase (AMPK) negatively regulates Nox4-dependent activation of p53 and epithelial cell apoptosis in diabetes," *The Journal of Biological Chemistry*, vol. 285, no. 48, pp. 37503–37512, 2010.

[36] L. L. Zhou, F. F. Hou, G. B. Wang et al., "Accumulation of advanced oxidation protein products induces podocyte apoptosis and deletion through NADPH-dependent mechanisms," *Kidney International*, vol. 76, no. 11, pp. 1148–1160, 2009.

[37] K. Susztak, A. C. Raff, M. Schiffer, and E. P. Böttinger, "Glucose-induced reactive oxygen species cause apoptosis of podocytes and podocyte depletion at the onset of diabetic nephropathy," *Diabetes*, vol. 55, no. 1, pp. 225–233, 2006.

[38] J. Xu, Z. Li, P. Xu, and Z. Yang, "Protective effects of leukemia inhibitory factor against oxidative stress during high glucose-induced apoptosis in podocytes," *Cell Stress and Chaperones*, vol. 17, no. 4, pp. 485–493, 2012.

[39] J. Toyonaga, K. Tsuruya, H. Ikeda et al., "Spironolactone inhibits hyperglycemia-induced podocyte injury by attenuating ROS production," *Nephrology Dialysis Transplantation*, vol. 26, no. 8, pp. 2475–2484, 2011.

[40] A. Papadimitriou, E. B. M. I. Peixoto, K. C. Silva, J. M. Lopes de Faria, and J. B. Lopes de Faria, "Increase in AMPK brought about by cocoa is renoprotective in experimental diabetes mellitus by reducing NOX4/TGFβ-1 signaling," *The Journal of Nutritional Biochemistry*, vol. 25, no. 7, pp. 773–784, 2014.

[41] S. Greiber, T. Münzel, S. Kästner, B. Müller, P. Schollmeyer, and H. Pavenstädt, "NAD(P)H oxidase activity in cultured human podocytes: effects of adenosine triphosphate," *Kidney International*, vol. 53, no. 3, pp. 654–663, 1998.

[42] R. Nistala, A. Whaley-Connell, and J. R. Sowers, "Redox control of renal function and hypertension," *Antioxidants & Redox Signaling*, vol. 10, no. 12, pp. 2047–2089, 2008.

[43] T. Etoh, T. Inoguchi, M. Kakimoto et al., "Increased expression of NAD(P)H oxidase subunits, NOX4 and p22phox, in the kidney of streptozotocin-induced diabetic rats and its reversibity by interventive insulin treatment," *Diabetologia*, vol. 46, no. 10, pp. 1428–1437, 2003.

[44] Y. S. Kanwar, L. Sun, P. Xie, F.-Y. Liu, and S. Chen, "A glimpse of various pathogenetic mechanisms of diabetic nephropathy," *Annual Review of Pathology: Mechanisms of Disease*, vol. 6, pp. 395–423, 2011.

[45] L. Zhang, S. Pang, B. Deng et al., "High glucose induces renal mesangial cell proliferation and fibronectin expression through JNK/NF-κB/NADPH oxidase/ROS pathway, which is inhibited by resveratrol," *The International Journal of Biochemistry & Cell Biology*, vol. 44, no. 4, pp. 629–638, 2012.

[46] L. Xia, H. Wang, H. J. Goldberg, S. Munk, I. G. Fantus, and C. I. Whiteside, "Mesangial cell NADPH oxidase upregulation in high glucose is protein kinase C dependent and required for collagen IV expression," *American Journal of Physiology—Renal Physiology*, vol. 290, no. 2, pp. F345–F356, 2006.

[47] C. Whiteside, H. Wang, L. Xia, S. Munk, H. J. Goldberg, and I. G. Fantus, "Rosiglitazone prevents high glucose-induced vascular endothelial growth factor and collagen IV expression in cultured mesangial cells," *Experimental Diabetes Research*, vol. 2009, Article ID 910783, 11 pages, 2009.

[48] Y. Maeda, T. Inoguchi, R. Takei et al., "Inhibition of chymase protects against diabetes-induced oxidative stress and renal dysfunction in hamsters," *American Journal of Physiology—Renal Physiology*, vol. 299, no. 6, pp. F1328–F1338, 2010.

[49] K. N. Campbell, L. Raij, and P. Mundel, "Role of angiotensin II in the development of nephropathy and podocytopathy of diabetes," *Current Diabetes Reviews*, vol. 7, no. 1, pp. 3–7, 2011.

[50] Y. Gorin, J. M. Ricono, N.-H. Kim, B. Bhandari, G. G. Choudhury, and H. E. Abboud, "Nox4 mediates angiotensin II-induced activation of Akt/protein kinase B in mesangial cells," *American Journal of Physiology—Renal Physiology*, vol. 285, no. 2, pp. F219–F229, 2003.

[51] J. C. Jha, S. P. Gray, D. Barit et al., "Genetic targeting or pharmacologic inhibition of NADPH oxidase Nox4 provides renoprotection in long-term diabetic nephropathy," *Journal of the American Society of Nephrology*, vol. 25, no. 6, pp. 1237–1254, 2014.

[52] Y. Gorin, J. M. Ricono, B. Wagner et al., "Angiotensin II-induced ERK1/ERK2 activation and protein synthesis are redox-dependent in glomerular mesangial cells," *The Biochemical Journal*, vol. 381, part 1, pp. 231–239, 2004.

[53] L. Yu, Y. Liu, Y. Wu et al., "Smad3/Nox4-mediated mitochondrial dysfunction plays a crucial role in puromycin aminonucleoside-induced podocyte damage," *Cellular Signalling*, vol. 26, no. 12, pp. 2979–2991, 2014.

[54] R. Das, S. Xu, X. Quan et al., "Upregulation of mitochondrial Nox4 mediates TGF-β-induced apoptosis in cultured mouse podocytes," *American Journal of Physiology—Renal Physiology*, vol. 306, no. 2, pp. F155–F167, 2014.

[55] V. W. Dennis and K. Robinson, "Homocysteinemia and vascular disease in end-stage renal disease," *Kidney International, Supplement*, vol. 50, no. 57, pp. S11–S17, 1996.

[56] F. Yi and P.-L. Li, "Mechanisms of homocysteine-induced glomerular injury and sclerosis," *American Journal of Nephrology*, vol. 28, no. 2, pp. 254–264, 2008.

[57] A. Gupta and K. Robinson, "Hyperhomocysteinaemia and end stage renal disease," *Journal of Nephrology*, vol. 10, no. 2, pp. 77–84, 1997.

[58] A. Erol, M. G. Çnar, C. Can, M. Olukman, S. Ülker, and S. Koşay, "Effect of homocysteine on nitric oxide production in coronary microvascular endothelial cells," *Endothelium: Journal of Endothelial Cell Research*, vol. 14, no. 3, pp. 157–161, 2007.

[59] K. Chow, F. Cheung, T. T. H. Lao, and O. Karmin, "Effect of homocysteine on the production of nitric oxide in endothelial cells," *Clinical and Experimental Pharmacology & Physiology*, vol. 26, no. 10, pp. 817–818, 1999.

[60] X. Liu, F. Luo, J. Li, W. Wu, L. Li, and H. Chen, "Homocysteine induces connective tissue growth factor expression in vascular smooth muscle cells," *Journal of Thrombosis and Haemostasis*, vol. 6, no. 1, pp. 184–192, 2008.

[61] H. Guo, J.-D. Lee, H. Uzui et al., "Effects of heparin on the production of homocysteine-induced extracellular matrix metalloproteinase-2 in cultured rat vascular smooth muscle cells," *The Canadian Journal of Cardiology*, vol. 23, no. 4, pp. 275–280, 2007.

[62] F. Yi, M. Xia, N. Li, C. Zhang, L. Tang, and P.-L. Li, "Contribution of guanine nucleotide exchange factor Vav2 to hyperhomocysteinemic glomerulosclerosis in rats," *Hypertension*, vol. 53, no. 1, pp. 90–96, 2009.

[63] S. Shastry, A. J. Ingram, J. W. Scholey, and L. R. James, "Homocysteine induces mesangial cell apoptosis via activation of p38-mitogen-activated protein kinase," *Kidney International*, vol. 71, no. 4, pp. 304–311, 2007.

[64] F. Yi, A. Y. Zhang, N. Li et al., "Inhibition of ceramide-redox signaling pathway blocks glomerular injury in hyperhomocysteinemic rats," *Kidney International*, vol. 70, no. 1, pp. 88–96, 2006.

[65] L. Pin-Lan, Y. Fan, and L. Ningjun, "Hyperhomocysteinemia: association with renal transsulfuration and redox signaling in rats," *Clinical Chemistry and Laboratory Medicine*, vol. 45, no. 12, pp. 1688–1693, 2007.

[66] F. Yi, E. A. Dos Santos, M. Xia, Q.-Z. Chen, P.-L. Li, and N. Li, "Podocyte injury and glomerulosclerosis in hyperhomocysteinemic rats," *American Journal of Nephrology*, vol. 27, no. 3, pp. 262–268, 2007.

[67] C. Zhang, J.-J. Hu, M. Xia et al., "Protection of podocytes from hyperhomocysteinemia-induced injury by deletion of the gp91^{phox} gene," *Free Radical Biology & Medicine*, vol. 48, no. 8, pp. 1109–1117, 2010.

[68] C. Zhang, J.-J. Hu, M. Xia, K. M. Boini, C. Brimson, and P.-L. Li, "Redox signaling via lipid raft clustering in homocysteine-induced injury of podocytes," *Biochimica et Biophysica Acta—Molecular Cell Research*, vol. 1803, no. 4, pp. 482–491, 2010.

[69] C. Zhang, M. Xia, K. M. Boini et al., "Epithelial-to-mesenchymal transition in podocytes mediated by activation of NADPH oxidase in hyperhomocysteinemia," *Pflugers Archiv European Journal of Physiology*, vol. 462, no. 3, pp. 455–467, 2011.

[70] C.-X. Li, M. Xia, W.-Q. Han et al., "Reversal by growth hormone of homocysteine-induced epithelial-to- mesenchymal transition through membrane raft-redox signaling in podocytes," *Cellular Physiology and Biochemistry*, vol. 27, no. 6, pp. 691–702, 2011.

[71] J. M. Abais, C. Zhang, M. Xia et al., "NADPH oxidase-mediated triggering of inflammasome activation in mouse podocytes and glomeruli during hyperhomocysteinemia," *Antioxidants and Redox Signaling*, vol. 18, no. 13, pp. 1537–1548, 2013.

[72] A. J. Ingram, J. C. Krepinsky, L. James et al., "Activation of mesangial cell MAPK in response to homocysteine," *Kidney International*, vol. 66, no. 2, pp. 733–745, 2004.

[73] Z.-Z. Yang and A.-P. Zou, "Homocysteine enhances TIMP-1 expression and cell proliferation associated with NADH oxidase in rat mesangial cells," *Kidney International*, vol. 63, no. 3, pp. 1012–1020, 2003.

[74] F. Yi, A. Y. Zhang, J. L. Janscha, P.-L. Li, and A.-P. Zou, "Homocysteine activates NADH/NADPH oxidase through ceramide-stimulated Rac GTPase activity in rat mesangial cells," *Kidney International*, vol. 66, no. 5, pp. 1977–1987, 2004.

[75] C. Zhang, F. M. Yi, M. Xia et al., "NMDA receptor-mediated activation of NADPH oxidase and glomerulosclerosis in hyperhomocysteinemic rats," *Antioxidants and Redox Signaling*, vol. 13, no. 7, pp. 975–986, 2010.

[76] J. R. Diamond, "Hyperlipidemia of nephrosis: pathophysiologic role in progressive glomerular disease," *American Journal of Medicine*, vol. 87, no. 5N, pp. 25N–29N, 1989.

[77] S. Anderson, A. J. King, and B. M. Brenner, "Hyperlipidemia and glomerular sclerosis: an alternative viewpoint," *The American Journal of Medicine*, vol. 87, no. 5, pp. 34N–38N, 1989.

[78] V. S. Kamanna, D. D. Roh, and M. A. Kirschenbaum, "Hyperlipidemia and kidney disease: concepts derived from histopathology and cell biology of the glomerulus," *Histology and Histopathology*, vol. 13, no. 1, pp. 169–179, 1998.

[79] W. F. Keane, M. P. O'Donnell, B. L. Kasiske, and P. G. Schmitz, "Lipids and the progression of renal disease," *Journal of the American Society of Nephrology*, vol. 1, no. 5, pp. S69–S74, 1990.

[80] J. A. Joles, U. Kunter, U. Janssen et al., "Early mechanisms of renal injury in hypercholesterolemic or hypertriglyceridemic rats," *Journal of the American Society of Nephrology*, vol. 11, no. 4, pp. 669–683, 2000.

[81] B. L. Kasiske, M. P. O'Donnell, W. J. Garvis, and W. F. Keane, "Pharmacologic treatment of hyperlipidemia reduces glomerular injury in rat 5/6 nephrectomy model of chronic renal failure," *Circulation Research*, vol. 62, no. 2, pp. 367–374, 1988.

[82] K.-P. Shen, H.-L. Lin, W.-T. Chang et al., "Eugenosedin-A ameliorates hyperlipidemia-induced vascular endothelial dysfunction via inhibition of α1-adrenoceptor/5-HT activity and NADPH oxidase expression," *Kaohsiung Journal of Medical Sciences*, vol. 30, no. 3, pp. 116–124, 2014.

[83] H. Scheuer, W. Gwinner, J. Hohbach et al., "Oxidant stress in hyperlipidemia-induced renal damage," *American Journal of Physiology-Renal Physiology*, vol. 278, no. 1, pp. F63–F74, 2000.

[84] L. He, L. Hao, X. Fu, M. Huang, and R. Li, "Severe hypertriglyceridemia and hypercholesterolemia accelerating renal injury: a novel model of type 1 diabetic hamsters induced by short-term high-fat / high-cholesterol diet and low-dose streptozotocin," *BMC Nephrology*, vol. 16, article 51, 2015.

[85] J. P. Tolins, B. G. Stone, and L. Raij, "Interactions of hypercholesterolemia and hypertension in initiation of glomerular injury," *Kidney International*, vol. 41, no. 5, pp. 1254–1261, 1992.

[86] M. Oda, Y. Satta, O. Takenaka, and N. Takahata, "Loss of urate oxidase activity in hominoids and its evolutionary implications," *Molecular Biology and Evolution*, vol. 19, no. 5, pp. 640–653, 2002.

[87] O. S. P. Sah and Y. X. Qing, "Associations between hyperuricemia and chronic kidney disease: a review," *Nephro-Urology Monthly*, vol. 7, no. 3, Article ID e27233, 2015.

[88] G. K. Glantzounis, E. C. Tsimoyiannis, A. M. Kappas, and D. A. Galaris, "Uric acid and oxidative stress," *Current Pharmaceutical Design*, vol. 11, no. 32, pp. 4145–4151, 2005.

[89] R. J. Johnson, D.-H. Kang, D. Feig et al., "Is there a pathogenetic role for uric acid in hypertension and cardiovascular and renal disease?" *Hypertension*, vol. 41, no. 6, pp. 1183–1190, 2003.

[90] L. Li, C. Yang, Y. Zhao, X. Zeng, F. Liu, and P. Fu, "Is hyperuricemia an independent risk factor for new-onset chronic kidney disease?: a systematic review and meta-analysis based on observational cohort studies," *BMC Nephrology*, vol. 15, no. 1, article 122, 2014.

[91] A. Stack, A. J. Manolis, and E. Ritz, "Detrimental role of hyperuricemia on the cardio-reno-vascular system," *Current Medical Research and Opinion*, vol. 31, supplement 2, pp. 21–26, 2015.

[92] D.-H. Kang and T. Nakagawa, "Uric acid and chronic renal disease: possible implication of hyperuricemia on progression of renal disease," *Seminars in Nephrology*, vol. 25, no. 1, pp. 43–49, 2005.

[93] P. Dousdampanis, K. Trigka, C. G. Musso, and C. Fourtounas, "Hyperuricemia and chronic kidney disease: an enigma yet to be solved," *Renal Failure*, vol. 36, no. 9, pp. 1351–1359, 2014.

[94] N. Ohashi, S. Ishigaki, S. Isobe et al., "Hyperuricaemia is associated with renal damage independently of hypertension and intrarenal renin-angiotensin system activation, as well as their circadian rhythms," *Nephrology*, vol. 20, no. 11, pp. 814–819, 2015.

[95] W.-J. Ho, W.-P. Tsai, K.-H. Yu et al., "Association between endothelial dysfunction and hyperuricaemia," *Rheumatology*, vol. 49, no. 10, pp. 1929–1934, 2010.

[96] M.-A. Yu, L. G. Sánchez-Lozada, R. J. Johnson, and D.-H. Kang, "Oxidative stress with an activation of the renin-angiotensin system in human vascular endothelial cells as a novel mechanism of uric acid-induced endothelial dysfunction," *Journal of Hypertension*, vol. 28, no. 6, pp. 1234–1242, 2010.

[97] L. G. Sánchez-Lozada, V. Soto, E. Tapia et al., "Role of oxidative stress in the renal abnormalities induced by experimental hyperuricemia," *American Journal of Physiology—Renal Physiology*, vol. 295, no. 4, pp. F1134–F1141, 2008.

[98] D.-H. Kang and S.-K. Ha, "Uric acid puzzle: dual role as antioxidantand pro-oxidant," *Electrolyte & Blood Pressure*, vol. 12, no. 1, pp. 1–6, 2014.

[99] L. G. Sánchez-Lozada, M. A. Lanaspa, M. Cristóbal-García et al., "Uric acid-induced endothelial dysfunction is associated with mitochondrial alterations and decreased intracellular ATP concentrations," *Nephron - Experimental Nephrology*, vol. 121, no. 3-4, pp. e71–e78, 2013.

[100] E.-S. Ryu, M. J. Kim, H.-S. Shin et al., "Uric acid-induced phenotypic transition of renal tubular cells as a novel mechanism of chronic kidney disease," *American Journal of Physiology—Renal Physiology*, vol. 304, no. 5, pp. F471–F480, 2013.

[101] J. E. Quigley, A. A. Elmarakby, S. F. Knight et al., "Obesity induced renal oxidative stress contributes to renal injury in salt-sensitive hypertension," *Clinical and Experimental Pharmacology and Physiology*, vol. 36, no. 7, pp. 724–728, 2009.

[102] S. Darouich, R. Goucha, M. H. Jaafoura, S. Zekri, H. B. Maiz, and A. Kheder, "Clinicopathological characteristics of obesity-associated focal segmental glomerulosclerosis," *Ultrastructural Pathology*, vol. 35, no. 4, pp. 176–182, 2011.

[103] J. Habibi, M. R. Hayden, J. R. Sowers et al., "Nebivolol attenuates redox-sensitive glomerular and tubular mediated proteinuria in obese rats," *Endocrinology*, vol. 152, no. 2, pp. 659–668, 2011.

[104] H. Cai and D. G. Harrison, "Endothelial dysfunction in cardiovascular diseases: the role of oxidant stress," *Circulation Research*, vol. 87, no. 10, pp. 840–844, 2000.

[105] L. M. Yung, F. P. Leung, X. Yao, Z.-Y. Chen, and Y. Huang, "Reactive oxygen species in vascular wall," *Cardiovascular and Hematological Disorders-Drug Targets*, vol. 6, no. 1, pp. 1–19, 2006.

Hindawi Publishing Corporation
Oxidative Medicine and Cellular Longevity
Volume 2016, Article ID 9047821, 13 pages
http://dx.doi.org/10.1155/2016/9047821

Research Article

High Fat Diet-Induced Skeletal Muscle Wasting Is Decreased by Mesenchymal Stem Cells Administration: Implications on Oxidative Stress, Ubiquitin Proteasome Pathway Activation, and Myonuclear Apoptosis

Johanna Abrigo,[1,2] Juan Carlos Rivera,[1,2] Javier Aravena,[1,2] Daniel Cabrera,[3,4] Felipe Simon,[2,5] Fernando Ezquer,[6] Marcelo Ezquer,[6] and Claudio Cabello-Verrugio[1,2]

[1]*Laboratorio de Biologia y Fisiopatologia Molecular, Departamento de Ciencias Biologicas, Facultad de Ciencias Biologicas y Facultad de Medicina, Universidad Andres Bello, 8370146 Santiago, Chile*
[2]*Millennium Institute on Immunology and Immunotherapy, 8370146 Santiago, Chile*
[3]*Departamento de Ciencias Quimicas y Biologicas, Facultad de Salud, Universidad Bernardo O Higgins, 8370993 Santiago, Chile*
[4]*Departamento de Gastroenterologıa, Facultad de Medicina, Pontificia Universidad Católica de Chile, 8330024 Santiago, Chile*
[5]*Laboratorio de Fisiologia Integrativa, Departamento de Ciencias Biologicas, Facultad de Ciencias Biologicas y Facultad de Medicina, Universidad Andres Bello, 8370146 Santiago, Chile*
[6]*Centro de Medicina Regenerativa, Facultad de Medicina, Clinica Alemana, Universidad del Desarrollo, 7710162 Santiago, Chile*

Correspondence should be addressed to Claudio Cabello-Verrugio; claudio.cabello@unab.cl

Received 17 March 2016; Accepted 14 June 2016

Academic Editor: Saeid Golbidi

Obesity can lead to skeletal muscle atrophy, a pathological condition characterized by the loss of strength and muscle mass. A feature of muscle atrophy is a decrease of myofibrillar proteins as a result of ubiquitin proteasome pathway overactivation, as evidenced by increased expression of the muscle-specific ubiquitin ligases atrogin-1 and MuRF-1. Additionally, other mechanisms are related to muscle wasting, including oxidative stress, myonuclear apoptosis, and autophagy. Stem cells are an emerging therapy in the treatment of chronic diseases such as high fat diet-induced obesity. Mesenchymal stem cells (MSCs) are a population of self-renewable and undifferentiated cells present in the bone marrow and other mesenchymal tissues of adult individuals. The present study is the first to analyze the effects of systemic MSC administration on high fat diet-induced skeletal muscle atrophy in the tibialis anterior of mice. Treatment with MSCs reduced losses of muscle strength and mass, decreases of fiber diameter and myosin heavy chain protein levels, and fiber type transitions. Underlying these antiatrophic effects, MSC administration also decreased ubiquitin proteasome pathway activation, oxidative stress, and myonuclear apoptosis. These results are the first to indicate that systemically administered MSCs could prevent muscle wasting associated with high fat diet-induced obesity and diabetes.

1. Introduction

Skeletal muscle is the most abundant tissue in the human body and has a wide variety of physiological functions. Therefore, muscle loss results not only in physical dysfunction but also in metabolic impairment [1, 2]. Related to this, recent studies have shown that obesity is associated with skeletal muscle loss and dysfunction and the development of muscle atrophy [3]. Indeed, mice fed with a high fat diet (HFD) develop the typical features of muscle wasting, such as weakness, the loss of muscle mass, and decreased fiber diameter [4].

Skeletal muscle is composed of a variety of fast and slow fiber types and subtypes (i.e., slow: I; fast: IIb, IId, and IIa; or mixtures) [5]. Moreover, muscle fibers are versatile and capable of changing phenotypic properties in response to

muscle wasting, showing modifications in the expression of MHC isoforms. Therefore, when fast muscles atrophy, a fast-to-slow transition occurs (e.g., IIb→IId→IIa→I) [5, 6].

Ubiquitin proteasome pathway (UPP) overactivation, oxidative stress, and myonuclear apoptosis are some of the mechanisms involved in muscle atrophy induced by obesity and other causes [4, 7]. Overactivation of the UPP in muscle atrophy is characterized by an increased expression of two muscle-specific ubiquitin E3-ligase F-box proteins, muscle atrophy F-box (MAFbx)/atrogin-1 and muscle ring-finger protein 1 (MuRF-1). These proteins increase the ubiquitination of targets such as the myosin heavy chain (MHC), which are further degraded by the proteasome [8–11].

Oxidative stress is produced by increased reactive oxygen species (ROS) and/or decreased antioxidant mechanisms [12]. Oxidative stress has been associated with several models of muscle atrophy, including that induced by obesity [3, 13, 14]. Another mechanism involved in muscle atrophy is myonuclear apoptosis, which is related to muscle wasting induced by cachexia and obesity [4]. In atrophic muscle, several parameters of myonuclear apoptosis increase, such as the Bax/Bcl2 ratio, caspase-3 levels and activity, and apoptotic nuclei [15].

Stem cell-based interventions act through multiple mechanisms and provide a clear advantage when treating diseases with a complex pathophysiology, such as HFD-induced obesity. This type of intervention is arguably better in therapeutic terms than single-agent, drug-based treatments [16, 17]. Multipotent mesenchymal stromal cells, also referred to as mesenchymal stem cells (MSCs), are a heterogeneous adult stem cell population. These are a potentially ideal tool for stem cell-based interventions since they can be isolated from bone marrow and other mesenchymal tissues, including adipose tissue, dental pulp, the placenta, and the umbilical cord, and subsequently rapidly expanded *ex vivo* [18, 19]. As immunomodulatory cells, MSCs can limit inflammation in damaged tissue [20], produce a broad range of trophic factors that protect parenchymal cells from apoptotic death, and promote the proliferation and differentiation of endogenous precursors [21].

The present study is the first to provide evidence that systemic MSC administration can prevent the loss of muscle strength and mass, the decrease in fiber diameter and MHC protein levels, and the transition of fiber type in a murine model of HFD-induced muscle wasting. Prevention of the several parameters of muscle atrophy, among them UPP overactivation, increased ROS levels, and activation of myonuclear apoptosis, was also found in this model, which would explain the observed antiatrophic effects of MSC administration.

2. Materials and Methods

2.1. Animals. Male 12-week-old C57BL/10 mice were housed at a constant temperature (22 ± 2°C), with 60% relative humidity, and with a 12 : 12 light : dark cycle. Mice had *ad libitum* access to food and autoclaved water. Mice were fed with either a standard diet (control group, 10 cal% fat, 20 cal% proteins, and 70 cal% carbohydrates, Champion S.A., Chile) or a high fat diet (HFD group, 60 cal% fat, 20 cal% proteins, and 20 cal% carbohydrates, D12492 Research Diets Inc., USA). After 30 weeks of HFD feeding, mice were separated into two groups matched by average body weight. Then, for an additional eight weeks, one group received a vehicle treatment (HFD), while the other was treated with MSCs (HFD + MSCs). At the end of the 38-week experimental period, the mice were euthanized under anesthesia, and the tibialis anterior (TA) muscles were dissected, removed, and rapidly frozen and stored at −80°C until processing. All protocols were conducted in strict accordance with and with the formal approval of the Animal Ethics Committees of Universidad Andrés Bello and Universidad del Desarrollo.

2.2. Isolation and Administration of MSCs. Six-to-eight-week-old C57BL/10 male mice were sacrificed by cervical dislocation. Bone marrow cells were obtained by flushing the femurs and tibias with sterile PBS. After centrifugation, the cells were resuspended in an α-Minimum Essential Medium (Gibco, USA) supplemented with 10% selected fetal bovine serum (Hyclone, USA) and 80 μg/mL gentamicin (Laboratorio Sanderson, Chile) and plated at a density of 1×10^6 nucleated cells per square centimeter. Nonadherent cells were removed after 72 h by changing the medium. When the foci reached confluence, adherent cells were detached with 0.25% trypsin and 2.65 mM EDTA, centrifuged, and subcultured at 7,000 cells per square centimeter. After two subcultures, adherent cells were phenotypified and characterized according to the adipogenic and osteogenic differentiation potential, as previously described [6]. Then, 0.5×10^6 MSCs were resuspended in 0.2 mL of 5% mouse plasma (vehicle) and administered via the tail-vein to anesthetized mice. Untreated mice were given 0.2 mL of vehicle.

2.3. Weightlifting Strength Test. At the end of the treatment, the muscle strength of the mice was measured through a weightlifting test, as previously described [22]. Briefly, the apparatus consisted in a series of increasingly long chain links attached to a ball of tangled fine wire. The number of links ranged from two to seven, with total weights between 15.5 and 54.1 g. Before performing the test and prior to treatments, the mice were trained once per day for two weeks. To perform the test, the mouse grasped the different weights with its forepaws and a score was assigned. The final score was calculated as the summation of the product between the link weight and the time the weight was held. The average of three measures from each mouse was normalized against body weight [23].

2.4. Contractile Properties. The TA muscles removed from sacrificed mice were placed in a dish containing oxygenated Krebs-Ringer solution (in mmol/L: NaCl: 118; $NaHCO_3$: 25; D-glucose: 20; KCl: 4.7; $CaCl_2$: 3.2; KH_2PO_4: 1.2; $MgSO_4$: 1.2). The TA muscles were firmly tied with surgical silk at the bottom end of the tendon and at a portion of the knee bone. The muscle was transferred to a custom-built Plexiglas bath filled with oxygenated Krebs-Ringer solution that was thermostatically maintained at room temperature for optimal

oxygen diffusion. The muscles were vertically aligned and tied directly between a fixed hook and a force transducer (MLT 1030/D, AD Instruments, USA). Two platinum plate electrodes were positioned in the organ bath so as to flank the length of the muscles. Muscles were field-stimulated by supramaximal square wave pulses (S48 Stimulator, Grass, USA), which were amplified to increase and sustain current intensity at a level sufficient for producing a maximum isometric tetanic contraction. Optimum muscle length (Lo) and stimulation voltage were determined from the micromanipulation of muscle length to produce maximum isometric twitch force. All stimulation parameters and contractile responses were controlled and measured using Power Lab 4/35 (AD Instruments, USA). All obtained data were computed with the LabChart analysis software (AD Instruments, USA). Maximum isometric tetanic force (Po) was determined from the plateau of the frequency-force relationship after successive stimulations between 10 and 150 Hz for 850 ms, with 2 min rest periods between the stimuli. After testing, the muscles were removed from the bath and the tendons and any adherent nonmuscle tissues were trimmed, blotted once on filter paper, and weighed. Muscle mass and Lo were used to calculate specific net force or the normalized force of each total muscle fiber cross-sectional area (mN/mm^2) [24–27].

2.5. Blood Triglycerides, Cholesterol, Glucose, and Insulin Determination. After 4 h of fasting, mice were sacrificed and blood samples were collected. Serum triglycerides and cholesterol levels were determined in the ARCHITECT c8000 Clinical Chemistry Analyzer (Abbott, USA). Blood glucose levels were measured with the Accu-Chek Performance glucometer system (Roche Diagnostic, Germany). Plasma insulin levels were assayed using the Ultrasensitive Mouse-Insulin ELISA Kit (Mercodia, Sweden).

2.6. RNA Isolation, Reverse Transcription, and Quantitative Real-Time PCR. Total RNA was isolated from the TA muscles using TRIzol (Invitrogen, USA). The total RNA (1 μg) was reverse transcribed to cDNA using random hexamers and Superscript II reverse transcriptase (Invitrogen, USA). TaqMan quantitative real-time PCR reactions were performed in triplicate, using an Eco Real-Time PCR System (Illumina, USA) with predesigned primer sets for mouse *atrogin-1*, *MuRF-1*, and the housekeeping gene *18S* (TaqMan Assays-on-Demand, Applied Biosystems, USA). The mRNA expression was quantified using the comparative ΔCt method ($2^{-\Delta\Delta Ct}$), with 18S as the reference gene. The mRNA levels were expressed relative to the mean expression in the vehicle-treated mice [23, 28].

2.7. Western Blot Analysis. The muscles were homogenized in Tris-EDTA buffer with a cocktail of protease inhibitors and 1 mM phenylmethanesulfonyl fluoride. Proteins were subjected to SDS-PAGE, transferred onto polyvinylidene difluoride membranes (Millipore, USA), and probed with mouse anti-MHC (1 : 1,000) (MF-20, Developmental Studies, Hybridoma Bank, University of Iowa, USA), mouse anti-tubulin (1 : 5,000), mouse anti-GAPDH (1 : 5,000), rabbit anti-Bax (1 : 500), rabbit anti-Bcl2 (1 : 500), rabbit anti-caspase-3 (1 : 500), rabbit anti-Ub proteins (1 : 500) (Santa Cruz Biotechnology, USA), rabbit anti-LC3B (1 : 1,500) (Cell Signaling, USA), and rabbit anti-p62 (1 : 1,500) (Abcam, USA). All immunoreactions were visualized by enhanced chemiluminescence (Thermo Scientific, USA). Images were acquired using Fotodyne FOTO/Analyst Luminary Workstation Systems (Fotodyne, Inc., USA).

2.8. Muscle Histology and Fiber Diameter Determination and Quantification. Fresh-frozen TA muscles were sectioned, and cryosections (8 μm) were stained with hematoxylin and eosin (H&E) or Alexa-Fluor 594 tagged wheat germ agglutinin (WGA) (Life Technologies, USA) according to standard procedures. Wheat germ agglutinin-stained fibers were assessed through blind analysis using the Image J software (NIH, USA), with fiber sizes determined for seven randomly captured images from each experimental condition. Fibers were handled manually, and the minimal Feret diameter of each fiber was computed by the software [28, 29].

2.9. Immunohistochemical Analysis. For immunohistochemistry, fresh-frozen TA muscle cryosections (8 μm) were fixed in acetone and incubated overnight in 1% bovine serum albumin in PBS with anti-MHC IIa (clone SC-71-s; 1 : 20) and anti-MHC IIb (clone BF-F3-s; 1 : 20) (Developmental Studies, Hybridoma Bank, University of Iowa, USA). Then, cryosections were blocked for 15 min in 3% methanol-H_2O_2 and incubated for 30 min with the Envision Dual Link System-HRP (Dako, USA). Enzyme activity was detected with a 3′,3′-diaminobenzidine tetrahydrochloride liquid system (Dako, USA). Nuclei were stained with hematoxylin [26, 30].

2.10. ROS Detection. For ROS detection, fresh-frozen TA muscle cryosections (8 μm) were incubated for 30 min at 37°C with 10 μM CM-H_2DCF-DA dye (Molecular Probes, Eugene, Oregon, USA) in Hank's buffered salt solution. Then, the muscles were fixed in 4% paraformaldehyde in PBS for 10 min at room temperature. The nuclei were stained with Hoechst 33258 (1 : 5,000) in PBS. After rinsing, the muscles were mounted with a fluorescent mounting medium (Dako, USA) under a glass slide and viewed and photographed using the Motic BA310 epifluorescence microscope [31].

2.11. Terminal Deoxynucleotidyl Transferase Mediated dUTP Nick End Labelling (TUNEL) Technique. Breaks in the DNA strand as a result of endonuclease activity were detected by the TUNEL labelling technique using the commercial Dead-End Colorimetric TUNEL Kit (Promega, USA). The label was developed with a DAB 3,3′-diaminobenzidine horseradish peroxidase substrate that produces a dark-brown reaction product. A blinded field quantification of TUNEL-positive nuclei was then performed on five randomly captured images of the TA taken from four mice and for each experimental condition [15].

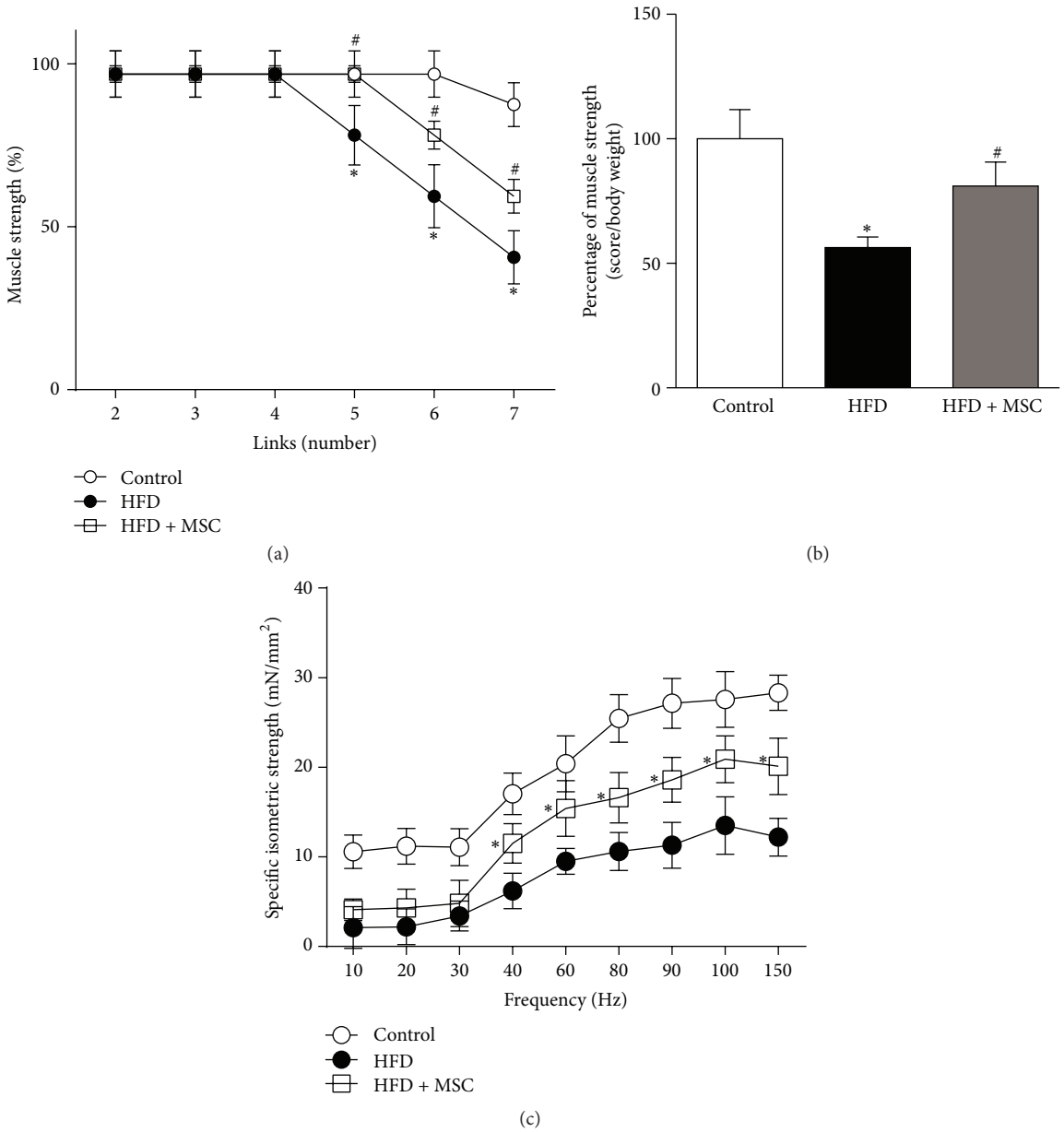

Figure 1: Mesenchymal stem cells (MSCs) administration inhibits the decreased muscle strength induced by a high fat diet (HFD) in mice. C57BL/10J male mice were fed with a standard chow (control) or HFD for 38 weeks. At week 30, a subgroup of HFD mice received MSC injected through the tail-vein. At week 38, all mice were subjected to the following: (a) A weightlifting test to determine limb muscle strength: values represent the percentage of muscle strength reached by the mice with each weight and correspond to the mean ± SD ($n = 8$; $^{*}P < 0.05$ versus control; $^{\#}P < 0.05$ versus HFD, two-way ANOVA). (b) A weightlifting test: the values represent the scores normalized by body weight. The values correspond to the mean ± SD ($n = 8$; $^{*}P < 0.05$ versus control; $^{\#}P < 0.05$ versus HFD, two-way ANOVA). (c) Maximal isometric strengths (mN/mm^2) against stimulation frequencies (Hz) in the tibialis anterior (TA) muscles: values represent the mean ± SD ($n = 8$; $^{*}P < 0.05$ versus HFD, two-way ANOVA).

2.12. Caspase-3 Activity. The activity of caspase-3 was determined in the TA protein extract using the commercial Caspase-3 Colorimetric Assay Kit (BioVision Inc., USA). A 405 nm absorbance value for each experimental condition was expressed as a fold of induction relative to control muscle [15].

2.13. Statistics. For statistical analysis, two-way analysis of variance (ANOVA) was used with a *post hoc* multiple-comparison Bonferroni test (Prisma). Differences were considered statistically significant at $P < 0.05$.

3. Results

3.1. Systemic Administration of Mesenchymal Stem Cells Reverts the Decreased Muscle Strength Induced by a High Fat Diet. After receiving a HFD for 38 weeks, live mice evidenced decreased muscle strength, as evaluated by a weightlifting

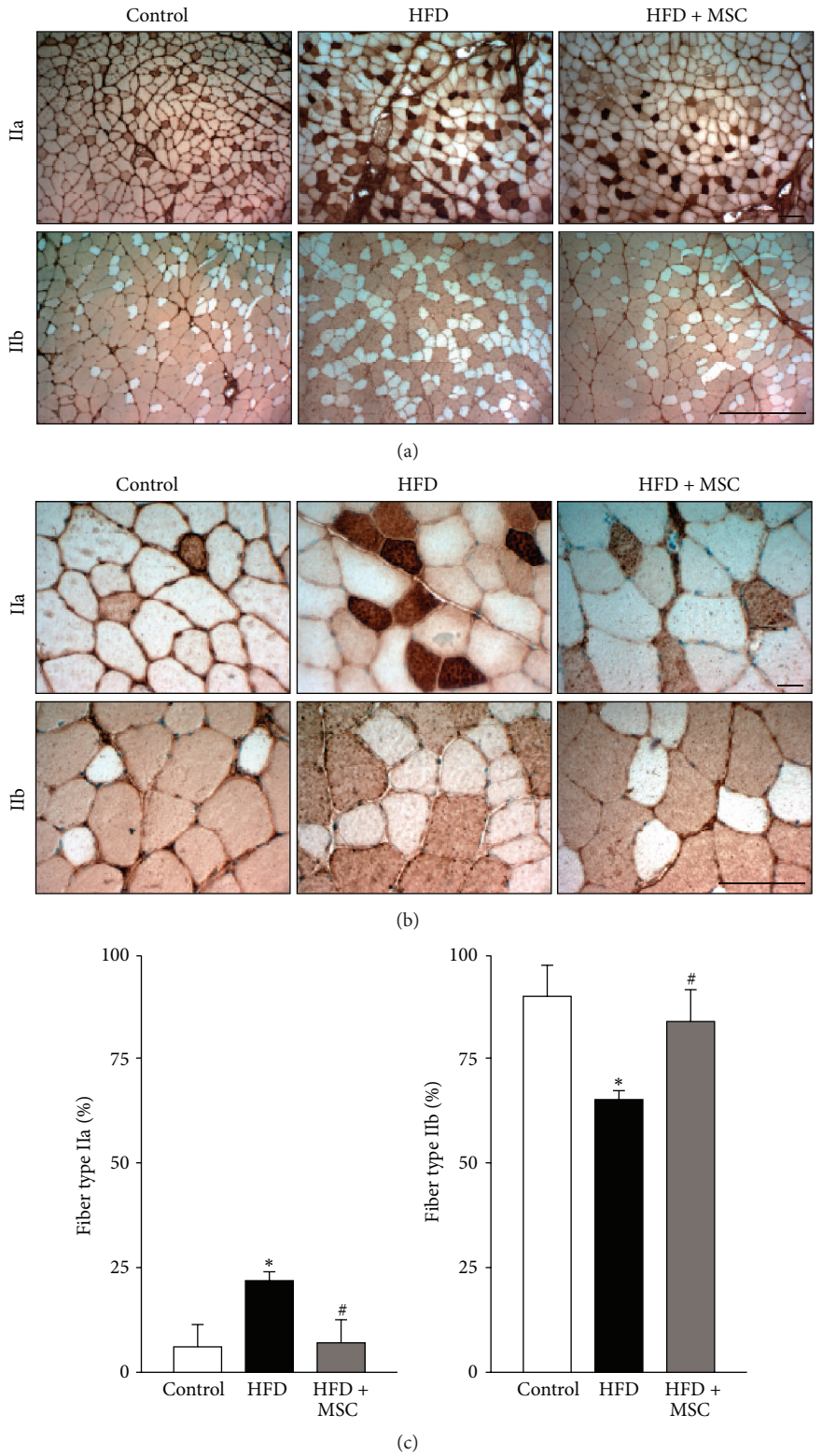

Figure 2: Systemic mesenchymal stem cells (MSCs) administration inhibits fiber type transitions in the tibialis anterior (TA) muscle of mice fed with a high fat diet (HFD). C57BL/10J male mice were fed with a standard chow (control) or HFD for 38 weeks. At week 30, a subgroup of HFD mice received MSC injected through the tail-vein. At week 38, all mice were sacrificed and the TA was analyzed to determine fiber type through the immunohistochemical detection of myosin heavy chain isoforms (IIa and IIb). Images obtained at 10x (a) and 40x (b) magnification show fiber types IIa (upper panel) and IIb (lower panel). Quantitative analysis of the fiber type is shown in (c). Graph representing the percentage of specific fiber types relative to the total fibers counted per field. Values represent the mean ± SD ($n = 8$; $^{*}P < 0.05$ versus control; $^{\#}P < 0.05$ versus HFD, two-way ANOVA).

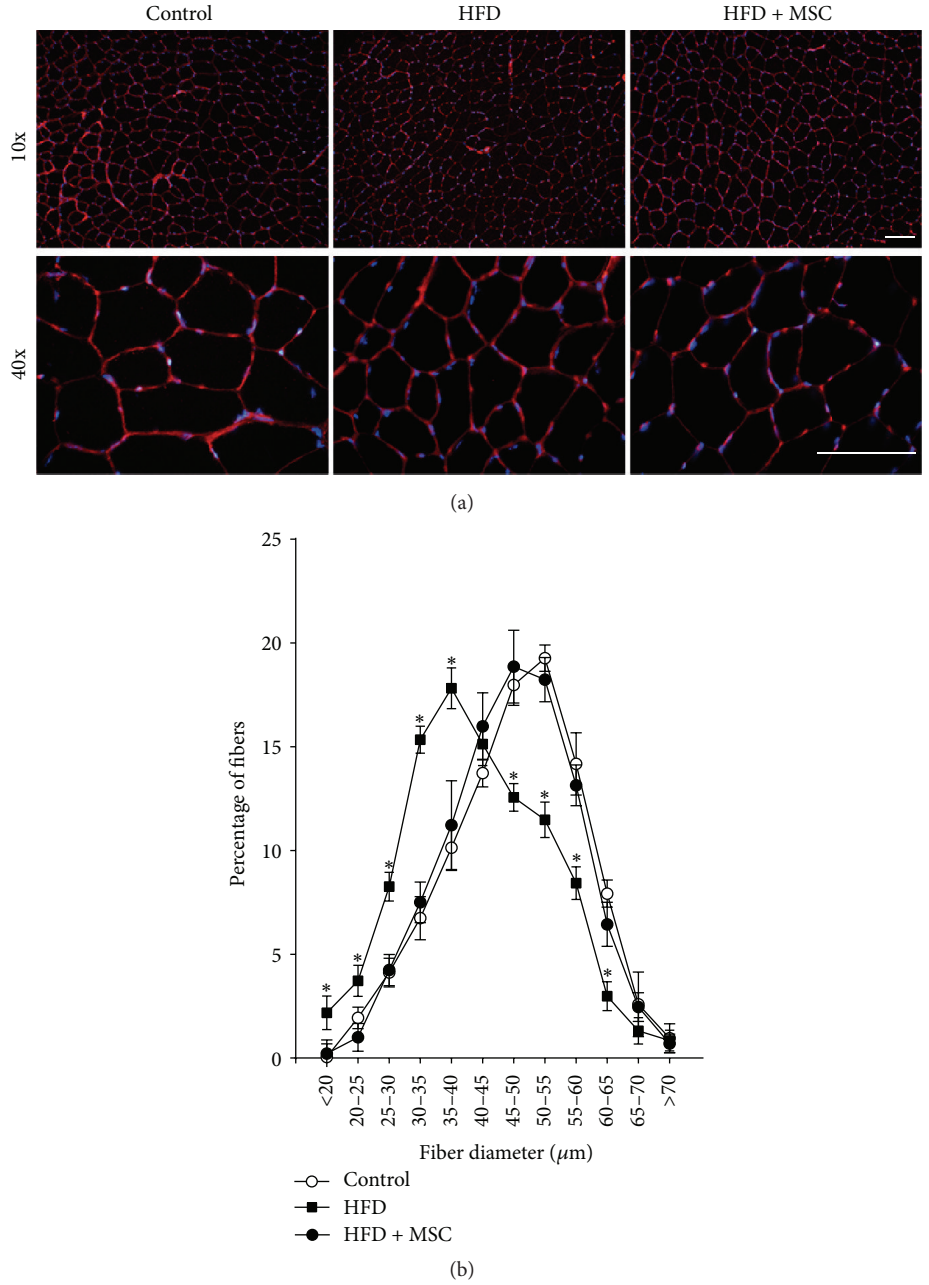

Figure 3: Mesenchymal stem cells (MSCs) administration prevents the decreased fiber diameter of the tibialis anterior (TA) muscle in high fat diet- (HFD-) induced skeletal muscle atrophy. TA muscles were obtained from C57BL/10J male mice fed with standard chow (control), a HFD, or a HFD-MSC treated. Muscle cross sections were stained with wheat germ agglutinin to delimit muscle fiber sarcolemma. (a) Images were obtained at 10x and 40x magnification. Bars correspond to 150 μm. (b) Minimal Feret diameters were determined in TA cross sections from (b). Fiber diameters were grouped and ranged from 0 to 70 μm. Values are expressed as a percentage of the total quantified fibers. Values correspond to the mean ± SD ($n = 8$; $^*P < 0.05$ versus control, two-way ANOVA).

assay (Figure 1(a)). However, HFD + MSC mice showed a partial recovery of muscle strength after MSC treatment (Figures 1(a) and 1(b)).

Muscle strength was also measured through electrophysiological assays of tetanic force in isolated TA muscles. While the muscle force of HFD mice decreased in all of the assessed frequency ranges (Figure 1(c)), muscle strength was recovered, albeit not completely, following MSC treatment. This recovery reached approximately 50% for frequencies from 40 to 150 Hz and was without differences in lower frequencies.

These results suggest that MSC administration can prevent the decreased muscle strength induced by a HFD in mice.

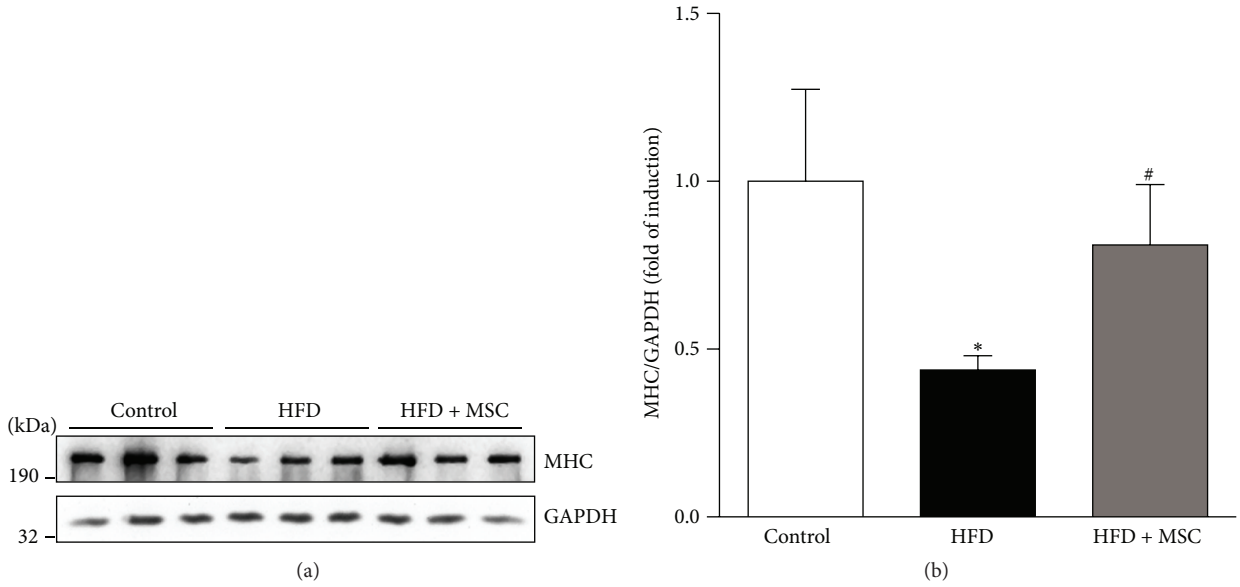

Figure 4: Systemic mesenchymal stem cells (MSCs) administration prevents the decreased myosin heavy chain (MHC) levels in the tibialis anterior (TA) muscle of mice fed with a high fat diet (HFD). C57BL/10J male mice were fed with a standard chow (control) or HFD for 38 weeks. At week 30, a subgroup of HFD mice received MSC injected through the tail-vein. After eight weeks, all mice were sacrificed and the TA was excised and homogenized to evaluate the following: (a) MHC protein levels through Western blot analysis (GAPDH levels were used as the loading control; molecular weight markers are shown in kDa) and (b) quantitative analysis of the experiments from (a). The levels of MHC normalized to GAPDH are expressed relative to control mice ($^{*}P < 0.05$ versus control; $^{\#}P < 0.05$ versus HFD).

3.2. Mesenchymal Stem Cells Prevent Fiber Type Transition, Decreased Fiber Diameter, and the Myosin Heavy Chain Levels Induced by a High Fat Diet. The most abundant fiber type in the TA is IIb. When the TA is atrophied, IIb fibers transition towards IIa fibers [5, 6]. This was observed in the present study, where a HFD produced a shift to IIa fibers in affected mice, increasing the quantity of IIa fibers from 4.3 to 24.5% and decreasing the quantity of IIb fibers from 92.8 to 69.4% (Figures 2(a) and 2(b)). This transition was prevented in the HFD + MSC group, which showed a similar proportion of IIb fibers as the control group (Figures 2(a) and 2(b)). The graphs in Figure 2(c) show the quantitative analysis of Figures 2(a) and 2(b).

The architecture of the TA muscles was conserved without evident changes and without foci of necrotic or damaged fibers (Supplemental Figure S1) (see Supplementary Material available online at http://dx.doi.org/10.1155/2016/9047821). However, when fiber size was evaluated (Figure 3(a)), the HFD mice showed a notable displacement towards smaller sized fibers, a situation that was reversed to the normal values in the HFD + MSC group (Figures 3(a) and 3(b)).

A characteristic feature of muscle atrophy is a decrease in the levels of the myofibrillar proteins such as MHC. In line with this, the HFD decreased MHC protein levels in the TA to only 40% of levels in control TA. In contrast, in HFD + MSC mice, the administration of MSC partially prevented lowered MHC levels, which reached 82% of the levels presented in control TA (Figures 4(a) and 4(b)).

3.3. Mesenchymal Stem Cell Administration Reverts Ubiquitin Proteasome Pathway Overactivation, the Increases in Reactive Oxygen Species, and the Myonuclear Apoptosis Induced by a High Fat Diet. Increased UPP activity was demonstrated by high levels of ubiquitinated proteins in the TA of HFD mice (Figures 5(a) and 5(b)). In contrast, HFD + MSC mice were able to decrease protein ubiquitination, reaching UPP activity levels similar to the control group. To corroborate this result, *atrogin-1* and *MuRF-1* expression, which increase under most muscle atrophy conditions, were also evaluated. A HFD induced increased *atrogin-1* and *MuRF-1* gene expression (Figures 5(c) and 5(d)). However, MSC treatment in HFD + MSC mice completely prevented increased *atrogin-1* expression and partially prevented increased *MuRF-1* expression in the TA (Figures 5(c) and 5(d)). When autophagy was evaluated, the levels and processing of LC3B and p62 did not show differences between the controls, HFD, and HFD + MSC mice (Supplemental Figures S2A, B, and C).

The levels of ROS were also evaluated in the TA of HFD mice. For this, a DCF probe was used to detect (Figure 6(a)) and quantify (Figure 6(b)) ROS. HFD increased ROS levels 7.22-fold relative to the control, while MSC administration partially prevented this increase (3.83-fold relative to the control).

Another mechanism recently described in relation to HFD-induced muscle wasting is myonuclear apoptosis [4]. Proapoptotic Bax levels and antiapoptotic Bcl2 levels were measured (Figure 7(a)). The Bax/Bcl2 ratio increased in the TA of HFD mice as compared to the control group (Figure 7(b)). However, HFD + MSC mice presented a decreased Bax/Bcl2 ratio in the TA as compared to the HFD group. Additionally, HFD-induced caspase-3 protein levels

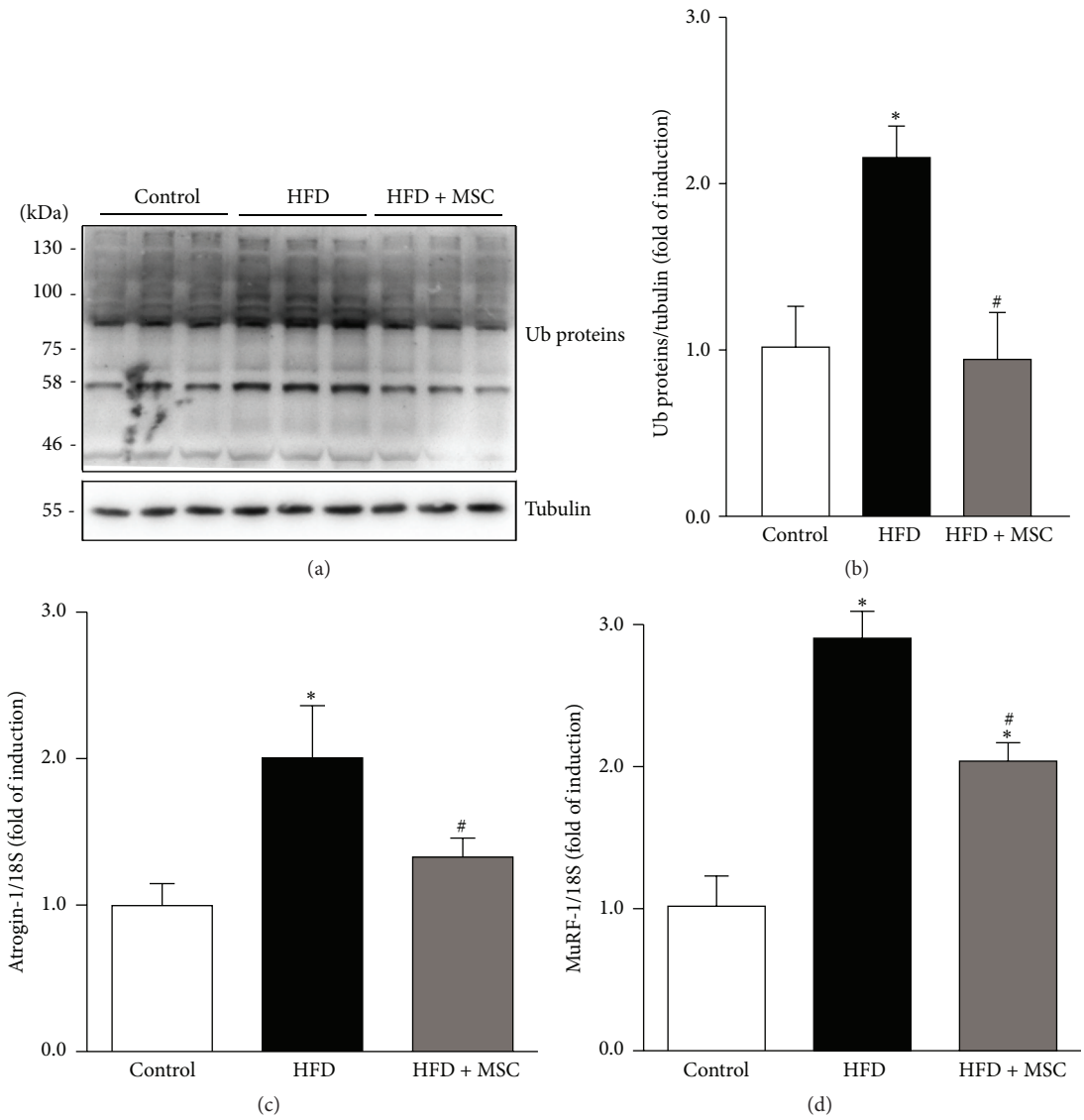

Figure 5: Mesenchymal stem cells (MSCs) administration inhibits increases in ubiquitinated proteins and atrogin-1 and MuRF-1 gene expression levels induced by a high fat diet (HFD) in mice. C57BL/10J male mice were fed with a standard chow (control) or HFD for 38 weeks. At week 30, a subgroup of HFD mice received MSC injected through the tail-vein. At week 38, all mice were sacrificed and the TA was excised and homogenized to evaluate the following: (a) total ubiquitinated (Ub) protein levels through Western blot analysis (tubulin levels were used as the loading control; molecular weight markers are shown in kDa) and (b) quantitative analysis of the experiments from (a). The levels of Ub normalized to tubulin are expressed relative to control mice ($^{*}P < 0.05$ versus control; $^{\#}P < 0.05$ versus HFD). Detection of atrogin-1 (c) and MuRF-1 (d) mRNA levels through RT-qPCR using 18S as the reference gene. Expressions are shown as the fold of induction relative to the TA from control mice, and the values correspond to the mean ± SD ($^{*}P < 0.05$ versus control; $^{\#}P < 0.05$ versus HFD).

(Figure 7(c)) were decreased by MSC administration (Figure 7(d)). Similarly, MSC injection decreased HFD-induced caspase-3 activity in the TA (Figure 7(e)). Finally, apoptotic nuclei were evaluated by TUNEL analysis (Figure 7(f)). The results revealed that a HFD increased the number of apoptotic nuclei in the TA (165.4% relative to the control), while MSC injection fully prevented this increase in HFD + MSC mice (Figure 7(g)). Together, these results indicate that MSC administration decreases myonuclear apoptosis in the TA of HFD mice.

4. Discussion

It is well reported that HFD impairs muscle function and, specifically, produces muscle atrophy [32–34]. HFD induces skeletal muscle atrophy through the induction of several mechanisms, such as UPP overactivation, increased oxidative stress, and the generation of myonuclear apoptosis [4, 7]. In this context, the present study corroborated that HFD can produce phenotypical changes in skeletal muscle, many of which also occur in muscle atrophy caused by other

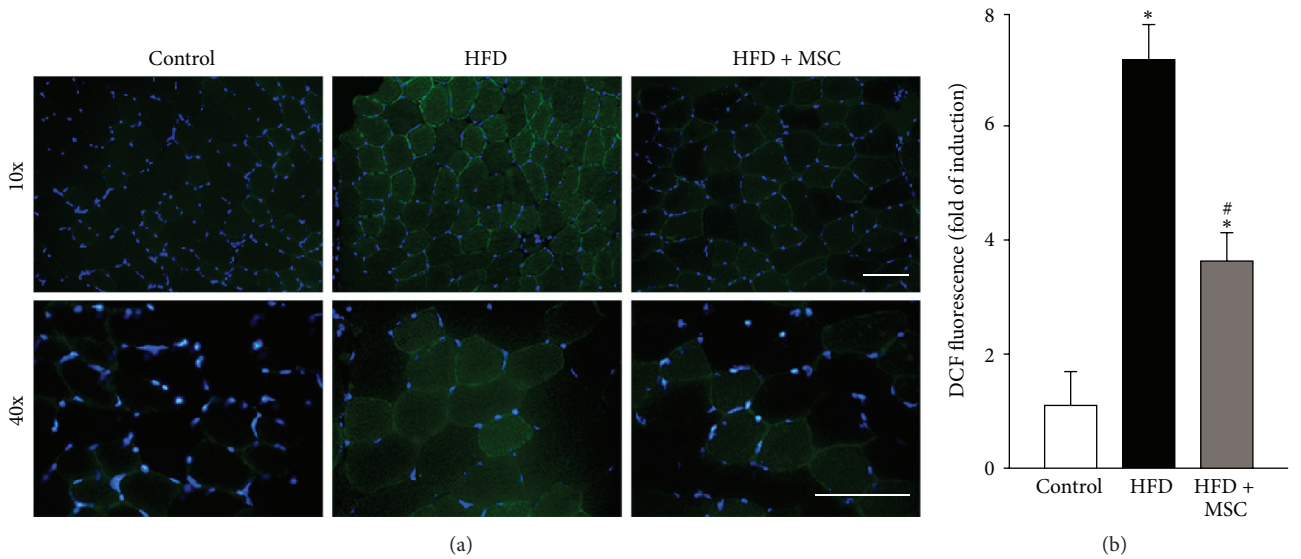

Figure 6: Systemic mesenchymal stem cells (MSCs) administration prevents increased reactive oxygen species (ROS) levels in the tibialis anterior (TA) of mice fed with a high fat diet (HFD). C57BL/10J male mice were fed with a standard chow (control) or HFD for 38 weeks. At week 30, a subgroup of HFD mice received MSC injected through the tail-vein. At week 38, all mice were sacrificed. (a) Cryosections obtained from the TA were incubated with a DCF probe for ROS detection through fluorescence microscopy. Nuclei were labelled via Hoechst staining. (b) Quantification of ROS levels from experiments showed in (a). The values are expressed as the fold of induction of the DCF probe intensity. Values correspond to the mean ± SD ($n = 8$; $^{*}P < 0.05$ versus control; $^{\#}P < 0.05$ versus HFD, two-way ANOVA).

stimuli, such as by immobilization, sepsis, or cachexia. These changes include decreased muscle strength and fiber size, fiber type transitions (e.g., IIb→IIa), the downregulation of MHC levels, the upregulation of atrogenes such as atrogin-1 and MuRF-1, and increased oxidative stress and myonuclear apoptosis. Interestingly, all of these features of HFD-induced muscle wasting were prevented when MSC was systemically administrated to mice.

One feature of obesity is an increase of some circulating factors that can affect muscle function and structure, producing muscle atrophy. These factors include angiotensin II and TNF-α [7, 35, 36]. Thus, the next step in our model of study is to know if the MSC administration alters the circulating and tissue levels of angiotensin II and TNF-α. The mechanisms through which angiotensin II and TNF-α induce muscle wasting include increased oxidative stress, UPP overactivation, and myonuclear apoptosis [7, 37–39]. These studies are in line with the present results, which show that MSC treatment prevented oxidative stress, UPP overactivation, and myonuclear apoptosis. Building on this result, it is important that future studies elucidate the possible participation of the angiotensin II and TNF-α induced pathways in the improvements observed when MSC is given to obese mice.

Despite the fact that one of the effects observed by MSC treatment is the decrease of myonuclear apoptosis, the cell type responsible for or sensible to this effect is not studied. We cannot rule out the possibility that apoptotic signaling may have occurred by a combination of muscle (fiber or satellite cells) and nonmuscle cells (e.g., endothelial cells and resident fibroblast) that reside inside muscles *in vivo*. Moreover, we cannot be sure that apoptotic myonuclei are intramuscular or associated with satellite cells. However, considering that the main and more abundant cell type in skeletal muscle is the muscle fibers and the evidences that describe the fibers as main source of apoptotic myonuclei in models of muscle atrophy by unloading [40], then we can speculate that at least this cell type significantly contributes to the changes in apoptotic signaling induced by high fat diet (HFD) and therefore it is sensitive to MSC treatment. This suggestion is supported by other studies that show the muscle fiber as the main cell source of the myonuclear apoptosis induced by HFD [4, 41]. Despite these evidences, we cannot discard that part of the atrophic effect observed under HFD can be attributed to another cell type, specifically to satellite cells whose dysfunction has been reported in atrophied muscles [42, 43], opening another cell target to the effect of MSC administration. Thus, further studies, such as specific immunolocalization of apoptotic marker, must be performed to detect and clarify the cell types responsible for the myonuclear apoptosis in the skeletal muscle under HFD, evaluating in addition the effect of MSC treatment.

The use of stem cell therapy to improve muscle disorders has been previously evaluated in models of muscle regeneration or dystrophy, mainly using the graft strategy [44, 45]. However, the efficiency of these procedures has been poor. In turn, the present results indicate that systemic MSC administration improves skeletal muscle atrophy associated with a HFD. Importantly, the effects of MSC administration were not related to obesity reversion, since HFD mice remained obese, hypercholesterolemic, hyperglycemic, and hyperinsulinemic (Supplemental Table S1).

Also worth noting, the MSCs incorporated into the muscle tissue of HFD mice were undetected in posttreatment

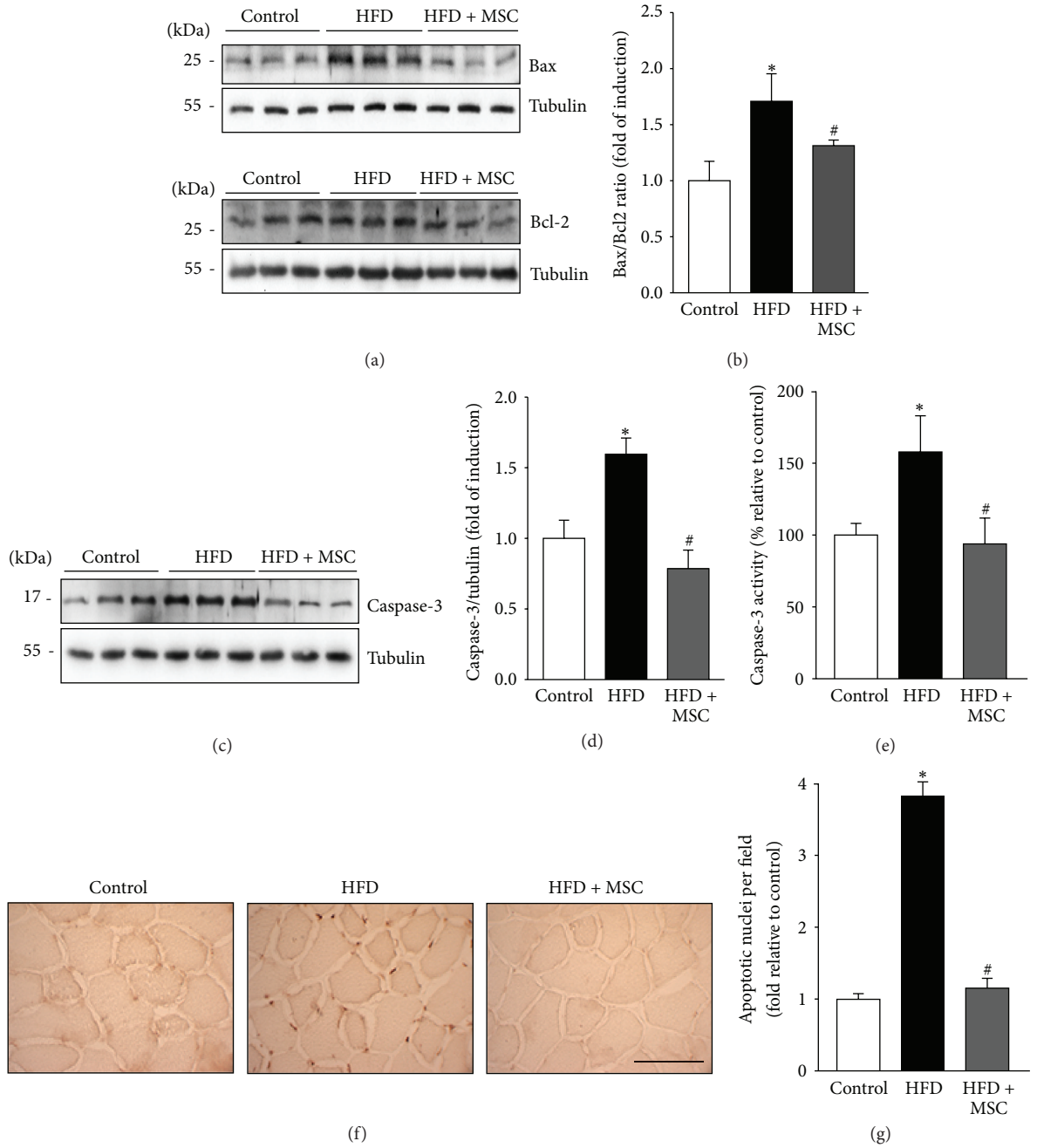

Figure 7: Mesenchymal stem cells (MSCs) administration inhibits the increased myonuclear apoptosis induced by a high fat diet (HFD) in mice. C57BL/10J male mice were fed with a standard chow (control) or HFD for 38 weeks. At week 30, a subgroup of HFD mice received MSC injected through the tail-vein. At week 38, all mice were sacrificed and the tibialis anterior (TA) was excised and homogenized to evaluate (a) Bax and Bcl2 protein levels through Western blot analysis; (b) Bax/Bcl2 ratio analysis (the values are expressed as fold of induction relative to the control and correspond to the mean ± SD ($n = 8$; $^{*}P < 0.05$ versus control; $^{\#}P < 0.05$ versus HFD, two-way ANOVA)); (c) cleaved caspase-3 levels detected by Western blot analysis; (d) quantification of caspase-3 levels from experiments shown in (c). The values are expressed as fold of induction relative to the control and correspond to the mean ± SD ($n = 8$; $^{*}P < 0.05$ versus control; $^{\#}P < 0.05$ versus HFD, two-way ANOVA). For (a) and (c), the levels of tubulin are shown as the loading control. The molecular weights are shown in kDa. (e) Caspase-3 activity was measured and expressed as fold of induction relative to the control, with values corresponding to the mean ± SD ($n = 8$; $^{*}P < 0.05$ versus control; $^{\#}P < 0.05$ versus HFD; two-way ANOVA). (f) Cryosections of TA were used to perform the TUNEL assay. The bar corresponds to 50 μm. (g) Blinded quantification of TUNEL-positive nuclei per field in five randomly captured images. The values are expressed as the fold of induction relative to the control and correspond to the mean ± SD ($n = 8$; $^{*}P < 0.05$ versus control; $^{\#}P < 0.05$ versus HFD, two-way ANOVA).

analyses (data not shown). Diverse studies have shown that <1% of systemically administered MSCs remain present one week after administration in any organ, including the lungs, heart, kidneys, liver, spleen, and gut [16, 46, 47]. However, the clinical benefits associated with MSC administration can be observed for a much longer period. Considering this, it is possible to speculate that the impaired muscle function and features of muscle atrophy were prevented by some indirect event dependent on the MSCs. For example, MSCs secrete a broad range of bioactive growth factors, such as VEGF, bFGF, IGF, HGF, and EGF [21]. Therefore, MSCs could provide trophic support for injured tissue by modifying the microenvironment, thus inducing local precursor proliferation and differentiation to improve damaged tissue irrigation and prevent parenchymal cell apoptosis [17, 21]. Considering this, the impaired muscle function and features of muscle atrophy could be prevented by some indirect or paracrine event dependent on MSCs, as has been previously found in relation to the secretion of trophic factors [21, 48]. If this is the mechanism by which the effects of MSCs occur, it is possible that MSCs increase the secretion of trophic factors such as EGF and bFGF [21]. In skeletal muscle, EGF and bFGF also stimulate growth and prevent muscle atrophy [49, 50].

Through MSC administration, the muscle function affected by sepsis-induced skeletal muscle wasting was partially recovered, mainly through improving the function of satellite cells, the primary cell population responsible for repairing skeletal muscle [51]. Considering differences in MSC administration between Gao et al. [46] and the present study, it is possible that, in the present model of HFD-induced muscle wasting, MSC treatment could induce the secretion of soluble factors that finally improve muscle strength. This possible mechanism could be mediated by an effect on satellite cells or another cell population that participates in muscle repair. One such population is a muscle-resident population of nonsatellite progenitor cells that are termed bipotent fibro/adipogenic progenitors and are located in the muscle interstitium and neighbor muscle-associated blood vessels. These cells could contribute to preventing muscle atrophy by secreting paracrine factors such as IL-6, IGF-1, and Wnt1 [52, 53].

Alternatively, MSC administration produces an anti-inflammatory response in several models and pathologies. Systemic inflammation can increase during obesity, resulting in increased proinflammatory cytokines such as IL-1β and TNF-α [54], which induce muscle wasting [55]. Therefore, it is possible that the presently obtained results are due to decreased TNF-α plasma levels, which, in turn, could decrease the atrophic effect on skeletal muscle.

5. Conclusions

The present study is the first to demonstrate that systemically administered MSCs could prevent the muscle wasting associated with HFD-induced obesity, by preventing the decreased MHC levels, increased UPP activity, increased myonuclear apoptosis, and oxidative stress.

Competing Interests

The authors declare that there is no conflict of interests regarding the publication of this paper.

Authors' Contributions

Johanna Abrigo and Juan Carlos Rivera contributed equally to the present work.

Acknowledgments

This study was supported by research grants from the Association-Française Contre Les Myopathies AFM 16670 (Claudio Cabello-Verrugio); FONDECYT 1161646 (Claudio Cabello-Verrugio), 1150589 (Marcelo Ezquer), 1161288 (Felipe Simon), and 3140396 (Daniel Cabrera); the Millennium Institute on Immunology and Immunotherapy, P09-016-F (Claudio Cabello-Verrugio and Felipe Simon); and UNAB DI-741-15/N (Claudio Cabello-Verrugio and Felipe Simon). Johanna Abrigo and Juan Carlos Rivera thank CONICYT for a Ph.D. Scholarship 21161353 and 21141242.

References

[1] R. T. Jagoe, S. H. Lecker, M. Gomes, and A. L. Goldberg, "Patterns of gene expression in atrophying skeletal muscles: response to food deprivation," *The FASEB Journal*, vol. 16, no. 13, pp. 1697–1712, 2002.

[2] J. L. Bailey, "Insulin resistance and muscle metabolism in chronic kidney disease," *ISRN Endocrinology*, vol. 2013, Article ID 329606, 14 pages, 2013.

[3] B. A. Bhatt, J. J. Dube, N. Dedousis, J. A. Reider, and R. M. O'Doherty, "Diet-induced obesity and acute hyperlipidemia reduce IκBα levels in rat skeletal muscle in a fiber-type dependent manner," *American Journal of Physiology—Regulatory Integrative and Comparative Physiology*, vol. 290, no. 1, pp. R233–R240, 2006.

[4] B. Sishi, B. Loos, B. Ellis, W. Smith, E. F. Du Toit, and A.-M. Engelbrecht, "Diet-induced obesity alters signalling pathways and induces atrophy and apoptosis in skeletal muscle in a prediabetic rat model," *Experimental Physiology*, vol. 96, no. 2, pp. 179–193, 2011.

[5] D. Pette and R. S. Staron, "Myosin isoforms, muscle fiber types, and transitions," *Microscopy Research and Technique*, vol. 50, no. 6, pp. 500–509, 2000.

[6] K. Higashino, T. Matsuura, K. Suganuma, K. Yukata, T. Nishisho, and N. Yasui, "Early changes in muscle atrophy and muscle fiber type conversion after spinal cord transection and peripheral nerve transection in rats," *Journal of NeuroEngineering and Rehabilitation*, vol. 10, no. 1, article 46, 2013.

[7] C. Cabello-Verrugio, M. G. Morales, J. C. Rivera, D. Cabrera, and F. Simon, "Renin-angiotensin system: an old player with novel functions in skeletal muscle," *Medicinal Research Reviews*, vol. 35, no. 3, pp. 437–463, 2015.

[8] S. C. Bodine, E. Latres, S. Baumhueter et al., "Identification of ubiquitin ligases required for skeletal muscle atrophy," *Science*, vol. 294, no. 5547, pp. 1704–1708, 2001.

[9] B. A. Clarke, D. Drujan, M. S. Willis et al., "The E3 ligase MuRF1 degrades myosin heavy chain protein in dexamethasone-treated skeletal muscle," *Cell Metabolism*, vol. 6, no. 5, pp. 376–385, 2007.

[10] M. J. Eddins, J. G. Marblestone, K. G. Suresh Kumar et al., "Targeting the ubiquitin E3 ligase MuRF1 to inhibit muscle atrophy," *Cell Biochemistry and Biophysics*, vol. 60, no. 1-2, pp. 113–118, 2011.

[11] V. C. Foletta, L. J. White, A. E. Larsen, B. Leger, and A. P. Russell, "The role and regulation of MAFbx/atrogin-1 and MuRF1 in skeletal muscle atrophy," *Pflügers Archiv: European Journal of Physiology*, vol. 461, no. 3, pp. 325–335, 2011.

[12] P. G. Arthur, M. D. Grounds, and T. Shavlakadze, "Oxidative stress as a therapeutic target during muscle wasting: considering the complex interactions," *Current Opinion in Clinical Nutrition and Metabolic Care*, vol. 11, no. 4, pp. 408–416, 2008.

[13] D. E. Kelley, J. He, E. V. Menshikova, and V. B. Ritov, "Dysfunction of mitochondria in human skeletal muscle in type 2 diabetes," *Diabetes*, vol. 51, no. 10, pp. 2944–2950, 2002.

[14] C. S. Stump, E. J. Henriksen, Y. Wei, and J. R. Sowers, "The metabolic syndrome: role of skeletal muscle metabolism," *Annals of Medicine*, vol. 38, no. 6, pp. 389–402, 2006.

[15] C. Meneses, M. G. Morales, J. Abrigo, F. Simon, E. Brandan, and C. Cabello-Verrugio, "The angiotensin-(1–7)/Mas axis reduces myonuclear apoptosis during recovery from angiotensin II-induced skeletal muscle atrophy in mice," *Pflugers Archiv*, vol. 467, pp. 1975–1984, 2015.

[16] S. Schrepfer, T. Deuse, H. Reichenspurner, M. P. Fischbein, R. C. Robbins, and M. P. Pelletier, "Stem cell transplantation: the lung barrier," *Transplantation Proceedings*, vol. 39, no. 2, pp. 573–576, 2007.

[17] D. G. Phinney and D. J. Prockop, "Concise review: mesenchymal stem/multipotent stromal cells: the state of transdifferentiation and modes of tissue repair—current views," *STEM CELLS*, vol. 25, no. 11, pp. 2896–2902, 2007.

[18] R. J. Deans and A. B. Moseley, "Mesenchymal stem cells: biology and potential clinical uses," *Experimental Hematology*, vol. 28, no. 8, pp. 875–884, 2000.

[19] M. J. Hoogduijn, M. G. H. Betjes, and C. C. Baan, "Mesenchymal stromal cells for organ transplantation: different sources and unique characteristics?" *Current Opinion in Organ Transplantation*, vol. 19, no. 1, pp. 41–46, 2014.

[20] I. Rasmusson, "Immune modulation by mesenchymal stem cells," *Experimental Cell Research*, vol. 312, no. 12, pp. 2169–2179, 2006.

[21] A. I. Caplan and J. E. Dennis, "Mesenchymal stem cells as trophic mediators," *Journal of Cellular Biochemistry*, vol. 98, no. 5, pp. 1076–1084, 2006.

[22] R. M. Deacon, "Measuring the strength of mice," *Journal of Visualized Experiments*, no. 76, article e2610, 2013.

[23] M. G. Morales, H. Olguín, G. Di Capua, E. Brandan, F. Simon, and C. Cabello-Verrugio, "Endotoxin-induced skeletal muscle wasting is prevented by angiotensin-(1–7) through a p38 MAPK-dependent mechanism," *Clinical Science*, vol. 129, no. 6, pp. 461–476, 2016.

[24] C. Cabello-Verrugio, M. G. Morales, D. Cabrera, C. P. Vio, and E. Brandan, "Angiotensin II receptor type 1 blockade decreases CTGF/CCN2-mediated damage and fibrosis in normal and dystrophic skeletal muscles," *Journal of Cellular and Molecular Medicine*, vol. 16, no. 4, pp. 752–764, 2012.

[25] M. G. Morales, D. Cabrera, C. Céspedes et al., "Inhibition of the angiotensin-converting enzyme decreases skeletal muscle fibrosis in dystrophic mice by a diminution in the expression and activity of connective tissue growth factor (CTGF/CCN-2)," *Cell and Tissue Research*, vol. 353, no. 1, pp. 173–187, 2013.

[26] M. G. Morales, C. Cabello-Verrugio, C. Santander, D. Cabrera, R. Goldschmeding, and E. Brandan, "CTGF/CCN-2 overexpression can directly induce features of skeletal muscle dystrophy," *The Journal of Pathology*, vol. 225, no. 4, pp. 490–501, 2011.

[27] P. Gregorevic, D. R. Plant, K. S. Leeding, L. A. Bach, and G. S. Lynch, "Improved contractile function of the mdx dystrophic mouse diaphragm muscle after insulin-like growth factor-I administration," *The American Journal of Pathology*, vol. 161, no. 6, pp. 2263–2272, 2002.

[28] F. Cisternas, M. G. Morales, C. Meneses et al., "Angiotensin-(1–7) decreases skeletal muscle atrophy induced by angiotensin II through a Mas receptor-dependent mechanism," *Clinical Science*, vol. 128, no. 5, pp. 307–319, 2015.

[29] C. Meneses, M. G. Morales, J. Abrigo, F. Simon, E. Brandan, and C. Cabello-Verrugio, "The angiotensin-(1–7)/Mas axis reduces myonuclear apoptosis during recovery from angiotensin II-induced skeletal muscle atrophy in mice," *Pflugers Archiv—European Journal of Physiology*, vol. 467, no. 9, pp. 1975–1984, 2015.

[30] M. G. Morales, J. Abrigo, C. Meneses, F. Cisternas, F. Simon, and C. Cabello-Verrugio, "Expression of the Mas receptor is upregulated in skeletal muscle wasting," *Histochemistry and Cell Biology*, vol. 143, no. 2, pp. 131–141, 2014.

[31] J. Abrigo, J. C. Rivera, F. Simon, D. Cabrera, and C. Cabello-Verrugio, "Transforming growth factor type beta (TGF-β) requires reactive oxygen species to induce skeletal muscle atrophy," *Cellular Signalling*, vol. 28, no. 5, pp. 366–376, 2016.

[32] N. H. Le, C.-S. Kim, T. Park et al., "Quercetin protects against obesity-induced skeletal muscle inflammation and atrophy," *Mediators of Inflammation*, vol. 2014, Article ID 834294, 10 pages, 2014.

[33] S.-R. Lee, A. V. Khamoui, E. Jo et al., "Effects of chronic high-fat feeding on skeletal muscle mass and function in middle-aged mice," *Aging Clinical and Experimental Research*, vol. 27, no. 4, pp. 403–411, 2015.

[34] Y. Shpilberg, J. L. Beaudry, A. D'Souza, J. E. Campbell, A. Peckett, and M. C. Riddell, "A rodent model of rapid-onset diabetes induced by glucocorticoids and high-fat feeding," *Disease Models and Mechanisms*, vol. 5, no. 5, pp. 671–680, 2012.

[35] I. Peluso and M. Palmery, "The relationship between body weight and inflammation: lesson from anti-TNF-α antibody therapy," *Human Immunology*, vol. 77, no. 1, pp. 47–53, 2016.

[36] H. Khodabandehloo, S. Gorgani-Firuzjaee, G. Panahi, and R. Meshkani, "Molecular and cellular mechanisms linking inflammation to insulin resistance and β-cell dysfunction," *Translational Research*, vol. 167, no. 1, pp. 228–256, 2016.

[37] P. Plomgaard, A. R. Nielsen, C. P. Fischer et al., "Associations between insulin resistance and TNF-α in plasma, skeletal muscle and adipose tissue in humans with and without type 2 diabetes," *Diabetologia*, vol. 50, no. 12, pp. 2562–2571, 2007.

[38] Y.-P. Li, Y. Chen, J. John et al., "TNF-α acts via p38 MAPK to stimulate expression of the ubiquitin ligase atrogin1/MAFbx in skeletal muscle," *FASEB Journal*, vol. 19, no. 3, pp. 362–370, 2005.

[39] N. Carbó, S. Busquets, M. van Royen, B. Alvarez, F. J. López-Soriano, and J. M. Argilés, "TNF-α is involved in activating DNA fragmentation in skeletal muscle," *British Journal of Cancer*, vol. 86, no. 6, pp. 1012–1016, 2002.

[40] Y. Hao, J. R. Jackson, Y. Wang, N. Edens, S. L. Pereira, and S. E. Alway, "β-hydroxy-β-methylbutyrate reduces myonuclear apoptosis during recovery from hind limb suspension-induced muscle fiber atrophy in aged rats," *American Journal of*

Physiology—Regulatory Integrative and Comparative Physiology, vol. 301, no. 3, pp. R701–R715, 2011.

[41] S. J. Lessard, D. A. Rivas, K. So et al., "The AMPK-related kinase SNARK regulates muscle mass and myocyte survival," *The Journal of Clinical Investigation*, vol. 126, no. 2, pp. 560–570, 2016.

[42] X. Fu, M. Zhu, S. Zhang, M. Foretz, B. Viollet, and M. Du, "Obesity impairs skeletal muscle regeneration through inhibition of AMPK," *Diabetes*, vol. 65, no. 1, pp. 188–200, 2016.

[43] M. L. Messi, T. Li, Z. M. Wang, A. P. Marsh, B. Nicklas, and O. Delbono, "Resistance training enhances skeletal muscle innervation without modifying the number of satellite cells or their myofiber association in obese older adults," *Journals of Gerontology Series A: Biological Sciences and Medical Sciences*, 2015.

[44] F. S. Tedesco, A. Dellavalle, J. Diaz-Manera, G. Messina, and G. Cossu, "Repairing skeletal muscle: regenerative potential of skeletal muscle stem cells," *The Journal of Clinical Investigation*, vol. 120, no. 1, pp. 11–19, 2010.

[45] A. Bareja and A. N. Billin, "Satellite cell therapy—from mice to men," *Skeletal Muscle*, vol. 3, article 2, 2013.

[46] J. Gao, J. E. Dennis, R. F. Muzic, M. Lundberg, and A. I. Caplan, "The dynamic in vivo distribution of bone marrow-derived mesenchymal stem cells after infusion," *Cells Tissues Organs*, vol. 169, no. 1, pp. 12–20, 2001.

[47] R. H. Lee, A. A. Pulin, M. J. Seo et al., "Intravenous hMSCs improve myocardial infarction in mice because cells embolized in lung are activated to secrete the anti-inflammatory protein TSG-6," *Cell Stem Cell*, vol. 5, no. 1, pp. 54–63, 2009.

[48] S. Jose, M. L. Hughbanks, B. Y. K. Binder, G. C. Ingavle, and J. K. Leach, "Enhanced trophic factor secretion by mesenchymal stem/stromal cells with Glycine-Histidine-Lysine (GHK)-modified alginate hydrogels," *Acta Biomaterialia*, vol. 10, no. 5, pp. 1955–1964, 2014.

[49] S. Chen, J. Murphy, R. Toth, D. G. Campbell, N. A. Morrice, and C. Mackintosh, "Complementary regulation of TBC1D1 and AS160 by growth factors, insulin and AMPK activators," *Biochemical Journal*, vol. 409, no. 2, pp. 449–459, 2008.

[50] S. Yamada, N. Buffinger, J. DiMario, and R. C. Strohman, "Fibroblast growth factor is stored in fiber extracellular matrix and plays a role in regulating muscle hypertrophy," *Medicine and Science in Sports and Exercise*, vol. 21, no. 5, pp. S173–S180, 1989.

[51] P. Rocheteau, L. Chatre, D. Briand et al., "Sepsis induces long-term metabolic and mitochondrial muscle stem cell dysfunction amenable by mesenchymal stem cell therapy," *Nature Communications*, vol. 6, article 10145, 2015.

[52] A. W. B. Joe, L. Yi, A. Natarajan et al., "Muscle injury activates resident fibro/adipogenic progenitors that facilitate myogenesis," *Nature Cell Biology*, vol. 12, no. 2, pp. 153–163, 2010.

[53] M. D. Boppart, M. D. Lisio, K. Zou, and H. D. Huntsman, "Defining a role for non-satellite stem cells in the regulation of muscle repair following exercise," *Frontiers in Physiology*, vol. 4, article 310, 2013.

[54] M. Debnath, S. Agrawal, A. Agrawal, and G. P. Dubey, "Metaflammatory responses during obesity: pathomechanism and treatment," *Obesity Research & Clinical Practice*, vol. 10, no. 2, pp. 103–113, 2016.

[55] S. Cohen, J. A. Nathan, and A. L. Goldberg, "Muscle wasting in disease: molecular mechanisms and promising therapies," *Nature Reviews Drug Discovery*, vol. 14, no. 1, pp. 58–74, 2015.